Proceedings of a Symposium on

PRELIMINARY RESULTS FROM THE SEPTEMBER 1979 RESEARCHER/PIERCE IXTOC-I CRUISE

Key Biscayne, Florida, June 9-10, 1980

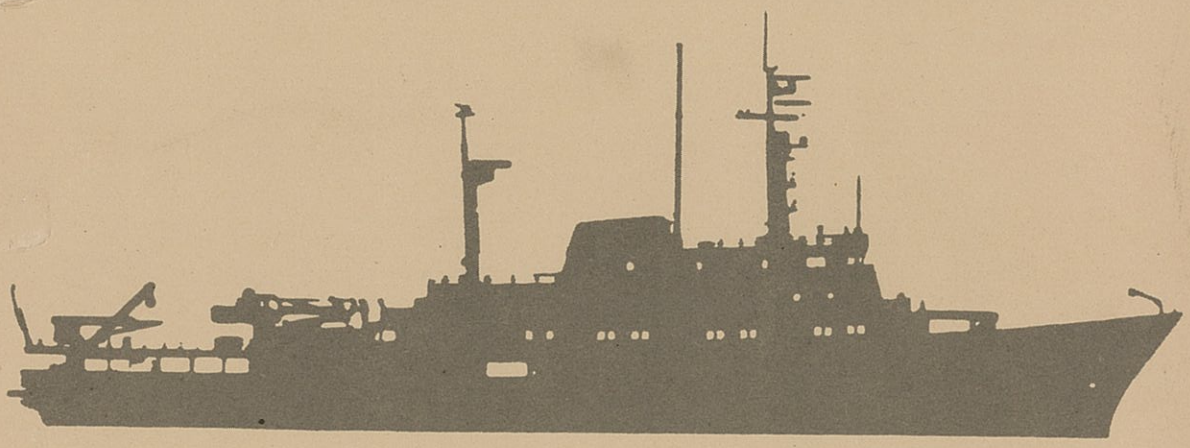

December 1980

U.S. DEPARTMENT OF COMMERCE
National Oceanic and Atmospheric Administration
Office of Marine Pollution Assessment

NOTICE

Mention of a commercial company or product does not constitute an endorsement by NOAA/Office of Marine Pollution Assessment. Use for publicity or advertising purpose of information from this publication concerning proprietary products or the tests of such products is not authorized.

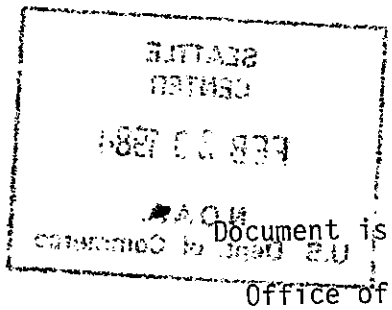

Document is available from:

Office of the Director
NOAA/ERL
Atlantic Oceanographic and Meteorological Laboratories
15 Rickenbacker Causeway
Miami, FL 33149

or

Publications Office
NOAA/RD/MP3
Office of Marine Pollution Assessment
325 Broadway
Boulder, CO 80303

FOREWORD

This symposium volume provides a description of the research cruise by the NOAA Ship RESEARCHER and R/V G. W. PIERCE to the IXTOC-I oil spill in September 1979, and of the initial results from the analyses of data and samples from that cruise. The purpose of this symposium was to provide a forum for early release of these results to the public and to allow the investigators participating in the effort to conduct a scientific dialogue. Given the large number of samples to be analyzed and the complexity of the analytical chemistry, as well as of the geochemical and microbiological results, there is still much to be done, especially as regards interrelation of results from various groups and efforts. Nevertheless, it was decided that the data were of sufficient interest and importance to those involved on a day-to-day basis with oil pollution research and responding to oil spills to warrant a report at this time. This was done with the recognition that scientists, and others interested in this topic, will not find this report as useful as the more comprehensive and complete scientific and layman's version, which will follow within a one-year period.

A complete listing of the types and numbers of samples collected is given in Appendix I of this report. Appendix II describes the sample coding used in tracking all samples collected during the cruise. We feel that the results described herein, on the analysis of these samples, are interesting and significant. Compounds resulting from photooxidation experiments conducted on IXTOC-I crude oil were the same as those found in situ in the area of the spill plume. Interestingly, these same compounds were formed by microbial action in microcosm experiments conducted in the dark on board the RESEARCHER, but in differing amounts and ratios. It is also clear that the entire microbial community responds to the spilled oil and that a population of petroleum degrading bacteria can grow rapidly enough to consume the oil at relatively rapid rates. However, the growth of these bacterial populations in the tropical surface waters of the Bay of Campeche was nutrient-limited. These facts lead to an interesting hypothesis that spraying oil spilled in such an environment with solutions of nutrients (fertilizer) might be an effective method for enhancing the natural ability of the ecosystem to cleanse itself and for combating future spills. It is at least an approach which should be tested. We hope that these and the other detailed results described in the individual pages of this volume are of use to the scientific community and welcome any comments or feedback of ideas individuals might want to put forward.

Dr. Donald K. Atwood
Chief Scientist
IXTOC-I Research Cruise

CONTENTS

	Page
FOREWORD	iii
CRUISE SCIENCE PERSONNEL	viii
PARTICIPATING GROUPS AND THEIR FUNCTION	ix
ACKNOWLEDGMENTS	xi
THE MISSION OF THE SEPTEMBER 1979 RESEARCHER/PIERCE IXTOC-I CRUISE AND THE PHYSICAL SITUATION ENCOUNTERED Donald K. Atwood, John A. Benjamin and John W. Farrington	1
MARINE OIL SPILL RESEARCH PRIOR TO THE IXTOC BLOWOUT IN JUNE 1979 George R. Harvey	19
IXTOC-I OIL BLOWOUT S. L. Ross, C. W. Ross, F. Lepine and R. K. Langtry	25
INTERCALIBRATION OF ANALYTICAL LABORATORIES William D. MacLeod, Jr. and James R. Fischer	41
GASEOUS AND VOLATILE HYDROCARBONS IN THE GULF OF MEXICO FOLLOWING THE IXTOC-I BLOWOUT James M. Brooks, Denis A. Wiesenburg, Roger A. Burke, Mahlon C. Kennicutt and Bernie B. Bernard	53
TRACING THE DISPERSAL OF THE IXTOC-I OIL USING C, H, S, AND N STABLE ISOTOPE RATIOS R. E. Sweeney, R. I. Haddad and I. R. Kaplan	89

Page

HORIZONTAL AND VERTICAL TRANSPORT OF DISSOLVED AND PARTICULATE-BOUND HIGHER-MOLECULAR-WEIGHT HYDROCARBONS FROM THE IXTOC-I BLOWOUT 119
J. R. Payne, G. S. Smith, P. J. Mankiewicz, R. F. Shokes, N. W. Flynn, V. Moreno and J. Altamirano

SUBSURFACE DISTRIBUTIONS OF PETROLEUM FROM AN OFFSHORE WELL BLOWOUT - THE IXTOC-I BLOWOUT, BAY OF CAMPECHE 169
David L. Fiest and Paul D. Boehm

MINERALOGY OF SUSPENDED AND BOTTOM SEDIMENTS IN THE VICINITY OF THE IXTOC-I BLOWOUT, SEPTEMBER 1979 189
Terry A. Nelson

ASPECTS OF THE TRANSPORT OF PETROLEUM HYDROCARBONS TO THE OFFSHORE BENTHOS DURING THE IXTOC-I BLOWOUT IN THE BAY OF CAMPECHE 207
Paul D. Boehm and David L. Fiest

SURFACE EVAPORATION/DISSOLUTION PARTITIONING OF LOWER-MOLECULAR-WEIGHT AROMATIC HYDROCARBONS IN A DOWN-PLUME TRANSECT FROM THE IXTOC-I WELLHEAD 239
J. R. Payne, N. W. Flynn, P. J. Mankiewicz and G. S. Smith

SURFACE WATER COLUMN TRANSPORT AND WEATHERING OF PETROLEUM HYDROCARBONS DURING THE IXTOC-I BLOWOUT IN THE BAY OF CAMPECHE AND THEIR RELATION TO SURFACE OIL AND MICROLAYER COMPOSITIONS . . . 267
Paul D. Boehm and David L. Fiest

PHOTO-CHEMICAL OXIDATION OF IXTOC-I OIL 341
Edward B. Overton, John L. Laseter, Wayne Mascarella, Christine Raschke, Ileana Nuiry and John W. Farrington

Page

CHEMISTRY AND NATURAL WEATHERING OF VARIOUS CRUDE OIL FRACTIONS FROM THE IXTOC-I OIL SPILL 387
Alfonso V. Botello and
Sylvia Castro-Gessner

MICROBIAL DEGRADATION OF HYDROCARBONS IN MOUSSE FROM IXTOC-I 411
Ronald M. Atlas, George Roubal,
Anne Bronner, and John Haines

DETAILED CHEMICAL ANALYSIS OF IXTOC-I CRUDE OIL AND SELECTED ENVIRONMENTAL SAMPLES FROM THE RESEARCHER AND PIERCE CRUISES 439
E. B. Overton, L. V. McCarthy,
S. W. Mascarella, M. A. Maberry,
S. R. Antoine, J. L. Laseter and
J. W. Farrington

ACOUSTIC OBSERVATIONS OF BIOLOGICAL VOLUME SCATTERING IN THE VICINITY OF THE IXTOC-I BLOWOUT 499
Michael C. Macaulay, Kendra Daly and
T. Saunders English

ACOUSTIC OBSERVATIONS OF SUBSURFACE SCATTERING DURING A CRUISE AT THE IXTOC-I BLOWOUT IN THE BAY OF CAMPECHE, GULF OF MEXICO 525
Donald J. Walter and John R. Proni

RESPONSE OF THE PELAGIC MICROBIAL COMMUNITY TO OIL FROM THE IXTOC-I BLOWOUT: I. IN SITU STUDIES 545
Frederic K. Pfaender, Earle N. Buckley
and Randolph Ferguson

RESPONSE OF THE PELAGIC COMMUNITY TO OIL FROM THE IXTOC-I BLOWOUT: II. MODEL ECOSYSTEM STUDIES 563
Earle N. Buckley, Frederic K. Pfaender,
Kristine L. Kylberg and
Randolph L. Ferguson

APPENDIX I 589

APPENDIX II 591

CRUISE SCIENCE PERSONNEL

NOAA/NATIONAL OCEAN SURVEY

NATIONAL OCEAN SURVEY PERSONNEL

Capt. Ronald L. Newsom, Commanding Officer, RESEARCHER

Lt. Cdr. Richard L. Permenter, Operations Officer, RESEARCHER

Lt. Cdr. H. Bruce Arnold, Operations Officer assigned to G. W. PIERCE

Chief Robert L. Hopkins, Chief Survey Technician, RESEARCHER

SCIENTIFIC PERSONNEL - RESEARCHER

Dr. Donald Atwood	NOAA/AOML, Chief Scientist
Dr. John Farrington	Woods Hole Oceanographic Institution, Senior Chemist
Dr. Randy Ferguson	NOAA/NMFS, Beaufort, North Carolina, Senior Biologist
Dr. James Payne	SAI (Science Applications, Inc.), La Jolla, California
Dr. Fred Pfaender	University of North Carolina
Mr. Earle Buckley	University of North Carolina
Mr. Larry McCarthy	University of New Orleans
Mr. David Fiest	ERCO (Energy Resources Co., Inc.), Cambridge, Massachusetts
Mr. George Perry	ERCO (Energy Resources Co., Inc.)
Ms. Dale Finch	NOAA/AOML
Mr. Ricardo Klimek	Departamento de Pescas, Mexico, D.F.
Mr. Victor Moreno	Departamento de Pescas, Mexico, D.F.
Mr. Jose Altamirano	Instituto Mexicano del Petroleo, Mexico
Mr. Michel Marchand	Centre National pour l'Exploration des Oceans, Paris, France
Mr. Glen Aurelius	Helicopter Pilot
Mr. Gary Freeman	Helicopter Mechanic

SCIENTIFIC PERSONNEL - G. W. PIERCE

Mr. Donald Walter	NOAA/AOML, Senior Scientist
Mr. Mahlon Kennicutt	Texas A&M University
Mr. Keith Hausknecht	ERCO (Energy Resources Co., Inc.)
Mr. Jack Barbash	ERCO (Energy Resources Co., Inc.)
Ms. Kendra Daly	University of Washington
Ms. Anne Bronner	University of Louisville (Kentucky)
Mr. George Roubel	University of Louisville (Kentucky)
Mr. Antonio Puig	NOAA/AOML
Mr. Paul Dammon	NOAA/AOML
Mr. Lawrence Guest	NOAA/AOML

PARTICIPATING GROUPS AND THEIR FUNCTIONS

NOAA/Office of Marine Pollution Assessment

- Project Coordination and Funding

NOAA/ERL Atlantic Oceanographic and Meteorological Laboratories

- Cruise logistics and procurement
- Science coordination
- Chemistry contract monitoring

NOAA/National Marine Fisheries Service, Southeast Fisheries Center

- Microbiology contract monitoring
- Coordination of cruise biology efforts

NOAA/National Marine Fisheries Service, National Analytical Facility

- Intercalibration on hydrocarbons and NSO polar compounds

NOAA/National Ocean Survey

- RESEARCHER
- Procurement and contract monitoring for R/V PIERCE

Woods Hole Oceanographic Institution

- Organic geochemistry
- Coordination of cruise chemistry efforts

Texas A&M University

- Sampling and analysis of C_1-C_4 gases and volatile organic compounds

University of Washington

- Zooplankton distributions

Energy Resources Co., Inc.

- Organic geochemistry

Science Applications, Inc.

- Organic geochemistry

Global Geochemistry Corporation

- Isotopic ratios in spilled IXTOC-I crude oil

Center for Bio-Organic Studies, University of New Orleans

Photooxidation of IXTOC-I crude oil
Chemical analysis of microcosm experiments

University of North Carolina

Microcosm experiments on microbial degradation of IXTOC-I crude oil

University of Louisville

In-situ studies of microbial degradation of IXTOC-I crude oil

Tracor Marine, Inc.

R/V PIERCE

Crescent Airways

Helicopter and crew

ACKNOWLEDGMENTS

The following acknowledgments are to persons or groups whose names do not appear elsewhere in this volume as authors or cruise participants but who, nevertheless, made significant contributions to the success of the efforts described.

Mr. George Berberian of NOAA/AOML, who coordinated the publication of this volume.

Ms. Janice R. Adamson of NOAA/AOML, who made all the necessary arrangements for the Symposium.

Dr. Louis Butler and Ms. Judith Roales of the NOAA/Office of Marine Pollution Assessment, who coordinated the funding for the entire project and follow-up work.

Mr. P. D. Jiron and Ms. Joan Wagner of NOAA/AOML, who accomplished difficult emergency procurement actions prior to the cruise.

Mr. John W. Kofoed of NOAA/AOML, who arranged loan of a laboratory van to the RESEARCHER for SAI, and Dr. Thomas O'Connor of the NOAA/Ocean Dumping Research and Monitoring Office, who arranged loan of a freezer van to the RESEARCHER and two laboratory vans to the PIERCE.

Capt. William Jeffers of the NOAA/Commissioned Officer Corps, for coordinating the efforts to locate a keel-cooled contract research vessel.

Mr. John Robinson, Dr. Nancy Maynard and Dr. Jerry Galt of the NOAA/Office of Marine Pollution Assessment, for their helpful suggestions and information throughout the cruise.

The Office of Naval Research, which supplied salary and support to Dr. John W. Farrington for his efforts as Senior Chemist during the cruise and cruise follow-up.

Dr. George R. Harvey of NOAA/AOML, who served as COTR for all of the chemistry-related contracts and his significant help in staging up for the cruise.

Mrs. Amada Cortes Rubio of the Instituto Mexicano de Petroleo, for supplying, through Dr. Ian Kaplan, samples of fresh IXTOC-I crude oil.

Dr. Patrick Parker of the University of Texas, Port Aransas Marine Laboratory, for his helpful suggestions and information.

Mr. Larry Chesal of NOAA/AOML, for his assistance in preparing the extraction van aboard the RESEARCHER.

Dr. Robert Gagosian and Dr. Oliver Zafiriou of Woods Hole Oceanographic Institution, for the loan of glass Bodman bottles and carboys.

Mr. Steve Carson and Drs. Taro Takahashi and Pierre Biscaye, for the provision of a box corer on short notice.

Mr. William Erb of the U.S. Department of State, Washington, D.C., and Mr. Charles Finan at the U.S. Embassy in Mexico City, for arranging ship clearance for the RESEARCHER and PIERCE to work in Mexican waters.

Ms. Jan Witte of NOVA University in Dania, Florida, who edited this entire volume.

Ms. Roxanne Caballero of NOAA/AOML, who performed many, many hours of editorial tasks essential to publication of this volume.

Dr. James Mattson of NACOA, whose persistence made it all happen.

Ms. Rosa Lee Echard and Ms. Salli Ann Schiffmacher of NOAA/OMPA, who performed the final preparations for publication of this volume.

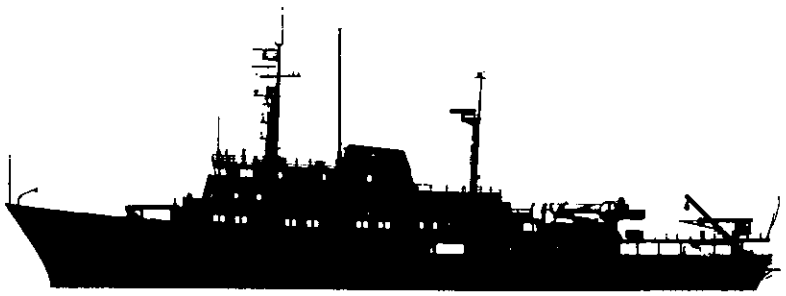

THE MISSION OF THE SEPTEMBER 1979 RESEARCHER/PIERCE IXTOC-I CRUISE AND THE PHYSICAL SITUATION ENCOUNTERED

Donald K. Atwood and John A. Benjamin
Atlantic Oceanographic and Meteorological Laboratories
National Oceanic and Atmospheric Administration
15 Rickenbacker Causeway
Miami, Florida 33149

John W. Farrington
Woods Hole Oceanographic Institution
Woods Hole, Massachusetts 02543

1. INTRODUCTION

The IXTOC-I well blew out on June 9, 1979, with an initially estimated flow of about 30,000 bbl of oil per day. Although this flow seemed to some observers to lessen during the summer, there was still a considerable discharge of oil into the Gulf of Mexico in August, 1979, three months later. A detailed account of the blowout and subsequent events up to late November, 1979, is available in testimony before the U.S. Senate (Campeche Oil Spill: Joint hearing before the Committee on Commerce, Science & Transportation, and the Committee on Energy and Natural Resources--December 5, 1979, Serial No. 9666).

In September, 1979, the NOAA Ship RESEARCHER and the Tracor-Marine-owned-and-operated R/V PIERCE conducted a research cruise to the site of the IXTOC-I blowout in the southern Bay of Campeche and then proceeded along the coast of the western Gulf of Mexico (Figures 1 and 2). This cruise was part of NOAA's overall response to this oil spill. The specific mission of the cruise was limited to conducting research on the biogeochemistry of the spilled oil, e.g., the kinds and rates of chemical and microbial weathering.

The purpose of this paper is to provide basic information on the cruise, the physical situation encountered during the cruise, and the overall strategy as background for other papers in this volume.

The primary vessel for the cruise was the NOAA Ship RESEARCHER, which is equipped with extensive laboratory space. This space was augmented by one laboratory van and a portable freezer unit. A helicopter landing platform was placed aboard for a four-passenger helicopter, leased from Crescent Airways, Inc., along with its crew. This helicopter proved to be absolutely essential to operating the vessels and to the research. It allowed observation of oil coverage over large areas and was consistently used to observe the position of the well discharge plume and the positions of the two ships relative to it. Since the RESEARCHER's engine cooling system does not permit entry into heavily oiled waters, a second, keel-cooled vessel, the R/V PIERCE, was leased from Tracor Marine to accompany the RESEARCHER to the blowout site. This vessel's laboratory space also was augmented by two portable laboratory vans. During the cruise, the R/V PIERCE sampled in the well output plume, up to within a few hundred meters of the flame at the wellhead. At the same time, the RESEARCHER sampled along the edge of the plume and provided extensive laboratory space for sophisticated sample workup and underway experiments. Sample transfer between the two vessels was accomplished using small boats and the helicopter.

Both ships staged up for the cruise in Miami, Florida, and departed that port on September 11. A timetable for the cruise is given in Table 1, and the overall cruise track is shown in Figure 1. Figure 2 shows the detail of stations occupied in the immediate vicinity of the blowout and along the blowout plume.

Table 1. Timetable for RESEARCHER/PIERCE IXTOC-I Cruise (September 1979).

Date	Activity
11 September	Departed Miami
13 September	Commenced helicopter reconnaissance
14 September	Cleared Arrecife, Alcaran, off Yucatan; set up first control (R2, P1) station at 21°41'N, 90°24'W
15 September	Arrived at NE extremity of plume; set up second control station (R4, P2) at 19°48'N, 91°22'W
16 September	PIERCE arrived at wellhead, RESEARCHER commenced sampling plume
16-21 September	Both ships sampled in vicinity of wellhead and plume
22 September	Both ships sampled off Veracruz, Mexico (R12, P16, P17)
23 September	PIERCE departed for Galveston, Texas, RESEARCHER sampled off Tampico, Mexico
24 September	RESEARCHER sampled sediment transect south of U.S./Mexico border
25 September	RESEARCHER sampled off Brownsville, Texas; sampled BLM sediment transect off Brownsville
26 September	RESEARCHER sampled off Corpus Christi, Texas
27 September	RESEARCHER and PIERCE tied up in Galveston, Texas

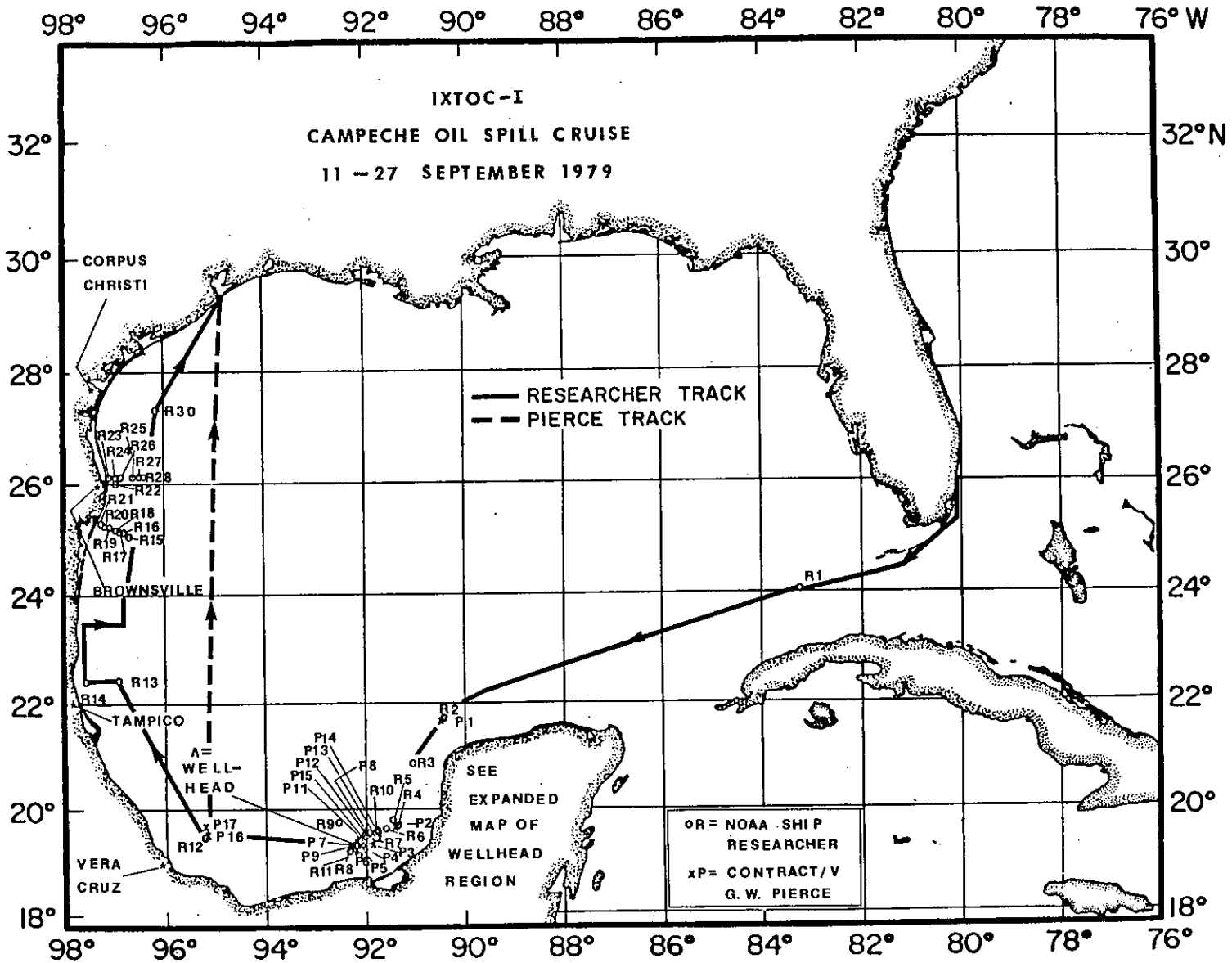

Figure 1. IXTOC-I Campeche oil spill cruise, 11-27 September 1979.

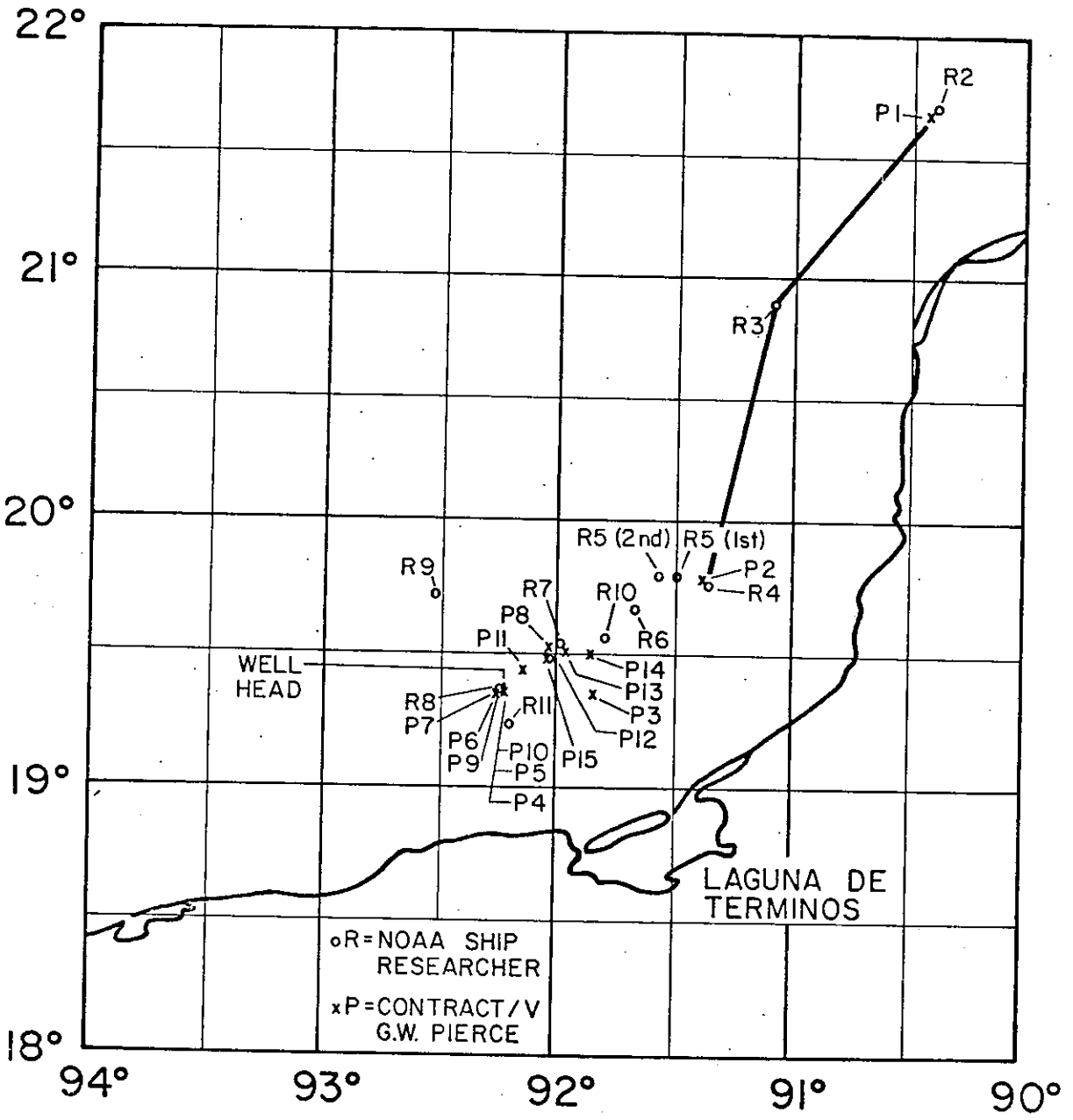

Figure 2. IXTOC-I Campeche oil spill cruise, 11-27 September 1979, expanded wellhead region.

2. PHYSICAL SITUATION

2.1 Effects of Gulf Circulation on IXTOC-I Oil

At the time of the cruise, the Gulf Loop Intrusion was at a maximum, with the northern extremity reaching very close to the Mississippi River Delta. The extent of this intrusion was maintained at least through April of 1980, with no formation of major eddies as a result of pinching off the intrusion as described by Maul (1977) and Molinari (1978). Nor was there any evidence of relic eddies in the northern or western Gulf. The western boundary current, described by Sturges and Blaha (1976) as existing along the coasts of Mexico and Texas, was operative throughout the summer of 1979 and constituted a northerly flow (Galt, personal communication). Flow in the western Gulf of Mexico carried IXTOC oil northwesterly through June, July, and August of 1979, so that major concentrations occurred mostly in a triangle with apexes at the IXTOC-I wellhead, Veracruz, Mexico, and at Cabo Rojo, Mexico, which is just south of Tampico. In late July and early August, beaches along the south Texas coast were heavily oiled by IXTOC oil that had moved considerably north of this triangle. This was not the case in September when the RESEARCHER/PIERCE cruise was in progress. Seasonal current shifts resulted in minimal amounts of oil being found within the above-described triangle. Instead, major surface concentrations of oil were found to the northeast, east, and southeast of the well. This will be discussed further below.

2.2 Climatic Factors

Immediately prior to departure of the vessels from Miami, Hurricane Frederick crossed the western tip of Cuba and traversed the eastern Gulf of Mexico with a landfall at Mobile Bay on September 13. During the early stages of work in the wellhead and blowout plume area (September 14-17), Tropical Storm Henri developed off Yucatan and moved in an erratic course across the southwestern Gulf. The fringes of this storm were felt in the plume area on the 16th and 17th of September, resulting in seas in excess of fifteen feet. Both vessels operated throughout this storm period with minimal time loss. However, all drilling rigs in the vicinity of IXTOC I were evacuated and any oil cleanup operations in progress were abandoned.

Wind speeds and directions observed by RESEARCHER personnel are given in Table 2 for the dates during which that vessel operated in the wellhead/plume area and off Veracruz, Tampico, Brownsville, and Corpus Christi. As can be seen, except for the 16th of September when Henri was just north of the operating area, wind speeds seldom exceeded 15 knots. These winds did not appear to control the direction of oil flow, as evidenced by the fact that wind direction was often 180° to direction of the plume flow. The wind may have had significant effects on weathering and weathering rates, as will be discussed below.

Table 3 is a listing of wet and dry bulb temperatures recorded by the RESEARCHER Quartermaster Department during the cruise. As can be seen, daytime dry bulb temperatures in the southern Bay of Campeche were consistently above

Table 2. Wind speed and direction observed during the RESEARCHER/PIERCE IXTOC-I Cruise (September 1979).

Date	Time (Local/Miami)	Speed (Knots)	Dir. (True)	Position	
14 September	0800	05	010	21°42.3'N	090°23.5'W
	1500	14	015	21°40.2'N	090°23.8'W
	2000	08	000	21°24.0'N	090°46.0'W
15 September	0800	12	010	20°54.6'N	091°10.8'W
	1500	12	320	19°30.2'N	091°29.8'W
	2000	Lt. Airs		19°48.8'N	091°21.7'W
16 September	0800	15	215	19°55.8'N	091°14.3'W
	1500	16	220	19°49.4'N	091°32.6'W
	2000	24	215	19°58.8'N	091°32.0'W
17 September	0800	10	130	19°49.5'N	091°33.5'W
	1500	Lt. Airs		19°34.9'N	091°46.7'W
	2000	08	075	18°58.2'N	091°54.0'W
18 September	0800	10	090	19°32.2'N	091°59.1'W
	1500	Lt. Airs		19°34.7'N	091°57.9'W
	2000	11	340	19°21.0'N	091°51.8'W
19 September	0800	07	030	19°34.3'N	092°19.8'W
	1500	12	330	19°44.8'N	092°30.2'W
	2000	12	000	19°19.8'N	091°59.0'W
20 September	0800	10	250	19°30.6'N	091°50.1'W
	1500	13	260	19°19.5'N	091°56.8'W
	2000	16	250	19°17.5'N	092°08.3'W
21 September	0800	12	225	19°19.1'N	092°13.0'W
	1500	15	300	19°18.4'N	092°12.8'W
	2000	13	305	19°15.1'N	093°11.0'W
22 September	0800	12	355	19°15.1'N	095°10.8'W
	1500	14	330	19°14.2'N	094°56.2'W
	2000	17	350	19°56.0'N	095°15.1'W
23 September	0800	15	350	22°00.1'N	096°40.6'W
	1500	16	360	22°30.0'N	096°58.0'W
	2000	13	035	22°22.6'N	097°31.7'W
24 September	0800	12	340	23°38.6'N	097°20.2'W
	1500	13	000	24°09.1'N	096°32.1'W
	2000	12	025	25°03.2'N	096°42.9'W
25 September	0800	16	015	25°58.7'N	096°48.6'W
	1500	17	005	26°10.0'N	097°01.0'W
	2000	18	020	26°10.1'N	096°20.0'W
26 September	0800	16	030	27°17.2'N	096°11.0'W
	1500	15	010	27°41.7'N	095°48.5'W
	2000	14	080	28°20.3'N	095°10.9'W

Table 3. Wet and dry bulb temperatures observed during the RESEARCHER/PIERCE IXTOC-I Cruise (September 1979).

Date	Time (Local/Miami)	Wet Bulb	Dry Bulb	Position	
14 September	0800	26.5	30.5	21°42.3'N	090°23.5'W
	1500	25.7	29.1	21°40.2'N	090°23.8'W
	2000	26.5	29.0	21°24.0'N	090°46.0'W
15 September	0800	27.0	29.5	20°54.6'N	091°10.8'W
	1500	26.3	28.6	19°30.2'N	091°29.8'W
	2000	26.0	26.5	19°48.8'N	091°21.7'W
16 September	0800	26.0	28.0	19°55.8'N	091°14.3'W
	1500	25.0	26.8	19°49.4'N	091°32.6'W
	2000	25.0	27.0	19°58.8'N	091°32.0'W
17 September	0800	24.0	27.0	19°49.5'N	091°33.5'W
	1500	22.1	27.4	19°34.9'N	091°46.7'W
	2000	23.5	27.5	18°58.2'N	091°54.0'W
18 September	0800	25.0	28.5	19°32.2'N	091°59.1'W
	1500	25.2	28.2	19°34.7'N	091°57.9'W
	2000	25.0	26.5	19°21.0'N	091°51.8'W
19 September	0800	24.5	27.5	19°34.3'N	092°19.8'W
	1500	23.8	26.0	19°44.8'N	092°30.2'W
	2000	24.5	27.0	19°19.8'N	091°59.0'W
20 September	0800	26.0	28.0	19°30.6'N	091°50.1'W
	1500	24.4	27.6	19°19.5'N	091°56.8'W
	2000	24.0	27.0	19°17.5'N	092°08.3'W
21 September	0800	25.5	28.0	19°19.1'N	092°13.0'W
	1500	24.5	28.0	19°18.4'N	092°12.8'W
	2000	24.0	26.5	19°15.1'N	093°11.0'W
22 September	0800	23.5	27.0	19°15.1'N	095°10.8'W
	1500	23.3	26.5	19°14.2'N	094°56.2'W
	2000	24.0	26.0	19°56.0'N	095°15.1'W
23 September	0800	22.5	27.5	22°00.1'N	096°40.6'W
	1500	22.5	26.9	22°30.0'N	096°58.0'W
	2000	23.5	26.5	22°22.6'N	097°31.7'W
24 September	0800	23.5	26.0	23°28.6'N	097°20.2'W
	1500	22.0	26.6	24°09.1'N	096°32.1'W
	2000	22.0	26.0	25°03.2'N	096°42.9'W
25 September	0800	20.0	26.0	25°58.7'N	096°48.6'W
	1500	18.1	25.4	26°10.0'N	097°01.0'W
	2000	20.5	25.5	26°10.1'N	096°20.0'W
26 September	0800	22.0	27.0	27°17.2'N	096°11.0'W
	1500	20.2	25.1	27°41.7'N	095°48.5'W
	2000	22.5	25.0	28°20.3'N	095°10.9'W

27°C, with maximum daily values ranging from 26.0°C to 30.5°C. Nighttime (2000 hours) temperatures were not much lower, with a maximum difference between night and day dry-bulb values being only 2°C.

2.3 Water Characteristics

Water column characteristics in the vicinity of the well and plume were variable and typical of subtropical coastal environments. Surface temperatures were in excess of 28°C and the water column was isothermal to at least 10 m and often to as deep as 40 or 50 m. Water temperatures below 25°C were not observed above 50 m in the vicinity of the well.

Surface salinities in the vicinity of the well and plume varied from about 34.5°/oo to 36.6°/oo and were variable over that range throughout the water column. In general, when low (<35.0°/oo) salinities were observed they occurred at the surface. Below 10 m salinities were generally in excess of 35.5°/oo.

Water in the vicinity of the well and plume was quite turbid, with a greenish color. This color extended from the shore to 1 to 5 nm seaward of the wellhead. This turbidity apparently was a general coastal feature at that time and the interface between it and the clear, blue waters of the open Bay of Campeche was very sharp. A paper by Nelsen describing the suspended matter within the water column is included in this volume.

Dissolved oxygen concentrations measured by Winkler titrations on samples collected from throughout the water column varied from 4.20 to 5.05 ml/l in the vicinity of the well and plume, indicating that the water was fully saturated with oxygen.

3. LOCATION OF OIL

The extent of the oiled area throughout the period of September 15-20 is generally indicated by the locations of stations depicted in Figure 2. In that figure, P1, P2, R2, R3, R4, and R9 are all control-type stations outside of the plume. The rest of the stations are either in or at the edge of the plume proper. Very little oil was noted on the surface west of the wellhead, and what was observed in that direction was assumed to be older oil moving back past the well due to changes in the circulation noted above. Throughout this period, the ouput plume trended northeast from the wellhead (045° to 055° true) and extended for 40 to 50 nm. At times, the plume took sharp meanders, which were generally to the south. As mentioned above, the direction of oil flow on the surface seemed independent of wind speed or direction.

On September 21, the output plume swung to a southeasterly direction over about a 12-hour period. When the RESEARCHER departed, at about sunset on that date, the plume output was flowing at about 135° true.

Virtually no oil was found elsewhere during the cruise, with the exception of some surface sheen and small balls of chocolate-mousse-like emulsion (see below) at P17 off Veracruz and some small "fingernail-sized" flakes of mousse at R30 off Corpus Christi.

4. PHYSICAL DESCRIPTION OF OIL

The physical state of the oil, based on visual observations during the cruise, is best described in terms of zones within the output plume. These zones are described below. Their relative size and position appeared to be a function of many factors, such as sunlight intensity, wind stress, and flow rate. Chemical and physical characteristics of the oil types mentioned are discussed in more detail in various other papers included in this volume.

4.1 Zone 1

This zone is characterized by a continuous light-brown-colored light emulsion of water and oil on the surface (plate 1). The zone existed in the immediate vicinity of the flames and extended for no more than a few hundred m down the plume.

4.2 Zone 2

This zone is characterized by a 30% to 50% coverage of the sea surface by a light brown water and oil emulsion in disoriented streaks (plate 2). The zone started a few hundred m down-plume from the burn and extended out to a maximum of 1 or 2 nm, depending on wind stress. However, at times it was virtually absent.

4.3 Zone 3

This zone is characterized by a 20% to 50% coverage of the sea surface by light brown water and oil emulsion oriented in Langmuir "streaks" parallel to the wind direction. The width of these "streaks" varied from a few cm to a few m, and the length varied from one to tens of meters. These dimensions depended on wind stress (plate 3). In general, these Langmuir "streaks" were surrounded by a light to heavy sheen of oil. This zone extended from as close as a few hundred m from the flames to several nm down the plume.

4.4 Zone 4

This zone is characterized by a darkening of the light brown water and oil emulsion until the streaks were black. This was assumed to result from oxidation of the oil, and the rate seemed to be dependent on sunlight intensity. Commonly, Langmuir "streaks" were blackened in the center and light brown at

the edges where emulsification may have been occurring. At times, these "streaks" coalesced into long lines of blackened oil that extended for several kilometers. In the brown edges of these lines or "streaks," small balls of chocolate-mousse-like emulsion (hereafter called mousse) broke off (plates 4 and 5). (The operational "definition" used for mousse during this cruise was surely different from that for other such events, e.g., the AMOCO CADIZ spill. There is a definite need for a clearer definition of such terms in order to allow adequate comparison of data from future events. In this report, mousse is considered to be an oil and water emulsion of a very thick and viscous consistency that forms into sticky but discrete balls. These balls readily coalesce into larger balls upon contact with each other.) At other times, the wind rolled portions of a streak up onto itself; this also served as a mechanism for the formation of mousse, as did passage of a boat hull or seeding by debris such as sugar cane stalks. Varying concentrations of these balls often covered the sea surface and, like the light brown emulsion, lined up in Langmuir lines or cells. In some instances, these balls reached grapefruit size and/or coalesced into huge "rafts" of mousse up to 50 or 60 m in diameter (plate 6). In one instance, one of these "rafts" was sampled and found to be approximately 1 m thick. This zone began from 5 to 15 nm from the burn and extended out to about 20 nm. The extent of the zone and rate of mousse formation apparently were dependent on sunlight intensity and wind stress. A light to heavy sheen of surface oil was always present in this zone.

4.5 Zone 5

This zone is characterized by an extensive light to heavy sheen of oil that covered >50% of the surface. Usually this sheen was in the form of Langmuir lines (plates 7 and 8). This zone overlapped zones 2, 3, and 4 and extended out to the farthest extremity of the plume.

It is important to remember that:

(1) The description of the zones is based on a combination of detailed observations from RESEARCHER, PIERCE, and small boats coupled with observations from eleven helicopter flights in the vicinity of the oil plume from September 15 to 21, 1979.

(2) These descriptions are operative only for the period of this cruise.

(3) There were no distinct boundaries between these various zones, and they tended to interweave at the transitions, more so on some days than on others.

Plate 1. Zone 1.

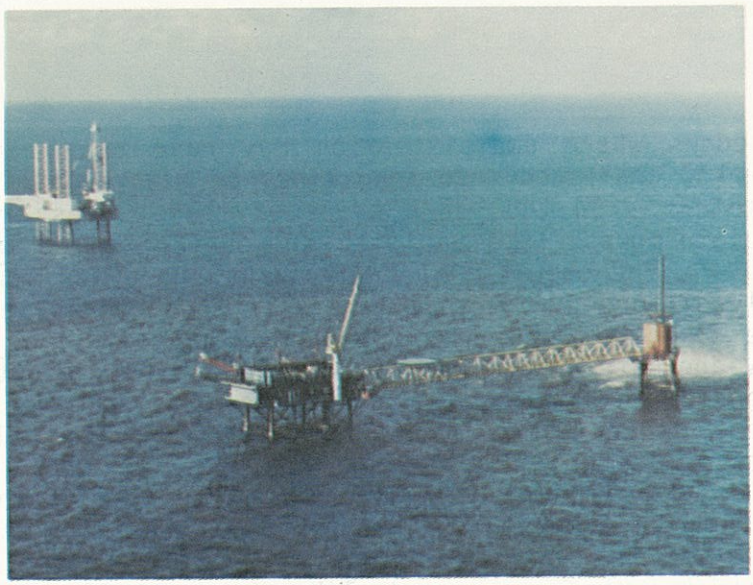

Plate 2. Zone 2.

Plate 3. Zone 3.

Plate 4. Zone 4.

Plate 5. Zone 4.

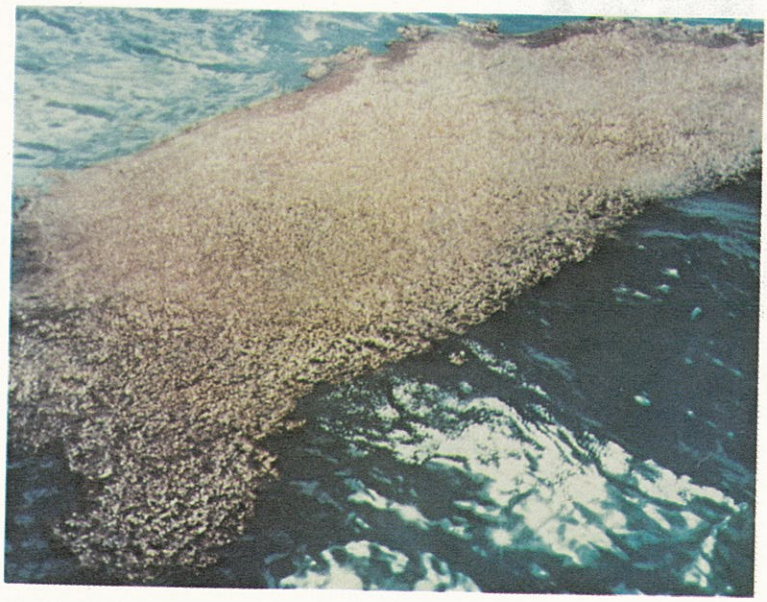

Plate 6. Zone 4.

Plate 7. Zone 5.

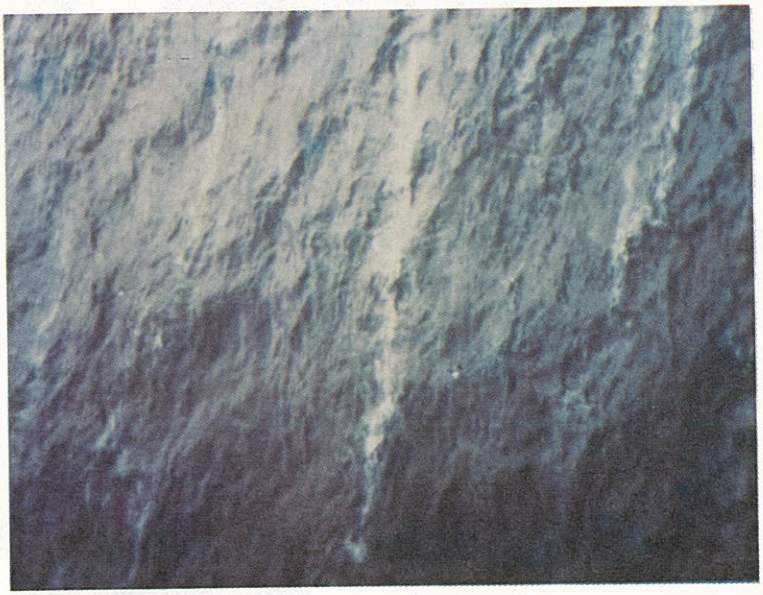

Plate 8. Zone 5.

5. SAMPLING STRATEGY

The initial sampling strategy for the cruise was developed in August and called for the following sequence:

(1) Sampling of fresh oil and "mousse" in its early stages of formation would be done near the well site. This would be accompanied by air, water, and slick sampling near the well site.

(2) The two ships would proceed along the western Gulf of Mexico about 100 to 150 nm offshore, sampling mousse of progressively older age as the coast of Texas was approached. Water and surface sheen in contact with this older mousse would also have been sampled.

The sampling strategy had to be extensively modified once it was clear that the circulation of the Gulf had changed by the time the ship arrived. This was apparent after the first helicopter flight to the well site area as the RESEARCHER and PIERCE approached. As a result, it was decided to focus more of the cruise effort at the well site area, sampling intensively at the edges of the plume and in the plume itself. One goal of this strategy was to provide some broad coverage of sampling stations for general investigation of processes active in controlling the fate of the discharge oil and gas near the well site, and progressively farther away in the area of the visually recognizable slick. This included air sampling for C_5 and higher-molecular-weight compounds; surface slick sampling for heavier-molecular-weight compounds; water sampling for gases, volatile compounds in the range of C_7 to C_{17} hydrocarbons, and higher-molecular-weight particulate and dissolved compounds; surface sediment sampling; and a few sediment trap samples. The water column was sampled in most of the same locations for microbiological studies. Plankton tows were obtained under the slick from the PIERCE, and neuston tows were obtained from the RESEARCHER. A listing of the sample type collected and the number of each is given in Appendix I. Appendix II is an explanation of the sample code designation used during the cruise.

Two different acoustic arrays were operated on the PIERCE to guide the sampling under the slick. These are described in other papers in this volume.

A second goal was the intensive sampling of mousse in an attempt to gain further insight into the relationship between physical form, chemical composition, and microbial processes. It was hypothesized that the chemical analyses and microbial studies would provide clues as to how the mousse formed, what its fate would be, and the extent to which toxic compounds were incorporated in the mousse or produced during mousse formation. This was, and is, an important area of investigation because "rafts" of mousse were transported across the Gulf of Mexico to distances of over 500 nm to the coast of Mexico near Tampico and on up to the U.S. coast near Brownsville and Port Aransas, Texas.

A third goal was the sampling of surface sediments on two transects in the area off the coast near the U.S. Department of Interior, Bureau of Land Management Outer Continental Shelf Environmental Studies. There had been earlier reports of slicks and mousse in the waters in this general area. If this had resulted in extensive contamination of surface sediments, analyses of these sediment samples could provide definitive data. If the analyses showed no detectable IXTOC-I oil, then these samples would provide a set of clean sediment analyses for the area in case of further incursions of IXTOC-I oil.

Most of the types of sampling gear used on the cruise are described in the papers that follow or are referenced therein. For further details, the reader should contact the NOAA Office of Marine Pollution Assessment.

After the cruise, time and funds placed constraints on the number of samples that could be analyzed as of the date of this symposium. Two analytical strategy meetings after the cruise provided guidance to all involved as to priorities of analyses and specific sample sets and types to be analyzed in the laboratory. The general approach was again to focus on (1) the samples close to the well site and near the slick, to gain information about the immediate fate of the oil over days to weeks; (2) samples of mousse collected throughout the cruise.

The papers that follow present the data and initial interpretations from these analyses. We emphasize here, as in the Foreword, that these papers are actually reports from the principal investigators of this research effort to each other, with some clarification added, to aid our colleagues conducting oil pollution research in understanding the data as presented. The overall interpretation and individual data set interpretations for the general scientific community and the public will follow within a year. Our intent here is to make available as much information and data as possible so that those having to respond to similar events and undertake similar cruises will have access to this information from the start.

6. REFERENCES

Maul, G. A. (1977): The annual cycle of the Gulf Loop Current part I: Observations during a one year time series. J. Mar. Res., 35: 29-47.

Molinari, R. L. (1978): Current variability and its relation to sea-surface topography in the Carribbean Sea and Gulf of Mexico. Mar. Geodesy, 3: 149-419.

Sturges, W., and J. P. Blaha (1976): A western boundary current in the Gulf of Mexico. Science, 192: 367-369.

MARINE OIL SPILL RESEARCH PRIOR TO THE IXTOC BLOWOUT IN JUNE 1979

George R. Harvey
Atlantic Oceanographic and Meteorological Laboratories
National Oceanic and Atmospheric Administration
15 Rickenbacker Causeway
Miami, Florida 33149

During the 1970's, marine scientists studied about six oil spills rather intensely. These include the Santa Barbara blowout off California, the grounding of the METULA in the Magellan Straits, the groundings of the FLORIDA in Buzzards Bay, Massachusetts, the TSESIS in the Stockholm channel, the AMOCO CADIZ off Brest, France, and the breakup of the ARGO MERCHANT on Nantucket Shoals. Most of those spills occurred in high latitudes in turbulent seas and usually required a hurried response from the scientific community before the oil dispersed or was removed by clean-up operations. Before 1979 there were almost no studies of oil behavior in tropical seas.

Nevertheless, much information on rates of evaporation and weathering was acquired. However, since most spills in the past have involved oiled beaches and marshes, the greatest effort in those cases was usually directed at the intertidal zone. Such studies have been conducted for over ten years now on Bermuda and in the Great Sippewisset Marsh on Buzzards Bay. Usually sampling efforts at sea were prematurely curtailed due to weather and time constraints. One case in point was the ARGO MERCHANT, which broke up off New England in rough seas during the Christmas holidays. Thus, before IXTOC, very little was known about the distribution of oil in the water column beneath surface slicks or floating tar.

During the study of the AMOCO CADIZ spill on the French coast, the cakes of brown, oil-seawater emulsions were aptly described as chocolate mousse. It was not possible at that time to study how, when, or why mousse formation occurred. Yet, within several hours after a spill into the sea, mousse is the predominant physical form of the oil. Several papers in this symposium will address these phenomena directly.

Prior to the IXTOC studies, it was generally thought that oil in seawater stimulated the growth of just the oil-consuming bacteria. Results of a study which was designed to test that hypothesis will be presented at this symposium.

The best summary of knowledge of the fate of oil in the marine environment before IXTOC is given by the updated reports and studies, No. 6 of the Working Group of GESAMP (Group of Experts for Scientific Advice on Marine Pollution), 1980, sponsored by the United Nations Environmental Program. Following is an abstract of that report (UNESCO, Paris, 1980):

> A variety of simultaneous physico-chemical processes govern the distribution and fate of the oil immediately following a spillage.
>
> Spreading on the surface is the initial dominating process. Evaporation of short-chained volatile compounds proceeds rapidly and this is highly temperature dependent. For example, at 20°C, compounds with up to 12 carbon atoms largely evaporate within a few hours. Partial loss by evaporation occurs within a few days for compounds with up to 22 carbon atoms.
>
> The formation of water-in-oil emulsions begins immediately after discharge of oil into the marine

environment. The rate of emulsion formation depends upon turbulence. Oil-in-water emulsions are formed more slowly, being of importance in the period days to weeks following the introduction of oil into the marine environment. The dissolution of oil components in water progresses continuously, but being dependent on the surface area of the oil it is most pronounced when a dispersion of oil-in-water is formed. Evaporation of lighter fractions and incorporation of denser suspended solids will eventually cause most oil residues to sink. This process is usually significant for crude oils within weeks of the discharge.

Photolysis, photochemical and other oxidative processes are at their greatest relative importance during the first weeks after the incident.

Over 90 species of micro-organisms including open ocean, coastal and estuarine bacteria, fungi and yeasts, capable of degrading petroleum by biological oxidation, have been identified. Their action does not become important until a week or so after an oil discharge. All kinds of oils are susceptible to microbiological degradation. Assuming the presence of appropriate micro organisms and recognizing the other physical and chemical factors involved, the most important factor which influences the biodegradability of hydrocarbons seems to be the molecular configuration. Alkanes are attacked by more microbial species more rapidly than either aromatic or naphthenic compounds.

Tar balls, because of varying size and density, are distributed throughout the water column - from the surface to the sea bed but may concentrate at a thermocline. Some are formed soon after oil is discharged from tanker washings, others from crude oil and heavy oil products over a longer period of time in the marine environment.

Bioconcentration has been demonstrated, but while possible under certain conditions, there is little convincing evidence of accumulation or biomagnification of oil. In general, higher trophic organisms show lower concentrations of hydrocarbons.

The only disappointment related to the RESEARCHER cruise in the western Gulf of Mexico was not finding a continuous sheet of oil laid out in a 0-4 month-old path from the well head to the south Texas islands. This was the setting in August 1979 and would have allowed detailed studies of rates of weathering of pelagic oil. The reasons that this important objective was made impossible in September 1979 is the subject of another paper in this symposium.

IXTOC-I OIL BLOWOUT

S. L. Ross and C. W. Ross
Environment Canada

F. Lepine
Energy, Mines & Resources Canada

R. K. Langtry
Indian Affairs & Northern Development Canada

1. BACKGROUND

Mexico has emerged on the international stage as a major factor in the world's petroleum situation. The country is currently developing four geographic areas for production, and the hydrocarbon deposits in these areas indicate a large quantity of proven and probable reserves.

One of these areas, the Bay of Campeche, having 8000 square km of area, is particularly promising (see Figure 1). Geophysical studies in conjunction with drilling to date have shown that huge deposits exist here with an oil-impregnated rock mass of over one thousand m in depth in some places. At the present time, there is much offshore drilling activity in the area, with plans in 1979 to complete the installation of 10 stationary drilling platforms, six production platforms, and one connecting platform.

All of this activity in Mexico is controlled by the national oil company, Petroleos Mexicanos (PEMEX), which is one of the most integrated oil companies in the world, taking part in all petroleum activities ranging from exploration to distribution of products. The company, with an annual budget of $11 billion, is Mexico's largest enterprise and largest employer.

2. BLOWOUT IN CAMPECHE BAY

On 3 June 1979, at 0330 hours, the exploratory (field outpost) well IXTOC-I, located approximately 80 km NNW of Ciudad del Carmen (19°24'29.418"N; 92°19'36.690"W) in the Bay of Campeche, was the site of an uncontrolled oil blowout (see Figure 1). The SEDCO 135 semisubmersible platform, with BOP stack situated on the seafloor, was drilling in 51.5 m of water. This was the first well drilled in that particular geological structure. Perforaciones Marinas del Golfo S. A. of Mexico City had contracted the platform from SEDCO, Inc. of Dallas, Texas, and then leased it to PEMEX. The well had been drilled to the top of the known productive interval at approximately 3500 m. Production casing had been run and cemented at that depth and the well had been deepened another 30 m when the mud "circulation" was totally lost. The operator spent approximately 48 hours attempting to regain circulation, determining fluid levels in the annulus and watching for indications of flow from the productive zone. A decision was made then to pull the pipe out of the well to remove the drilling bit. The drill pipe was pulled out of the hole without incident and apparently without any sign of the well's flowing until the drill collars reached the rig floor. At this point, the 4-3/4" drill collars extended through the blowout preventers. The well then started to kick and the driller shut the annular preventer which closed off the annulus. However, the gas and oil started flowing up through the drill collars onto the derrick. At this point, the annular preventer failed and the drill collars began rising from the hole.

When this happened, all of the crew but two individuals abandoned the drilling unit. Before leaving, they attempted to shear the drill collars with the

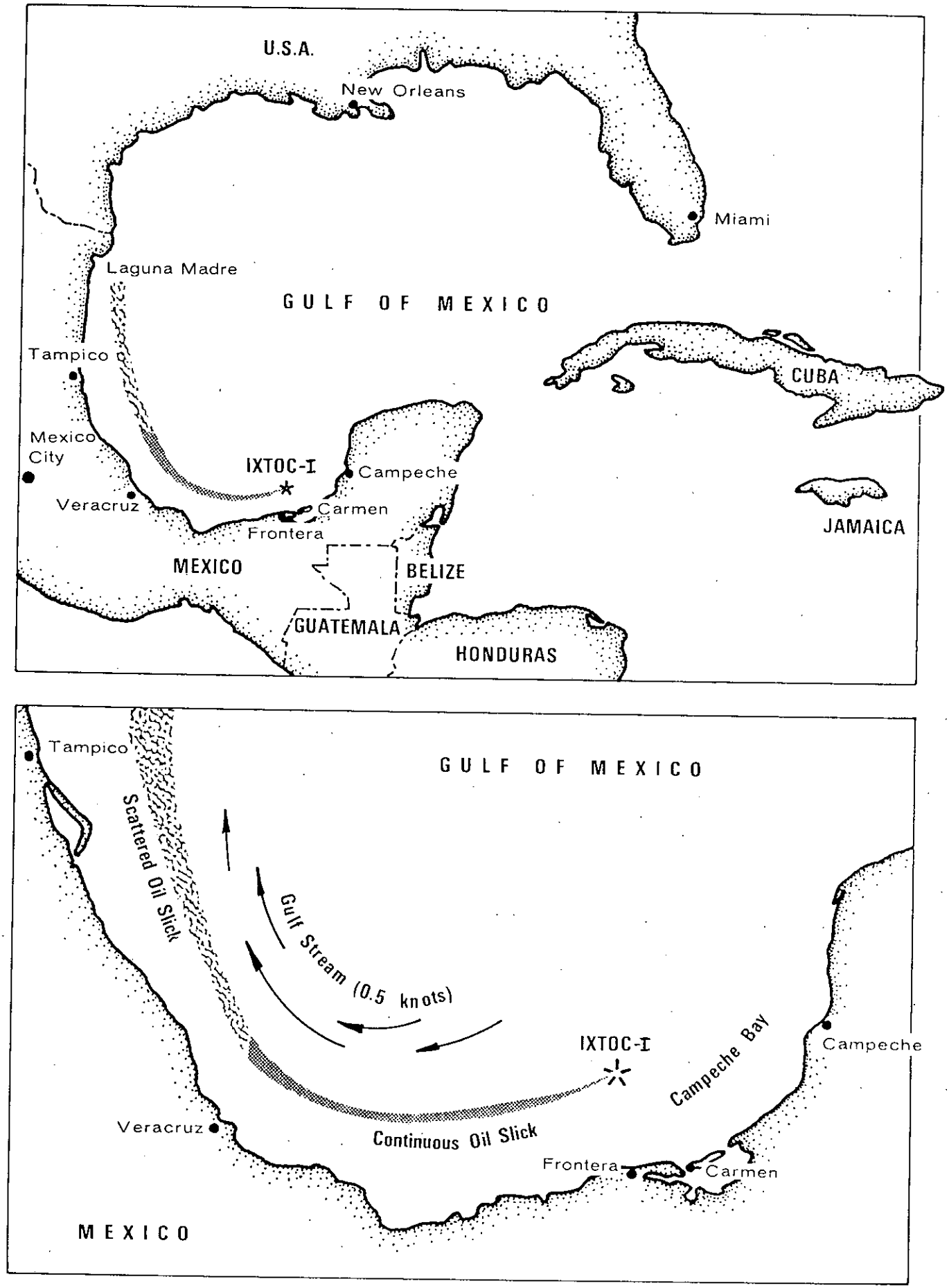

Figure 1. The site of the IXTOC-I blowout.

shear rams; however, they were unable to do so. (The shear rams are designed to cut only thin-walled drill pipe and casing. The other rams in the BOP's were sized to fit the drill pipe--3-1/2"--and therefore could not seal off against the drill collars.) They then attempted to cut the anchor lines so that the unit would or could be moved away from the site. They had cut about half of the lines (4 of 9) when they were forced to leave the unit by the heat and fire from the oil and gas which had by this time ignited. After about 15 hours, the substructure that supports the hoisting equipment and derrick collapsed as a result of the fire, and derrick, riser, hoisting equipment, etc., fell into the water. (Subsequent inspection by divers showed that this equipment did not land on the BOP's and that the BOP's did not seem to be damaged.) The rest of the drilling unit remained floating and was pulled away from the site the next day (4 June 1979). The burned-out hulk is considered a write-off at an estimated loss of $22 million.

3. OIL PLUME AND SLICK CHARACTERISTICS

Gas and oil were being discharged at the top of the undamaged BOP stack, about 12 m above the seafloor, in pulses of about 80 per minute, as viewed by remote-controlled videotape cameras. The oil is believed to be light with a low sulphur content (33° API, 1.5% sulphur). Estimates of the amount of oil have varied. Originally PEMEX indicated the flow was 30,000 barrels of oil per day, but later appraisals put the flow at 5,000 to 10,000 barrels per day. Calculations based on inexact measurement of the oil slick flowing on the water surface place the flow rate in the 20,000- to 30,000-barrel-per-day range.

A large fire, about 50 m in diameter and 7 m in height, was burning on the water's surface directly above the stack. The fire was essentially yellowish-orange and generally smoke-free, with occasional discharges of grey-black smoke. There was continuous upwelling of water within this fire diameter. Around the main fire and within 20 m of it are much smaller random surface fires which appeared and disappeared periodically. These were easily extinguished by the surrounding turbulent surface waters. Ringing the fire and extending out about 150 m on each side of the flame, a tan- to rust-colored oil slick could be seen on the surface of the water. This oil was being swept in the direction of the wind and current and expanded from the 400 m width at the fire to about 1 km approximately 2 km downstream (see Figure 2).

The oil was heavily emulsified with water. It was thought that the oil from the blowout, in close association with the emerging gas, was quickly rising to the churning boil water of the plume and was mixing and frothing with seawater; this resulted in a fine emulsion of water droplets in the oil. At the same time the heat from the gas fire was evaporating and burning the light fractions of the oil. The heavily mixed water-in-oil emulsion in the boil area eventually was swept out of the turbulent plume area and rose to the surface of the calmer waters surrounding the fire. Based on preliminary chemical analyses, the emulsion on the water surface was found to contain about 70% water and 30% oil and to be viscous (350cp) and heavy (SG = 0.99). It is a very stable water-in-oil emulsion containing fine droplets of water coated with a thin

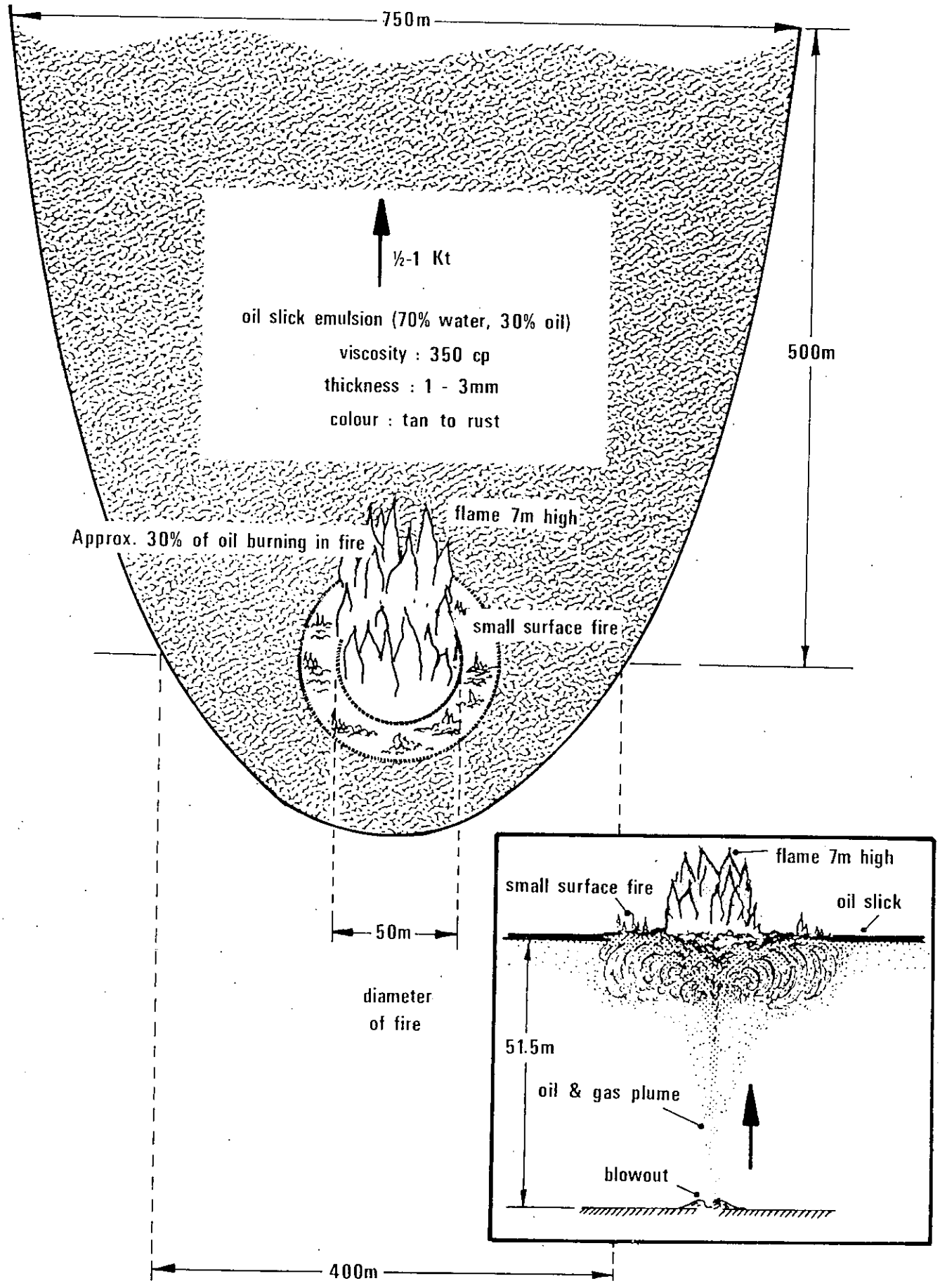

Figure 2. Schematic diagram of IXTOC-I blowout site.

viscous layer of oil. Analysis of the oil indicates that almost all of the light fractions of the oil (lighter than C_{10}) are missing, having burned or evaporated in the fire or heat zone (Figure 3). It is thus estimated that about 30% of the discharging oil was being consumed in the fire. The emulsion slick surrounding the fire and being swept downstream appeared to be approximately 1 to 3 mm thick. In addition, close to the blowout plume there apparently was a cloudy suspension of very fine emulsion particles within the upper few m of the water column.

Surface currents in the area ranged from approximately 0.5 to 1.0 knots, depending on the direction and force of the winds and tidal currents. The water temperature was 25 to 27°C and the air temperature varied from about 30 to 40°C during the day. Sea-state condition generally was in the Beaufort 1-2 range.

4. WELL CONTROL

PEMEX gave well control top priority for the use of the manpower and equipment assigned to the IXTOC-I blowout. The options available for control were either to plug or cap the well or to drill an adjacent relief well to intersect the existing one. Although plans included drilling two relief wells, as of 23 June (day 20) only one jack-up platform, Azteca, was in place about 1 km NE of the blowout. It had penetrated approximately 500 m below the seafloor by 17 June, but was expected to take 3 months to complete its task. The second drilling rig will move to its drilling site shortly.

The fire at the blowout could be extinguished at any time, but it was felt that the explosion hazard that would be associated with the unburned gas would far outweigh any problems caused by the existing flames.

Since videotapes and diver observations of the BOP stack suggested that it may not have been seriously damaged by the debris collapsing around it from the burning drilling platform, it was hoped that the oil flow could be terminated quickly with the remaining valves. The plan was to leave the debris in place for fear that in the process of removing it the stack might be destroyed. Instead, divers would work around these obstacles and attach a series of hydraulic hoses to the controls for various valves so that the valves could be operated from a surface barge. The intention was first to open the rams so that any debris stuck in the BOP would either fall into the well or blow out, then to close the valves and cut the oil flow.

Unfortunately, attempts at attaching the hoses to the stack were handicapped by a number of circumstances. While diving conditions around the stack had been acceptable during the first few days of operation, as the slick moved to an easterly bearing, underwater visibility was reduced to about 0.3 m, and a surface current of 3.5 knots was recorded near the boil of the spewing oil. These factors made diving extremely difficult.

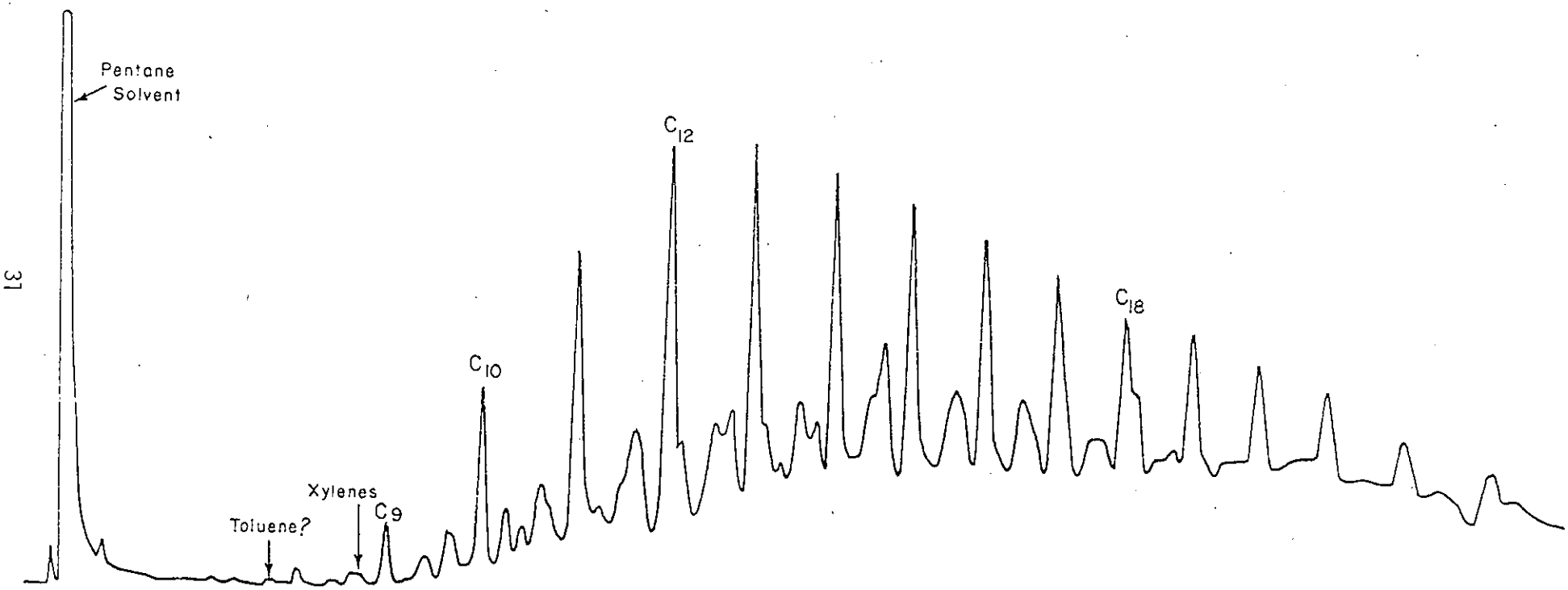

Figure 3. G.C. of pentane extract of IXTOC emulsion.

By 22 June, three of the eight required hydraulic lines had been successfully attached to the BOP and by 26 June (day 23), attempts were made to activate the valves. Unfortunately, the BOP failed to respond satisfactorily. Another attempt was made several days later, but this too failed.

5. OIL SLICK MOVEMENT AND DISTRIBUTION

The oil originating directly from the blowout had tended to become heavily mixed with water and reduced of its lighter fractions, ultimately appearing on the surface as an emulsion 1 to 3 mm in thickness. There its movement was subject to the action of the prevailing winds and currents with little thinning of the 350 cp emulsion occurring.

For the first nine days of the blowout, the oil slick moved at about 0.5 knot to the west in the general direction of the Gulf Stream. By 8 June (day 5), the slick extended 70 km from the blowout site and was 50 km wide. However, on 12 June, the prevailing offshore winds started moving the oil in a direction clockwise from its original location until it settled on an easterly bearing at about 0.7 knot. As a result, by 15 June (day 12) large patches of oil with various estimated thicknesses were distributed around the IXTOC site (Figure 4). Fortunately, the offshore winds continued to keep the oil away from the coast. The nearest confirmed oil observation occurred approximately 16 km from land on 16 June. Other observers estimated oil to be closer to shore on 15-21 June, but in most cases these sightings turned out to be only very small areas of sheen.

On 17 June, the slick again shifted but turned counterclockwise to a NE bearing and to NNE by the following day. Finally, on 21 June (day 18) the direction of the oil slick suddenly changed 120° counterclockwise to a westerly direction, approaching a bearing typical of the first days of the blowout.

On 22 June, several American scientists arrived on-site to study the characteristics of the slick and to collect wind and current input data for spill trajectory models. According to a USCG spill prediction model, the oil will likely impact the Tamaulipas, Mexico, coast between Tampico and Lower Laguna Madre in August 1979.

6. OIL SPILL COUNTERMEASURES

The countermeasures operation to deal with the oil slick had two components: physical recovery of the oil by skimmers in the immediate vicinity of the IXTOC site, and dispersing of the patches of oil threatening shorelines.

Although the amount of oil-skimming equipment at the site was impressive, only a very small fraction of the oil being discharged from the blowout had been picked up by equipment. (By 20 June, it was estimated that less than 20,000 barrels of oil emulsion (70% water) had been recovered since the start

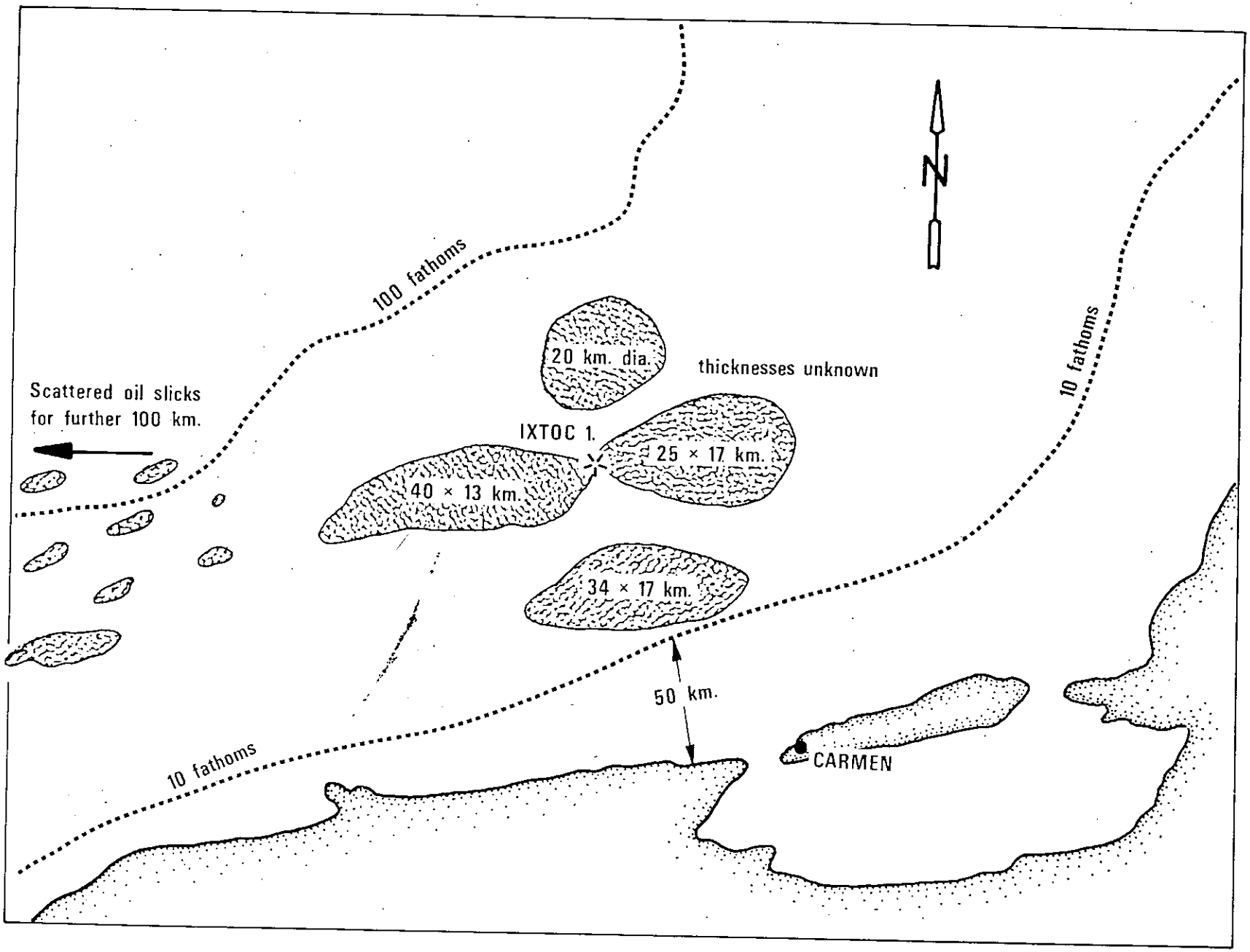

Figure 4. Sketch of oil slick locations.

of the skimming operations.) There are two major reasons for this. First, at times the ideal configuration and operation of the control and cleanup equipment had not been permitted because of potential interference with the blowout control efforts at the site, which, of course, took precedence; second, although support or ancillary equipment was available (there are 23 large tugs and ships at the site), allocation problems and unsuitable deployment equipment had hampered the implementation of an effective cleanup program. Most of these problems, which are due to a lack of experience and are common to many large spill control operations, will undoubtedly be corrected as the cleanup team gains daily invaluable experience.

A Norwegian team of approximately 15 technical persons from the government, STATOIL, and equipment manufacturing companies arrived in Mexico with two FRAMO skimmers and three TK-series high-capacity pumps. Each of these skimming systems has the potential for collecting thousands of barrels of oil per day. PEMEX provided an unpowered flat barge (a platform with no tankage) on which the skimmers were welded. A second barge was tied alongside the first to serve as a receptacle for the collected oil. The intention was to use several hundreds of meters of Norwegian oil boom (NOFI) to deflect and concentrate the oil, using a V-shaped configuration, into the apex of the V, where the skimmers were located on the barge. Unfortunately, the boom was severed on several occasions by the tug traffic in the area. Without booms, it was decided to anchor the 150 m barge broadside to the flowing slick about 500-1000 m downstream from the blowout. The barge acted as a barrier to the flowing oil and tended to concentrate the 1 to 3 m oil slick to several centimeters along the length of the barge. Unfortunately, the FRAMO skimmers could remove oil only from a few meters alongside the barge on each side of the units. Also, it was found on many occasions that by the time all anchors to the barge were in place, the slick would move in a new direction because of changing currents, leaving the skimmers in relatively oil-free water. As of 20 June (day 17), it was estimated that the Norwegian units had collected only a few thousand barrels of oil emulsion since the operation began.

A more productive operation involved the application of oleophilic rope devices manufactured by Oil Mop, Inc. These machines essentially are comprised of a continuous loop of polypropylene strands that are woven together, travel over the surface of the oil slick, and are wrung out in a roller apparatus. By 22 June, four 9" diameter rope Oil Mop machines and a 16" rope machine, all mounted on a 100,000-barrel barge and in a configuration similar to that described for the Norwegian system, collected perhaps 15,000 barrels of oil emulsion. (The 16" device can collect 100 barrels/hour of emulsion, which is 70% water; the 9" units can remove 30 barrels/hour of emulsion.) Unlike the FRAMO units, the oil that is concentrated alongside the barge can be collected by the oleophilic ropes that are run along the water surface next to the barge. PEMEX planned to operate the Oil Mop machines 14 hours a day; it was reported that 10 additional Oil Mop units would be sent to the site, including Oil Mop, Inc.'s ZRV dynamic skimmers. It was reported in the Oil Spill Intelligence Report that as of 9 July, the Mop machines located on barges 150 meters from the well site had recovered 50,000 barrels of emulsion.

Shell Oil of Houston offered PEMEX the use of its experimental "Sock" skimmer. Unfortunately, due to its experimental nature, the "Sock" had not been debugged, and it proved to be structurally underdesigned. As a result, it picked up very little oil and had to be permanently retired on 20 June. Test runs indicated that the "Sock" may be capable of picking up about 150 bbl/hour of oil/water emulsion.

As of 9 July, more equipment had been delivered to Ciudad del Carmen for use on the slick. Two complete BP Vikoma systems, including Seapack and Seaskimmer, were in Carmen as well as a Cyclonet 150 open ocean skimmer from the Southern California Petroleum Contingency Organization.

The other major countermeasure effort involved the use of chemical dispersants applied aerially. Conair Aviation Ltd. of Abbottsford, B.C., was contracted by PEMEX to apply the oil spill dispersant COREXIT, a product of EXXON Chemical, to portions of the slick threatening shorelines. Since 9 July, Conair had sprayed more than 170,000 gallons of COREXIT 9517, COREXIT 9527, and COREXIT 7664 during one-to-four hour spraying missions per day. Conair had applied 3500 gallons of dispersant per flight, over an area of 500 to 600 hectares. A Conair DC6B, fitted with about 34 m of spray boom, had been flying 15 m above the water at a speed of 150 knots and applying the dispersant at a rate of 350 gallons per minute.

The swath width had ranged from 80 m to 200 m, depending on the wind speed, direction, and other environmental factors. The plane had been spraying from 1.8 to 3.0 gallons of dispersant per acre (1 acre = 0.405 hectare). EXXON had been manufacturing 400 drums of dispersant per day in Houston, Texas; about two-thirds of the dispersant used had been COREXIT 9517. The market price for the EXXON dispersants is about $8 per gallon. Under contract to PEMEX, Southern Air of Houston and Pacific Western of Vancouver, B.C., had been flying a total of three flights per day to transport the dispersant to Ciudad del Carmen, Mexico, from Houston to a cost of $16,000 per flight.

PEMEX had been dispatching regular observation flights over the spill site to monitor the spill movement and to determine the targets for dispersant spraying.

As of the end of June, no "ground-truthing" mission had been mounted to take and analyze samples of water in order to determine the effectiveness of the dispersing operation. There may be a possibility that the chemicals are indeed "herding" the oil and not dispersing it into the water column. This "herding" action would give the appearance of "dispersing" as seen from a surveillance aircraft.

7. ENVIRONMENTAL CONCERNS

The normally clear turquoise water of the Bay of Campeche is nutrient-rich due to the upwelling at the nearby edge of the continental shelf. The area supports a wide variety of fish species, oysters, shrimp, and porpoises.

Although many types of marine animals are fished commercially, the shrimp fishery is of greatest importance. Ciudad del Carmen (pop. 77,000), the largest shrimp port in the world, takes in an annual catch valued at about $110 million.

In spite of the commercial importance of the Gulf fishery, many areas have not been well documented as regards their biological resources. Figure 5 outlines some of the areas known to contain important habitats. The lagoon area south of Carmen is believed to be one of the most biologically productive areas in the world. At this time of the year, thousands of juvenile shrimp are migrating to sea in a westerly direction along the coast from nursery areas in the lagoon. Although oil covered areas where commercial fishing boats are operating, as of 22 June it had not inundated "critical" areas such as the nursery area or shallow coastal waters. This has been due largely to the predominantly offshore winds.

Natural oil seeps exist in the Bay of Campeche and there is some evidence that a direct correlation exists between the presence of seeps and the abundance of shrimp. This possibly relates to local upwelling induced by these seeps. Certainly, the videotapes of the BOP stack indicated that the disturbance of the bottom during the blowout had attracted large numbers of fish to the site. In addition, large schools of fish and some barracuda were occasionally observed at the edge of the oil slick.

To study the environmental impact of the IXTOC-I spill, PEMEX has contracted CIFSA, a consulting firm in Mexico City. CIFSA plans a three-month program to sample the water and benthos in the lagoons, inlets, and offshore areas in the spill region and then analyze the samples for their physical, biological, and chemical properties. The research program will study the impact of the dispersant on the marine environment and analyze the populations of plankton and other marine organisms.

As of 9 July, this program had not yet begun. It is reported that an EXXON-sponsored research team and a Norwegian consulting firm will also be doing some biological sampling and impact-assessment work.

8. PROGNOSIS

Fortunately, the prevailing currents and winds in the vicinity of IXTOC-I tended to keep oil away from the shoreline and minimized potential environmental damage. Hurricanes or tropical storms, which occur in the Gulf of Mexico during July and August, may inundate significant portions of the coast with oil, greatly increasing the impact and cost of this blowout. The potential for acutely toxic effects in the water column is probably minimal due to the loss of low-boiling-point aromatics through burning and evaporation. Environmental damage in littoral areas may still occur through the physical coating of habitat and organisms and aesthetically pleasing beaches. PEMEX is planning research programs that will document the physical and chemical fate of the oil and monitor possible biological effects.

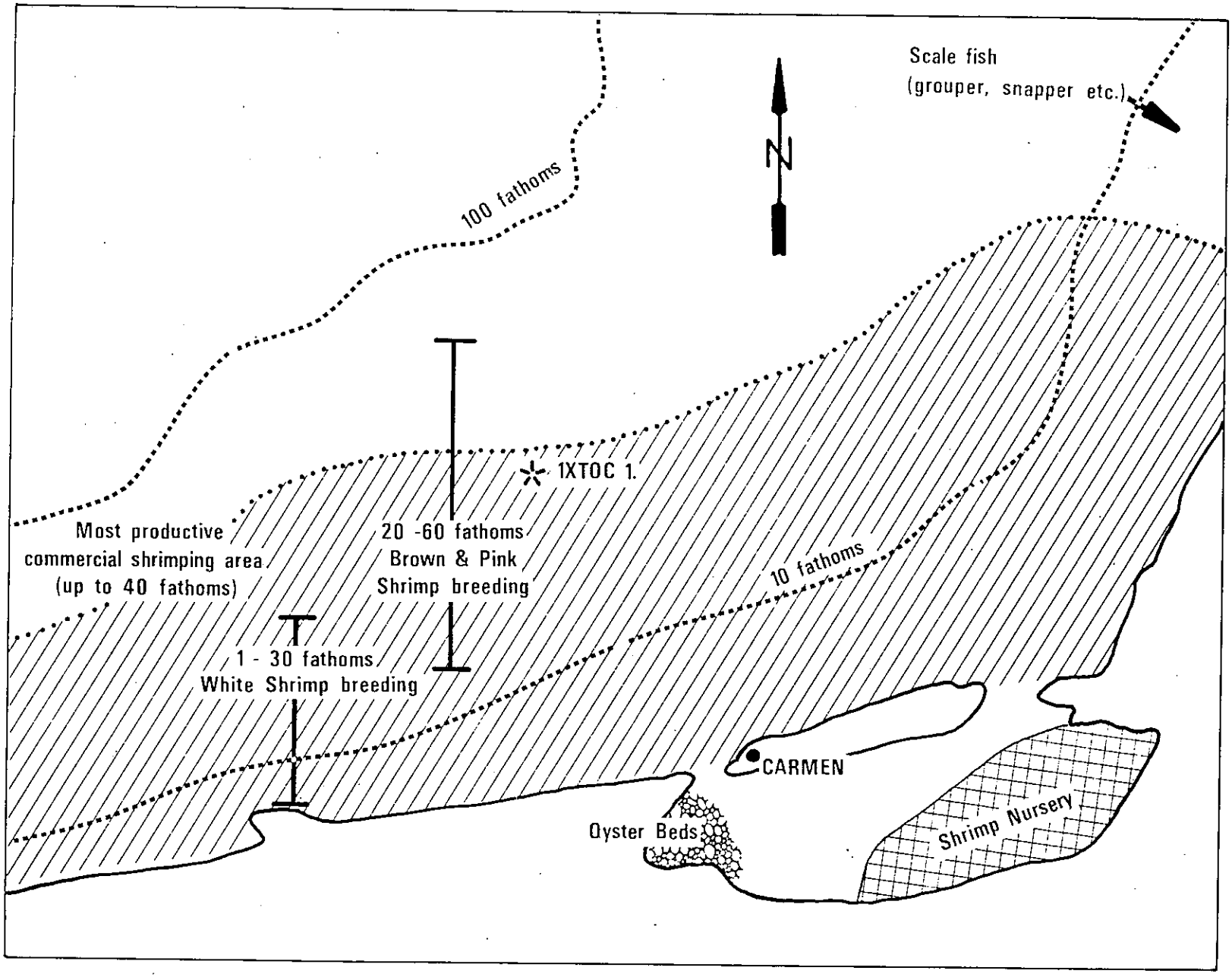

Figure 5. Sketch of some important fisheries habitats.

To reduce the potential environmental impact of the spill, the most important countermeasure activity that took place, aside from relief-well drilling, was the oil spill removal operation at the blowout location. The oil recovery device at the site had the capacity to recover a large percentage of the oil on the water surface, if properly deployed. Other countermeasure techniques for dealing with the oil on the water showed less promise. Burning of the oil spill had been ruled out because the oil is intimately mixed with much water and is already partially burned. The continuing efforts to chemically disperse the viscous oil emulsion also have been of questionable value.

It is impossible to predict whether this oil spill, which is one of the world's largest, will lead to extensive environmental damage and cleanup costs, or will dissipate naturally and harmlessly into the warm and vast Gulf waters.

INTERCALIBRATION OF ANALYTICAL LABORATORIES

William D. MacLeod, Jr. and James R. Fischer
NOAA National Analytical Facility
Environmental Conservation Division
Northwest and Alaska Fisheries Center
National Marine Fisheries Service
2725 Montlake Boulevard East
Seattle, Washington 98112

1. INTRODUCTION

Qualification to analyze environmental samples for hydrocarbons for NOAA's R/V RESEARCHER/IXTOC-I Project was predicated on a prior satisfactory performance by the participating laboratories. Considering the state of the art, the four laboratories listed in Table 1 have shown analytical capability for hydrocarbons in their analyses of an Interim Reference Material (IRM) developed by NOAA's Outer Continental Shelf Environmental Assessment Program (OCSEAP). This IRM was a well-mixed shoreline sediment from an active harbor. The National Analytical Facility (NAF) had previously documented the hydrocarbon composition of the IRM in multiple replicate analyses according to four procedures. A comparison of the results and precision among the methods appeared in the American Chemical Society monograph, Petroleum in the Marine Environment (Brown et al., 1980). NAF's published data from that study were used as a reference in evaluating the data of the Project analytical laboratories in this report.

Table 1. RESEARCHER/IXTOC-I Project Analytical Laboratories.

University of New Orleans New Orleans, Louisiana (UNO)	Energy Resources Co., Inc. Cambridge, Massachusetts (ERCO)
Science Applications, Inc. La Jolla, California (SAI)	University of Louisville Louisville, Kentucky (UL)

2. IRM ALKANES

NAF's analyses of the IRM for nineteen alkanes (n-C_{14} to n-C_{30}, plus pristane and phytane) had a relative standard deviation* (RSD) ($1\sigma_r$) of 21% for NAF's tumbler extraction procedure (Brown et al., 1979) and a RSD of 19% for a common Soxhlet procedure (Farrington and Tripp, 1975). Thus, NAF's precision for alkanes averaged 20% RSD for two established analytical procedures. This intralaboratory RSD was employed in comparing the IRM results from the four Project laboratories with NAF's more extensive data.

The intralaboratory RSD was used in conjunction with an empirical rule that differences in analytical results between comparable laboratories can, in general, be expected to have about twice the uncertainty (e.g., RSD) as that within a given laboratory. Thus, if 20% is NAF's relative standard deviation ($1\sigma_r$) for IRM alkanes, about twice that value ($2\sigma_r$) may be employed when comparing the IRM alkanes between NAF and other comparable laboratories. In applying this empirical rule, we calculated the differences between each result

*Standard deviation x 100/mean.

for an individual alkane reported by a Project laboratory and our counterpart result. These differences were expressed in terms of twice the intralaboratory RSD ($2\sigma_r$) and graphed according to frequency of occurrence.

Figure 1 shows the frequency vs. $2\sigma_r$ graphs comparing the Project laboratories to NAF with respect to the IRM alkanes. The graphs show that the data from UNO and SAI correspond well with those of NAF, with ERCO next closest (see Table 1 for laboratory abbreviations). Although the UL graph shows a greater divergence between their results and ours, the majority of UL's results still lie within the first $2\sigma_r$ interval.

Comparisons between analytical laboratories, clearly, are soundest when the analytical procedures are most alike. Thus, we compare only the IRM alkane data from a Project laboratory to NAF's corresponding data, using their tumbler or shaker results vs. our tumbler results, or their Soxhlet results vs. our Soxhlet results. The importance of this distinction is seen in a frequency vs. σ_r comparison within NAF's own tumbler and Soxhlet data (Figure 2). While the correlation of data shown in Figure 2A (alkanes) is encouraging from a methods-comparison viewpoint, the moderate disparity between the results obtained by the two methods in our laboratory demonstrates the need to compare analogous procedures between laboratories.

3. IRM AROMATICS

Data for nine aromatic compounds (Table 2) from the OCSEAP IRM intercalibration were similarly compared between NAF and the Project laboratories. In this instance, NAF's intralaboratory RSD ($1\sigma_r$) for aromatics was 33%; hence, the RSD intervals ($2\sigma_r$) for interlaboratory comparison of aromatics became 66% under the empirical rule discussed above. Frequency vs. $2\sigma_r$ graphs comparing the four laboratories with NAF are shown in Figure 3. Overall, the high incidence of correspondence is quite encouraging.

Table 2. Aromatic Compounds Used for Comparisons.

Dibenzothiophene	Pyrene	Benzo[e]pyrene
Phenanthrene	Benz[a]anthracene	Benzo[a]pyrene
Fluoranthene	Chrysene	Perylene

Figure 2 indicates a less precise relationship between our tumbler and Soxhlet data for the selected aromatics (Fig. 2B) than for the alkanes (Fig. 2A). Therefore, for these aromatics it is all the more important that analagous methods be compared between laboratories.

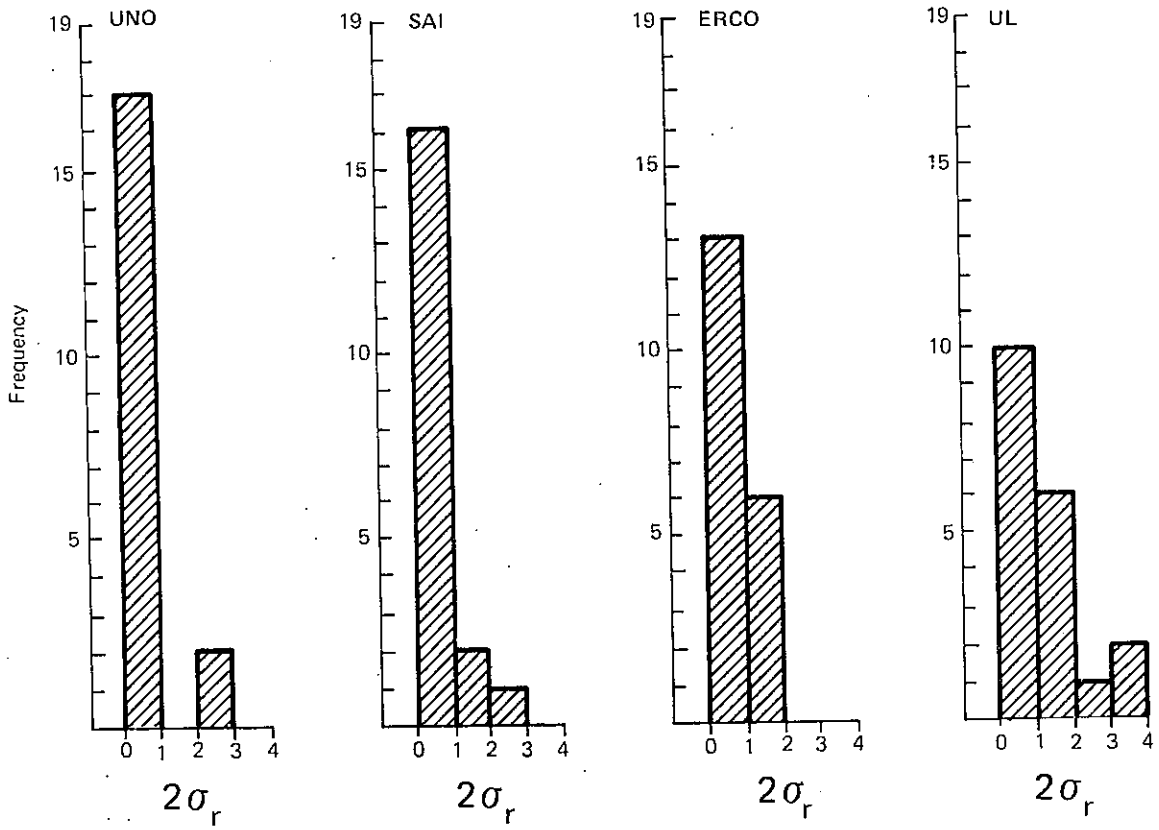

Figure 1. Frequency vs. precision comparisons between Project laboratories and NAF. Parameters compared: amounts of each of 19 alkanes from the OCSEAP IRM sediment: σ_r is NAF's RSD for alkanes (20%). Data compared only from closely corresponding methods, i.e., Soxhlet vs. NAF Soxhlet or tumbler/shaker vs. NAF tumbler.

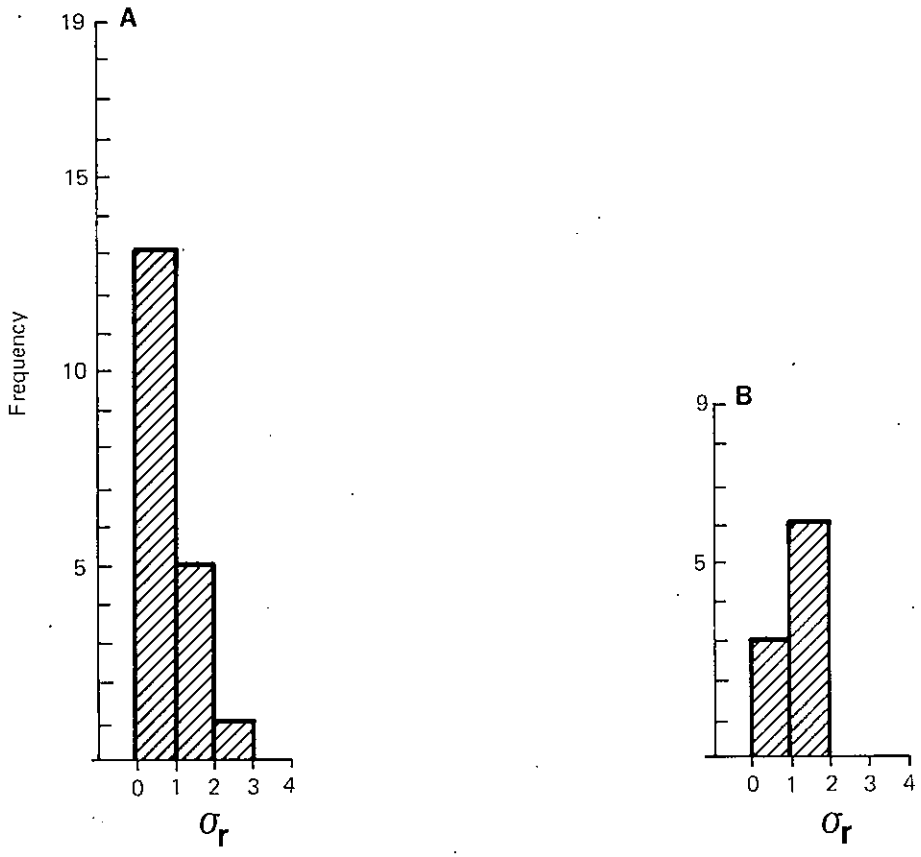

Figure 2. Frequency vs. precision comparisons between NAF Soxhlet and NAF tumbler extraction procedures with the OCSEAP IRM sediment. A. Parameters compared: amounts of each of 19 alkanes; σ_r is NAF's RSD for alkanes (20%). B. Parameters compared: amounts of each of 9 aromatics; σ_r is NAF's RSD for aromatics (33%).

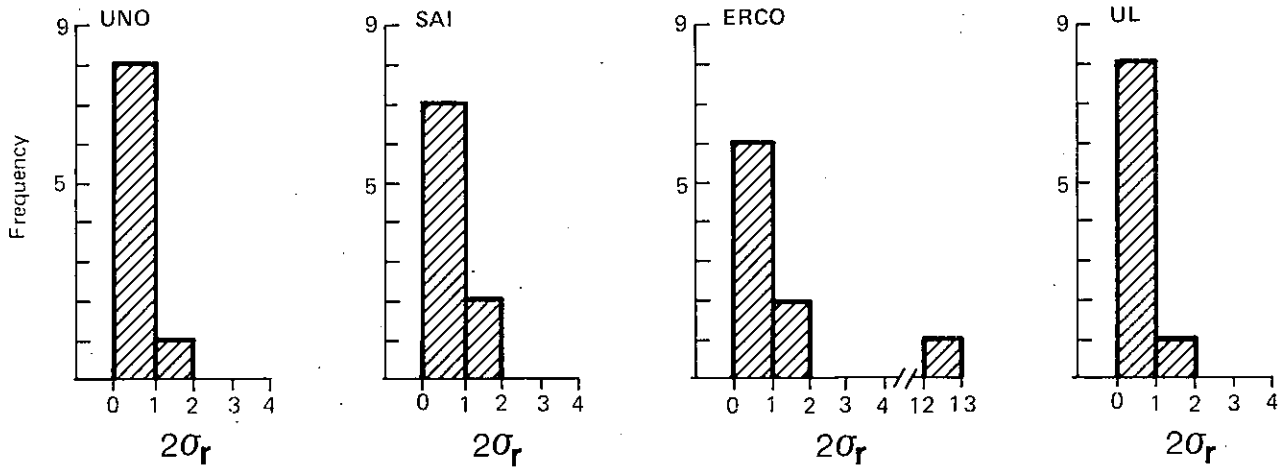

Figure 3. Frequency vs. precision comparisons between laboratories indicated and NAF. Parameters compared: amounts of each of 9 aromatics from the OCSEAP IRM sediment; σ_r is NAF's RSD for aromatics (33%). Data compared only from closely corresponding methods, i.e., Soxhlet vs. NAF Soxhlet or tumbler/shaker vs. NAF tumbler.

4. WEATHERED MOUSSE COMPOUNDS

As a further exercise in interlaboratory calibration, the UNO group supplied us with a portion of a solid weathered mousse (sample RIX23S001). Both UNO and NAF analyzed the mousse surface for alkanes in the first chromatographic fraction (f_1); the results are shown in Table 3. All the counterpart data fell within the first $2\sigma_r$ interval.

In the aromatic hydrocarbon fraction (f_2), UNO reported a trace of two-carbon alkylated dibenzothiophenes (C_2-DBT's), whereas NAF found 1-2 parts-per-million (ppm) of 1-methylphenanthrene, pyrene and chrysene by gas chromatography (GC). NAF further analyzed f_2 by GC/mass spectrometry (GC/MS) and found the following alkylated aromatics:

a. DBT's (ppm)

C_1 - (0.01)	C_4 - (0.04)
C_2 - (0.08)	C_5 - (0.03)
C_3 - (0.08)	

b. Napthobenzothiophenes (ppm)

C_1 - (0.03)	C_4 - (0.02)
C_2 - (0.02)	C_5 - (0.01)
C_3 - (0.01)	

c. Phenanthrenes/Anthracenes (ppm)

C_2 - (0.03)	C_4 - (0.01)
C_3 - (0.03)	C_5 - (0.02)

d. Chrysenes (ppm)

C_1 - (0.07)	C_3 - (0.02)
C_2 - (0.02)	

plus traces of DBT, C_3-naphthalenes and benzo[e]pyrene.

NAF collected a third chromatographic fraction (f_3) of the mousse surface sample by eluting the column with methanol. After concentration, GC/MS analysis of f_3 revealed a series of trace multiple peaks that suggested a homologous series of isomeric compounds. The mass spectra of these compounds were consistent with their structural formulation as long-chain saturated alcohols. Experiments are underway to provide further evidence for this interpretation and to determine whether primary, secondary or tertiary saturated alcohols predominate.

Table 3. Parts-per-thousand (°/oo) of individual alkanes found in surface portion of weathered mousse (sample RIX23S001) by NAF and UNO.

Alkane	NAF °/oo	UNO °/oo	SAI* °/oo
n-C_{15}	0.01	--	0.02
n-C_{16}	0.01	--	0.05
n-C_{17}	0.11	0.11	0.20
pristane	0.04	0.04	0.05
n-C_{18}	0.20	0.18	0.21
phytane	0.10	0.10	0.10
n-C_{19}	0.25	0.23	0.25
n-C_{20}	0.27	0.26	0.28
n-C_{21}	0.27	0.24	0.26
n-C_{22}	0.25	--	0.24
n-C_{23}	0.23	--	0.22
n-C_{24}	0.20	--	0.20
n-C_{25}	0.18	0.15	0.16
n-C_{26}	0.17	0.13	0.17
n-C_{27}	0.13	--	0.12
n-C_{28}	0.12	0.09	0.10
n-C_{29}	0.08	--	0.09
n-C_{30}	0.10	--	0.08
n-C_{31}	0.10	--	0.07
n-C_{32}	0.08	--	--

*Added during proof.

5. ACKNOWLEDGMENTS

Dr. Edward Overton, Center for Bio-Organic Studies, UNO, kindly supplied weathered mousse sample RIX23S001. Donald W. Brown and his NAF associates provided technical assistance. This study was supported by the Office of Marine Pollution Assessment, National Oceanic and Atmospheric Administration.

6. REFERENCES

Brown, D. W., L. S. Ramos, A. J. Friedman, and W. D. MacLeod, Jr. (1979): Analysis of marine sediments using a solvent slurry extraction procedure. In: Trace Organic Analysis: A New Frontier in Analytical Chemistry, H. S. Hertz and S. N. Chesler (Eds.), Special Publ. 519, National Bureau of Standards, Washington, DC, pp. 161-168.

Brown, D. W., L. S. Ramos, M. Y. Uyeda, A. J. Friedman, and W. D. MacLeod, Jr. (1980): Ambient-temperature extraction of hydrocarbons from marine sediments--comparison with boiling-solvent extractions. In: Petroleum in the Marine Environment, L. Petrakis and F. T. Weiss (Eds.), Advances in Chemistry Series 185, American Chemical Society, Washington, DC, pp. 313-326.

Farrington, J. W., and B. W. Tripp (1975): A comparison of analysis methods for hydrocarbons. In: Surface Sediments, Marine Chemistry in the Coastal Environment, T. M. Church (Ed.), Symposium Series No. 18, American Chemical Society, Washington, DC, pp. 267-284.

GASEOUS AND VOLATILE HYDROCARBONS IN THE GULF OF MEXICO FOLLOWING THE IXTOC-I BLOWOUT

James M. Brooks, Denis A. Wiesenburg, and Roger A. Burke
Department of Marine Science
University of South Florida
830 First Street South
St. Petersburg, Florida 33701

Mahlon C. Kennicutt
Department of Geosciences
University of Tulsa
Tulsa, Oklahoma 74104

Bernie B. Bernard
School of Geology and Geophysics
The University of Oklahoma
830 Van Vleet Oval
Norman, Oklahoma 73019

ABSTRACT

Low-molecular-weight (LMWH) and volatile liquid hydrocarbons (VLH) were determined in water and oil samples taken around the IXTOC-I well blowout on the Campeche shelf between 15 and 21 September 1979. During this time period, oil and gas from the wellhead were burning at the ocean surface and large volumes of crude oil and gas were being discharged at the sea surface. Methane, ethane, propane, and butane concentrations as high as 530, 93, 85, and 30 μl/L were observed at stations closest to the wellhead. LMWH concentrations decreased by approximately 1, 1.5, 2, and 3 orders of magnitude at stations increasing in distance from the blowout site, 6, 12, 18, and 24 miles downstream, respectively. This concentration decrease is principally the result of mixing with noncontaminated seawater containing much lower concentrations of LMWH. LMWH from the blowout were concentrated in the upper 20 m of the water column. These gases resulted from gas being discharged by the well and were not due to solution from the oil. A significant correlation was found between high levels of LMWH and VLH.

VLH as high as 400 μg/L were observed in the vicinity of the blowout. High values near the well site were partially due to dispersed oil in the water column. At 6 and 12 miles downplume from the blowout, VLH had decreased to 63 and 4 μg/L, respectively. The VLH away from the immediate vicinity of the blowout were dominated by light aromatics (benzene $\rightarrow$ o-xylene). Most VLH in solution in the water column originated at the wellhead and not from dissolution from floating oil/mousse. Samples of oil/mousse had lost 98% of the $<C_{12}$ n-alkanes after drifting only 12 miles from the wellhead.

1. INTRODUCTION

Well blowouts occurring at offshore platforms rarely result in platform losses. Such losses, however, are the inevitable result of accidents where heavy equipment, flammable materials, large number of employees, and reliance on complex technology are involved. In many cases, these catastrophic incidents result in large inputs of gaseous and/or liquid hydrocarbons into the marine environment. Previously, most well blowouts in the Gulf of Mexico have occurred in the upper Gulf coast region (see, for example, Brooks, et al., 1978) where offshore operations have been underway for over 20 years. With increasing offshore drilling operations on the Mexican continental shelf, there was an increased probability that the lower Gulf coast would experience similar inputs of hydrocarbons from a major offshore incident. Such an incident occurred on 3 June 1979 when a Petroleos Mexicanos well (IXTOC-I) blew out. IXTOC-I is located in the lower Gulf of Mexico on the Campeche Shelf at 18°24.4'N, 92°12.2'W (Figure 1). Shortly after the blowout, the escaping gas and oil ignited, forcing evacuation of the rig (Royce and Robertson, 1979). This well blowout resulted in the introduction of several million barrels of oil into western Gulf of Mexico waters during a period of many months.

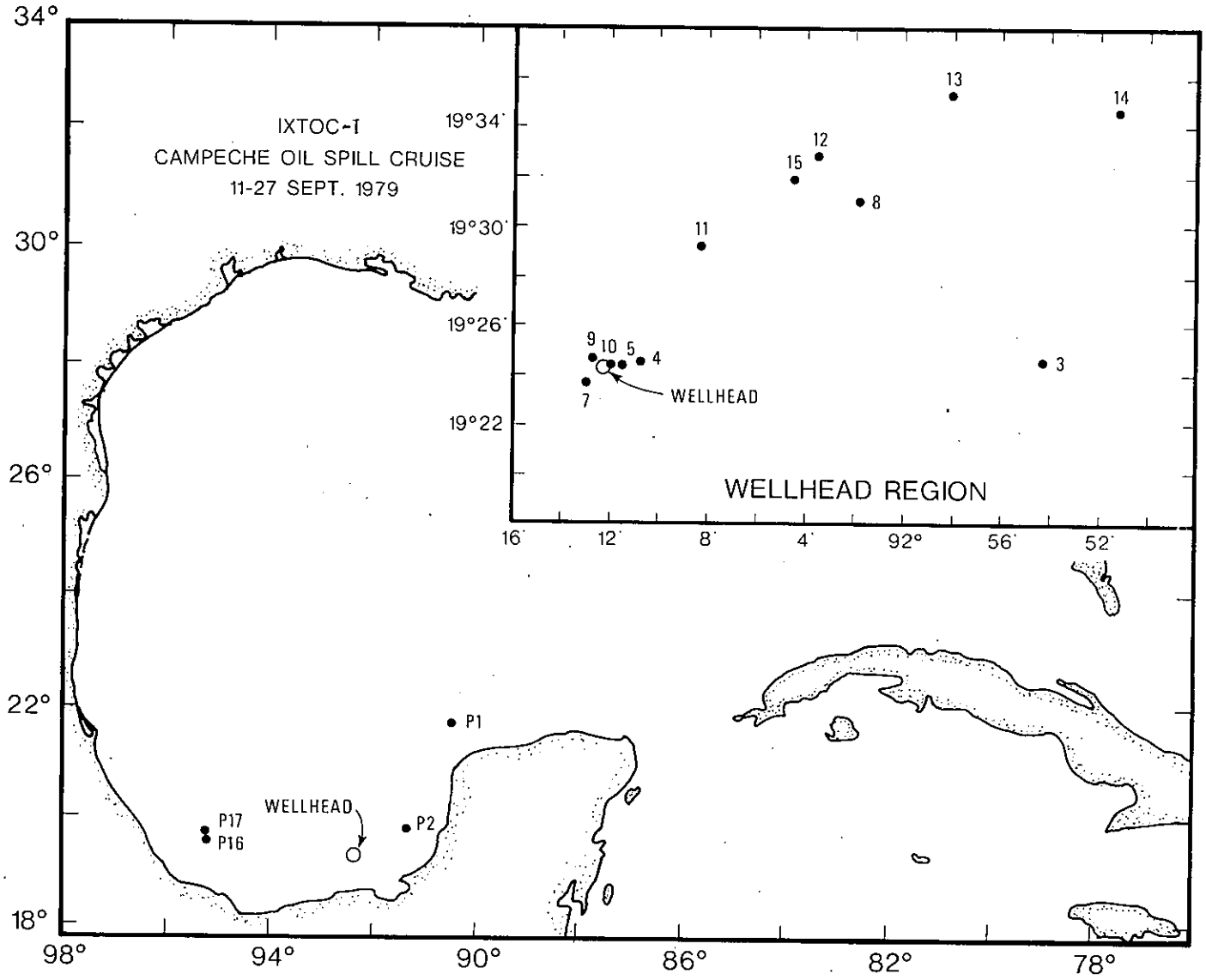

Figure 1. Wellhead and sampling locations taken on the G. W. PIERCE.

On 11 September 1979 a National Oceanic and Atmospheric Administration (NOAA) sponsored expedition was undertaken aboard the NOAA Ship RESEARCHER and the contract vessel G. W. PIERCE to investigate the environmental contamination produced by this blowout. These ships arrived at the wellhead on 15 September and departed the region on 21 September. During that week, the gas and oil from the well was on fire and large volumes of crude oil were being added to the sea surface. Flames from the well covered approximately 4000 m^2 (Atwood, personal communication). Two relief well platforms, Azteca and Interocean II, were located within 0.25 mile of the burning wellhead. Visual examination of the area, upon arrival on 15 September, showed an oil slick from the well directed to the northeast at about 055° true. The visible plume extended northeast for at least 35 miles. The slick continued to drift northeast until 20 September, when it started to swing to a southerly direction. On 21 September the slick drift was approximately 145° true.

Crude oil can be divided into three categories, based on compound molecular weights and vapor pressures. The C_1-C_5 aliphatic hydrocarbons are gaseous, low-molecular-weight compounds. They are easily removed from water by helium sparging at room temperature. The compounds above C_{15} have very low vapor pressures and are easily removed from water by solvent extraction. Between these two extensively studied groups of hydrocarbons are the volatile liquid hydrocarbons in the range of C_6-C_{14}. These hydrocarbons can be extracted only by more vigorous gas stripping techniques than are required for gasous hydrocarbons, yet are lost during solvent extraction and concentration techniques used for high-molecular-weight hydrocarbons. The volatile liquid hydrocarbons are important since they contain the light aromatics (benzenes → naphthalenes), the most immediately toxic components of petroleum (Blumer, 1971; Baker, 1970; McAuliffe, 1977a). This study represents the first detailed sampling for gaseous and volatile hydrocarbons around a major oil spill.

The gaseous and volatile hydrocarbon results reported here were obtained from samples collected aboard the vessel G. W. PIERCE. Figure 1 shows the location of the sampling stations for this hydrocarbon study. Table 1 gives the types of samples obtained at each station, the date sampled, and sample location.

2. METHODS

2.1 Sampling

Samples of IXTOC-I oil/mousse were collected from the ocean surface for hydrocarbon analysis. Seawater samples from depths of 1 to 40 m were taken for LMWH and VLH analysis. Samples for gaseous and volatile hydrocarbons were taken using a stainless-steel submersible pumping system, 10-liter teflon-line Niskin Go-Flow bottles, or Bodman bottles. The pumping system consisted of 2.5-m lengths of stainless-steel tubing fitted with flexible Swagelock connectors. The pumping system had a depth capability of 25 m. Samples for gaseous hydrocarbons were transferred from the sampling devices by gravity flow and stored in 200-ml glass bottles. Sample bottles were flushed with twice their

Table 1. Sample stations for gaseous and volatile hydrocarbons aboard the G. W. PIERCE.

Station	Location		Date	Sample Type			Distance from Wellhead
				Water (C_1-C_4)	Water (C_5-C_{14})	Oil/Mousse	
1	21°41'N	090°25'W	9/14/79	X	X		Control
2	19°49.0'N	090°21.7'W	9/16/79	X	X		Control
3	19°39'N	091°45'W	9/16/79			X	18 NM E
5	19°21'N	092°18'W	9/17/79	X	X	X	0.75 NM E
7	19°18'N	092°21'W	9/18/79	X	X		1 NM SW
8	19°30.9'N	092°01.8'W	9/18/79	X	X	X	12 NM NW
9	19°18'N	092°19'W	9/19/79	X	X		0.6 NM WNW
10	19°23'N	092°17'W	9/19/79			X	0.5 NM E
11	19°26'N	092°09'W	9/19/79	X	X	X	6 NM NE
12	19°28'N	092°01'W	9/19/79	X	X		12 NM NE
13	19°31'N	091°56'W	9/19/79	X	X	X	18 NM NE
14	19°30'N	091°50'W	9/20/79	X	X	X	24 NM NE
15	19°27'N	092°03'W	9/21/79			X	10 NM NE
16	19°15.6'N	095°10.1'W	9/22/79	X	X		Off Veracruz
17	19°40'N	095°13'W	9/22/79			X	Off Veracruz

volume, poisoned with sodium azide, and capped with no headspace. Samples for volatile hydrocarbons were taken in a similar manner in combusted, hydrocarbon-free, 2-liter ground-glass-stoppered bottles. These samples were stored in the dark in an air-conditioned van on the ship and at 4°C in the laboratory. Oil/mousse samples taken from the vessel G. W. PIERCE were collected from a bucket sampler or by using the pumping system. All oil/ mousse samples were stored at 4°C in 20-ml capped glass bottles.

2.2 Analysis

LMWH were analyzed either by the multiple-phase equilibrium method of McAuliffe (1971) or by the purge and trap technique (Brooks et al., 1977). The equilibrium technique was used for samples containing µl/L concentrations. It involves equilibrating 25 ml of seawater with 25 ml of helium in a 50-ml syringe for 20 minutes on a mechanical shaker. Over 98 percent of the LMWH partitioned from the water into the helium. The equilibrated gas was injected onto a Porapak Q column and analyzed with a HP5710A gas chromatograph with a HP3380A integrator, using a flame ionization detector. Duplicate analyses were averaged and compared against standards. The purge and trap technique was used for samples containing nl/L concentrations. It involves stripping the gases from solution by purging with purified helium for 5 minutes at a flow rate of 200 ml/min and concentrating on a 0.6-cm O.D. copper trap containing 60/80-mesh Porapak Q at liquid nitrogen temperatures. When the LMWH had been quantitatively transferred to the cold trap, the trap was isolated and heated to 100°C. The trap was then switched into the chromatographic stream using a 6-port gas sample value. Sample separation and analyses were performed using the same conditions as described for the equilibrium technique.

VLH were extracted from the seawater samples using the dynamic headspace sampling technique developed by Sauer (1978). This method is a modification of the technique presented by Bertsch et al. (1975) and May et al. (1975). The volatile organics were stripped from a heated (70°C), stirred, 2-liter seawater sample by purging with ultrapure helium using a coarse frit. Volatile organics were trapped on a 0.5-cm I.D. x 15-cm column of solid polyphenyl ether absorbent (Tenax-GC), which has excellent retention characteristics for liquid hydrocarbons, retains very little water, and exhibits negligible column bleed at temperatures under 300°C (Butler and Burke, 1976). The all-glass headspace sampling apparatus was designed such that the stripping of the volatiles was done in the sample bottle itself. Contamination from the atmosphere and loss of volatiles due to absorption on sample bottle walls were thus minimized. Samples were helium-stripped for 90 minutes at 120 ml/min, a time sufficient for complete stripping of most volatile hydrocarbons.

After the volatile organics were stripped from the water sample, the volatile components trapped on the Tenax-GC were desorbed by heating (250°C) using an on-line heating unit. They were transferred by helium flow to a liquid-nitrogen-cooled trap for sample consolidation. This trap, attached to a 6-port sample valve, was isolated and then heated to transfer the trapped hydrocarbons (using the GC carrier stream) as a plug onto a gas chromatographic column for sample separation and analysis. The column was a 0.3-cm x 305-cm stainless-

steel chromatographic column packed with 10% SP-2100 on 80/100 Supelcoport. The column was temperature programmed at 50°C for 10 minutes, 50 to 180°C at 4°/min, and at 180°C for 20 minutes. Peak confirmation was performed using the aforementioned VLH extraction system coupled to a HP5992 gas chromatograph/quadrapole mass spectrometer supported by a HP 9885 M/S flexible-disk data system. Mass spectra identifications were confirmed by comparison with spectra given by Heller and Milne (1978).

Samples of oil/mousse (2-3 g) were dissolved in 3 g of reagent-grade carbon disulfide for VLH analysis. Five μl of the sample were injected onto an identical chromatographic column as described previously and analyzed using an HP5830A gas chromatograph. The same chromatographic conditions were used as described above. Confirmation of component identification was made using the HP5992 GC/MS.

3. RESULTS AND DISCUSSION

3.1 Low-Molecular-Weight Hydrocarbons

Table 2 shows low-molecular-weight (C_1-C_4) hydrocarbon (LMWH) concentrations in seawater samples taken from aboard the vessel G. W. PIERCE. Methane concentrations varied from 50 nl/L (10^{-9} liters of gas at NTP/liter of seawater) at a control station to 500,000 nl/L near the wellhead. Methane, ethane and propane concentrations (ranging from 50 to 90, 0.4 to 1.5, and 0.3 to 1.0 nl/L, respectively) observed at station 1 were typical of open-ocean LMWH concentrations (Brooks and Sackett, 1973). The LMWH levels at the control station, as in any noncontaminated oceanic area, were influenced by air-sea exchange and possibly by small amounts of "in-situ"-produced gas (Scranton and Brewer, 1977). All other stations in this study that were sampled for light hydrocarbons showed anthropogenic inputs.

The highest LMWH concentrations were observed at station 5 on 17 September. Profiles of methane and ethane concentrations versus depth for ten stations are shown in Figures 2 and 3. The horizontal scales on these figures are four cycle logarithms of concentration. These figures indicate that there was rapid dilution of LMWH away from the wellhead in the northwest direction (direction of slick drift). Methane concentrations decreased by approximately 1, 1.5, 2, and 3 orders of magnitude within 6, 12, 18, and 24 miles downstream, respectively. This decrease resulted both from loss to the atmosphere and from mixing with water containing lower levels of LMWH. Stations 8 and 12, taken approximately the same distance and direction from the wellhead on separate days, indicated that the degree of dilution was very direction-, current-, and/or sea-state-dependent. Ethane, propane, and butane concentrations showed the same general trends with distance from the wellhead.

Samples taken immediately upstream of the blowout (stations 7 and 9) showed methane, ethane, and propane concentrations of 270 to 470, 12 to 36, and 0.8 to 15 nl/L, respectively. Although these concentrations are three orders of magnitude below concentrations approximately the same distance downstream of

Table 2. Low-molecular-weight hydrocarbons in seawater samples taken aboard the vessel G. W. PIERCE (see Figure 1 for station locations).

Station	Depth (m)	Sampler	Methane nl/L	Ethane nl/L	Propane nl/L	Isobutane nl/L	Butane nl/L	C_1/C_2+C_3
1	1	Pump	55	1.2	1.0	n.d.	n.d.	25
	2	Pump	58	1.5	0.9	n.d.	n.d.	24
	4	Pump	60	0.4	0.4	n.d.	n.d.	75
	6	Pump	52	0.4	0.3	n.d.	n.d.	74
	8	Pump	63	0.4	0.4	n.d.	n.d.	79
	10	Pump	65	0.4	0.3	n.d.	n.d.	93
	12	Pump	55	0.5	0.3	n.d.	n.d.	69
	14	Pump	70	0.6	0.3	n.d.	n.d.	78
	20	Bodman	207	39*	8*	0.5	0.3	4.4
	20	Go-Flow	89	0.4	0.3	n.d.	n.d.	127.0
2	1	Pump	274	--	--	--	--	--
	2	Pump	151	11*	6.3*	14	--	8.7
	4	Pump	123	3.6*	2.4*	4	--	21.0
	6	Pump	155	25*	4.7*	3	--	5.2
	6	Bodman	203	41*	4.9*	3	--	4.4
	6	Go-Flow	161	42*	3.8*	3	--	3.5
	8	Pump	167	19*	4.3*	3	--	7.2
	10	Pump	170	20*	5.4*	3	--	6.7
	12	Pump	171	20*	5.6*	3	--	6.7
	14	Pump	157	27*	4.6*	5	--	5.0
	16	Pump	175	29*	5.1*	5	--	5.1
	20	Bodman	357	22*	5.0*	4	--	13.0
			µl/L	µl/L	µl/L	µl/L	µl/L	
5	2	Bodman	258	44	39	3.5	9.1	3.1
	6	Bodman	530	93	85	7.4	22	3.0
	20	Bodman	160	25	15	1.7	2.2	4.0
			nl/L	nl/L	nl/L			
7	1	Pump	409	19	8.0	--	--	15
	2	Pump	410	22	15	--	--	11
	4	Pump	440	29	7.0	--	--	12
	6	Pump	410	24	8.1	--	--	13

(*) Peak includes unsaturate (ethene plus ethane, or propene plus propane).
(--) Indicates compound was not determined.
(n.d.) Indicates compound was not detected.

Table 2. (Continued)

Station	Depth (m)	Sampler	Methane nl/L	Ethane nl/L	Propane nl/L	Isobutane	Butane	C_1/C_2+C_3
7	10	Pump	449	23	7.7	--	--	15
	12	Pump	458	23	8.0	--	--	15
	14	Pump	460	21	12	--	--	14
	14	Bodman	443	36	11	--	--	9.4
	20	Bodman	465	34	12	--	--	10
			µl/L	µl/L	µl/L	µl/L	µl/L	
8	1	Pump	99	10	0.2	0.9	0.2	9.7
	2	Pump	77	10	1.0	1.2	0.3	7.0
	4	Pump	111	17	5	1.2	0.4	5.0
	6	Pump	118	20	9	2.0	1.7	4.1
	6	Bodman	1.6	0.5	0.02	--	--	3.1
	8	Pump	120	19	3.6	1.2	0.2	5.3
	10	Pump	142	22	10	1.7	0.9	4.4
	12	Pump	154	26	20	1.7	5.8	3.3
	14	Pump	164	28	18	1.9	3.5	3.5
	16	Pump	75	12	4	0.7	0.3	4.7
	19	Pump	12	2.9	2.7	--	--	2.1
			nl/L	nl/L	nl/L			
	20	Bodman	465	25	6	--	--	15
	40	Bodman	471	32	12	--	--	11
			nl/L	nl/L	nl/L			
9	6	Go-Flow	309	13	1.0	n.d.	n.d.	22
	20	Go-Flow	270	12	0.8	n.d.	n.d.	21
			µl/L	µl/L	µl/L	µl/L	µl/L	
11	1	Go-Flow	95	17	16	1.4	4.7	2.8
	6	Go-Flow	78	14	13	2.0	2.7	2.9
	20	Go-Flow	47	6.6	0.58	0.14	0.21	6.5
			µl/L	µl/L	µl/L	µl/L	µl/L	
12	1	Go-Flow	23	3.2	1.1	0.05	0.04	5.3
	6	Go-Flow	28	3.5	0.34	0.04	0.06	7.3
	20	Go-Flow	2.5	0.22	0.1	--	--	8.3

Continued

(--) Indicates compound was not determined.
(n.d.) Indicates compound was not detected.

Table 2. (Continued)

Station	Depth (m)	Sampler	Methane µl/L	Ethane µl/L	Propane µl/L	Isobutane µl/L	Butane µl/l	C_1/C_2+C_3
13	1	Go-Flow	5.5	0.85	1.0	0.02	0.02	3.0
	6	Go-Flow	2.3	0.42	0.16	0.01	0.01	4.0
	20	Go-Flow	2.8	0.24	0.11	0.03	0.02	8.0
			nl/L	nl/L	nl/L			
14	1	Go-Flow	388	16	0.5	n.d.	n.d.	24
	1	Pump	388	13	0.6	n.d.	n.d.	29
	2	Pump	389	18	0.5	n.d.	n.d.	21
	4	Pump	381	18	0.5	n.d.	n.d.	21
	6	Pump	395	17	0.6	n.d.	n.d.	22
	8	Pump	501	23	0.7	n.d.	n.d.	21
	10	Pump	496	21	2.0	n.d.	n.d.	22
	12	Pump	492	23	2.3	n.d.	n.d.	19
	14	Pump	665	37	6.1	n.d.	n.d.	15
			nl/L	nl/L	nl/L			
16	1	Pump	121	3.4	0.4	n.d.	n.d.	32
	2	Pump	113	3.8	0.4	n.d.	n.d.	27
	4	Pump	142	5.7	0.5	n.d.	n.d.	23
	6	Pump	115	3.0	0.4	n.d.	n.d.	34
	8	Pump	117	3.4	0.4	n.d.	n.d.	31
	12	Pump	120	4.4	0.4	n.d.	n.d.	25
	18	Pump	181	4.5	0.4	n.d.	n.d.	37
	90	Go-Flow	134	5.1	0.5	n.d.	n.d.	24

(n.d.) Indicates compound was not detected.

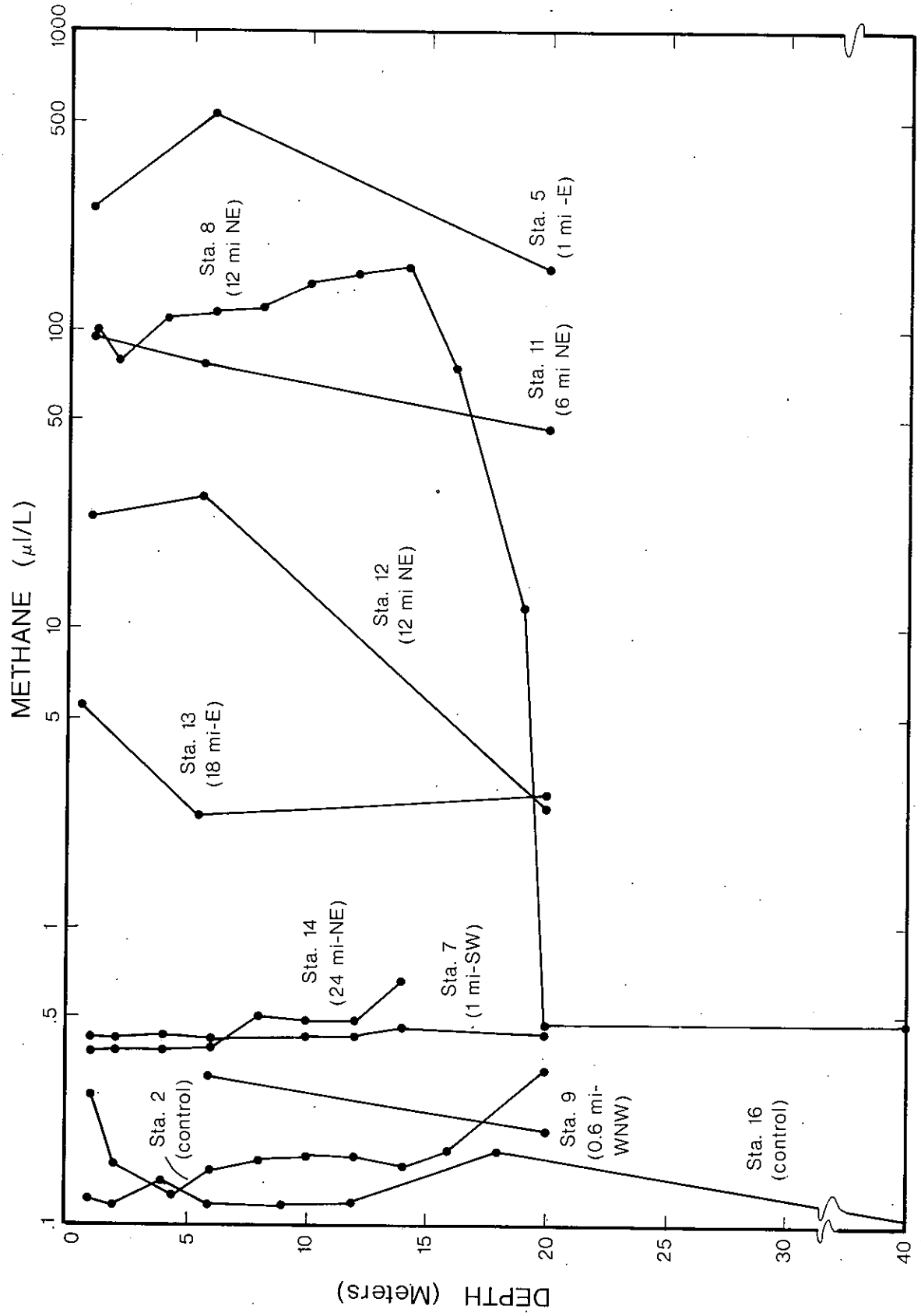

Figure 2. Vertical methane profiles in the IXTOC-I blowout region.

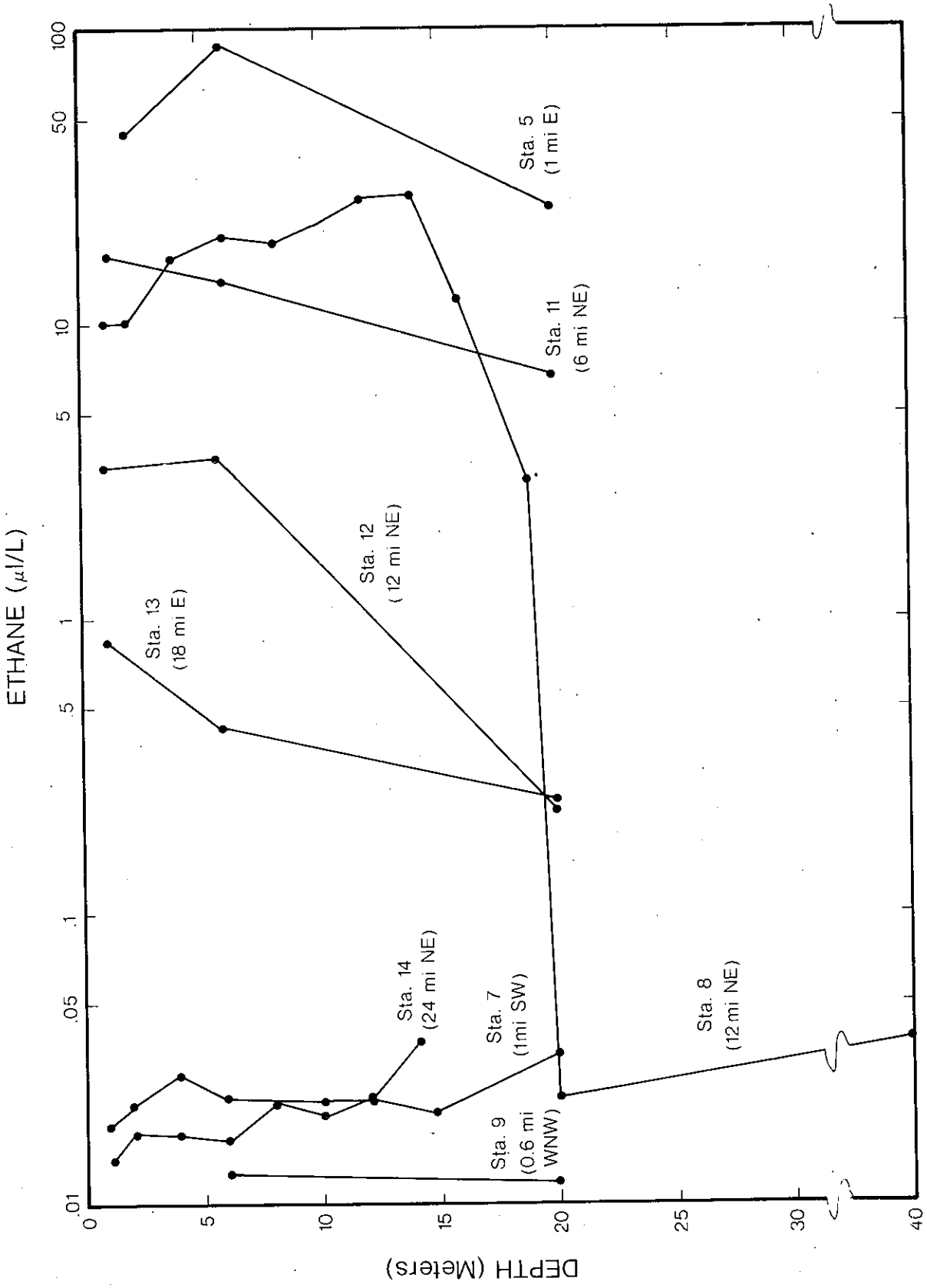

Figure 3: Vertical ethane profiles in the IXTOC-I blowout region.

the wellhead (i.e., station 5), they are still an order of magnitude above baseline levels. The source of these upstream anthropogenic LMWH is no doubt the IXTOC-I blowout. However, whether or not they resulted from mixing by the churning water directly at the blowout site or from the variable current pattern in the blowout region carrying LMWH-laden water back to the wellhead is unknown.

The most probable source of the LMWH to the water column in the blowout region is gaseous hydrocarbons escaping from the wellhead along with the oil, not dissolution of these components from the oil. This concept is confirmed by examation of the vertical profiles at stations 5, 8, 11, 12, 13, and 14 (Figures 2 and 3). These profiles do not show a decreasing gradient from the surface, which would be expected if LMWH were originating from dissolution oil floating on the surface. The vertical profile from station 8 (down to 40 meters) indicates that LMWH are relatively uniform in the upper 14 meters of the water column. However, between 14 and 20 meters there is a decrease of two orders of magnitude in concentration. One explanation for this distribution is that the riser from which the oil and gas are escaping was broken approximately 20 meters below the surface. If the gas and oil were escaping near the seafloor, one would expect increasing concentrations to the bottom because of increased hydrostatic pressure with depth. A second possibility is that since station 8 was 12 miles from the blowout, a different water mass below the thermocline (approximately 20 m) was carrying the plume from the blowout in a different direction at that depth.

A few aberrations in the data in Table 1 are apparent. Methane, ethane, and propane were higher in Bodman bottle samples at stations 1 and 2 than in pump and Niskin Go-Flow samples. The source of this contamination is unknown, but it might have come from previous use of the bottles in waters containing higher levels of LMWH. At all other stations, the Bodman sampler gave results consistent with both the pump samples and the Niskin bottle samples. The ethane and propane concentrations at station 2 include their unsaturate analogs (i.e., ethane and propane, respectively). The Bodman sample at 6 m at station 8 was not representative of the rest of the profile for either LMWH or volatile liquid hydrocarbon (VLH) concentrations. The main hydrocarbon plume must have been missed in this downcurrent station. Methane and ethane concentrations at station 16, almost 170 miles from the wellhead, were higher than typical open-ocean concentrations. Whether these higher concentrations resulted from the IXTOC-I blowout or from another source is unknown. Tar balls and floating mousse were observed in the surface waters near this station.

LMWH in marine waters and sediments can result from either biogenic or petrogenic sources. These two sources can be easily distinguished by molecular and isotopic analysis. Biogenic gas consists almost exclusively of methane, carbon dioxide, and hydrogen sulfide, having $C_1/(C_2+C_3)$ ratios greater than 1000 and carbon isotope ratios ($\delta^{13}C$ values) of methane more negative than $-60^{o}/oo$. Petroleum-related (thermocatalytic) hydrocarbon gases generally have $C_1/(C_2+C_3)$ ratios less than $50^{o}/oo$ and isotopic ratios of methane greater than $-50^{o}/oo$. These two parameters were used by Bernard, et al. (1977) to characterize LMWH gas sources using a simple geochemical model constructed from the field of $C_1/(C_2+C_3)$ ratios and $\delta^{13}C$ values found in marine natural gases.

The $C_1/(C_2+C_3)$ ratios for samples from this study are given in Table 2. These ratios are very low (i.e., 3 to 15) at stations taken in the immediate vicinity of the blowout, whereas stations farther away show a higher ratio, indicating a decreasing influence of the blowout on LMWH concentrations with increasing distance from the wellhead.

Table 3 shows carbon isotopic ratios of methane, ethane and propane in water column samples taken in the immediate vicinity of the blowout. These values are typical of an oil-related gas.

3.2 Volatile Hydrocarbons

Although volatile liquid hydrocarbons (VLH) are a major fraction of crude oil [approximately 19 percent for South Louisiana crude oil (Clark and Brown, 1977)], little information is available on this fraction in waters associated with oil spills. The lack of VLH data is mainly due to the fact that until recently, analytical methodologies have not been available to measure VLH at ng/L levels (Sauer, 1978, 1980; Schwarzenbach et al., 1978). McAuliffe (1977b), using a multiple-phase equilibrium technique sensitive only to µg/L concentrations, found C_2 to C_{10} hydrocarbons under oil slicks at concentrations of 2 to 60 µg/L during the first 30 minutes. These concentrations were attributed to dispersed oil droplets and not to solution. Sauer (1978, 1980) and Sauer et al. (1978) reported VLH in coastal, shelf and open-ocean waters of the Gulf of Mexico using the dynamic headspace stripping technique. Open-ocean surface waters of the Gulf that are relatively free of petroleum pollution contained VLH concentrations of ~60 ng/L. Louisiana shelf coastal waters, believed to contain some hydrocarbon pollution, reached levels of ~500 ng/L. Aromatic hydrocarbons constituted 60-85% of the total VLH in these surface waters. Cycloalkanes ranged from 60 to 100 ng/L (20% of the total VLH) and total alkanes ranged up to 40 ng/L in Louisiana shelf waters. Brooks et al. (1977) reported VLH concentrations around a well blowout on the Texas shelf. Although no oil was associated with this gas well blowout, VLH levels of 20 µg/L were measured. The major VLH measured around this Texas shelf blowout were unresolved in an envelope of branched alkanes and substituted cycloalkanes. Total aromatics were below 90 ng/L and n-alkanes were less than 200 ng/L.

VLH data from stations near the IXTOC-I blowout, as well as at two control stations, are shown in Tables 4 and 5. Typical VLH chromatograms are shown in Figures 4 to 8. VLH in these samples ranged from approximately 300 ng/L to over 400,000 ng/L near the wellhead. At control station 1, the ~300ng/L VLH observed would be typical of Louisiana shelf waters. No baseline values for VLH on the Campeche shelf are available. Control station 2, nearer the wellhead, showed higher VLH levels, possibly indicating an influence from the blowout. Figure 4 shows a typical chromatogram for station 2. Calculated values of total n-alkanes, aromatics, VLH, and the unresolved-area concentrations for the chromatograms shown in Figures 4 to 8 are given in Table 4. In the Figure 4 chromatogram, the light aromatics (benzene → o-xylene) are the dominant peaks, although n-C_5 and n-C_6 were also present. Station 16, taken 170 miles to the west of the blowout in conjunction with mousse/tar observations, also

Table 3. $\delta^{13}C$ values for methane, ethane, and propane in seawater samples near the IXTOC-I well blowout.

Station	Depth (m)	Methane	Ethane	Propane
5	2	-43.8	-35.4	-32.2
	6	-43.2	-34.4	-29.7
	20	--	-35.9	-29.0
8	1	-46.4	--	--
11	1	-44.5	--	--

Values are in $^{o}/oo$ relative to PDB.

Table 4. Volatile hydrocarbons (C_5-C_{14}) in seawater samples ($\mu g/L$) taken in the vicinity of the IXTOC-I well blowout.

Station	Depth (m)	Sampler	Total N-alkanes	Total Aromatic	Unresolved Area	Total VLH
2	4	Pump	0.3 (58%)	0.13 (25%)	n.d.	0.52
5	2	Bodman	38.0 (11%)	42.0 (12%)	95.0 (28%)	340.0
5	6	Bodman	39.0 (9%)	57.0 (14%)	100.0 (24%)	420.0
8	1	Pump	2.0 (4%)	17.0 (35%)	3.1 (6%)	49.0
8	2	Pump	2.0 (4%)	23.0 (44%)	1.5 (3%)	52.0
11	1	Go-Flow	5.8 (9%)	9.1 (14%)	6.5 (10%)	63.0
12	1	Go-Flow	0.3 (8%)	1.1 (30%)	0.2 (6%)	3.6

(n.d.) Indicates compound was not detected.

Table 5. Volatile liquid aromatic hydrocarbons in seawater samples taken aboard the vessel G. W. PIERCE (see Figure 1 for station locations).

Station	Depth (m)	Sampler	Benzene	Toluene	Ethylbenzene	m, p-Xylene	o-Xylene	Mesitylene	Total Aromatic
1	1	Pump	26.0	25.0	8.0	22	n.d.	n.d.	81
	2	Pump	18.0	34.0	7.8	27	8.0	n.d.	95
	4	Pump	66.0	40.0	11.0	59	7.0	n.d.	180
	10	Pump	12.0	19.0	8.7	44	12.0	n.d.	96
	14	Pump	38.0	31.0	7.0	27	n.d.	n.d.	100
	20	Bodman	18.0	22.0	4.3	31	13.0	n.d.	88
	20	Go-Flow	40.0	42.0	5.3	31	n.d.	n.d.	120
2	1	Pump	14.0	34.0	21.0	110	240.0	2.1	420
	2	Pump	38.0	54.0	36.0	360	490.0	25.0	1,000
	4	Pump	23.0	41.0	5.8	41	23.0	n.d.	130
	6	Bodman	17.0	25.0	13.0	40	15.0	3.5	110
	10	Pump	22.0	33.0	6.1	17	24.0	2.6	100
	14	Pump	16.0	18.0	3.6	21	37.0	2.1	98
	20	Bodman	39.0	26.0	11.0	37	25.0	1.1	140
5	2	Bodman	13,900.0	6000.0	380	1580	13,700.0	6,100.0	41,700
	6	Bodman	17,600.0	5500.0	780	2370	20,200.0	10,100.0	56,600
7	1	Pump	32.0	6.3	4.1	26	20.0	10.0	100
	1	Pump	32.0	3.5	3.7	26	16.0	9.6	91
	2	Pump	4.5	4.8	2.1	15	8.3	4.0	39
	6	Pump	3.5	2.7	1.8	13	6.7	3.6	31
	14	Pump	15.0	5.6	3.9	21	23.0	6.0	75
	14	Bodman	16.0	3.8	2.7	19	8.5	9.8	60
	20	Bodman	17.0	3.1	1.7	11	5.2	5.5	44

Continued

Table 5. (Continued)

Station	Depth (m)	Sampler	Benzene	Toluene	Ethylbenzene	m, p-Xylene	o-Xylene	Mesitylene	Total Aromatic
8	1	Pump	4400	4900	162.0	243	5200	1700.0	16,600
	2	Pump	3000	7600	1000.0	5700	4000	1500.0	22,800
	6	Pump	6300	4600	202.0	500	7700	3000.0	22,300
	6	Bodman	82	140	35.0	194	97	41.0	590
	10	Pump	7000	1400	480.0	650	1400	750.0	11,700
	19	Pump	37	20	21.0	63	36	21.0	200
	20	Bodman	22	19	11.0	64	30	36.0	180
	40	Bodman	28	20	6.5	39	22	10.0	130
9	6	Go-Flow	41	18	6.2	39	25	7.6	140
	20	Go-Flow	33	17	6.4	44	30	13.0	140
11	1	Go-Flow	5800	1200	380.0	615	426	700.0	9120
12	1	Go-Flow	330	190	75.0	350	130	29.0	1110
13	1	Go-Flow	1800	1100	120.0	730	330	76.0	4160
14	1	Go-Flow	50	23	7.7	45	28	13.0	170
	1	Pump	270	160	13.0	78	38	8.9	570
	4	Pump	30	12	7.7	34	22	9.3	110
	10	Pump	660	240	17.0	110	36	3.4	1070
	14	Pump	180	26	13.0	49	30	11.0	310
16	1	Pump	27	23	7.8	39	16	3.1	120
	2	Pump	40	50	36.0	170	180	8.2	480
	8	Pump	42	24	8.5	44	18	1.4	140

(n.d.) Indicates compound was not detected.

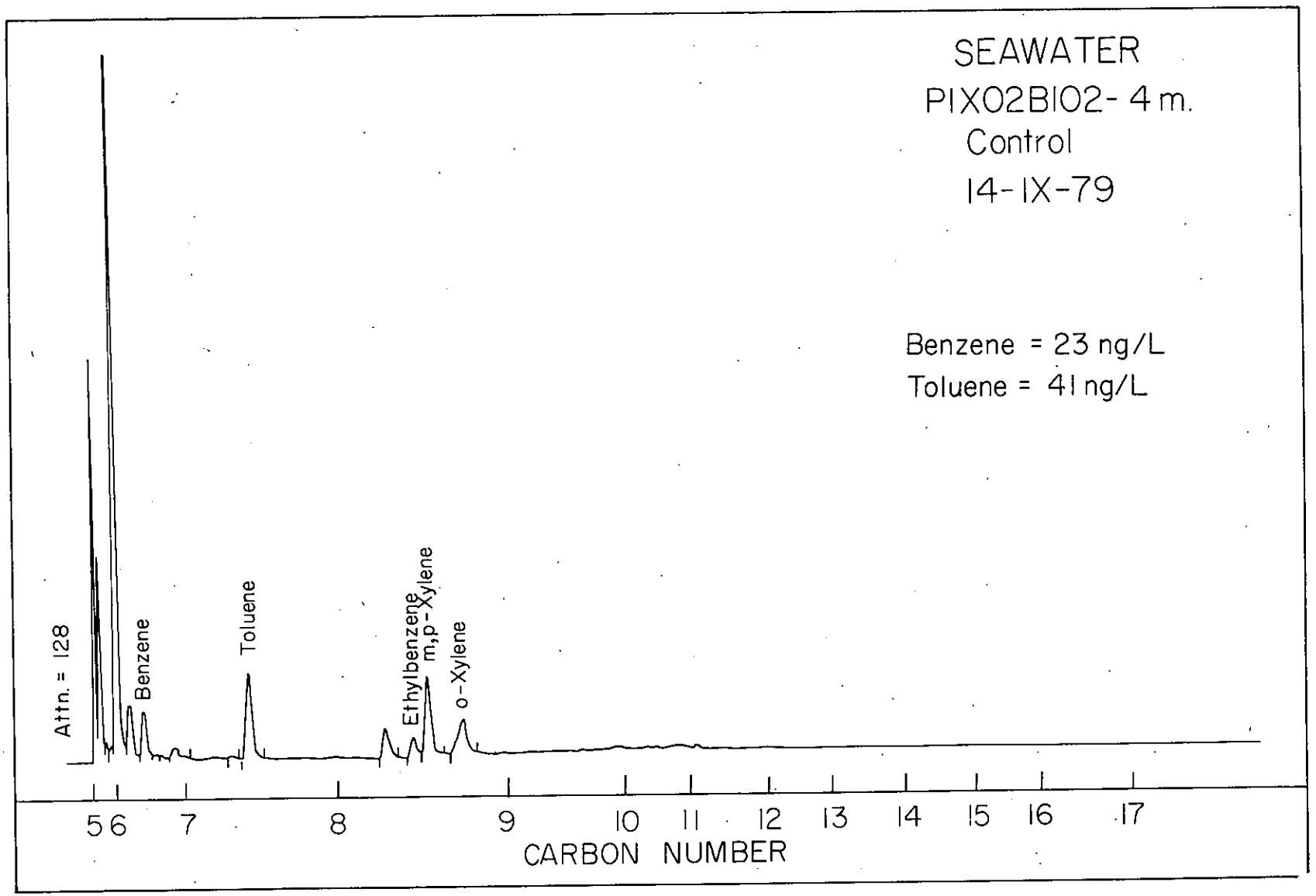

Figure 4. Volatile hydrocarbons at control station 2 (4 meters) on the Campeche shelf.

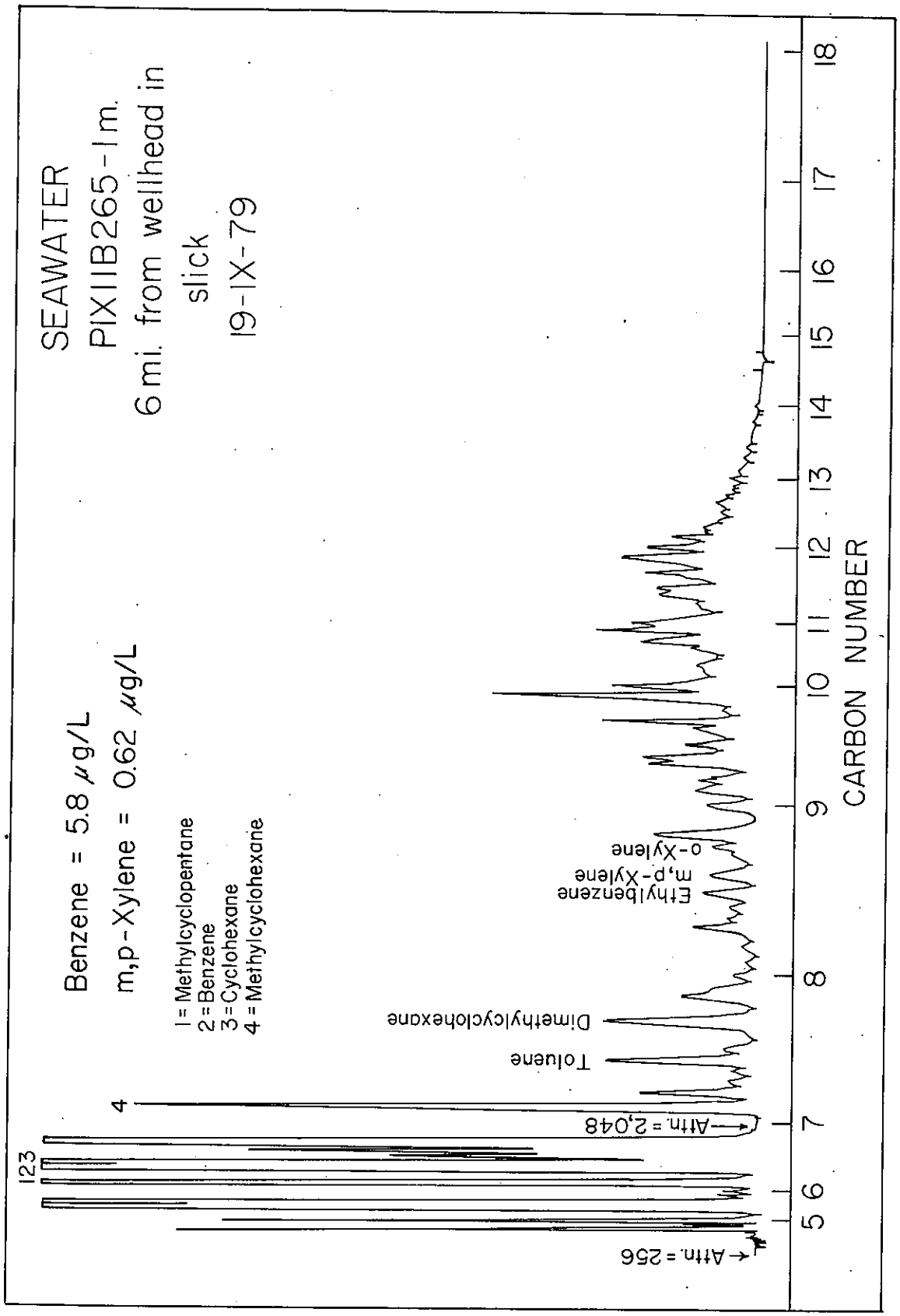

Figure 5. Volatile hydrocarbons at station 11 (1 meter) near the IXTOC-I well blowout.

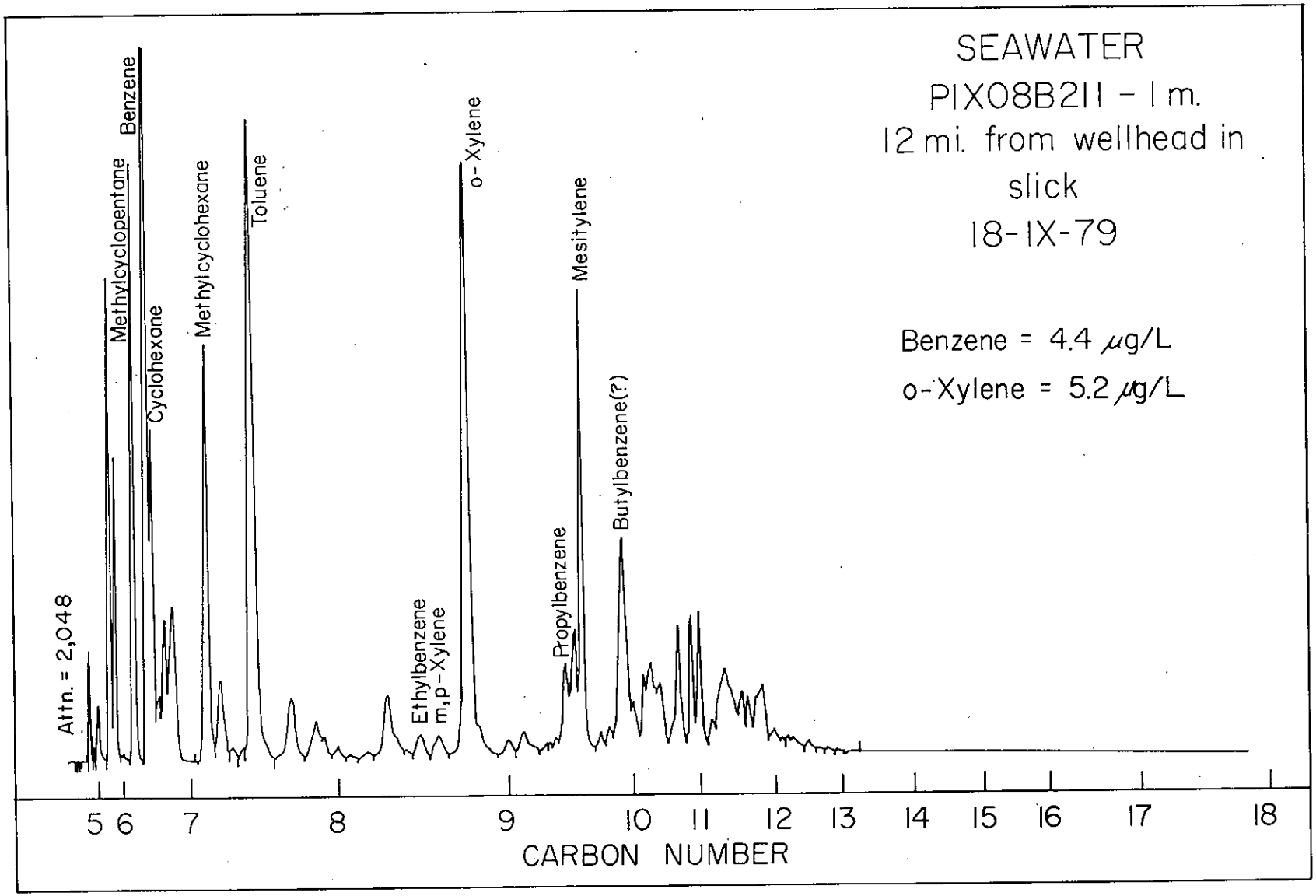

Figure 6. Volatile hydrocarbons at station 8 (1 meter) near the IXTOC-I well blowout.

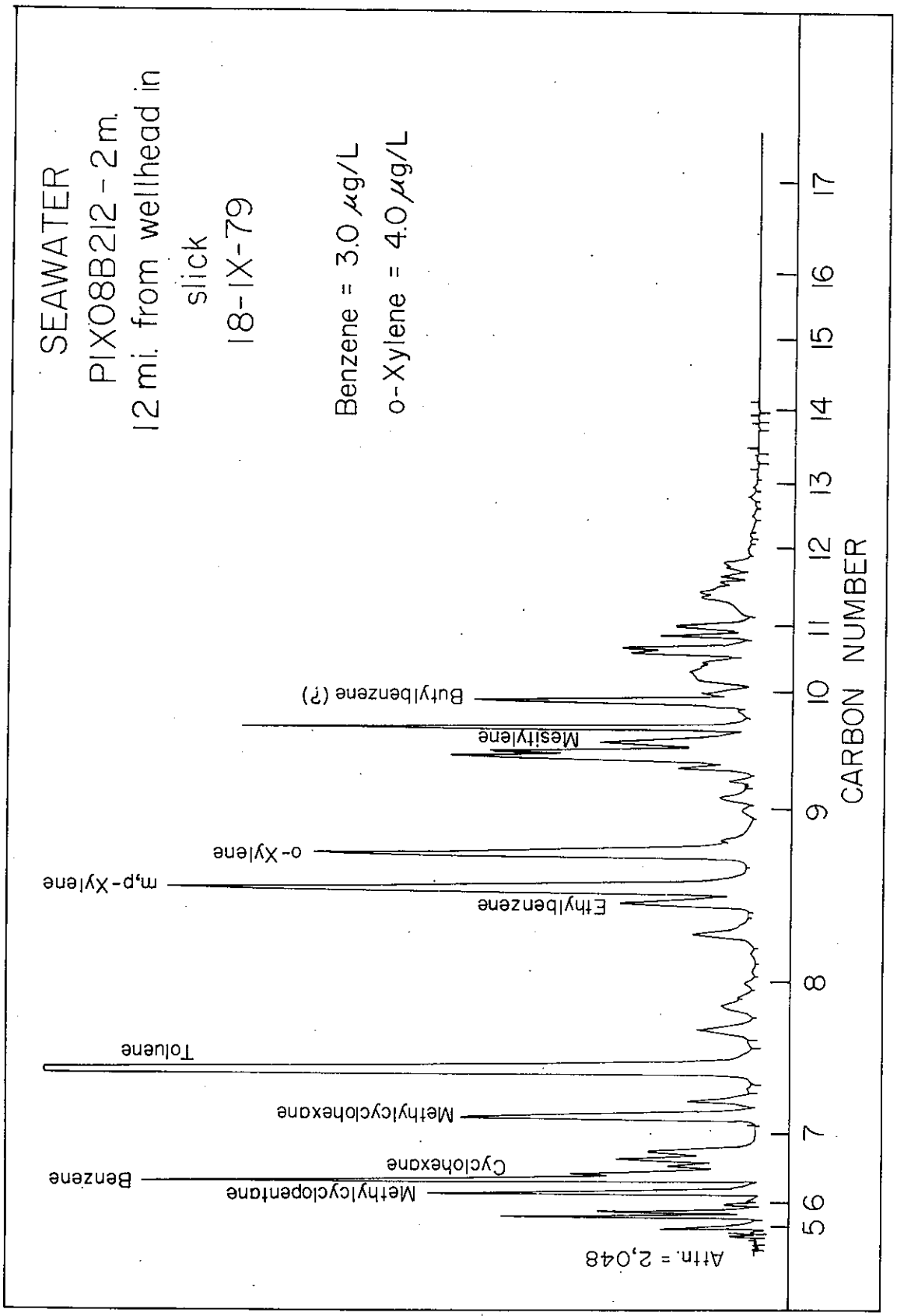

Figure 7. Volatile hydrocarbons at station 8 (2 meters) near the IXTOC-I well blowout.

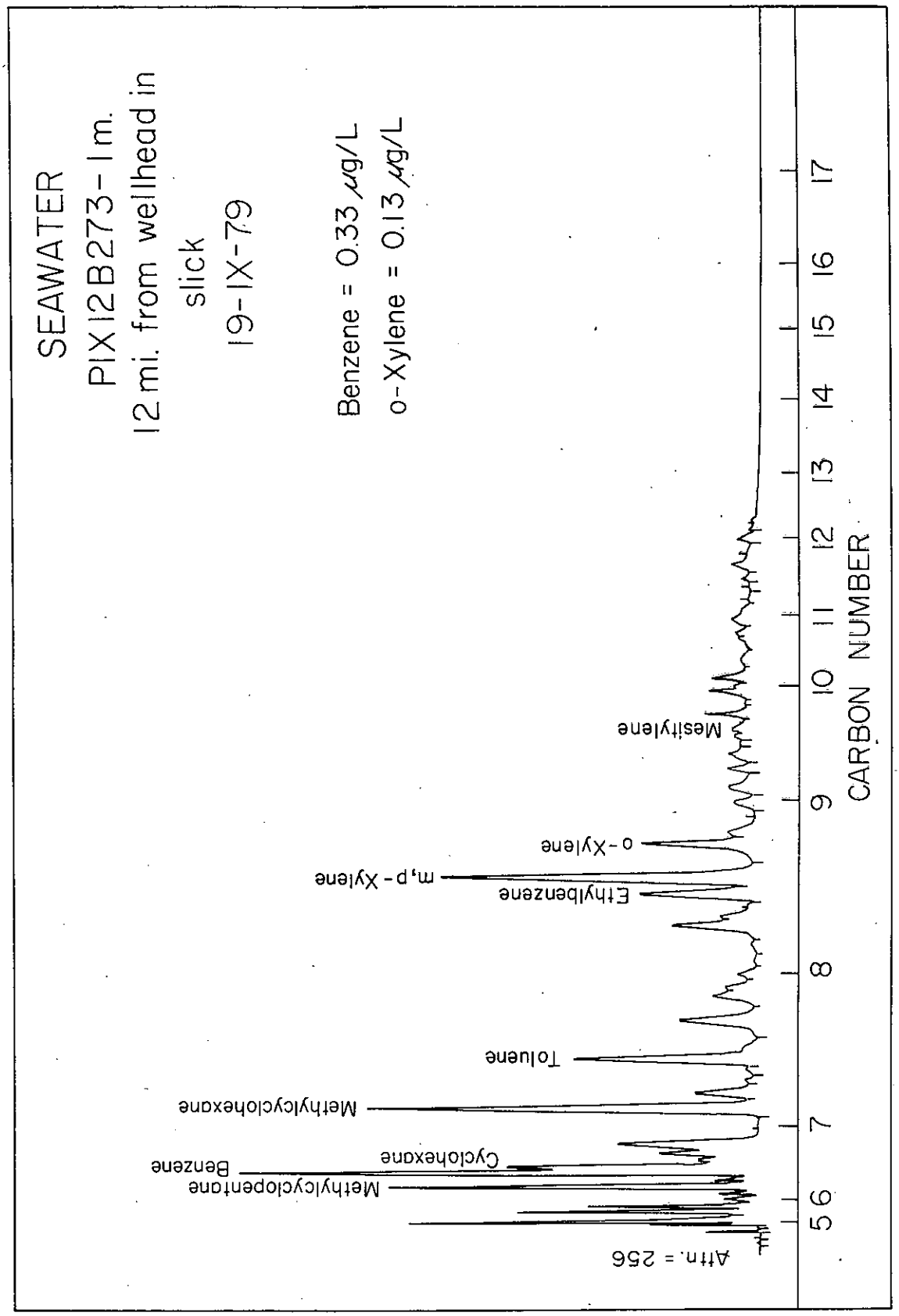

Figure 8. Volatile hydrocarbons at station 12 (1 meter) near the IXTOC-I well blowout.

had higher VLH levels than did station 1. The influence of the IXTOC-I well blowout on VLH levels and particularly on aromatic levels was possibly observed over a wide area of the Campeche shelf.

VLH levels in the immediate vicinity of the wellhead (station 5) were ~400 μg/L. Visual observations of the sample bottles and the presence of a large unresolved envelope (~25% of VLH) in station 5 chromatograms indicated that these samples contained dispersed oil. Total aromatics and n-alkanes comprised approximately 10 and 13 percent, respectively, of the VLH at this station. At station 11 (Figure 5), 6 miles downplume, VLH levels dropped from ~400 to 63 μg/L. The unresolved chromatographic envelope comprised only about 10% of the VLH at this station, compared to 25% at station 5 near the wellhead. This change possibly indicates lower amounts of dispersed oil in the samples farther from the wellhead. Identified in Figure 6 are several cycloalkanes in the VLH chromatogram (station 8). A large fraction of the VLH between n-C_6 and n-C_9 are substituted one-ring cycloalkanes. These components are major constituents of the naphtha fraction of many oils. Their intermediate solubility between aromatics and alkanes contributes to their presence in the VLH chromatograms. Between 6 and 12 miles from the wellhead, the percent aromatic component of the VLH increased by at least a factor of two in the water, while percent n-alkanes and unresolved area decreased. These changes can be observed by examining the data in Table 4 and Figures 5 and 6. These compositional changes can be explained either by variations in the dispersed oil content in the samples, or by greater solution of the volatile aromatics relative to aliphatics from the surface slick. However, Figure 11 shows that oil sampled 6 miles away from the blowout had few aromatics that could be lost to the water column. Thus, this dissolution process may not account for the aromatic increase over the 6-12 mile range. VLH showed similar distributions with depth and distance from the wellhead to distributions of LMWH.

Brooks et al. (1977), Sackett and Brooks (1975), and Sauer (1978) have used LMWH as tracers of the more toxic and soluble VLH. A regression analysis of the data in Tables 1 and 2 gave

$$\delta CH_4 = -3.17 + 0.0077 \text{ Total Aromatics}$$

with a coefficient variation of 0.92. Correlations between CH_4 and aromatics were most significant for methane concentrations in the μl/L range. The fact that a high correlation was observed between LMWH and VLH at the stations in the plume downstream from the wellhead indicates that similar processes were controlling their concentrations in the study area. Since LMWH are assumed to be introduced as a point source at the wellhead from the rising gas plume, a gaseous hydrocarbon total aromatic correlation confirms theoretical and experimental data (see following section) which predict that solution of VLH from an oil slick is a minor process compared with partitioning to the atmosphere. If significant amounts of VLH were being added to the water column from dissolution from the surface oil slick as currents transport it away from the wellhead, a strong correlation between VLH and LMWH would not exist. The introduction of ~400 μg/l VLH in the immediate vicinity of the wellhead is not unrealistic, since Brooks et al. (1978) found VLH levels near 20 μg/L over a gas well blowout containing a large biogenic gas component. The release of large

quantities of condensate-rich gas from the IXTOC-I well could input the quantities of VLH observed in the water column without any dissolution from the surface oil slick. The positive correlation that was observed also confirms that LMWH are good tracers of soluble, higher-molecular-weight hydrocarbons.

3.3 Loss of Volatiles from Oil

Immediately upon the introduction of oil onto the sea surface, evaporation and solution act to reduce volatile hydrocarbons in the oil slick. These processes are simultaneous and competitive. The rate of these changes depends upon the nature of the oil, wind velocity, sea state, and water temperature (McAuliffe, 1977a). Experimental studies (McAuliffe, 1977b; Harrison et al., 1975; Sivadier and Mikolaj, 1973; Smith and MacIntyre, 1971) have shown that hydrocarbons up to about 12 carbon atoms are rapidly lost from a surface slick in a few hours. Harrison et al. (1975) developed a theoretical model to describe the loss of VLH from an oil slick by evaporation and solution. This model predicts that compounds up to n-C_{12} disappear in 3 to 8 hours. McAuliffe (1977b) showed that the rate of loss of C_2-C_{12} hydrocarbons was in accordance with their vapor pressure. The trimethylbenzenes, the slowest of these to weather, were gone from the oil in 4 to 8 hours.

Theoretical (Harrison et al., 1975), laboratory (McAuliffe, 1971, 1974), and field studies (McAuliffe, 1977b) indicate that only a small percentage of VLH lost from a slick enters the water column. The majority of VLH are lost from an oil slick by evaporation. Hydrocarbons lost by solution should dissolve in the water from an oil slick in amounts relative to their mole fraction in oil and inversely proportional to their molecular weights. Theoretical calculations show that evaporation dominates over dissolution 20 (benzene) to 75 (cumene) times. However, for naphthalene the loss from evaporation is almost the same as from dissolution. The aliphatics show evaporation to be greater than dissolution by 10^3 to 10^4. For each homologous series (i.e., aliphatics, aromatics, cycloalkanes) the ratio of evaporation/solution increases with molecular weight. McAuliffe (1977b) found the rates of loss of benzene and cyclohexane, which have similar vapor pressures but very different solubilities (1780 and 55 ppm), to be similar. Figures 9 to 12 also show the rates of disappearance of the benzene and cyclohexane peaks to be identical. If solution were a significant loss mechanism of these hydrocarbons, the percent benzene remaining in the oil should be lower than percent cyclohexane. Harrison, et al. (1975) also found similar loss rates of hydrocarbons with similar vapor pressures but widely different solubilities.

Table 6 shows the n-alkane distribution in the eleven IXTOC-I oil/mousse samples collected during this study. Figures 9 to 12 illustrate the loss of volatile hydrocarbons from the oil/mousse samples with distance from the wellhead. Samples PIX10B258 (Figure 9) and PIX05B117 (Figure 10), taken within 0.75 mile of the blowout, had C_5-C_{12} n-alkane concentrations of approximately 11,000 µg/g. No attempt was made to separate water from the oil/mousse samples before analysis. Therefore, on a water-free basis, the n-alkane concentration in a sample could be as much as 50 percent low. However, the fresh oil samples

Table 6. N-alkane distributions in oil/mousse samples from the IXTOC-I blowout.

Sample	Date	Distance from Wellhead (miles)	n-Alkane Concentration ($\mu g/g$)[1]														TOTAL	
			C_5	C_6	C_7	C_8	C_9	C_{10}	C_{11}	C_{12}	C_{13}	C_{14}	C_{15}	C_{16}	C_{17}	C_{18}	C_5-C_{12}	C_5-C_{18}
PIX10B258	9/19	0.5	200	350	450	570	770	1500	3400	4600	6800	6800	9900	11100	13400	8800	11800	68500
PIX05B117	9/17	0.75	90	130	170	180	820	2100	3800	3900	5200	5200	4600	6400	5400	5500	11200	43500
PIX11b266	9/19	6	3.9	8.8	9.8	15	35	68	160	330	810	810	3700	5600	8400	5300	630	25300
PIX08B183	9/18	12	6.2	3.6	3.8	6.1	15	35	75	150	220	220	1600	2900	4500	3300	290	13000
PIX03B114	9/16	18	8.4	6.3	2.8	--	6	8.8	10	17	48	49	510	1600	1700	1700	64	5700
PIX13B281	9/19	18	10	8.2	2.5	--	3	7.4	15	30	60	63	620	1400	3100	2700	76	8000
PIX08B184	9/18	12	2.4	2.7	--	--	--	--	0.4	8.6	130	130	910	2100	3700	1800	14	8800
PIX05B116[2]	9/17	1	4.3	2.7	--	--	--	2.3	1.7	6.5	30	30	580	1700	2100	2100	18	6600
PIX14B282	9/20	24	0.6	3.2	--	--	--	0.7	5.5	32	160	160	1500	2300	3100	2600	42	9900
PIX15B326	9/21	10	1.3	3.4	--	--	--	--	--	10	39	44	751	1700	3100	2400	15	8000
PIX17B360	9/22	170	2.1	3.0	--	--	--	--	--	2.1	15	120	550	1200	2700	2400	7	7000

[1]Concentrations include oil plus water.

[2]Appeared to be older mousse blown back to well by a wind change.

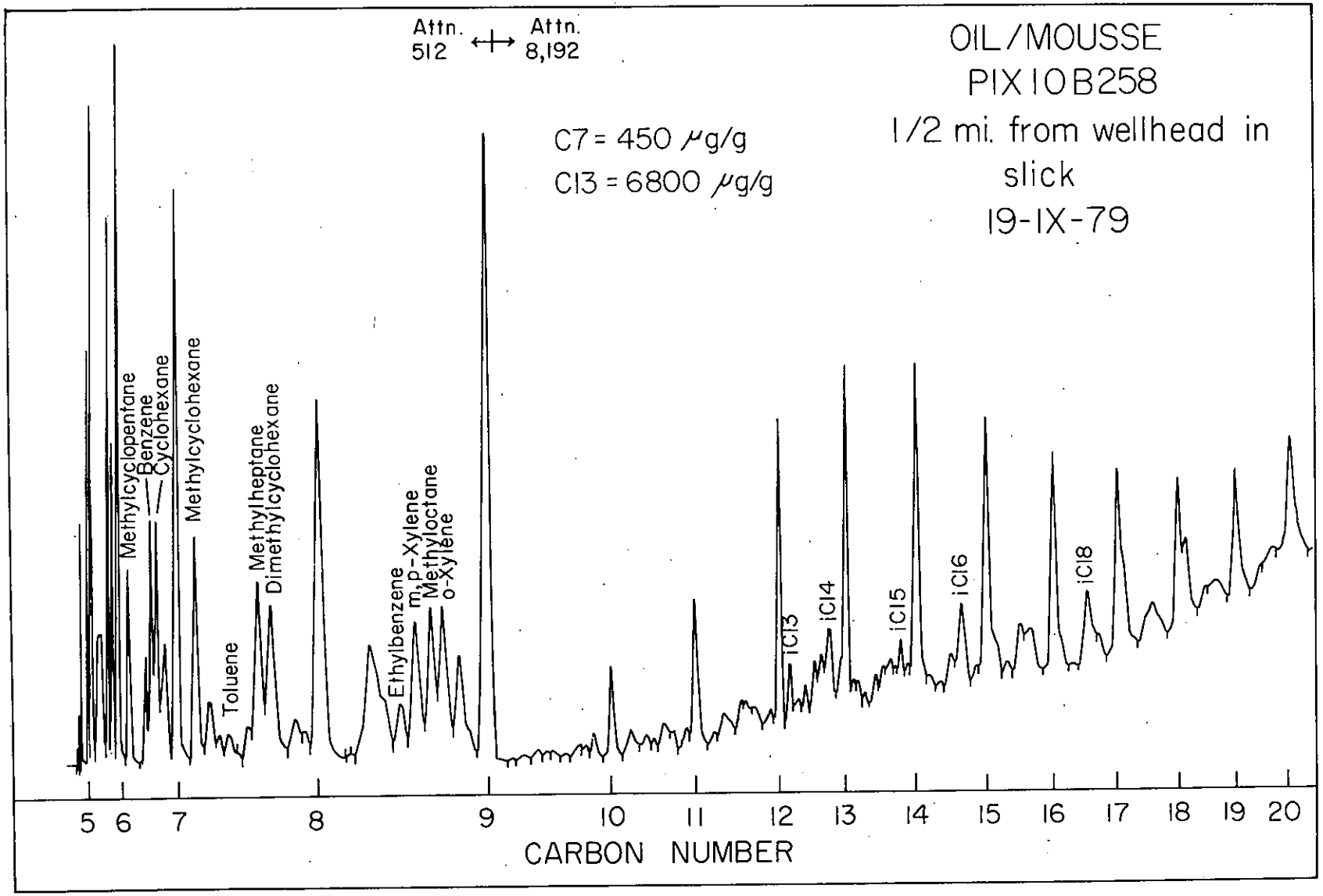

Figure 9. Oil/mousse sample from the IXTOC-I well blowout collected at station 10.

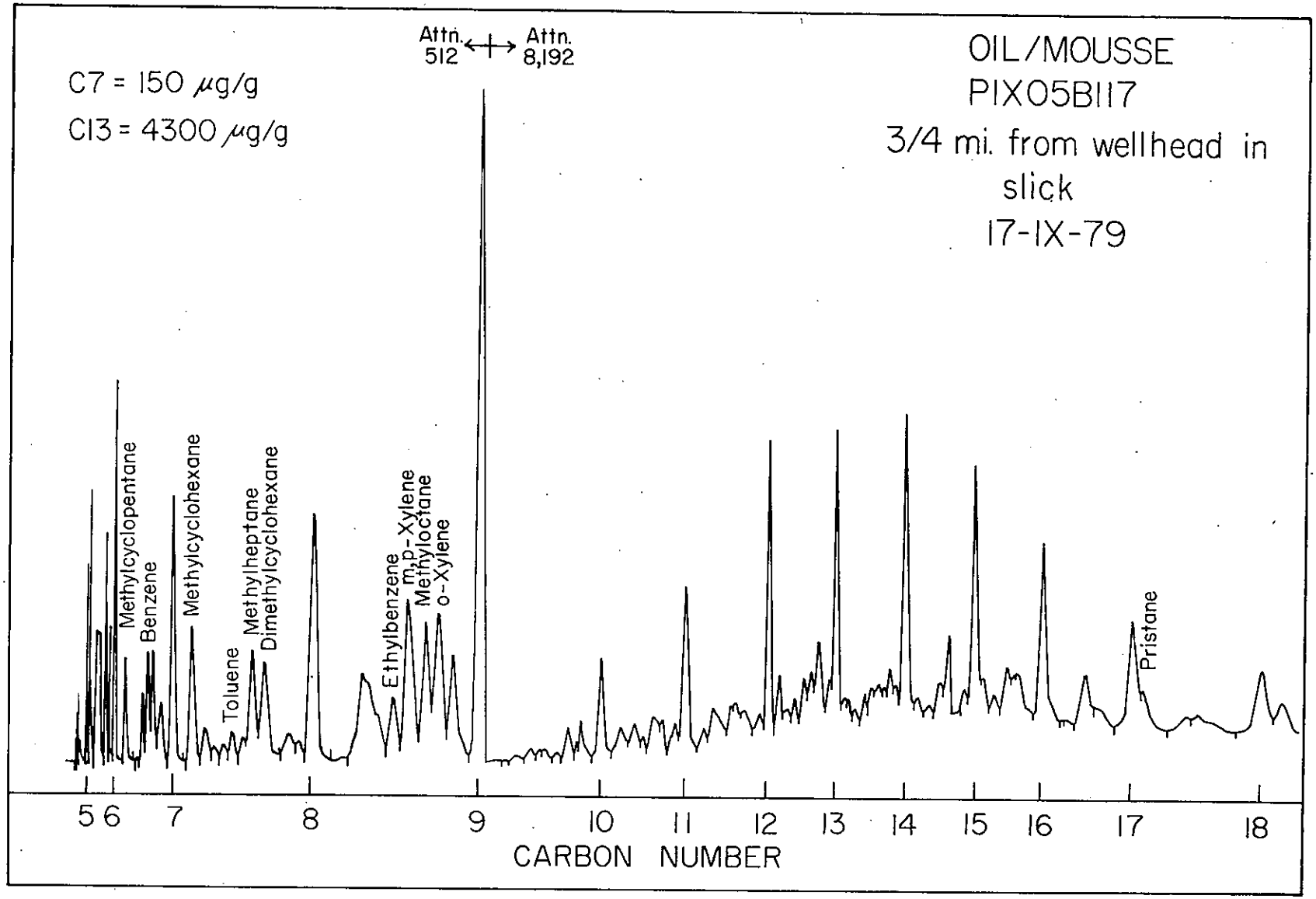

Figure 10. Oil/mousse sample from the IXTOC-I well blowout collected at station 5.

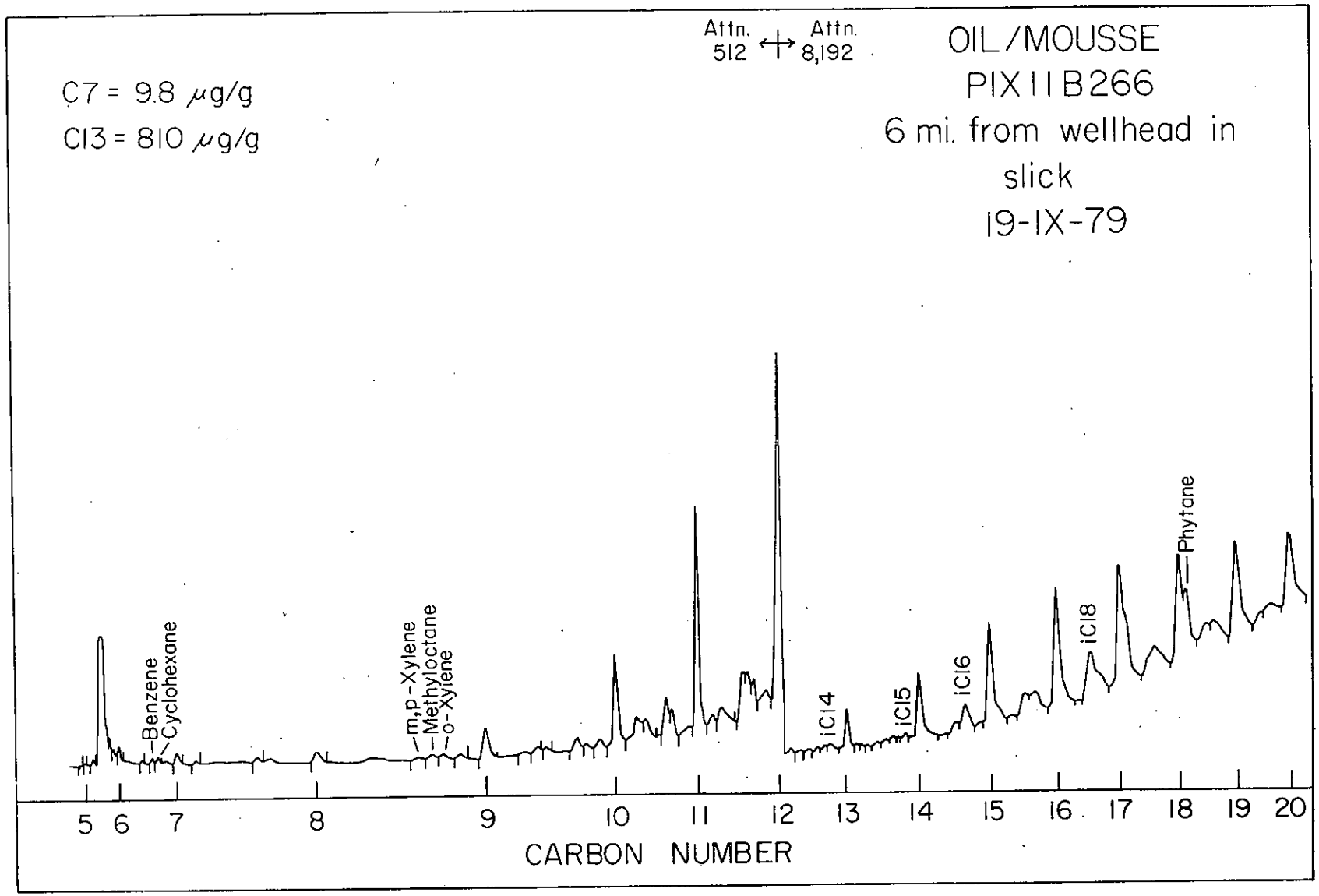

Figure 11. Oil/mousse sample from the IXTOC-I well blowout collected at station 11.

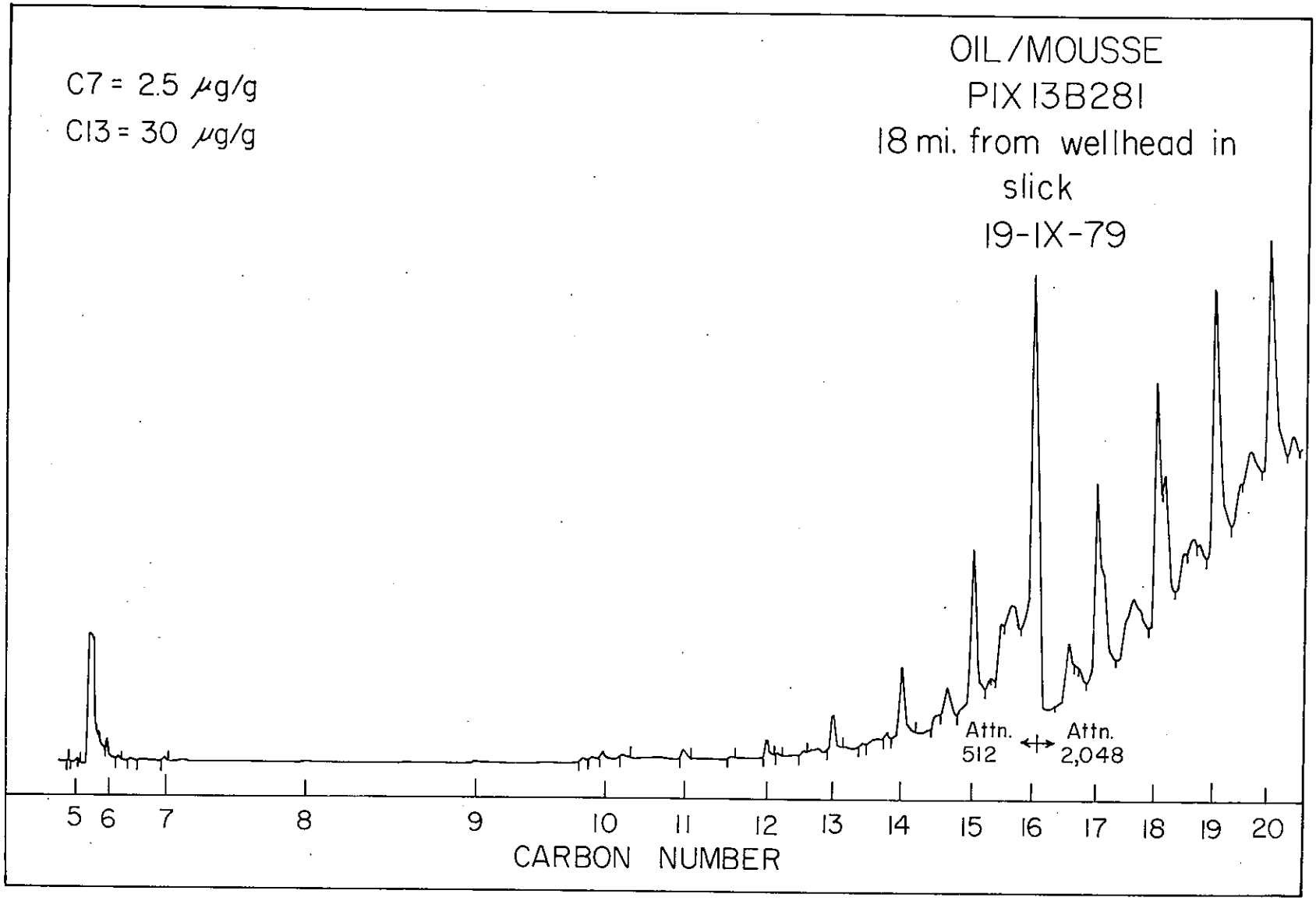

Figure 12. Oil/mousse sample from the IXTOC-I well blowout collected at station 13.

(PIX10B258 and PIX05B117) had little water and even the mousse samples tended to separate from seawater with storage. Sample PIX11B266, taken 6 miles from the blowout, had lost 95% of the n-C_5–n-C_{12} relative to oil taken within a mile of the blowout. Samples taken between 10-12 and 18-24 miles lost 97.5% to 99.8% and about 94.4% of C_5-C_{12} n-alkanes, respectively. Assuming a current speed of one knot, there is almost complete loss of C_5-C_{12} hydrocarbons from the IXTOC-I oil within 12 hours.

Sample PIX05B116, which was taken within a mile of the wellhead, had C_5-C_{12} n-alkanes of around 18 μg/g. It was recognized at the time of collection of this sample that it appeared to be older mousse that had been blown back to the wellhead by changing wind conditions. The chemical analysis confirmed these visual data. PIX17B360, a tar sample taken 170 miles to the east of the IXTOC-I wellhead, had only 7 μg/g of C_5-C_{12} n-alkanes. The C_5 and C_6 n-alkanes observed in this sample were unexpected, considering the total loss of C_7-C_{11} hydrocarbons; thus they may represent contamination. Table 6 indicates that n-alkanes lost from the surface slick were at least as high as n-C_{18}.

Figures 9 and 10 indicate that the main resolved components of the oil/mousse samples were n-alkanes. However, several light aromatics were observed in the chromatograms between n-C_6 and n-C_{11}. The light aromatics (e.g., benzene, toluene, xylenes) also were rapidly lost from the IXTOC-I slick. Cycloalkanes (Figures 9 and 10) are also major components of the VLH fractions. It was mentioned earlier that benzenes and cyclohexane have similar loss rates in this set of samples, indicating that evaporation is the major loss mechanism of VLH from the slick.

4. CONCLUSIONS

Gaseous and volatile hydrocarbons introduced into Campeche shelf waters by the IXTOC-I well blowout resulted mainly from condensate-rich gas escaping along with oil from the wellhead. Some of the ~400 μg/L volatile liquid hydrocarbons (VLH) observed in surface waters in the immediate vicinity of the wellhead were attributed to dispersed oil in the water column. VLH in oil emanating as a surface plume from the wellhead were rapidly lost, principally to the atmosphere, within a few miles downstream. During the September 1979 sampling, over 98% of both aliphatic and aromatic C_5-C_{12} hydrocarbons were lost from the downcurrent slick within 12 miles of the wellhead. Several lines of evidence indicate that VLH were not introduced in significant amounts to the water column by the surface slick. First, rapid loss of volatiles from the oil/mousse precludes significant additions more distant than a few miles from the wellhead. Second, the observed correlation between methane and total aromatics could not occur if there had been a flux of VLH from the oil to the water with increasing distance from the wellhead. Third, if a VLH flux to the water had occurred, benzene and cyclohexane, with similar vapor pressures but with widely different solubilities, would have been lost from the slick at different rates. This was not observed. Thus, our results are in agreement with

previously reported theoretical, laboratory and field experiments that indicate that solution is a minor mechanism for VLH loss from a slick.

Although low-molecular-weight hydrocarbons (LMWH) and VLH were introduced to the IXTOC-I well blowout region as essentially a point source, they were found to be distributed over a large area. LMWH also served as good tracers of the dispersion of the VLH. Elevated levels of both of these components were found at stations 2 and 16, tens of miles away from the wellhead. Although the LMWH are relatively nontoxic gases, VLH contain the most immediately toxic components of petroleum, the light aromatics (e.g., benzene, toluene, xylenes, naphthalene). The parts-per-billion concentrations of these components in the immediate vicinity of the wellhead may have a damaging effect on the marine ecosystem. The effects of parts-per-trillion levels of VLH over a much broader area of the Campeche shelf are unknown.

5. ACKNOWLEDGMENTS

This work was supported by the U.S. Department of Commerce, National Oceanic and Atmospheric Administration, under grants NA-79-RCA-00827 and NA-80-RCA-00006.

6. REFERENCES

Baker, J. M. (1970): The effect of oil on plants. Environ. Pollut., 1:27-44.

Bernard, B. B., J. M. Brooks, and W. M. Sackett (1977): A geochemical model for characterization of hydrocarbon gas sources in marine sediments. In Proc. Ninth Ann. Offshore Technol. Conf., OTC 2934, Houston, Texas: 435-438.

Bertsch, W., E. Anderson, and G. Holzer (1975): Trace analysis of organic volatiles in water by gas chromatography--mass spectrometry with glass capillary columns. J. Chromatogr., 112: 701-718.

Blumer, M. (1971): Hydrocarbons in the marine environment. Environ. Affairs, 1: 54-73.

Brooks, J. M., B. B. Bernard and W. M. Sackett (1977): Input of low-molecular-weight hydrocarbons from petroleum operations into the Gulf of Mexico. In Fate and Effects of Petroleum Hydrocarbons in Marine Organisms and Ecosystems, D. A. Wolfe (Ed.), Pergamon Press, New York: 373-384.

Brooks, J. M., B. B. Bernard, T. C. Sauer, and H. Abdel-Reheim (1978): Environmental aspects of a well blowout in the Gulf of Mexico. Environ. Sci. Technol., 12: 695-703.

Brooks, J. M. and W. M. Sackett (1973): Sources, sinks, and concentrations of light hydrocarbons in the Gulf of Mexico. J. Geophys. Res., 78: 5248-5258.

Butler, L. D. and M. F. Burke (1976): Chromatographic characterization of porous polymers for use as absorbents in sampling columns. J. Chromatogr. Sci., 14: 112-117.

Clark, R. C., Jr. and D. W. Brown (1977): Petroleum: Properties and analysis in biotic and abiotic systems. In Effects of Petroleum on Arctic and Subarctic Marine Environments and Organisms, Vol. 1, Academic Press, New York: 91-223.

Harrison, W., M. A. Winnik, P. T. Y. Koong, and D. MacKay (1975): Crude oil spills: Disappearance of aromatic and aliphatic components from small sea-surface slicks. Environ. Sci. Technol., 9: 231-234.

Heller, S. R. and C. W. A. Milne (1978): EPA/NIH Mass Spectral Data Base, Vol. 1. U.S. Gov't Printing Office, Washington, DC, 988 pp.

May, W. E., S. N. Chester, S. P. Cram, B. H. Gump, H. S. Hertz, D. P. Enagonio, and S. M. Dyszel (1975): Chromatographic analysis of hydrocarbons in marine sediments and seawater. J. Chromatogr. Sci., 13: 535-540.

McAuliffe, C. D. (1971): GC determination of solutes by multiple phase equilibrium. Chem. Technol., 1: 40-51.

McAuliffe, C. D. (1974): Determination of C_1-C_{10} hydrocarbons in water. Marine Pollution Monitoring (Petroleum), NBS 409 U.S. Gov't: 38-42.

McAuliffe, C. D. (1977a): Dispersal and alteration of oil discharged on a water surface. In Fate and Effects of Petroleum Hydrocarbons in Marine Organisms and Ecosystems, D. A. Wolfe (Ed.), Pergamon Press, New York: 19-35.

McAuliffe, C. D. (1977b): Evaporation and solution of C_2 to C_{10} hydrocarbons from crude oils in the sea surface. In Fate and Effects of Petroleum Hydrocarbons in Marine Organisms and Ecosystems, D. A. Wolfe (Ed.), Pergamon Press, New York: 363-372.

Royce, C. and R. Robertson (1979): IXTOC-I blowout draws massive control effort. Offshore, 39: 43-49.

Sackett, W. M. and J. M. Brooks (1975): Origin and distribution of low-molecular-weight hydrocarbons in the Gulf of Mexico coastal waters. In Marine Chemistry in the Coastal Environment, T. M. Church (Ed.), ACS Symposium Series 18: 211-230.

Sauer, T. C., Jr. (1978): Volatile liquid hydrocarbons in the marine environment. Ph.D. dissertation, Texas A&M University, College Station, Texas, 317 pp.

Sauer, T. C., Jr. (1980): Volatile liquid hydrocarbons in waters of the Gulf of Mexico and Caribbean Sea. Limnol. Oceanogr., 25: 338-351.

Sauer, T. C., Jr., W. M. Sackett, and L. M. Jeffrey (1978): Volatile liquid hydrocarbons in the surface coastal waters of the Gulf of Mexico. Mar. Chem., 7: 1-16.

Schwarzenbach, R. P., R. H. Bromund, P. M. Gschwend, and O. C. Zafiriou (1978): Volatile organic compunds in coastal seawater, preliminary results. J. Org. Geochem., 1:93-107.

Scranton, M. I., and P. G. Brewer (1977): Occurrence of methane in near-surface waters of the western subtropical North Atlantic. Deep-Sea Res., 82: 4947-4953.

Sivadier, H. O., and P. G. Mikolaj (1973): Measurement of evaporation rates from oil slicks on the open ocean. Proc. Joint Conf. on Prevention and Control of Oil Spills, Am. Petrol. Institute, Washington, DC: 475-484.

Smith, C. L. and W. G. MacIntyre (1971): Initial aging of fuel oil films on seawater. Proc. Joint Conf. on Prevention and Control of Oil Spills, Am. Petrol. Institute, Washington, DC: 457-461.

TRACING THE DISPERSAL OF THE IXTOC-I OIL USING C, H, S, AND N STABLE ISOTOPE RATIOS

R. E. Sweeney and R. I. Haddad
Global Geochemistry Corporation
6919 Eton Avenue
Canoga Park, California 91303

I. R. Kaplan
Institute of Geophysics and Planetary Physics
and
Department of Earth and Space Sciences
Los Angeles, California 90024

ABSTRACT

A suite of seventy-two samples, including 48 mousse samples, 6 tarballs collected from the water, 10 beach samples, and 8 clean beach tars, were analyzed. The isotopic ratios of carbon and hydrogen were measured on all samples and were compared to those for the IXTOC-I oil and a sample of oil collected by the MOP near the wellhead. The $\delta^{13}C$ values of the oil and wellhead oil are $-26.97^{o}/oo$ and $-26.89^{o}/oo$, respectively. The $\delta^{13}C$ values for 43 of the mousse samples are in the narrow range $-26.53^{o}/oo$ to $-27.11^{o}/oo$, and the other five range from $-25.96^{o}/oo$ to $-26.22^{o}/oo$. The latter group of mousse samples is considered to have been isotopically altered during transport. The δD values for all mousse range from $-25^{o}/oo$ to $-82^{o}/oo$ compared to $-83^{o}/oo$ for the crude oil and wellhead MOP oil. The positive δD values for the mousse are due to contamination by entrained seawater, which is not removable by vacuum desiccation. The δD values of the aliphatic and aromatic fraction of mousse range from $-86^{o}/oo$ to $-1000^{o}/oo$, indicating that entrained water can be eliminated by extraction of the mousse with organic solvents and column separation.

The ranges of $\delta^{13}C$ and δD values for clean beach tars ($-26.82^{o}/oo$ to $-27.02^{o}/oo$ and $-78^{o}/oo$ to $-84^{o}/oo$) from beaches extending from the Yucatan Peninsula to Brownsville, Texas, are isotopically similar to IXTOC-I crude oil. However, several tars collected by the NOAA Ship RESEARCHER from beaches near Tephnales, La Marina, and Brownsville have isotopic ratios distinctly different from that of the IXTOC oil. Measurement of the isotopic composition of C, S, and N on the asphaltene fraction supports the conclusion that several non-IXTOC-derived beach tar samples were collected.

The content (1.10% to 3.48%) and isotopic composition ($-4.73^{o}/oo$ to $-0.81^{o}/oo$) of sulfur in the asphaltene fractions of the mousse are different from the asphaltene fractions of the tars, crude oil, and MOP oil ($2.98^{o}/oo$ to $5.04^{o}/oo$ and $-5.65^{o}/oo$ to $-4.72^{o}/oo$). Since the asphaltenes of the mousse are different from the crude, fractionation or incorporation of external sulfur (e.g., seawater sulfate) may have taken place during mousse genesis. Because the isotopic properties of the asphaltene fraction of the crude oil and tars are so similar for many of the samples studied, we suggest that tar forms directly from spilled oil and does not involve a mousse intermediate.

1. INTRODUCTION

The leak from the IXTOC-I oil well in Campeche Bay, Gulf of Mexico, was the largest accidental release of petroleum in the history of drilling and production. The spill resulted in the release of more than 110 million barrels of oil into the Gulf of Mexico. By comparison, the AMOCO CADIZ spill, which caused significant environmental and economical damage along the French coast in 1978, released approximately 1.5 million barrels (IXTOC-I Oil Spill Damage Assessment Program, 1979).

The blowout on the IXTOC-I drilling rig occurred on June 3, 1979. After the blowout, the oil was carried northward by the Gulf currents from June through September and impacted along the coastal environments of Texas. A mid-September change in the prevailing winds and currents caused the oil to retreat and move southward. From this time until April 1980, when the leak was effectively shut off, the oil remained in Mexican waters.

The IXTOC-I oil spill was harmful to the environment, but not disastrous. As with other regions of the world, an increase in shipping traffic and the exploration and production of petroleum will cause the Gulf Coast to continue to suffer from exposure to oil spills from various sources. With this in mind, a concerted effort was made to study the environmental impacts on the Gulf of Mexico region following the initial release of IXTOC-I oil.

The objectives of this operation were twofold: (1) to monitor molecular changes that occur during weathering of crude oil in the natural environment, and (2) to test the effectiveness of various tracer techniques in order to characterize and correlate residual petroleum samples to their source.

The stable isotope ratios of both carbon and sulfur have been used to determine the origin of beach tars on the southern California coast (Reed and Kaplan, 1977; Sweeney and Kaplan, 1978; Hartman, 1978; Venkatesan et al., 1981). Most conventional chemical methods that use the identification of molecular species to characterize petroleums suffer from the unavoidable obliteration of the chemical fingerprints during weathering. By contrast, the stable isotope ratio of the elements appears to be relatively unaltered during the processes of biodegradation, water washing, evaporation, etc. For this reason, 74 samples from the NOAA-sponsored program for the investigation of the IXTOC-I oil spill were analyzed for isotopic composition. The isotopic ratios of carbon, hydrogen, sulfur, and nitrogen were determined for various samples.

2. EXPERIMENT

2.1 Samples

The majority of the samples analyzed for stable isotope composition were collected on the NOAA-sponsored IXTOC-I Campeche oil spill cruises from September 11 to 27, 1979. Two ships were involved in the collection. Fifty-three samples were collected on the NOAA Ship RESEARCHER and are denoted by RIX (Table 1). The following numbers, 0-23, indicate the collection site in Figures 1 and 2. Ten samples were collected on the contract ship G. W. PIERCE. They are denoted by PIX in Table 1; the station locations are shown in Figures 1 and 2. Eight beach tars were collected in August-September, 1979, from Yucatan State beach, Mocambo beach near Vera Cruz, Barra del Mezquital Beach, Isla del Lobos beach, Rio Bravo beach of Matamoros (all in Mexico), and South Padre Island, Texas. The samples were supplied to Global Geochemistry Corporation (GGC) by PEMEX. PEMEX also supplied a sample of the IXTOC-I oil and a sample of oil near the wellhead picked up by an oil MOP in September 1979.

Table 1. List of samples, locations, and collection agencies. RIX and PIX coordinates are given in the RESEARCHER and PIERCE cruise logs, respectively. Locations for beach tars collected by PEMEX are general. The weathered oil was picked up by an oil MOP in September 1979.

Sample	Cruise/Location		Agency	Sample	Cruise/Location		Agency
RO-1	RIX	0A0015	UNO	R10-5	RIX	10E572	ERCO
RO-2		0C0039	UNO	R11-1		110028	UNO
RO-3		0C0041	UNO	R11-2		110029	UNO
RO-4		0C0042	UNO	R11-3		110030	UNO
RO-5		0C0044	UNO	R11-4		11E581	ERCO
RO-6		0D0045	UNO	R11-5		11E582	ERCO
RO-7		00F070	UNO	R11-6		11E583	ERCO
RO-8		00F071	UNO	R11-7		11E584	ERCO
RO-9		00F072	UNO	R11-8		11E585	ERCO
RO-10		00F073	UNO	R11-9		11E588	ERCO
RO-11		00F074	UNO	R11-10		11E589	ERCO
RO-12		00F075	UNO	R12-1		12F058	UNO
RO-13		00F077	UNO	R23-1		235009A	SAI
RO-14		00F078	UNO	R23-2		235010A	SAI
RO-15		00F079	UNO	RX10		STX1013	UNO
RO-16		00F080	UNO	R23-4		235012	ERCO
RO-17		00F081	UNO	P3-1	PIX	03E048	ERCO
RO-18		00F096	UNO	P5-1		05E050	ERCO
R6-1		060014	UNO	P6-1		06E068	ERCO
R6-2		06F015	UNO	P14-1		14E154	ERCO
R6-3		06F016	UNO	P14-2		14E155	ERCO
R6-4		06E525	ERCO	P17-1		17E186	ERCO
R6-5		06E526	ERCO	P17-2		17E187	ERCO
R6-6		06E530	ERCO	P17-3		17E190	ERCO
R6-7		06E533	ERCO	PPI		Padre Island	ERCO
R7-1		07F019	UNO	P5-2		05B166	ERCO
R7-2		07F020	UNO	FI		near well	COB
R7-3		07F023	UNO	M1		Yucatan state	PEMEX
R7-4		07E024	UNO	M2		Mocambo, V.C.	PEMEX
R7-5		07E539	ERCO	M3		Mocambo, V.C.	PEMEX
R7-6		07E542	ERCO	M4		B. Mezquital	PEMEX
R7-7		07E543	ERCO	M5		B. Mezquital	PEMEX
R7-8		07E545	ERCO	M6		Padre Island	PEMEX
R10-1		10FTOW-5	UNO	M7		Isla de Lobes	PEMEX
R10-2		10E566	ERCO	M8		Matamoros	PEMEX
R10-3		10E567	ERCO	IXTOC-I		Crude oil	PEMEX
R10-4		10E571	ERCO	MOP oil			PEMEX

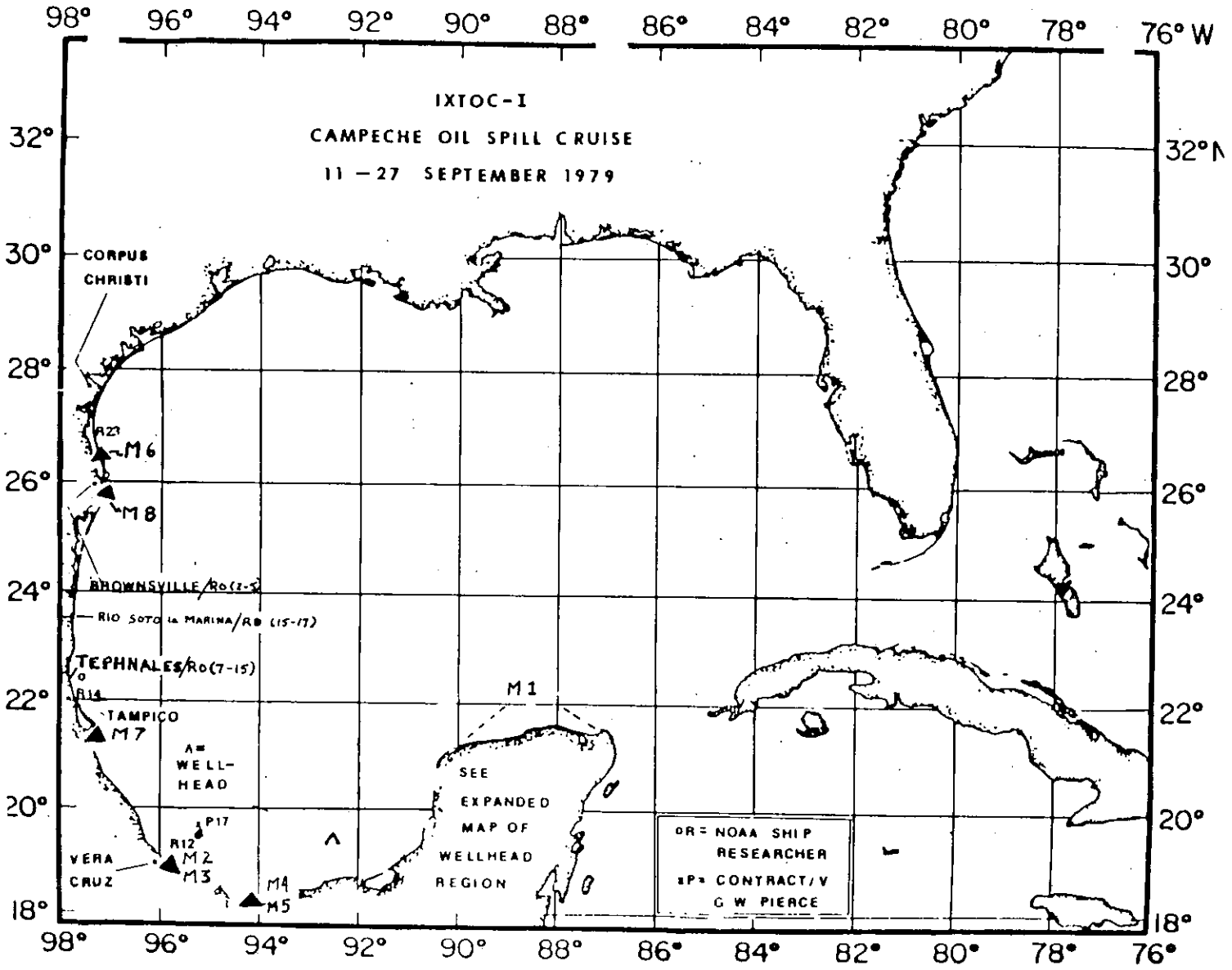

Figure 1. Location map showing collection sites throughout the Gulf of Mexico.

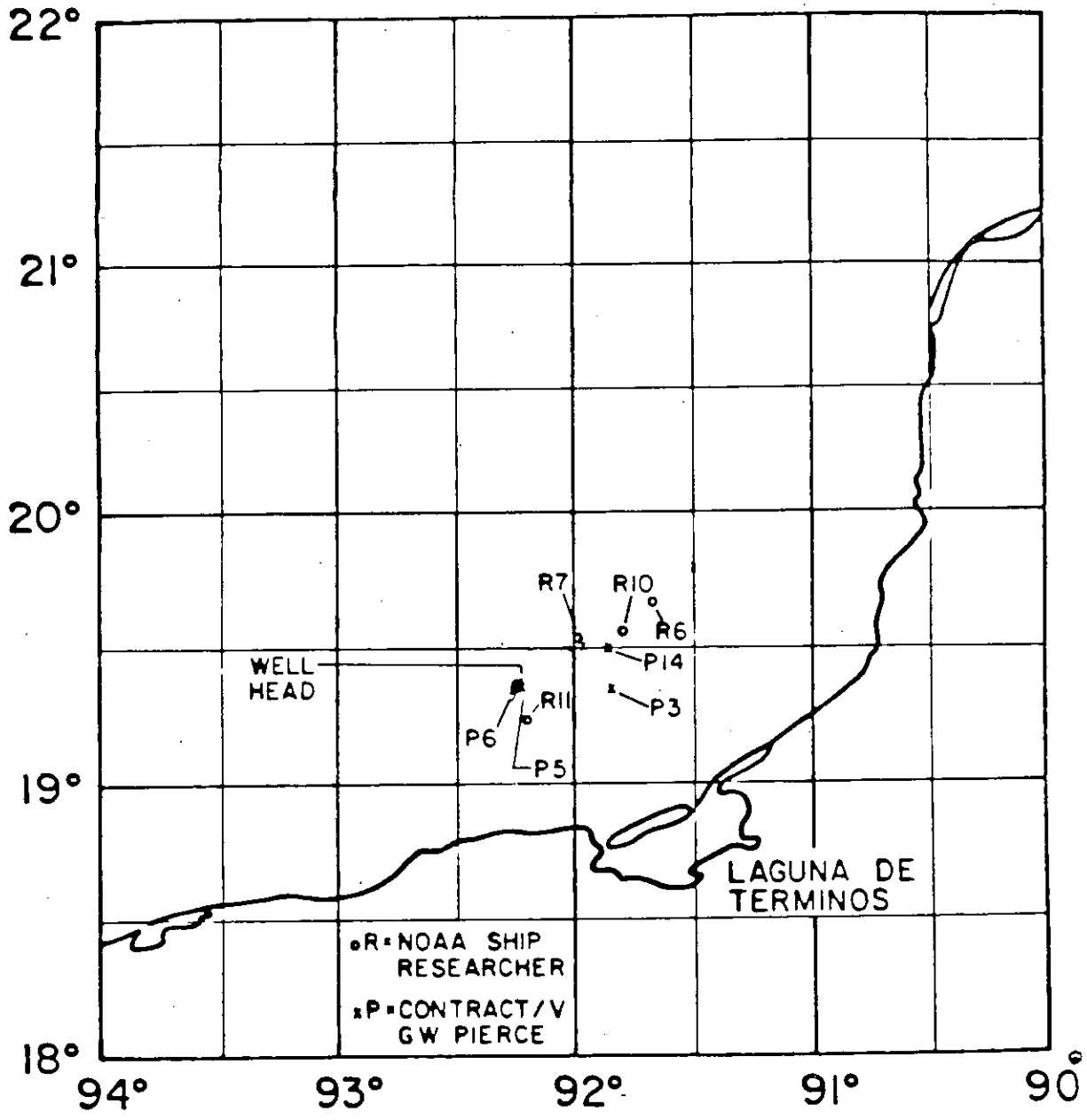

IXTOC-I
CAMPECHE OIL SPILL CRUISE
11-27 SEPTEMBER 1979
EXPANDED WELLHEAD REGION

Figure 2. Location map showing collection sites near well head.

An additional sample of mousse, collected near the well in July 1979, was received from Mr. Marchand, Centre Oceanologique de Bretagne, Brest, France.

For comparative purposes, the weathered (altered) crude oil is divided into two classifications, depending on physical texture: (1) mousse, a shimmering, brownish-colored, highly viscous fluid--an oil-water emulsion with a consistency similar to that of thick fudge syrup; (2) tar, of a blackish, dull luster--very granular-appearing, well-congealed balls. A total of 48 mousse samples were measured for isotopic composition. In almost all cases, the samples were collected in the water column; 23 samples were classified as tars. These samples were predominantly derived from beaches. Also included in the samples were black beach sand layers that were believed to be high in residual petroleum.

Figures 1 and 2 show the locations of the various sample sites. Sampling site locations lie near the wellhead (R2-11 and P3-P14), near Vera Cruz (R12, P17), or near Brownsville (RO, R23). Beach samples were collected from a variety of beaches extending from Yucatan to Brownsville (Table 2). The samples supplied by PEMEX were very clean tar balls, but tar samples collected by NOAA cruises contained much external debris. The locations of the PEMEX samples are shown in Figure 1.

2.2 Procedures

Unfractionated samples received at GGC were washed to remove salts, freeze-dried, and then analyzed for carbon and hydrogen isotope ratios. One (1) mg of each sample was combusted at 900°C in the presence of cupric oxide and silver metal (Stump and Frazer, 1973). The produced CO_2 was purified and collected for isotope analysis. The water produced by the combustion was converted to hydrogen gas by reaction with uranium turnings at 800°C and collected on activated charcoal at liquid nitrogen temperature in a sample tube.

Nitrogen and sulfur isotope analyses were performed on the asphaltene fraction of selected samples. These samples were cleaned of foreign debris and separated from entrapped sand by extraction with methylene chloride. The asphaltene components were precipitated in pentane and separated by centrifugation and freeze-drying.

Nitrogen was produced by the same combustion procedure described above (Stump and Frazer, 1973). The produced N_2 gas was measured volumetrically by use of a Toepler pump-manometer system and collected on activated charcoal at liquid nitrogen temperature in a sample tube.

Total sulfur content was determined by Parr bomb combustion of 0.5 gm of asphaltene in 30 atmospheres of oxygen, and the produced sulfate subsequently precipitated as $BaSO_4$ (Parr Instrument Company, 1965). Sulfur dioxide was prepared for isotopic analysis by direct combustion of the barium sulfate with quartz powder at high temperature (Bailey and Smith, 1972).

Table 2. Carbon and hydrogen isotope ratios for organic matter in beach sands. Samples marked with * had no extractable components and the δ values are for kerogen or humic material (these results are not included in Table 3).

Sample	$\delta^{13}C$ (°/oo)	δD (°/oo)	Location
RO-2	-25.82	-77	Beach south of Brownsville, Texas
RO-3	-26.86	-78	" " " " "
RO-4	-26.72	-62	" " " " "
RO-5	-26.11	-67	" " " " "
RO-7	-27.19	-110	Beach due west of R14 near Tephnales
RO-8	-28.32	-114	" " " " "
RO-9	-27.29	-105	" " " " "
RO-10*	-22.86	-89	" " " " "
RO-11	-26.80	-100	" " " " "
RO-12*	-11.66	-64	" " " " "
RO-13*	-17.72	-81	" " " " "
RO-14*	-18.55	-97	" " " " "
RO-15	-26.10	-54	Beach north of Rio Soto La Marina
RO-16	-26.88	-77	" " " " "
RO-17	-23.73	-78	" " " " "

Aliphatic and aromatic fractions supplied by the University of New Orleans (UNO) or Energy Resources Co. (ERCO) were analyzed for carbon and hydrogen isotopic ratios in a similar manner to that used for the unfractionated samples.

Stable isotopic ratio determinations for C, H, and N were carried out using a MAT 250 Varian mass spectrometer. The sulfur isotope ratio was determined using a Nuclide 6" - 60° RMS mass spectrometer.

All isotopic data are expressed in the standard δ notation:

$$\delta X \text{ sample } (^{o}/oo) = \frac{R \text{ sample} - R \text{ standard}}{R \text{ standard}} \times 1000$$

where X represents the element of interest and R the ratio of the rare to the most abundant isotope of that element (e.g., $^{13}C/^{12}C$). The isotopic standards used for carbon, hydrogen, nitrogen, and sulfur are Chicago Pee Dee Beleminite (PDB), standard mean ocean water (SMOW), atmospheric nitrogen, and Canyon Diablo meteorite troilite sulfur, respectively. Analytical precision of the reported values is $0.10^{o}/oo$ for carbon, $1.0^{o}/oo$ for hydrogen, $0.5^{o}/oo$ for nitrogen, and $0.3^{o}/oo$ for sulfur.

3. RESULTS

Table 1 gives a list of the 74 samples used in this study. All whole samples were analyzed for $\delta^{13}C$ and δD. These values are listed in Table 3. The $\delta^{13}C$ of the crude is $-26.97^{o}/oo$ and the oil picked up near the wellhead (MOP) is $-26.89^{o}/oo$. The range in $\delta^{13}C$ values for mousse near the wellhead (R6-R11, P3-P14) is $-26.33^{o}/oo$ to $-27.08^{o}/oo$, with a mean of $-26.86^{o}/oo$. The values for mousse collected near Vera Cruz ($-26.79^{o}/oo$ to $-27.11^{o}/oo$) also have $\delta^{13}C$ values essentially identical to those measured on the mousse near the emission source. The mousse samples collected near Brownsville have a different range for $\delta^{13}C$ ($-25.96^{o}/oo$ to $-26.22^{o}/oo$), indicating either isotopic alteration during transport or the inclusion of samples from an alternative source.

The range in $\delta^{13}C$ values for the clean tars collected from various Mexican beaches by PEMEX is $-26.82^{o}/oo$ to $-27.02^{o}/oo$, identical to that of IXTOC-I oil and related mousse. The range of $\delta^{13}C$ values for tars collected by NOAA is $-23.73^{o}/oo$ to $-28.32^{o}/oo$, significantly greater than the spread values measured on the wellhead mousse and PEMEX tars. This would suggest that tars from other sources have probably been sampled in this group. Table 2 gives a list of the samples collected from the Brownsville, Tephnales, and Rio Soto La Marina beaches. Four samples (denoted by asterisks) were not included in Table 3, because there was no extractable organic matter. Only one of the eight samples from Tephnales and one of the three samples from La Marina have $\delta^{13}C$ values comparable with values for the IXTOC-I material. The four tars from Brownsville Beach have $\delta^{13}C$ values in a narrow range, $-25.85^{o}/oo$ to $-26.88^{o}/oo$, which are different from the IXTOC material but similar to values of the mousse collected at the nearby station, R-23.

Table 3. Carbon and hydrogen stable isotope ratios for whole samples. Each sample is classified generally as either mousse or tar.

Sample Type	Sample Number	$\delta^{13}C$ (‰)	δD (‰)	Sample Type	Sample Number	$\delta^{13}C$ (‰)	δD (‰)
IXTOC-I crude oil		-26.97	-83	mousse	R11-10	-26.72	-52
					R23-1	-26.00	-56
					R23-2	-26.18	-74
mousse	R0-1	-26.86	-30		RX10	-26.22	-43
	R0-4	-26.72	-62		R23-4A	-27.59	-66
	R0-6	-25.96	-55		R23-4B	-26.91	-82
	R0-15	-26.10	-54		P3-1	-26.79	-46
	R6-1	-26.86	-44		P5-1	-26.53	-35
	R6-2	-26.65	-50		P6-1	-26.84	-37
	R6-3	-26.88	-39		P14-1	-26.57	-54
	R6-4	-26.96	-42		P14-2	-26.71	-58
	R6-5	-26.83	-57		P17-1	-26.81	-52
	R6-6	-27.08	-51		P17-2	-27.11	-45
	R6-7	-26.88	-52		P17-3	-26.79	-41
	R7-1	-26.66	-54		PPI	-26.77	-42
	R7-2	-26.88	-50		FI	-26.86	-25
	R7-3	-27.21	-79				
	R7-4	-26.63	-37	tar	R0-2	-25.82	-77
	R7-5	-26.91	-58		R0-3	-26.86	-78
	R7-6	-27.00	-57		R0-5	-26.11	-67
	R7-7	-27.08	-52		R0-7	-27.19	-110
	R7-8	-26.86	-52		R0-8	-28.32	-114
	R10-1	-26.84	-46		R0-9	-27.29	-105
	R10-2	-26.82	-53		R0-11	-26.80	-100
	R10-3	-27.02	-54		R0-16	-26.88	-77
	R10-4	-26.85	-53		R0-17	-23.73	-78
	R10-5	-26.97	-53		R0-18	-26.67	-84
	R11-1	-26.73	-42		R12-1	-26.18	-76
	R11-2	-26.74	-46		M1	-27.02	-78
	R11-3	-26.97	-35		M2	-26.95	-84
	R11-4	-26.89	-48		M3	-26.94	-83
	R11-5	-27.08	-47		M4	-26.91	-82
	R11-6	-26.77	-54		M5	-26.90	-81
	R11-7	-26.92	-43		M6	-26.93	-84
	R11-8	-26.89	-51		M7	-26.82	-79
	R11-9	-26.94	-57		M8	-26.90	-84

Shown also in Tables 2 and 3 are the δD values for the various samples. The δD values of the crude MOP oil are the same (-83°/oo). The δD values for every mousse sample (-25°/oo to -82°/oo, mean -49°/oo) are more positive than the crude oil values. The δD values for the PEMEX tars range from -78°/oo to -84°/oo and are equivalent to that of the crude. The range in δD values for the tars collected by NOAA is larger, -67°/oo to -114°/oo, but is not skewed as much to isotopic heavy values as the mousse material.

Figure 3 is a plot of $\delta^{13}C$ versus δD for the various beach tar samples and the MOP oil. The data points for the PEMEX tars and the MOP oil fall into a tight group, along with some tars from Brownsville and La Marina. Other tars from these beaches fall into a group more positive in both $\delta^{13}C$ and δD than the MOP oil. The tars from the beach sands near Tephnales have values more negative than the other samples.

Figure 4 is a plot of $\delta^{13}C$ versus δD for the various mousse samples, the MOP oil, and the PEMEX tars. With the exception of the mousse samples collected from RO and R23, the $\delta^{13}C$ values fall in the same range as the MOP oil and the PEMEX tars. The $\delta^{13}C$ values for some of the samples from stations RO and R23 are more positive than the mousse samples collected near the wellhead and fall into a similar range as that for the Brownsville and La Marina beach tars (Figure 4). The δD values for all mousse samples are more positive than those for the MOP oil or the PEMEX tars.

The asphaltene fraction was separated for the IXTOC-I crude, the MOP oil, 17 mousse samples, and 7 beach tars. This fraction was chosen in order to concentrate the nitrogen and sulfur, which are in low abundance in the IXTOC-I oil. The sulfur and nitrogen content, the isotopic composition, and the $\delta^{13}C$ value for the asphaltenes were determined and are listed in Table 4. The data for some of the samples are not given because the amount of material received at GGC was too small to provide sufficient asphaltene for analysis.

Figure 5 gives a plot of sulfur content versus $\delta^{34}S$. The sulfur content of the MOP oil is higher than that for most of the tars and mousse. The value is -4.97°/oo, compared to the ranges -5.65°/oo to -3.85°/oo (mean = -5.04°/oo) for the PEMEX tars and -5.75°/oo to +0.81°/oo (mean = -3.38°/oo) for the mousse samples. Mousse A and B are samples from the surface and center of a patty collected at station R23. With the exception of the patty, the $\delta^{34}S$ is more positive and the sulfur content is lower for mousse than for tar. Also different are tars from Tephnales beach (R08, R09) and one tar from Brownsville Beach (R03).

The nitrogen content and isotopic composition are listed in Table 4. With the exception of the two mousse samples collected near Vera Cruz (1.3% and 1.7%), the nitrogen content in the asphaltene fraction of all other samples ranges between 0.7% and 1.0%. The $\delta^{15}N$ values of the crude and MOP oil are +0.63°/oo and -0.34°/oo, respectively. The $\delta^{15}N$ values of the samples range from -0.80°/oo to +0.99°/oo, with the exception of R11-4 and RO-3, which are -1.20°/oo and -1.21°/oo, respectively. Only these samples have $\delta^{15}N$ values outside the range of IXTOC-I oil. The sulfur/nitrogen weight ratios range from 0.1 to 6.7 and are plotted versus $\delta^{34}S$ in Figure 6.

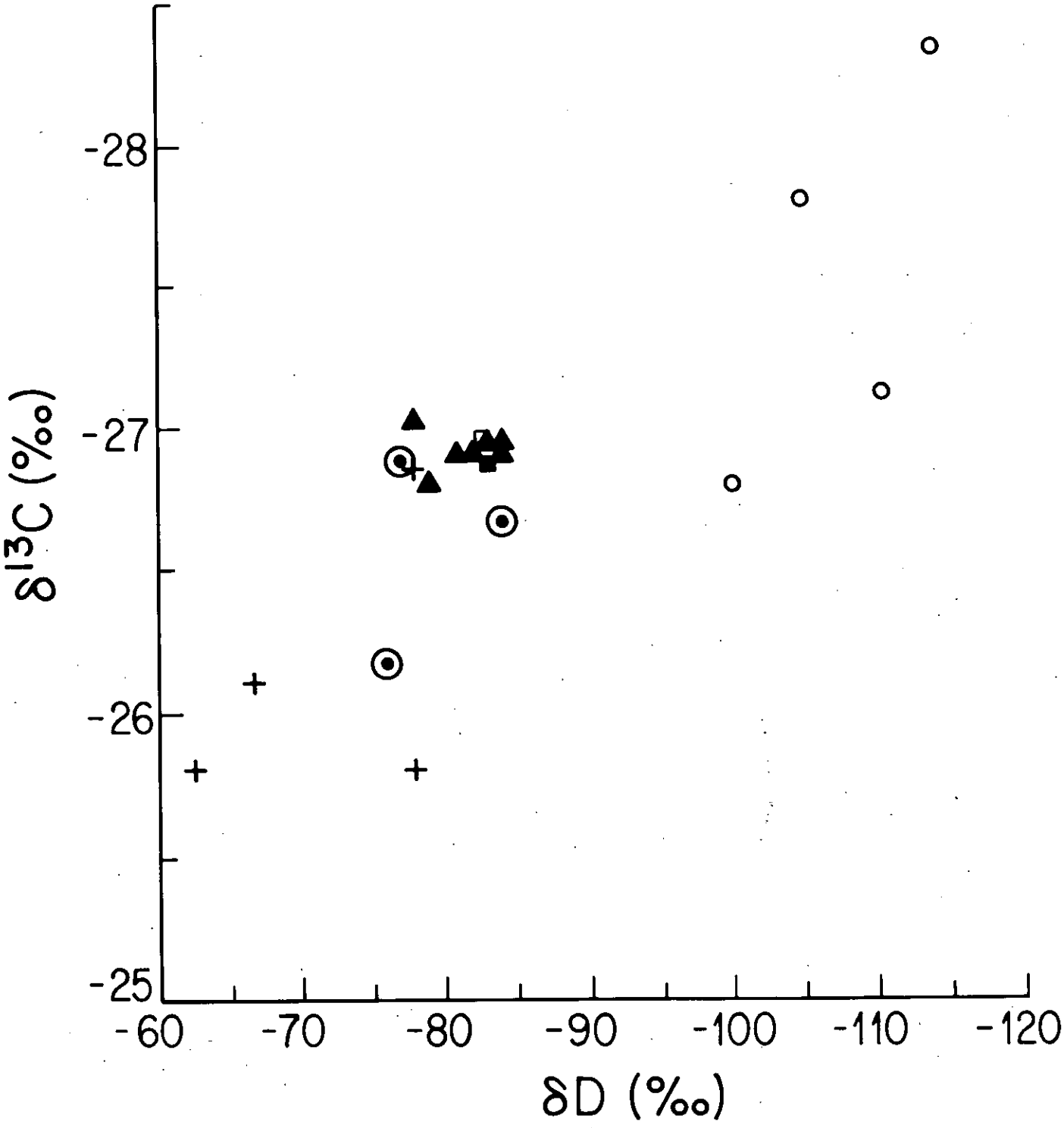

Figure 3. Plot of $\delta^{13}C$ vs. δD for tars, MOP oil, and IXTOC-I crude □ oil. Tars are separated by collection site: Brownsville +, Rio Soto La Marina ◉, Tephnales ○, and PEMEX ▲.

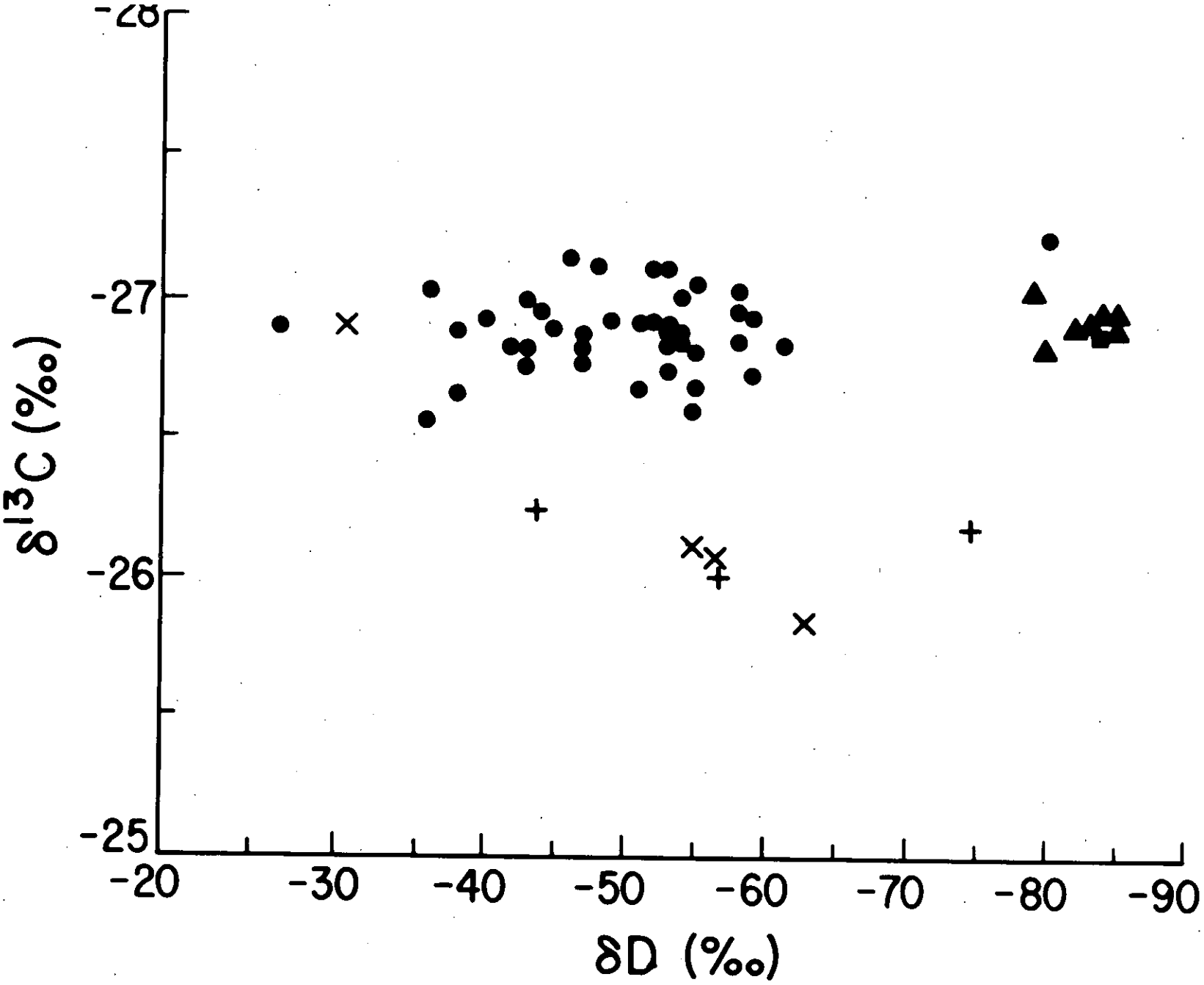

Figure 4. Plot of $\delta^{13}C$ vs. δD for mousse, MOP oil, and PEMEX tars. Mousse samples are differentiated by stations: station RO ×, station 23 +, all other ●, PEMEX tars ▲, and MOP oil ■.

Table 4. Sulfur and nitrogen content, $\delta^{34}S$, $\delta^{15}N$, and $\delta^{13}C$ for asphaltene fraction of certain samples listed in Tables 1 and 3.

Sample		S (%)	$\delta^{34}S$ (°/oo)	N (%)	$\delta^{15}N$ (°/oo)	S/N	$\delta^{13}C$
IXTOC-I crude		5.72	---	1.0	+0.63	5.7	-27.13
MOP oil		5.04	-4.97	1.0	-0.34	5.0	---
mousse	R6-1	2.81	-3.74	0.9	+0.51	3.1	---
	R6-4	2.71	-3.46	0.9	+0.25	3.0	---
	R7-1	1.97	-2.65	---	---	---	---
	R7-6	2.22	-3.45	0.9	+0.18	2.5	---
	R10-3	2.23	-0.81	---	---	---	---
	R11-2	3.18	-4.54	0.7	-0.13	4.5	-27.12
	R11-3	1.12	-2.88	0.9	+0.23	1.2	-26.84
	R11-4	2.44	-3.61	0.7	-1.20	3.4	---
	R11-5	2.76	-4.12	---	---	---	---
	R11-7	2.90	-2.79	---	---	---	---
	R23-2	2.72	-4.97	0.8	+0.99	3.4	-26.90
	R23-4A	5.16	-4.73	0.8	-0.31	6.5	-26.83
	R23-4B	3.48	-5.75	0.8	-0.37	4.4	-27.01
	P17-1	2.81	-3.72	1.3	-0.17	2.2	---
	P17-3	2.28	-3.69	1.7	+0.13	1.3	---
	PPI	3.21	-2.39	0.7	+0.09	4.6	---
	FI	1.10	-1.84	---	---	---	---
tar	R0-3	6.37	+2.85	1.0	-1.21	6.7	-27.30
	R0-8	0.05	+1.82	0.7	+0.16	0.1	---
	R0-9	0.10	+5.37	0.8	-0.15	0.1	---
	R0-11	0.66	-6.84	---	---	---	---
	R0-16	3.81	-4.72	0.8	+0.53	4.8	-26.26
	M1	2.98	-5.29	0.8	-0.80	3.7	-26.95
	M2	3.61	-5.31	0.9	+0.61	4.0	-26.75
	M4	3.10	-5.65	0.9	-0.40	3.4	-26.95
	M5	3.24	-5.50	0.8	-0.02	4.1	-26.90
	M6	3.35	-4.91	0.7	-0.40	4.8	-26.93
	M7	3.70	-4.73	0.8	-0.08	4.6	-26.88
	M8	3.79	-3.85	0.8	-0.18	4.7	-26.97

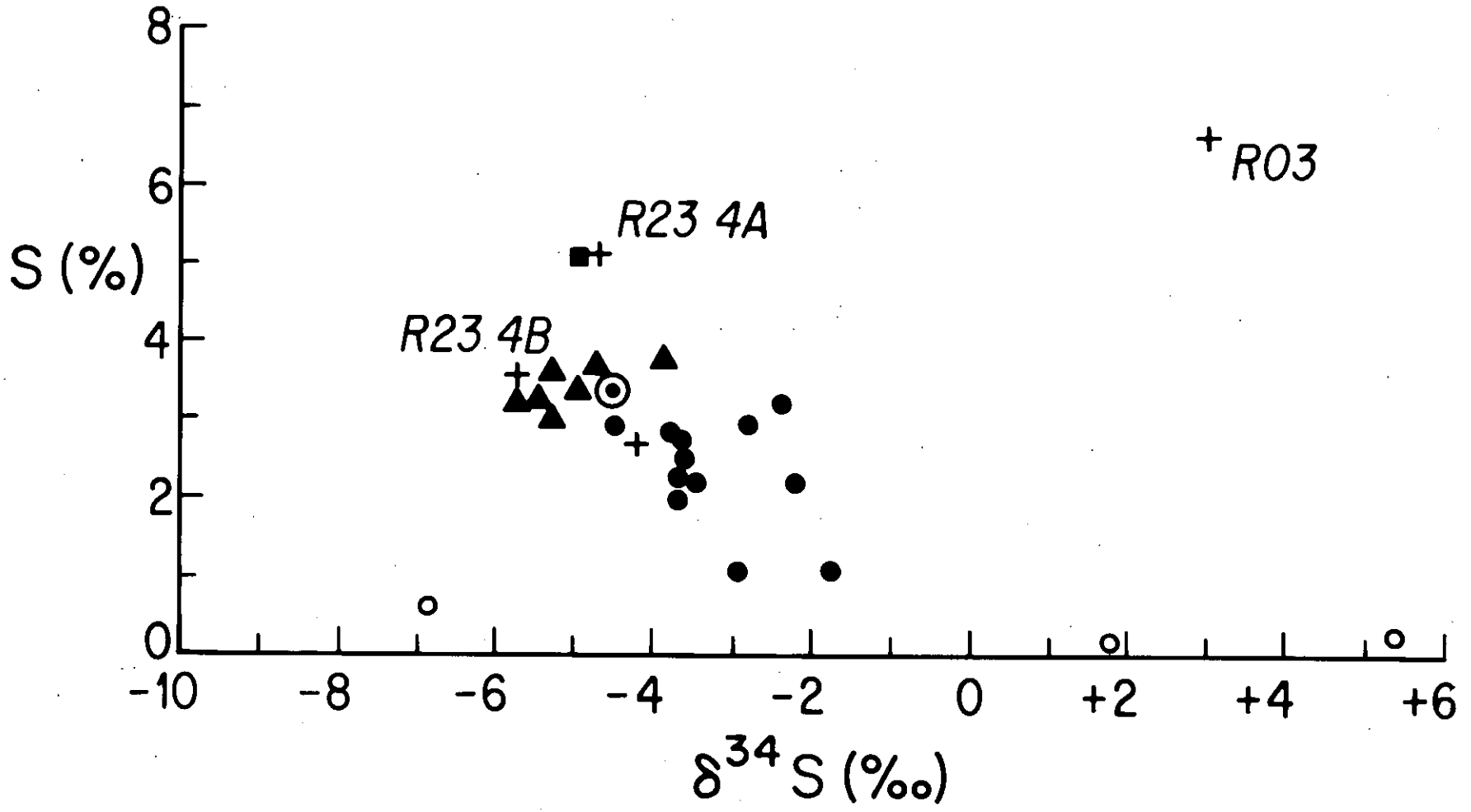

Figure 5. Plot of sulfur content vs. $\delta^{34}S$ for the asphaltene fraction of selected samples. Tars are differentiated by location: Brownsville +, Tephnales ○, Rio Soto La Marina ◉, and PEMEX ▲. Mousse samples are denoted by ● and MOP oil ■.

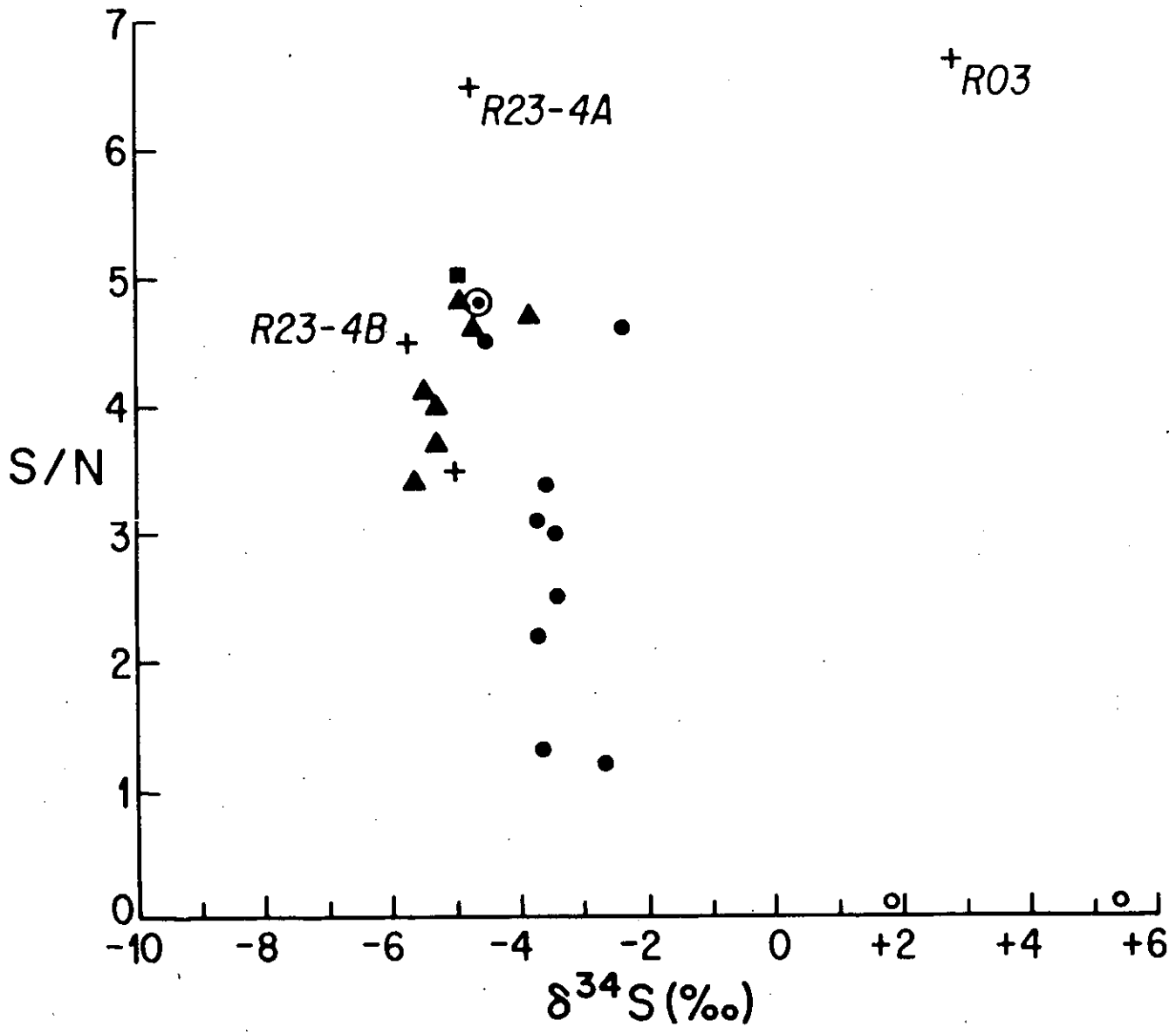

Figure 6. Plot of $\delta^{34}S$ vs. the S/N ratio for selected samples. Tars are differentiated by location: Brownsville +, Tephnales ○, Rio Soto La Marina ⊙, and PEMEX ▲. Mousse samples are denoted by ● and MOP oil ■.

The $\delta^{13}C$ values were measured for several of the asphaltene fractions. The results are listed in Table 4 and are plotted versus $\delta^{13}C$ of the whole sample in Figure 7. The asphaltene fraction of the MOP oil was not measured, so the values for the crude are shown for comparison. The $\delta^{13}C$ values of the skin and core of the mousse patty (A and B) are different for the whole sample but the same for the asphaltene fraction. The $\delta^{13}C$ values for the asphaltene fraction of the two tars collected by the RIX cruise (RO-3, RO-16) are more negative than the others.

Several of the mousse samples were column-separated at the UNO and ERCO laboratories and sent to GGC. The aliphatic and aromatic fractions were measured for carbon isotopic composition, and the samples from UNO were measured for hydrogen isotope composition. The IXTOC oil was column-separated and measured at GGC. The results are listed in Table 5 and presented graphically in Figures 8 and 9.

The ranges and standard deviations for the $\delta^{13}C$ results are $-27.13^{o}/oo$ to $-28.05^{o}/oo$ (0.28) and $-26.74^{o}/oo$ to $-26.92^{o}/oo$ (0.21) for the aliphatic and aromatic fractions, respectively. For comparison, the range and standard deviation for the whole mousse measurement is $-26.53^{o}/oo$ to $-27.02^{o}/oo$ (0.14) for these samples. All results are comparable to the IXTOC-I crude.

The ranges in the δD values for the aliphatic and aromatic fractions are $-86^{o}/oo$ to $100^{o}/oo$ and $-92^{o}/oo$ to $-100^{o}/oo$, in comparison with $-35^{o}/oo$ to $-57^{o}/oo$ for the equivalent whole mousse samples. These values for the aliphatic and aromatic fractions are more comparable with the δD values of the IXTOC-I crude and the PEMEX beach tars.

4. DISCUSSION

In this investigation a series of mousse and tar samples was collected from a variety of locations in the Gulf of Mexico. Each sample was measured for carbon and hydrogen isotopic composition. Chosen samples were separated into the aliphatic, aromatic, or asphaltene fractions. The $\delta^{13}C$ values were determined on most of these separates. The asphaltene fractions were processed for sulfur and nitrogen content and isotope ratio determination. The results are listed in Tables 2-5 and will be discussed with respect to two topics: (1) compare the isotope data to determine which samples were derived from sources other than IXTOC-I oil, and (2) determine whether certain isotopic fractionation or partitioning has occurred during exposure to the marine environment.

4.1 Correlation of Mousse and Tar to IXTOC-I Oil

The IXTOC-I oil has a $\delta^{13}C$ value of $-26.97^{o}/oo$ and the MOP oil, collected near the wellhead, has a $\delta^{13}C$ value of $-26.89^{o}/oo$. Of the 48 mousse samples collected, 43 have $\delta^{13}C$ values in the narrow range $-26.53^{o}/oo$ to $-27.11^{o}/oo$, or equivalent to the MOP oil. The 5 remaining mousse samples have $\delta^{13}C$ values in

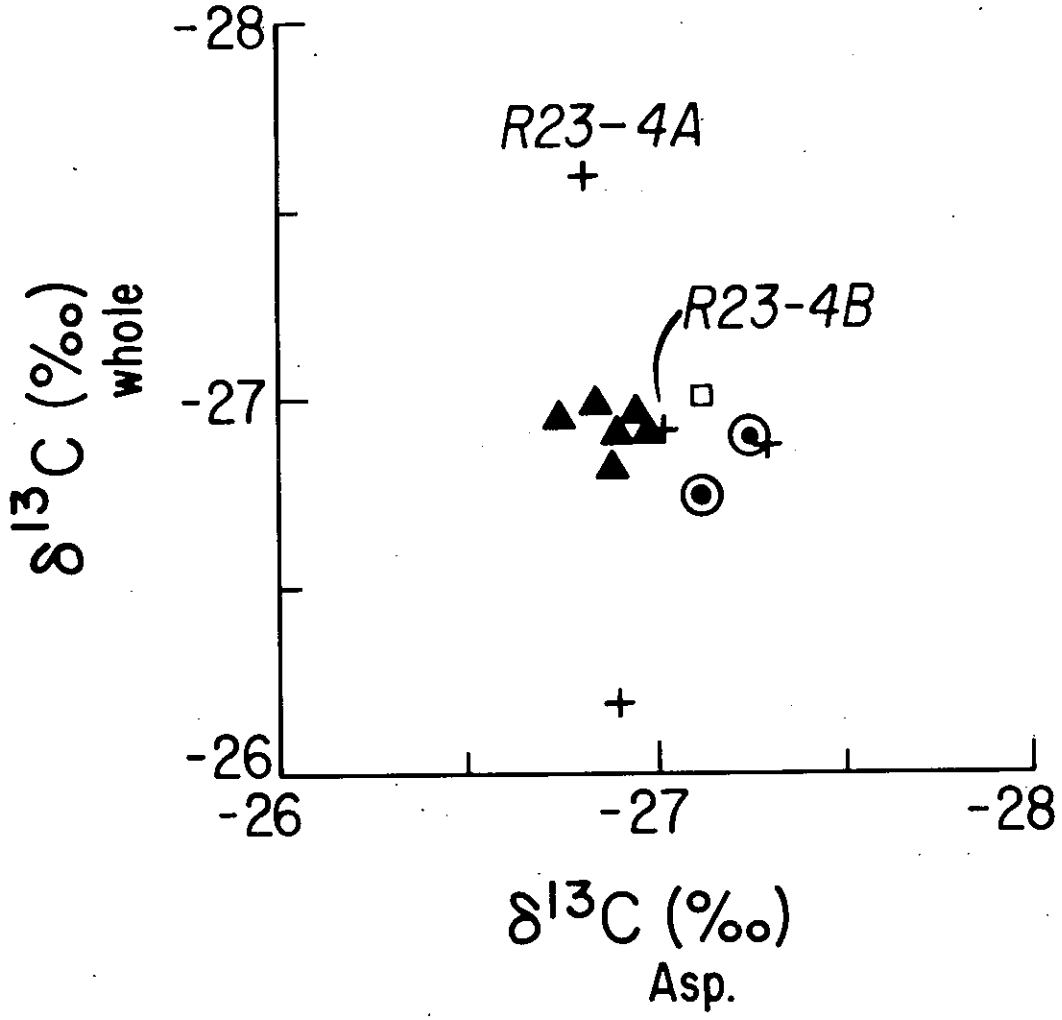

Figure 7. Plot of $\delta^{13}C$ whole sample vs. $\delta^{13}C$ asphaltene fraction. IXTOC-I oil is denoted by □ and samples are differentiated by location: Brownsville +, Rio Soto La Marina ⊙, and PEMEX ▲.

Table 5. Carbon and hydrogen stable isotope ratios on certain fractions of mousse samples. The fractions were separated at the agencies noted.

Sample	$\delta^{13}C$ (‰)		δD (‰)		Agency
	Ali	Aro	Ali	Aro	
Crude	-27.40	-26.70	---	---	GGC
R10-1	-27.59	-26.86	-95	-100	UNO
R10-3	-27.97	-26.23	-96	-98	UNO
R10-4	-27.47	-26.83	-93	-94	UNO
R11-9	-27.84	-26.59	-86	-87	UNO
R11-10	-27.66	-26.74	-100	-100	UNO
P5-1	-27.13	---	-93	-92	UNO
R10-2	-28.05	-26.55	-93	-99	UNO
R10-2	-27.81	-26.84	---	---	ERCO
R6-7	-28.06	-26.62	---	---	ERCO
R7-6	-27.79	-26.98	---	---	ERCO
R11-8	-27.41	-26.47	---	---	ERCO
P5-2	-27.74	-26.92	---	---	ERCO

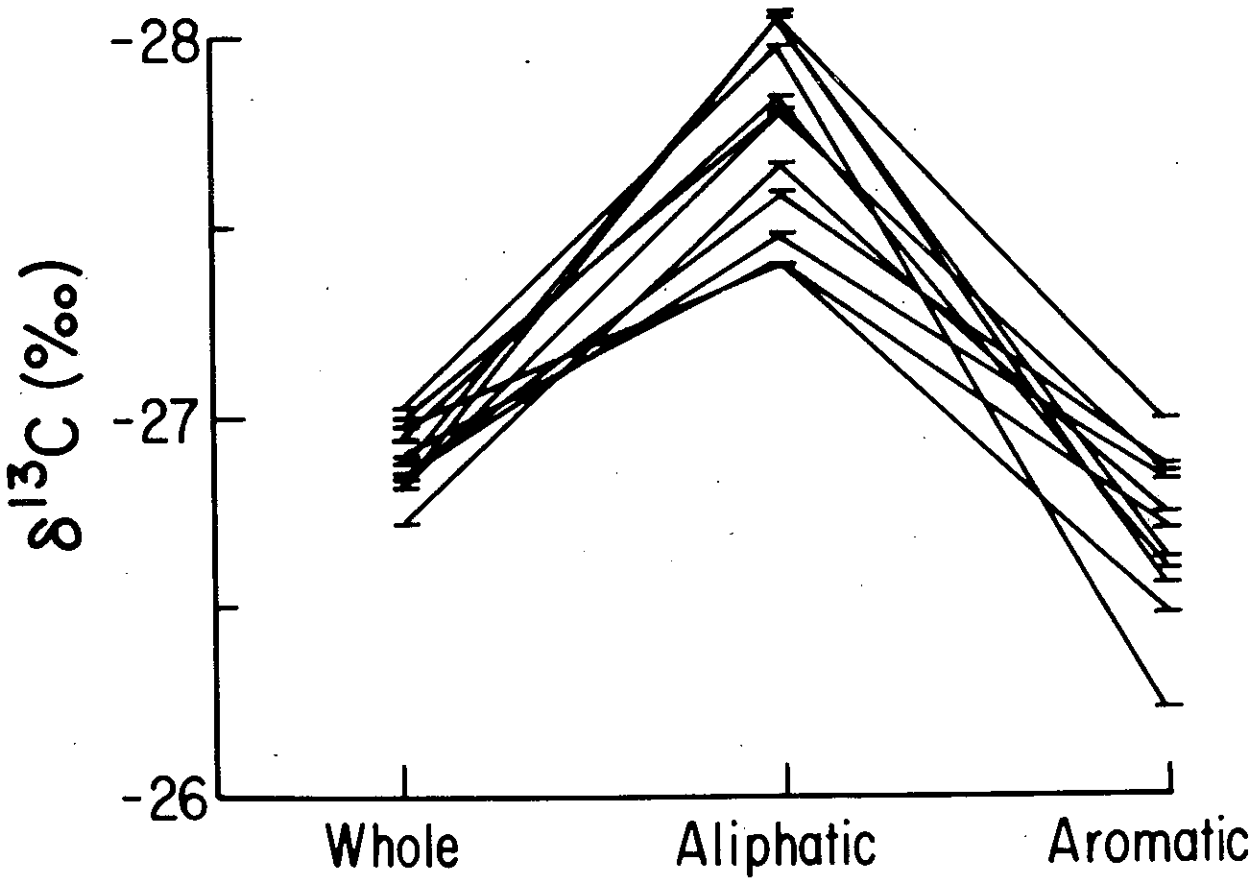

Figure 8. Comparison of $\delta^{13}C$ values of whole samples and the aliphatic and aromatic fractions.

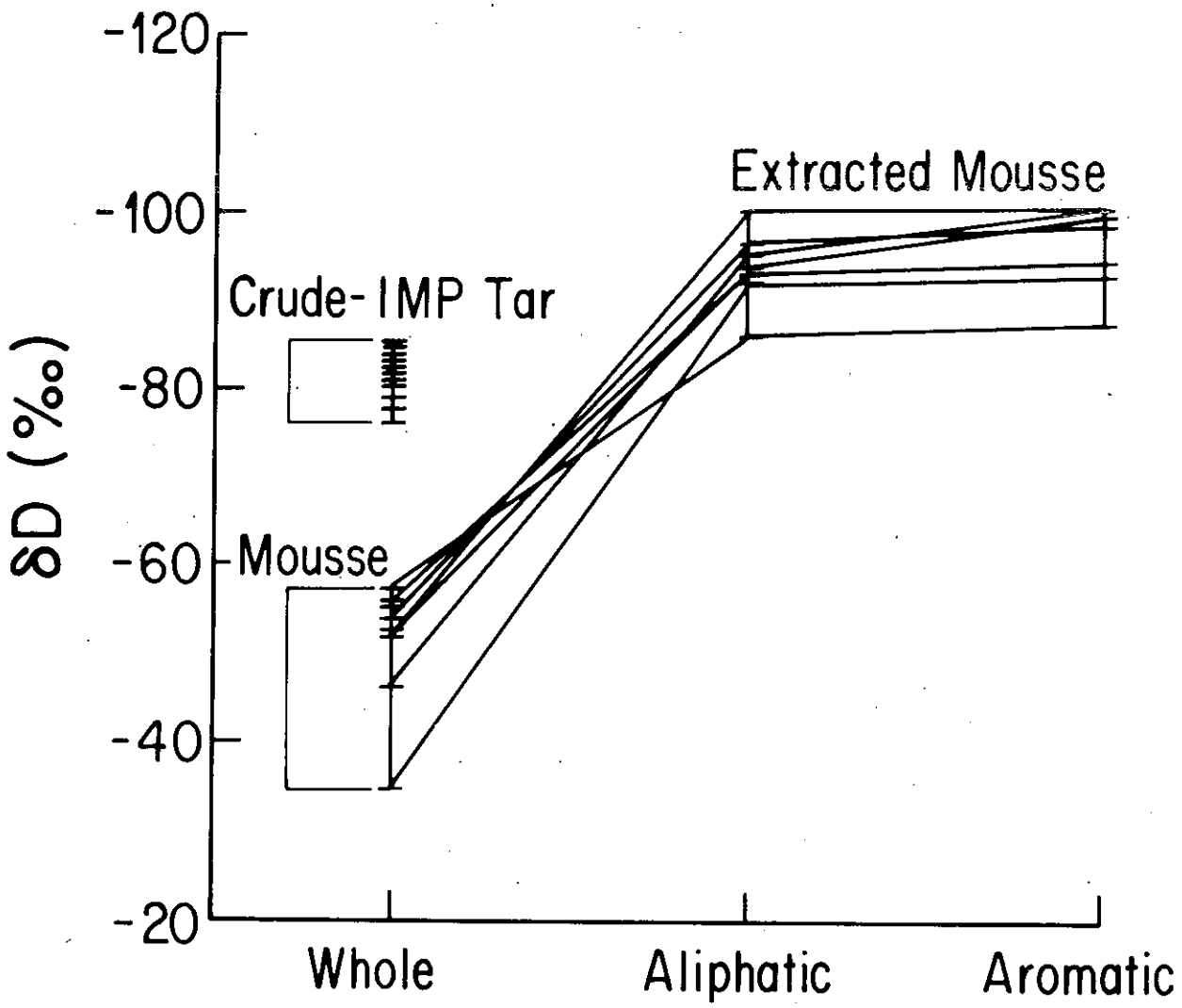

Figure 9. Comparison of δD values of whole samples and the aliphatic and aromatic fractions.

the range -25.96°/oo to -26.22°/oo. The latter group of mousse samples was from locations RO and R23 (Figure 1), more distant from the wellhead than the others (results summarized in Table 6). It is possible that the mousse at these locations came from a separate source. However, it is also likely that there was a 0.5°/oo shift in the $\delta^{13}C$ value during transport and weathering. The asphaltene fraction for sample R23-2 was analyzed for isotopic composition. The $\delta^{13}C$, $\delta^{34}S$, and $\delta^{15}N$ were all comparable to the MOP oil (Table 7). It would appear, therefore, that these mousse samples are derived from IXTOC oil.

Two tars from the beaches near Brownsville and one from the beach near Vera Cruz have $\delta^{13}C$ values which correspond to the isotopically heavy mousse (Table 7). Other tar samples have $\delta^{13}C$ values similar to the MOP oil values (Table 2). The remaining tars are listed in group B, Table 7. Two of these tars (RO-3 and RO-11) have $\delta^{13}C$ values similar to those of the IXTOC-I oil. However, RO-3 has isotopic ratios of S, N, and C in the asphaltenes which do not match the oil, and RO-11 has a $\delta^{34}S$ and sulfur content which are different (Figure 6).

Four samples collected from the beach sand near Tephnales did not have an extractable component (RO-10, 12, 13, 14) and are obviously not IXTOC-related. Sample RO-17 is isotopically more positive (123.73°/oo) and could be contaminated by marine organic matter (about -20°/oo). Three samples (RO-7, 8, 9) from near Tephnales have $\delta^{13}C$ values more negative than IXTOC oil. In addition, the δD values are more negative. (Why more negative δD values are considered to indicate an alternative source will be discussed later.) For the asphaltene fractions of RO-8 and RO-9, the $\delta^{34}S$ values (Table 7) and the sulfur content do not correspond to those of IXTOC oil (Figures 5 and 6).

In summary, all of the mousse samples collected from the various agencies and the tar samples provided by PEMEX are considered to have been derived from IXTOC-I oil. Several of the tars collected by the RIX cruise are considered to be either contaminated or derived from another source.

4.2 Isotopic Fractionation or Partitioning

The most apparent anomalies in the isotope data presented in Table 3 are for the δD values of the mousse samples. The values are, on an average, 40°/oo more positive than the tars or oil (Figure 4). The samples were all dehydrated in the same manner: freezing followed by freeze-drying for three days. An additional 15-minute evacuation was performed on the vacuum line immediately before sealing the sample for reaction with cupric oxide. This procedure is routine for a variety of organic materials. Although no recognizable problem has been identified for other types of organic material similarly treated, the mousse, being an oil-water emulsion, adheres more strongly to adsorbed seawater. To test this hypothesis, several mousse samples were extracted with methylene chloride and column-separated into the aliphatic and aromatic fractions. The δD values for these samples are listed in Table 5 and are presented schematically in Figure 9. The δD values for the separated alkanes and aromatics are about 50°/oo more negative than those for the whole mousse. These values are about 10°/oo more negative than those for the crude or the PEMEX tars.

Table 6. The range, mean, and standard deviation for mousse and tar samples ($\delta^{13}C$) collected at the different locations. (Note that the Brownsville mousse and tar are about 0.6°/oo more positive than the mousse samples near the wellhead.)

	Range (°/oo)		Mean x (°/oo)	Standard Deviation (σ)
MOUSSE				
near wellhead	-26.53	-27.08	-26.85	0.12
near Vera Cruz	-26.81	-27.11	-26.90	0.17
near Brownsville	-26.00	-26.86	-26.29	0.35
TAR				
PEMEX	-26.82	-27.02	-26.92	0.06
RIX Brownsville	-25.82	-26.86	-26.26	0.54
RIX Tephnales	-26.11	-28.32	-27.40	0.65
RIX Rio Soto La Marina	-23.73	-26.88	-25.76	1.76

Table 7. List of the isotope ratios for samples which did not directly correspond to IXTOC-I oil. The (A) group is considered IXTOC-I-related with a shift in $\delta^{13}C$ of the sample due to evapo-transport. The (B) group is considered unrelated or contaminated.

		WHOLE		ASPHALTENES		
		$\delta^{13}C$ (‰)	δD (‰)	$\delta^{34}S$ (‰)	$\delta^{15}N$ (‰)	$\delta^{13}C$ (‰)
GROUP A						
Mousse	RO-6	-25.96	-62			
	RO-15	-26.10	-55			
	R23-1	-26.00	-56			
	R23-2	-26.18	-74	-4.97	+0.99	-26.90
	RX10	-26.22	-43			
Tar	RO-2	-25.82	-77			
	RO-5	-26.11	-67			
	R12-1	-26.18	-76			
GROUP B						
Tar	RO-3	-26.86	-78	+2.85	-1.21	-27.30
	RO-7	-27.19	-110			
	RO-8	-38.32	-114	+1.82	+0.16	
	RO-9	-27.29	-105	+5.37	-0.15	
	RO-10*	-22.86	-89			
	RO-12*	-11.66	-64			
	RO-13*	-17.72	-81			
	RO-14*	-18.55	-97			
	RO-17	-23.73	-78			
Weathered Crude		-26.89	-83	-4.97	+0.63	-27.13

*No extractable organic matter.
Underlined results are not compatible with IXTOC-I origin.

The more comparable data for the crude and the extracted mousse samples indicate that contamination of adhered water (δD about $0^{o}/oo$) was the cause of the more positive δD values for the mousse. Because extracted samples are slightly more negative than the tars and IXTOC oil, there may be indications that the latter contains a small amount of adhered water. The most negative δD measured for the extracted samples is $-100^{o}/oo$. Any δD value more negative than this cannot be contributed to adhered water (note samples in Table 7).

It has already been noted that certain mousse and tar samples have $\delta^{13}C$ values that are about $0.5^{o}/oo$ more positive than the IXTOC oil or the mousse near the wellhead. An alternative source for this material was not supported by the isotope ratios of the asphaltenes (Table 7). It is possible that the oil released from the well has not been isotopically constant with time. However, the mousse (F1) collected in June is isotopically the same as the weathered oil collected in September ($-26.86^{o}/oo$ compared to $-26.89^{o}/oo$). Also, the $\delta^{13}C$ of the asphaltene fraction of R23-2 is in the range of the PEMEX tars ($-26.90^{o}/oo$ compared to $-26.75^{o}/oo$). Since the more volatile molecules of crude oil are isotopically light (Silverman, 1964), evaporation during transport would tend to leave the remaining oil isotopically heavy, or with a more positive $\delta^{13}C$ than it contained previously. This trend is consistent with the carbon isotope shift suggested for some of the mousse and tar samples collected many miles from the wellhead. The fact that a continuous change was not apparent from the data indicates that this process is not simple and probably depends on other factors, such as surface tension, roughness of the sea, size of accumulations, etc.

A third, and very interesting, correlation between sulfur content and $\delta^{34}S$ is shown in Figures 5 and 6. The content and $\delta^{34}S$ of sulfur in the asphaltene fraction of the mousse are different from those in the asphaltene fraction of the oil or tars. If it is considered that the oil evolves through the mousse to tar, then it would not be expected that the mousse would have less sulfur (and different $\delta^{34}S$) in the asphaltene fraction. An interpretation more consistent with the data is that the tars collected in this study did not evolve from mousse. The actual asphaltene fraction for the mousse may not be representative of the released oil. Not only do processes such as water washing and evaporation affect the light ends of the oil, but also a partitioning of asphaltene molecules may occur in mousse formation. Dehydration of the mousse samples should produce tar that would not correspond in sulfur content or isotopic composition to the original oil.

5. SUMMARY

The stable isotope ratio of carbon in the unfractionated samples was sufficiently diagnostic to correlate the majority of the IXTOC-related material to the original oil. However, extraction by methylene chloride, followed by precipitation of the asphaltenes on which measurements can be performed, is preferable. Using this scheme, (1) minerals and nonextractable contaminants are eliminated, (2) mousse oil is dehydrated so that the characteristic hydrogen stable isotope may be measured, (3) nitrogen and sulfur compounds are

concentrated sufficiently for isotope measurement, and (4) carbon isotope alteration due to volatilization on transport is minimal in the asphaltene fraction. Because the processes responsible for defining the stable isotope ratios of C, N, H, and S in oil are generally unrelated (Grizzle et al., 1979), the measurement of these isotope ratios on the separated asphaltene fraction can yield four independent parameters for source correlation.

As a consequence of comparing the isotopic ratios between mousse and tar, certain conclusions can be reached related to mousse formation. First, vacuum desiccation is not sufficient to separate the water-oil emulsion, but extraction by methylene chloride is. Second, partitioning of asphaltene molecules in the mousse does not discriminate for nitrogen, but apparently does for sulfur-containing constituents. A simple explanation of the differences in sulfur content and $\delta^{34}S$ between mousse tar and asphaltenes is that seawater sulfate could not be washed out of the former. However, isotopic ratios in the asphaltene fraction of tar samples are similar to those for crude oil, indicating that the mousse phase may not have been an intermediate step in formation of the tar.

6. ACKNOWLEDGMENTS

We thank Dr. Amada Cortes Rubio (Instituto Mexicano Del Petroleo), Dr. Ed Overton (UNO), Mr. Dave Fiest (ERCO), Dr. Jim Payne, Science Applications, Inc. (SAI), and Dr. Manchard (Brest) for supplying samples for analysis. Mr. Wai Ho, Ms. Louise Lasnick, Mr. Brian Wilcher, and Ms. Jackie Schmidt aided in stable isotope preparation, and D. Winter was the mass spectroscopist. This work was supported by contract # NA80RAC00040, National Oceanic and Atmospheric Administration.

7. REFERENCES

Bailey, S. A., and J. W. Smith (1972): Improved method for preparation of sulfur dioxide from barium sulfate for isotope ratio studies. Anal. Chem., 44: 1542-1543.

Grizzle, P. L., H. J. Coleman, R. E. Sweeney, and I. R. Kaplan (1979): Correlation of crude oil source with nitrogen, sulfur and carbon stable isotope ratios. Symp. Reprints, ACS/CSJ Div. of Petroleum Chem., Honolulu, HI, Apr. 1-6, 1979: 39-57.

Hartman, B. A. (1978): The use of carbon and sulfur isotopic ratios and total sulfur content for identifying the origin of beach tars in Santa Monica, California. M.Sc. Thesis, University of Southern California, Los Angeles, CA.

NOAA, and EPA Region Six Program Plan (1979): IXTOC-I Oil Spill Damage Assessment Program.

Parr Instrument Company (1965): Oxygen bomb colorimetry and combustion methods. Tech. Manual: 130.

Reed, W. E., and I. R. Kaplan (1977): The chemistry of marine petroleum seeps. J. Geochem. Explor., 7: 255-293.

Silverman, S. R. (1964): Investigations of petroleum origin and evolution mechanisms by carbon isotope studies. In Isotopic and Cosmic Chemistry. H. Craig, S. L. Miller, and G. L. Wasserburg, (Eds.), Amsterdam, North Holland Publications: 92-102.

Stump, R. K., and J. W. Frazer (1973): Simultaneous determination of carbon, hydrogen and nitrogen in organic compounds. Nucl. Sci. Abstr., 28: 7848.

Sweeney, R. E., and I. R. Kaplan (1978): Characterization of oils and seeps by stable isotope ratio. Proc. Energy/Environment California, SPIB: 281-293.

Venkatesan, M. I., P. Mankiewicz, W. K. Ho, R. E. Sweeney, and I. R. Kaplan (1981): Determination of petroleum contamination in marine sediments by organic geochemical and stable sulfur isotope analysis. (In preparation.)

HORIZONTAL AND VERTICAL TRANSPORT OF DISSOLVED AND PARTICULATE-BOUND HIGHER-MOLECULAR-WEIGHT HYDROCARBONS FROM THE IXTOC-I BLOWOUT

J. R. Payne, G. S. Smith, P. J. Mankiewicz,
R. F. Shokes, and N. W. Flynn
Science Applications, Inc.

V. Moreno
Departamento de Pescas Gobierno de Mexico

J. Altamirano
Instituto Mexicano de Petroleos

1. INTRODUCTION

When oil is released subsurface in a natural water body, it immediately begins a number of interactive processes with its environment that alter its composition. All of these processes occur at different rates and their degrees of impact vary; however, collectively they determine the ultimate fate of the released oil and the effects these will have on sensitive components of the aqueous environment. The low-molecular-weight ($<C_{12}$) components of released oil are most affected by dissolution and then evaporation once they have reached the water surface. The components of lower volatility and solubility, however, are most affected by processes that alter their bulk density (flocculation, agglomeration, association with suspended particulates) and chemical nature (photo- and microbial degradation).

Sampling during the NOAA RESEARCHER/PIERCE IXTOC-I cruise in September 1979 has afforded investigators the opportunity to characterize many of these processes that impact oil after its release under special environmental conditions. This report contains results of water column sampling and analysis aimed at elucidating several of the phenomena that act to distribute the high-molecular-weight components of oil after a spill. Filtered water and suspended particulates were collected and analyzed in an effort to describe the distribution of IXTOC oil with elapsed time after the subsurface blowout. As an extension of our examination of the effects of oil dispersing processes, several samples of floating mousse were collected and analyzed for time-dependent chemical alteration.

2. METHODS

2.1 Sampling Methods

Although high levels of petroleum hydrocarbons were anticipated in the water column as a result of the IXTOC-I blowout, extensive precautions were nevertheless undertaken to insure that elevated hydrocarbon levels would not be artificially introduced and measured due to contamination from shipboard activities. Two 90-L Bodega-Bodman water samplers (Figure 1) were used to collect all of the water and suspended particulate material samples. These samplers were modified and constructed from the original design of the Bodman sampler (Bodman et al., 1961) by scientists at the University of California - Bodega Marine Laboratory and SAI in collaboration with R. Hamlin, Oceanic Industries, Osterville, Mass. (Payne et al., 1978; de Lappe et al., 1980).

The sampler design incorporates a 12 kHz pinger with a double pulse rate option which allows continuous shipboard monitoring of the open/closed status and depth of the sampler. The construction is of anodized aluminum, stainless steel, Teflon, and Viton, to minimize contamination from sampler materials, and it is designed to pass closed through the air/sea interface to avoid potential internal contamination from surface slicks. Once beneath the surface, the sampler is opened by means of a one-way relief valve and cocking line at a depth

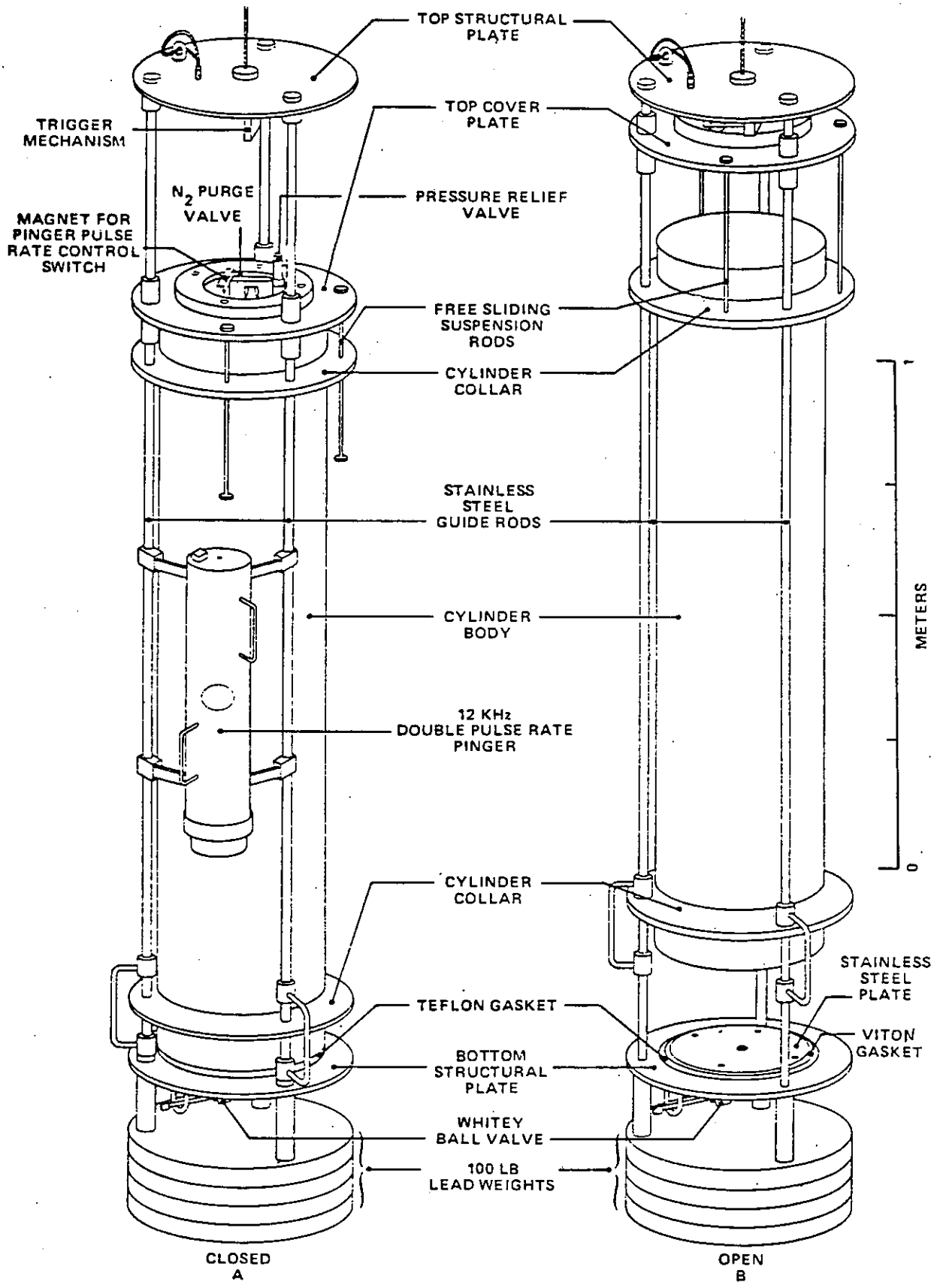

Figure 1. The Bodega-Bodman 90-liter seawater sampler.

of 3-5 meters. It is then lowered open through the water column to the desired sampling depth.

During the IXTOC-I cruise aboard the RESEARCHER, discrete 90-L samples were obtained using a conventional "messenger" for subsurface and mid-depth samples and by means of a bottom pilot-weight-tripping mechanism for near-bottom samples, approximately 5 meters above the sediment/water interface. Once a sample was obtained, the Bodega-Bodman sampler was retrieved and a 25-ml aliquot was transferred to a Pierce septum-capped vial and then refrigerated at 3°C for later analysis of volatile organics (as described in Payne et al., 1980). The remaining 90 liters of sample were then transferred via stainless-steel lines to a "clean van" specially modified and mounted on the fantail of the vessel. While transferring the sample, the volume of water removed was displaced with pre-purified nitrogen or charcoal and molecular seive-filtered air to minimize potential contamination from generator or main engine exhausts.

The "clean van" was an oceanographic van supplied by NOAA/AOML and outfitted by NOAA and SAI personnel before the cruise. An air-recirculating charcoal filter was installed within the van to remove any airborne hydrocarbons from the ship's exhaust and also to minimize airborne solvent fumes generated in the course of the extraction of samples. The stainless-steel transfer line from the Bodega-Bodman sampler rack was attached to a bulkhead fitting into the interior of the van where it was then connected to a top-mounted Millipore filter holder secured to a laboratory bench. Kiln-fired 0.4 µm Gelman glass fiber filters (293 mm diameter) were used to remove suspended particulate material from the whole water samples. A collection carboy located immediately below the counter and elevated by an adjustable lab-jack was attached to the Millipore filtering apparatus by means of stainless-steel tubing and a two-hole Teflon stopper with a Viton O-ring. Flexible Teflon tubing was used to connect the collection carboy to an oiless vacuum pump, and charcoal filters and Dri-Rite traps were installed in-line between the collection carboy and pump.

The Bodega-Bodman water samples were pumped into the clean van carboys at approximately 1 L/min, depending on the particulate load. A total of three 19-L collection carboys were obtained for each sample, resulting in approximately 56 L of seawater being extracted within the clean van for each. The remaining 30 L of each Bodega-Bodman sample were then filtered to obtain a total particulate burden on the glass fiber filter from a 90-L sample. Because of time, solvent quantities, and logistical constraints, the last 30 L of seawater were not extracted for dissolved-phase organic contents.

Following collection, the three carboys containing the filtered seawater were extracted three times with 150 ml Burdick and Jackson "distilled in glass" methylene chloride. Each extraction was performed by mechanical agitation with a variable-speed drill and a stainless-steel mixing blade with pivoting propellor blades. The methylene chloride from each extraction was pressure-forced from the collection carboy with pre-purified molecular seive, charcoal-filtered nitrogen into amber bottles and then stored at ambient temperature until concentration and subsequent analysis (at SAI's La Jolla laboratory). After the full 90-L sample filtration was completed, each particulate filter was removed

with stainless-steel spatulas and tongs, folded into kiln-fired, solvent-rinsed aluminum foil, and immediately frozen. The particulate samples remained frozen until laboratory extraction and analysis. The total volume of the extracted seawater sample was then measured and the water discarded from the vessel. Collection carboys were then cleaned between stations with Alkonox and fresh water and rinsed with Burdick and Jackson acetone and methylene chloride. This operation was always completed upwind of the ship's main engine exhaust.

The amber bottles containing methylene chloride extracts from each station were capped at the time of collection with Teflon sheeting as liners to the plastic reagent bottle screw caps. Part way through the sampling (after station RIX 11), it was discovered upon examination of several of the extracts that the Teflon was permeable to the methylene chloride solvent and that some extraction of the plastic cap liners had occurred. At that time new Teflon-sheet liners were placed on all of the sample containers on hand and then capped with kiln-fired and solvent-rinsed aluminum foil before the plastic caps were replaced. Cap blanks were also prepared at that time with methylene chloride, Teflon sheets, and plastic caps with and without the aluminum foil layer. Examination of FID glass capillary gas chromatograms of fractionated extracts of these blanks showed the same n-alkane series (nC_{22} to nC_{30}) where no aluminum foil was used. After we began using the foil, no further contamination of the samples was noted.

Because of the higher-molecular-weight n-alkane contamination in the dissolved fraction, any contributions from their extraneous presence were deleted from samples before RIX 12 during data reduction. The distribution of the parent hydrocarbons in the fresh IXTOC crude indicated that the unique n-alkane nC_{22} - nC_{30} suite was clearly not from the oil, and it was easily identifiable as cap contamination whenever encountered.

2.2 Laboratory Analysis

2.2.1 Preparation of Methylene Chloride Extracts for Liquid Column Chromatography

All methylene chloride extracts and blanks derived from the shipboard clean van were stored under refrigeration at our laboratory until analysis. In the laboratory each extract was transferred to a 1-L round-bottom flask and reduced to a volume of about 100 ml by solvent evaporation over a 60°C water bath using a Kuderna-Danish (K-D) apparatus. Residual water was removed by passing the concentrated sample through a 2-cm I.D. column packed with 15 cm of cleaned and activated sodium sulfate, which was then rinsed with 400 ml of methylene chloride. Each sample was further concentrated to about 2 ml, and the methylene chloride was then exchanged with hexane by adding 10 ml of hexane and repeating the K-D evaporation at 80-90°C to a final volume of about 2 ml.

2.2.2 Preparation of Particulate Filters for Liquid Column Chromatography

All filter pads were kept frozen prior to preparation. Each filter was dissected into small pieces (1 x 2 cm) and placed in a 500-ml round-bottom flask under 300 ml of 27% methanol in methylene chloride (an azeotropic mixture of boiling point 30°C). The mixture was refluxed for four hours and the solvent was then transferred to a 1000-ml round-bottom flask and partitioned into hexane. Refluxing was repeated with 300 ml of methylene chloride, again for four hours. The methanol-water portion from the first reflux was separated from the hexane and back-extracted with additional methylene chloride. The hexane and methylene chloride extracts were combined in a 1000-ml round-bottom flask and reduced to a volume of 10 ml by K-D concentration. Each sample was then transferred to a 20-ml vial and reduced to a volume of 2 ml under a gentle stream of dry, purified nitrogen.

2.2.3 Liquid Column Chromatography

A five-fraction liquid column chromatography (LC) procedure was developed for the separation of aliphatics, aromatics, nitrogen-sulfur-oxygen (NSO) heterocyclics, and carboxylic acids in the water, particulate, whole oil, and mousse samples. A 10-mm I.D. x 23-cm-long column, with a 16-ml pore volume, was packed with a hexane slurry of 60/200-mesh silica gel that had been cleaned with methylene chloride and activated overnight at 210°C. For the particulate extractions, an 11-cm layer of sodium sulfate was packed on top of the silica gel. This was necessary since some residual water was present in the particulate extracts. To minimize contamination, 30 ml of clean hexane were eluted through the column prior to sample loading.

The five-part fractionation scheme consisted of sucessive addition of the following solvents:

	Fraction	Amount
1.	Hexane	30 ml
2.	Hexane:Benzene (1:1)	45 ml
3.	10% CH_3OH in CH_2Cl_2	45 ml
4.	CH_2Cl_2:$EtOA_c$:CH_3OH (1:1:1)	~60 ml
5.	CH_3OH	45 ml

During the course of the study, the five-part fractionation was abbreviated to a three-part scheme for the methylene chloride water extracts since few, if any, compounds were found in the last two fractions of the five. The three-part scheme consisted of:

	Fraction	Amount
1.	Hexane	30 ml
2.	Hexane:Benzene (1:1)	45 ml
3.	50% CH_3OH in CH_2Cl_2	60 ml

Each fraction was collected in a 100-ml round-bottom flask, and the solvent reduced to about 1 ml using the K-D method at 80-90°C. All fractions were solvent-exchanged (if necessary) with 10 ml of hexane and again reduced to a volume of about 1 ml. Each sample was transferred to 3.7-ml glass vials and further concentration was accomplished by evaporation at ambient temperature using a stream of dry, purified nitrogen. Total sample volumes were measured after injection into the gas chromatograph and were on the order of 20-30 µl for waters and particulates and 200-2000 µl for oil and mousse samples. No extracts or fractions were allowed to go to dryness during any extraction or concentration step prior to gas chromatographic analysis.

2.2.4 Gas Chromatography Analysis

All gas chromatographic results were obtained on a Hewlett-Packard 5840A gas chromatograph equipped with an 18835A glass capillary inlet system and flame ionization detector. The microprocessor-based instrument was interfaced to a Texas Instruments Silent 7800 data terminal equipped with casette tape drive, allowing direct storage of calibration data, retention times, and peak areas required for the data reduction system.

A 30-m J&W Scientific Co. SE-54 wall-coated open tubular glass capillary column was utilized for the desired chromatographic separation of aromatic compounds. Temperature programming used with this column included:

Initial Temperature:	60°C for 5 minutes
Program Rate:	3.5°C/min
Final Temperature:	275° for 60 minutes

The injection port and detector were maintained at 250° and 350°C, respectively. All injections were made in the splitless mode of operation with an injection port backflush 1 minute into the run.

Constant injection volumes of 2.0 µl were analyzed automatically using a Hewlett-Packard model 7671A automatic liquid sampler, increasing precision substantially relative to manual injection.

2.2.5 Gas Chromatogram Data Reduction

Hydrocarbon concentrations for individual resolved peaks in each gas chromatogram were calculated on a DEC-10 System Computer using the formula given in equation 1. This particular example is of the program used for seawater analysis. Operator-controlled modification of the DEC-10 program allows similar data reduction on sediments, tissues, or individual oil (mousse) samples.

$$\mu g \text{ compound X/L seawater} = (A_X) \times (R.F.) \times \left[\frac{P.I.V. + 2}{Inj.S.Vol.} \quad \frac{Pre\text{-}C.S.\ Vol.}{Post\text{-}C.S.\ Vol.} \quad \frac{100}{\%NSL \text{ on } LC} \times \frac{100}{\%DW/FW} \times \frac{1}{liters}\right] \tag{1}$$

where:

A_X = the area of peak X as integrated by the gas chromatograph (in arbitrary GC area units)

R.F. = the response factor (in units of µg/GC area unit)

P.I.V. + 2 = the post-injection volume (in µl) from which a 2-µl aliquot had been removed for analysis by GC (measured by syringe immediately following sample injection)

Inj.S.Vol. = the volume of sample injected into the GC (always 2.0 µl as measured by an HP automatic liquid sampler)

Pre-C.S.Vol. & Post-C.S. Vol. = the total solvent volumes before and after an aliquot is removed for gravimetric analysis of a Cahn electrobalance

%NSL on LC = the percent of sample non-saponifiable lipid used for SiO_2 column chromatography

%DW/FW = the percent dry weight of wet weight in the sediment tissue, or oil sample being analyzed

liters = liters of seawater initially extracted (or grams wet weight of oil or sediment).

During analysis of the extracts, the 5840A gas chromatograph was recalibrated after every 8 to 10 injections, and individual response factors were calculated for all detected even and odd n-alkanes between nC_{12} and nC_{32}. Concentrations of other components (i.e., branched and cyclic) that eluted between the major n-alkanes were calculated by linear interpolation of the adjacent n-alkane response factors and the unknown compound peak's KOVAT index. By incorporating the post-injection volume (PIV) into the calculation, the amount of hydrocarbons measured in the injected sample was converted to the total hydrocarbon concentration in the sample.

Unresolved complex mixtures (UCM's) were measured in triplicate by planimetry; the planimeter area was converted to the gas chromatograph's standard area units at a given attenuation and then quantitated using the average response factors of all the n-alkanes occurring within the range of the UCM, as shown in equation 2.

$$\frac{\mu g\ UCM}{liter} = Area_p \times (Conf.\ F) \times \frac{S.\ Att.}{Ref.\ Att.} \times (\overline{R.F._{a-b}}) \times [\cdots] \qquad (2)$$

where:

Area = UCM area in arbitrary planimeter units,

Conv. F. = a factor for converting arbitrary planimeter units to GC area units at a specific GC attenuation,

S. Att. and Ref. Att. = the GC attenuation at which the sample chromatogram was run and the reference attenuation to determine the conversion factor (Conv. F.), respectively,

$R.F._{a-b}$ = the mean response factor for all sequential n-alkanes (with carbon numbers a to b) whose retention times fall within the retention time window of the UCM, and

$[\cdots]$ = the same parameters enclosed in brackets in equation 1.

Confirmation of KOVAT index assignment to n-alkanes was done by computer correlation with n-alkane standard retention times and direct data-reduction-operator input.

Assignment of a KOVAT index to each branched or cyclic compound eluting between the n-alkanes was done by interpolation using the unknown compound and adjacent n-alkane retention times. Assignment of KOVAT indices to peaks in the aromatic fraction was made by direct correlation of unknown peaks with retention times from the n-alkane-standard run completed prior to sample injection (Payne et al., 1978). This approach has been shown to yield equivalent or better results than those obtained using 4 or 5 specific aromatic compounds as individual standards.

2.2.6 Capillary Gas Chromatography Mass Spectrometry

Selected extractable organic compounds previously analyzed by glass capillary column-FID GC were also subjected to glass capillary GC mass spectrometry. A 30-meter J&W SE-54 glass capillary column (0.25-mm I.D. with a film thickness of 25 μm) was used to achieve chromatographic separation on the front end of a Finnigan 4021 quadrupole mass spectrometer. The capillary system was operated in the splitless (Grob-type) mode. The static time upon injection was 1.0 min, after which time the injector was backflushed with the split and septum sweep flows at a combined 35 ml/min. Linear velocity was set at 40 cm/sec, which gave a flow rate of 1.18 ml/min. The GC was programmed to remain isothermal at 50°C for 4.0 min following injection. It was then set to elevate at 3.5°C/min from 50-275°C, after which the oven was held isothermally at 275°C for approximately 20 minutes.

The column effluent from the capillary system was directly transferred through an all-glass line to the ion source, which was operated in the electron impact mode. The mass spectrometer ion source was operated at 70eV and the lens potentials optimized for maximum ion transmission. The quadrupole offset and offset programs were adjusted to yield a fragmentation ratio of perfluorotributylamine m/e 69-to-219 of 2.5:1. This tuning yields quadrupole electron impact spectra that are comparable to magnetic sector electron impact spectra, thereby allowing optimal matches in the computer search routines used in the INCOS data system that scans the quadrupole rods from 35-550 amu in 0.95 sec. A hold time of 0.05 sec between scans allows the electronics to stabilize prior to the next scan. The mass spectrometer was tuned at the beginning of each day using perfluorotributylamine. A calibration was accomplished with a routine diagnostic fit of 2% mass accuracy. Prior to analysis of samples, a standard mixture of n-alkanes, pristane, phytane, and mixed aromatic hydrocarbons was injected.

Several aromatic fractions of mousse, crude oil, water filtrates, and particulates were analyzed by glass capillary GCMS techniques. For each sample, the ionization current of the molecular ions of the parent through the tetra-alkyl analogs of naphthalenes, fluorenes, phenanthrenes, and dibenzothiophenes was integrated to determine the change in the relative abundance of the various aromatic types and their homologs in the different sample types. Although this technique may under-represent the higher alkyl homologs (because of greater fragmentation relative to the parent compound), it allows an accurate distributional comparison between samples and sample types.

For the crude oil and mousse samples, the abundance of the mono-substituted (m/e 91), di-substituted (m/e 105), and substituted (m/e 119) benzenes were also documented as a function of carbon number.

3. RESULTS

3.1 Spiked Recovery Data

In order to assess the extraction efficiency of our analytical procedures, one sample was spiked at sea with a series of aliphatic, cycloalkane, and alkyl substituted aromatic hydrocarbons. These standards were diluted in acetone and added to the carboys before methylene chloride extraction. Table 1 includes the spiked and recovered amounts of these hydrocarbons, suggesting that yields in the range of 35 to 40% can be expected with these methods. This implies that the actual dissolved hydrocarbon burdens may be as much as a factor of two higher than the results reported here. The relative concentrations from site to site are still useful, however, in evaluating the fate and distribution of the higher-molecular-weight hydrocarbons released from the IXTOC blowout.

Assessment of extraction efficiency for particulate-bound hydrocarbons was undertaken by spiking a Gelman 293-mm diameter, kiln-fired glass-fiber filter with a mixture of n-alkanes and aromatic hydrocarbons. These recovery data are

Table 1. Particulate and dissolved spike recovery results.

Compound	Actual Amount µg/l	Recovered Amount µg/l	% Recovered µg/l
PARTICULATES			
nC_{12}	0.0197	0.011	56
nC_{13}	0.0204	0.012	59
nC_{14}	0.0221	0.013	59
nC_{15}	0.0204	0.012	59
nC_{17}	0.0218	0.015	69
pristane	0.0218	0.014	64
nC_{18}	0.0207	0.0155	75
phytane	0.0323	0.0233	72
nC_{20}	0.0314	0.0255	81
nC_{21}	0.0850	0.0698	82
nC_{22}	0.0327	0.0260	80
nC_{23}	0.0620	0.0505	81
nC_{31}	0.0165	0.0140	85
nC_{32}	0.0215	0.0190	88
n-propylbenzene	0.081	0.22	27
naphthalene	0.077	0.034	44
anthracene	0.072	0.037	51
pyrene	0.080	0.042	53
WATERS			
nC_{20}	3.0	1.05	35
hexamethylbenzene	0.54	0.075	14
hexaethylbenzene	0.67	0.28	42

also shown in Table 1. In examining our own past data and those of others, we have considered the possibility that hydrocarbons dissolved in the water column may be preferentially adsorbed onto the glass filter or suspended particulate material during filtration. As a result, we have reported hydrocarbon concentrations for both dissolved-phase and particulate-bound loads as well as the sum of the particulate and dissolved fractions. Thus, the data presented herein represent total water column burdens as derived by graphically summing the particulate-bound and dissolved hydrocarbon component loads.

3.2 Results of Intercalibration Sample Analyses

Tables 2 and 3 present the triplicate determinations of total resolved and unresolved complex mixtures in the aliphatic and aromatic fractions, respectively, of an intercalibration sample distributed among the participants of the IXTOC RESEARCHER/PIERCE cruise. This sample was a water parcel obtained from the PIERCE by Go-Flo sampler; it was extracted with methylene chloride by scientists from Energy Resources Company (ERCO) and the University of New Orleans. An aliquot of the methylene chloride extract was distributed to each of the participating laboratories; each laboratory fractionated the extract according to its own protocol and analyzed it by flame ionization detector glass capillary gas chromotography.

Table 4 presents the abundance of selected aromatic compounds relative to phenanthrene in the intercalibration extract. This approach to quantitation of the observable GC peaks was hampered by several inherent problems:

- phenanthrene coelutes with alkyl benzene,
- C_1-dibenzothiophene-C (DBT) coelutes with C_1-phen-A,
- naphthalene-A coelutes with several other compounds,
- the valley-to-valley integration algorithm of the HP5840 GC under-represents the concentration of those peaks which are not fully resolved.

Despite these GC "problems," we were able to generate the data in Table 4 as representative using GC/MS mass chromatograms to confirm the GC quantitation.

3.3 Water Column Concentration Data

Figures 2 and 3 present overviews of the Gulf of Mexico and the IXTOC-I vicinity showing the RESEARCHER/PIERCE station locations; Table 5 includes the dissolved and particulate-bound hydrocarbon concentrations as measured by flame ionization detector gas chromatography. Figures 4 and 5 present these data in graphical form in which the total dissolved and particulate-bound fractions are compared. The most striking features of these data are the extremely low

Table 2. Aliphatic (F1) fraction intercalibration results, sample PIX 05E050.

	1	2	3
Total resolved hydrocarbons	3320	3150	3570
Total unresolved hydrocarbons	6470	6260	7020
n-alkane: branched hydrocarbons	2.22	1.96	1.88

Concentrations (μg/ml of supplied extract)

	Replicate (1)	(2)	(3)	Mean	Coefficient of variation	Rel. to nC_{20}
C_{10}	12	32	34	26	40%	0.245
C_{11}	58	88	98	81	21	0.771
C_{12}	140	160	179	171	17	1.621
C_{13}	184	190	213	196	6	1.855
C_{14}	213	206	212	217	5	2.057
C_{15}	238	201	249	229	9	2.174
C_{16}	201	186	206	198	4	1.874
C_{17}	197	180	195	190	4	1.807
Pristane*	0	0	0	0	0	0
C_{18}	143	132	145	140	4	1.327
Phytane	57	49	55	54	6	0.507
C_{19}	116	107	116	113	5	1.060
C_{20}	109	100	108	106	4	1.000
C_{21}	98	88	96	113	4	1.071
C_{22}	89	80	87	85	4	0.806

*Not integrated

Table 2. (Continued)

	Replicate (1)	(2)	(3)	Mean	Coefficient of variation	Rel. to nC_{20}
C_{23}	82	73	80	78	5	0.739
C_{24}	76	67	73	72	5	0.583
C_{25}	72	64	71	69	5	0.657
C_{26}	54	47	52	51	6	0.484
C_{27}	47	41	46	45	6	0.424
C_{28}	42	18	41	40	5	0.383
C_{29}	38	32	36	36	7	0.366
C_{30}	46	32	38	39	14	0.365
C_{31}	40	32	34	35	10	0.334
C_{32}	32	29	30	31	3	0.289
C_{33}	29	27	26	27	5	0.183
C_{34}	19	20	19	19	2	0.183
TOTAL	2260	2080	2330	2220	5	

Table 3. Aromatic (F2) and polar (F3) fraction intercalibration results, sample PIX 05E050.

Total resolved hydrocarbons	484	458	430
Total unresolved hydrocarbons	4200	4240	4090

COMPARISON OF SELECTED PEAKS

Kovat Index		Replicate (μg/ml) (1)	(2)	(3)	Mean	Coefficient of variation
1298	C_1-Naphthalene	21	16	19	19	10%
1315	C_1-Naphthalene	12	10	11	11	9%
1409	C_2-Naphthalene	23	22	19	21	8%
1423	C_2-Naphthalene	13	10	11	11	9%
1509	C_3-Naphthalene	9	8	7	8	8%
1540	C_3-Naphthalene	11	10	9	10	6%
1712	C_4-Naphthalene	12	14	12	12	6%
1758	DBT	9	9	8	9	5%
1860	C_1-DBT	16	18	16	16	6%
1985	---	8	9	9	9	8%
2008	---	9	10	10	10	7%
2055	---	10	11	10	10	6%

FRACTION 3 - INTERCALIBRATION RUNS

SAMPLE PIX05E050

	1	2	3
Resolved hydrocarbons	4	243	4
Unresolved hydrocarbons	206	244	68
TOTAL	210	268	72

Table 4. Abundance of selected aromatics relative to phenanthrene for inter-calibration.

	Replicate No.			Mean	C.V.
	1	2	3	4	5
Naphthalene	-not resolved-	--	--	--	--
C_1 naphthalene "A"	2.03	1.60	1.85	1.83	12
C_1 naphthalene "B"	1.89	1.49	1.73	1.70	12
TOTAL C_1 Naphthalenes (A+B)	3.92	3.09	3.58	3.53	12
Dibenzothiophene (DBT)	1.20	1.27	1.21	1.22	3
C_1 DBT A	2.50	2.85	2.65	2.67	7
C_1 DBT B	1.60	1.76	1.67	1.68	5
C_1 DBT C	0.76	0.98	0.92	0.89	13
TOTAL C_1 DBT (A+B+C)	4.86	5.59	5.24	5.23	7
Phenanthrene (PHEN)	1.00	1.00	1.00	--	--
C_1 PHEN A	0.63	0.77	0.72	0.71	10
C_1 PHEN B	0.93	1.10	1.17	1.07	12
C_1 PHEN C	1.59	1.80	1.68	1.69	6
C_1 PHEN D	0.86	1.02	1.05	0.98	10
TOTAL C_1 PHEN (A+B+C+D)	4.01	4.69	4.62	4.44	8

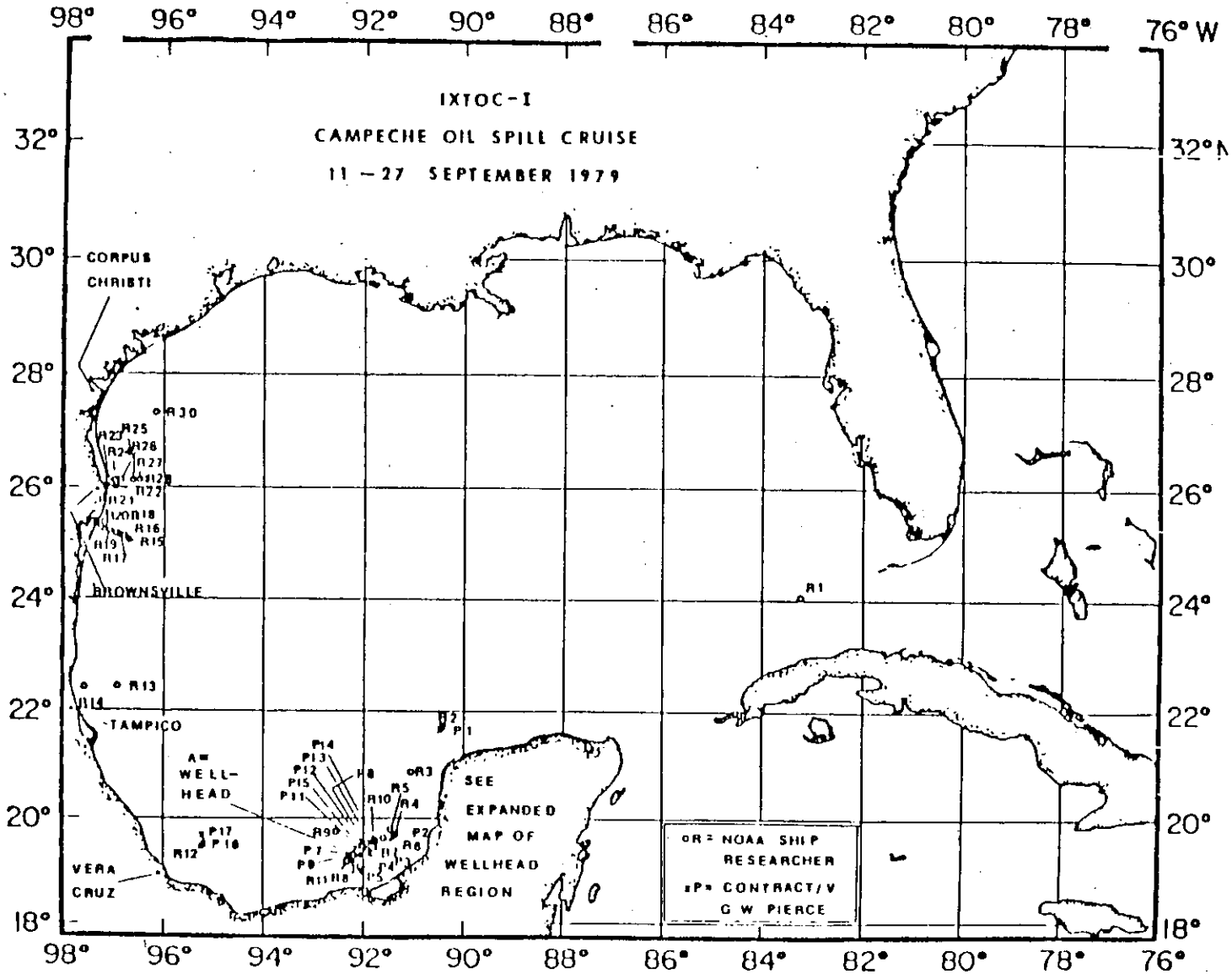

Figure 2. IXTOC-I oil spill cruise stations, 11-27 September 1979.

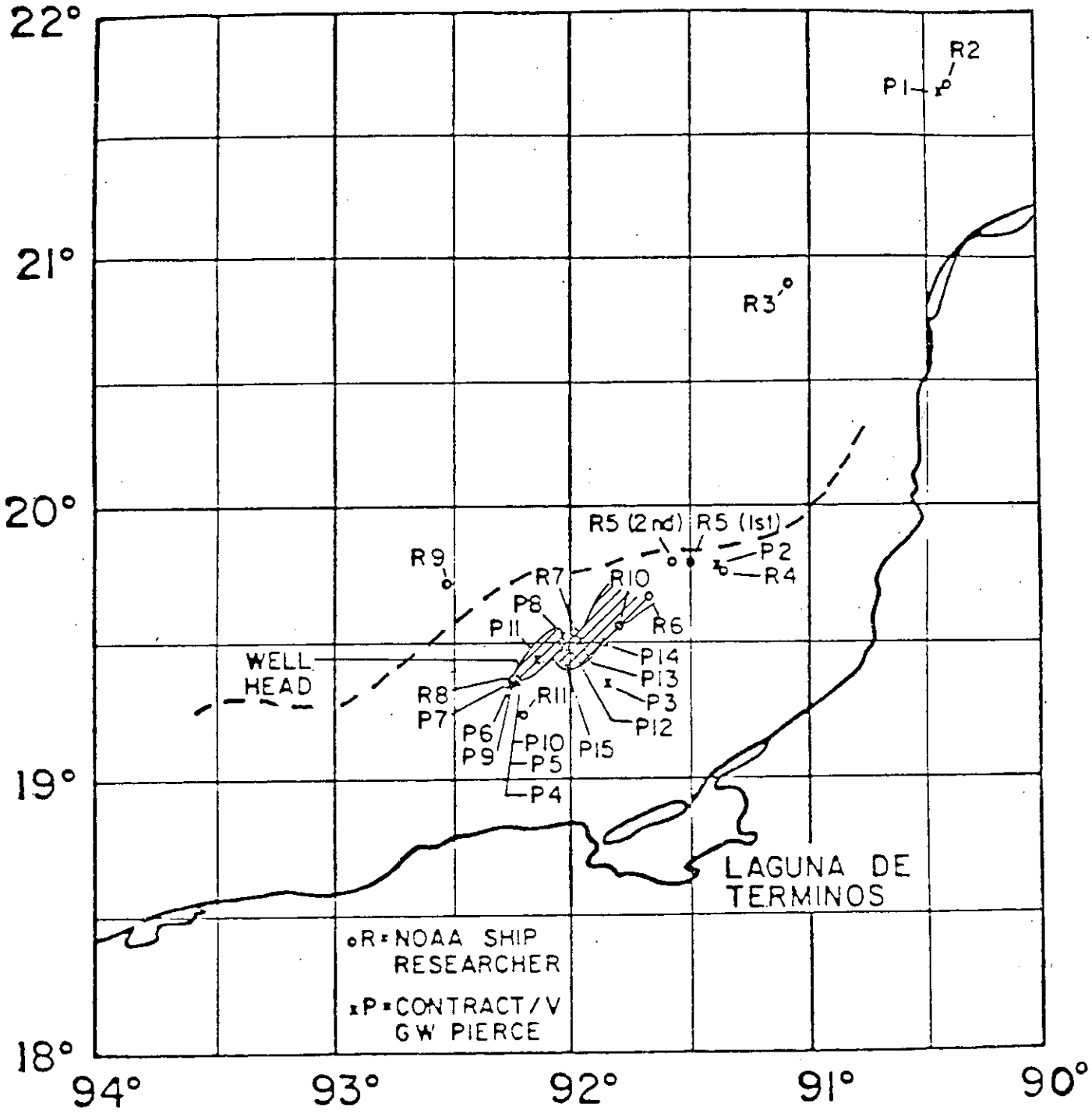

Figure 3. IXTOC-I Campeche oil spill cruise, 11-27 September 1979. Expanded wellhead region.

------ Green (sediment laden) blue water front
Spproximate oil plume track

Table 5. Dissolved and particulate-bound hydrocarbon concentrations from RESEARCHER/PIERCE IXTOC stations.

Sample	Distance from Wellhead (mi)	Latitude / Longitude	Depth (m)	Hydrocarbon Concentration µg/l: Dissolved F-1 Resolved / Unresolved	Dissolved F-2	Particulates F-1 Resolved / Unresolved	Particulates F-2
RIX 11 S001	8.1	19°16'N / 92°11'W	1-3	0.0484 / 0.58	0.125 / 0.316	0.144 / 0.861	0.001
RIX 11 S003	12.9	19°16'N / 92°09'W	1-3	1.632 / 1.164	1.173	0.048	0.016
RIX 11 S002	12.9	19°16'N / 92°09'W	28	0.0179	<0.00048	<0.00048	0.005
RIX 07 S002	20.0	19°34'N / 91°50'W	1-3	0.0281 / 0.1045	0.005 / 0.08347	0.032	<0.00048
RIX 07 S003	20.0	19°34'N / 91°50'W	43	0.0663	<0.00048	0.145 / 0.327	0.022
RIX 10 S001	28.5	19°39'N / 91°48'W	1-3	0.0359	0.0179	0.0014	0.085
RIX 10 S003	28.5	19°39'N / 91°48'W	42	<0.00048	<0.00048	0.081 / 0.374	0.007 / 0.078
RIX 05 S001	48.4	19°50'N / 91°30'W	1-3	0.019	0.0162	0.364 / 1.498	0.049 / 0.75
RIX 05 S002	48.4	19°50'N / 91°30'W	32	<0.00048	<0.00048	0.038836	0.0006

Table 5. (Continued)

RIX 05 S003	50.1	19°50'N / 91°34'W	18	0.0023	0.0512	0.0362	0.011 / 0.028
RIX 04 S001	57.2	19°40'N / 91°22'W	1-3	0.0097	<0.00048	0.0204	0.0086
RIX 04 S002	57.2	19°40'N / 91°22'W	22	<0.00048	<0.00048	0.08 / 0.042	0.03
RIX 02 S004	174.0	21°42'N / 90°26'W	1-3	1.233 / 21.55	0.807 / 22	<0.00048	0.006 / 0.026
RIX 02 S005	174.0	21°42'N / 90°26'N	33	0.0487 / 0.1487	<0.00048	<0.00048	0.0013
RIX 02 S006	175.0	21°42'N / 90°25'W	20	0.0356	0.0424	0.0066	0.0046
RIX 12 S001	178.0	19°15'N / 95°10'W	1-3	0.142	0.008	0.002	0.00096
RIX 12 S004	178.0	19°15'N / 95°10'W	60	0.059	0.0636	<0.00048	<0.00048
RIX 12 S003	178.0	19°15'N / 95°10'W	90	0.0122	<0.00048	0.012	0.0004
RIX 13 S001	342.0	22°27'N / 91°07'W	1-3	0.0026	0.0055 / 0.049	<0.00048	<0.00048
RIX 13 S002	342.0	22°27'N / 91°07'W	31	0.0246	0.74 / 1.185	0.006	0.0005
RIX 14 S001	367.0	22°24'N / 97°32'W	1-3	0.02656	<0.00048	0.003	0.003
RIX 14 S002	367.0	22°24'N / 97°32'W	1-3	<0.00048	<0.00048	0.0018	0.0012

Table 5. (Continued)

RIX 22 S001	481.0	26°00'N / 96°45'W		0.001	0.1339	0.034	0.01
RIX 22 S002	481.0	26°00'N / 96°45'W		<0.00048	<0.00048	0.0067	0.0016
RIX 30 S001	490.0	27°18'N / 96°10'W	1-3	0.00212	0.0184	0.021	0.007
RIX 30 S003	490.0	27°18'N / 96°10'W	43	0.0005	0.004	0.019	<0.00048
RIX 30 S002	490.0	27°18'N / 96°10'W	271	<0.00048	0.0215	<0.00048	<0.00048

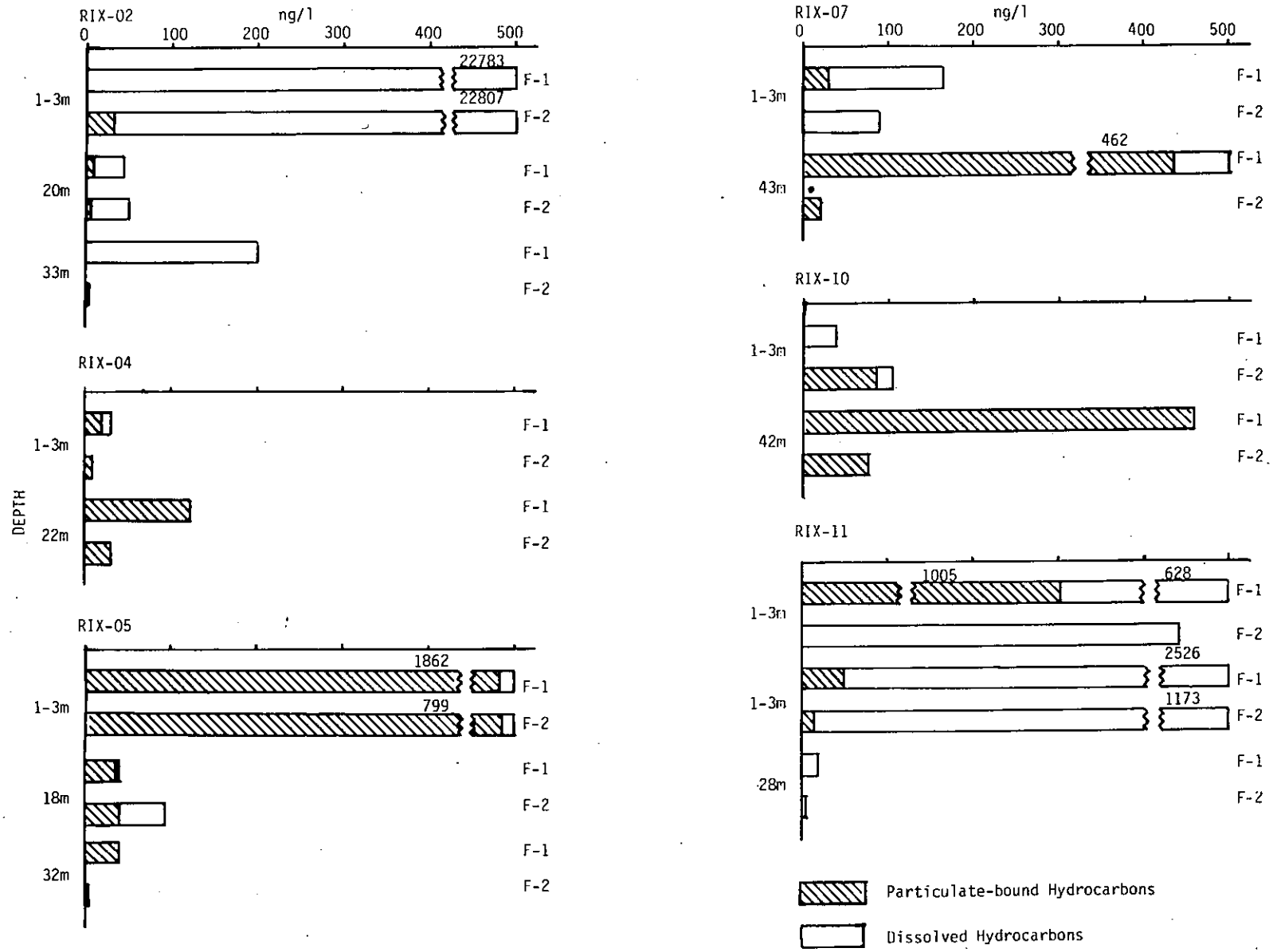

Figure 4. Dissolved and particulate-bound hydrocarbon burdens measured from Bodega-Bodman water sample casts.

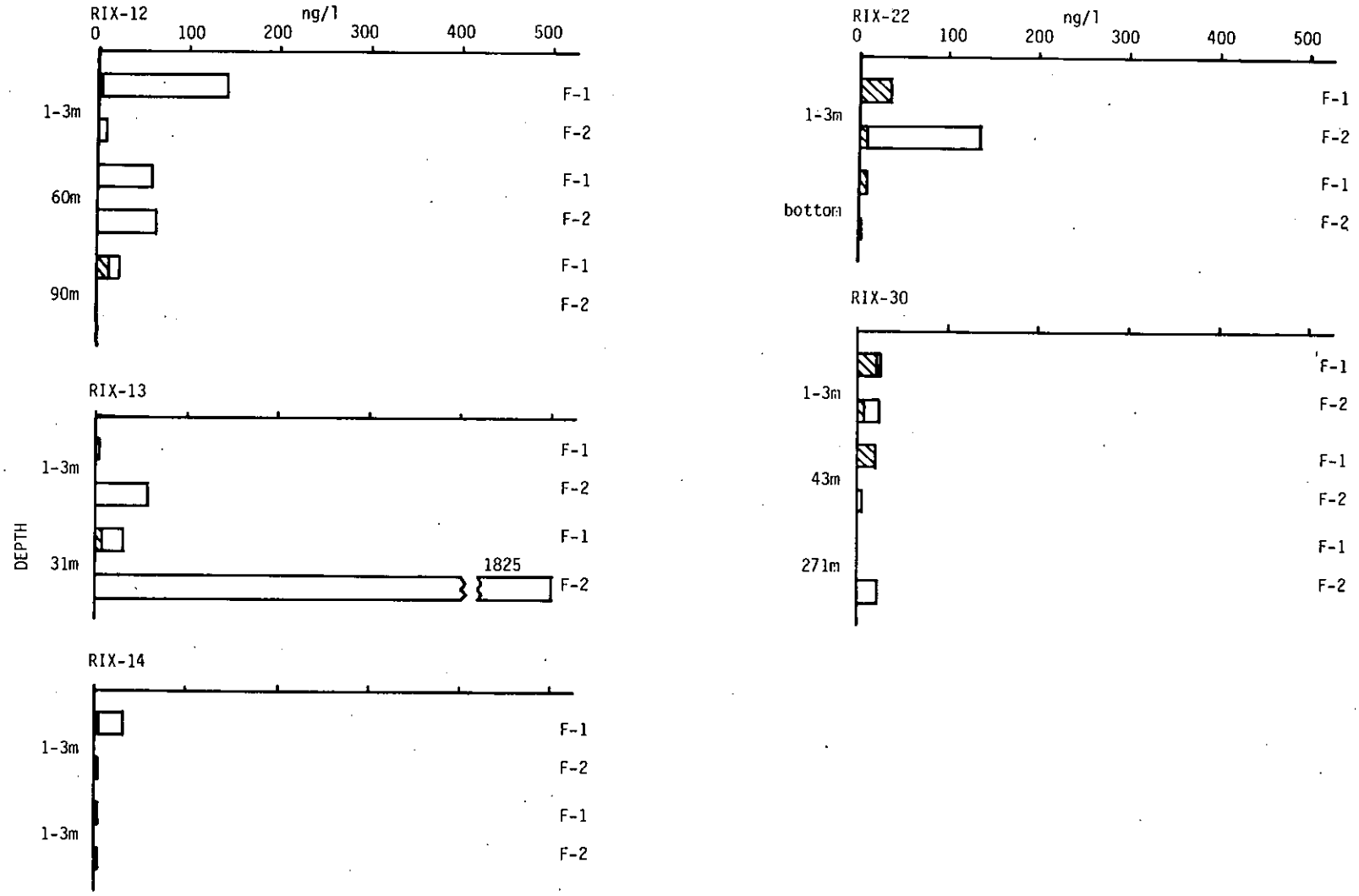

Figure 5. Dissolved and particulate-bound hydrocarbon burdens measured from Bodega-Bodman water sample casts (far field from well site).

levels of petroleum hydrocarbons detected and the predominance of hydrocarbons associated with the particulate phase.

Several explanations can be offered for these values. First, prior to arriving in the vicinity of the IXTOC blowout, two hurricanes passed through the Gulf, greatly disturbing the bottom and its overlying water column. Excessive levels of resuspended sediment were apparent from both shipboard and helicopter observations, and a blue-green oceanic front of a nearshore boundary layer of suspended sediment was clearly evident north of the IXTOC wellsite (see Figure 3) and in the near-coastal water along the entire Bay of Campeche.

During all of the near-well and near-plume RESEARCHER and PIERCE stations, the water was a light turquoise/blue-green in color. In many of the Bodega-Bodman samples, extremely large amounts of suspended particulate material were recovered; in fact, the particulate load was so high in several instances (e.g., RIX 07 and RIX 11) that the filter pads plugged during filtration on the first 40 liters of sample. In these instances the filter was removed and wrapped in foil, and a second filter was inserted. Both filters were later combined for extraction and analysis.

Figure 6 presents the aliphatic and aromatic fraction chromatograms from the subsurface and near-bottom dissolved and particulate samples obtained at station RIX 07. This station was near the northeast edge of the plume in an area covered by a light to moderate sheen. Heavily oiled areas could not be investigated directly from the RESEARCHER because the vessel's saltwater intakes were located just below the water line. (The G. W. PIERCE was able to enter the areas of heavy slick and mousse, however, so subsurface samples were able to be obtained; the results of those analyses are presented elsewhere.) Nevertheless, the near-plume samples in the chromatogram shown in Figure 6 illustrate the differences in dissolved and particulate-bound oil with regard to total water column loading. At this and several of the other stations it was not uncommon to observe order-of-magnitude higher levels of hydrocarbons in the particulate phase relative to the dissolved. An exception to this was station RIX 02, just to the north of the Yucatan Peninsula, which was sampled just before Hurricane Henri passed through the area.

Our data suggest that once the oil had been adsorbed onto particulates, it was then subject to subsurface horizontal and vertical advective transport. Under these conditions it could then be transported a considerable distance before eventually settling to the bottom. In several cases dissolved and particulate-bound oil were found where surface slicks were not readily apparent from the research vessel, and in one instance a definite subsurface lens (or "plume") of dissolved and particulate-bound oil was detected in association with a very strong thermocline and halocline at mid-depth. Some of the highest measured levels of dissolved and particulate oil were obtained at station RIX 05, located to the northeast of the wellhead; however, at the time of sampling only a slightly visible surface sheen was observed near the ship, with windows of what appeared to be slick or light sheen surrounding the vessel. Figure 7 presents the STD cast data from stations RIX 05, RIX 07, and RIX 10. Station RIX 05 was occupied around midnight GMT on 16-17 September while there was still a fairly stable and stratified water column (i.e., prior to the mixing

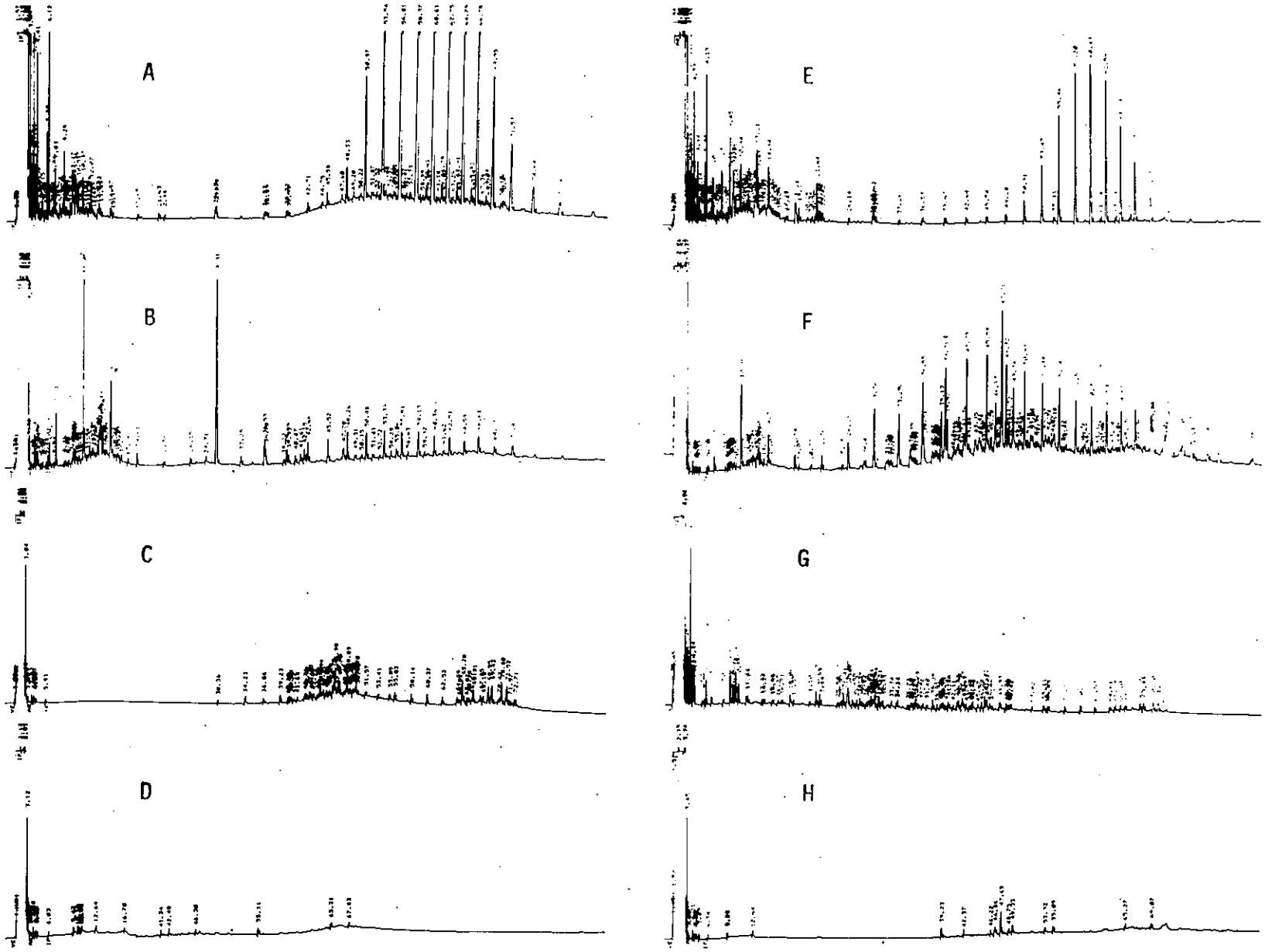

Figure 6. Aliphatic fraction chromatograms of surface dissolved (A) and particulate (B), and bottom dissolved (E) and particulate (F); aromatic fraction chromatograms for surface dissolved (C) and particulate (D) and bottom dissolved (G), and particulate (H) samples from station RIX 07. (Note dissolved fraction cap contamination n-alkanes in A and E as noted in section 2.1-Sampling Methods.)

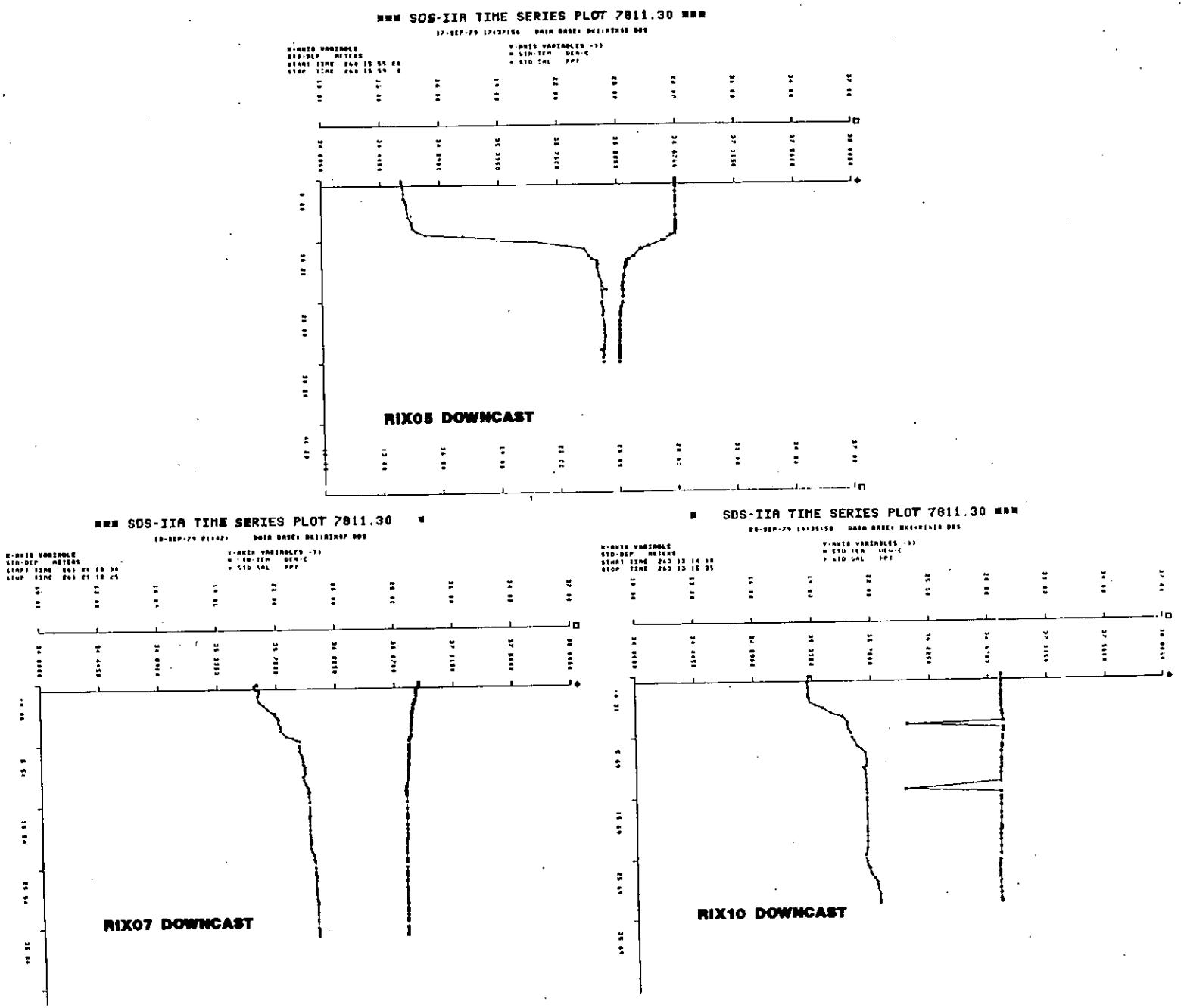

Figure 7. STD data from RESEARCHER stations RIX 05, RIX 07, RIX 10.

effects of the hurricanal storm). Clearly, there was a sharp density gradient at approximately 12 to 16 meters. Examination of the data in Table 5 and Figure 4 reveals a significant concentration of particulate-bound oil (2600 ng/L) in the subsurface 1-3 m sample and close to background levels (less than 150 ng/L) of dissolved and particulate oil in the water sampled at 18 meters (approximately 5 m below the density gradient) and at 32 m (5 m above the bottom). Elsewhere, at RIX 07 and RIX 10, there was no clear stratification of the water column, and near-bottom levels of particulate-bound oil were elevated with respect to the subsurface samples. Both of these stations were located at the edge of the visible plume (north and south, respectively) after Hurricane Henri had caused complete mixing of the water column. It is not possible from our data to determine whether or not the near-bottom levels reflect sinking particulate-bound oil or resuspended bottom sediment that had previously been contaminated with IXTOC oil.

Concentration abundance of the n-alkanes for the more heavily oiled particulate samples is illustrated in Figure 8. The common trend for the particulate samples is the increase in biogenic hydrocarbons (nC_{15}) and enhancement of the higher paraffins with distance from the well. Whether this reflects the removal of the lower-molecular-weight paraffins with distance from source (dissolution and evaporation) or indicates selective adsorption with a change in particulate type (terrestrial vs. pelagic) is not known. It should be noted that in addition to the distributional change in the paraffins, as nC_{15} becomes more prominent, certain prominent biogenic olefins (KOVAT 2078, 2045, and 2139) at station RIX 07 were absent from RIX 10 and RIX 05. Furthermore, the polar fractions (F-3) of stations RIX 10 and RIX 05 contained increasingly abundant C_{14} fatty acids and C_{14} fatty acid methyl esters (increases of 100 ng/L), also indicative of pelagic sediments.

Figure 9 shows a plot of the saturate concentration (F-1) versus the concentration of nC_{15} for the more heavily oiled particulates. It is readily apparent that a rough correlation exists, possibly implying that the concentration of nC_{15} reflects greater biogenic particulate loading and associated scavenging of oil.

As the RESEARCHER cruise track moved into clear waters to the west of the IXTOC blowout site, hydrocarbon values drastically decreased, as illustrated by the dissolved and particulate levels in Table 5 and Figure 5.

While elevated levels of hydrocarbons were found in water samples collected from the PIERCE within the plume, such levels were not observed in any of the samples obtained by the Bodega-Bodman operations aboard the RESEARCHER (out of the plume only). Given the high particulate load in the vicinity of the well, it is not unreasonable to speculate that most of the oil released was scavenged and removed by primary and secondary sedimentary processes before it reached the sampling locations at greater distances from the source. Other researchers (Gearing et al., 1979) have found in test-tank studies that lower-molecular-weight aromatic compounds (including up to three-ring aromatics) tend to partition into the dissolved phase before partitioning onto suspended particulate matter (and subsequently sinking). The excessive particulate loads in the vicinity of the well at the time of our sampling may have altered this

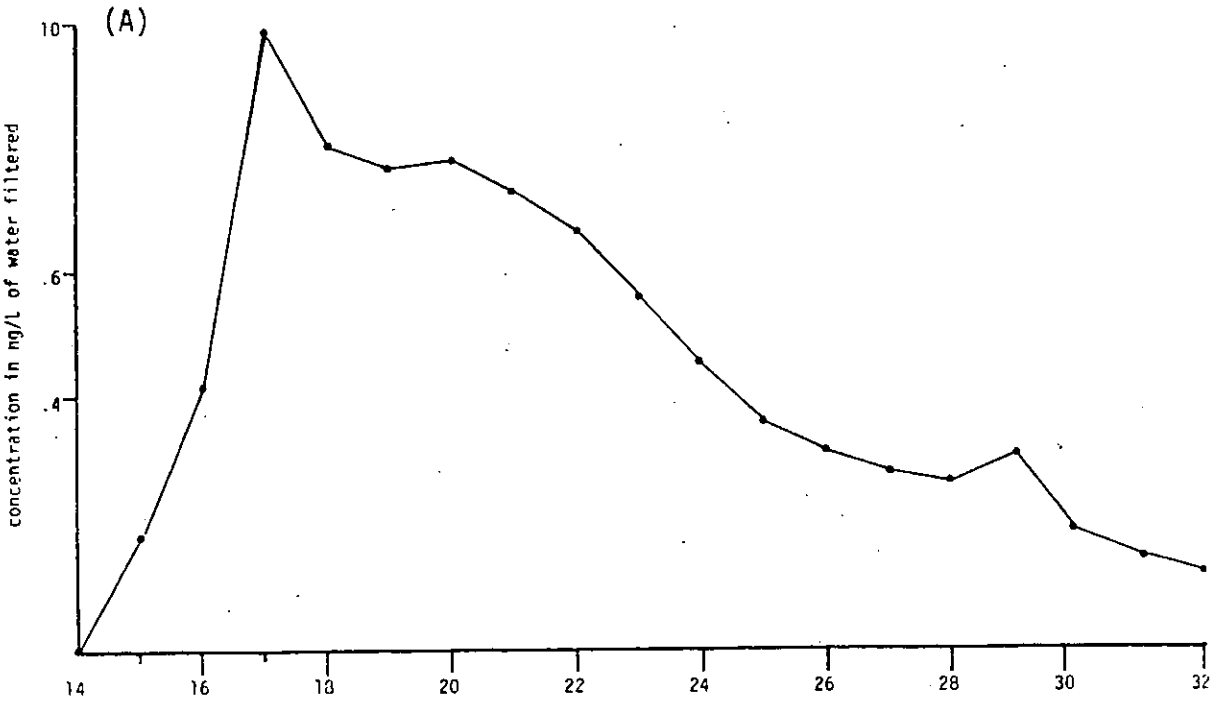

Figure 8A. Concentration abundance of N-alkanes in particulates, RIX 07 near bottom.

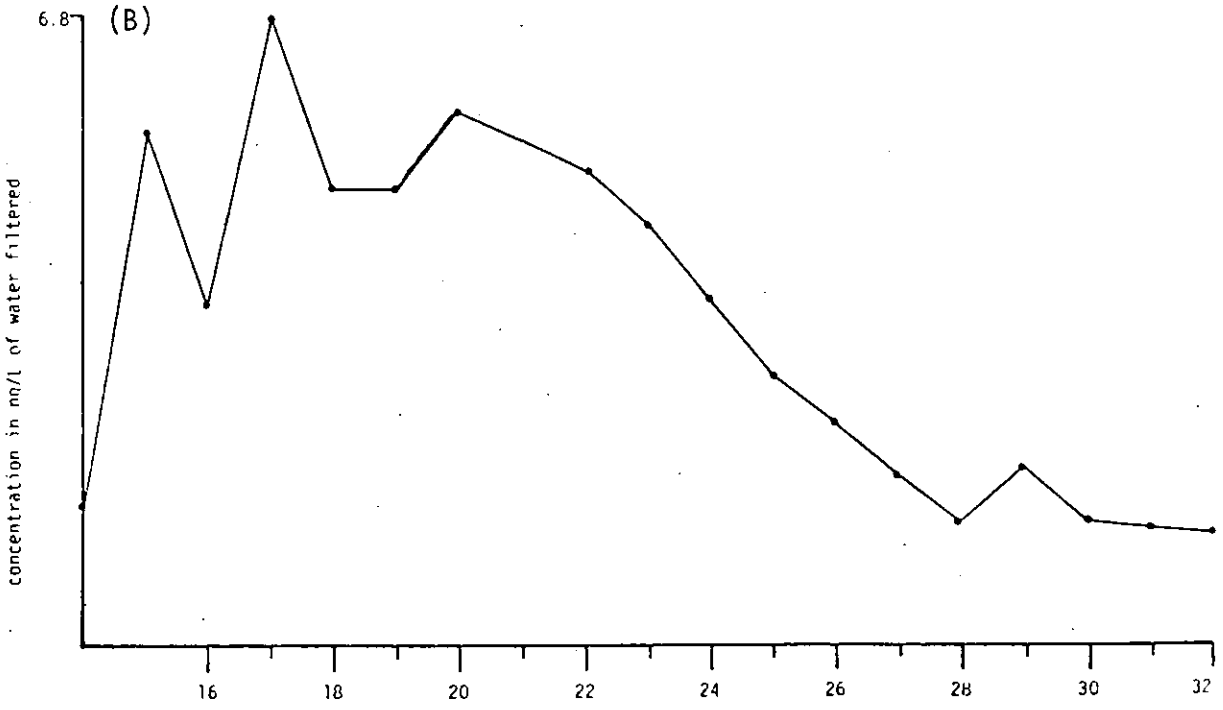

Figure 8B. Concentration abundance of N-alkanes in particulates, RIX 10 near bottom.

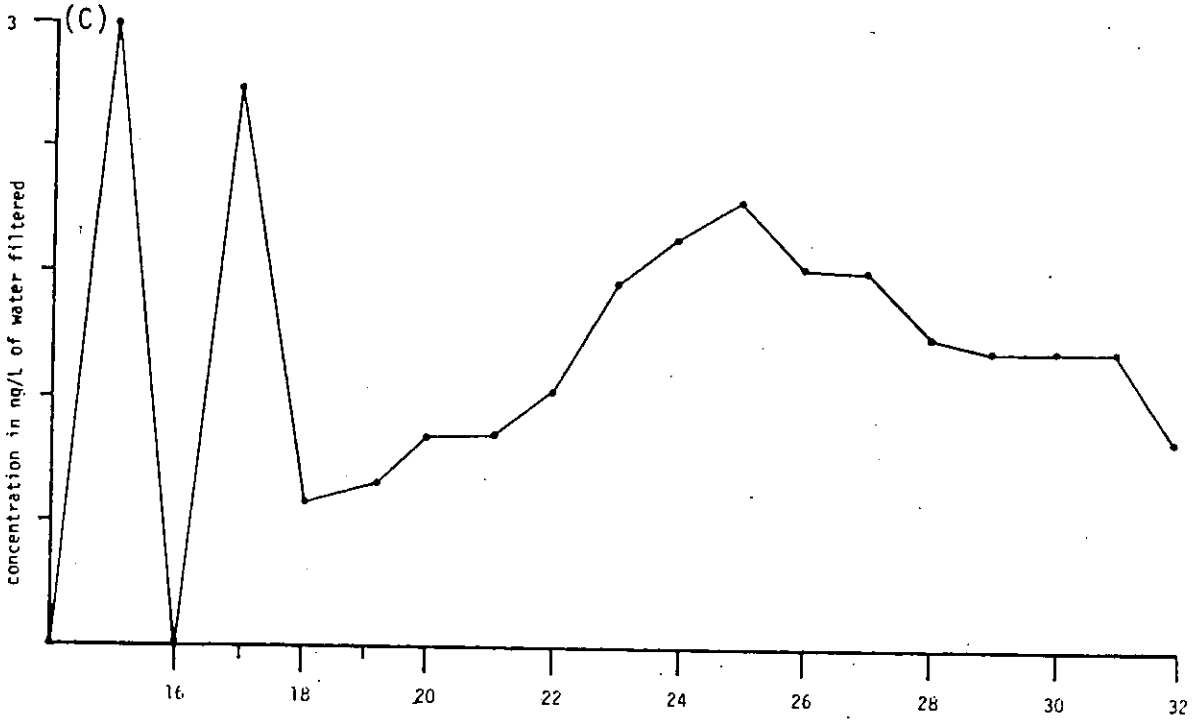

Figure 8C. Concentration abundance of N-alkanes in particulates, RIX 05 near bottom.

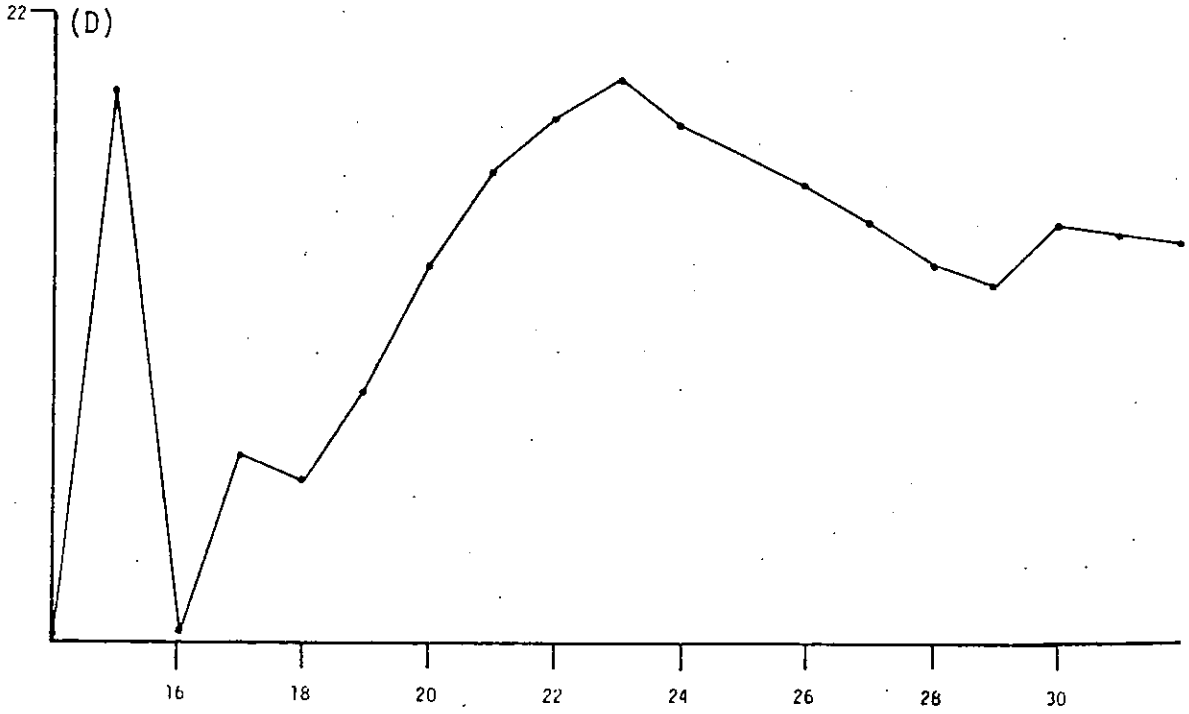

Figure 8D. Concentration abundance of N-alkanes in particulates, RIX 05 near surface.

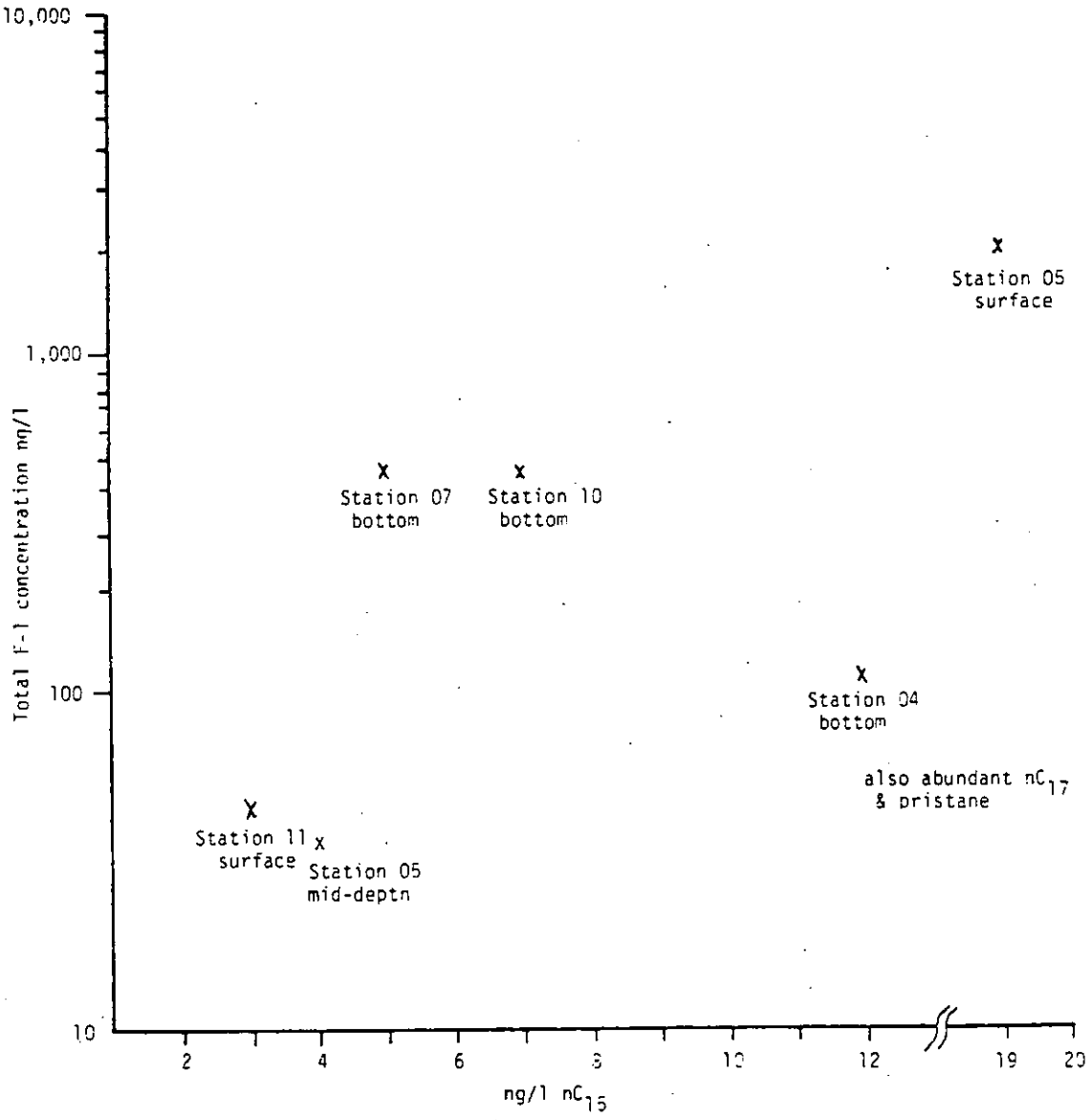

Figure 9. Relationship between total aliphatic (F-1) concentrations and the concentrations of nC_{15} in "OILED" particulates as a function of biogenic character.

usual behavior. Other data collected in this study (Payne et al., 1980) suggest that, in fact, lower-molecular-weight aromatics such as benzene, toluene, ethylbenzene, and xylenes do remain in the water column at exceedingly high (1 µg/L) levels despite the high particulate loads observed.

Several authors (Gearing et al., 1979; Meyers and Quinn, 1973; Wheeler, 1978; Winters, 1978; Zurcher and Thuer, 1978; Zurcher et al., 1980) have also suggested that particulate/oil interactions are dominant processes in the ultimate disposition of petroleum. The density of seawater is such that only limited amounts of detrital material or particulate matter are required to cause sedimentation of several times their volume of oil. Differences in partitioning of the particulate material also appear to be a function of oil composition. The chromatograms in Figure 6 illustrate that the lower-molecular-weight aromatic compounds tend to predominate in the dissolved phase, whereas the higher-molecular-weight materials, including polynuclear aromatics, tend to associate with the suspended particulates. Winters (1978) found similar results in laboratory studies in which petroleum-derived alkanes were approximately ten times greater in the particulate fraction than were the aromatics. Conversely, the aromatic compounds were at least five times more concentrated in the dissolved state.

3.4 Higher-Molecular-Weight Aromatic Distributions in Crude Oil, Water Filtrate, Particulate, and Mousse Samples

The GC-mass spectral data from the aromatic fractions of several selected samples were obtained so that information regarding the distributional changes of aromatic hydrocarbons could be elucidated. By comparing the distributions of aromatics in several sample types (air, water, mousse), the direction and possibly the degree of partitioning of aromatic compound suites can be addressed. Specifically, we examined the occurrence of the aromatic compounds naphthalene, fluorene, dibenzothiophene, and phenanthrene and their mono- through tetra-alkyl homologs. Data for the crude oil and mousse flakes from station PIX 13 (about 18 miles from the wellhead) are illustrated in Figure 10. The aromatic abundance plots indicate that the majority of the naphthalenes in the crude have been removed and that the dominant aromatic suite consists of the dibenzothiophenes. This trend is similar to that observed by Calder (1979) in the AMOCO CADIZ spill.

Figure 11 also shows that the abundance maximum for each aromatic type is shifted by one carbon number between the crude oil and the mousse sample. For example, in the crude oil, the dominant homologs for fluorene are C-1, whereas in the mousse they are C-2; similar trends occur for the other aromatic compound suites studied. Also, the relative abundances of the alkyl-substituted benzenes for both crude and mousse were plotted as a function of carbon number (Figure 12). In contrast to the multi-ringed aromatics that shifted one carbon, the alkyl benzenes appear to have shifted three carbons toward the higher homologs, with an almost total depletion of those consituents lighter than C_{12}-substituted benzenes.

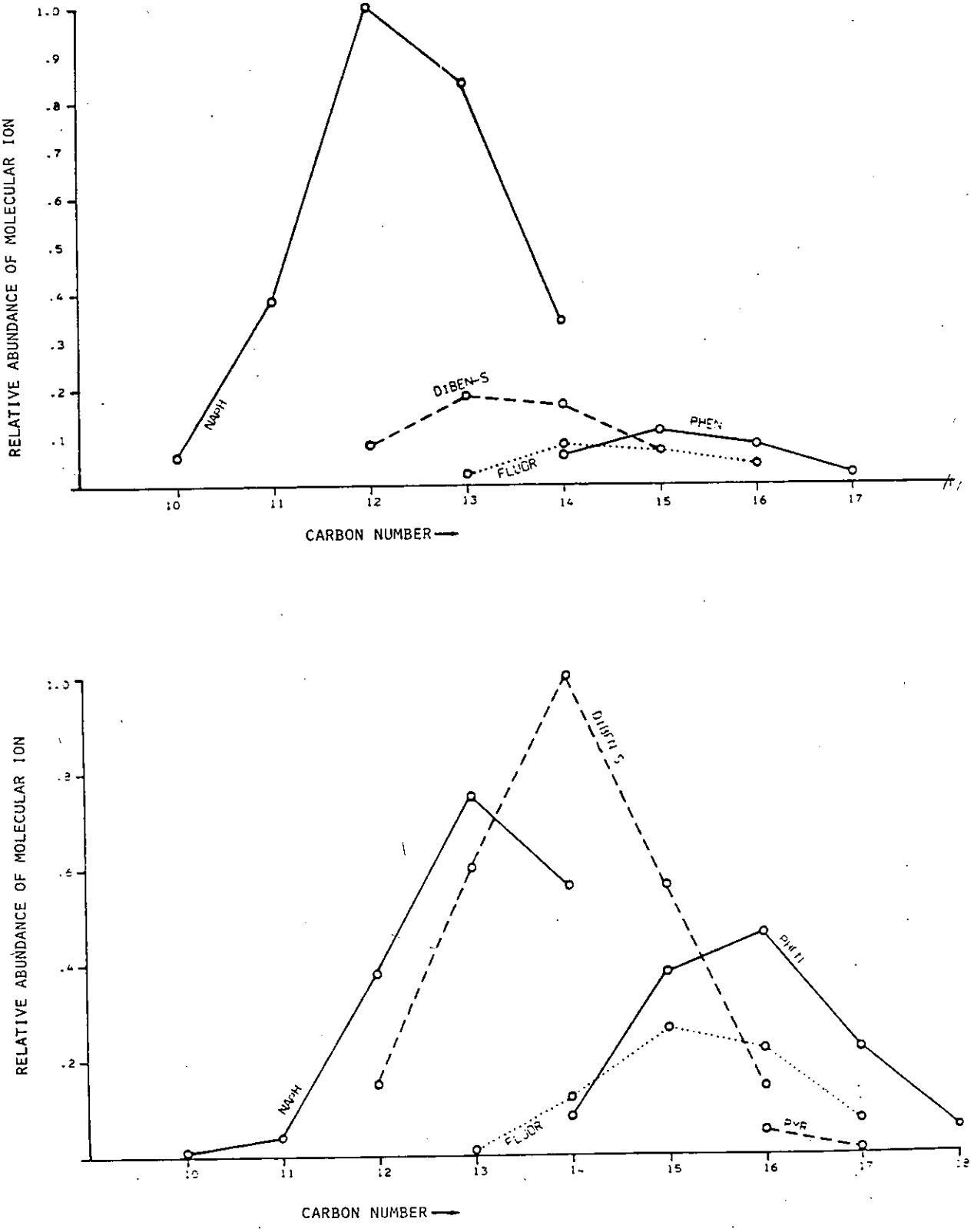

Figure 10. Relative abundance of PNA's in IXTOC crude oil (top) and mousse flakes (bottom).

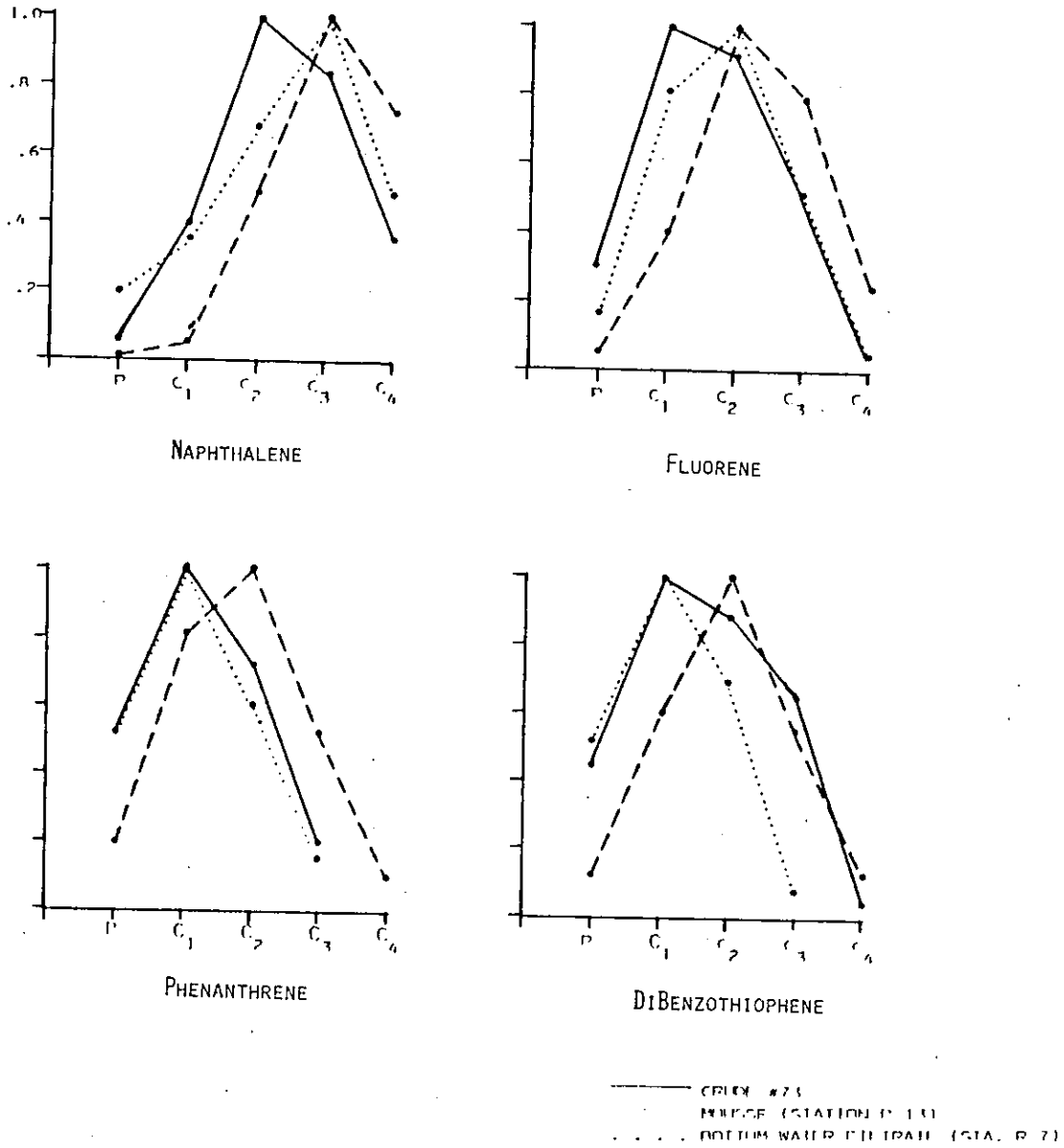

Figure 11. Comparison of the distribution of aromatic hydrocarons for mousse, crude oil, and a water filtrate.

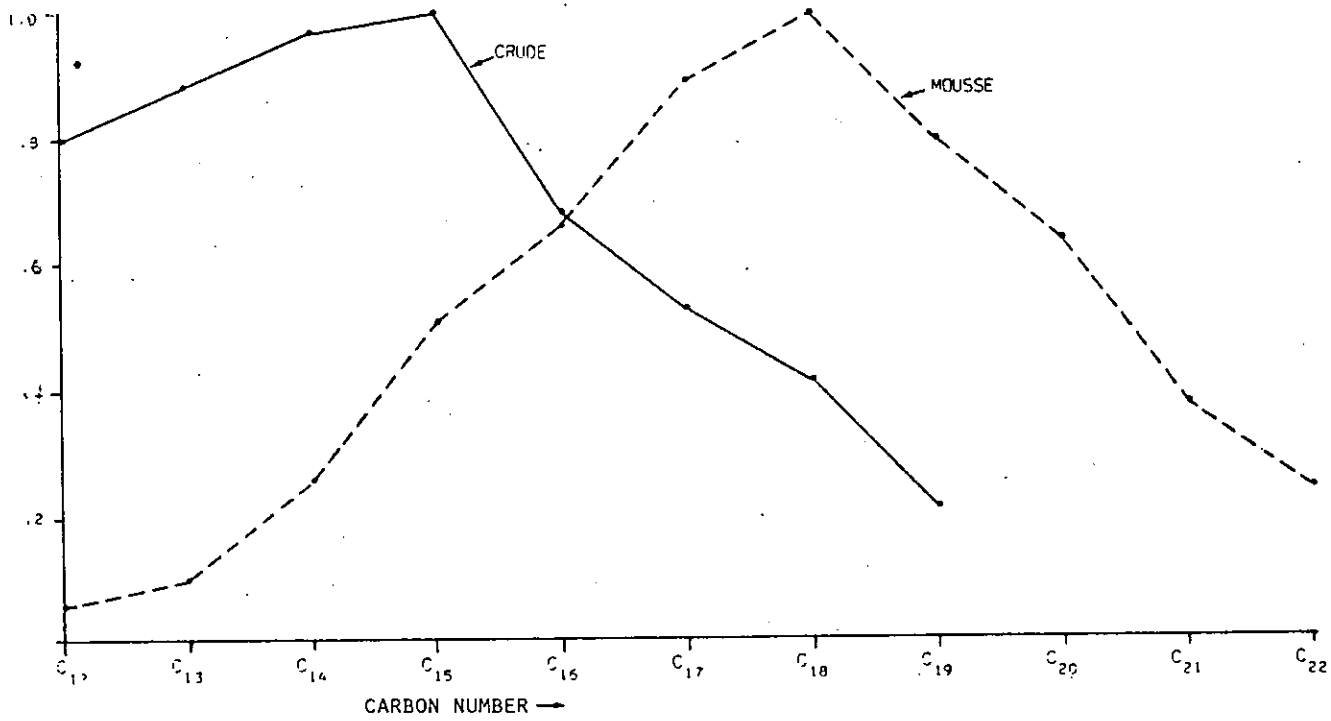

Figure 12. Relative abundance of alkl substituted benzenes (m/e 105 and m/e 119).

Three water filtrates and one particulate were analyzed for their aromatic distributions. In all cases no appreciable alkyl benzenes were detected, and in the particulate sample (station RIX 07, near-bottom), the only aromatic series identified was the phenanthrenes. Figure 13 summarizes the aromatic distributions as a function of carbon number for the filtrates, mousse, and crude oil samples with the abundance of the individual aromatic types shown in Figure 14. The high naphthalene content in the bottom water filtrate from station RIX 07 is likely due to its proximity to the plume and wellhead relative to the more distant station (RIX 04) and the station south of the well (RIX 11, which contained the lowest relative abundance of naphthalenes for the water filtrates examined). The depletion at RIX 11 is probably due to its location well outside of the path of plume transport, rather than its distance from the source.

The concentration data for mousse samples collected from the PIERCE (stations PIX 11 and PIX 13) and those from a beached mousse sample (RIX 23) are listed in Table 6. The concentration differences in most of the samples appear to be a function of water content and/or detrital dilution (e.g., by sand).

Although stations PIX 11 and PIX 13 were located in the oil plume, certain of their samples (PIX 11-4 and PIX 13-5) contained a relatively high proportion of saturated components (i.e., a saturate/aromatic ratio greater than 5). This depletion in aromatic constituents could indicate excessive weathering; however, more likely it may indicate non-IXTOC oil (or possibly even oil that had been treated with a dispersant).

The distribution of n-alkanes relative to nC_{20} is shown in Figure 15 for the crude oil, beached mousse, and mousse collected at PIX 13. It is clearly evident that within 18 miles of the well site a majority of the paraffins (approximately 40-50%) have been removed by evaporation and dissolution.

Figure 16 illustrates a plot of the concentration of hydrocarbons as a function of depth in a beached mousse "log" collected at RIX 23 about 480 miles from the wellhead. Included in Figure 16 are ratios of the concentration of total saturate to total aromatic hydrocarbons. The concentrations are lower and saturate enrichment is greater for those samples nearest the air/mousse interface; however, it is not clear whether the concentration differences are due to differential weathering or to detrital dilution from entrained sand. Interestingly, the total n-alkane-to-C_{20} character of the PIX 13 (18 miles from well site) suggests that very little, if any, additional chemical weathering occurred to the material as it traveled and agglomerated into the larger "log."

Table 7 lists ratios of nC_{25}/nC_{19}, nC_{25}/nC_{16}, and phytane/nC_{18} with depth into the RIX 23 mousse log. Excluding sample RIX 23-02, there is a general trend of light paraffin removal at the fringes of the mousse log, but very little microbial degradation (i.e., phytane/nC_{18} is constant). The only anomalous sample is RIX 23-02, which shows much more extensive weathering of the

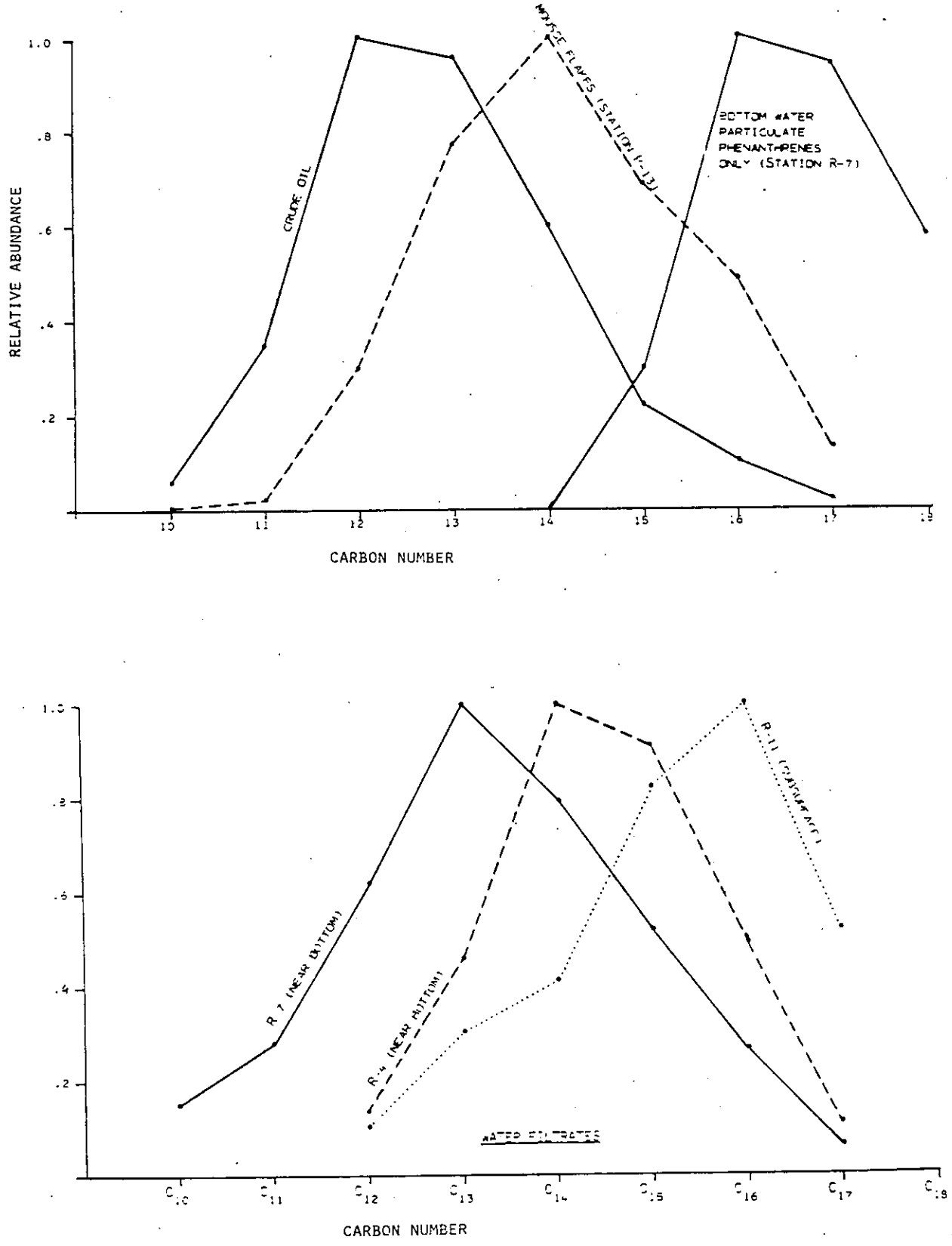

Figure 13. Relative abundance plots of total PNA's (naphthalenes, fluorenes, dibenzothiophenes, and phenenthrenes) for the GCMS analyses of mousse, crude oil, and particulates (top) and water filtrate (bottom).

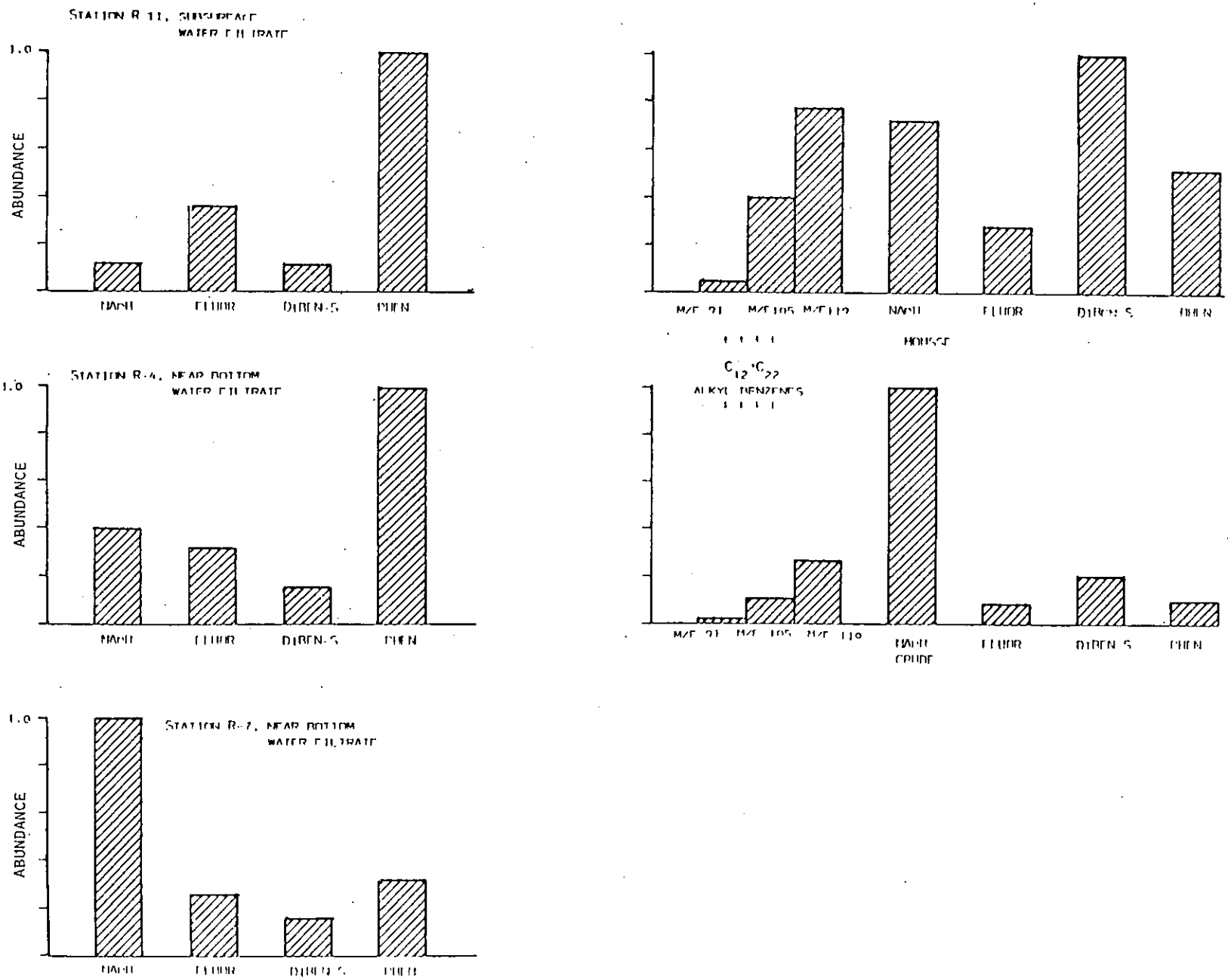

Figure 14. Relative abundance of the aromatic hydrocarbon types in the IXTOC crude, and mousse flakes and water filtrates.

Table 6. Concentration data for oil and mousse samples.

Sample	Distance from Wellhead (mi)	Latitude / Longitude	Water Depth	Hydrocarbon Concentration µg/g: Mousse F-1 Resolved / Unresolved	Mousse F-2	Mousse F-3-5 Sum Resolved / Unresolved
PIX 11 S002	4.3	19°16'N / 92°09'W	Surface oil slick	3370 / 8020	86 / 2500	52
PIX 11 S004	6.2	19°20'N / 92°00'W	Surface oil slick	5990 / 18100	130 / 3820	<0.00048
PIX 13 S004	17.8	19°32'N / 91°56'W	Surface oil flakes	13000 / 57000	1180 / 40600	11
PIX 13 S005	17.8	19°32'N / 91°56'W	Larger surface oil flakes	5250 / 32900	69 / 1280	12 / 613
PIX 13 S006	17.8	19°32'N / 91°56'N	Surface mousse balls	11400 / 42700	641 / 13400	372
PIX 13 S007	17.8	19°32'N / 91°56'N	Surface oil flakes	9680 / 36800	467 / 11200	127
PIX 13 S008	17.8	19°32'N / 91°56'N	Surface mousse ball (5 cm dia)	13400 / 49600	637 / 14330	20

Table 6. (Continued)

RIX 06 S003	36.9	19°49'N 91°40'W	Surface beached mousse pancake	6451 25900	218 9860	2
RIX 23 S001-1	486.0	25°49'N 97°09'W	Surface skin 3 mm	3280 14400	102 4780	<0.00048
RIX 23 S001-2	486.0	25°49'N 97°09'W	3-8 mm from surface skin	5950 29700	86 6180	<0.00048
RIX 23 S001-3	486.0	25°49'N 97°09'W	8-13 mm from surface skin	6000 25400	306 8250	<0.00048
RIX 23 S001-4	486.0	25°49'N 97°09'W	16-23 mm from surface skin	12200 50400	573 20900	<0.00048
RIX 23 S001-5	486.0	25°49'N 97°09'W	Weeds in center of mousse	<0.00048	<0.00048	<0.00048
RIX 23 S001-6	486.0	25°49'N 97°09'W	5-10 mm from bottom skin	9300 33500	600 14500	<0.00048
RIX 23 S001-7	486.0	25°49'N 97°09'W	Bottom 5 mm of mousse	8600 37000	150 16300	<0.00048

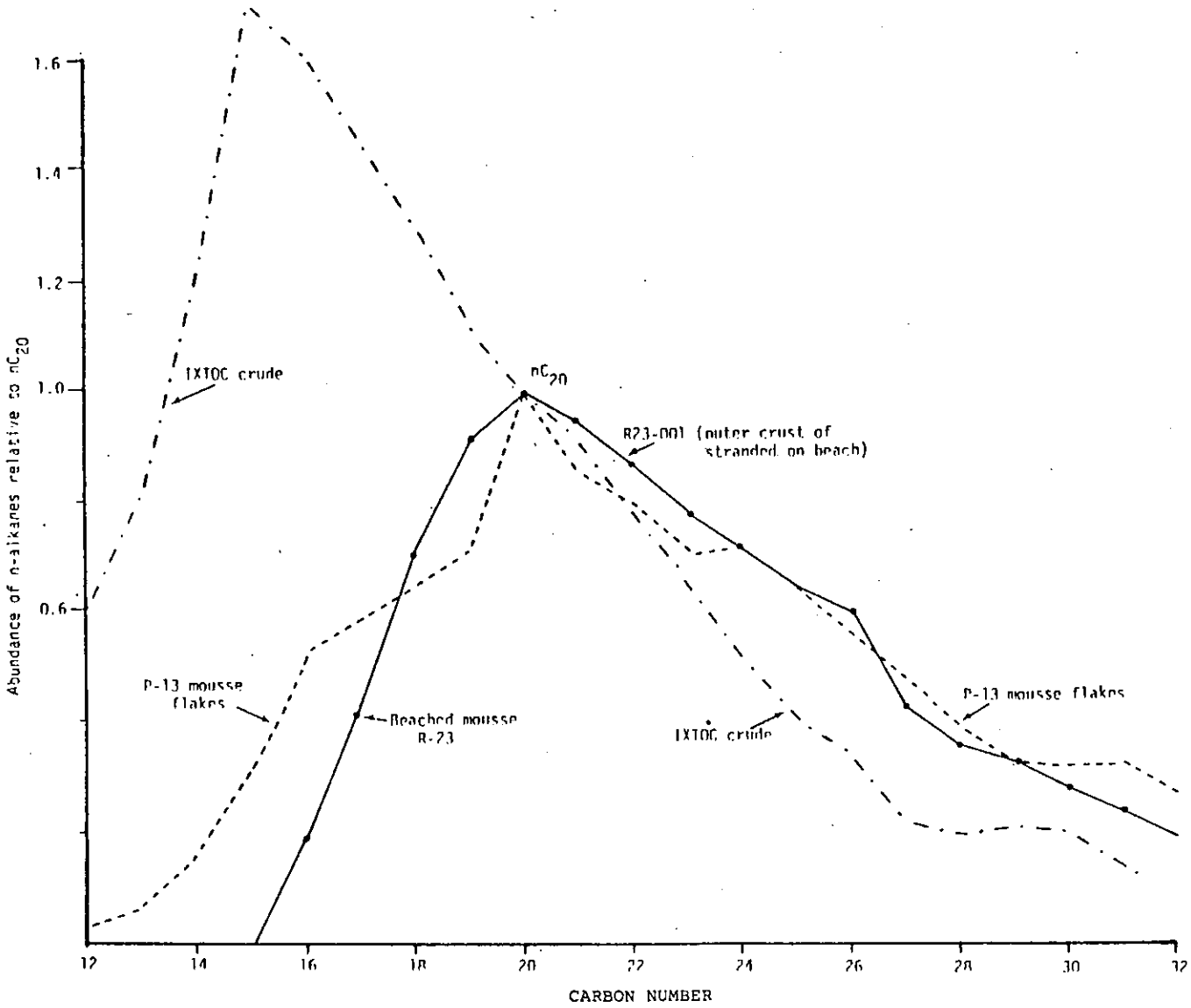

Figure 15. Abundance of N-alkanes relative to nC_{20}, in beached mousse (R23), mousse flakes (P13), and IXTOC crude.

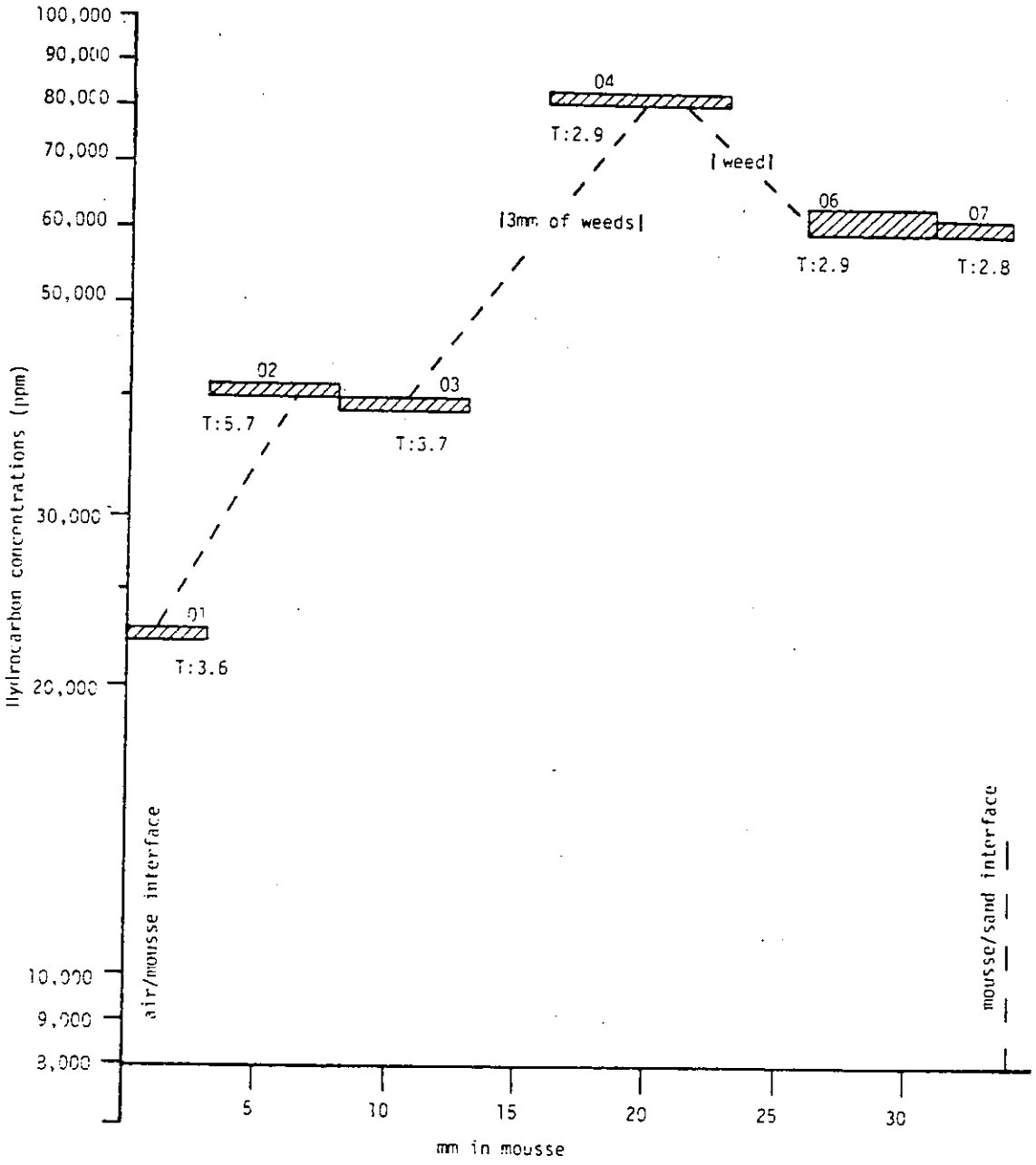

Figure 16. Hydrocarbon concentration relative to depth into (below the skin of) a "beached" mousse log from RIX 23 (480 miles from IXTOC site).

Table 7. Selected component ratios for a dissected mousse sample at station RIX 23.

Sample	Depth Below Skin	nC_{25}/nC_{16}	nC_{25}/nC_{19}	Phytane/nC_{18}
01	surface 3 mm	3.1	0.66	0.46
02	3-8 mm	4.3	1.05	0.42
03	8-13 mm	2.6	0.63	0.46
04	16-23 mm	2.3	0.61	0.44
05		---	Weeds	----
06	5-10 m from bottom	2.4	0.69	0.44
07	bottom 5 mm	2.9	0.79	0.46

*01 represents the sample from the air/mousse interface and 07 that from the sand/mousse interface.

paraffins than the other samples. This is difficult to explain, but it may involve different "histories" of mousse formation.

4. CONCLUSIONS

In examining the data from this study, we must consider the impact caused by the passage of Hurricane Henri across the Yucatan shelf several days before our sampling began. Conditions were drastically changed by this storm, and extremely high suspended particulate loads were noted from both helicopter overflights and the vessels RESEARCHER and G. W. PIERCE. A prevailing light turquoise-green water color extended from north of the wellhead, into the Yucatan shelf and along the southern coast of the Bay of Campeche, and into the eastern Gulf. On several occasions floating oil or patches of mousse were observed along the blue-green front of the particulate-loaded water and the (more seaward) clear oceanic water. Presumably because of turbulent mixing, most of the surface oil remnant that would be expected from the blowout had sunk by the time we arrived at the wellhead; the observable slick extended for only about 36 miles (see Figure 3). These conditions are in contrast to those found earlier in the summer when surface oil was contaminating much of the western Gulf of Mexico from the Bay of Campeche to the south Texas coast.

Extremely low levels of hydrocarbons were consistently found in the dissolved and particulate samples collected in the vicinity of the well. In fact, the total hydrocarbon burdens encountered appear similar to those that have been previously reported from more pristine environments (Payne et al., 1978; de Lappe et al, 1979; Brown and Huffman, 1976). In contrast to the quite low dissolved higher-molecular-weight hydrocarbon concentrations, monocyclic and lower-molecular-weight alkyl-substituted aromatics were found at relatively high concentrations in the plume and in the outside waters surrounding the wellhead. Generally, aromatic levels in the range of 40 to 80 µg/L were found under the plume and 3-4 µg/L levels were observed in the clear water surrounding it. Background levels of aromatic hydrocarbons, specifically benzene, toluene, and xylenes were also found in the ng to low µg/L range elsewhere in the Gulf.

We believe that the extremely low levels of dissolved and particulate hydrocarbons found in the vicinity and to the east of the well site were due to rapid adherence of oil onto the particulates. As noted, particulate loads were extremely high at the time of our sampling, and the oil that had initially been in solution could have been readily scavenged and sedimented. RIX stations 05, 07, and 10 clearly show much higher particulate burdens compared to the dissolved phase. Certainly, a great deal of the fresh oil that was being released at the wellhead was probably being adsorbed onto particulates as it moved away. Interestingly, Boehm and Fiest (1980) found relatively low levels of sediment-bound hydrocarbons at the time of the RESEARCHER/PIERCE sampling, most likely due to the extensive bottom material resuspension from the severe storm activity. Also, it is possible that the surface sediment/oil layer could have been disturbed and lost during the Smith-McIntyre grab sampling operations, and this would result in lower-than-expected oil levels.

Figure 4 shows particulate-to-dissolved ratios in the vicinity of the wellhead to range from 10:1 to 100:1. Similarly, Gearing et al. (1979) reported that the lower aromatic fractions specifically partitioned into the water column, whereas the higher-molecular-weight aliphatic and aromatic compounds partitioned onto the suspended particulate material. Also, the ratio of aromatics-to-aliphatics in the sediments was much less than that in the parent oil. They found from 2 to 34% of the higher-molecular-weight aliphatic, acyclic, and three-ring aromatic compounds in the suspended particulate material, while only about 0.1% of naphthalenes and methylnaphthalenes appeared in that phase (the naphthalenes were the dominant compounds in the starting oil).

Winters (1978) examined two simulated oil spills and the distribution of alkanes and aromatic standards on particulates in spill-tank tests. He found the alkane concentration to be ten times greater in the particulates and the aromatic fraction partitioning to ten times greater in the dissolved phase. The parent aromatics and the mono-methyl aromatics were particularly enriched in the aqueous phase, while those of higher aliphatic character were skewed toward the particulate load. A similar partitioning phenomenon was observed by Parker and Macko (1978) in coastal waters where they conducted a transect perpendicular from the Texas coast into the western Gulf, as part of the STOCS program sponsored by BLM. The higher-molecular-weight alkane and polynuclear aromatic compounds on the particulates appeared to be enriched relative to the lower-molecular-weight compounds, apparently as they drifted farther from the shore and their presumed source.

De Lappe et al. (1980) also observed differential partitioning with respect to molecular species onto particulates in near-coastal waters. N-alkanes and branched aliphatics in the range of C_{22} to C_{35} tended to be associated with the suspended particulate material, whereas n-alkanes in the range of C_{12} to C_{22} were skewed toward the dissolved phase. Similar partitioning of low- and high-molecular-weight chlorinated hydrocarbon species has been reported by Risebrough et al. (1976) and Dexter and Pavlou (1978).

Other investigators have demonstrated that the nature of the particulate matter is also critical in the dissolution-particulate partitioning process. Myers and Quinn (1973) studied the adsorption efficiency of a variety of mineral types with No. 2 fuel oil, finding that for particulates of 44 μm (diameter), adsorption efficiency was found to decrease in the order: bentonite>kaolinite>illite>montmorillonite. They also noted that the GC-resolved hydrocarbon species tended to associate with particulates more effectively than the more polar materials typical of the GC-unresolved complex mixture. When sediment from Narragansett Bay was treated with 30% peroxide to remove humic substances, its adsorption efficiency was increased by a factor of three, which led to the conclusion that the removal of a particle's organic coating frees up "active" sites. Suess (1968), on the other hand, suggested that a 3-4% lipophillic coating may increase oil coating onto particulates.

Zurcher and Thuer (1978) conducted a comprehensive laboratory study in which the dissolution, suspension, agglomeration, and particulate adsorption of oil were studied under experimental conditions that minimized evaporative loss. They used kaolinite as a substrate and a fuel oil of molecular distribution in

the benzene-to-nC_{24} range. Using infrared spectrometry and gas chromatography, they demonstrated that the lower-molecular-weight aromatics between benzene and methylnaphthalene remained dissolved in the water column and that the particulate fraction adsorbed most of the hydrocarbons in the nC_{14} to nC_{32} range. When the oil was agitated vigorously, an agglomeration formed as the oil-enriched particulates rapidly entrained more oil as droplets. This oil/particulate agglomeration then settled rapidly when the agitation was discontinued and the gas chromatographic profile of the oil/particulate phase was extremely characteristic of the original oil. Following this treatment, however, the ligher aromatics were found still to be in solution; specific components included benzene, toluene, ethylbenzene, (o, m, p)-xylene, C-3 and C-4 benzenes, and naphthalenes.

From Zurcher and Thuer's experiments, it was estimated that a total of 200 mg of oil could be scavenged by one kg of dry kaolinite in approximately ten hours. In further studies, they found that this load did not increase in a period of up to 100 hours. A similar value of 162 mg oil per kg for dry kaolinite was reported by Meyers and Quinn (1973). When agitation of the oil/particulate/water mixture was incorporated into Zurcher and Thuer's experiment, the oil droplets became dispersed in the mixture of oil/kaolinite agglomerates and rapidly settled to the bottom. The loading (or oil removal) for this agglomerated mixture increased up to 20 g oil per kg of dry-weight clay (a factor of 100 over that simply removed by adsorptive processes). Data generated by Nelsen (1980) clearly demonstrate that kaolinite was one of the major minerals present in the resuspended sediment in the vicinity of the IXTOC-I well site.

Even higher values of suspended oil/particulate loading were estimated by Bassin and Ichiye (1977). Using southern Louisiana crude oil, they found that oil and suspended particulate material could form spontaneous flocculations of colloids or colloidal electrolytes in the presence of dissolved salts. They reported that the oil coated the clay with a thin film that disrupted the electrolytic interaction between the charged clay particle and the surrounding waters. This resulted in an overall rapid flocculation of "oiled" particulate material, and they reported that between 250 and 3000 grams of oil could be taken up per kg of clay. Their studies also showed that rapid flocculation would lead to entrapment of oil, similar to the results reported by Zucher and Thuer. The floccules formed during these rapid formations had extremely coarse structures, and because of oil incorporation they were lighter than anticipated, leading to a longer residence time in the water and subsequently to greater dispersion. Similar observations were made at the time of the IXTOC sampling as oil/clay, cornflake, or snowflake floccules were found at great distances from the well.

Malinky and Shaw (1979) have suggested that perhaps particulate adsorption of oil is not the major means of removal; however, their study was conducted with glacial sediments, which are low in carbonates and organic carbon. In southern Alaska, ambient particulate levels as high as 1 g/L are typical, and Malinky and Shaw were interested in determining whether this condition would be an effective mechanism for oil removal. In a study using C-14-labeled decane and biphenyl at near-saturation levels, they found that only 30 percent (by

weight) partitioned into the clay. The results of our work and others, however, suggest that the molecular weights of decane and biphenyl are too low to be representative of the types of compounds that should be expected to readily adsorb onto particulates. Further, their study involved no agitation, so it is not directly comparable to the results of Zurcher and Thuer or to the field data obtained in the IXTOC-I study.

All of the laboratory studies mentioned, as well as field observations in previous, more confined situations, tend to support our findings from the IXTOC-I study. That is, a major storm can be expected to generate high levels of resuspended sediment, which in turn will readily scavenge the more insoluble, higher-molecular-weight hydrocarbons. This scavenging then affects subsequent dispersion and/or agglomeration, depending on the mixing forces at work. The more soluble, lower-molecular-weight aromatics, on the other hand, tend to undergo rapid dissolution. An interesting comparison could be made by sampling the IXTOC-I area at a subsequent time. A survey of water, particulate, and sediment loads should explain a great deal relative to the ultimate fate of the spilled oil.

5. ACKNOWLEDGMENTS

The authors extend appreciation to Bill Paplaswky, Gary Favara, Randy Jordan, Martha Kopplin, and Marti Wright for dedicated technical support in analysis and data reduction; to Lorelei Jones for typing, editing, and transcribing much of the text and tabulated data; to Cheryl Fish and Randee Luedecke for figure drafting and final report production; and to NOAA for committed scientific interest and financial support through Contract NA80RCA00013.

6. REFERENCES

Bassin, N. J., and T. Ichiye (1977): Flocculation behavior of suspended sediments and oil emulsions. J. Sed. Pet., 47: 671-677.

Bodman, R. H., L. V. Slabaugh, and V. T. Bowen (1961): A multipurpose large volume sea water sampler. J. Mar. Res., 19: 141-148.

Boehm, P. D., and D. L. Fiest (1980): Aspects of the transport of petroleum hydrocarbons to the offshore benthos during the IXTOC I blowout in the Bay of Campeche. Presented at the NOAA RESEARCHER/PIERCE IXTOC-I Program Symposium, Miami, Florida, June 9-10.

Brown, R. A., and H. L. Huffman, Jr. (1976): Hydrocarbons in open ocean waters. Science, 191: 847-849.

Calder, J. (1979): Weathering effects on chemical composition of the AMOCO CADIZ oil. Presented at the Annual Meeting of the American Association for the Advancement of Science, Houston, Texas.

deLappe, B. W., R. W. Risebrough, J. C. Shropshire, E. F. Letterman, W. R. Sistek, and W. Walker II (1979): Hydrocarbons in the waters of the Southern California Bight in 1977. Submitted to U. S. Department of Interior, Bureau of Land Management, as Science Applications, Inc., Report No. SAI-77-917-LJ: 50 pp.

deLappe, B. W., R. W. Risebrough, A. M. Springer, T. T. Schmidt, J. C. Shropshire, E. F. Letterman, and J. R. Payne (1980): The sampling and measurement of hydrocarbons in natural waters. In: Hydrocarbons and Halogenated Hydrocarbons in the Aquatic Environment, B. K. Afghan and D. Mackey (Eds.). Plenum Press, New York: 29-68.

Dexter, R. N., and S. P. Pavlou (1978): Mean solubility and aqueous activity coefficients of stable organic chemicals in the marine environment: Polychlorinated biphenyls. Mar. Chem., 6: 41-53.

Gearing, J. N., P. J. Gearing, T. Wade, J. G. Quinn, H. B. McCarty, J. Farrington, and R. F. Lee (1979): The rates of transport and fates of petroleum hydrocarbons in a controlled marine ecosystem and a note on analytical variability. In: Proceedings of the 1979 Oil Spill Conference (Prevention, Behavior, Control, Cleanup), Los Angeles, California: 555-564.

Malinky, G., and D. G. Shaw (1979): Modeling the association of petroleum hydrocarbons and sub-arctic sediments. In: Proceedings of the 1979 Oil Spill Conference (Prevention, Behavior, Control, Cleanup), Los Angeles, California: 621-624.

Meyers, P. A., and J. G. Quinn (1973): Association of hydrocarbons and mineral particulates in saline solutions. Nature, 244: 23-24.

Nelsen, T. A. (1980): Mineralogy of suspended and bottom sediments in the vicinty of the IXTOC-I blowout, September 1979. Presented at the NOAA RESEARCHER/PIERCE IXTOC-I Program Symposium, Miami, Florida, June 9-10.

Parker, P. L., and S. Macko (1978): An intensive study of the heavy hydrocarbons in the suspended particulate matter of seawater, South Texas Outer Continental Shelf Study (Chapter 11). Submitted to U. S. Department of Interior, Bureau of Land Management, from Univ. of Texas Marine Science Inst.

Payne, J. R., J. R. Clayton, Jr., B. W. deLappe, P. L. Millikan, J. S. Parkin, R. K. Okazaki, E. F. Letterman, and R. W. Risebrough (1978): Hydrocarbons in the Water Column, Southern California Baseline Study. Submitted to U. S. Department of Interior, Bureau of Land Management as Science Applications, Inc. Report No. SAI-76-809-LJ: 149 pp.

Payne, J. R., N.W . Flynn, J. E. Nemmers, P. J. Mankiewicz, and G. S. Smith (1980): Surface evaporation/dissolution partitioning of lower molecular weight aromatic hydrocarbons in a down-plume transect from the IXTOC-I wellhead. Presented at the NOAA RESEARCHER/PIERCE IXTOC-I Program Symposium, Miami, Florida, June 9-10.

Risebrough, R. W., B. W. deLappe, and T. T. Schmidt (1976): Bioaccumulation factors of chlorinated hydrocarbons between mussels and seawater. Mar. Pollut. Bull., 7: 225-228.

Suess, E. (1968): Calcium carbonate interactions with organic compounds. Ph.D. Thesis, Lehigh Univ., Bethlehem, Pa.

Wheeler, R. B. (1978): The fate of petroleum in the marine environment. Exxon Production Research Co., Special Report.

Winters, J. K. (1978): Fate of petroleum-derived aromatic compounds in seawater held in outdoor tanks and South Texas Outer Continental Shelf Study (Chapter 12). Submitted to U. S. Department of Interior, Bureau of Land Management, from Univ. of Texas Marine Science Inst.

Zurcher, F., and M. Thuer (1978): Rapid weathering processes of fuel oil in natural waters - analysis and interpretations. Environ. Sci. and Technol., 12: 838-843.

Zurcher, F., M. Thuer, and J. A. Davis (1980): Importance of particulate matter on the load of hydrocarbons of motorway runoff and secondary effluents. In: Hydrocarbons and Halogenated Hydrocarbons in the Aquatic Environment, B. K. Afghan and D. Mackay (Eds.). Plenum Press, New York: 373-386.

SUBSURFACE DISTRIBUTIONS OF PETROLEUM FROM AN OFFSHORE WELL BLOWOUT - THE IXTOC-I BLOWOUT, BAY OF CAMPECHE

David L. Fiest and Paul D. Boehm
Environmental Sciences Division
Energy Resources, Co., Inc. (ERCO)
185 Alewife Brook Parkway
Cambridge, Massachusetts 02138

ABSTRACT

Concentrations of oil were measured in seawater in the vicinity of the blowout of the exploratory well IXTOC-I located in the Bay of Campeche (Gulf of Mexico) during the month of September 1979. Seawater samples from more than 20 stations located within 100 km of the blowout were analyzed aboard ship for petroleum hydrocarbons by synchronous fluorescence spectroscopy. Concentrations of oil ranged from 5 µg/L at a distance of 80 km to 10,600 µg/L within several hundred meters of the blowout. A subsurface plume of oil droplets suspended in the top 20 m of the water column extended 25 km to the northeast of the blowout. The physical processes which might be controlling the behavior of the oil in the plume are discussed.

1. INTRODUCTION

A significant part of the oil released to the marine environment from a tanker spill or a well blowout may be retained and dispersed in the water column. The relative amount of oil which resides in the water column is a function of a number of factors, including the chemical and physical nature of the oil, the point of release, the sea surface turbulence, and other hydrographic conditions. During an undersea well blowout, very favorable conditions exist for retention and transport of particulate, dispersed, and dissolved oil in the water column. For example, the turbulent subsurface release of the oil is expected to enhance the formation of small droplets of oil. These droplets can be retained in the water column for a period of time during which ocean currents can carry them away from the blowout. The formation of droplets increases the surface area of the oil, thereby increasing the rates of physical/chemical and biological processes such as dissolution and microbial attack. Measurements of the concentrations of oil in seawater are important for assessing the potential impact on marine organisms and for predicting the dispersion and weathering pattern of the oil.

Concentrations of hydrocarbons in seawater have been measured in coastal water following oil spills (Grahl-Nielsen, 1978; Grosse and Mattson, 1977; Levy, 1971; Boehm et al., 1978; Boehm, 1979; Calder et al., 1978) in oil spill test tanks (Gordon et al., 1976) and in uncontaminated seawater (Gordon et al., 1974; Berryhill, 1977; Brown et al., 1973). Reported concentrations generally are < 1 µg/L for "clean" open ocean seawater, 2-100 µg/L for oil spills in nearshore environments, and 100-800 µg/L in heavily polluted urban environments (e.g., Boston Harbor). Prior to this study of the IXTOC-I blowout, few measurements of oil concentrations in the vicinity of a well blowout had been reported. The notable exceptions are those reported by Mackie et al. (1978) and Grahl-Nielsen (1978), after the Ekofisk blowout in the North Sea, and Brooks et al. (1978), after a gas well blowout in the northwestern Gulf of Mexico.

The exploratory well IXTOC-I, located in 48 m of water 80 km northwest of Ciudad del Carmen, Mexico, in the Bay of Campeche (Gulf of Mexico), blew out on June 3, 1979. Estimates of the rate of release of oil during the first four months range from 10,000 to 30,000 barrels per day (OSIR, 1980). The oil slick was transported to the north and west of the well from June until early September 1979. However, in mid-September, a shift in prevailing currents transported the spilled oil to the east and south of the platform. Floating booms and oil dispersants were used periodically in the vicinity of the blowout to mitigate the impact of the oil. A continuous fire at the blowout site consumed an unknown fraction of the gaseous and volatile components of the oil. The liquid portion of the oil underwent emulsification with seawater either during or subsequent to its release to the water column.

The data presented here were collected as part of a NOAA-sponsored study of the IXTOC-I well blowout. Scientists aboard the ships R/V RESEARCHER and C/V PIERCE conducted a research cruise in the western Gulf of Mexico from September 11 to October 3, 1979. While samples were being collected near the well, no booming or dispersant spraying operations were being conducted. Hurricane Henri passed near the well on September 15-16 and caused extensive flooding in adjacent onshore areas and subsequent freshwater runoff. The station locations are shown on the chart of the study area (Figure 1); they are oriented for the most part along the observed axis of the surface oil plume.

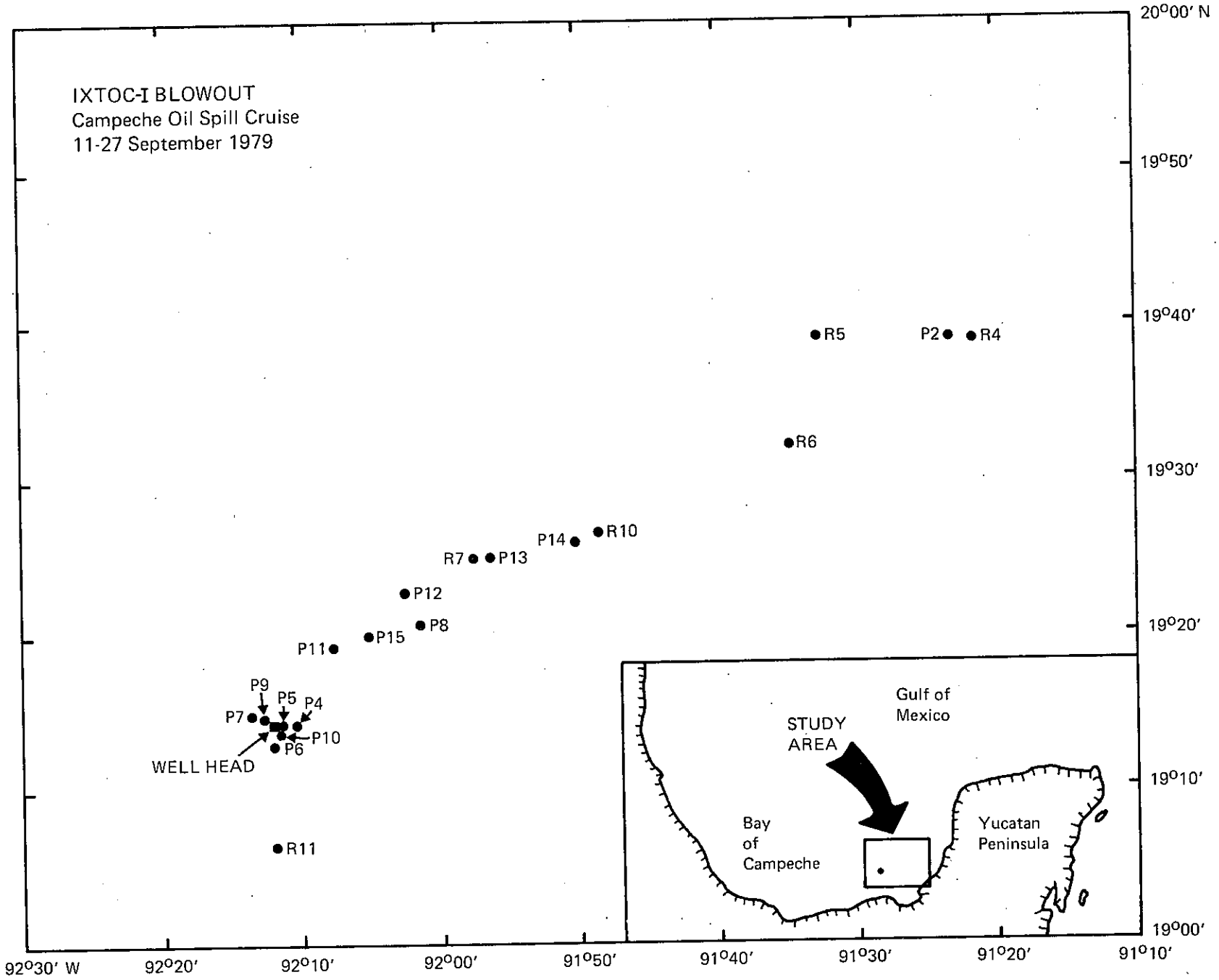

Figure 1. Detailed map of wellhead region.

2. EXPERIMENT

Samples from the immediate vicinity of the IXTOC-I blowout were collected between September 14 and 21, 1979. Seawater was collected with a 10-liter Teflon-lined GO-FLO Sampler (General Oceanics), a 30-liter glass Bodman bottle (Gagosian et al., 1979), a 90-liter aluminum Bodega Bodman bottle (Payne et al., 1977), or a submersible pumping system. The pumping system consisted of a submersible pump (Cole Parmer Model 7111: nylon impeller, silicone rubber gaskets, Viton seals) and 2-m sections of stainless steel tubing (0.5-inch O.D. type 903) connected with 0.5-m flexible stainless steel joints and stainless steel quick connects (Swagelock: Viton seals). Immediately following collection, a 1-liter sample was drawn from each sampler, preserved with 100 ml of dichloromethane (Burdick and Jackson, UV grade) and stored at ambient temperature awaiting extraction.

The unfiltered water sample was transferred to a 1-liter separatory funnel and extracted three times with 50 ml of dichloromethane. At a few stations, the seawater collected by the pumping system was pressure filtered through a 142-mm, 0.45-μ glass fiber filter held in a stainless steel filter holder (Millipore) prior to extraction. The solvent extract was dried over sodium sulfate, transferred to a Kuderna-Danish apparatus, and concentrated to 1 ml. The dichloromethane was displaced by repeatedly adding hexane (Burdick and Jackson, UV grade) and evaporating under a stream of purified nitrogen.

The hexane extracts were analyzed for petroleum hydrocarbons using a synchronous fluorescence spectroscopy technique (Wakeham, 1977; Gordon and Keizer, 1974). In summary, a measured aliquot of the sample extract was dissolved in a known volume of hexane. The intensity of the fluorescence emission was measured from 250 to 500 nm while synchronously scanning at an excitation wavelength 25 nm shorter than the wavelength at which the emission was measured. This technique measures aromatic hydrocarbons with a two to five-ring aromatic structure (Lloyd, 1971). The analysis was done on board the R/V RESEARCHER using a Farrand Mark I spectrofluorometer equipped with corrected excitation and emission modules. The instrument conditions were as follows: excitation slit - 2.5 nm, emission slit - 5.0 nm, scan speed - 50 nm per minute, sample cell - single 10 mm non-fluorescing quartz cell.

The intensities of the fluorescence spectra were measured at several wavelengths which correspond to peak maxima present in an IXTOC-I reference oil sample. The fluorescence spectra were converted to relative concentration units by comparing the peak height at 312 nm to that of a No. 2 fuel oil standard (API Reference No. 2). The No. 2 fuel oil is comprised primarily of two-ring aromatics which are responsible for the fluorescence in the 312-nm region of the spectra.

The concentrations of oil in No. 2 fuel oil equivalents were converted to absolute concentrations by multiplying by a factor of 2.30. This factor was determined from a linear regression of oil concentrations in No. 2 fuel oil equivalents versus concentrations measured by gravimetry using a Cahn electrobalance. The samples used for this calibration had gravimetric concentrations of oil which ranged from 74 to 1700 μg/L by gravimetry. The fluorescent material in samples with low concentrations (< 20 μg/L) differs chemically from the material in the samples used for the regression. Although a lower conversion factor should have been used because of this discrepancy, none is available from existing data and the same conversion factor was used for all calculations.

3. RESULTS

The concentrations of oil in the water column ranged from values of less than 5 µg/L at a distance of 80 km from the blowout to peak values of 10,600 µg/L within a few hundred meters of the blowout. The highest concentrations were observed within 25 km of the blowout in the top 6 m of the water column. The higher values reported here may be an underestimate, since some oil was visibly adsorbed onto the walls of the bottle samplers during sampling in the plume.

The concentration data are summarized in Figure 2, which is a contoured vertical cross section of the oil concentrations along the plume axis. Elevated concentrations of oil occurred 40 km to the northeast of the well. At distances greater than 40 km to the northeast and 2 km to the south and west, concentrations were, with a few exceptions, less than 5 µg/L. The northeastern orientation of the oil-contaminated seawater plume coincided with the observed direction of movement of the surface plume of oil. However, emulsified oil was observed floating on the ocean surface at distances greater than the apparent extent of the oil-contaminated seawater plume, whereas, surface oil was found 80 km or more to the northeast of the well; elevated concentrations of oil in the water column were limited to within 40 km. It is apparent that somewhat dissimilar processes are controlling the transport of surface and subsurface oil.

Several distinct spectral patterns were observed among the samples that were collected (Figure 3). Samples containing low concentrations (< 5 µg/L) had a spectrum with a single fluorescence peak at 308 nm (Type A). This spectrum results from either background fluorescent material in seawater or low-level contaminants from the sample workup. Samples with concentrations from 5 to 20 µg/L had a single peak spectrum with a peak maximum at 312 nm (Type B). This peak results from a predominance of petroleum-derived, two-ring aromatics which fluoresce from 310 to 330 nm (Lloyd, 1971). As discussed below, this spectral type reflects the selective dissolution by seawater of two-ring aromatics from the whole oil released from the blowout. Spectral Type D is characterized by a series of flourescent peaks at 312 nm, 328 nm, 355 nm, and 405 nm. This spectrum was predominant for samples with concentrations greater than 20 µg/L. The series of peaks results from two-, three-, four-, five- and larger-ring polycyclic aromatic compounds (Lloyd, 1971). Type D spectra were similar to spectra of the whole oil collected from surface mousse samples.

At a few stations, samples of both whole seawater and filtered seawater through a 0.45-µm glass fiber filter from the same depth were analyzed. At stations with low concentrations of oil (PIX 01, PIX 02, and PIX 14), no systematic differences between the filtered and unfiltered samples were found. However, at Station PIX 08, the concentrations of oil in the filtered samples were 21 and 28% of the concentrations in unfiltered samples collected at 6 and 16 m, respectively (Table 1). In both cases, the spectrum of the filtered sample was depleted in the three- to five-ring region compared to the unfiltered sample.

The distinction between the three spectral types was confirmed by glass capillary gas chromatography analysis (Boehm and Fiest, this symposium). The saturated (f_1) and unsaturated (f_2) fractions of samples with Type D, whole

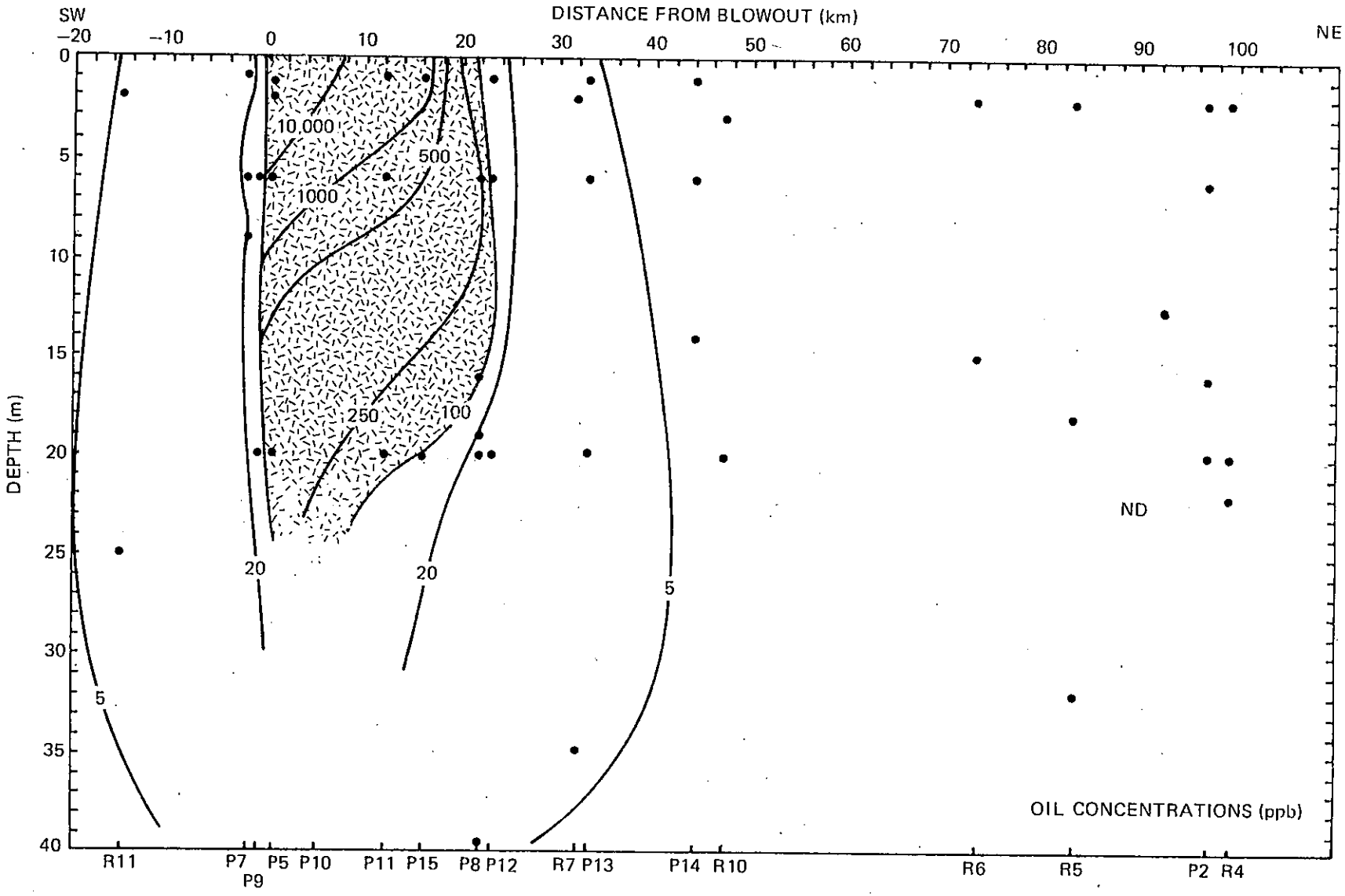

Figure 2. Concentrations of oil along a transect oriented to the northeast of the IXTOC-I blowout, September 1979.

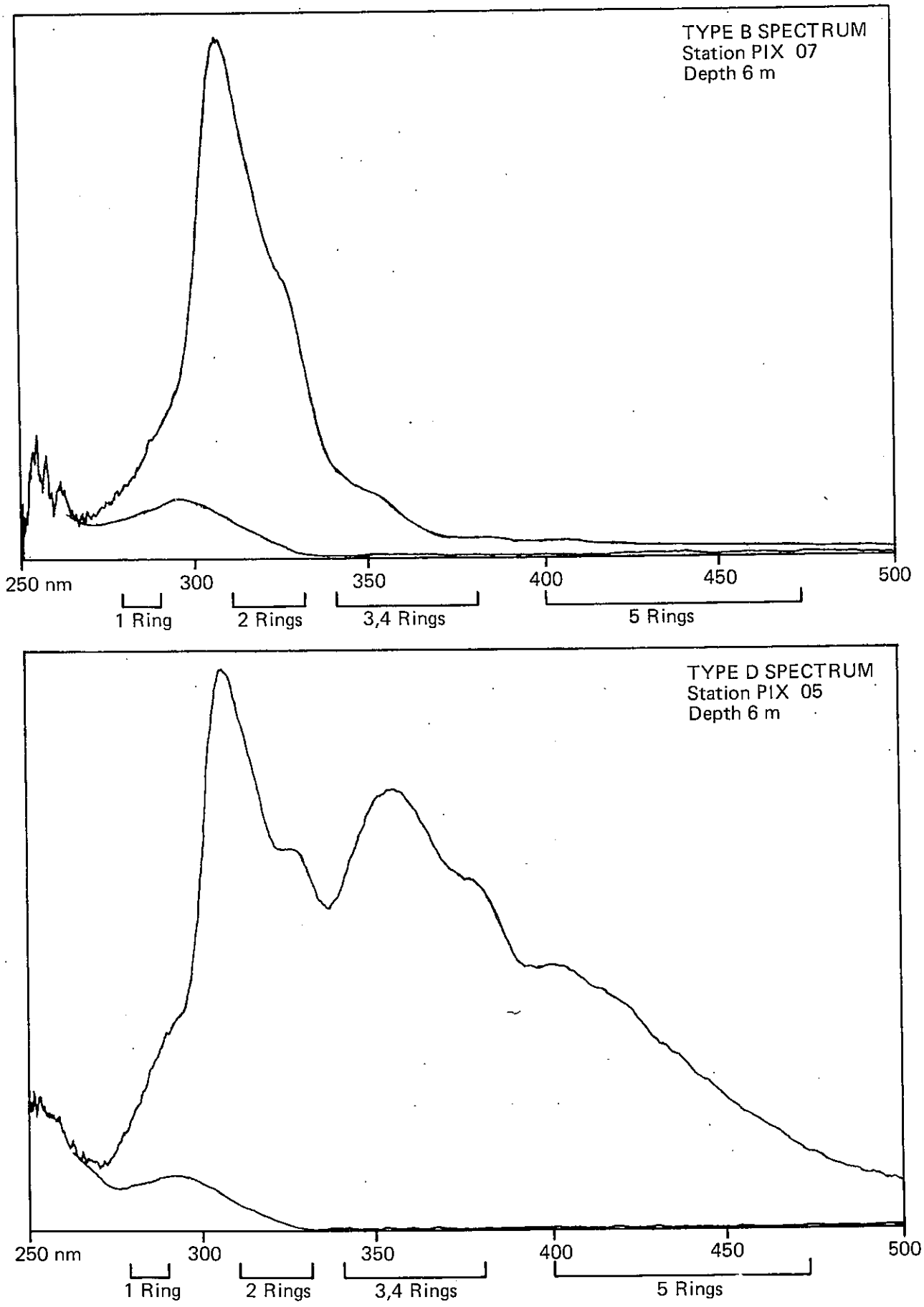

Figure 3. Representative synchronous fluoresence spectra of seawater samples collected near the IXTOC-I blowout.

Table 1. Concentrations of oil in filtered versus unfiltered water samples.

Station	Depth (m)	Concentration (μg/L) Unfiltered Sample	Filtered Sample	Filtered/ Unfiltered
PIX 08	6	416	87	0.21
	16	133	37	0.28

oil, spectra contained petroleum hydrocarbons in a boiling range equivalent to that of < n-C_{10} to n-C_{30} (Figure 4). The glass capillary gas chromatogram of the f_2 confirmed the presence of polycyclic aromatic hydrocarbons (PAH) with two to five rings. Normal alkanes from < n-C_{10} to n-C_{34} and a low-boiling unresolved complex mixture predominated in the f_1. Samples with Type B, dissolved oil, spectra contained predominantly substituted one- and two-ring aromatic hydrocarbons. Relatively small amounts of PAH with more than two rings and saturated hydrocarbons were present. Samples with Type A spectra contained very low amounts of material.

In summary, higher concentrations (> 20 µg/L) of oil were associated with Type D (whole oil) spectra and were found at shallow water depths (< 20 m) within 25 km northeast of the well. Moderate concentrations of oil (5-20 µg/L) occurred to the south and west of the well and from 25 to 40 km to the northeast of the well. Samples collected in this region were of spectral Type B, which is characterized by soluble two-ring aromatics. A comparison of oil concentrations in filtered and unfiltered seawater supports the contention that oil in the water column occurred in both a whole oil (droplet) form and a fractioned oil ("dissolved") form, although the operational definition of the material in the filtrate can include dissolved and colloidal oil as well as small oil droplets if the filter is overwhelmed.

4. DISCUSSION

Those samples with concentrations of oil greater than 20 µg/L had Type D spectra which contained two-, three-, and four-ring aromatic hydrocarbons. The high concentrations of oil in samples collected near the blowout probably resulted from suspension of oil droplets in the water column. This hypothesis is consistent with laboratory studies of the formation of oil-in-water dispersions (Zurcher and Thuer, 1978; Shaw and Reidy, 1979; Prouse et al., 1976). These studies have shown that under vigorous mixing conditions, droplets of oil, which contain two-, three-, four-, and five-ring aromatic compounds, are entrained in the water, and a Type D spectrum results. Since the high shear associated with an undersea blowout enhances the formation of oil-in-water dispersions (i.e., droplets), the predominance of oil droplets in the water samples is not unexpected.

Seawater samples with less than 20 µg/L of oil were collected at distances greater than 25 km from the blowout and have Type B spectra which are dominated by two-ring aromatic hydrocarbons. Two-ring aromatic hydrocarbons are one to two orders of magnitude more soluble than three- and four-ring structures (Mackay and Shiu, 1977). Laboratory studies have confirmed that under gentle mixing conditions, two-ring aromatics in oil are selectively dissolved by seawater which would result in a Type B spectrum dominated by a single peak. The same selection for two-ring aromatics occurs if the large (> 1 µm) droplets are removed from the vigorously mixed dispersion by filtration (Shaw and Reidy, 1979) or centrifugation (Zurcher and Thuer, 1978). In samples with Type B spectra, oil is present in a "dissolved" state. Two of the three filtered seawater samples collected within the oil plume also had Type B spectra. These two samples contained approximately 20 to 30% (37 and 87 µg/L) of the oil in the unfiltered sample.

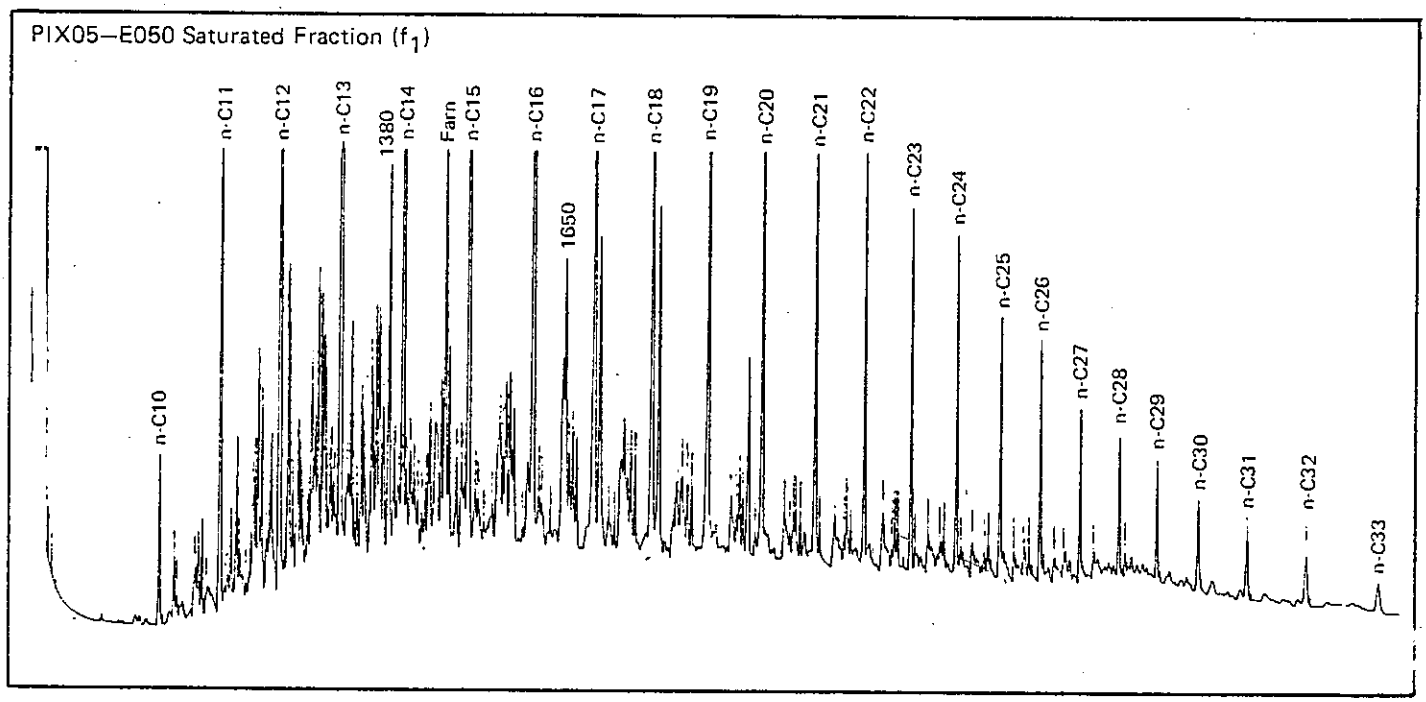

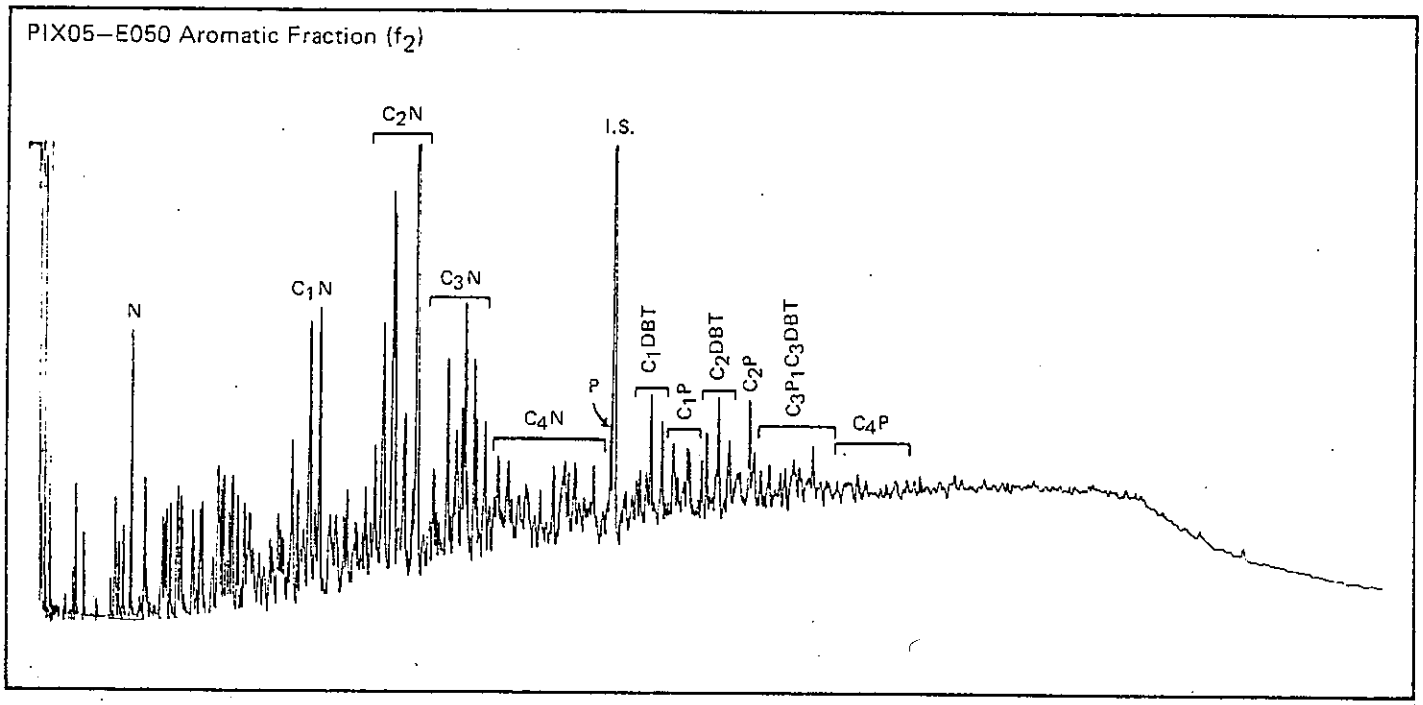

Figure 4. Glass capillary gas chromatograms of "reference oil."

We postulate that within the subsurface oil plume (within 5 km), high concentrations (> 600 µg/L) of oil droplets with diameters of > 0.45 µm predominated. Near the downstream edge of the oil-contaminated plume, 25 km from the blowout, moderate concentrations (100-300 µg/L) of oil droplets with diameters > 0.45 µm comprised 70-80% of the oil in the water. The remaining 20-30% consisted of two-ring aromatics "dissolved" in the water. Droplets of oil with diameters < 0.45 µm were not found near the edge of the plume, and low concentrations (< 20 µg/L) of "dissolved" two-ring aromatics predominated.

The absence of high concentrations of oil at depths below 20 m in the plume may have been the result of three processes. First, the plume of oil and water streaming from the blowout in the sea bed had a net upward velocity that could have caused it to rise quickly to the surface where it spread horizontally in response to prevailing currents. Second, the positive buoyancy of the oil droplets within the plume may have caused them to move vertically within the plume and remain close to the surface. Third, droplets of oil could have been generated by turbulence at the air/oil interface and subsequently driven down into the water column. The slightly positive buoyancy of the droplets would have retained them near the surface. Although we have no evidence to favor one hypothesis over another, it is apparent that the formation of oil droplets acts to concentrate the oil close to the surface.

Laterally, the subsurface oil plume was limited to within 25-40 km to the northeast of the blowout. Based on the assumption that the subsurface oil was moving to the northeast at a minimum speed of 0.5 knots, it would take approximately 28 hours for the oil to reach Stations PIX 08 and PIX 12 at the edge of the plume. Since these stations were sampled two to four days after Hurricane Henri had left the study site, oil streaming from the blowout would have had more than ample time to travel beyond these stations and reestablish a quasi-steady state subsurface plume. Processes other than simply the rate of advection of the oil must have been responsible for establishing the horizontal limitation of the subsurface plume.

One such process may have been a progressive agglomeration of smaller droplets to form larger droplets as oiled seawater was carried away from the blowout. According to Stokes Law, the formation of larger droplets would increase the positive buoyancy and upward velocity of the oil (Thuer and Stumm, 1977). Such a process would remove oil from the subsurface plume to the ocean surface as the oiled water moved away from the blowout.

Alternately, a frontal zone may have restricted the horizontal advection or diffusion of the plume. A vertical cross section of σ_T along the plume axis (Figure 5) suggests the possibility of such a front. The profile, which was generated from STD profiles and salinity and temperature measurements of discrete water samples at stations occupied over a five-day period of time, suggests the presence of a lens of less saline, less dense water to the northeast of the blowout. This lens may have resulted from freshwater runoff from the adjacent land, which had experienced heavy rains and flooding both prior to and during Hurricane Henri. The southward extent of the lens occurred between 25 and 40 km from the blowout, which was the location of both the strong subsurface oil concentration gradient and the loss of definition of the surface oil plume. Since the hydrographic data were collected over several days, they are not synoptic, and this hypothesis may be somewhat

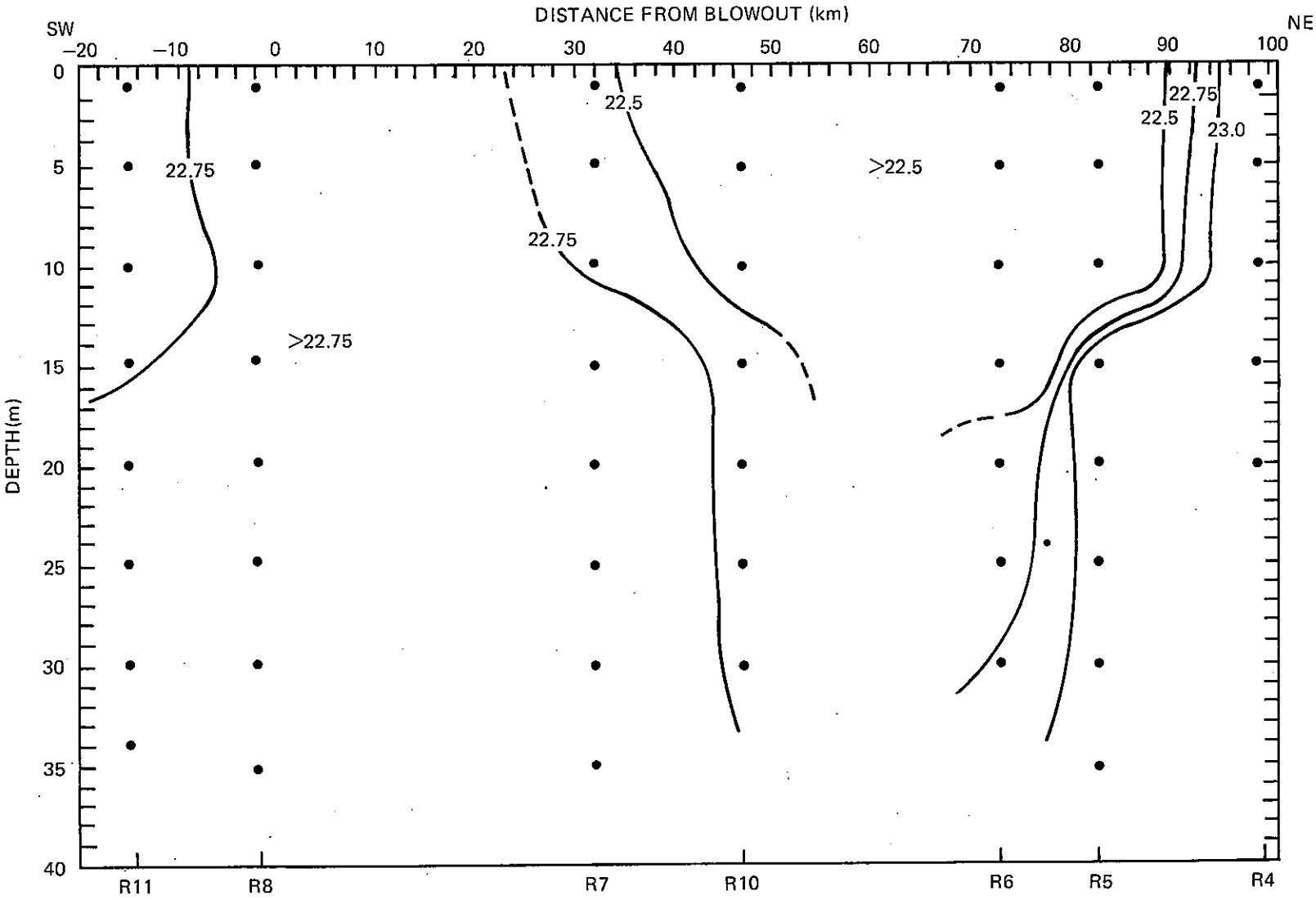

Figure 5. Sigma-t along a transect oriented to the northeast of the IXTOC-I blowout, September 1979.

speculative. Samples were not taken on either side of the transect near the gradient, which would allow the three-dimensional behavior of the oiled seawater plume to be better defined.

Low concentrations (< 20 µg/L) of oil occurred to the south and west of the well (Stations PIX 07, PIX 09, PIX 06, RIX 11). This demonstrated the strong influence of advection on the dispersion of oil from the blowout. During our sampling, the subsurface plume of oiled seawater and the surface plume were similarly aligned to the northeast under the presumed influence of oceanic currents. The wind vector was generally perpendicular to the direction of the movement of oil on the surface from the blowout. However, by the time the last station (RIX 11) in the vicinity of the blowout was occupied, the direction of the surface plume had shifted to a more southerly direction. Slightly elevated levels of oil found within the water column at this station may have resulted from the shift in plume orientation.

5. CONCLUSIONS

Oil released from the IXTOC-I blowout tended to form a plume of oil droplets suspended in the top 10-20 m of the water. The oiled seawater plume moved in a northeasterly direction, presumably in response to ocean currents rather than wind. The northeasterly horizontal diffusion/advection of the oiled seawater plume may have been inhibited or deflected by a lens of less saline water situated to the northeast of the blowout. Alternatively, the sharp boundary between the oiled seawater plume could have been the result of agglomeration and upward movement of the oil droplets in the plume.

Concentrations of oil within the plume ranged from 20 to > 10,000 µg/L. The highest concentrations of oil (up to 10,600 µg/L), which may have been underestimated due to absorption in the sampling systems, were found within the oiled seawater plume near the IXTOC-I blowout. These values were in the same range as concentrations found underneath oil slicks during experimental surface spills in the New York Bight (McAuliffe et al., 1980). During these spills maximum concentrations within the top 3-9 m of water ranged from 950 µg/L under an untreated slick to 17,800 µg/L under a slick treated with dispersant. Concentrations of oil (2-300 µg/L) measured in the vicinity of the Ekofisk blowout in the North Sea (Mackie et al., 1978; Grahl-Nielsen, 1978) were comparable to concentrations at the outside edge of the oil plume at the IXTOC-I blowout. The higher concentrations of subsurface oil found during the IXTOC-I blowout resulted from the subsurface release of oil rather than a release at or above the ocean's surface, as occurred during the Ekofisk blowout.

The horizontal and vertical limitations of the size of the oiled seawater plume from the IXTOC-I blowout suggest that both the physical properties of the oil (i.e., droplet size and density) and the density and current structure of the seawater controlled the dispersal of oil from this undersea blowout. Oceanic frontal systems may act as barriers to subsurface transport of oil and may also act as conduits for subsurface movement of oil along the frontal axis.

6. ACKNOWLEDGMENTS

The authors acknowledge the valuable assistance given by the following individuals to the intensive shipboard sampling effort: Keith Hausknecht, Jack Barbash, and George Perry (ERCO); John Farrington (Woods Hole Oceanographic Institution); James Payne (Science Applications, Inc.); Larry McCarthy (University of New Orleans); Donald Atwood, Chief Scientist (NOAA); and the officers and crew of the R/V RESEARCHER and C/V PIERCE.

This work was supported by a research contract from the National Oceanic and Atmospheric Administration Office of Marine Pollution Assessment (No. NA 79 RAC 00151).

7. REFERENCES

Barbier, M., D. Joly, A. Saliot, and D. Tourres (1973): Hydrocarbons from Sea water. Deep-Sea Res., 20: 305-314.

Berryhill, H. L. (1977): Environmental studies. South Texas outer continental shelf, 1975: An atlas and integrated summary. U.S. Bureau of Land Management, New Orleans, Louisiana.

Boehm, P. D. (1979): Evidence for the decoupling of dissolved, particulate and surface microlayer hydrocarbons in Northwestern Atlantic continental shelf waters. Mar. Chem. (in press).

Boehm, P. D., G. Perry, and D. Fiest (1978): Hydrocarbon chemistry of the water column of Georges Bank and Nantucket Shoals, February-November, 1977. In: Proceedings of a Symposium: In the Wake of the ARGO MERCHANT, 11-13 January 1978, URI, Kingston, R.I.

Brooks, J. M., B. B. Bernard, T. C. Sauer, Jr., and H. Abel-Reheim (1978): Environmental aspects of a well blowout in the Gulf of Mexico. Environ. Sci. Tech., 12: 695-703.

Brown, R. A., T. D. Searl, J. J. Eliot, B. G. Phillips, D. E. Brandon, and P. H. Monaghan (1973): Distribution of heavy hydrocarbons in some Atlantic Ocean waters. Joint Conference on Prevention and Control of Oil Spills, API, Washington, D.C.: 505-519.

Calder, J. A., J. Lake, and J. Laseter (1978): Chemical composition of selected environmental and petroleum samples from the AMOCO CADIZ oil spill. NOAA/EPA Special Report. The AMOCO CADIZ Oil Spill: A Preliminary Scientific Report: 283 pp.

Gagosian, R B., J. P. Dean, Jr., R. Hamblin, and O. C. Zafiriou (1979): A versatile interchanageable chamber seawater sampler. Limnol. Oceanogr., 24: 583-588.

Gordon, D. C., Jr., and P. D. Keizer (1974): Estimation of petroleum hydrocarbons in seawater by fluorescence spectroscopy: Improved sampling and analytical methods. Fisheries Research Board, Canada, Technical Report No. 481.

Gordon, D. C., Jr., P. D. Keizer, and J. Dale (1974): Estimates using fluorescence spectroscopy of the present state of petroleum hydrocarbon contamination in the water column of the Northwest Atlantic Ocean. Mar. Chem., 2: 251-261.

Gordon, D. C., Jr., P. D. Keizer, W. R. Hardstaff, and D. G. Aldous (1976): Fate of crude oil spilled on seawater contained in outdoor tanks. Environ. Sci. Tech., 10: 580-585.

Grahl-Nielsen, O. (1978): The Ekofisk Bravo blowout. Petroleum hydrocarbons in the sea. In: Proceedings of the Conference on Assessment of Ecological Impacts of Oil Spills. AIBS, 14-17 June 1978, Keystone, CO.

Grosse, P. L., and J. S. Mattson (1977): The ARGO MERCHANT oil spill. A preliminary scientific report. U. S. Department of Commerce, NOAA/ERL, Boulder, CO.

Iliffe, T. M., and J. A. Calder (1974): Dissolved hydrocarbons in the eastern Gulf of Mexico loop current and the Caribbean Sea. Deep-Sea Res., 21: 481-488.

Levy, E. M. (1971): The presence of petroleum residues off the east coast of Nova Scotia. Water Res., 5: 723-733.

Lloyd, J. B. F. (1971): The nature and evidential value of the luminescence of automobile engine oil and related materials. In: Synchronous excitation of fluorescence emission. J. Forensic Science Soc., 11: 83-94.

Mackay, D., and W. Y. Shiu (1977): Aqueous solubility of polynuclear aromatic hydrocarbons. J. Chem. Eng. Data, 22: 399.

Mackie, P. R., R. Hardy, and K. J. Whittle (1978): Preliminary assessment of the presence of oil in the ecosystem at Ekofisk after the blowout, April 22-30, 1977.

McAuliffe, C. D, G. P. Canevari, T. D. Searl, J. C. Johnson, and S. H. Greene (1980): The dispersion and weathering of chemically treated crude oils on the sea surface. In: Proceedings of the International Conference of Petroleum and the Marine Environment, 27-30 May, 1980, Monaco.

Oil Spill Intelligence Report (OSIR) (1980): Special Report: Ixtoc I. January 4, 1980 Newsletter. Center for Short-Lived Phenomena, Cambridge, MA.

Payne, J. R., J. R. Clayton, Jr., B. W. de Lappe, P. L. Millikin, J. S. Parkin, R. K. Okazaki, E. F. Letierman, and R. W. Risebrough (1977): Hydrocarbons in the water column. Southern California Baseline Study, Vol. III, Report 3.2.3. Final Report, submitted to the Bureau of Land Management, Washington, D.C.: 1-207.

Prouse, N. J., D. C. Gordin, Jr., and P. D. Keizer (1976): Effects of low concentrations of oil accommodated in sea water on the growth of unialgal marine phytoplankton cultures. J. Fish. Res. Board Can., 33: 810-818.

Shaw, D. G., and S. K. Reidy (1979): Chemical and size fractionation of aqueous petroleum dispersions. Environ. Sci. Tech., 13: 1259-1263.

Thuer, M., and W. Stumm (1977): Sedimentation of dispersed oil in surface water. Prog. Wat. Tech., 9: 183-194.

Wakeham, S. G. (1977): Synchronous fluorescence spectroscopy and its application to indigenous and petroleum-derived hydrocarbons in lacustrine sediments. Environ. Sci. Tech., 11: 272-276.

Zurcher, F., and M. Thuer (1978): Rapid weathering processes of fuel oil in natural waters: Analyses and interpretations. Environ. Sci. Tech., 12: 838-843.

MINERALOGY OF SUSPENDED AND BOTTOM SEDIMENTS IN THE VICINITY OF THE IXTOC-I BLOWOUT, SEPTEMBER 1979

Terry A. Nelsen
Marine Geology and Geophysics Laboratory
National Oceanic and Atmospheric Administration
15 Rickenbacker Causeway
Miami, Florida 33149

1. INTRODUCTION

On June 3, 1979, the IXTOC-I well on the continental shelf west of the Yucatan Peninsula blew out and began spilling oil into the Bay of Campeche. In the following months, the National Oceanic and Atmospheric Administration of the U.S. Department of Commerce sponsored an oceanographic cruise, known as IXTOC-I, to study the dispersal and subsequent chemical changes of this oil in the marine environment. During the course of this cruise, several storms and a hurricane (Henri) impacted the study area in the vicinity of the IXTOC-I site. Although this inclement weather hampered working operations at the time, it may have provided us with an insight into the storm response of the study area which would not have been possible during calm weather.

It was noted during the IXTOC-I cruise (Donald K. Atwood, personal communication) that the continental shelf water in the vicinity of the well site was quite turbid. This turbid zone extended landward at least to the landward-most sample station and seaward past the well site for four to five miles. At this point, an abrupt transition took place seaward of which clear blue Gulf water existed. Because of the relatively shallow depths (i.e., < 60 m) encountered in this section of the Campeche Shelf, coupled with the high-energy storm activity at that time, one could pose the following questions:

(1) Was there mineral matter suspended in the water column at the time of the IXTOC-I cruise that could have added to or been the source of water turbidity in the vicinity of the IXTOC-I well?

(2) If so, is it just a surface effect due to runoff from the land, is it resuspension from the bottom, or both?

(3) What minerals, if any, are present and what is their potential for sorption of hydrocarbon materials?

(4) Can mineralogy distribution patterns, if decipherable, give us hints as to the long-term dispersal patterns in the study area?

It will be the object of this study to attempt to answer these questions with the available sample suite taken during the IXTOC-I cruise.

From the limited amount of geological literature on the study area available to the author, some insight into the regional sediment types and mineralogy can be obtained. It is clear from a study by Logan et al. (1969) that the entire Yucatan Shelf south to approximately 20°N latitude is composed entirely of biogenic carbonate sediments. In a study of Terminos Lagoon, just south of Logan's area, Phleger and Ayala-Castanares (1971) note that the lagoon is on the boundary of the carbonate province which is to the east and northeast and the terrigenous province, which is to the west. This is diagiamatically shown in Figure 1. Their work also shows that net water flow through the lagoon is inward at the eastern inlet and outward through the western inlet. At present,

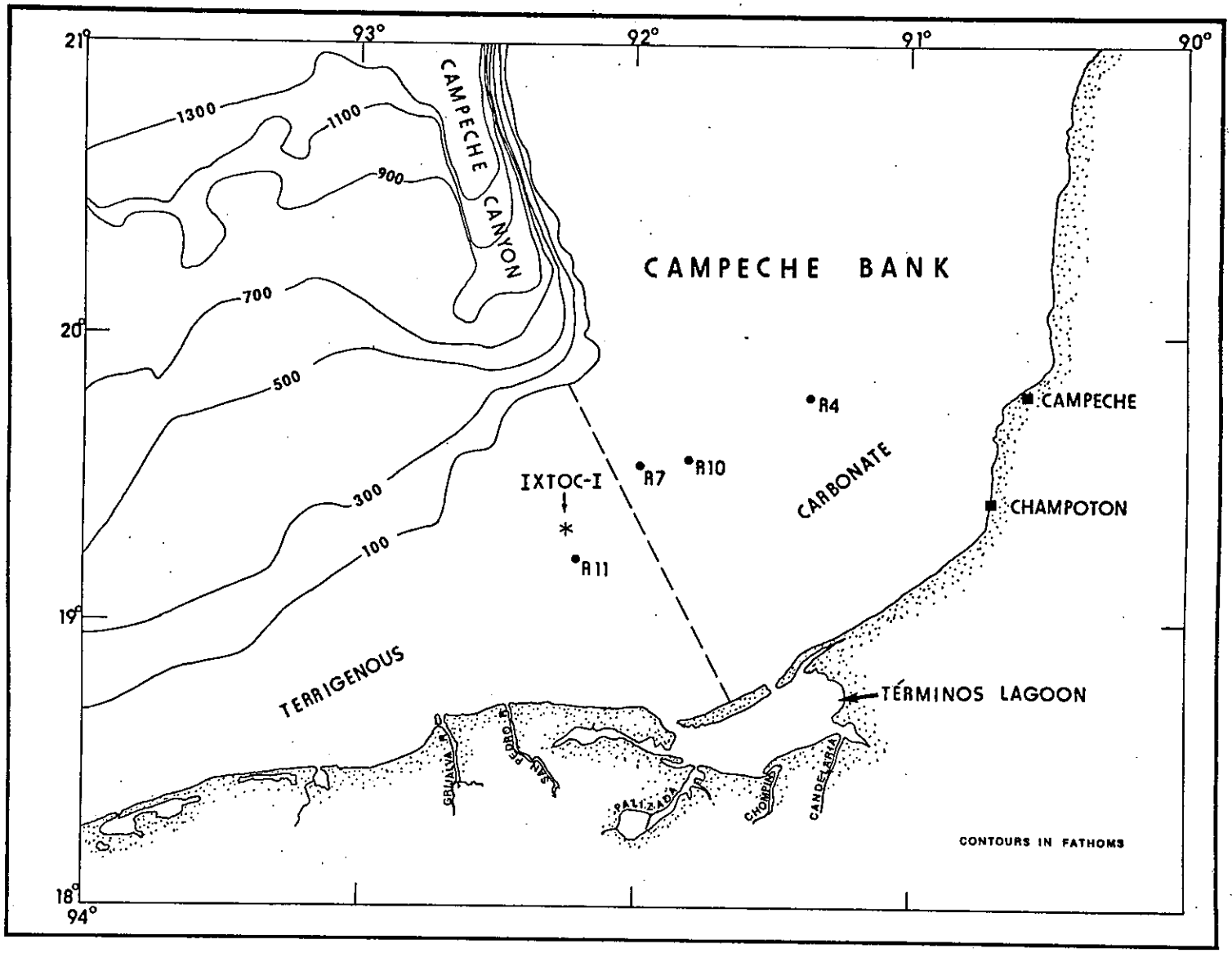

Figure 1. General bathymetry and continental shelf configuration (after Creager, 1958) in the vicinity of the IXTOC-I well site showing the RESEARCHER station locations considered in this study. The dashed line represents an approximate boundary between the carbonate province to the east and the terrigenous province to the west.

river-borne terrigenous sediments delivered to the filled lagoon are bypassing it and are being distributed westward along the nearshore zone of the shelf under the influence of the predominant circulation pattern noted above. This is well illustrated in Figure 2, which is a space photograph from Gemini-5 from Phleger and Ayala-Castanares (1971, their Fig. 9).

The terrigenous mineralogy in this area has been shown to contain quartz, feldspar, and heavy minerals in the sand-sized fraction (Freeland, 1971) with kaolinite, illite, and smectite (montmorillonite) in the fine silt to clay fraction (Creager, 1958).

2. METHODS

2.1 Sampling Strategy

Because water column sampling during the cruise was not done with suspended mineralogy in mind, the mineralogy portion of the IXTOC Program had to rely on samples collected initially for organic chemical analysis. In order to evaluate the potential role of resuspension to the water turbidity near the well site, only sample stations at which bottom sediment were collected in conjunction with water column samples could be considered. This reduced the choices to four stations (RIX-4, 7, 10, and 11). Their locations relative to the IXTOC-I well, the shelf and slope bathymetry, and the landmass of Mexico are shown in Figure 1, while their exact locations, depths, and sample numbers are recorded in Table 1. These four stations, as well as the IXTOC-I well site have also been superimposed on Figure 2. Although the weather conditions, as well as the phase of the tide, were unknown before and during the time of the photo, it can be seen that a turbid plume extends from the nearshore zone adjacent to the western (exit) inlet of the lagoon outward across the shelf toward station RIX-11 (R-11). This indicates a potential high-level (i.e., water column) transfer of material from terrigenous sources to the shelf. Since the differences in mineralogy, if any, between the lagoon and the open shelf sediments were unknown to the author, five bottom sediment samples from within the lagoon were also analyzed. Figure 3 shows the locations of these samples (#4, 8, 9, 14, 16) which were collected during another project.

2.2 Sample Preparation

Samples collected in the water column were taken initially with only organic chemistry in mind, and for this reason were filtered onto glass fiber filters. Initial sample treatment was for extraction and analysis of organic material, the results of which are presented elsewhere in this volume. The organic extraction of each filter pad consisted of tearing the filter into small fragments and refluxing in 27% methanol/73% hexane for four hours, followed by a four-hour reflux with methylene chloride. It was the opinion of this author that these extraction techniques would have no deleterious effects

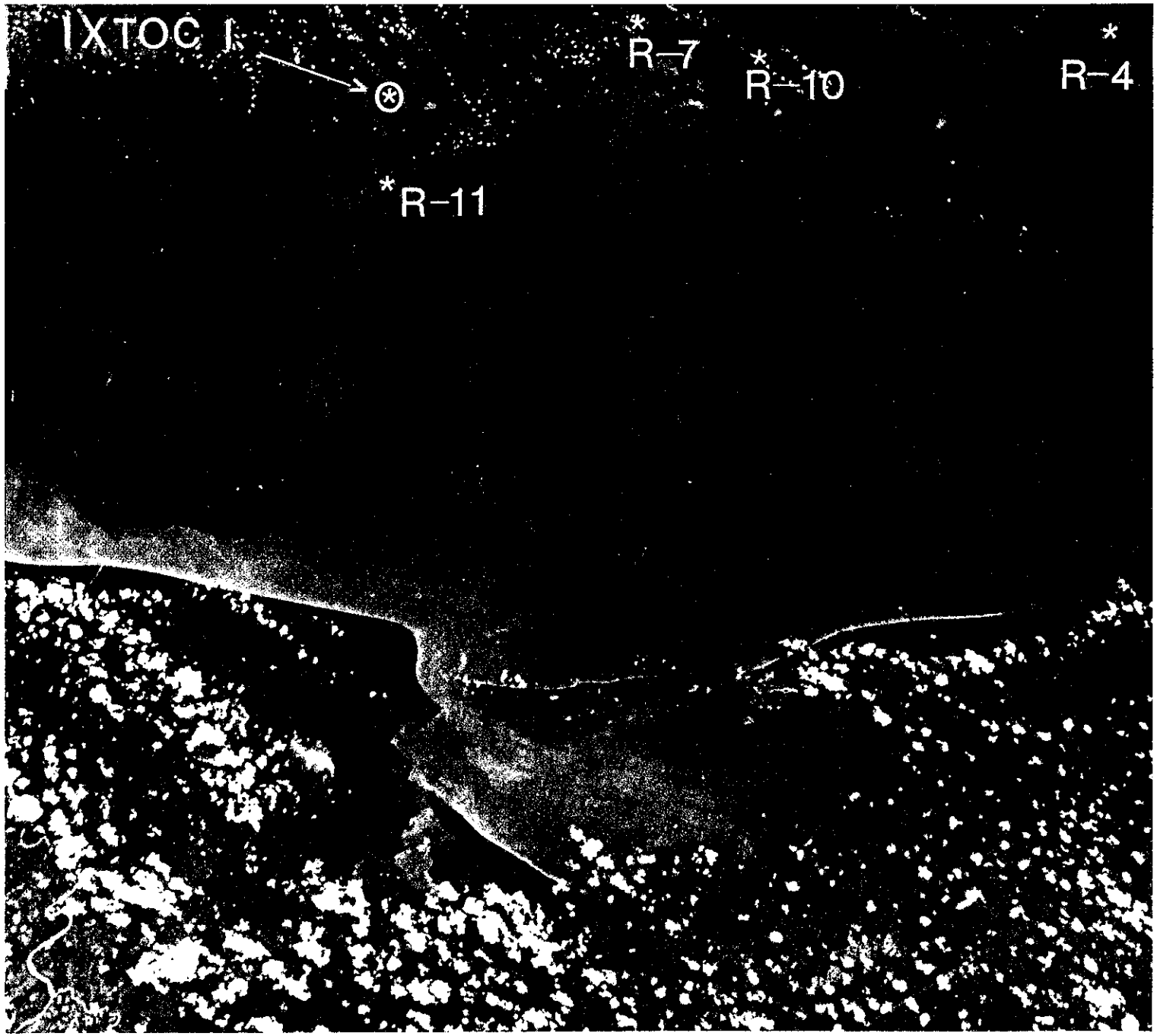

Figure 2. A Gemini-5 space photograph of Terminos Lagoon (from Phleger and Ayaly-Castanares, 1971) with the IXTOC-I well site and RESEARCHER sample stations superimposed.

Table 1. RIX Sampled Locations

Station RIX-04: 19°48'N Lat, 91°22'W Long

RIX - 04-S001	@	1-3 m, suspended sediment
RIX - 04-S002	@	22 m, suspended sediment
RIX - 04-F007	@	28 m, bottom sediment

Station RIX-07: 19°33'N Lat, 91°59'W Long

RIX - 07-S002	@	1-3 m, suspended sediment
RIX - 07-S003	@	43 m, suspended sediment
RIX - 07-F025	@	55 m, bottom sediment

Station RIX-10: 19°36.1'N Lat, 91°49.4'W Long

RIX - 10-S001	@	surface, suspended sediment
RIX - 10-S003	@	42 m, suspended sediment
RIX - 10-F038	@	"bottom," bottom sediment

Station RIX-11: 19°06'N Lat, 92°12'W Long

RIX - 11-S001	@	1-3 m, suspended sediment
RIX - 11-S002	@	28 m, suspended sediment
RIX - 11-F046	@	39 m, bottom sediment

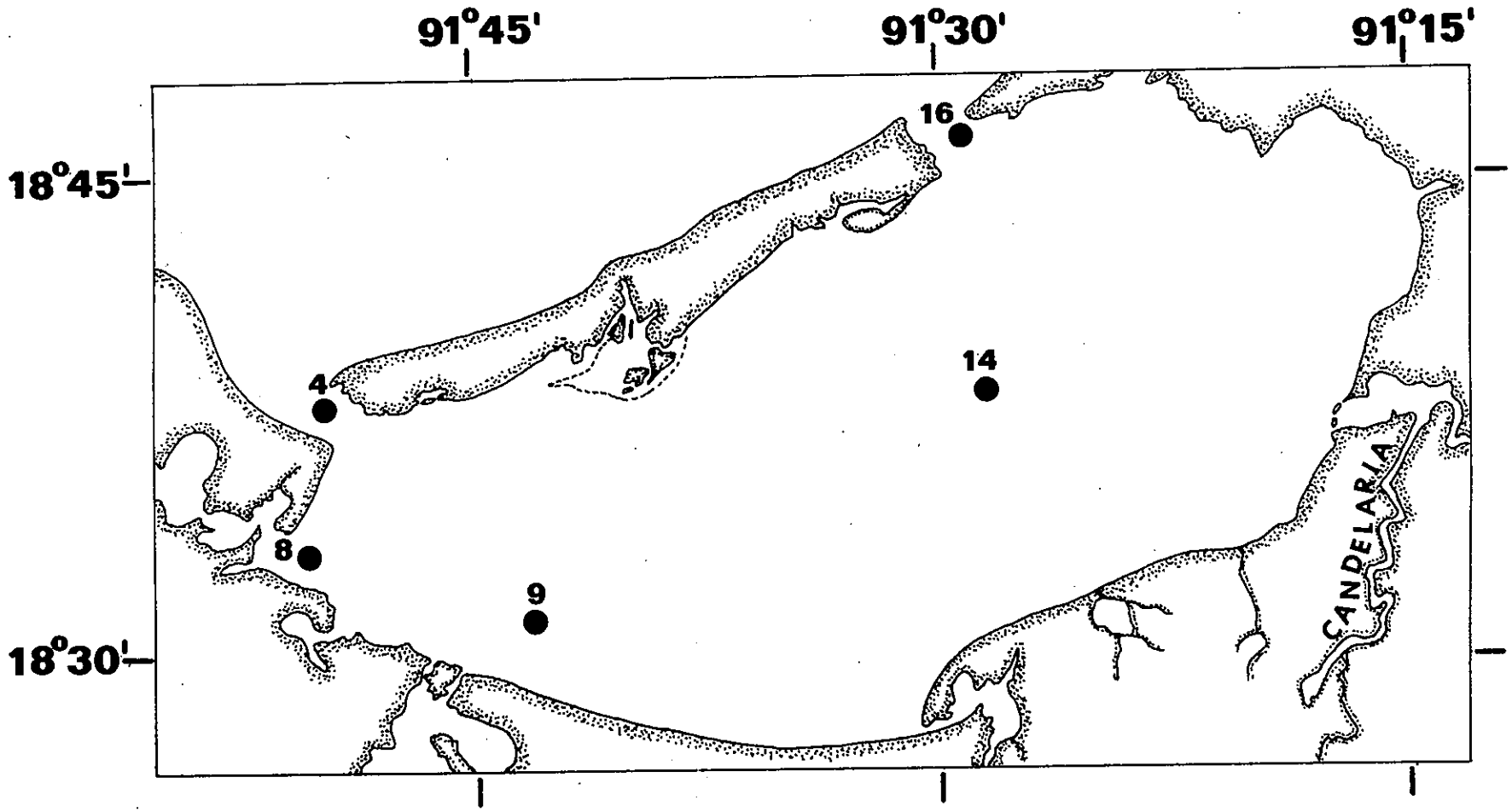

Figure 3. Terminos Lagoon showing bottom sediment sample locations.

on any mineral matter present. This was seemingly borne out by the data to be presented later.

Quantitative measurements of suspended sediment concentrations were not made during the cruise. However, estimates of concentration of mineral matter on the filters ranged from very low to nearly nonexistent, based on visual inspection with a light microscope. Concentration variation between the different sample pads, as well as between the fragments of any one pad could, however, be estimated by color variation, although few or no individual grains could be resolved by the microscope. Color ranged from the natural white of the filter to light shades of tan, and as such formed the criterion for isolating filter pad fragments with the highest potential mineral concentration.

The glass fiber which constitutes the filter pad is made of borosilicate glass, which has a density of 2.23 g/cm^3, and as such is less dense than most mineral matter (i.e., quartz = 2.65, carbonates 2.8, clays 2.2-3.1 g/cm^3). Initial attempts at mineral isolation and concentration involved ultrasonification of filter fragments in acetone followed by centrifigal heavy-liquid (density = 2.30 g/cm^3) density separation. After making numerous attempts at using this method, it was clear that no visible residue was collecting at the bottom of the separating funnels; hence, isolation and concentration of mineral matter from these filters was not possible. As a consequence of this, the remaining choice was to X-ray the filter directly, and this was the method finally used in this study. The filter fragments were visually sorted on the basis of color for maximum potential mineral concentration, mosaiced together on a glass slide, bonded to the slide with rubber cement, and then X-rayed.

The bottom sediments were present in adequate quantities so that they could be sieved, ground, washed and mounted by standard methods. Because bottom resuspension probably affects only the silt- and clay-sized particles of the sediment, the sand-sized (> 62μ) and coarser particles were selectively removed from samples RIX-4, 7, 10, and 11 during sample preparation. The bottom sediments from Terminos Lagoon were received in powdered form; hence, no such separation was possible. A two-gram representative sample was next wet-ground for one hour in a Fisher Mortar Grinder under tert-butyl alcohol. The alcohol acted as a coolant and lubricant to prevent potential damage to the mineral crystal structures, while the grinding reduced and optimized the grain size as well as homogenized the material. After grinding, the samples were washed with acetone and then distilled water, dried, and finally powder-mounted for initial X-ray analysis. After the initial X-ray analysis, the samples were weighed to the nearest 0.01 g and then placed in acetic acid, buffered with 1.0 N sodium acetate to pH = 5, for carbonate removal. After overnight soaking, the samples were distilled-water-washed, dried, and reweighed for carbonate loss calculations. After weighing, the samples were rewetted with water and pipetted onto silver filters under vacuum and then allowed to dry to room humidity (70%). This final X-ray mount analysis served two purposes. First, it oriented the clay minerals in such a way as to enhance their detection due

to improved orientation of their basal d spacings. The second objective was to detect mineral components which may have been masked by the numerous carbonate diffraction peaks.

2.3 X-Ray Diffraction Procedures

The samples were analyzed on a Philips X-ray diffraction system using a Cu target X-ray tube set at 35 kv and 25 ma. The radiation was monochromatized with a graphite curved crystal monochrometer set to transmit Cu_{K_a} radiation with a mean wavelength of 1.5418 Å. The goniometer scanned each sample from 3-45° 2θ at a rate of 1° 2θ/minute; the data was recorded on a strip chart recorder that moved at a rate of 0.5 inch/minute.

2.4 Mineral Identification

Terrigenous materials were identified with the aid of Carroll (1970), Brown (1961), and the Joint Committee on Powder Diffraction Standards (JCPDS) Inorganic Index (1972) and card file. Guidance for identification of carbonate minerals was provided by Milliman (1974). These mineral identification criteria are summarized in Table 2, which contains both the diagnostic d spacings of each mineral and the respective Miller indices (hkl) for the crystal planes whose spacings are those d-values.

3. RESULTS

Despite the visual lack of mineral matter on the filters, each sample's X-ray diffractogram revealed the presence of at least three mineral species. The complete list of mineral species present in each sample is recorded in Table 3. In all, six terrigenous and four carbonate minerals were identified. The terrigenous suite contained quartz, plagioclase feldspar, and the clay minerals chlorite, smectite (montmorillonite), illite, and kaolinite, while the carbonate suite contained aragonite, calcite, dolomite, and Mg-calcite. Figures 4a-c are given as exemplary diffractograms, showing the three samples at station RIX-07 in descending order from the surface sample (Fig. 4a) through to the bottom sediment (Fig. 4c). Two points are obvious from this sequence of diffractograms. The first is that despite the apparent lack of visible mineral material on the surface of the filters, beyond discoloration, the diffractograms of the filtered samples (Figs. 4a and 4b) show strong identifiable diffraction peaks. The second observation is that the mineralogy for all three samples is identical, as shown in Table 3. It should be noted here that Figures 4a and 4b contain peaks for gypsum and halite, while Figure 4c does not. This is not considered significant, since these minerals are precipitates resulting from the direct filtration of seawater through the subsequently unwashed filters.

The mineral distributions recorded in Table 3 show several noteworthy patterns. The first is that quartz, plagioclase, chlorite, calcite, and aragonite

Table 2. Mineral Identification Criteria.

TERRIGENOUS MINERALS

Mineral	d Spacing (Å)	hkl
Chlorite	14-14.3	001
	7-7.15	002
	4.7-4.75	003
	3.53-3.69	004
Smectite	15-18	001
	4.98-5.01	003
	4.48-4.50	001,020
	3.78	004
Illite	9.9-10.1	002
	4.48-4.50	020,110
	3.33	006
Kaolinite	7.15-7.18	001
	4.48	02-
	3.57	002
Quartz	4.26	100
	3.34	101
	2.28	102
	2.24	111
	2.13	200
Plagioclase	4.0-4.05	$20\bar{1}$ (?)
	3.76	111
	3.69	$1\bar{3}0$
	3.26	$2\bar{2}0$
	3.20	040
	2.98-3.01	$1\bar{3}1$
	2.46	$\bar{2}41$
Aragonite	3.40	111
	3.27	021
	2.70	012
	2.48	200
	2.37	112
	2.34	130
Calcite	3.87	102
	3.04	104
	2.50	110
	2.29	113
	2.10	202
Dolomite	2.89	104
	2.19	113
Mg-Calcite	2.95-3.01	104

Table 3. Mineral species at each sample location.

	Terrigenous Minerals						Carbonate Minerals				
RIX*	Chlorite	Smectite	Illite	Kaolinite	Quartz	Plagioclase	Aragonite	Calcite	Dolomite	Mg-Calcite	% Carbonate
04-S001	-	-	-	-	X	-	X	X	-	-	
04-S002	X	-	-	?	X	X	X	X	X	X	
04-F007	X	X	X	?	X	X	X	X	X	X	76
10-S001	X	X	X	-	X	?	X	X	-	?	
10-S003	X	X	X	X	X	X	X	X	-	-	
10-F038	X	X	X	X	X	X	X	X	X	X	53
07-S002	X	X	X	?	X	X	X	X	?	X	
07-S003	X	X	X	X	X	X	X	X	?	X	
07-F025	X	X	X	X	X	X	X	X	-	X	38
11-S001	X	X	X	X	X	X	X	X	-	-	
11-S002	X	X	X	X	X	X	X	X	-	-	
11-F046	X	X	X	X	X	X	X	X	X	?	59
Lagoon											
Sample 4	X	X	X	?	X	X	X	X	X	X	26
Sample 8	X	-	X	-	X	X	X	X	X	-	47
Sample 9	X	-	X	-	X	X	X	X	X	-	
Sample 14	X	X	X	-	X	X	X	X	X	-	
Sample 16	?	-	-	-	X	X	X	X	X	-	92

* East-west order.

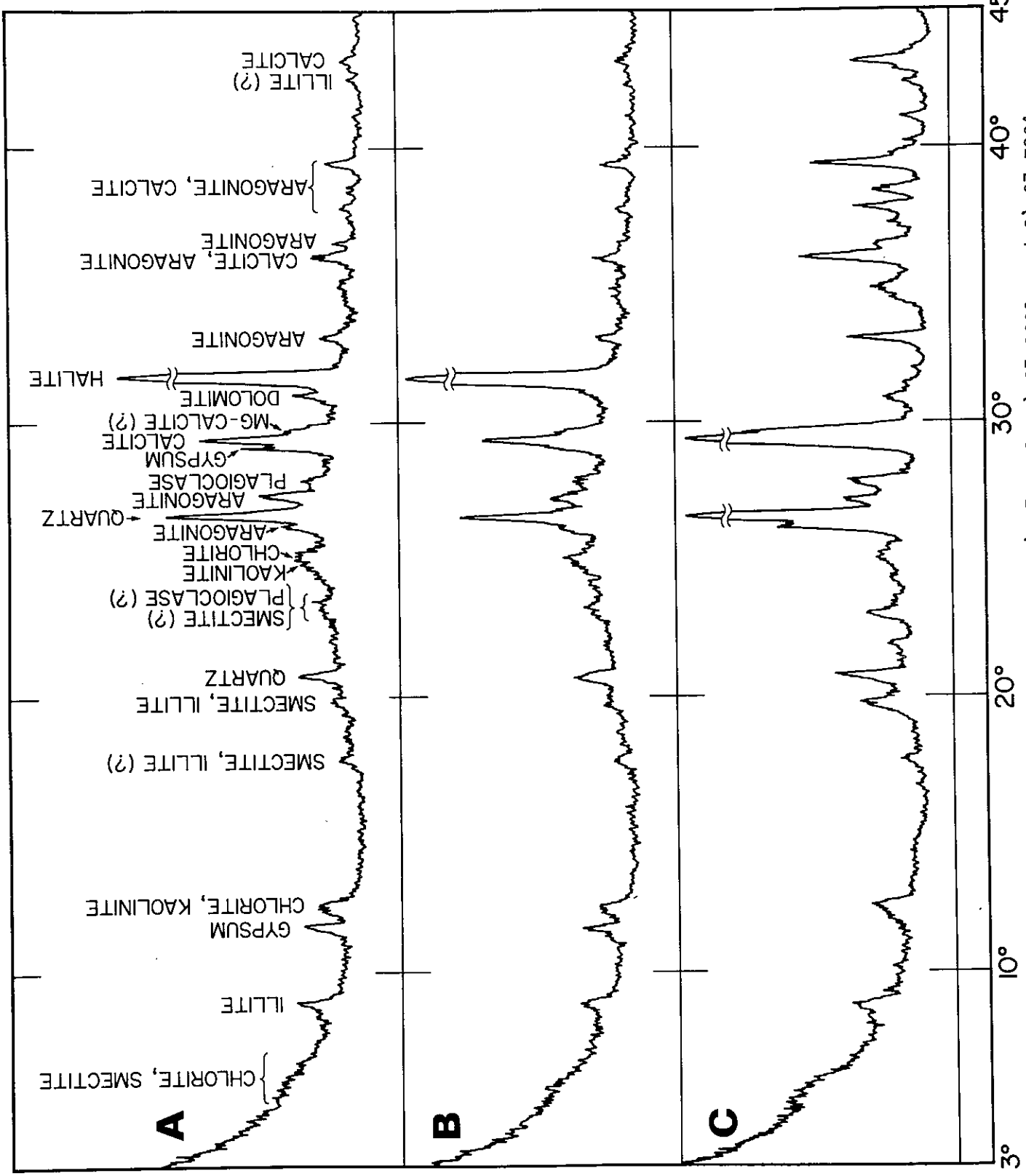

Figure 4. X-ray diffractograms of RIX stations A) 07-S002, B) 07-S003, and C) 07-F004.

are essentially ubiquitous at all sample stations and levels. Secondly, no mineral species occur in the water column that do not occur in the sediment directly below. Finally, all of the mineral species that were identified occurred in all of the shelf-bottom sediments (i.e., RIX 04-F007, 10-F038, 07-F025, and 11-F046) as well as in the western inlet (Sample 4) of Terminos Lagoon. This will be discussed further in the next section.

The results of the carbonate percentage analyses for each bottom sediment are recorded in Table 3. From these data it can be seen that the results of this analysis conform to prior work (Phleger and Ayala-Castanares, 1971) in that this shelf region is the juncture for carbonate and terrigenous sediments (i.e., RIX-10-F038, 53% carbonate; -07-F025, 38%; and -11-F046, 59%) with an increase in carbonate material to the east and northeast (i.e., RIX-04-F007, 76%). In the Terminos Lagoon, Phleger and Ayala-Castanares (1971) report net longshore transport to the west with tidal inflow into the lagoon through the eastern inlet and outflow bearing terrigenous material through the western inlet. The carbonate percentages presented here seemingly sustain that conclusion, with 92% carbonate (Sample 16) for the eastern inlet and 26% carbonate (Sample 4) for the western inlet.

4. DISCUSSION AND CONCLUSIONS

From the data presented above, answers to the four questions posed in the Introduction are now available. In response to the first question, "Was there mineral matter present in the water column?," the data in Figures 4a and 4b, as well as Table 3, clearly indicate that there was. Visual, low-power microscopic inspection of numerous filter fragments did not reveal the presence of biota fragments or tests. This leads one to the conclusion that the water turbidity was most likely the result of suspended mineral matter.

The second question as to whether the turbidity was from surface runoff, resuspension, or both is more difficult to answer using the available data. Figure 5 shows the temperature and salinity data recorded during the hydrocasts in which water column samples were collected for the stations considered in this report. Figure 5a shows a slight thermocline at station RIX-04. These data were collected just before the storm, which was generated by Hurricane Henri, hit the area. Figures 5b-d show stations RIX-07, -10, and -11, respectively, all of which were occupied after the storm. It is obvious that the water is isothermal and that any thermocline that may have existed at those stations was destroyed by the storm. The data, however, show a mild halocline that may be the result of direct at-sea precipitation or land runoff resulting from torrential rains that occurred in the area at that time (Donald Atwood, personal communication). The mineralogy gives no clear guidance here, in that the bottom sediments on the shelf and in the lagoon are essentially identical to each other and to the material suspended in the water column for stations RIX-07, -10, and -11. Prior work with suspended particulate matter in shelf environments, with depths similar to those in the IXTOC-I area, has shown that intense storms (Nelsen, 1979) and hurricanes (Rodolfo et al., 1971) are capable of resuspending large amounts of bottom materials into the water column

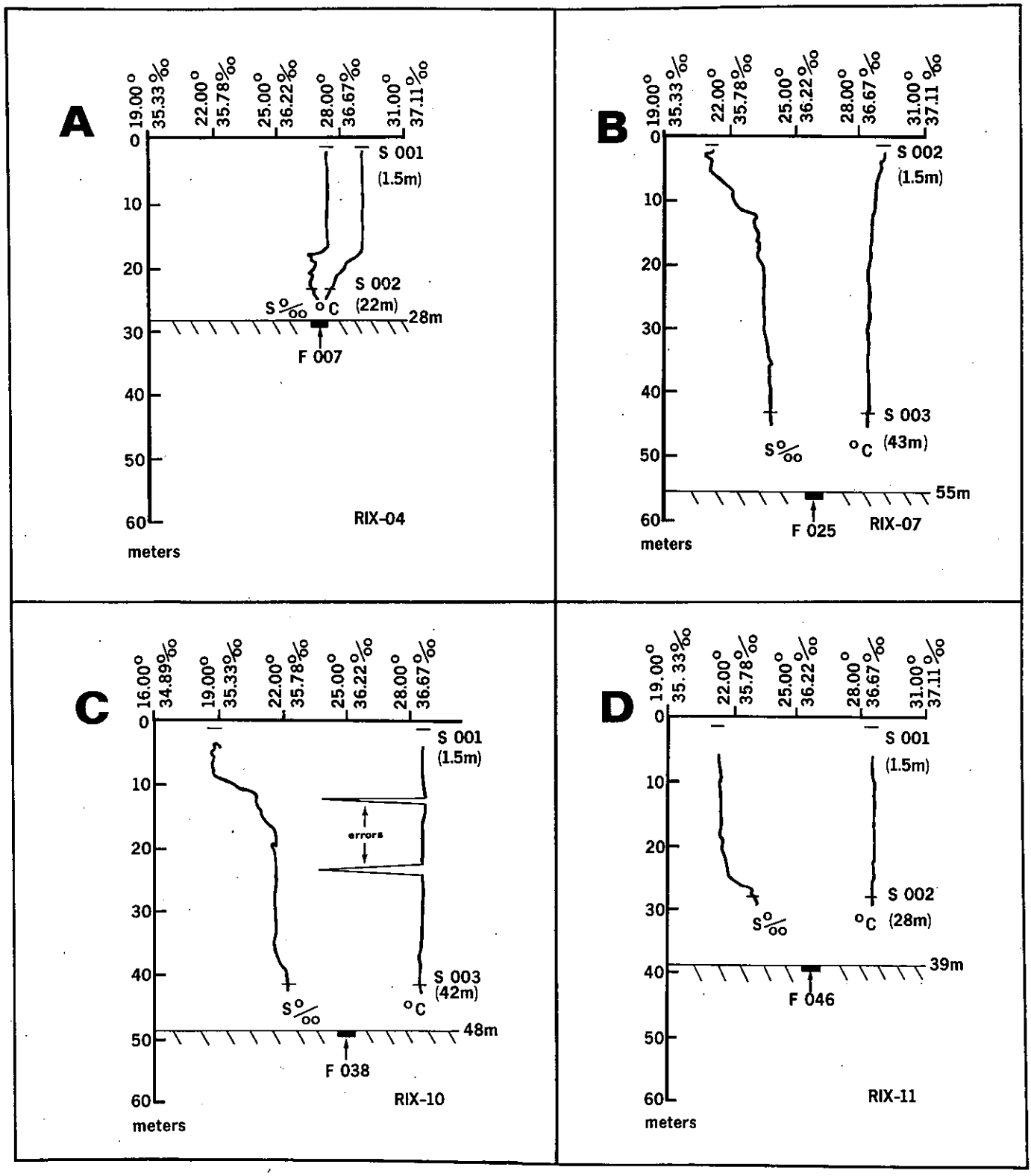

Figure 5. Temperature and salinity of the water column taken concurrently with the RIX samples at the stations marked on each profile.

for several days. However, under conditions of strong thermal stratification, resuspension may be reduced or inhibited, even under brief hurricane conditions (Young, 1978). Because prestorm stratification was weak (Fig. 5a) and post-storm conditions were isothermal (Figs. 5b-d), it is the opinion of this author that resuspension was the primary, if not the sole, cause of mineral matter in the water column.

In addressing the third question, the hydrocarbon sorption properties of the minerals present, at least three minerals have been shown to have that capacity. In a study by Meyers and Quinn (1973), it was shown that marine sediments (of unspecified mineralogy), as well as kaolinite, illite, and smectite have the capacity for significant sorption of petroleum hydrocarbons in saline solution. It is therefore reasonable to conclude that at least three of the minerals present in the IXTOC-I study area are capable of scavenging and forming sinks for petroleum hydrocarbons.

The final question, concerning mineral distributions and long-term dispersal patterns in the study area, can be addressed only in a speculative manner due to the limited data base available to this study.

During the time period over which the samples of this study were collected, the general trajectory of the discharging oil was to the east-northeast (Donald Atwood, helicopter observation log), with a landward shift near the end of this observational period. As such, the oil entered the carbonate province and possibly the nearshore zone. If suspended mineral particles acted as sorption sites for the petroleum hydrocarbons, their long-term dispersal in the study area may take two paths. From the work of Phleger and Ayala-Castanares (1971), it has already been noted that longshore drift in the area of Terminos Lagoon is from the east to the west and that the net tidal exchange consists of inflow through the eastern inlet and outflow from the western inlet. As such, this provides the Terminos Lagoon with a potential mechanism for intake of contaminated particulates from the nearshore zone. The second possibility is dispersal to abyssal depths. It is known from the work of Davies (1968) that a considerable volume of abyssal plain sediments contains carbonate turbidite sequences derived from the Campeche Bank. These turbidites have been shown to contain foraminifera from the very shallow inner shelf environment. From this, it is reasonable to conclude that contaminated particulates can be brought to the shelf-edge by process such as storm resuspension, and under proper conditions they can be delivered to abyssal depths by turbidite flow mechanisms.

5. ACKNOWLEDGMENTS

Alfonso Vasquez Botello, of the Centro de Cienias del Mar y Limnologia, UNAM, Mexico, provided bottom sediments from the Terminos Lagoon. David Fiest and John C. Yarko, of ERCO, Cambridge, Massachusetts, provided the RIX-04, -07, -10, and -11 bottom sediments, while James Payne and Gary Smith, of Science Applications, La Jolla, California, provided the suspended sediment samples from those stations. Robert R. Lankford, UNESCO Marine Geologist, San Jose, Costa Rica, suggested background source information for the study area. Robert

Glaccum, of the University of Miami, shared his wisdom about mineralogy with me. Frances Nastav drafted all figures. To the above persons I express my gratitude for their assistance and guidance.

6. REFERENCES

Brown, G. (1961): The X-ray Identification and Crystal Structures of Clay Minerals. Mineralogical Society, London: 544 pp.

Carroll, D. (1970): Clay minerals: A guide to their X-ray identification. GSA Spec. Paper 126: 80 pp.

Creager, J. S. (1958): Bathymetry and sediments of the Bay of Campeche. Texas A & M Tech Report 58-12F: 188 pp.

Davies, D. K. (1968): Sedimentary Petrology. In Study of the Continental Shelf of the Gulf of Mexico, A. H. Bouma, W. R. Bryant, D. K. Davies, and T. T. Tieh (Eds.), Texas A & M Tech. Report 68-2T: 49-94.

Freeland, G. L. (1971): Carbonate sediments in a terrigenous province: The reefs of Veracruz, Mexico. Ph.D. Dissertation, Rice University, Houston, Texas: 267 pp.

JCPDS Inorganic Index (1972): Powder Diffraction File. Pub. by Joint Committee on Powder Diffraction Stds, 1601 Park Lane, Swarthmore, Pa.: 432 pp.

Logan, B. W., J. L. Harding, W. M. Ahr, J. D. Williams, and R. G. Snead (1969): Carbonate sediments and reefs, Yucatan Shelf, Mexico. In A.A.P.G. Memoir 11: Pub. by AAPG, Tulsa, OK, 1-198.

Meyers, P. A., and J. G. Quinn (1973): Association of hydrocarbons and mineral particles in saline solution. Nature, vol. 244, 23-24, pub. Macmillan Journals Ltd, London.

Milliman, J. D. (1974): Marine Carbonates: Part I - Recent Sedimentary Carbonates, Springer-Verlag, New York: 375 pp.

Nelsen, T. A. (1979): Suspended particulate matter in the New York Bight Apex: Observations from April 1974 through January 1975, NOAA Tech. Memo. ERL MESA-42: 78 pp.

Phleger, F. B., and A. Ayala-Castanares (1971): Processes and history of Terminos Lagoon, Mexico. Bull. Amer. Assoc. Petrol. Geol., 55: 2130-2140.

Rodolfo, K. S., B. A. Buss, and O. H. Pilkey (1971): Suspended sediment increase due to Hurricane Gerda in continental shelf waters off Cape Lookout, N.C. J. Sed. Pet., 41: 1121-1125.

Young, R. A. (1978): Suspended-matter distribution in the New York Bight Apex related to Hurricane Belle. Geol., 6: 301-304.

ASPECTS OF THE TRANSPORT OF PETROLEUM HYDROCARBONS TO THE OFFSHORE BENTHOS DURING THE IXTOC-I BLOWOUT IN THE BAY OF CAMPECHE

Paul D. Boehm and David L. Fiest
Environmental Sciences Division
Energy Resources Co., Inc. (ERCO)
185 Alewife Brook Parkway
Cambridge, Massachusetts 02138

ABSTRACT

An investigation of the areal extent and nature of oil in offshore surface sediments from the IXTOC-I blowout in the Bay of Campeche was undertaken by sampling surface sediment from the blowout region and along its Mexico-to-Texas path of movement. Sediment traps deployed in the blowout region collected actively sedimenting material.

Synchronous scanning spectrofluorometric, glass capillary gas chromatographic, and gas chromatographic mass spectrometric analytical techniques were used to investigate both the distribution and the detailed nature of sedimenting and sedimented oil. Petroleum hydrocarbons captured in trap arrays were undegraded by microorganisms but weathered by evaporation/dissolution. Hydrocarbons transported to the sediments were associated with phytoplanktonic material and grayish suspended carbonates. Oil from IXTOC-I was found in surface sediment at station 30, at 50 km from the blowout site, and possibly off the Texas coast in deep water in concentrations as high as 100 ppm. Sedimentary petroleum hydrocarbons exhibit chemical characteristics of petroleum in its early stages of microbial degradation. Alkyl phenanthrenes and alkylated dibenzothiophenes dominate the aromatic hydrocarbons in the sediments.

Mass balance calculations indicate that 1% to perhaps 3% of the spilled oil is to be found in offshore sediments, a conclusion that is in agreement with the weathering (fates) model of Mackay et al. (1979).

1. INTRODUCTION

When released into the marine environment, the behavior and fate of petroleum hydrocarbons are dictated by a variety of physical/chemical, chemical, and biological processes which result in hydrocarbon dissolution, evaporation, emulsification, dispersion (mixing), adsorption, sedimentation, photo-oxidation, and hence their active and passive biological uptake. The rates of these "weathering" processes and their relative significance in a three-dimensional mass balance have been the subject of several significant modeling efforts (Mackay and Paterson, 1978; Kolpack and Plutchak, 1976; Mackay et al., 1979; Mattson and Grose, 1979). The most important quantitative processes predicted to influence the fate of oil in a spill's early stages are evaporation and dissolution. The rates of both of these processes are dependent not only on the water temperature and other environmental variables, but also on mixing energy that disperses oil into the water column in fine droplets, hence increasing dissolution and sorption of petroleum hydrocarbons. Sedimentation of oil in the offshore environments is thought to be a minor sink for hydrocarbons (Mackay et al., 1979), the extent of which is dependent on suspended sediment loading and biological production (i.e., planktonic concentrations).

It is clear that the extent of long-term biological effects of most oil pollution events studied to date is directly dependent on the extent of oiling of the benthic substrate in and upon which organisms dwell. The specific

gravity of most crude and refined oils spilled at sea does not exceed that of seawater (—1.025; Ferraro and Nichols, 1972) and hence direct sinking of petroleum residues at sea is rare. Notable exceptions are spillages associated with the ANNE MILDRED BROVIG collision in the North Sea (Mattson and Grose, 1979), the USNS POTOMAC (Grose et al., 1979) during which some sinking of oil appears to have occurred, probably due to weathering and subsequent fractionation of the oil, and the SANSINENA Bunker C spill (Kolpack et al., 1978) during which the burning of the cargo resulted in the sinking of the residuals.

Studies of the IXTOC-I emulsified crude oil (mousse) masses off the Texas coast during August 1979 (Patton et al., 1980; Patton and Amos, unpublished data) found that photochemical and evaporative processes presumably resulted in skinning-over and subsequent flaking of mousse patches, and that wind-driven dispersion (apparent sinking) drove these particles into the water column. These particles were neutrally or positively buoyant (Patton et al., 1980) and thus did not passively sink.

Petroleum hydrocarbons have become associated with intertidal and subtidal sediments following many spills during which landfall, substrate oiling, and offshore transport of affected sediment have occurred. Long-term association of hydrocarbons with sediments has occurred during the West Falmouth (Teal et al., 1978), Chedabucto Bay ARROW (Cretney et al., 1978; Keizer et al., 1978), and AMOCO CADIZ (Beslier et al., 1980; Boehm et al., 1980b) spill events, to name a few. Similar landfall followed by offshore and hence subtidal transport undoubtedly occurred to a great extent during the IXTOC-I blowout; the only documented observations were recorded off the southern Texas coast (OSIR, 1980).

There have been few studies directly pertaining to the transport of oil to the offshore continental shelf benthos via the important phenomenon of adsorption of oil on living or detrital particulate matter (or vice versa) followed by sedimentation to the benthos. An evaluation of the extent of this process is extremely important in order to predict the exposure of important benthic resources to petroleum hydrocarbons released from offshore blowouts. This process is dependent on the availability and concentration of suspended particulates and their surface area (Poirier and Thiel, 1941; Mattson and Grose, 1979; National Academy of Sciences, 1975; Thüer and Stumm, 1977). Another possible route of transport to the benthos is by ingestion of oil by zooplankters followed by fecal pellet transport (Conover, 1971). These two processes are those most likely to result in water-column-to-benthos transport of petroleum hydrocarbons in continental shelf environments.

Several recent studies have addressed transport of oil to the benthos following offshore platform blowouts and tanker spills. Kolpack (1971) and Kolpack et al. (1971) have attributed the large concentrations of oil in sediments following the Santa Barbara blowout to the interaction of petroleum hydrocarbons with sediment-rich river plumes, followed by sorption and sinking. Low but significant concentrations of oil in sediments were observed following the Ekofisk BRAVO blowout in the North Sea (Johnson et al., 1978), although no specific mechanism was investigated. McAuliffe et al. (1975) have associated the spilled oil in sediments in the vicinity of the Chevron platform blowout at

the mouth of the Mississippi River with sorption and sedimentation processes. Boehm et al. (1980a) have examined the detailed chemistry of sedimenting oil captured in sediment traps deployed during the TSESIS tanker spill in Sweden. They found that microbial degradation caused rapid alteration of the chemical composition of the spilled cargo, and that the hydrocarbon composition of benthic deposit feeders (Macoma balthica) echoed this composition. Johansson et al. (1980) estimated that 15 to 20 percent of the oil spilled during the TSESIS event was transported to the benthos by sorption and sedimentation and/or by ingestion and zooplankton fecal pellet transport.

The continuous seabed blowout event of the IXTOC-I drilling platform in the Bay of Campeche introduced at least 140 million gallons (3.5 million bbl $\cong$500 thousand metric tons) of oil into the offshore waters of the Bay of Campeche over a 10-month period (OSIR, 1980). This study was intended to place the magnitude, nature, and areal extent of the sedimentation processes in the perspective of the overall behavior of the released petroleum hydrocarbons by examining and comparing the concentrations and composition of hydrocarbons of actively sedimenting particles (sediment traps), particulate oil, source material (weathered mousse), and surface sediments themselves.

2. METHODS

2.1 Sampling

Samples were obtained during the R/V RESEARCHER and C/V PIERCE Campeche oil spill cruise, 11-27 September 1979. This research expedition was designed to examine the three-dimensional distribution of petroleum hydrocarbons, the concentration gradients from the blowout source, and the compositional changes occurring, and to postulate a comprehensive mass balance for the spilling petroleum.

Surface sediments were obtained from a larger set of sediment samples from 10 stations occupied by the RESEARCHER; one series was in close proximity to the wellhead (the closest station was RIX 07 at 30 km), and a second series was along the historical path of surface slick movement from the wellhead to Texas coastal waters (Figures 1 and 2). All samples were obtained with a Smith-MacIntyre grab sampler. A subsample from the top 3-4 cm of sediment was taken from each grab after it was brought on deck. Samples were immediately frozen at -10°C and remained so until analyses were begun.

Sediment traps were constructed quite simply by attaching wide-mouth jars to a weighted Kevlar-coated hydrowire at several depths (2.5, 5, and 15 m) along the wire. Duplicate traps were deployed from the C/V PIERCE at three stations near the wellhead (Figure 1) along the observed direction of movement of the surface oil, as well as at one control station. The traps remained deployed for approximately 8 hr, at which point they were retrieved. During retrieval the trap strings were slowly brought on board and each jar was capped before breaking the sea surface. The jars' contents were poisoned with methylene chloride and frozen at -10°C until analyses were begun.

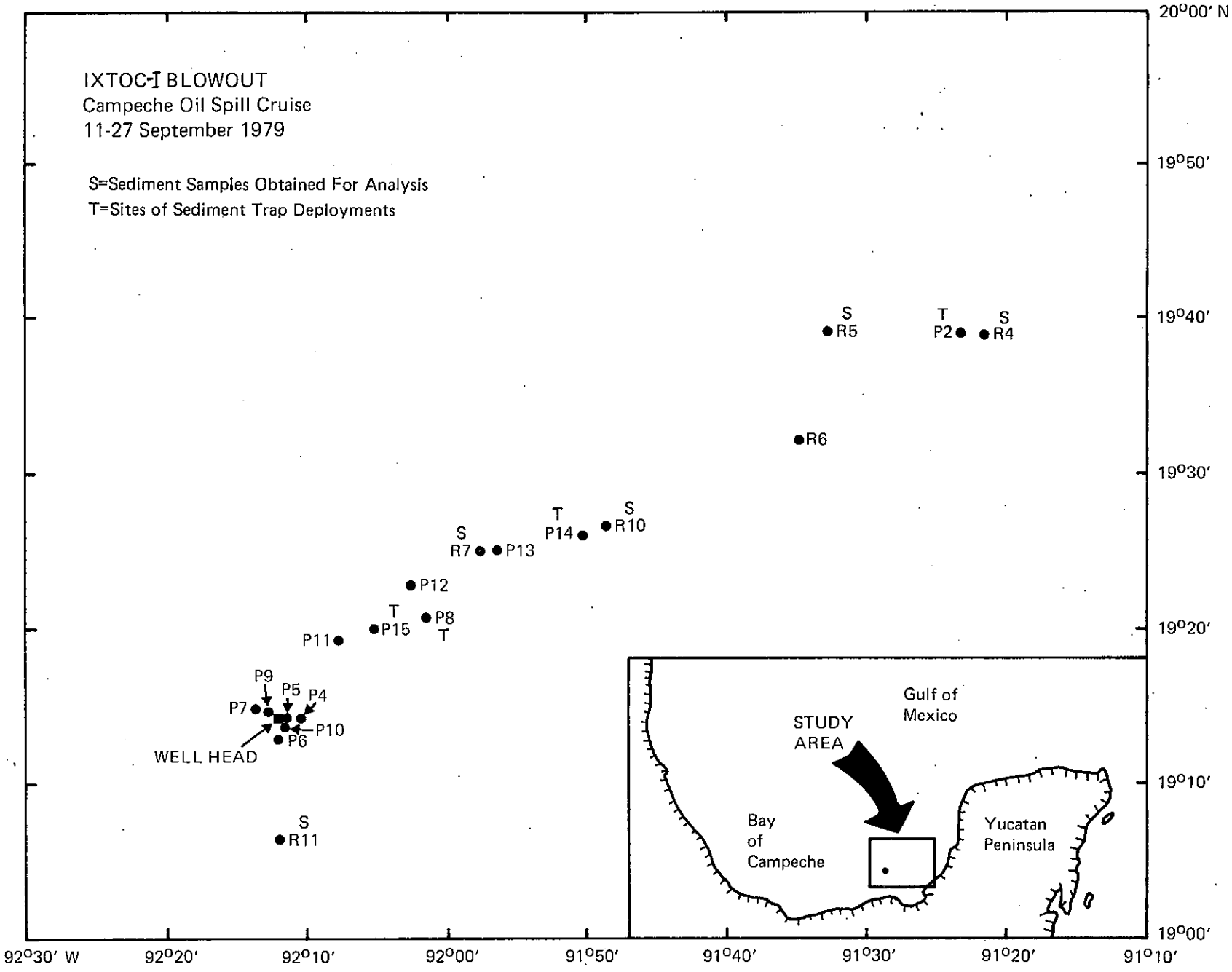

Figure 1. Detailed map of wellhead region.

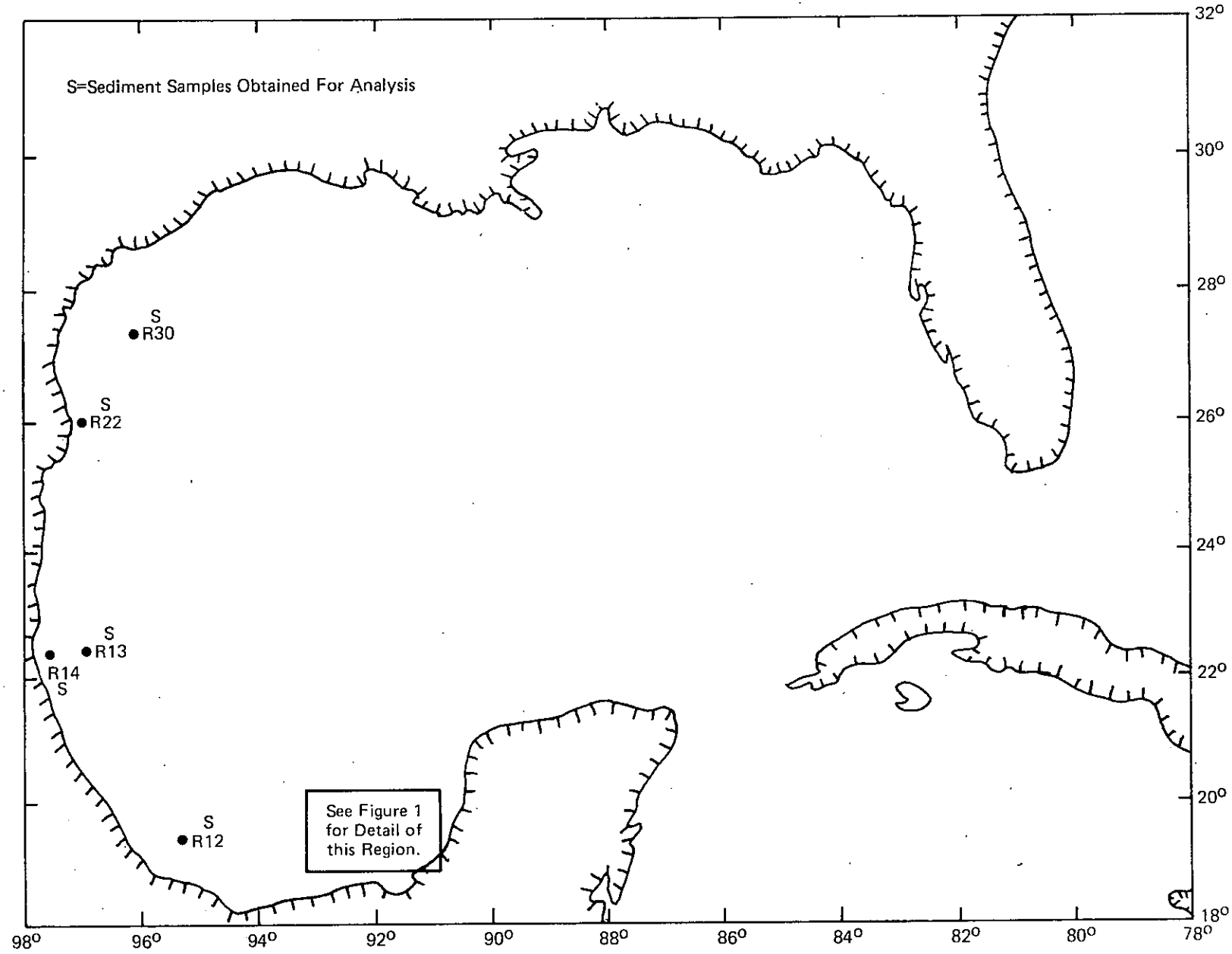

Figure 2. Sampling stations along the historical path of IXTOC-I surface oil movement.

Particulate water column samples were obtained through an all-stainless-steel pumping system designed specifically for oil-spill studies (Boehm and Fiest, this symposium). A submersible pump (nylon bushings) attached to an alterable series of 2-m lengths of 1/2" I.D. stainless-steel tubing, linked by flexible stainless couplings and quick-connect fittings, was deployed outside the area of heavy slick. Once in the water the ship, and hence the string of tubing, was allowed to drift into the heavy oil. Vertical profiles down to 20 m were obtained by adding lengths to the tubing. The hydrocarbon content of pumped seawater was monitored continuously through a Turner fluorometer. Particulate samples were obtained by channeling the flow through a 142-mm precombusted Gelman AE glass fiber filter held in a stainless filter holder. Ten to 20 liters of water were filtered to obtain a single sample. The filter was removed and frozen immediately.

2.2 Analyses

The overall analytical strategy was geared to determining the comparative detailed hydrocarbon chemistries (saturates: n-C_{10} to n-C_{34}; aromatics: alkylbenzenes to benzopyrenes) of samples by a combination of analytical techniques: glass capillary gas chromatography (FID-GC) and capillary gas chromatographic mass spectrometry (GC/MS).

The hydrocarbon compositions of the surface sediments were screened by synchronous scanning spectrofluorometry (Wakeham, 1977; Gordon et al., 1976; Fiest and Boehm, 1980). Approximately 3 g dry weight of sediment was transferred to a centrifuge tube, solvent was added, and the tube was agitated using a vibrating mixer for several minutes. Use of different solvent mixtures (hexane, methylene chloride/methanol, hexane/methylene chloride) was tried to compare extraction methods. Hexane compared quite favorably with methylene chloride mixtures in its ability to qualitatively extract fluorescent compounds from wet sediment and was subsequently used in all screenings to address the qualitative sedimentary hydrocarbon distributions. Hexane extracts were analyzed directly on a Farrand MK-1 scanning spectrofluorometer by offsetting the excitation and emission monochronometers 25 nm, and scanning both simultaneously and monitoring the resultant emission spectrum of the sample. Families of aromatics (Lloyd, 1971) are revealed by this method. Twelve samples were chosen on the basis of their fluorescence spectra for more detailed GC and GC/MS analyses. Those samples whose spectra revealed the probable presence of IXTOC-I oil or those whose spectra illustrated a "typical background" distribution of fluorescent polycyclic aromatic hydrocarbons were chosen for further scrutiny.

The solvent extraction, silica gel column chromatographic fractionation, GC, GC/MS, and quantification procedures are described in detail elsewhere (Boehm et al., 1980b; Atlas et al., 1980; Brown et al., 1979; Boehm and Fiest, this symposium). Briefly, 50-100 g of wet sediment are added to a Teflon canister and internal standards are spiked to the sediment. The sediment is dried by shaking with methanol, extracted by a methylene-chloride:methanol azeotrope (9:1), the methanol is back-extracted with methylene chloride, all extracts are combined, reduced in volume, displaced with hexane, and charged to

a silica gel/alumina column. Two fractions (f_1 = hexane eluate = saturated hydrocarbons; f_2 = hexane/methylene chloride eluate = unsaturated = aromatic and olefinic hydrocarbons) are eluted, reduced in volume, weighed on a Cahn electrobalance, and analyzed by glass capillary GC and GC/MS/computer using 30-meter, AA, SE-30 columns (J&W Scientific).

Sediment trap samples consisted of a 500-ml jar of seawater with zero to about 50 mg of sediment at the bottom. To lower the analytical detection limit and to avoid handling losses, the three to four jars comprising each trap array string were combined and treated as water samples (i.e., added to a separatory funnel and extracted vigorously with three 100-ml portions of methylene chloride). The extracts were treated as were the sediment extracts.

3. RESULTS

The analytical results of a series of sediments, selected sediment trap, and particulate hydrocarbons are presented in this section.

3.1 Ultraviolet Spectrofluorometry: Sediments

The synchronous spectrofluorometric determinations provided a rapid and clear picture as to the basic nature of the hydrocarbon composition of the surface sediments from those stations shown in Figure 1. The spectra fall into three nontrivial (nonzero) categories illustrated in comparison to a reference oil-in-water dispersion sampled at the wellhead (Figures 3A-E). The spectrum of Figure 3B is characteristic of all sediment samples examined from stations RIX 07 and RIX 10, approximately 30 and 50 km from the wellhead, respectively, and RIX 30, in deep water off Texas. These spectra compare quite favorably with the reference oil, with wavelength maxima at 312 and 350 nm and significant shoulders at 322 and 400 nm. The 312- and 322-nm responses are attributable to families of 2-ringed aromatic hydrocarbons, while the 350- and 400-nm maxima are due to 3-ringed compounds and minor amounts of 4-ringed aromatic structures (Lloyd, 1971). The 312- and 322-nm peaks are depleted relative to the presumed source material (Figure 3A), undoubtedly due to weathering of the petroleum hydrocarbon mixture.

The second type of spectra was observed in sediment samples from station RIX 12 off Veracruz (Figure 3C). The prominent multiple maxima between 290 and 315 nm are quite distinct and represent several biaromatic responses. The broad band and shoulders from 345 to 450 nm with a maximum at 370 nm is attributable to a set of 3- and 4-ringed compounds other than that associated with the spilled oil and hence another pollutant source.

The third spectral type, illustrated in Figure 3D, is characteristic of a prominent set of 2-ringed aromatic compounds as revealed by two spectral maxima at 295 nm and 305 nm. A small degree of triaromaticity is revealed by a small band centered at 345 nm. These spectra, common to RIX 14 sediments north of Tampico, are quite unlike those from other stations examined from the study

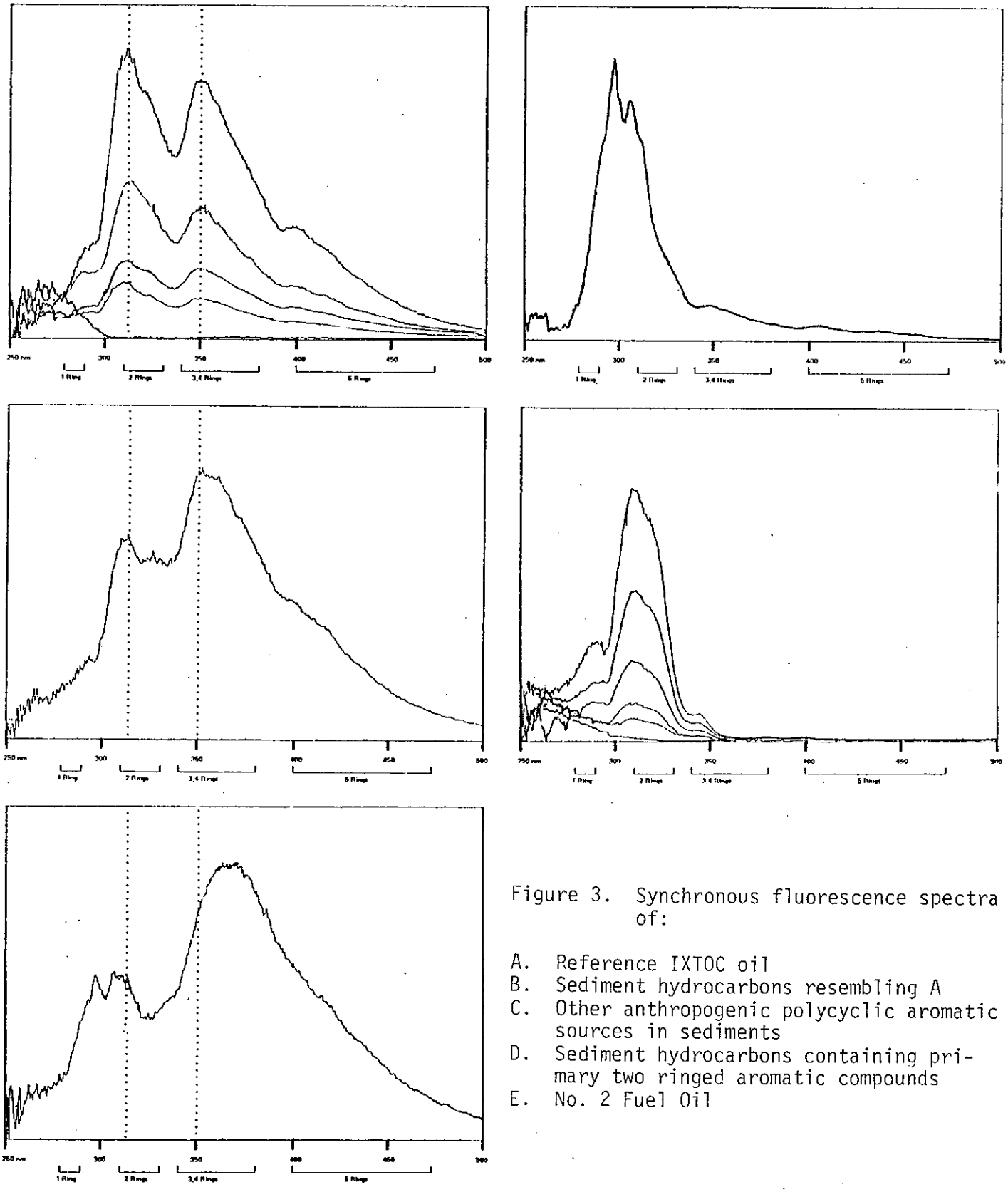

Figure 3. Synchronous fluorescence spectra of:

A. Reference IXTOC oil
B. Sediment hydrocarbons resembling A
C. Other anthropogenic polycyclic aromatic sources in sediments
D. Sediment hydrocarbons containing primary two ringed aromatic compounds
E. No. 2 Fuel Oil

area and are most similar to a light distillate oil (e.g., No. 2; see Figure 3E). However, GC and GC/MS data do not reveal the presence of any marked distillate pollution; therefore, the origin of this distribution is unknown. Sample contamination is possible but unlikely, in view of the fact that two of the three samples examined from RIX 14, and no others, contain this unique distribution of fluorescent compounds.

3.2 GC, GC/MS, Quantitative Aspects: Sediments

The hydrocarbon content (f_1 and f_2) of sediments from the wide geographic region examined ranged from 15.1 μg/g at station RIX 14 to 143.6 μg/g at RIX 10 (Table 1). A direct relationship between absolute hydrocarbon levels and the presence of IXTOC-I oil does not seem to exist, although the presence of petroleum hydrocarbons attributable to IXTOC-I was noted at stations RIX 07 and RIX 10. The background distributions of hydrocarbons are related to the organic content of the sediments. RIX 22 and RIX 30 contain hydrocarbon contents greater than non-oiled sediments farther south, due to riverine influences, not to IXTOC-I influences.

Gas chromatograms of oil from the sea surface at the blowout site (Figure 4A, B) are characterized by a distribution of n-alkanes (n-C_{10} to n-C_{36}), isoprenoid hydrocarbons, aromatic hydrocarbons (alkyl benzenes through alkyl phenanthrenes), and aromatic hetero compounds (dibenzothiophenes). The important features of the GC distribution are presented in Table 2.

The major processes affecting the compositions of petroleum in the water column, evaporation/dissolution and biodegradation, can be evaluated through three parameter ratios and are discussed in greater detail elsewhere (Boehm and Fiest, this symposium). A ratio of n-alkanes (C_{10}-C_{25}/C_{17}-C_{25}) approaches 1.0 as a fresh oil is weathered through partitioning of lower-boiling components into aqueous and gaseous phases. The ratio of selected n-alkanes (n-$C_{14,15,16,17,18}$) to isoprenoids in the same boiling region (retention indices 1380, 1470 [farnesane], 1650, 1710 [pristane], and 1812 [phytane]) decreases as microbial degradation of the more readily degraded n-alkanes proceeds (Boehm, et al., 1980a, b). The information in Table 2 compares source material with unweathered water-column particulate oil and, in turn, with sediment trap and surface sediments containing recent petroleum inputs associated with IXTOC-I oil.

Particulate hydrocarbons (Boehm and Fiest, this symposium) at those stations where oil was detected in sediments (RIX 07, RIX 10) and sediment traps (PIX 08, PIX 14) are comprised of a weathered version of the source oil (Figures 5A, B), with components lighter than n-C_{15} largely depleted due to physical/chemical weathering (primarily evaporation). Aromatic hydrocarbons in the naphthalene and fluorene series have partitioned into the dissolved and/or vapor phases, thus decreasing the aromatic weathering ratio (AWR; Table 2). Petroleum hydrocarbons in the water column in this spill are relatively unaffected by biodegradative processes compared to other well-studied spill scenarios (AMOCO CADIZ: Calder et al., 1979; TSESIS: Boehm et al., 1980a).

Table 1. Surface sediment data summary.

Station	Hydrocarbon Content (μg/g) (Gravimetric)			Composition
	f_1	f_2	Total	
RIX 04	5.4	19.2	25.1	B
RIX 07-1	11.4	18.8	30.2	I/B
RIX 07-2	26.3	54.0	80.3	I/B
RIX 10-1	33.6	110.0	143.6	I/B
RIX 10-2	23.5	38.0	61.5	I/B
RIX 12	8.3	16.4	24.7	T
	9.6	17.3	28.9	T
RIX 14-1	6.7	12.3	19.0	T/C
RIX 14-2	5.1	10.0	15.1	T/C
RIX 22	17.9	20.5	38.4	C/T
RIX 30	16.8	30.0	46.8	T/B/C/I
Blank	2.0	2.0	4.0	---

KEY:

I = predominantly IXTOC-I oil in f_1; weathered aromatics and biogenics (olefins, sterenes) in f_2.

B = biogenic inputs in f_1 and f_2.

T = terrigenous biogeneous biogenic inputs (i.e., n-C_{23}, n-C_{25}, n-C_{27}, n-C_{29}, n-C_{31}, n-alkanes = vascular plant waxes).

C = chronic pollution; unresolved hump in f_1; pyrogenic polynuclear aromatic hydrocarbon inputs in f_2.

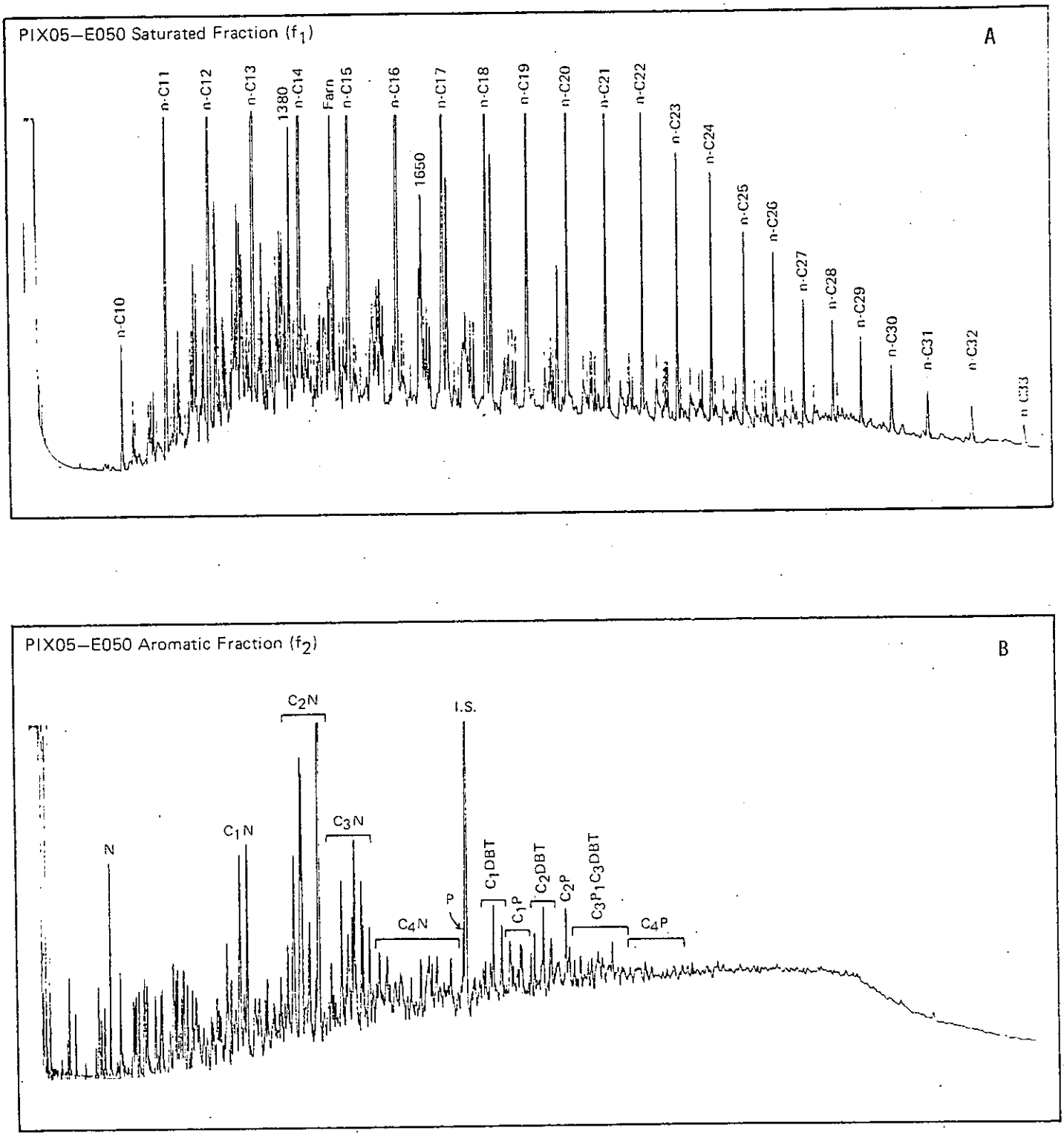

Figure 4. Glass capillary gas chromatograms of "reference oil."

Table 2. Summary of compositional information and parameter ratios for the various sample types.

Sample Type	Alkane Boiling Range	ALK/ISO	SHWR	AWR	Location
Reference Dispersion	$n\text{-}C_9\text{-}n\text{-}C_{36}$	4.1	2.7	2.2	PIX 05
Fresh Mousse	$n\text{-}C_{10}\text{-}n\text{-}C_{36}$	3.8	2.7	2.5	PIX 05/10
Weathered Mousse	$n\text{-}C_{15}\text{-}n\text{-}C_{36}$	3.1-3.5	1.1	1.2	RIX 06
Fresh Particulates	$n\text{-}C_{10}\text{-}n\text{-}C_{36}$	3.5-4.0	2.5	2.1	PIX 10
Weathered Particulates	$n\text{-}C_{15}\text{-}n\text{-}C_{36}$	3.5-4.0	1.1	1.0	PIX 14
Sediment Traps	$n\text{-}C_{11}\text{-}n\text{-}C_{34}$	4.5	1.0-1.6	---	PIX 08/14
Surface Sediments	$n\text{-}C_{13}\text{-}n\text{-}C_{36}$	1.1-1.9	1.0	1.1	RIX 07/10

$$\text{ALK/ISO} = \frac{\text{normal alkanes}}{\text{isoprenoids}} = \frac{(C_{14} + C_{15} + C_{16} + C_{17} + C_{18})}{\text{RI 1380 + farnesane + RI 1650 + pristane + phytane}}$$

$$\text{SHWR} = \text{saturated hydrocarbon weathering ratio} = \frac{\P\text{n-alkanes } (C_{10}\text{-}C_{20})}{\P\text{n-alkanes } (C_{15}\text{-}C_{20})}$$

$$\text{AWR} = \text{aromatic weathering ratio} = \frac{\text{Total naphthalenes + fluorenes + phenanthrenes + dibenzothiophenes}}{\text{Total phenanthrenes + dibenzothiophenes}}$$

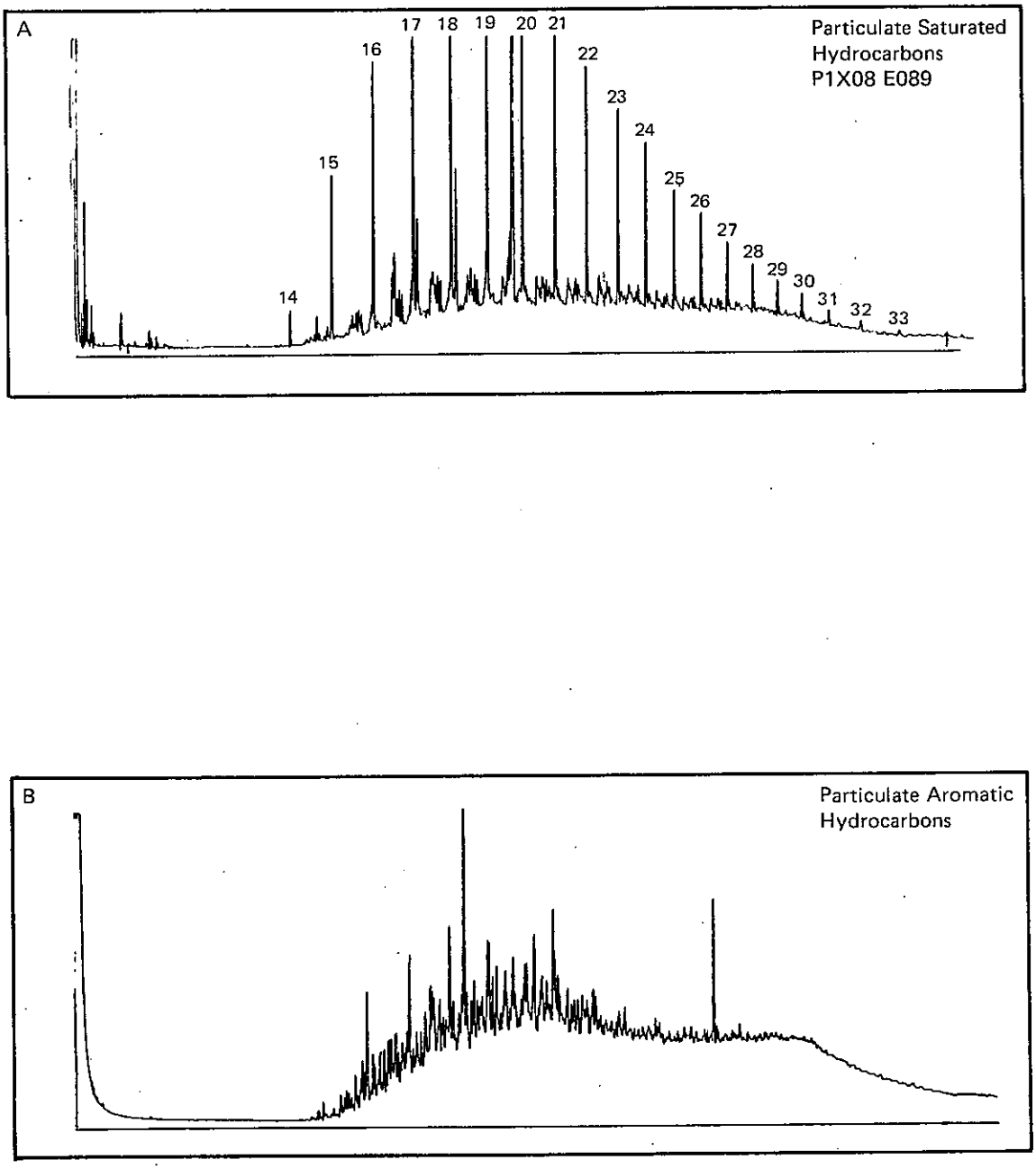

Figure 5. Glass capillary gas chromatograms of representative hydrocarbon-bearing particulates.

The capillary GC traces of hydrocarbons in the sediments illustrate the major compositional features referred to in Tables 1 and 2. Background aliphatic hydrocarbon distributions are characterized by marine biogenic distributions (Figure 6A), terrigenous biogenic distributions (Figure 6B), and a combination of chronic pollution and biogenic inputs (Figure 6C). The unsaturated (f_2) fractions of most samples are comprised of prominent sets of normal and branched olifinic compounds and compounds of the triterpene series (Figure 7). Several of the compounds reveal mass spectral fragments characteristic of this series (m/e = 191; MW 368, 380; Ensminger et al., 1975; Bieri et al., 1978), which probably originate in the marine microbiota (Ensminger et al., 1975). Those sediment samples that do contain significant quantities of petroleum hydrocarbons (RIX 07, RIX 10) exhibit a moderately weathered n-alkane distribution overriding an unresolved complex mixture (UCM) resulting from weathering of the saturate fraction, which visually enhances the UCM on the GC traces and possibly results in the production of UCM compounds (cyclic saturated compounds) by marine bacteria (Atlas et al., 1980; Figure 8A). That biodegradation is proceeding is evidenced not only by the UCM prominence, but also by the decreasing ALK/ISO ratios (1.1-1.9) for these samples (Table 2).

The unsaturated fraction (f_2) of spill-impacted surface sediment contains major biogenic components (Figure 8B), as do the background samples. The petrogenic aromatic hydrocarbons are revealed only through GC/MS-generated reconstructed mass chromatograms. The quantitative results from the GC/MS examinations of the f_2 fractions are summarized in Table 3 and detailed in Figure 9. The prominent families of phenanthrene and dibenzothiophene homologs dominate the aromatic hydrocarbon distributions (Figure 8B) of RIX 07, RIX 10, and RIX 30. No naphthalene compounds were detected in the oil-impacted sediments. The quantities of the phenanthrene and dibenzothiophene series range from less than 1.0 ng/g to 36 ng/g. The dibenzothiophenes (13-40 ng/g) are associated with sediments containing petroleum hydrocarbons. In these cases the C_2 and C_3 alkylated dibenzothiophenes (m/e = 212 and 226) dominate, illustrating that the petroleum present is moderately weathered (Boehm, et al., 1980b). The phenanthrenes present (Figure 8C) when dibenzothiophenes, and hence oil, are absent, are the unsubstituted parent compound with lesser amounts of alkylated phenanthrenes. This small amount (1.0-3.0 ng/g) can be attributed, along with the polynuclear aromatic hydrocarbon (PAH; m/e 202, 228, and 252) components, to pyrogenic sources (i.e., combustion of fossil fuels; Youngblood and Blumer, 1975) introduced to the sediment probably through fallout and riverine runoff. The sediments of RIX 22 and RIX 30 (Figure 8C, D) contain greater quantities of these indicators of pyrogenic sources, most likely due to their proximity to the influence of the Rio Grande River. RIX 30 also contains dibenzothiophene and alkyl phenanthrene PAH compounds, which strongly suggest a petrogenic source. In addition, the synchronous spectrofluorometry spectrum of the RIX 30 sample suggests a similarity to IXTOC-I oil. However, other petroleum sources prevalent in the Texas Gulf coast region (platform drilling discharges, tanker discharges) may result in similar distributions. Therefore, assignment of the trace levels of petroleum hydrocarbons found in RIX 30 sediments to any particular source is quite ambiguous.

It should be noted that the olefinic and triterpenoid nonpetrogenic components of the unsaturate (f_2) fraction are present in quantities from 2 to 100

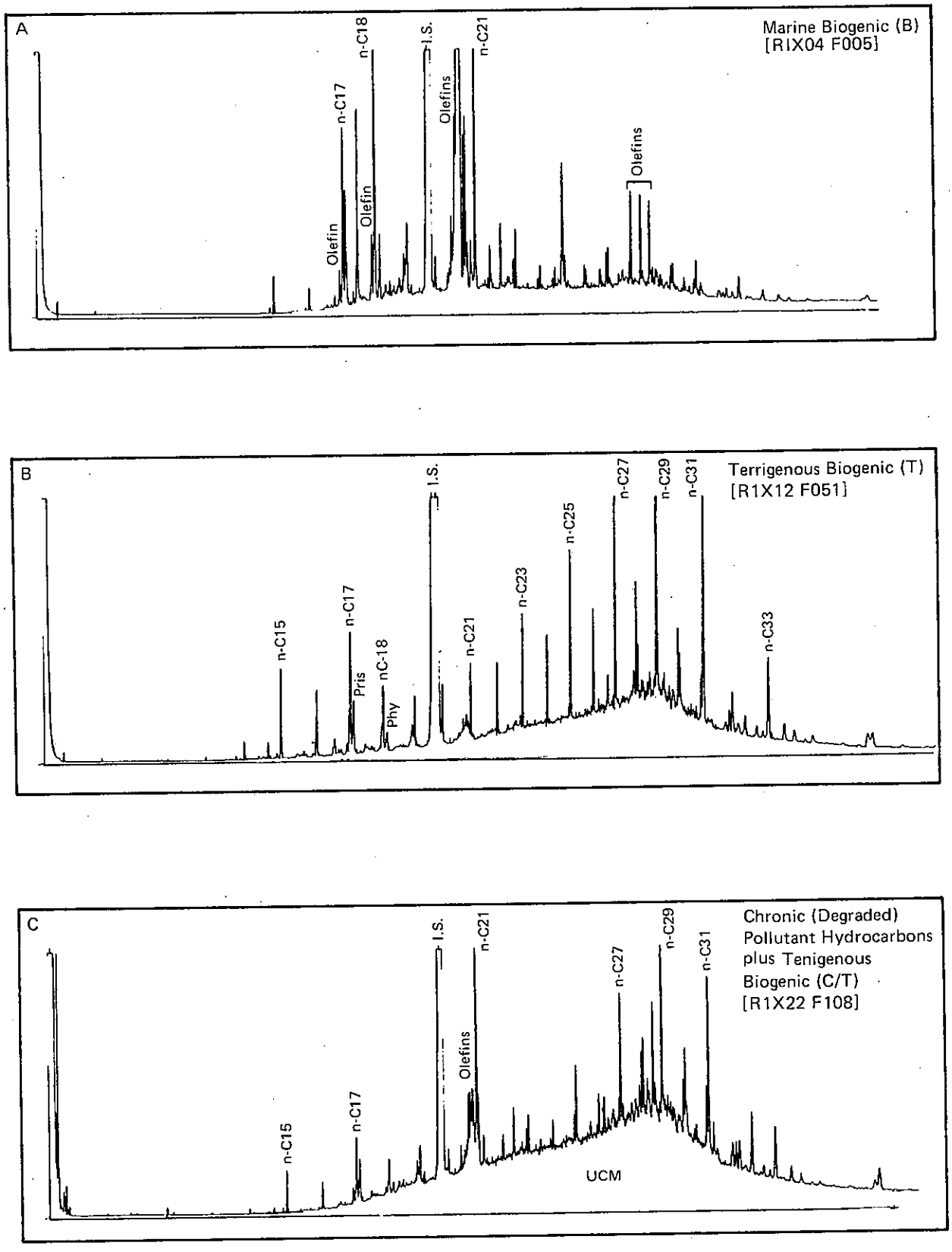

Figure 6. Glass capillary gas chromatograms of saturated hydrocarbons in non-oiled surface sediments.

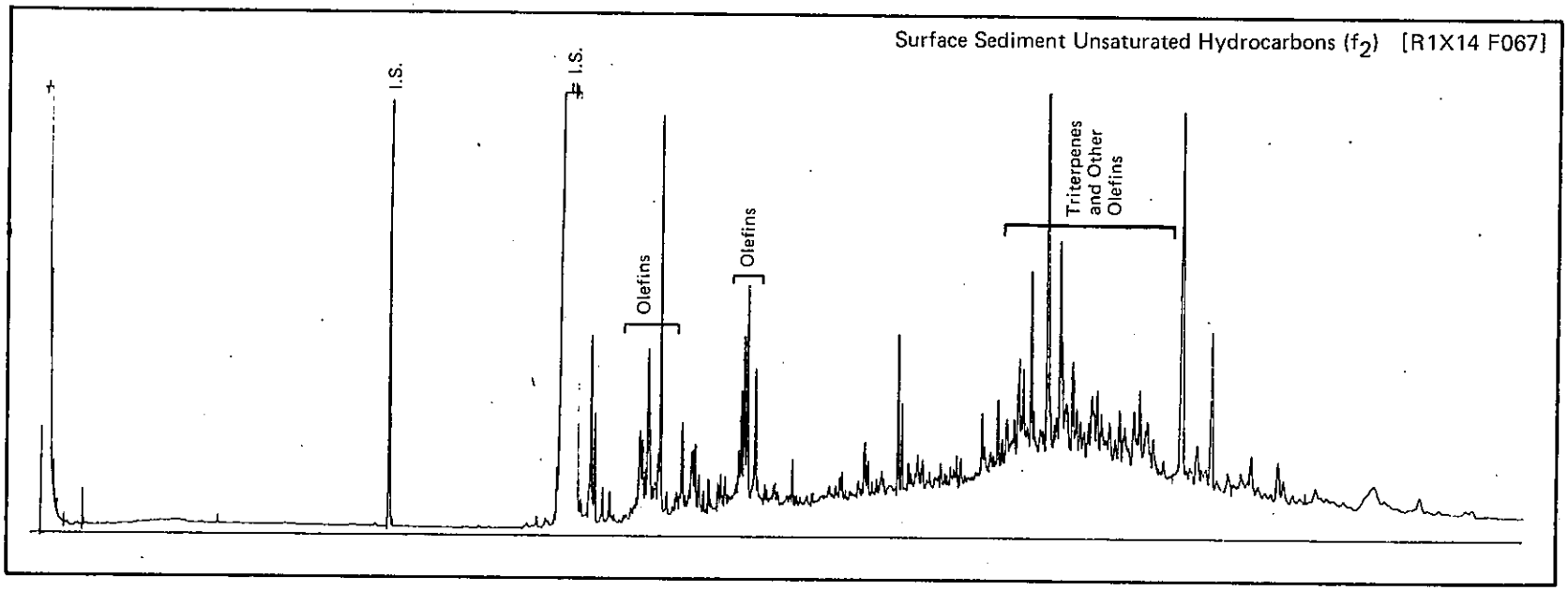

Figure 7. Glass capillary gas chromatogram of typical unsaturate (olefins + aromatic) fraction of surface sediment.

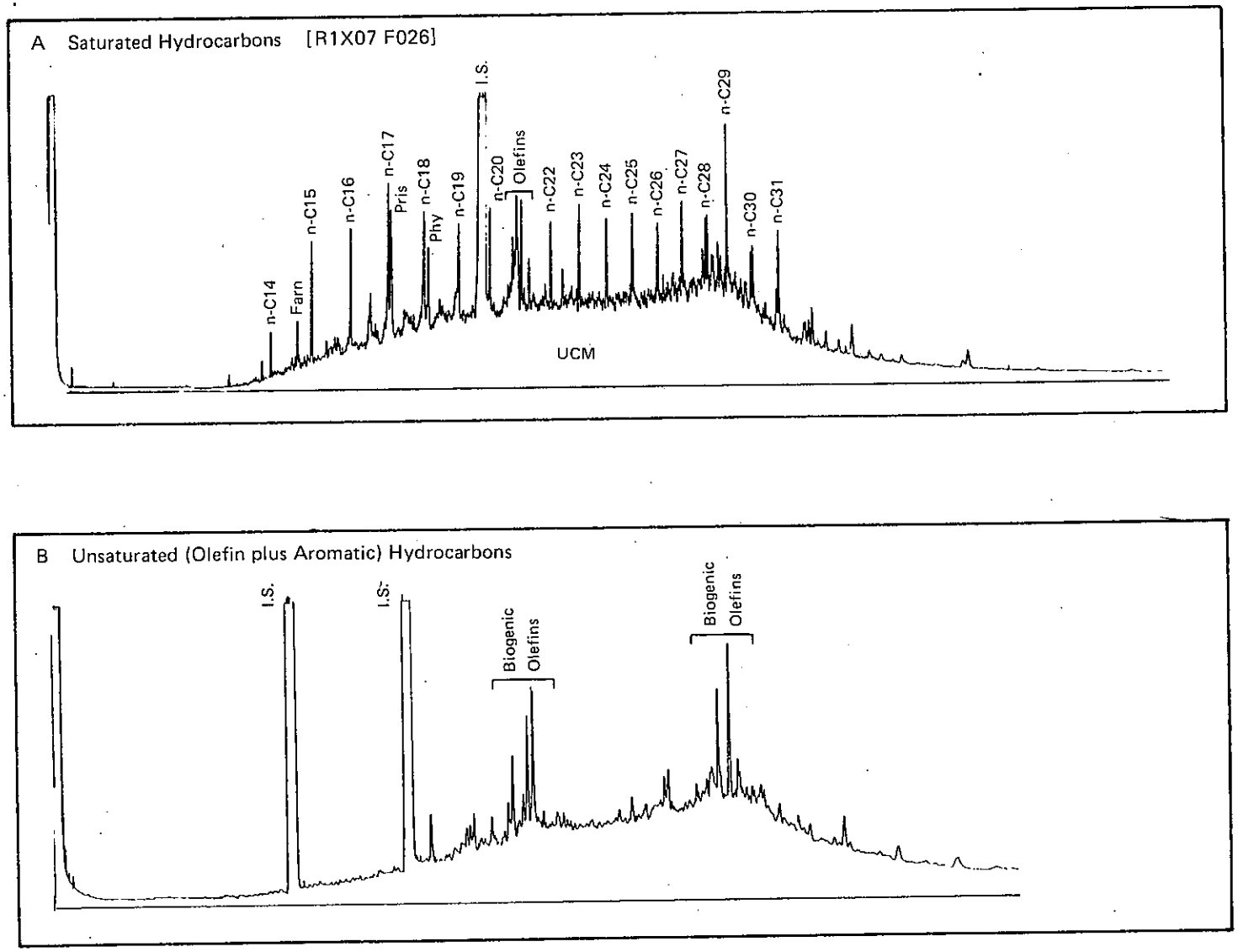

Figure 8. Glass capillary gas chromatograms of petroleum hydrocarbon-impacted surface sediment.

Table 3. Aromatic hydrocarbon levels in surface sediment (10^{-9} g/g dry wt.).

Station	Total P[a]	Total DBT[b]	m/e: 202[c]	m/e: 228[d]	m/e: 252[e]
RIX 7-1	8	16	<1	<1	2
7-2	13	36	n.d.	n.d.	5
RIX 10-1	6	13	--	--	5
10-2	10	13	--	--	2
RIX 12-1	2f	n.d.	2	2	13
12-2	<1f	n.d.	<1	--	10
RIX 14-1	--	--	3	1	14
14-2	--	--	2	--	7
RIX 22	3f	n.d.	12	8	42
RIX 30	6	13	3	3	25
RIX 4	--	--	1.5	--	--

[a]Total P = phenanthrene and alkyl phenanthrenes (C_1-C_4).

[b]Total DBT = dibenzothiophene and alkly dibenzothiophenes (C_1-C_3).

[c]m/e: 202 = fluoranthene and pyrene.

[d]m/e: 228 = benzanthracene and chrysene.

[e]m/e: 252 = benzofluoranthene, benzo(e)pyrene, and benzo(a)-pyrene and perylene.

[f]Comprised mainly of unsubstituted phenanthrene and small quantity of methlyphenanthrene (m/e 178 and 192, respectively).

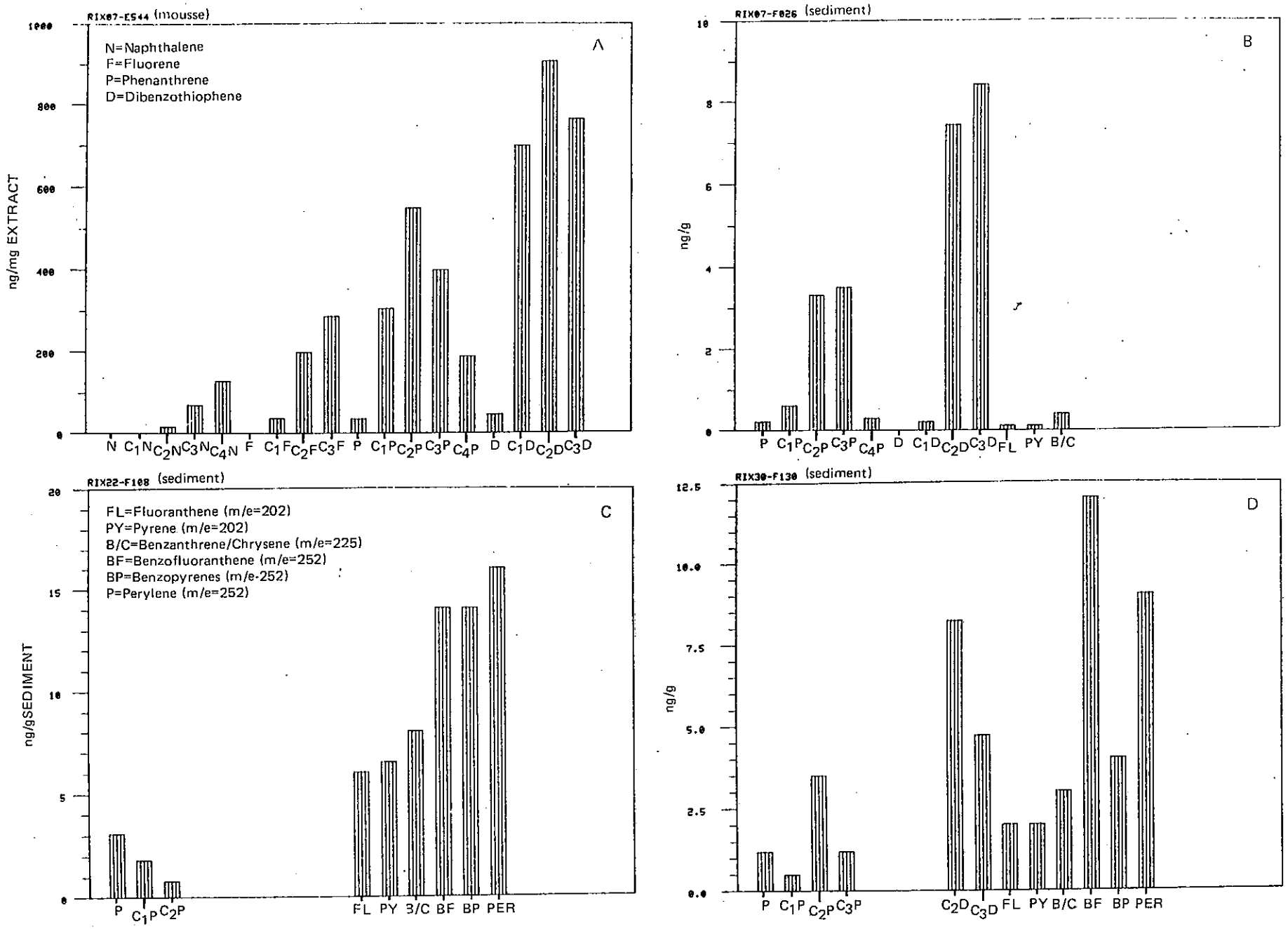

Figure 9. Histogram plots of GC/MS generated aromatic hydrocarbon data (note change in horizontal axis between mousse and sediment samples).

times greater than the PAH compounds. However, the unsaturate fraction of oil-impacted sediments contains UCM material that is quantitatively the most important group of compounds present in the samples. While the saturate fractions of oiled sediments contain resolved (peaks) features readily identifiable with a petroleum source, the f_1 UCM accounts for the majority of the concentration of this fraction.

We attempted to determine a pentacyclic triterpane "fingerprint" (Pym et al., 1975) of the IXTOC-I oil and to follow this relatively stable fingerprint as weathering proceeded in the water column and in petroleum-impacted sediment (Boehm et al., 1980b; Atlas et al., 1980). However, mass spectral searches for the m/e = 191 fragments associated with the hopane series yielded only a weak fingerprint with prominent norhopane and hopane compounds. Though all of the oil-impacted sediment exhibited a similar distribution of hopane compounds, so did several of the sediments classified as "clean" due to the preponderance of marine and/or terrigenous aliphatic hydrocarbon inputs. Therefore, in this instance we must assume that chronic petroleum and/or biogenic hydrocarbon inputs to the study region have left a refractory hopane fingerprint on the sedimentary geochemistry which, in combination with very low, nondiagnostic quantities of hopanes in the IXTOC-I oil, precludes the use of pentacyclic triterpanes as passive chemical source markers for this oil.

3.3 Sediment Traps

Several of the sediment trap composite samples analyzed do contain significant traces of what are believed to be actively sedimenting petroleum-hydrocarbon-bearing particulates. Both trap arrays deployed in the surface slick plume at PIX 08 (composites of traps at 2.5, 5, and 15 m), the combined 5-m and 15-m traps at PIX 14, and the array at PIX 15 contained detectable saturate hydrocarbon material primarily of a petroleum origin and likely associated with IXTOC-I oil. Figure 10 illustrates the nature of the captured material, which appears to consist of undegraded, physically/chemically weathered (primarily evaporation) IXTOC-I oil. The n-alkane distribution appears to be quite similar to the filtered particulate oil (Figure 5) and to the oil in sediments from nearby RIX 07 and RIX 10. Two noteworthy differences are apparent. The sedimentary petroleum hydrocarbon distribution appears to be richer in naphthenic (cyclic saturate) material in the UCM than the trapped particulates, presumably due to the lack of observed biodegradation in the water column and its increased role in the benthos. Secondly, the presence of phytoplanktonic material in the traps is signified by the prominence of n-C_{15} (pentadecane) and n-C_{17} (heptadecane) in the saturate capillary GC trace (Clark and Blumer, 1967). Neither the filtered particulate nor the sediment hydrocarbons in the blowout region show a planktonic influence, presumably due to masking by other more abundant compounds. Filtered particulates in control areas do contain phytoplanktonic hydrocarbons as the primary hydrocarbon input to the suspended particulate fraction (Boehm and Fiest, this symposium). Instead, the sediments containing petroleum appear to be influenced by a combination of petroleum and terrigenous biogenic inputs (n-C_{23}, n-C_{25}, n-C_{29}, n-C_{31}). Although there is no direct evidence for the association of oil with suspended mineral matter in the water column (Nelsen, this symposium), the observed presence of small

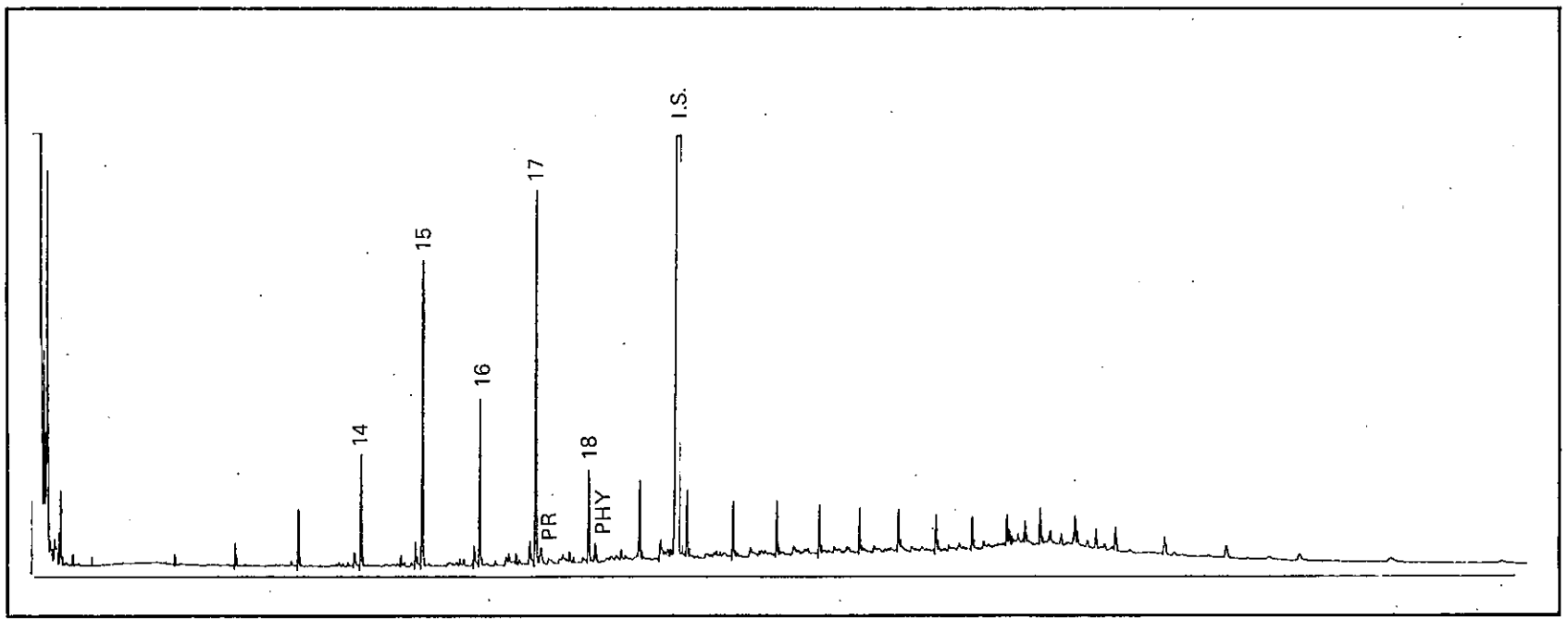

Figure 10. Capillary gas chromatogram of saturated hydrocarbons in sediment trap sample, PIX 8.

quantities of grayish carbonates in the traps suggests a possible association of suspended minerals with oil, resulting in their sinking. GC/MS examination of the aromatic (unsaturate) hydrocarbon fraction of the sediment traps revealed no detectable aromatic hydrocarbons, due undoubtedly to the very small amount of material captured rather than to any chemical fractionation process.

The absolute concentration of petroleum on the trapped hydrocarbon-bearing particulates is difficult to determine. The weight of trapped material was not measured due to fear of contamination and losses. However, we estimate that particulates in the traps ranged from 10 to 50 mg. Absolute quantities of oil in the traps ranged from 50 to 250 μg (8 hours after capture). Therefore, in those traps containing petroleum concentrations, the particulates may contain on the order of 1-25 μg petroleum hydrocarbons/mg settling particles, or the equivalent of 1-25 mg/g. Assuming a 150 cm^2 cross-sectional area of capture (the area of the openings of three jars/traps), and assuming ideal capture, a vertical flux of 1-5 $\mu g/cm^2$/day of oil is estimated. Admittedly, much uncertainty is associated with these calculations.

4. DISCUSSION

In our study of sedimenting petroleum-bearing particulates following the TSESIS spill (Boehm et al., 1980a; Johansson et al., 1980; Linden et al., 1980), two important factors emerged. First, oil transported recently to the sediment initially resides in the top few millimeters of the sediment, actually in the sediment floc. Conventional sediment sampling devices are nearly ineffectual in sampling this floc, as both sampler "bow waves" (corers and grabs) blow the floc aside and material may be lost in bringing grab samples on board. Hence, the TSESIS field study confirmed findings of the MERL experiments (Gearing et al., 1979). Secondly, rapid biodegradation was observed to greatly affect the composition of the TSESIS sediment-trap hydrocarbons. The same biodegraded pattern was found in the benthic-deposit-feeding bivalve (Macoma), which feeds on detritus in the top few millimeters of sediment.

Great care was exercised in obtaining sediment samples and grab subsamples aboard the R/V RESEARCHER. However, the determined concentrations of petroleum hydrocarbons in the sediment must be viewed as a result of a composite of the top 3-4 cm of sediment, which probably actually obscures a decreasing concentration gradient from surface to 3-4 cm and artificially lowers surface sediment (0-0.5 cm depth) concentrations. This fact has a bearing on determinations of both the areal extent of sedimentary impact of the IXTOC blowout and that part of the overall mass budget dealing with the offshore benthic sink. Furthermore, no bottom sediment samples were collected directly west or northwest of the well, the direction in which significant quantities of the oil had traveled prior to this cruise. For the purpose of calculating a budget, we assume a 30-km radius of detectable oil in the benthos, a depth of penetration into the sediment of 0.5 cm, and a conservative mean concentration in the top 0.5 cm of 150 μg/g (i.e., no oil in the 0.5- to 3-cm layer). Higher concentrations of oil in sediments probably can be found closer to the blowout source,

and levels undoubtedly increased from September to March of 1980 before the well was capped.

The budget summary presented in Table 4 indicates that a small percentage of oil is accountable in the offshore sediments. This value includes material directly transported to the offshore benthos but does not include that material in the nearshore subtidal/offshore bar system transported as a result of landfall followed by beach erosion and offshore deposition. This latter sink for IXTOC-I oil is probably an order of magnitude higher than for the offshore direct water-column-to-benthos transport.

The possibility that petroleum observed in the sediments was associated with pre-blowout drilling and lubricating mud discharges in the area cannot be entirely ruled out. However it seems unlikely in light of the detected presence of oil in the newly sedimenting water column hydrocarbon-bearing particulates.

That the actively settling material is undegraded seems remarkable in light of findings on TSESIS (Boehm et al., 1980a) and AMOCO CADIZ spills (Calder et al., 1979), both of which indicated that rapid biodegradation altered the composition of oil shortly after introduction into the marine system. However, findings of this work indicate that rapid biodegradation in some environments, perhaps limited by available nutrients, cannot be assumed to occur. Chemical (photochemical) weathering at the sea surface and physical chemical weathering (evaporation/dissolution) in the water column are the dominant, if not the only, weathering processes affecting the oil's aromatic and aliphatic composition within a 100-km radius of the blowout (this study) and along the entire path of slick movement (Laseter and Overton, this symposium; Patton et al., 1980). Biodegradation, albeit quite slow, is occurring in the sediments. The extent of weathering of oil in the sediments 3 months after the initial blowout approximates that observed in AMOCO CADIZ oil-impacted subtidal and intertidal sediments within a few weeks of deposition (Boehm et al., 1980b; Calder and Boehm, 1980; Atlas et al., 1980), thus confirming the retarded extent of biodegradation associated with all aspects of the IXTOC-I spill. The entire system seems nutrient-limited, thus accounting for imperceptible compositional changes due to microbial utilization of hydrocarbons. Significant biodegradation, however, did occur when petroleum particles became associated with land-derived plant matter and the decomposition of water-borne plants "feeding" the microbial degradation process on a microscale (Boehm and Fiest, this symposium).

Results from the sediment trap samples indicate that all mechanisms of transport of oil to the benthos appear to depend on the association of dispersed oil with phytoplankton by adsorptive processes. Indeed, the water column of the region appeared to be heavily influenced by living and detrital particulates at the time of sampling. Concentrations of suspended particulate matter are estimated to be on the order of 100 μg/l (Harvey, personal communication), with Secchi disc readings of 5 m as compared to normal Gulf of Mexico blue water with disc readings of 20 m or greater. The plankton/oil association could result from sorption of plankton on small oil droplets, resulting in increased density and hence sinking, or from ingestion of plankton and oil by zooplankters followed by fecal pellet transport. One or both of these

Table 4. Summary of mass budget for oil in sediments.

Estimated impact radius	30 km
Mean concentration of oil in top 0.5 cm	150 μg/g dry weight
Specific gravity of dry sediment	4 g/cm^3
Total IXTOC-I petroleum in sediment at the time of sampling	8.7 x 10^9 g
Volume of oil spilled	140 x 10^6 gallons = 550 x 10^9 cm^3
Density of oil	1 g/cm^3
Total weight of oil spilled	= 550 x 10^9 g
Percent of spilled oil in offshore sediments	= 8.7 x 10^9/550 x 10^9 = 1.5% of spillage

mechanisms, in addition to some association of petroleum with suspended (or resuspended) minerals in the water volume, result in sedimentation of a small percentage of the oil. In contrast, Kolpack et al. (1971) documented the sorption of oil from the Santa Barbara blowout onto terrigenous riverine suspended particulates followed by large-scale sedimentation of oil.

Clearly, the phenomenon of sedimentation of oil from tanker spills and offshore blowouts involves association of petroleum with available suspended particulates. The nature of the particulates (organic versus mineral), their surface area and concentration, result in a variety of scenarios both for the transport of water-borne petroleum hydrocarbons to the offshore continental shelf benthic environment and for their potential impact on sediment-dwelling detritovores. In these environments, suspended sediment or living particulate material must exceed 100-500 μg/l before significant (greater than a few percent) quantities of oil are transported to the benthos.

5. CONCLUSIONS

The study of sedimentation processes acting to transport IXTOC-I oil to the offshore benthos illustrates that:

(1) Minor quantities of the total oil spilled (0.5-3%) may reside in surface sediment layers within 50 km of the blowout site.

(2) Oil in the sediments is only marginally degraded by marine bacteria but has been weathered substantially by physical/chemical processes.

(3) Concentrations of oil in sediments were detected as high as 100 ppm but probably are much higher closer to the well and in the top layer (0-10 mm) of sediment.

(4) Actively sedimenting particles captured in trap arrays indicate that a significant amount of sedimenting oil is associated with phytoplanktonic material.

(5) The magnitude of direct transport of oil to the benthos agrees well with that predicted by the model of Mackay et al. (1979).

6. ACKNOWLEDGEMENTS

We would like to acknowledge the important role that Dr. John Farrington (Woods Hole) played in conceiving the sampling design and sediment samples aboard the R/V RESEARCHER. Keith Hausknecht and Jack Barbash of ERCO were instrumental in deploying and recapturing the sediment trap arrays. John Yarko, Adria Elskus, Lynn Kennedy, Neil Mosesman, and Ann Jefferies played important roles in the analytical chemistry segment of this study.

7. REFERENCES

Atlas, R. M., P. D. Boehm, and J. A. Calder (1980): Chemical and biological weathering of oil from the AMOCO CADIZ spillage within the littoral zone. Estuar. Coast. Mar. Sci. (in press).

Beslier, A., J. L. Berrien, L. Cabioch, J. L. Douville, C. Larsonneur, and L. Le Borgne (1980): Distribution et evolution de la pollution des bares de lannion et de morlaix par les hydrocarbures de l'AMOCO CADIZ. In Proceedings, AMOCO CADIZ, Fates and Effects of the Oil Spill, 19-22 November 1979, Brest, France, Centre National pour l'Exploitation des Oceans, COB, Brest.

Bieri, R. H., M. K. Cueman, C. L. Smith, and D. W. Su (1978): Polynuclear aromatic and polycyclic aliphatic hydrocarbons in sediments from the outer continental shelf. Internat. J. Environ. Anal. Chem.

Boehm, P. D., J. E. Barak, D. L. Fiest, and A. A. Elskus (1980a): A chemical investigation of the transport and fate of petroleum hydrocarbons in littoral and benthic environments: The TSESIS oil spill. (Submitted).

Boehm, P. D., D. L. Fiest, and A. A. Elskus (1980b): Comparative weathering patterns of hydrocarbons from the AMOCO CADIZ oil spill observed at a variety of coastal environments. In Proceedings, AMOCO CADIZ, Fates and Effects of the Oil Spill, 19-22 November 1979, Brest, France, Centre National pour l'Exploitation des Oceans, COB, Brest.

Brown, D. W., L. S. Ramos, A. J. Friedman, and W. D. Macloed (1979): Analysis of trace levels of petroleum hydrocarbons in marine sediments using a solvent/slurry extraction procedure. In Trace Organic Analysis: A New Frontier in Analytical Chemistry. National Bureau of Standards Special Publication 519, Washington, D.C.: 161-167.

Calder, J. A., and P. D. Boehm (1980): A one year study of weathering processes acting on the AMOCO CADIZ oil spill. In Proceedings, AMOCO CADIZ, Fates and Effects of the Oil Spill, 19-22 November 1979, Brest, France, Centre National pour l'Exploitation des Oceans, COB, Brest.

Calder, J. A., J. Lake, and J. Laseter (1979): Chemical composition of selected environmental and petroleum samples from the AMOCO CADIZ oil spill. In W. N. Hess, Ed., The AMOCO CADIZ Oil Spill--A preliminary scientific report. NOAA, Boulder, Colorado: 21-84.

Clark, R. C., Jr., and M. Blummer (1967): Distribution of paraffins in marine organisms and sediments. Limnol. Oceanogr., 12: 79-87.

Conover, R. J. (1971): Some relations between zooplankton and Bunker C oil in Chedocbueto Bay following the wreck of the tanker Arrow. J. Fish. Res. Board, Canada, 28: 1327-1330.

Cretney, W. J., C. S. Wong, D. R. Green, and C. A. Bawden (1978): Long term fate of a heavy oil in a spill contaminated B.C. coastal bay. J. Fish. Res. Board, Canada, 35: 521-527.

Ensminger, A., A. Van Dorsselaer, D. Spychkerelle, P. Albrecht, and G. Ourisson (1975): Pentacyclic triterpanes of the hopane type as ubiquitous geochemical markers: Origin and significance. In Advances in Organic Geochemistry, 1973. B. Tissot and F. Bienner (Eds.), Paris, France: 245-260.

Ferraro, E. P., and D. T. Nichols (1972): Analyses of 160 crude oils from 122 foreign oil fields. Bureau of Mines Information Circular 8542: 113 pp.

Fiest, D. L., and P. D. Boehm (1980): Mechanisms of subsurface transport of hydrocarbons from the IXTOC-I oil spill--spectrofluorometric determinations. Environ. Sci. Technol. (submitted).

Gearing, J. N., P. J. Gearing, T. Wade, J. G. Quinn, H. B. McCarty, J. Farrington, and R. F. Lee (1979): The rates of transport and fates of petroleum hydrocarbons in a controlled marine ecosystem and a note on analytical variability. In Proceedings 1979 Oil Spill Conference, Los Angeles, California, American Petroleum Institute, Washington, D.C.: 555-565.

Gordon, D. C., P. D. Keizer, W. R. Hardstaff, and D. G. Aldous (1976): Fate of crude oil spilled in seawater contained in outdoor tanks. Environ. Sci. Technol., 10: 580-585.

Grose, P. L., J. S. Mattson, and H. Petersen (1979): USNS Potomac oil spill, Melville Bay, Greenland 5 August 1977. Joint Report on the Scientific Studies and Impact Assessment by the NOAA-USCG Spilled Oil Research Team and the Greenland Fisheries Investigations, Ministry to Greenland, U.S. Department of Commerce, NOAA.

Johansson, S., U. Larsson, and P. Boehm (1980): The TSESIS oil spill. I. Impact of the pelogic ecosystem. Mar. Poll. Bull. (in press).

Johnson, J. H., P. W. Brooks, A. K. Aldridge, and S. J. Rowland (1978): Presence and sources of oil in sediments and the benthic community surrounding the Ekofisk field after the blowout at Bravo. In Proceedings of the Conference on Assessment of Ecological Impacts of Oil Spills, 14 and 17 June 1978, Keystone Co., American Institute of Biological Sciences, Washington, D.C.

Keizer, P. D., T. P. Ahearn, J. Dale, and J. A. Vandermeulen (1978): Residues of Bunker C oil in Chedabucto Bay, Nova Scotia, 6 years after the Arrow spill. J. Fish. Res. Board, Canada, 35: 528-535.

Kolpack, R. L., Ed. (1971): Biological and oceanographical survey of the Santa Barbara channel oil spill 1969-1970. In Physical, Chemical and Geological Studies, Vol. II of Biological and Oceanographic Surveys of the Santa Barbara Channel Oil Spill, University of Southern California, Allan Hancock Foundation, Los Angeles.

Kolpack, R. L., J. S. Mattson, J. B. Mark, Jr., and T. C. Tu (1971): Hydrocarbon content of Santa Barbara channel sediments. In Physical, Chemical and Geological Studies, Vol. II of Biological and Oceanographic Surveys of the Santa Barbara Channel Oil Spill, R. L. Kolpack, Ed., University of Southern California, Allan Hancock Foundation, Los Angeles, p. 276-295.

Kolpack, R. L., and N. B. Plutchak (1976): Elements of mass balance relationships for oil released in the marine environment. Proceedings of Symposium on Sources, Effects, and Sinks of Hydrocarbons in the Aquatic Environment, 9-11 August 1976, American Institute of Biological Sciences, Washington, D.C.

Kolpack, R. L., R. W. Stearns, and G. L. Armstrong (1978): Sinking of oil in Los Angeles Harbor, California following the destruction of the Sansinena. In Proceedings of the Conference on Assessment of Ecological Impacts of Oil Spills, 14-17 June 1978, Keystone, Colorado, American Institute of Biological Sciences.

Linden, O., R. Elingren, and P. Boehm (1980): The TSESIS oil spill: Its impact on the coastal ecosystem of the Baltic Sea. Ambio., 8: 244-253.

Lloyd, J. B. F. (1971): The nature and evidential value of the luminescence of automobile engine oils and related materials. J. Foren. Sci. Soc., 11: 83-94, 153-160, 235-253.

Mackay, D., I. Berist, R. Mascarenhas, and S. Paterson (1979): Oil spill processes and models. Report to Environmental Protection Service (Arctic Marine Oil Spill Program), DSS Contract No. 06SS-KE304-8-0680.

Mackay, D., and S. Paterson, Eds. (1978): Oil Spill Modelling. Proceedings of a workshop held in Toronto, Canada, 7-8 November 1978, Publication EE-12, Institute for Environmental Studies, University of Toronto, Toronto, Canada.

Mattson, J. S., and P. L. Grose (1979): Modeling algorithms for the weathering of oil in the marine environment. Final Report, Research Unit No. 499, Outer Continental Shelf Environmental Assessment Program, NOAA, Boulder, Colorado.

McAuliffe, C. D., A. E. Smalley, R. D. Grover, W. M. Welsh, W. S. Pickle, and G. E. Jones (1975): Chevron Main Pass block 41 oil spill: Chemical and biological investigations. In Proceedings, Joint Conference on Prevention and Control of Oil Spills, San Francisco, California, 1975: 555-566.

National Academy of Sciences (1975): Petroleum in the marine environment. NAS, Washington, D.C.: 107 pp.

OSIR (Oil Spill Intelligence Report) (1980): Volume III, Center for Short-Lived Phenomena, Cambridge, Massachusetts.

Patton, J. S., M. W. Rigler, P. D. Boehm, and D. L. Fiest (1980): The IXTOC-I oil spill: Flaking of surface mousse in the Gulf of Mexico. Science (submitted).

Poirier, O. A., and G. A. Thiel (1941): Deposition of free oil by sediments settling in seawater. Amer. Assoc. Petrol. Geol. Bull., 25: 2170-2180.

Pym, J. G., J. E. Ray, G. W. Smith, and E. V. Whitehead (1975): Petroleum triterpane fingerprinting of crude oils. Anal. Chem., 47: 1617-1622.

Teal, J. M., K. Burns, and J. Farrington (1978): Analyses of aromatic hydrocarbons in intertidal sediments resulting from two spills of No. 2 fuel oil in Buzzards Bay, Massachusetts. J. Fish. Res. Board, Canada, 35: 510-520.

Thuer, M., and W. Stumm (1977): Sedimentation of dispersed oil in surface waters. Prog. Wat. Tech., 9: 183-194.

Wakeham, S. G. (1977): Synchronous fluorescence spectroscopy and its application to indigenous and petroleum-derived hydrocarbons in lacustrine sediments. Environ. Sci. Technol., 11: 272-276.

Youngblood, W. W., and M. Blumer (1975): Polycyclic aromatic hydrocarbons in the environment: Homologous series in soil and recent marine sediment. Geochim. Cosmochim. Acta, 39: 1303-1314.

SURFACE EVAPORATION/DISSOLUTION PARTITIONING OF LOWER-MOLECULAR-WEIGHT AROMATIC HYDROCARBONS IN A DOWN-PLUME TRANSECT FROM THE IXTOC-I WELLHEAD

J. R. Payne, N. W. Flynn, P. J. Mankiewicz, and G. S. Smith
Science Applications, Inc.

1. INTRODUCTION

Most authorities have concluded that the combined processes of evaporation and dissolution are responsible for the most significant loss of lower-molecular-weight hydrocarbons (up to n-C_{12}) from crude oil that has been spilled into open waters (Clark and Brown, 1977; Clark and MacLeod, 1977; Karrick, 1977; McAuliffe, 1977a; Wheeler, 1978). Numerous investigations have suggested from observation that the majority of these lighter components of oil are rapidly and effectively lost to the atmosphere by evaporation relative to their dispersal by dissolution into the subsurface water column (Calder, 1979; Harrison et al., 1975; McAuliffe, 1977a and b; Regnier and Scott, 1975; Smith and McIntyre, 1971). However, virtually all of the data indicating the relative importance of evaporation over dissolution have been collected from surface open-water spills in which the crude oil being acted upon is confined to relatively limited contact with the bulk water column.

The IXTOC-I blowout represents a major subsurface "spill" in which a tremendous amount of oil was released at depth, increasing its exposure to the water column. Because many of the same properties and parameters affect both dissolution and evaporation (e.g., molecular size, molecular polarity, sea conditions, atmospheric conditions), an important question in such a case is that of the relative partitioning of lower-molecular-weight fractions between evaporative loss and solubilization throughout the water mass. Our approach to this question was to determine whether certain compounds were preferentially dissolved or evaporated compared to others and to determine the net relationships between compound solubility/volatility and compound partitioning preference under the conditions encountered in the post-IXTOC-I environment.

The results presented here represent volatile hydrocarbon data from samples of air and subsurface water collected along a 24-mile down-plume transect from the IXTOC-I wellhead. Sampling was performed on the NOAA RESEARCHER/G. W. PIERCE cruise between September 18 and 21, 1979.

2. EXPERIMENTAL METHODS

2.1 Field Sampling Techniques

Volatile hydrocarbons were sampled from the ambient air 1.5 m above the slick (or water surface) by vacuum-pumping measured volumes of air through 1/8 in. ID x 12 in. long stainless tubes packed with Tenax GC polymer. At each station two tubes were connected in series with Swagelock fittings, and prior to and immediately after sampling all tubes were sealed with Swagelock endcaps and plugs. Sampling was achieved by using a Gast Mfg. Corp. vacuum pump attached to the Tenax traps via flow regulators and flexible Teflon tubing.

The traps were positioned over the windward gunwale of the PIERCE, forward of the main engine exhaust stacks, and a telltail was positioned above the traps to monitor prevailing wind direction at all times during sampling.

Before obtaining each sample, the system's flow velocity was checked with a bubble flow meter. Approximately 1/2-hour samples (accurately timed) were obtained at flow rates ranging from 20 to 30 ml/min; thus, sample volumes ranged from 600-900 ml.

Water samples for analysis of dissolved lower-molecular-weight aliphatic and aromatic hydrocarbons were obtained by bucket casts, and subsamples were taken in Pierce septum-capped vials for subsequent purge and trap analysis by GC/MS techniques similar to those developed by Bellar and Lichtenberg (1974) and others.

Following collection, the water samples were refrigerated (no preservatives were added), and they were maintained at 3°C during shipment and storage before analysis. The plugged stainless-steel Tenax traps were stored at ambient temperature until analysis.

2.2 Analytical Techniques

2.2.1 Heat Desorption GC/MS Analysis of Tenax Columns

The Tenax air samples were analyzed by heat desorption followed by gas chromatography/mass spectrometry using a Finnigan 4021 quadrupole instrument. The GC/MS desorption was accomplished by installing the Tenax traps in a Tekmar liquid sample concentrator (LSC-2).

At the time of desorption (5 min. at 180°C at 20 ml/min He flow) the gas chromatographic column (packed 6 ft. x 22 mm I.D. SP-1000) and oven were cryogenically cooled to 30°C. Following desorption the oven was programmed rapidly (30°C/min) to 100°C and then from 100°C to 200°C at 10°C/min. The final temperature of 200°C was held for the duration of the chromatographic run. A GC column flow rate of 20 ml/min He was also used and the injector temperature was held at 200°C.

The effluent from the gas chromatograph passed through a glass jet separator for enrichment and then directly into the ion source, operated in the electron impact-mode at 300°C. Spectra were acquired by operating the ion source at 70eV from 35 to 300 amu in 1.95 sec. A hold time of 0.05 sec was used to allow the electronics to stabilize before the next scan. The ion source was tuned for maximum sensitivity with perfluorotributylamine. The ion fragments at m/e 69 and m/e 219 were calibrated to give a 2.5:1 ratio; the electron multiplier was operated at 1600V with the preamplifier gain at 10^{-7} amps/volt.

Data acquisition was initiated at the moment of desorption. Typically, 900-1000 scans were acquired for each data file.

2.2.2 Purge and Trap GC/MS Analysis for Volatiles in Water

The water samples stored in Pierce vials were allowed to come to room temperature and 5-ml aliquots were withdrawn and injected into the purge device of the LSC-2. Before purging, 100 ng each of three internal standards, dichlorobutane, (m/e 55), bromochloromethane (m/e 130), and bromochloropropane (m/e 77) were added. This allowed correction of recovered values for matrix effects and negated differences in ionization potential, lens voltage, etc., among runs.

Instrumental conditions were identical to those described for Tenax column analysis.

2.2.3 Data Reduction

Two methods of quantitation were used for determining concentrations of volatile hydrocarbons. First the base peak ionization was summed from GC-mass chromatograms as shown in Figure 1 by scanning the temperature-programmed GC run specifically at the molecular ion or base peak of the compound(s) of interest.

Base peak areas and mass spectra, together with standard compound retention times, were used as the basis for compound identifications. The equation used for calculation of individual hydrocarbon concentration levels is:

$$\text{Component concentration (ng/g or } \mu\text{g/L)} = \frac{\text{peak area of component}}{\text{reference peak area}} \times \frac{\text{reference concentration}}{\text{response factor}}$$

In the case of the Tenax trap (air) samples, a certain amount of pre-sampling calibration had to be conducted in order that proper data reduction could be performed. Before preparing for the field experiments, a series of recovery tests were completed using several organic solvents (including benzene) and raw gasoline as substrates. Figure 2 shows the reconstructed ion chromatograms obtained on the "front" and "back" columns used as a sampling train in this study. Mass chromatograms A and D in Figure 2 clearly show the presence of benzene and toluene trapped on the front column (note m/e 78 and 91), whereas the mass chromatograms of the secondary (back) columns in Figure 2 (B and E) show the lack of any breakthrough using a 1/2-hour sampling period at a flow rate of 20 ml/min. When actual field samples were analyzed, however, some breakthrough of lower-molecular-weight aliphatic and cycloalkane compounds did occur. As a result, all of the data presented in this report were generated from the sum of the compounds isolated in the front and back columns.

During the period of Tenax air sampling, the ambient air temperature varied from 25 to 28°C. Barometric pressure recorded on September 19 ranged from

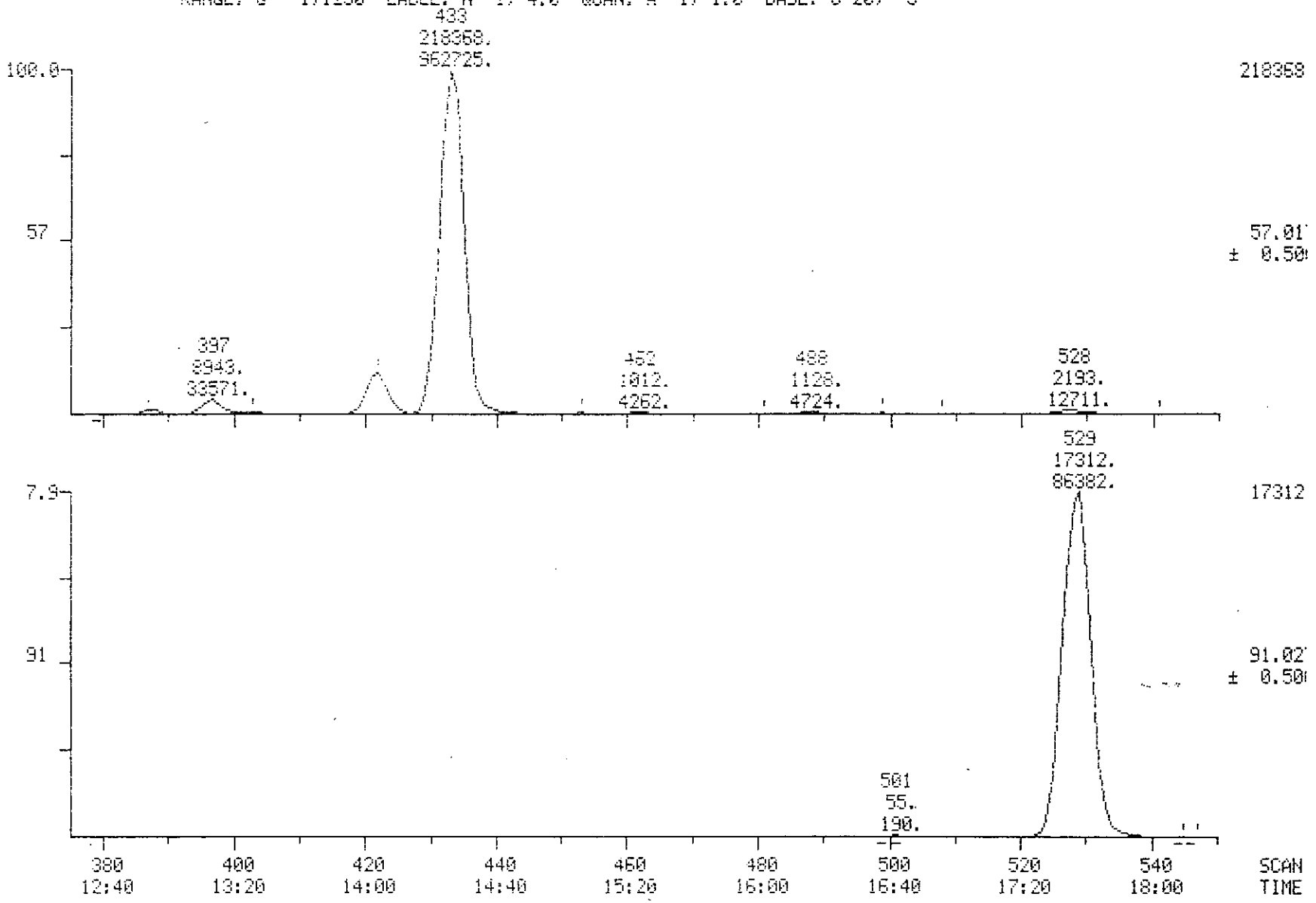

Figure 1. Mass chromatograms for m/e 57 and m/e 91 for quantitation of 2-methylpentane and toluene, respectively.

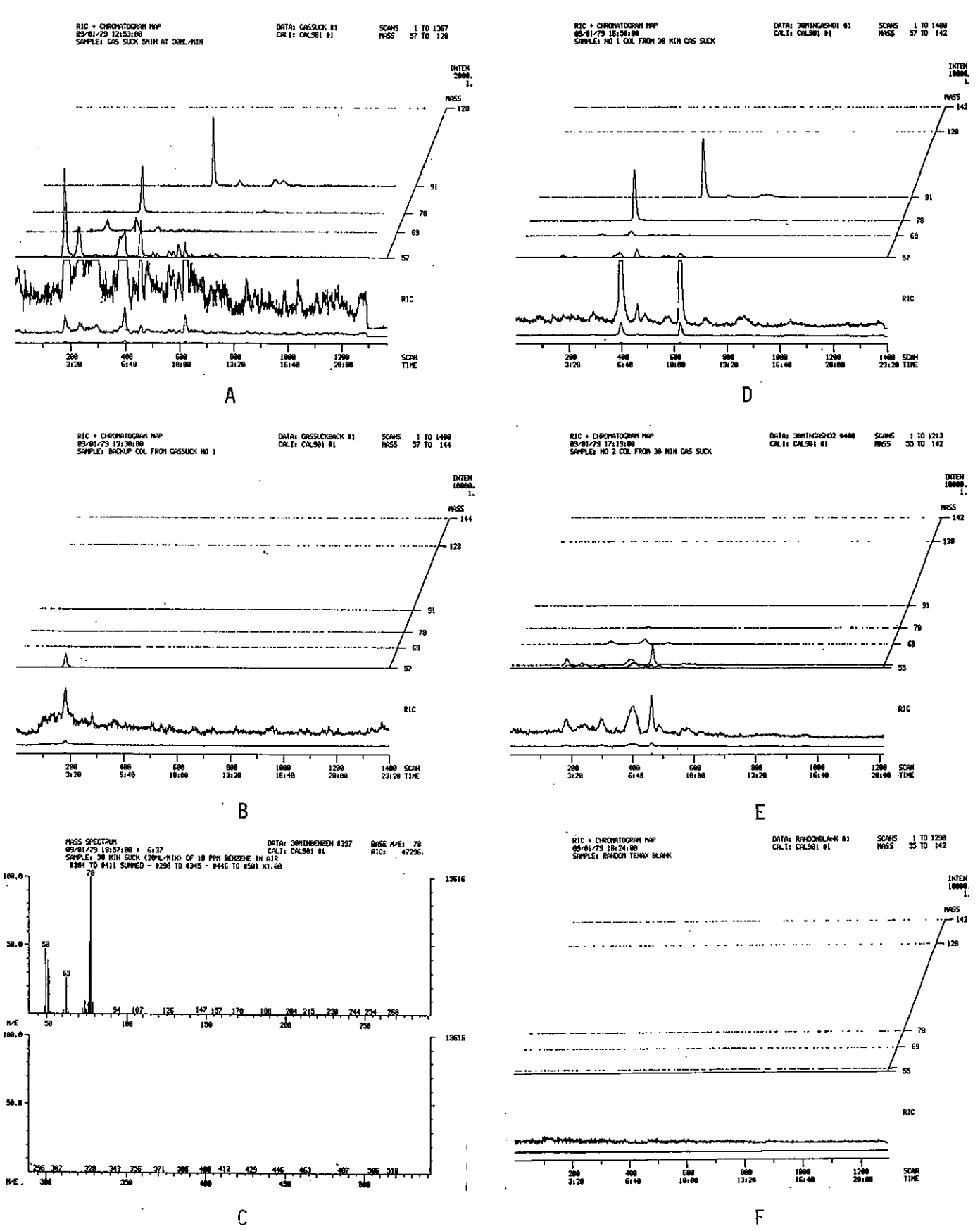

Figure 2. Reconstructed ion chromatograms obtained from heat desorbtion of Tenax columns used for trapping of volatile aromatic hydrocarbons from gasoline. A. front column obtained from 5 min air sample at 30 ml/min; B. secondary backup column from A; C. mass spectrum from scan number 397 from A identifying component as benzene; D. 30 min air sample from gasoline sample after 5 hr of exposure to atmospheric conditions (front column) E. secondary column from D above; and F. Tenax blank.

765 to 767 mm (Hg) and records from the PIERCE indicate that the barometric pressure may have varied from a low of 757 mm to a high of 767 mm (Hg) over the total time of the cruise. In calculating the concentrations of hydrocarbons in the air samples, the density of air was determined for these ranges of temperature and barometric pressure, and a mean density 0.001181 g/ml was derived. Differences in density due to fluctuations in temperature and atmospheric pressure over the range encountered result in a maximum variance of less than 2% in the calculated concentration data. For this reason the individual air sample concentrations were not corrected for the temperature and barometric pressure at the exact time of sampling. Corrections for atmospheric humidity were not made.

Standards for both the air samples and water samples were run daily and relative response factors were generated for pentane, thiophene, benzene, hexane, iso-octane, toluene, ethylbenzene, xylene (all three isomers), styrene, nonane, and dichloromethane. Rentention times, scan numbers, and relative response factors (compared to the internal standard, dichlorobutane) for these compounds are shown in Table 1.

All concentration data are reported as either ng/g air (Tenax samples) or µg/L seawater.

3. RESULTS

Figure 3 shows the station locations of the PIERCE during the 3-day, 24-mile down-plume transect. The majority of stations were occupied on one day (19 September). Background air samples were obtained northwest of the Yucatan Peninsula at station PIX 01 on 15 September, and additional near-wellhead samples were collected both west and east of the blowout site, at various distances, on 18 and 21 September.

Figure 4 (A and B) shows the reconstructed ion chromatograms with compound identifications for the front and back Tenax columns obtained from station PIX 11, located at 6.2 miles/40° true from the wellhead. The qualitative spectrum appearance and compound identifications shown in Figure 4 indicate that the majority of materials were trapped on the front column, with approximately 17% overall breakthrough onto the secondary trap. (If 17% breakthrough on the secondary trap occurred, then overall trapping efficiencies are still greater than 95%.) Compound identifications were made by comparing the mass spectrum of each major component to NBS/NIH library spectra contained in the INCOS data system of the Finnigan 4021 GC/MS. Best fits in connection with retention time reproducibility were the criteria used for absolute compound identifications.

Figure 5 presents the reconstructed ion chromatogram of the water sample (PIX 11E114) obtained at a depth of 1 m with a Go-Flo sampler simultaneously with the air sample shown in Figure 4. Clearly, the major components in the water sample are benzene, bromochloromethane (internal standard), methylpentane, toluene, xylene isomers, and an extraneous breakdown product from the Tenax trap. Table 2 presents the reduced data for all of the Tenax air samples

Table 1. Base peaks, scan numbers, and relative response factors for volatile compounds of interest.

		SIXV41080B#				SIXV41180#				SIXV41480				SIXV41580			
Compound	m/e	scan#	area	amt mg	RF	scan#	area	amt mg	RF	scan#	area	amt mg	RF	scan#	area	amt mg	RF
Dicholorobutane	55	500	23162	100.0	1.0	496	30233	100.0	1.0	424	34734	100.0	1.0	498	7272	100	
Pentane	43	325	34948	72.8	2.1	325	95649	72.8	4.3	327	54785	72.8	2.2	323	9117	72.8	1.7
Thiophene	84	335	29925	91.8	1.4	335	43330	91.8	1.6	336	39118	91.8	1.2	332	40417	91.8	6.1
Benzene	78	369	40076	73.4	2.4	366	66676	73.4	3.0	366	53696	73.4	2.1	362	58352	73.4	10.9
Hexane	57	481	33195	76.2	1.9	477	70154	76.2	3.0	478	82852	76.2	3.1	476	27738	76.2	5.0
Iso-octane	57	508	27495	71.4	1.7	504	83819	71.4	3.9	506	29238	71.4	1.2	505	6722	71.4	1.3
Toluene	91	527	44533	73.8	2.6	524	92570	73.8	4.1	526	64498	73.8	2.5	525	74046	73.8	13.8
Ethylbenzene	91	588	51190	80.2	2.8	584	89216	80.2	3.7	587	33589	80.2	1.2	586	59786	80.2	10.3
Xylene	91	649	37744	74.0	2.2	646	66304	74.0	3.0	650	22165	74.0	0.9	648	42216	74.0	7.8
Xylene (X2)	91	660	77474	148.0	2.3	656	128599	148.0	2.9	659	46479	148.0	0.9	658	84300	148.0	7.8
Styrene	104	646	28952	64.6	1.9	642	29655	64.6	1.5	646	5410	64.6	0.2	644	14357	64.6	3.1
Nonane	57	717	30543	77.0	1.7	713	79256	77.0	3.4	717	34552	77.0	1.3	715	44765	77.0	8.0
Naphthalene	128	1112	40353	73.0	ND	918	16521	73.0	0.7	---	ND	---	---	928	3821	73.0	0.2

Continued

Table 1. (Continued)

Compound	m/e	scan#	area	amt mg	RF	scan#	area	amt mg	RF	$\bar{X}$ response factor for days 4/10, 4/11, 4/16, and 4/17	Response factor coefficient of variation
Dicholorobutane	55	490	11083	100.0	1.0	496*	27246	100.0	1.0		
Pentane	43	328	9429	36.4	2.3	334	15863	36.4	1.6	2.6	46.2
Thiophene	84	339	8205	45.9	1.6	346	12065	45.9	1.0	1.4	21.4
Benzene	78	376	11516	36.7	2.8	384	17849	36.7	1.8	2.5	20.0
Hexane	57	476	2284	38.1	0.5	484	2839	38.1	0.3	1.4	92.9
Iso-octane	57	498	17537	35.7	4.4	503	32458	35.7	3.3	3.3	36.4
Toluene	91	519	16157	36.9	4.0	524	19781	36.9	2.0	3.2	31.3
Ethylbenzene	91	579	14984	40.1	3.4	585	24269	40.1	2.2	3.0	23.3
Xylene	91	641	10002	37.0	2.4	648	16830	37.0	1.7	2.3	21.7
Xylene (X2)	91	651	19546	74.0	2.4	658	38373	74.0	1.9	2.4	16.7
Styrene	104	637	5459	32.3	1.5	644	12786	32.3	1.5	1.6	12.5
Nonane	57	708	8113	38.5	1.9	714	15732	38.5	1.5	2.1	43.9
Naphthalene	128	---	ND	---	---	---	ND	---	---	---	---

*Acquisition started 0.5 min later - all scans are adjusted.
#Used for making average RF values.

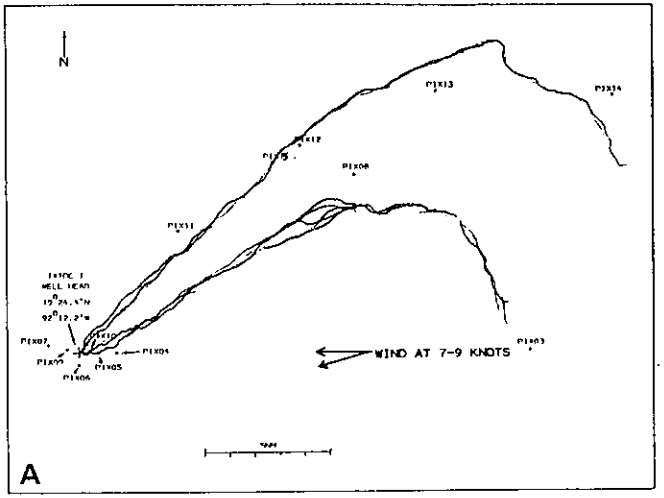

9-18-79
wind 75° to 90° true 7-9 knots
0911 - 1115 local Miami time

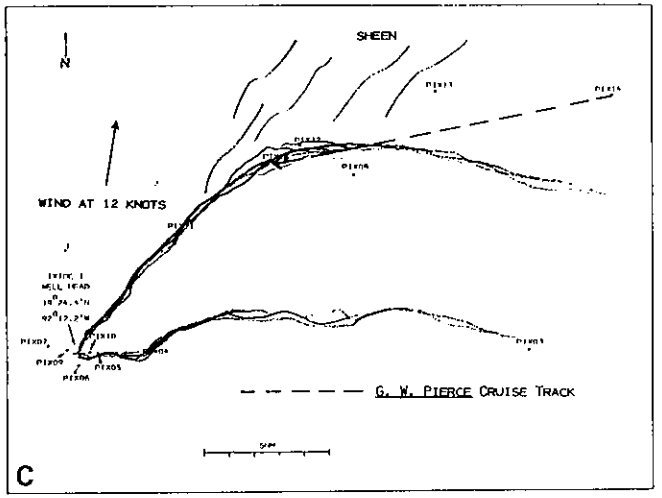

9-20-79
wind out of 190° true at 12 knots
0930-1100 local Miami time

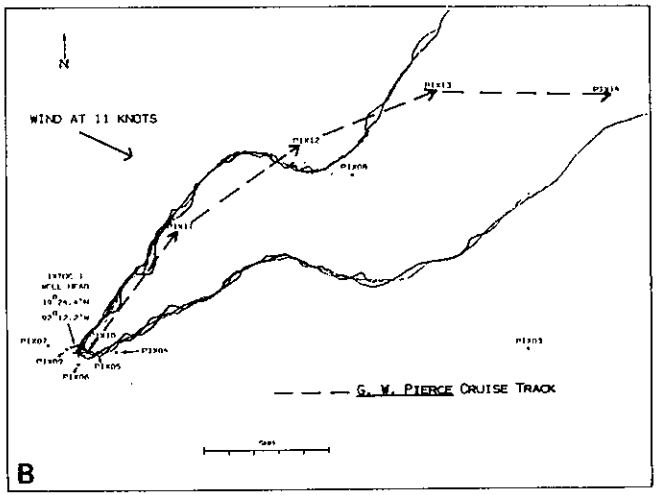

9-19-79
wind out of 295°T at 11 knots
0914-1050 local Miami time

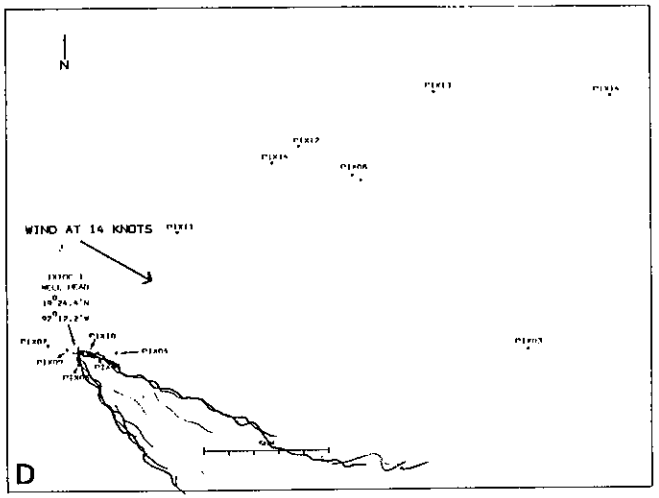

9-21-79
wind out of 300° true at 14 knots
1630 - 1800 local Miami time

Figure 3. IXTOC-I Oil Plume Drift and G. W. PIERCE station locations occupied on (A) 9-18-79, (B) 9-19-79, (C) 9-20-79 and (D) 9-21-79.

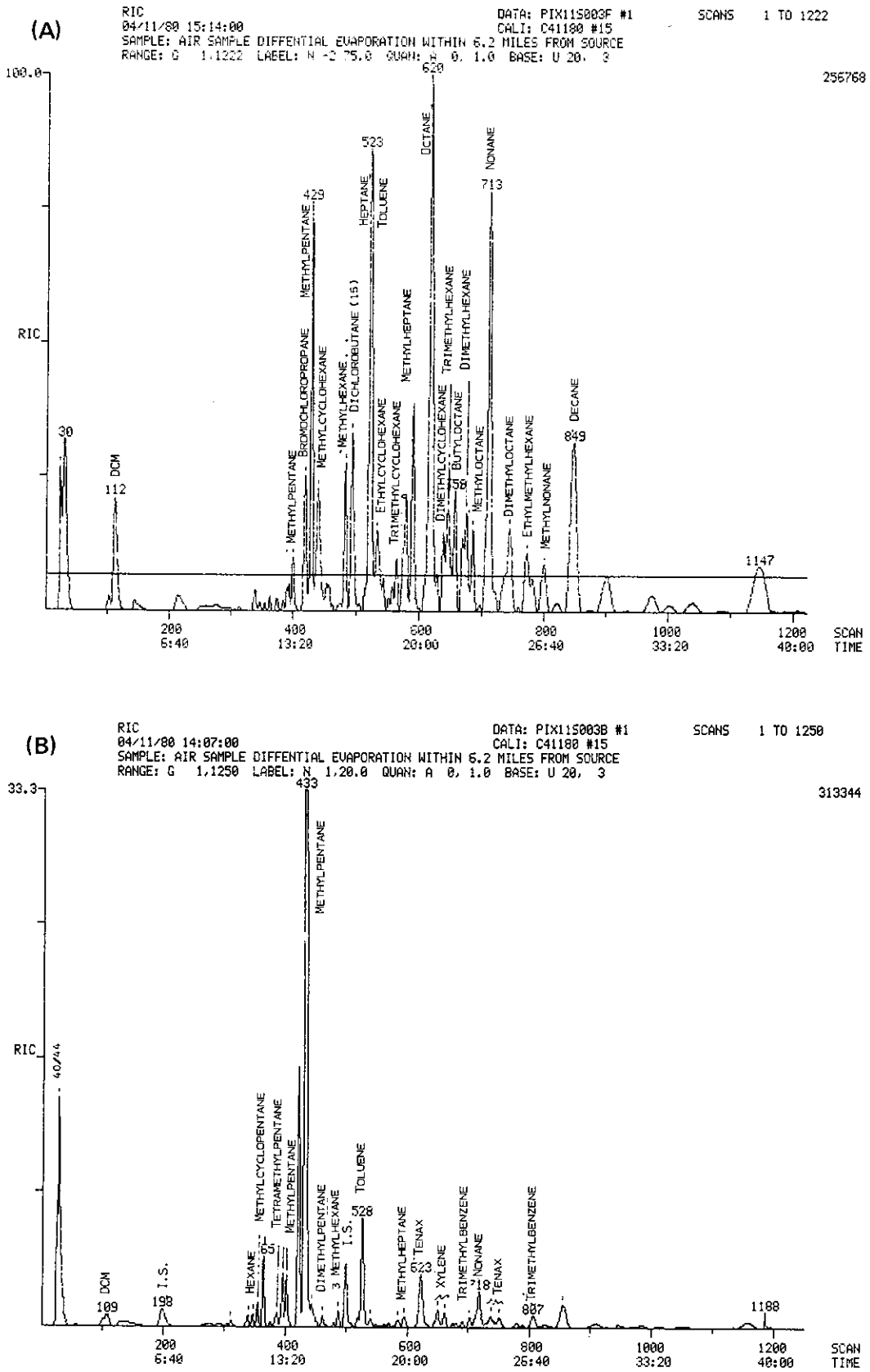

Figure 4. Reconstructed ion chromatograms for the "front" (A) and "back" (B) Tenax columne collected at Station PIX 11 (6.2 miles/40° true from IXTOC-I wellhead).

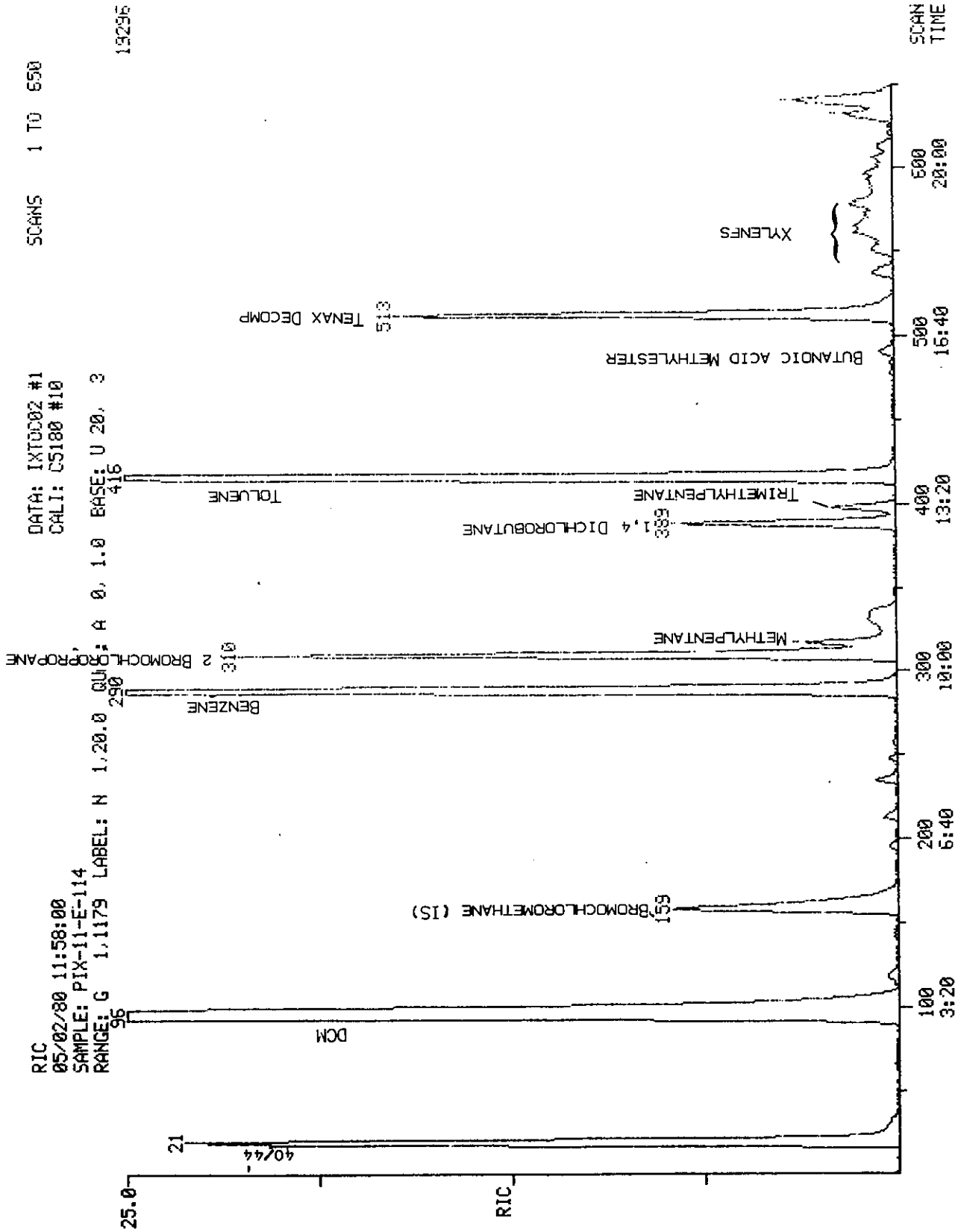

Figure 5. Reconstructed ion chromatogram of the 1 m deep water sample collected simultaneously with the Tenax trap sample shown in Figure 4 at Station PIX 11.

Table 2. Reduced concentration data for air- and water-borne volatile components along the G. W. PIERCE down-plume transect. (ng/g air; µg/L seawater).

SAI Sample No.	Distance and Direction from Wellhead	Sample Type	Water Depth	propane	pentane	methylcyclopentane	2-methylpentane	3-methylpentane	benzene	hexane	methylcyclohexane (X3)	toluene	heptane	ethylcyclohexane	trimethylcyclohexane	ethylbenzene	methylheptane	octane	trimethylcyclohexane	xylene	xylenes (X2)	dimethylcyclohexane	C_9-hexane	methylactane	nonane	Comments
PIX01S001	Background air						38	30																		
PIX10E103	0.4 mile E	air		+	+		1930		trace		+++	135	1800	+	++	375		1360		943	940		43		90	Background air on 9-15-79 21°41'N 90°25'W
PIX04E049	1.5 mile E	air		+	+	+	3850	4000			+	244			+	31	-	205		77	60	5			244	Background air on 9-15-79 21°41'N 90°25'W
PIX07E069	1.5 mile W	air					600	400	3			5								<2	<2				8	styrene
PIX11S001	3.2 miles NE	air		+	+	+	140	140		12	++	477				53	+	264		140	120				6200	stigene 215
PIX11S001A	3.2 miles NE	water	surf																							
PIX11S002	4.3 miles NE	air		+	+	+	510	3400			+++	14	+++		+	3	++	+		7	6				140	
PIX11S002A	4.3 miles NE	water	surf																							
PIX11S003	6.3 miles NE	air				+	1160				+	47	+		+	5	++	+		13	13	+	++		215	+ 2 methylnonane & decane
PIX11S003A	6.2 miles NE	water	surf																							
PIX11E114	6.2 miles NE	water	1 m				6	3	49			97								1.6	1.7					
PIX11E113	6.2 miles NE	water	6 m				5	7	2.1			5.7								3.2	2.3					
PIX11E110	6.2 miles NE	water	20 m				4	4	7.4			14								2	1					
PIX11S005	7 miles NE	air				+	1310				+	36	145	+		2	++			6	4				260	
PIX11S006	7 miles NE	water	surf					4	4.3			3.2								1.5	2.4					
PIX15S010	8.8 miles NE	air				+		2890				173	12							12						
PIX15S009	10 miles NE	air					960	3950		2		41	16			<1				<3	2					Return transect 9-20-80
PIX16S011	10.5 miles NE	water	surf					++	1.5			0.8														Return transect 9-20-80
PIX16S012	10.5 miles NE	water	1 m					++	1.0			0.8														Return transect 9-20-80
PIX11S007	10.5 miles NE	air		+	+			170				3				<1				<1					<1	Return transect 9-20-80
PIX11S008	11.3 miles NE	water	surf					10	3.2			5.0								2.2	3					(North of dog-leg not directly in plume)
PIX12S001	12 miles NE	air						360				2				<1				<1	<1					(North of dog-leg not directly in plume)
PIX12S002	12 miles NE	water	surf						1.1			1.2														(North of dog-leg not directly in plume)
PIX12E113	12 miles NE	water	1 m						1.2			0.9														(North of dog-leg not directly in plume)
PIX12E121	12 miles NE	water	6 m						0.5			0.2								0.4	0.6					(North of dog-leg not directly in plume)
PIX12S118	12 miles NE	water	12 m						0.5			0.3														(North of dog-leg not directly in plume)
PIX08SD75	12 miles E	air		+		5600	2400					19				1				1	1				4	Air sample obtained day before transect closer to center of plume
PIX13S001	17.8 miles NE	air				+		1700				860				<3				120	84				120	Back in center of plume track
PIX13S003	17.8 miles NE	water	surf						1.5			2.4								0.26	0.32					
PIX13E131	17.8 miles NE	water	6 m	49					89			92								0.7	1.0					
PIX13E127	17.8 miles NE	water	12 m				+	+	1.5			0.95														
PIX14S001	22 miles NE	air					550	2910				<2													<2	Sample obtained with Diesel engines on
PIX14S006	22 miles NE	air					3670	10600				8								<2					3	
PIX14S005	22 miles NE	water	surf				+		1.1			1.3														
PIX14S007	22 miles NE	water					+		1.1			0.7														
PIX14E149	24 miles NE	water							1.8			1.6														
PIX16S013	168 miles W	air		+			+			+		8.2				1									7	19°15.6'N 95°10.1'W
PIX16S014	168 miles W	water	surf						1.7			3.0														
PIX16S015	168 miles W	water	1 m						3.3			3.1								0.2	0.2					

toluene, xylene, and nonane are nearly identical to the nearer-source (PIX 10) values obtained several days earlier.

PIX 11S001 (air from 3.2 miles east of the wellhead) was obtained while the vessel was in a heavy slick, which emitted a very strong oil odor, for the first twenty minutes of sampling, and in a light slick for the last ten minutes. The concentrations of toluene, ethylbenzene, xylene, and nonane were higher at this location than at any other station occupied. PIX 11S002 (air from 4.3 miles from the wellhead), however, was obtained over an area characterized by a surface oil sheen but with no heavy slick. At the time PIX 11S002 was collected, the PIERCE was nearing the northern edge of the heavy oil slick plume.

PIX 11S003 (air from 6.2 miles from the wellhead) was found to have concentrations of volatile hydrocarbons similar to its water sample counterpart collected simultaneously, and to those collected within several hundred yards of the wellhead. PIX 11S005 (air from 7 miles from the wellhead) shows essentially unchanged (from the closer stations) volatile hydrocarbon distributions, while the dissolved component concentrations were found to be depressed as the cruise track approached the more northern edge of the surface slick area.

By the time station PIX 12 was occupied on 19 September, the PIERCE had left the direct plume (as shown in Figure 7) and was located in clear water. During this transition, the sea surface conditions went from having a light sheen with occasional patches of oil to being clear water with no visible sheen. Wind at this time was out of the northwest and the observable slick had taken a sharp dogleg track along approximately 120° true, leaving the PIERCE in clear water. PIX 12 was sampled two times, and in both cases the primary components in the air were methylpentane (at drastically reduced concentrations) with traces (less than 3 ng/g) of toluene. The corresponding water samples obtained at this station contained less than 1.0 µg/L of methylpentane and less than 0.5 µg/L of benzene, toluene, and mixed xylenes.

Also shown in Figure 6 are depth profiles of volatile hydrocarbons measured at 1, 6, and 20 m at PIX 11S003 (6.2 mile) and at 1, 6, and 12 m at PIX 12. At PIX 11S003, benzene and toluene concentrations of 90 and 100 µg/L, respectively, were found just below the surface of a relatively heavy slick. At a depth of 6 m these concentrations were reduced although they still approached 10 µg/L at a depth of 20 m. At PIX 12, which was north of the plume's track, water-borne concentrations of benzene and toluene barely approaching 1 µg/L were observed at depths of 6 and 12 m, respectively.

After leaving station PIX 12, the PIERCE was directed by helicopter back into the center of the plume, and on arriving at station PIX 13 (17.8 miles east of the wellhead), additional samples were collected. The air samples from PIX 13 clearly show the elevated levels of methylpentane, toluene, ethylbenzene, xylene, and nonane which were characteristic of the mid-slick area closer to the well. Higher levels of benzene and toluene in the water column are also readily apparent. At the beginning of the collection of the samples at PIX 13, there was a strong oil odor in the air and as the vessel approached the center of the plume, a light to very light sheen was noted. Small oil patches and oil

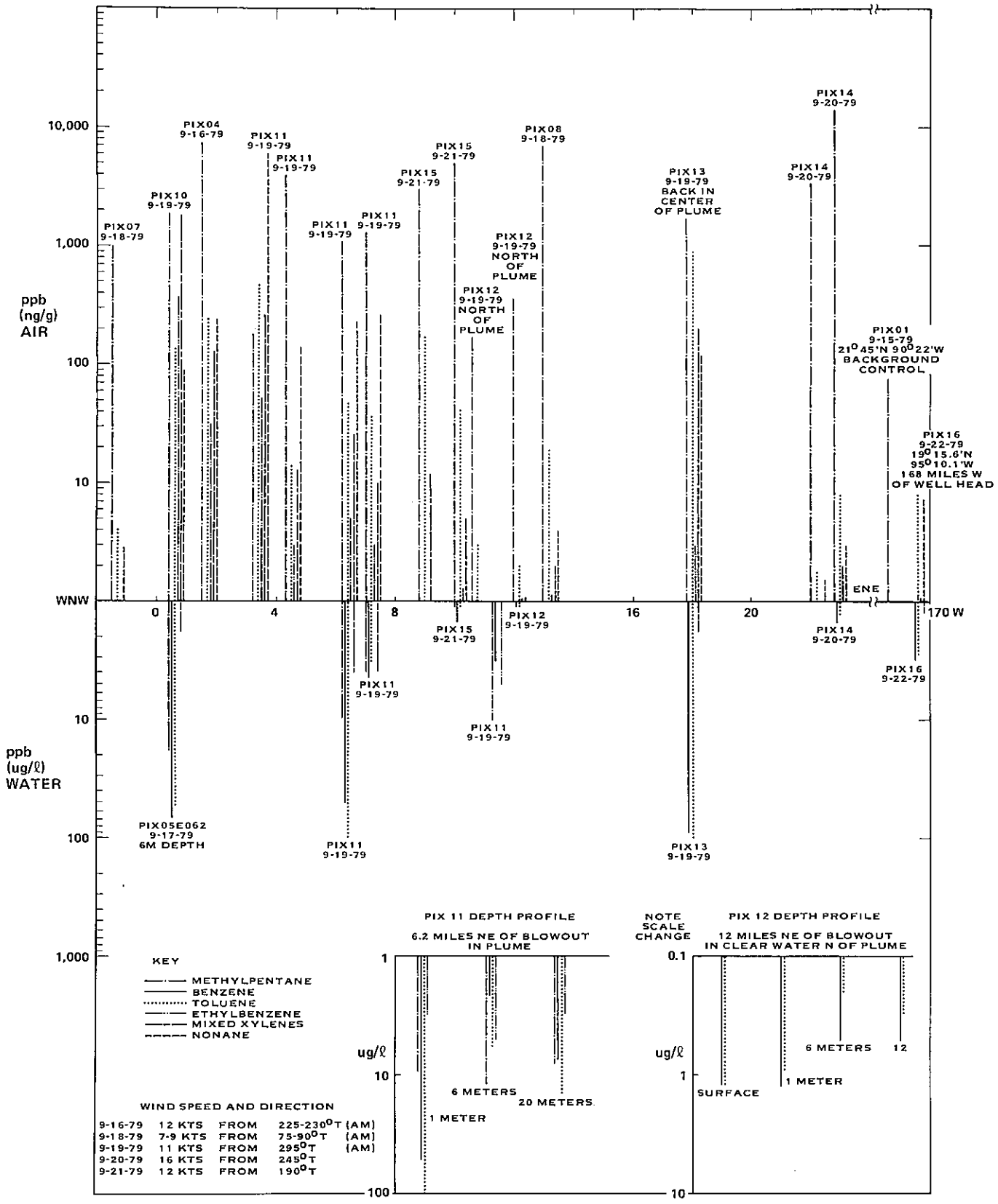

Figure 6. Display of the differential partitioning between evaporation and dissolution for selected volatile components along the G. W. PIERCE down-plume transect.

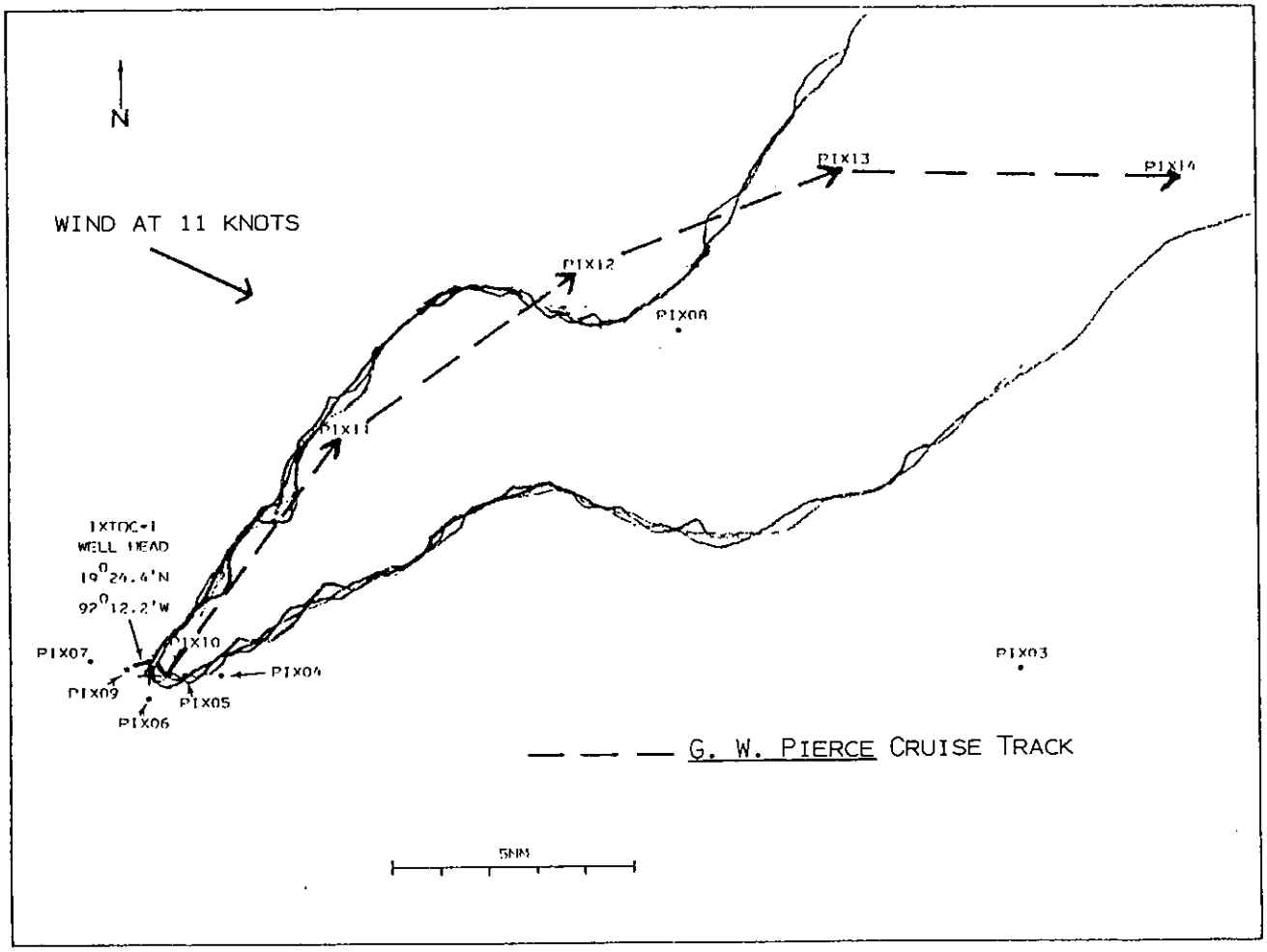

9-19-79
wind out of 295°T at 11 knots
0914-1050 local Miami time

Figure 7. G. W. PIERCE stations and plume drift from the IXTOC-I wellhead, on September 19, 1979.

droplets were also observed in the water. The sheen was predominantly "silver"; however, occasional colored patches, due to thicker concentrations of oil, were encountered.

In going from PIX 13 to PIX 14 (22 miles from the wellhead), much lower dissolved hydrocarbons were found. The first air sample from PIX 14 was collected with the hydrowinch diesel generator running in order to see whether exhaust fumes could be detected as possibly being responsible for some of the compounds that would later be identified in the laboratory. The Tenax traps were located at water level, however, so minimum contamination was expected, and the only component found in the sample was methylpentane. Following shutdown of the diesel generator, a second sample was obtained on the windward (westerly, 10-12 knots) side of the vessel. The major component in this sample again was methylpentane, although approximately 8 ng/g of toluene were measured. The benzene concentration in the water column at this station was less than 2 µg/L.

On 21 September the PIERCE re-occupied the location between 9 and 10 miles due east of the wellhead (PIX 12), this time designated PIX 15. At the time PIX 15 was sampled, however, the slick was beginning to turn to 120° true (as shown in Figure 8) under a wind of 12 knots from 190° true. As a result, while the air samples obtained at PIX 15 contained relatively high concentrations of methylpentane, toluene, and xylenes that were being released from the surface and were entrapped in the air mass blowing across the width of the slick, relatively low levels of hydrocarbons were found in the corresponding water samples at this station due to the shifting location of the slick. (Figure 9 shows the direction of the slick later during the same day, at which point it was definitely headed 120° true and the wind was blowing from 300° true at 14 knots.)

4. DISCUSSION

The major loss of low-molecular-weight components from crude oil discharged into water is due to evaporation and dissolution. These processes occur simultaneously and competitively, and understanding their relative importance under different conditions is a key part of evaluating the pathways and fates of these hydrocarbon materials. Since in an aqueous environment greater harmful impact is expected from chemical components actually dissolving in the water rather than from those that escape across the air/water interface, insight into the preferential evaporative loss and solubilization of specific aromatic and aliphatic compounds is important.

Under equivalent environmental conditions (e.g., wave action, air and water temperature, wind action), preferential partitioning between dissolution and evaporation should depend on the relative component characteristics of vapor pressure and solubility, which in turn rely on the molecular characteristics of size, weight, and polarity. However, in the typical case of oil being discharged on a water surface, evaporation has been found to exceed dissolution by several orders of magnitude just because of the large differences in

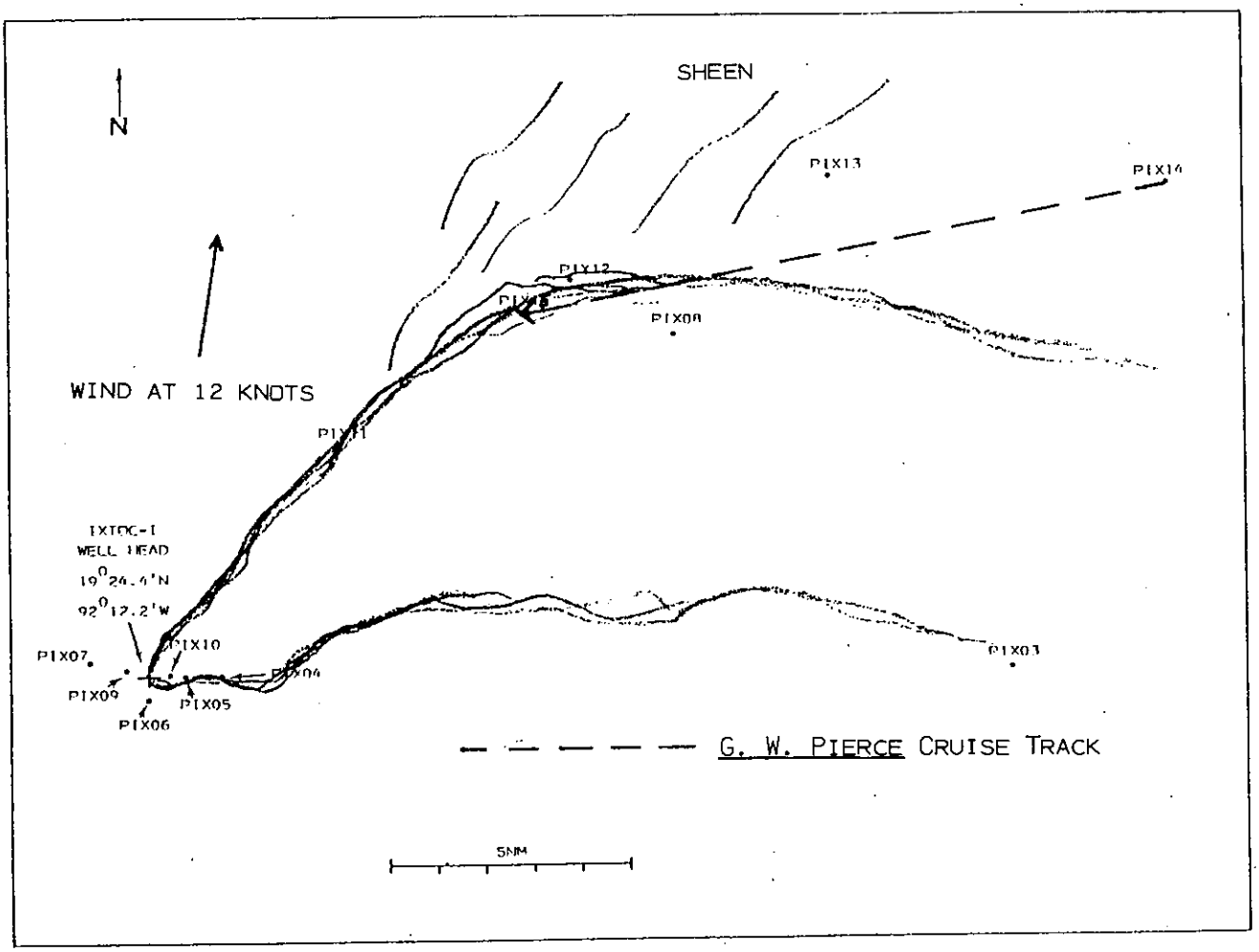

9-20-79
wind out of 190° true at 12 knots
0930-1100 local Miami time

Figure 8. G. W. PIERCE stations and plume drift from the IXTOC-I wellhead, on September 20, 1979.

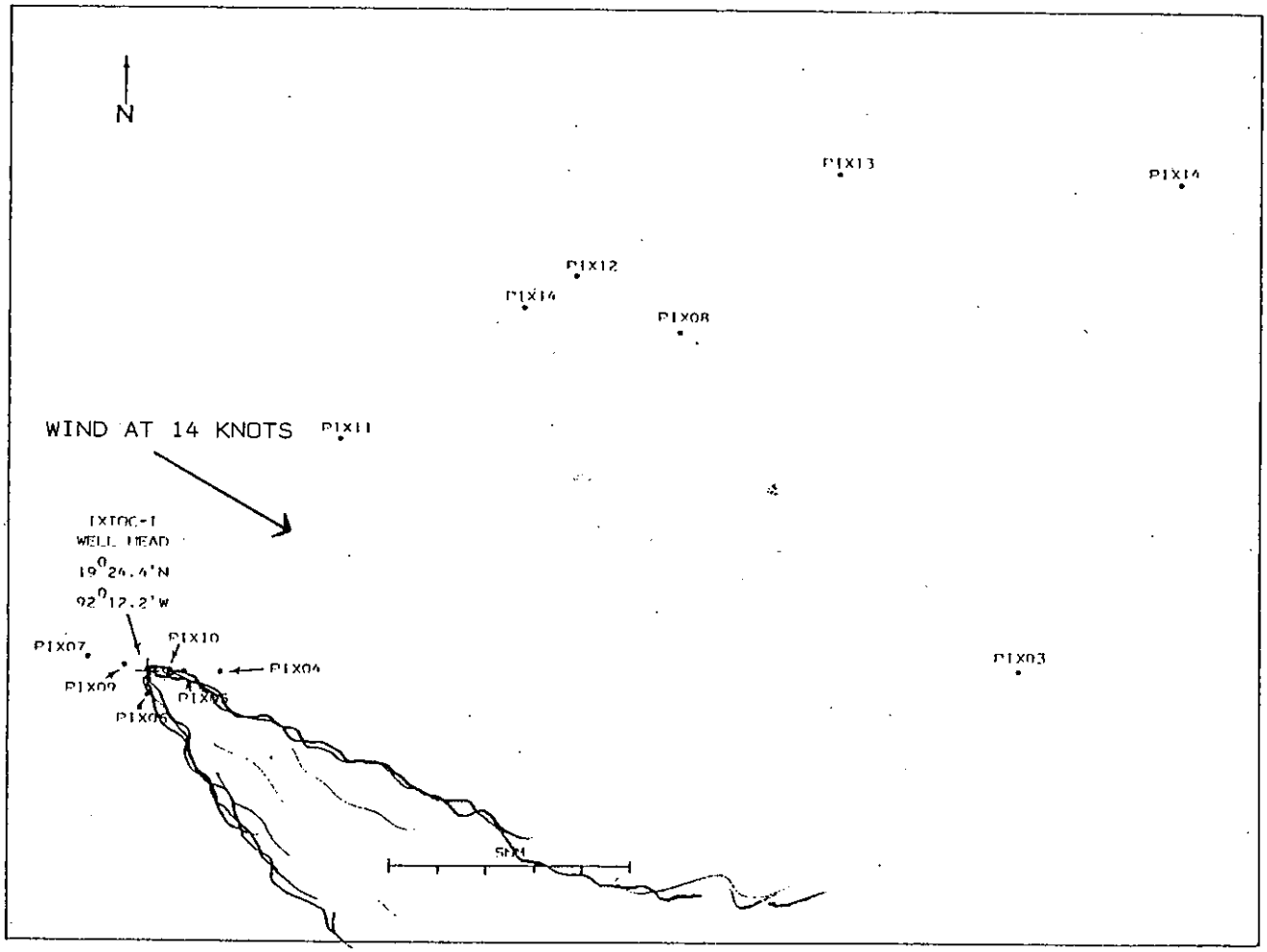

9-21-79

wind out of 300° true at 14 knots
1630 - 1800 local Miami time

Figure 9. G. W. PIERCE stations and plume drift from the IXTOC-I wellhead, on September 21, 1979.

exposure and the relative diffusion gradients across the oil/air interface and the oil/water interface.

Most studies of offshore surface spills, in fact, have found no detectable amounts of truly dissolved light hydrocarbons (from oil) in the water column (Harrison et al., 1975; McAuliffe, 1977b). One exception is a study completed by Koons and Brandon (1975), who examined levels of benzene and toluene in seawater at Coal Oil Point, California. Here the subsurface release of oil from natural seeps has been estimated to be between 50 and 100 bbl per day. In the vicinity of the seeps they found benzene and toluene at approximate concentrations of 0.08 µg/L each. In the case of the IXTOC spill, estimates of 15,000 to 30,000 bbl per day have been made for the amount of oil released. Extrapolating the levels found by Koons and Brandon to this higher amount of total oil released results in an estimate of 1.5 µg/L in ambient water. This value is similar to the benzene levels measured in the seawater surrounding the IXTOC blowout but not in or below the plume. Our levels in the plume were significantly higher, ranging between 60 and 100 µg/L depending on location.

McAuliffe (1977b) has studied the rate of loss of benzene and cyclohexane from surface slicks. Benzene and cyclohexane have similar vapor pressures (95.5 and 97.8 mm Hg, respectively) but drastically different solubilities in fresh water (1780 mg/L benzene and 55 mg/L cyclohexane; McAuliffe, 1966). When McAuliffe measured the rate of loss from the surface oil slick, benzene and cyclohexane were found to be removed at approximately the same rates. Harrison et al. (1975) have conducted a similar study for nonane and isopropylbenzene and found equivalent loss, again, as a result of surface slick evaporation.

McAuliffe (1977b) examined 68 water samples collected under four separate crude oil spills and found trace levels of C_2 to C_{10} hydrocarbons in only five of the samples analyzed. In the case of a Murban crude spill, the highest concentration of hydrocarbons was 60 µg/L at a depth of 5 feet under the spill, but this occurred after wind-wave agitation, forcing the surface slick into the water. Studies also were conducted to determine the maximum concentrations of benzene and toluene from Murban crude released into seawater when evaporation was prevented, and benzene concentrations up to 6,080 µg/L and toluene concentrations up to 6,160 µg/L were found.

To our knowledge this has been the first study that simultaneously measured concentrations of volatile aromatic and aliphatic hydrocarbons in the air above a slick and in the subsurface water.

In the case of these IXTOC spill studies, however, the oil was released with great pressure and agitated at a depth of 60 m below the surface. Thus there was considerable opportunity for the more soluble materials to partition into the water column.

It is significant, then, that dissolved benzene was elevated in the water column while the air sampled above the sea surface, even immediately adjacent to the well site, contained no measurable benzene. In contrast, the much less soluble aliphatic materials were found to be elevated in both the water column

and the overlying air. Also, the airborne concentrations of these less soluble components exhibited gradient patterns that were related to proximity to the well site and to intensity of the surface slick. Only toluene reflected the partitioning preference of benzene, although to a lesser extent.

In an effort to further elucidate the degree of differential evaporation and dissolution of benzene, cyclohexane, and toluene, a series of controlled laboratory experiments was conducted. A 1-L beaker was filled with seawater and 100 µl each of cyclohexane, benzene, and toluene were added to the bottom of the container with vigorous mixing. Tenax air samples were collected for one-half hour following the time of addition, and 5-ml water aliquots were taken at the end of that time and analyzed by the purge and trap technique. The experiment was then repeated, with 100-µl aliquots of cyclohexane, benzene, and toluene being added to the surface of 1 L of fresh seawater with moderate mixing.

The data from both experiments are presented in Table 3. Subsurface release of the components with mixing showed a preferential dissolution factor of 24 for benzene compared to cyclohexane. Likewise, benzene was preferentially dissolved into the water by a factor of 2.7 compared to toluene. These values very closely parallel the relative solubility of benzene, toluene, and cyclohexane in seawater (independent of their relative vapor pressures). When cyclohexane, toluene, and benzene were released at the surface, however, the water-to-air concentration ratios showed a two-order-of-magnitude increase in the amount of cyclohexane detected in the air relative to the water, and a 500-fold increase in the ratio of benzene released to the air as opposed to the subsurface water.

These data tend to substantiate our findings at the IXTOC wellhead, where the oil was released at a depth of 60 m with a great deal of turbulence. Even in the subsurface-release laboratory studies, there was nevertheless some loss of benzene to the atmosphere due to equilibrium partitioning at the water/air interface. The fact that similar partitioning into the atmosphere was not observed in the field is not unexpected. In the areas where these air samples were collected (directly above the slick) the oil coating may have acted as a barrier preventing equilibrium partitioning between the air and water column. By the time the oil reached the surface to form a slick, its benzene concentration had been drastically reduced, and the oil then effectively formed a barrier that would not allow equilibrium partitioning between the water column and the atmosphere on a time scale measurable under the experimental conditions in the field. Elevated levels of benzene in the smoke plume from the wellhead might have been expected; however, during the sampling period on the PIERCE, the vessel never was in the direct smoke plume. Significant concentrations of benzene also may be entrained in the gas that was released from the well, but this too would be directly downwind from the wellhead where samples were not obtained.

The concentrations of volatile hydrocarbons in the surface slick as analyzed by Brooks et al. (this volume) are very similar and very low for benzene and cyclohexane. Their water column data show greatly elevated levels of benzene compared to cyclohexane, however, suggesting (as our data do) that

Table 3. Laboratory-derived water/air partitioning ratios of selected hydrocarbons.

Compound	Water Solubility mg/l	Relative Water Solubility	Hydrocarbon mixture added below water surface with moderate turbulence		Hydrocarbon mixture added to water surface with gentle mixing	
			Ratio: $\frac{\text{water}}{\text{air}}$	Relative water/air Ratio	Ratio: $\frac{\text{water}}{\text{air}}$	Relative water/air Ratio
Cyclohexane	55	1.0	6.3	1	0.06	1
Benzene	1780	32.0	150.0	24	0.31	5
Toluene	535	9.7	57.0	9	0.44	7

preferential dissolution of benzene and toluene is occurring. In comparing our water column data to those of Brooks et al., the same general trends of decreasing dissolved aromatic concentrations with distance from the wellhead are observed. Absolute concentrations in the plume are different by as much as a factor of three in some instances, but this possibly reflects different methods of analysis. Brooks' quantitation was completed by a purge and Tenax trap of 2-L samples followed by flame ionization detection gas chromatography. Data generated in our study were from purge and trap treatment of 5-ml samples followed by heat desorption and analysis by gas chromatography--mass spectrometry. Alternatively, differences in Brooks' and our measured values in the water samples beneath the plume and those of Brooks et al. could reflect extreme patchiness of individual components within the water column.

In conclusion, eventual evaporation and loss to the atmosphere of the elevated levels of benzene and toluene may occur, but our data do not indicate that the process takes place to an appreciable extent after these water-soluble components have been thoroughly mixed into the water column. Clearly, if benzene-enriched water is advected to depth, elevated concentrations may exist in the water column for some time. Very little information exists on natural (or pre-IXTOC-I ambient) abundances of benzene and toluene in the Gulf of Mexico. Concentrations of 0.1 to 0.7 µg/L of each were reported by Koons and Monahan (1973) around offshore Louisiana drilling fields; the open Gulf was reported to be represented by 0.3 µg/L.

The large-scale impact of the dissolved benzene/toluene elevation is difficult to fully assess. We found concentrations of both benzene and toluene in the upper water column of from 1 to 4 µg/L; some correlation was seen with distance from the well site. Very limited depth profiling was performed; most of our samples came from the upper 60 m with only one "deep" sample of 90 m. This, coupled with the tremendous upper water column mixing caused by the major hurricane event prior to sampling, prevented us from measuring any real horizontal and/or vertical transport trends.

5. REFERENCES

Bellar, T. A., and J. J. Lichtenberg (1974): Determining volatile organics at micro-per-litre levels by gas chromatography. J. Am. Water Works Assoc., 66:739-744.

Brooks, J. M., D. A. Wissenburg, R. A. Burke, M. C. Kennicutt, and B. B. Bernard (1980): Gaseous and volatile hydrocarbons in the Gulf of Mexico following the IXTOC-I blowout. Unpublished IXTOC-I Symposium, 41 pp.

Calder, J. (1979): Weathering effects on chemical composition of the AMOCO CADIZ oil. Presented at the Annual Meeting of the American Association for the Advancement of Science, Houston, Texas.

Clark, R. C., and W. D. MacLeod, Jr. (1977): Inputs, transport mechanisms and observed concentrations in the marine environment. In Effects of Petroleum on Arctic and Subarctic Marine Environments and Organisms, D. C. Mailins (Ed.), Academic Press, New York: 91-223.

Clark, R. C., and D. W. Brown (1977): Petroleum: Properties and analysis in biotic and abiotic systems. In Effects of Petroleum on Arctic and Subarctic Marine Environments and Organisms, D. C. Mailins (Ed.), Academic Press, New York: 1-89.

Harrison, W., M. A. Winnik, P. T. Y. Kwong, and D. McKay (1975): Crude oil spills: Disappearance of aromatic and aliphatic components from small sea-surface slicks. Env. Sci. Technol., 9:231-234.

Karrick, N. L. (1977): Alterations in petroleum resulting from physiochemical and microbiological factors. In Effects of Petroleum on Arctic and Subarctic Marine Environments and Organisms, D. C. Mailins (Ed.), Academic Press, New York.

Koons, C. B., and D. E. Brandon (1975): Hydrocarbons in water and sediment samples from Coal Oil Point area. Offshore California, 3:513-521.

Koons, C. B., and P. H. Monahan (1973): Petroleum derived hydrocarbons in the Gulf of Mexico. 1973 Transactions of the Gulf Coast Association of the Geological Societies: 170-181.

McAuliffe, C. D. (1966): Solubility and water of paraffin, cycloparaffin, olefin, acetylene, cycloolefin, and aromatic hydrocarbons. J. Phys. Chem., 70: 1267-1275.

McAuliffe, C. D. (1977a): Dispersal and alterations of oil discharged on a water surface. In Fate and Effects of Petroleum Hydrocarbons in Marine Ecosystems and Organisms, D. A. Wolfe (Ed.), Pergamon Press, Oxford: 19-35.

McAuliffe, C. D. (1977b): Evaporation and solution of C_2 to C_{10} hydrocarbons from crude oils on the sea surface. In Fate and Effects of Petroleum Hydrocarbons in Marine Ecosystems and Organisms, D. A. Wolfe (Ed.), Pergamon Press, Oxford: 363-372.

Regnier, Z. R., and B. F. Scott (1975): Evaporation rates of oil components. Env. Sci. Technol., 9: 469-472.

Smith, C. L., and W. G. McIntyre (1971): Initial aging of fuel oil films on seawater. In Proceedings of 1971 Joint Conference on Prevention and Control of Oil Spills, American Petroleum Institute, Washington, DC: 457-461.

Wheeler, R. B. (1978): The fate of petroleum in the marine environment. Exxon Production Research Co. Special Report.

SURFACE WATER COLUMN TRANSPORT AND WEATHERING OF PETROLEUM HYDROCARBONS DURING THE IXTOC-I BLOWOUT IN THE BAY OF CAMPECHE AND THEIR RELATION TO SURFACE OIL AND MICROLAYER COMPOSITIONS

Paul D. Boehm and David L. Fiest
Environmental Sciences Division
Energy Resources Co., Inc. (ERCO)
185 Alewife Brook Parkway
Cambridge, Massachusetts 02138

ABSTRACT

A detailed chemical (GC, GC/MS) investigation of the concentrations, compositions, and transport paths of saturated and aromatic petroleum hydrocarbons in surface oil, surface microlayer, water column dissolved and particulate matter, and whole waters within and below (0-20 m) a surface oil plume (~ 60 km) from the IXTOC-I blowout in the Bay of Campeche was undertaken. Surface oil weathering patterns and compositions were compared to those of subsurface oil fractions and were found to differ substantially. Little hydrocarbon biodegradation was observed in the entire study area except for specialized nutrient-enhanced microenvironments. Samples of surface microlayer hydrocarbons emanating from surface mousse were more highly weathered and exhibited the possible presence of significant quantities of photo-oxidation products.

The existence of relatively unweathered subsurface oil plumes at considerable (~ 25 km) distances from the wellhead is postulated and evidence for their existence examined in detail. Significant quantitative and compositional gradients exist in the top 20 m of seawater beneath surface oil plumes and marked discontinuities and heterogeneities have been observed.

The use of two diagnostic chemical weathering ratios helps to sort out these heterogeneities and to examine the differential progressive weathering of surface oil/mousse and subsurface whole waters and hydrocarbon-bearing particulates. A budget for discharged oil transported within 25 km of the well indicates that approximately 1% may remain in the water column for considerable distances from the wellhead.

1. INTRODUCTION

The transport processes associated with the movement, weathering, and biogeochemical fates of petroleum hydrocarbons in intertidal and subtidal environments have been the subject of many research efforts in recent years. Most of these studies have addressed the subject of oil spills on the sea surface and have focused on the acute and chronic phases of spill impact on nearshore environments (e.g., METULA, ARGO MERCHANT, TSESIS, AMOCO CADIZ). Only a very small portion of the studies conducted during the early acute stages of these spill events addressed alterations in water column chemistry (e.g., Grose and Mattson, 1977; Calder et al., 1978). Offshore platform blowouts, in contrast to tanker spills, continually introduce large quantities of petroleum hydrocarbons, sometimes below the sea surface, until capping operations succeed. The dynamic changes in the seawater chemistry and the potential for profound biological effects to occur until sufficient dilution takes place remain a little studied and hence poorly understood aspect of oil spill research.

During a blowout, large shear forces (mixing) tend to form droplets of varying sizes (Shaw and Reidy, 1979), which have different dissolution kinetics and produce various biological effects. Depending on size and, hence, on buoyancy, these particles may remain in the water column and undergo compositional changes that are distinct from those of surface oil. These changes may have a marked effect on potential biological damage.

Knowledge of the physical/chemical dynamics of petroleum hydrocarbon water column chemistry during and after a blowout comes chiefly from the work of Brooks et al. (1978) on low-molecular weight gaseous and light hydrocarbons; from Grahl-Nielsen (1978), Boehm et al. (1980), and Boehm (1980) on high-molecular weight hydrocarbons; and from McAuliffe et al. (1980) on the transfer of oil to the water column following dispersant application on an experimental spill. Physical-chemical fractionation has been the subject of numerous laboratory studies (Zurcher and Thuer, 1978; Boehm and Quinn, 1975), and the solubility of hydrocarbons in seawater is well known (e.g., McAuliffe, 1966; Eganhouse and Calder, 1976; Sutton and Calder, 1974, 1975).

In recent years several important oil weathering models have been presented in the literature that attempt to mathematically define the rates and importance of the various significant physical (dispersion, emulsification), physical/chemical (evaporation, dissolution, sorption), chemical (photo-oxidation, auto-oxidation), and biological (hydrocarbon utilization, degradation, and metabolism) weathering processes (Mackay and Paterson, 1978; Leinonen and Mackay, 1977; Mackay et al., 1979; Kolpack and Plutchak, 1976; Mattson and Grose, 1979). These models are based on fundamental relationships and laboratory studies. There have been few cases in which a water column chemistry study of a design sufficiently rigorous to test such predictive models has been performed during the acute phases of an oil spill. Measurements of the dynamically changing concentrations and detailed compositions of hydrocarbons in various compartments in the water column (i.e., dissolved and particulate states), as compared to surface oil compositions, are required to refine such predictive models. Furthermore, there have been virtually no attempts to relate laboratory toxicity and sublethal stress studies to actual measured levels of individual toxic hydrocarbon components in the field.

Although difficult to accomplish, it is extremely important to sample both particulate and dissolved petroleum hydrocarbons and to measure levels of individual hydrocarbon components in each phase. Obtaining and analyzing only whole seawater for petroleum hydrocarbon analysis without fractionation may obscure important physical-chemical fractionations (Boehm, 1980), and hence the physical/chemical behavior (Shaw and Reidy, 1979; Zurcher and Thuer, 1978) and biological effects or bioavailability (Anderson et al., 1974) of pollutant compounds. Sampling beneath an oil-covered (oil, emulsified oil (mousse), surface films and sheens, and tar flakes, chips, tar balls, etc.) sea surface without contaminating the seawater being collected with surface material has been a challenge to chemical oceanographers for years. Sampling devices themselves are notorious for either contaminating the sample or sorbing components of interest (Gordon and Keizer, 1974; Boehm and Fiest, 1978; Zsolnay, 1978), thus altering the samples obtained.

Our study was undertaken as part of a larger effort to examine the transport processes affecting petroleum introduced from the IXTOC-I blowout in the Bay of Campeche into the offshore marine environment. This report and its companion report (Fiest and Boehm, this symposium) focus on the chemistry of the top 20 m of the water column beneath the surface oil plume emanating from the blowout source during September 17-21, 1979. Our goals were (1) to quantify the high-molecular weight hydrocarbons in particulate, selected filterable (dissolved), and whole water samples; (2) to determine the detailed changes in hydrocarbon chemistry and hence "weathering" of the hydrocarbons in the samples; (3) to examine vertical and horizontal concentration gradients and compositional changes; and (4) to examine the compositional relationships and, hence, the relative rates of weathering between petroleum hydrocarbons in the water column and oil/mousse and sheen (microlayer) at the sea's surface.

2. EXPERIMENTAL

Surface oil (mousse), surface microlayer, unfiltered and filtered seawater, and suspended particulate samples were collected and analyzed for their petroleum hydrocarbon content and composition (C_{10}-C_{32}). The methods used were glass capillary gas chromatography flame ionization detection (GC/FID) and combined glass capillary gas chromatography/mass spectrometry (GC/MS).

2.1 Sampling Sites

Two ships, the R/V RESEARCHER and the C/V PIERCE, operated in the vicinity of the IXTOC-I blowout between September 14 and 23, 1979. Samples were collected at stations along a 100-km transect oriented to the northeast of the blowout and at several stations more distant from the blowout (Figures 1 and 2). Stations occupied by the RESEARCHER and PIERCE were designated RIX and PIX, respectively. Samples were collected at Stations RIX 02, RIX 04, PIX 01, PIX 02, and PIX 03 during the two days just prior to the passage of Hurricane Henri through the study area on September 16-17. The remaining stations within 85 km of the well were sampled during the next four days. The hurricane's heavy rains and strong winds added to the abnormally high freshwater runoff from the adjacent land.

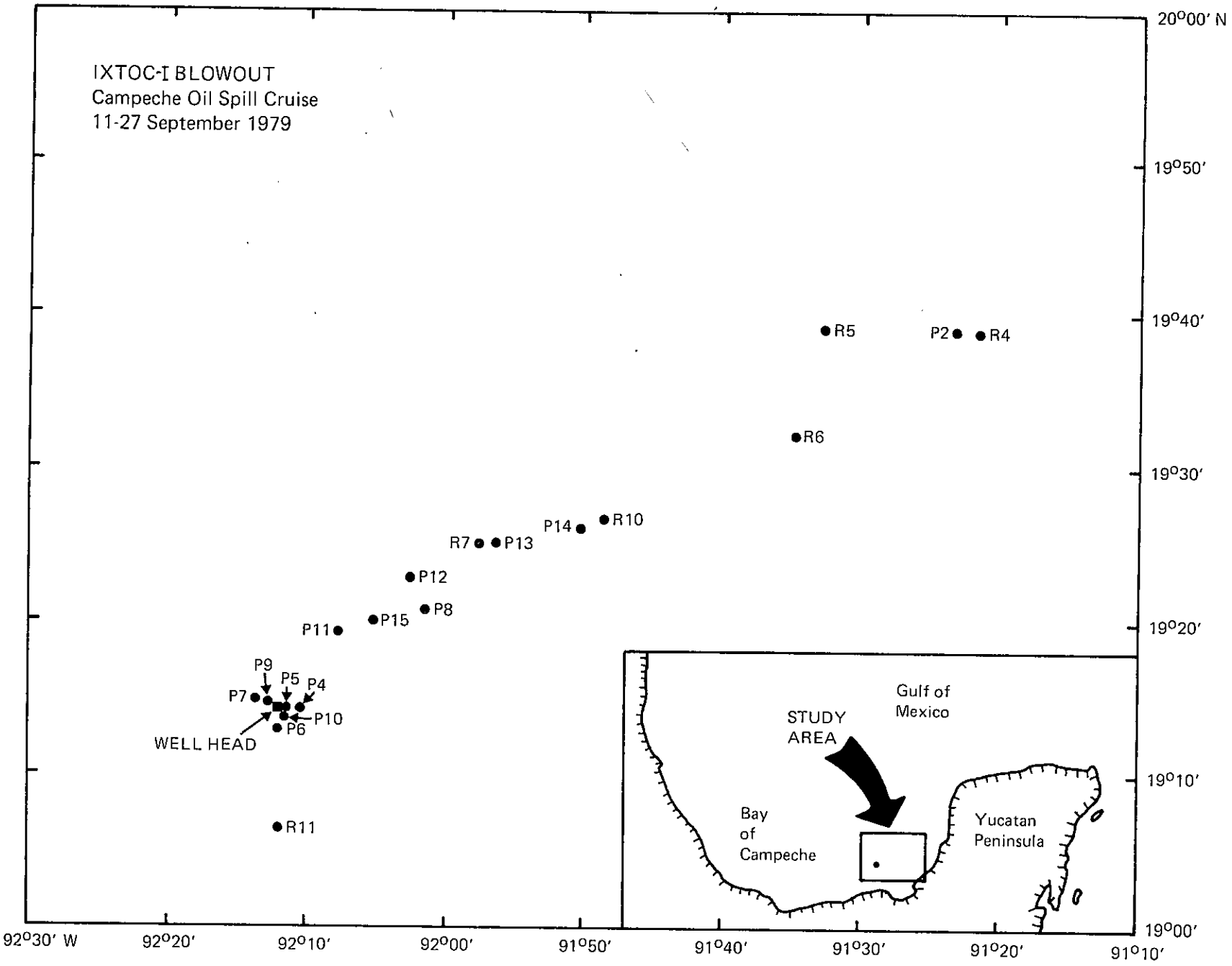

Figure 1. Detailed map of wellhead region.

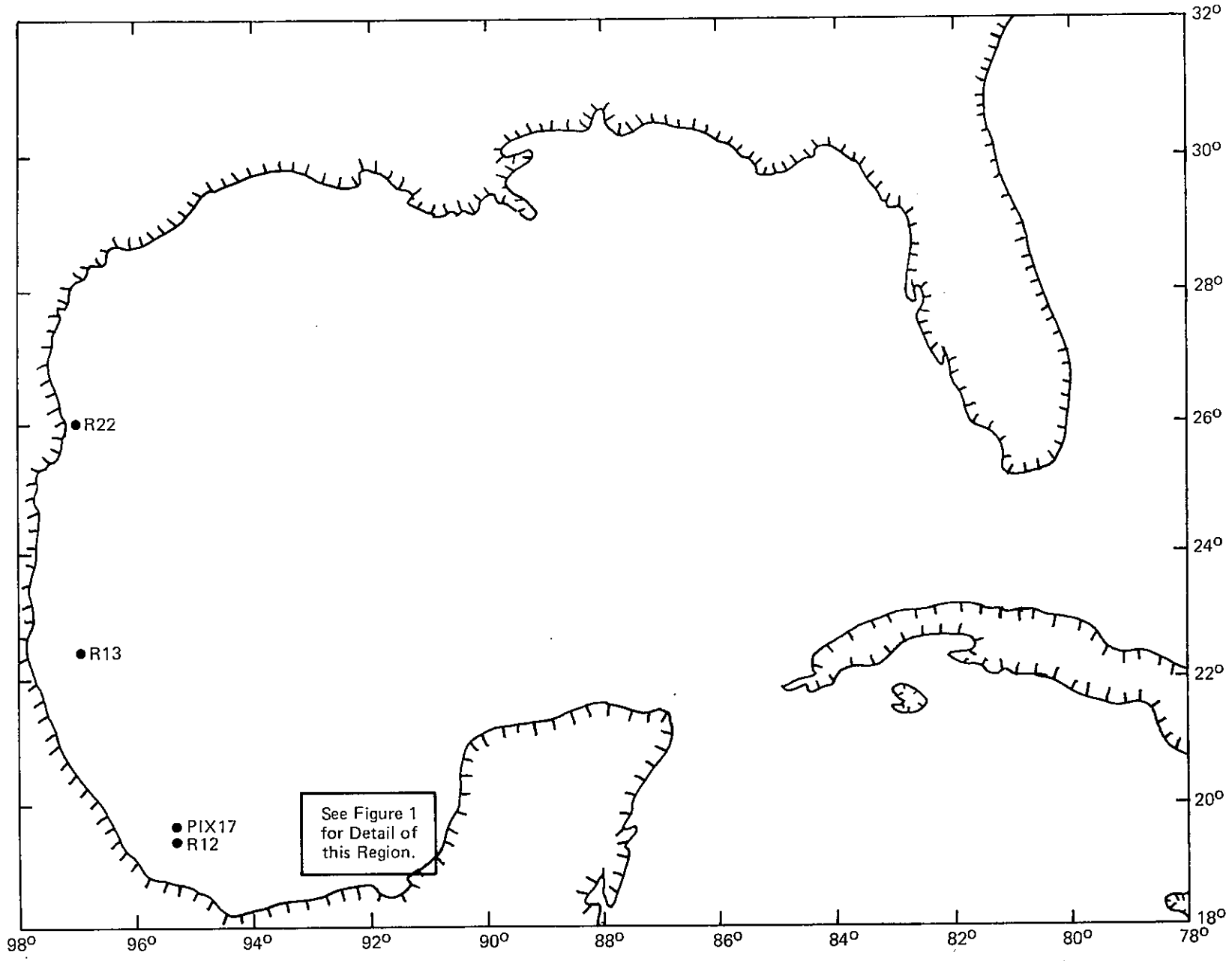

Figure 2. Sampling stations along the historical path of IXTOC-I surface oil movement.

The sampling equipment employed on the RESEARCHER included inflatable rafts, from which mousse and microlayer samples were collected, and 30-liter and 90-liter Bodman bottles with which large volumes of seawater outside the area of heavy surface oil coverage were collected (Payne et al., this symposium). Aboard the PIERCE, mousse samples were collected with a dip bucket and seawater samples with a non-contaminating pumping system, a 30-liter glass Bodman bottle and a 10-liter GO-FLO bottle. The results of this paper concern mousse and microlayer samples obtained by the scientific party aboard the RESEARCHER and mousse, whole water, and particulate and dissolved material in the top 20 m directly beneath heavy surface oil collected by scientists aboard the PIERCE.

2.2 Surface Oil/Mousse

Mousse samples were collected using a metal dip bucket from the ship's rail or a solvent-rinsed glass jar from an inflatable raft. The samples were frozen and stored in solvent-rinsed glass jars at -20°C.

In the laboratory, a small portion of mousse (0.5 g) was removed with a metal spatula and dissolved in 2 ml of dichloromethane (Baker Resi-Analyzed). The solution was dried by adding 2 g of sodium sulfate (Baker Analyzed; precombusted at 400°C for 16 hours) and then eluting the solution through a microcolumn consisting of glass wool and 3 g Na_2SO_4 in a glass pipette. An aliquot (10 µl) of the dry solution was weighed on a Cahn Model 25 electro-balance to determine the sample weight. An aliquot of sample weighing approximately 25 mg was removed, internal standards were added, and the dichloromethane was displaced with hexane (Burdick and Jackson; distilled in glass) prior to column chromatography and gas chromatographic analysis.

Density measurements were made on a few of the samples with a digital density meter (Mettler-Parr DMA46) aboard the ship. The instrument was calibrated in the density mode with air and distilled water at 30°C. Duplicate measurements were made on each sample by overfilling the sample cell using a plastic syringe, allowing the cell temperature to equilibrate to 30°C, and reading the density after the second decimal place remained unchanged for one minute. Replicate measurements agreed to the second decimal place.

2.3 Microlayer/Sheen

Microlayer samples were collected using a stainless steel screen (60 cm x 60 cm; Garrett, 1965) deployed from the upwind side of an inflatable boat positioned approximately 2 km upwind of the ship. The screens were cleaned with soap and water, rinsed with methanol and dichloromethane (Burdick and Jackson, UV grade), and wrapped in aluminum foil prior to each use. One liter of sample was collected with repeated dips of the screen, preserved by adding 50 ml of dichloromethane, and stored in a solvent-rinsed amber glass bottle at ambient temperatures.

In the laboratory, internal standards were added and the entire sample was extracted three times with 75 ml of dichloromethane in a separatory funnel. The dichloromethane was combined, dried over sodium sulfate, concentrated by rotary evaporation, and displaced with hexane prior to column

chromatography and gas chromatography analysis. This extraction procedure gives excellent (98%) recovery for petroleum hydrocarbons (Boehm, 1980).

2.4 Seawater (Whole Water and Dissolved Fraction)

Seawater samples were collected with a 10-liter Teflon-lined GO FLO sampler (General Oceanics), a 30-liter glass Bodman bottle (Gagosian et al., 1979), or a submersible pumping system. The pumping system consisted of a modified submersible pump (Cole Parmer Model 7111 with nylon impeller, silicone rubber gaskets, viton seals) connected to an in-line filtration system with alternate 2-m sections of stainless steel tubing (1.3-cm O.D. Type 903) and 0.5-m sections of flexible stainless steel couplings (Figure 3). The sections were alternately coupled with stainless steel unions and stainless steel quick connects (Swagelock with viton seals) to allow water to be pumped from depths of 1 to 20 m.

The pumping system was introduced in the water column in a clear area of sea surface and remained submerged until pumping was completed at a given station. The system was flushed at each sampling depth for several minutes before measurements and samples were taken. The outflow from the pumping system was split into two streams, one for collecting whole water samples and the other for filtering and measuring fluorescence. The filtration system stream flowed through an in-line stainless steel ball valve, which controlled the flow; a short fixed wavelength (254 nm) filter fluorometer (Turner Designs), which measured concentrations of dissolved oil; and a 142-mm stainless steel filter holder (Millipore) with a glass fiber filter (Gelman A/E), which removed particulates. The typical flow rate through the system was 1 liter/min, which corresponded to a linear velocity of 8 cm/sec and a flushing time of three minutes when pumping from a depth of 20 m. Seawater contacted only nylon, viton, silicone rubber, stainless steel, and Teflon.

One, four, or eighteen liters of seawater were transferred from the samplers to solvent-rinsed glass jars, preserved by adding dichloromethane, and stored at ambient temperature. One-liter samples were extracted with dichloromethane in a separatory funnel and analyzed by spectrofluorometry aboard the ship (see Fiest and Boehm, this symposium).

Samples larger than one liter were returned to the laboratory at the University of New Orleans (UNO) for initial processing. The seawater was extracted three times by stirring at high speed with 250 ml of dichloromethane per 20 liters of seawater. The extracts were combined, dried over sodium sulfate, concentrated by rotary evaporation, split into two aliquots, and sealed in glass ampules. Ampules were shipped to laboratories at Energy Resources Co., Inc. (ERCO) for analysis. At ERCO, the dichloromethane was removed from the ampules, spiked with internal standards, and displaced with hexane prior to analysis by column chromatography and glass capillary gas chromatography.

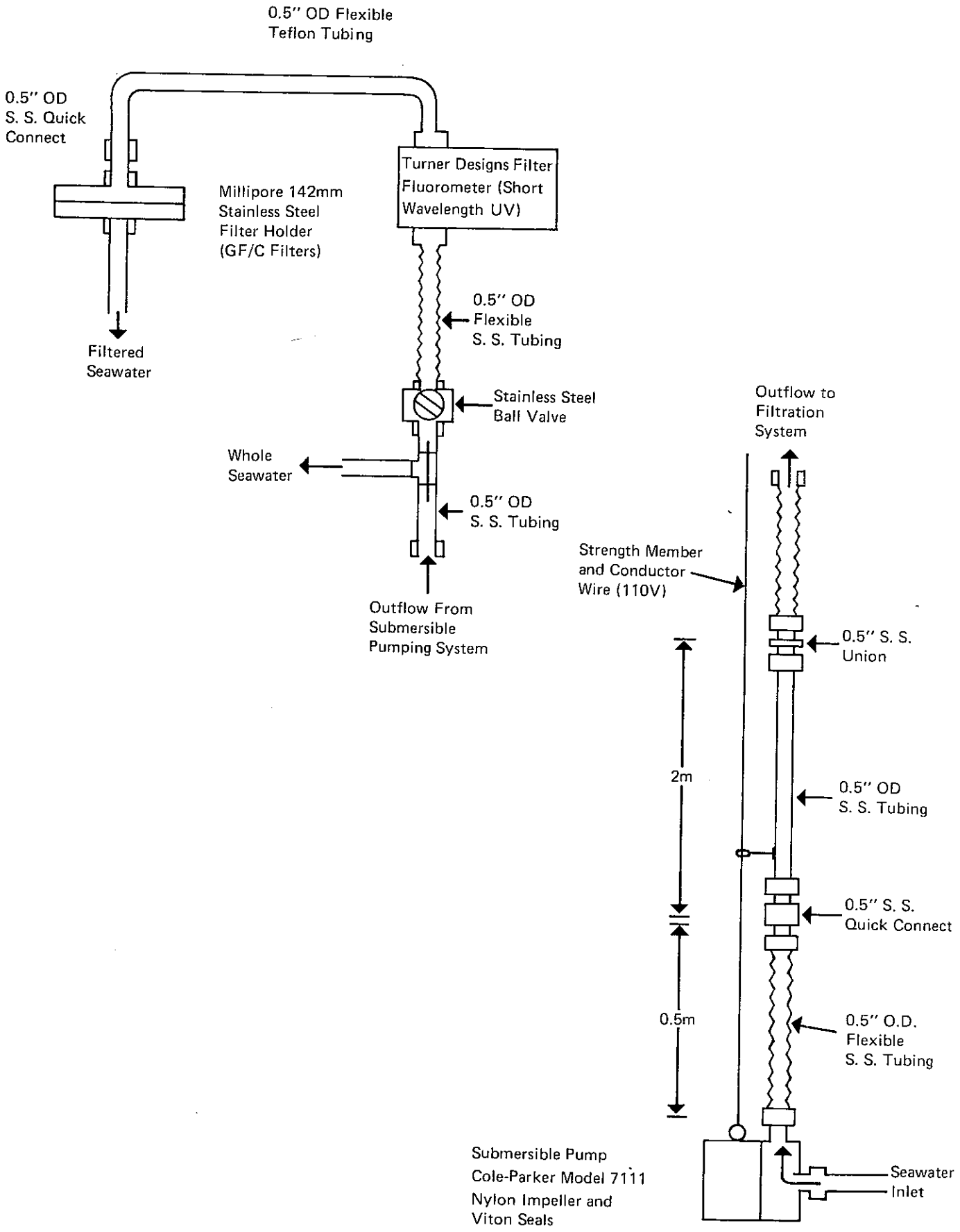

Figure 3. Design schematic for the submersible pumping system.

2.5 Particulates

Particulate samples were collected by pumping a measured volume (approximately 18 liters) of seawater through a 142-mm GF/A glass fiber filter held in a stainless steel filter holder with the pumping system described above. After pumping from a particular depth was completed, the filter was removed from the filter holder, folded face-to-face, placed in a solvent-rinsed aluminum foil packet, and stored at -20°C.

In the laboratory, the filters were thawed, cut into small pieces, placed in a 250-ml Teflon jar, and extracted three times with 100 ml of a 9:1 mixture of dichloromethane and methanol. The extracts were combined, concentrated, dried over sodium sulfate, and reconcentrated to 0.5 ml. The dichloromethane was displaced with hexane prior to analysis by column chromatography and glass capillary gas chromatography.

2.6 Column Chromatography

The hexane extracts of each sample type were fractionated by column chromatography prior to GC/FID and GC/MS analysis. Prior to chromatography, an aliquot (40 µl/1.0 ml) was weighed on a Cahn electrobalance. A maximum of 50 mg of sample was used for column chromatography.

A glass chromatography column (10.5-mm ID) with a Teflon stopcock was wet-packed with 11 g of silica gel (Davison 923; 100-200 mesh, 100% activated), 1 g of alumina (Fisher; 80-200 mesh, 5% deactivated), and 2 g of activated copper powder (Matheson; activated by rinsing with dilute HCl, organic-free water, methanol, dichloromethane, and hexane). Both alumina and silica were successively extracted for 24 hours with methanol and dichloromethane, air-dried, and activated for 16 hours at 140°C prior to use. After the column was packed and pre-eluted with 30 ml each of dichloromethane and hexane, the sample was charged to the column with 2 x 0.5 ml of hexane and successively eluted with 17 ml of hexane (f_1), 21 ml of 1:1 hexane:dichloromethane (f_2), and 25 ml of methanol (f_3). The f_1, f_2, and f_3 fractions contained saturated, aromatic, and polar compounds, respectively. The solvent in each fraction was concentrated and displaced with dichloro-methane. An aliquot of each fraction (40 µl/500 µl) was weighed on a Cahn electrobalance. The only exception to the procedure outlined above was for mousse samples for which the hexane was slurried with 0.25 g of silica gel before being transferred to the column.

2.7 Gas Chromatography and GC/MS Analysis

The f_1 and f_2 fractions were analyzed by a combination of GC/FID and GC/MS. A 1.0-µl aliquot of a dichloromethane solution of the sample was injected onto a 0.25-mm ID, 30-m SE-30 glass capillary column (J&W Scientific; AA grade), installed in a Hewlett-Packard 5840A gas chromatograph equipped with a splitless capillary injection port and a flame ionization detector and interfaced to a PDP-10 computer. Column conditions were as follows: carrier gas flow - 2 ml/min of helium, injection port temperature - 250°C, detector temperature - 300°C, and column oven temperature program - 60-275°C at a rate of 3°C/min.

Kovats retention indices were calculated by comparing retention times of the peaks in each sample with the retention times of n-alkanes in a standard mixture that was analyzed daily. Peaks in the chromatograms of samples were identified by comparing their retention indices with those of known compounds. These indices were measured by analyzing solutions containing known compounds or by identifying unknown peaks by GC/MS. The concentration of each peak was determined by comparing the area of the peak with the area of the internal standard, which was androstane for the f_1 and deuterated (D-10) anthracene for the f_2. Concentrations were reported in µg/L for seawater, particulate, and microlayer samples, and in mg/g of extractable oil for mousse samples.

Most of the f_2 fractions and selected f_1 fractions were analyzed on a Hewlett-Packard 5985 GC/MS system, which consists of a 5840A gas chromatograph, a quadrapole mass spectrometer, and a computer data system. The GC conditions were the same as for the GC/FID analysis. The GC/column was directly interfaced to the mass spectrometer with 0.3 in O.D. platinum-iridium tubing. The mass spectrometer conditions were as follows: ionization voltage - 70EV, scan 46-500 AMN, scan rate - 1 scan/4 seconds, and electron multiplier voltage 2200-2600 V. The mass spectrometer was tuned daily with PBTBA.

Aromatic hydrocarbon compounds were identified and quantified by a combination of selected ion searches for either the molecular ion (m+) or another characteristic ion of each compound, retention index matching, and matching of spectra with library spectra. The total ion current recorded for each peak in the selected ion search was compared to the area of the internal standard, D-10 anthracene. Response factors relative to D-10 anthracene were calculated from a regular analysis of a mixture of authentic aromatic compounds. When no standard was available, as was in the case for C_4 naphthalene, C_3, C_4 phenanthrene, C_2, C_3 fluorene, and C_1 through C_3 dibenzothiophenes, the response factor was obtained by extrapolation.

Four ratios of saturated and aromatic hydrocarbons were used to assist in the interpretation of the data. The carbon preference index (CPI) was used to evaluate the relative abundance of odd carbon number and even carbon number high molecular weight n-alkanes (Farrington and Meyers, 1975).

$$CPI_{26\text{-}30} = \frac{2(n\text{-}C_{27}) + 2(n\text{-}C_{29})}{(n\text{-}C_{26}) + 2(n\text{-}C_{20}) + (n\text{-}C_{30})}$$

The CPI approaches 1.0 as the abundance of odd and even alkanes becomes equal and petroleum, rather than biogenic hydrocarbons, predominate.

The alkane/isoprenoid ratio (ALK/ISO) was used to measure the extent of microbial depletion of n-alkanes relative to isoprenoids (Boehm et al., 1980). The numbers in parenthesis refer to the retention index of the compound on a 0.25 mm x 30 m SE-30 column. For example, the normal alkane tetradecane ($n\text{-}C_{14}$) has an index of 1400. The isoprenoid farnesane has a retention index of 1470 on this column indicating that it elutes between $n\text{-}C_{14}$ and $n\text{-}C_{15}$ at approximately 70% of the elapsed time between these two normal alkanes.

$$ALK/ISO_{14\text{-}18} = \frac{(1400) + (1500) + (1600) + (1700) + (1800)}{(1380) + (1470) + (1650) + (1708) + (1810)}$$

The ALK/ISO ratio approaches 0 as the n-alkanes are depleted.

The saturated hydrocarbon weathering ratio (SHWR) was used to measure the relative abundance of low-boiling and high-boiling n-alkanes.

$$SWHR = \frac{(\text{sum of n-alkanes from n-}C_{10}\text{ to n-}C_{25})}{(\text{sum of n-alkanes from n-}C_{17}\text{ to n-}C_{25})}$$

The SWHR approaches 1.0 as low-boiling saturated hydrocarbons (n-C_{10} to n-C_{17}) are lost by evaporation.

The aromatic weathering ratio (AWR) was used to measure the relative abundance of low- and high-boiling aromatics.

$$AWR = \frac{\text{Total naphthalenes + fluorenes + phenanthrenes + dibenzothiophenes}}{\text{Total phenanthrenes + dibenzothiophenes}}$$

The AWR approaches 1.0 as low-boiling aromatics are lost by evaporation and/or dissolution.

3. RESULTS

3.1 Surface Oil/Microlayer

3.1.1 Visual Observations

Surface oil samples were collected from stations located up to 600 km from the blowout. Near the blowout, the oil was present in a distinct plume oriented in the direction of the prevailing currents. Outside the plume, oil was observed in isolated patches, sometimes tens of meters in diameter and in windrows hundreds of meters long.

At a typical station, emulsified oil (mousse), a visible surface film, and oiled plant debris, such as water hyacinths, comprised the surface oil patch. Usually a visible sheen of oil covered the surface area between patches of emulsified oil. The incorporation of terrestrial plant material into the mousse patches suggested that in many cases the surface oil had been in the water for at least several weeks.

The emulsified oil took on a variety of physical forms, which reflected different weathering stages. Often several physical forms of mousse were found at a single location. Within the surface oil plume near the blowout,

the dominant form of oil was a continuous layer of emulsified oil. The oil was very watery and tended to stick tenaciously to any objects contacted.

Spherical clumps of mousse, 2-10 cm in diameter, were the most common form other than that in the immediate vicinity of the blowout. Small nodules were observed to adhere to each other at points of contact to form larger clumps with a cerebral-like appearance. These chunks were almost neutrally buoyant and floated with >95% of their volume submerged. Similar cerebral-like mousse clumps were observed during the Torrey Canyon spill (Smith, 1968, Plate 7B).

The most spectacular form of mousse found was in large coherent masses, or cylinders, at their largest 5 m wide, 30 m long, and 1 m thick. The shape and orientation of these masses of oil evolved with changes in the winds and swell, whereas at low wind speeds (< 5 knots), the long dimension of the mass was aligned with the trough of the swells, and at higher wind speeds (5-10 knots) the masses oriented with the wind. The exposed surfaces of several large patches of mousse encountered at Station RIX 10 had turned dark brown, probably as a result of exposure to sunlight and air.

Two additional forms of mousse were found less frequently than the mousse chunks and probably represented more advanced weathering stages of the mousse. Small pancakes, 2-4 cm in diameter and with about 10% of their volume exposed to the air, were found at station RIX 11. The exposed surface had a dark brown skin, which was much less sticky than the light brown submerged surface. The pancakes were clearly more buoyant than the mousse chunks and therefore more susceptible to the effects of sunlight. Small black flakes of oil, 0.5-2.0 cm in diameter, were found at Stations RIX 11 and RIX 13. These flakes may represent the dark-colored, hardened skin of mousse that was exposed to sunlight and air and had flaked off (Patton et al., 1980).

The densities of a number of mousse samples collected from Stations RIX 06 and RIX 07 were measured onboard (Table 1). At Station RIX 06, 73 km from the blowout, several samples of mousse clumps had densities between 1.00 and 1.01 ($T = 30^{o}C$). At Station RIX 07, 32 km from the blowout, the oil emulsion within the plume had a density of 0.99, and mousse outside of the plume had a density between 1.00 and 1.01. The density of the surface seawater at these stations was slightly higher ($\rho = 1.02$, $T = 30^{o}C$). As was visually apparent, the mousse had a density that made it slightly buoyant in seawater.

3.1.3 Chemical Measurements of Mousse Samples

The chemical composition of almost all of the mousse samples collected within 80 km of the blowout was remarkably constant (Table 2). The amounts of saturated hydrocarbons (f_1), aromatic hydrocarbons (f_2), and polar compounds (f_3) in the oil averaged 415 ± 52 mg/g, 239 ± 59 mg/g and 115 ± 26 mg/g, respectively. The proportions of high-molecular weight (> n-C_{22}) n-alkanes relative to n-C_{24} were virtually constant for these samples (Figure 4). The variability among the samples was primarily in the proportions of low-molecular weight n-alkanes and aromatics (Figures 4 and 5), which are most susceptible to evaporation and dissolution (Mackay et al., 1979). The compositional end members of mousse were the fresh oil collected at Station PIX 05 at the blowout and the mousse flakes collected off the Texas coast.

Table 1. Density of mousse collected near the IXTOC-I blowout.

Sample	(ρ-30°C)	Description
Mousse		
RIX 06-E525	1.01	Mousse chunks
RIX 06-E530	1.01	Mousse chunks in thick sheen
RIX 06-E533	1.01	Mousse chunks in no sheen
RIX 06-F014	1.00	Neuston tow
RIX 07-E544	0.99	Fresh plume mousse
RIX 07-E543	0.99	Fresh plume mousse
RIX 07-F012	0.99	Fresh plume mousse
RIX 07-F010	1.00	Mousse outside plume
RIX 07-E539	1.01	Old mousse - debris line
RIX 07-E537	1.01	Old mousse - outside of plume
Seawater		
Point Baker	0.99	Old mousse north of Tampico (July 1979)
RIX 04-E508	1.02	2-m depth
RIX 04-E509	1.02	20-m depth

Table 2. Summary of petroleum hydrocarbon composition of mousse samples.

Station	Distance from well (km)	Date	Sample ID	Visual Observations	Total f[1] mg/g	Total f[2] mg/g	Total f[3] mg/g	Residual mg/g	ALK/ ISO[1]	SHWR[1]	AWR[1]
PIX 05	0.4	9/17/79	B116		414	186	144	256	3.75	1.13	1.19
			E050	Fresh emulsion	471	407	77	45	4.12	2.69	2.23
PIX 10	0.5	9/19/79	B258	Fresh mousse	564	337	52	47	3.78	2.66	2.46
PIX 06	2.8	9/17/79	B068		403	216	89	292	3.32	1.10	1.16
RIX 11	14.8	9/21/79	E582	Mousse chunk	399	171	137	293	3.27	1.09	1.19
			E585	Black flake	385	234	111	270	2.91	1.08	1.26
			E588	Pancakes	393	232	140	235	3.14	1.09	1.13
			E589	Mousse chunk	412	215	128	245	3.08	1.07	1.22
PIX 08	21.8	9/18/79	B184		423	239	116	222	3.38	1.11	1.21
RIX 07	32.0	9/18/79	E544	Mousse in plume	427	194	124	255	3.40	1.06	1.19
			E542	Mousse out of plume	399	239	146	216	3.22	1.04	1.15
PIX 03	34.6	9/16/79	B114		404	181	109	306	3.39	1.11	1.18
PIX 14	43.8	9/20/79	E154	Mousse	468	312	123	97	4.10	1.34	1.59
			E155	Mousse	413	259	90	238	5.00	1.40	1.48
RIX 10 (mousse raft)	46.6	9/20/79	E566	Top of mousse	425	287	94	284	4.08	1.29	--
			E567	Crust of mousse	439	195	88	278	3.35	1.24	--
			E571	Bottom of mousse	455	255	113	177	3.85	1.31	1.51
			E572	Chunks of mousse	386	174	151	289	3.50	1.01	1.08
PIX 06	72.9	9/17/79	E525	Mousse chunk	409	248	123	220	3.80	1.13	1.37
			E523	Mousse chunk	368	212	149	271	3.20	1.07	1.15
PIX 17 Vera Cruz	314.0	9/22/79	E186	Mousse	391	288	112	209	3.38	1.13	1.22
RIX 13 Tampico	600.0	9/23/79	E602	Tar ball	274	178	133	415	0.19	no alkanes	
Texas Coast	> 600.0	8/79	Flake 1	Flake	464	150	316	70	2.51	1.01	--
			Flake 2	Flake	142	67	83	708	2.31	1.00	--
			Flake 3	Flake	73	39	54	834	2.94	1.00	--

[1]Refer to text (Experimental section) for explanation.

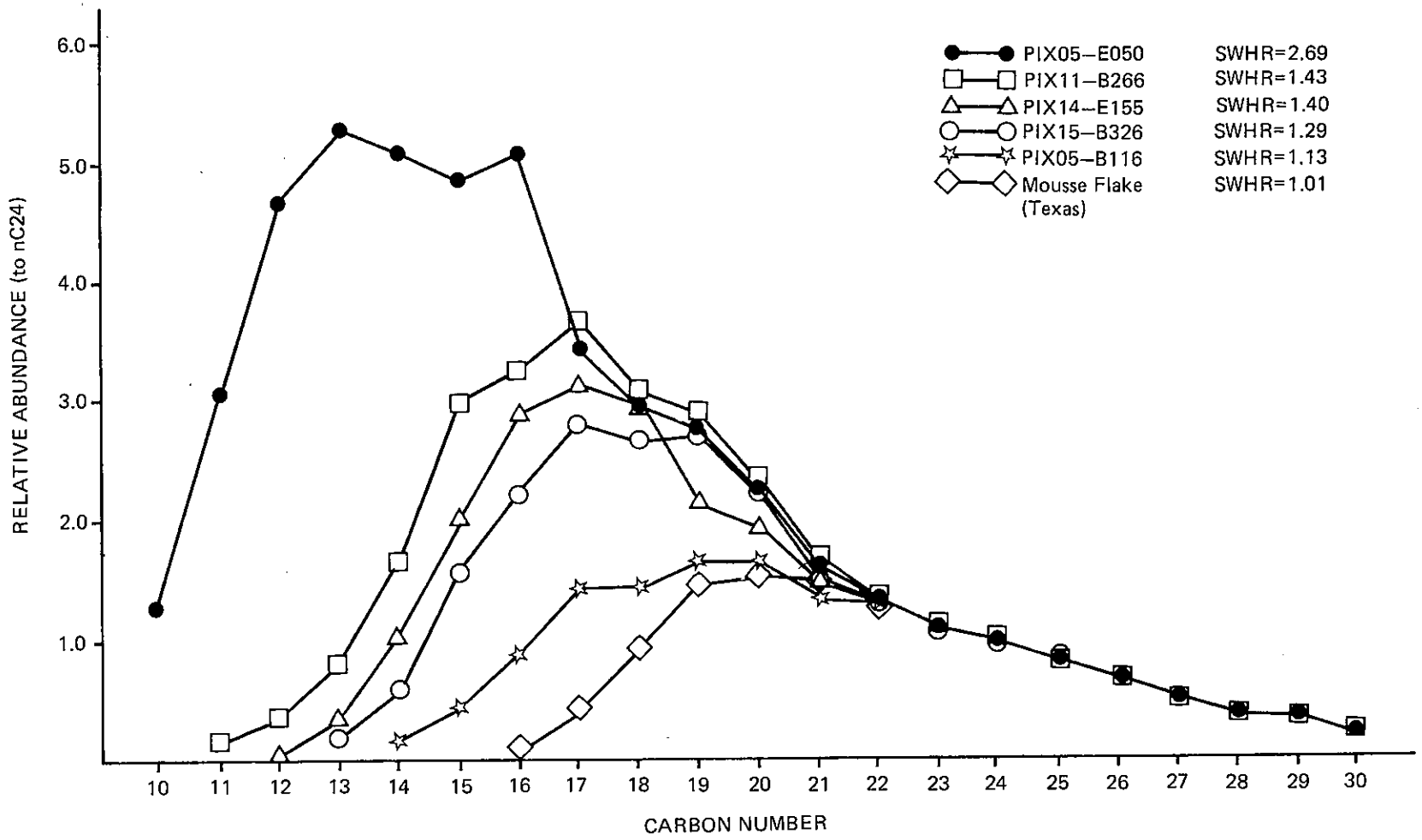

Figure 4. Relative abundance of n-alkanes in mousse samples.

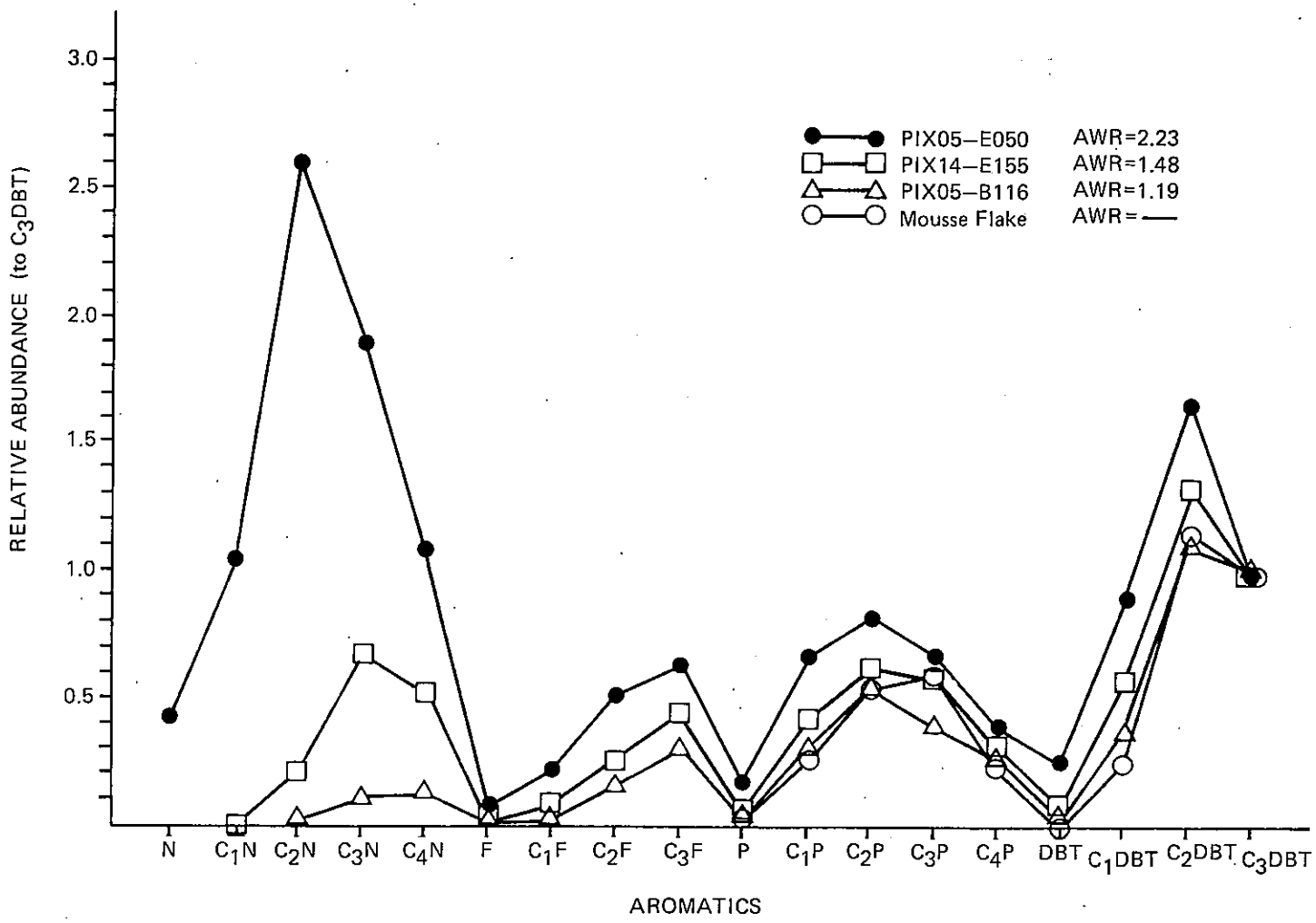

Figure 5. Relative abundance of aromatics in mousse samples.

Two samples collected at Stations PIX 05 and PIX 10, both located within 0.5 km of the well, were the least weathered mousse samples found. A suite of n-alkanes from < n-C_9 to n-C_{32} predominated in the saturate fraction (f_1) (Figure 6A). The aromatic fraction (f_2) was dominated by a series of substituted two- and three-ring aromatic hydrocarbons (Figure 6B). The saturated hydrocarbon weathering ratio (SHWR) and the aromatic weathering ratio (AWR) (see Table 2) for both of these samples were high (> 2). This confirms that relative to other mousse samples, little evaporative weathering of these samples had taken place. The high values of the alkane/isoprenoid ratio (>3.5), which is a measure of the microbial weathering of the oil (Boehm et al., 1980), confirm that little microbial degradation of these fresh oil samples had occurred.

The remaining samples collected near the blowout were weathered to a greater extent than the two fresh samples collected at the blowout site. Although the same suites of compounds, i.e., n-alkanes and substituted two-and three-ring aromatics, were present, the relative proportions of low-boiling compounds were lower than for the two fresh samples. The SHWR ranged from 1.00 to 1.40 and the AWR from 1.13 to 1.59. The high values of the ALK/ISO ratio, usually greater than 3.00, indicates that little microbial degradation of the oil had taken place.

Two exceptional samples are the mousse flakes and tar balls collected at Stations RIX 11 and RIX 13, respectively, which showed evidence of microbial degradation. The flakes from RIX 11 had undergone evaporative weathering to an extent similar to other mousse samples (SHWR = 1.08, AWR = 1.126). However, the alkane/isoprenoid ratio (ALK/ISO = 2.91) was lower than that for any other mousse sample collected near the blowout, indicating slight microbial degradation. Mousse flakes collected off the Texas coast showed microbial degradation similar to that for the flakes collected at RIX 11.

The tar ball collected at Station RIX 13, off Tampico, Mexico, was extensively weathered by microbial and evaporative processes (Figure 7). N-alkanes were virtually absent (ALK/ISO = 0.19), and isoprenoid peaks and an unresolved envelope dominated the f_1. The aromatics in the f_2 were similar to those of mousse samples for which no microbial degradation had occurred.

The striking feature of the composition of the mousse samples was a lack of relationship between the location at which the samples were collected and the chemical composition of the mousse. For instance, of the two samples collected at Station RIX 05, one was the freshest sample collected (SHWR = 2.69, AWR = 2.23) and the other was one of the most weathered (SHWR = 1.13, AWR = 1.19) found within 80 km of the blowout. No apparent correlation between chemical composition and distance from the blowout was found. This result was not totally unexpected, since old mousse patches were observed moving back into the fresh oil plume during helicopter overflights.

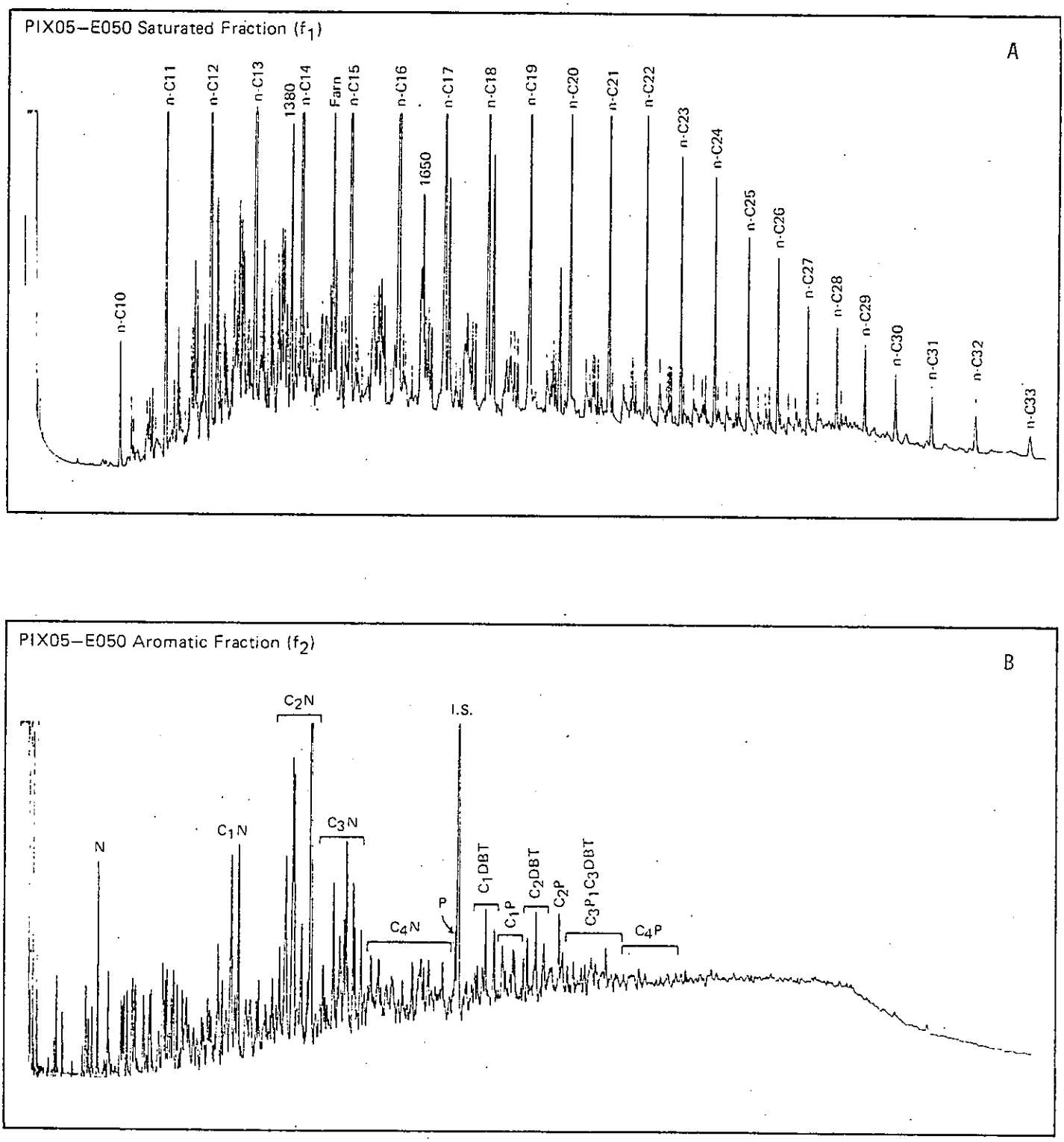

Figure 6. Glass capillary gas chromatograms of "reference oil."

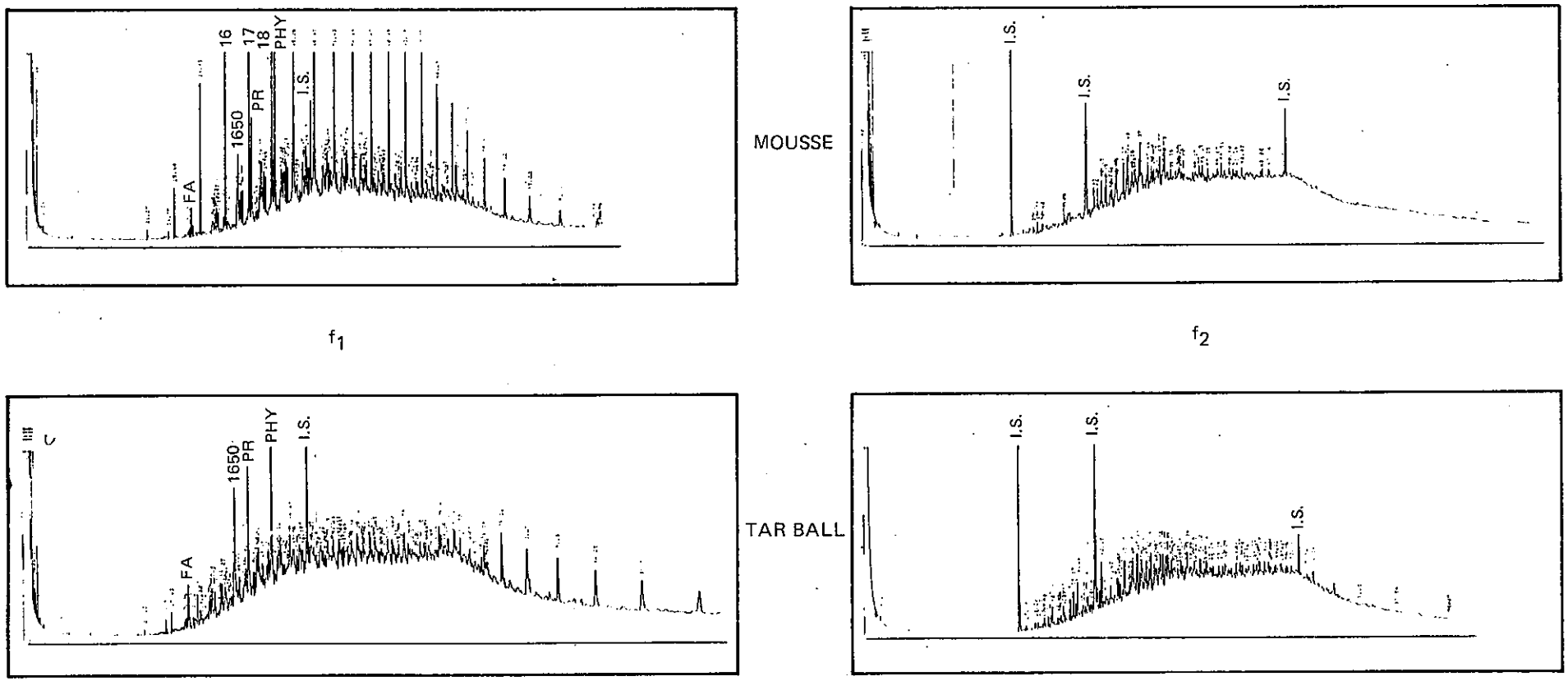

Figure 7. Comparison of mousse and tar ball samples collected at Stations P1X17 and R1X13, respectively (FA,1650,PR,PHY=Isoprenoid hydrocarbons).

3.1.4 Chemical Measurements of Microlayer Samples

The surface microlayer samples could be grouped into two classes, based on their hydrocarbon compositions (Table 3). Samples from Stations RIX 04, RIX 02, and RIX 12 fell into the first class and were characterized by having no detectable quantities of hydrocarbons. The remaining samples comprised the second class and contained levels of f_1 and f_2 hydrocarbons up to 2080 and 1370 µg/L, respectively. Detectable levels of hydrocarbons were found only in those microlayer samples collected at stations where mousse was also found. The chromatograms of the saturated fraction (f_1) were dominated by a series of n-alkanes from n-C_{16} to n-C_{32} superimposed on an unresolved envelope. The chromatograms of the aromatic fraction contained substituted two-, three-, and four-ring aromatics. The f_1 and f_2 chromatograms were similar to chromatograms of mousse samples but showed greater losses of low-boiling components (Figures 8 and 9).

The SHWR and AWR of the microlayer samples were all less than 1.02 and 1.15, respectively. These values were less than the lowest values reported for any mousse sample. The microlayer samples have evidently undergone a greater degree of evaporative and photooxidative weathering than the mousse samples. The ALK/ISO ratios for the microlayer samples are, with two exceptions, greater than or equal to 3.0, which suggests that, as with the mousse, minimal microbial degradation of the petroleum in the surface microlayer had occurred.

Microlayer samples collected in areas where a visible sheen was observed contained levels of f_1 and f_2 hydrocarbons greater than 1000 and 500 µg/L, respectively. At several sites, although no sheen was visible, detectable levels of oil were found. Samples with the lowest levels of hydrocarbons were depleted in aromatic hydrocarbons. Samples RIX 13-E599, RIX 12-E592, and RIX 06-E527 had a series of n-alkanes typical of the IXTOC-I mousse and no detectable aromatic hydrocarbons. Samples RIX 06-E528, RIX 07-E552, and RIX 07-E556 contained lower levels of aromatics than would be expected based on the concentration of n-alkanes. This trend was quantified by the ratio of the concentrations of an alkane (n-C_{17}) and aromatic compound (C_1 dibenzothiophenes) with similar volatility. The ratio of C_1DBT to n-C_{17} was greater than 0.20 for samples with total f_1 concentrations greater than 1,000 µg/L and less than 0.20 for samples with total f_1 concentrations less than 1000 µg/L. Apparently, as the thickness of the surface film decreases, the aromatics are selectively depleted from the film.

The aromatic (f_2) fraction of the microlayer sample collected downwind of a large mousse raft at station RIX 10 contained a series of compounds with retention indices ranging from 2380 to 2626 on a 0.25 mm ID x 30 m SE-330 glass capillary column. Although their identities are not yet known, the common occurrence of mass fragments with m/e 91, 105, 119, 143, 212, and 221 in mass spectra of the compounds suggests that they are related structurally (Figure 10). The concentrations range from 0.5 to 5 µg/L relative to D-10 anthracene as an internal standard. Since the material in the surface microlayer sample was emanating from a patch of mousse with a highly photo-oxidized surface, these compounds are likely to be photo-oxidation products which are dissolved in the surface microlayer. Similar compounds were found during the laboratory photo-oxidation experiment with IXTOC oil (Overton, personal communication).

Table 3. Summary of petroleum hydrocarbon composition of microlayer samples.

Station	Distance from well (km)	Date	Sample ID	Visual Observations	Total f^1 (µg/L)	Total f^2 (µg/L)	GC[1] f_1	GC[1] f_2	ALK/ ISO[2]	SHWR[2]	AWR[2]	$\frac{C_1 DBT^*}{n\text{-}C_{17}}$
RIX 11	15	9/21/79	E577	No sheen	134	< 100	n-alkanes	Envelope		1.01		
			E578	No sheen	173	< 100	n-alkanes	Envelope		1.00		
RIX 07	32	9/18/79	E553	Silver sheen	1670	565	n-alkanes	Envelope	2.99	1.00	1.08	0.35
			E556	Silver sheen	1090	653	n-alkanes	Envelope	3.40	1.02	1.15	0.25
			E557	No sheen	689	320	n-alkanes	Envelope	3.50	1.00	1.05	0.14
			E552	No sheen	693	489	n-alkanes	Envelope	2.57	1.00	1.06	0.16
RIX 10	47	9/20/79	E569	Silver sheen	2080	1370	n-alkanes	Envelope	3.10	1.01	1.11	0.37
RIX 06	73	9/17/79	E528	Silver sheen	2053	973	n-alkanes	Envelope	2.43	1.01	1.08	0.22
			E527	No sheen	169	< 100	n-alkanes	ND	4.00	1.01		<.15
RIX 04	99	9/16/79	E514	No sheen	< 100	< 100	ND	ND				
			E513	No sheen	271	< 100	ND	ND				
RIX 02	300	9/14/79	E503	No sheen	< 100	< 100	ND	ND				
			E504	No sheen	< 100	< 100	ND	ND				
RIX 12	300	9/22/79	E592	No sheen	< 100	< 100	n-alkanes	ND		1.01		
			E593	No sheen	< 100	< 100	ND	ND				
RIX 13	600	9/23/79	E598	No sheen	< 100	< 100	ND	ND				
			E599	No sheen	< 100	< 100	n-alkanes	ND		1.01		

[1]GC f_1 and GC f_2 are descriptions of the f_1 and f_2 gas chromatographs, respectively. The following descriptions were used: ND - nothing detected; n-alkanes - a homologous series of n-alkanes similar to IXTOC I oil dominates; envelope - an unresolved complex mixture (UCM) dominates.

[2]Refer to text for explanation.

$$\frac{*C_1 DBT}{n\text{-}C_{17}} = (\text{total } C_1 \text{ dibenzothiophenes})/n\text{-}C_{17}.$$

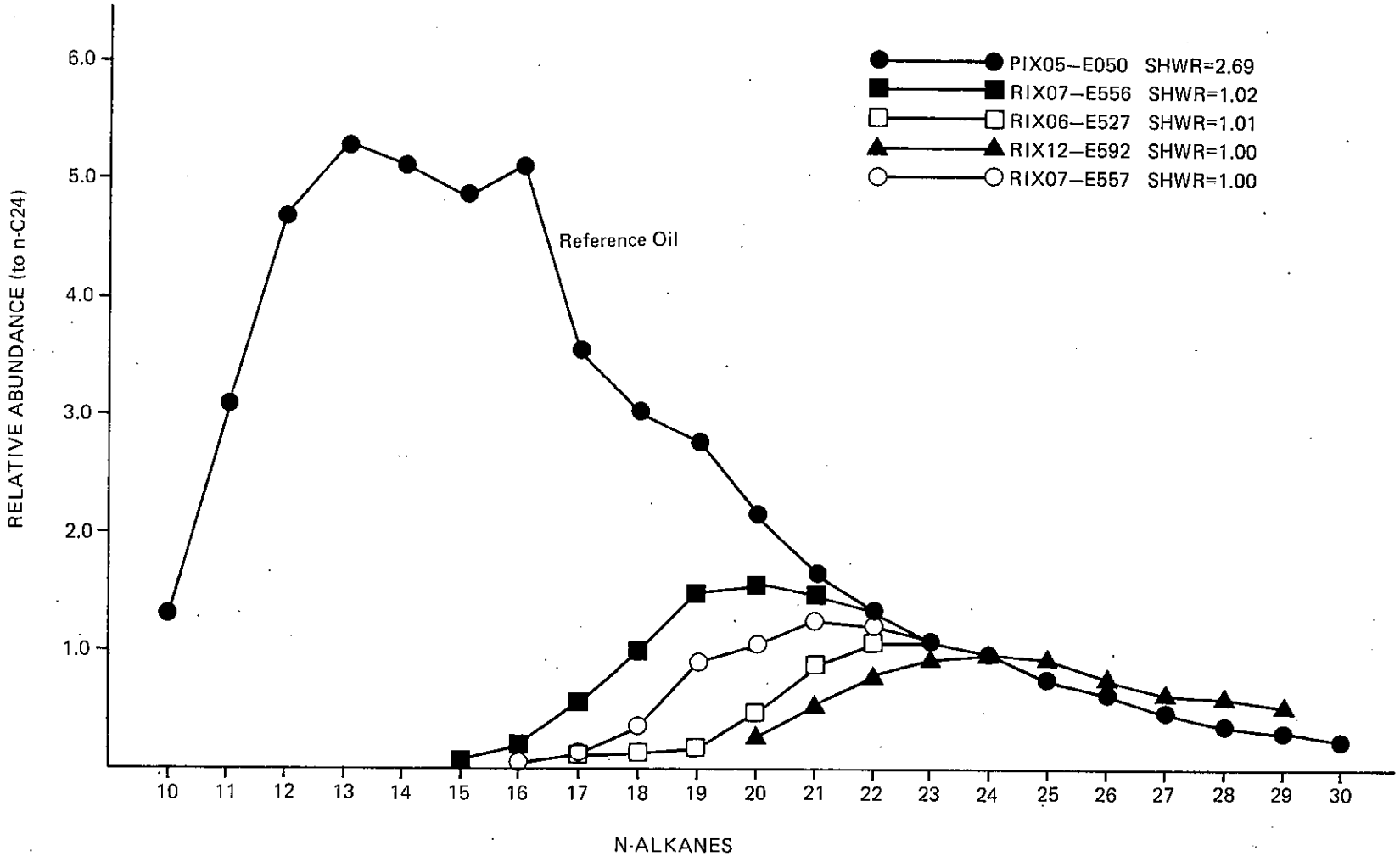

Figure 8. Relative abundance of N-alkanes of microlayer samples.

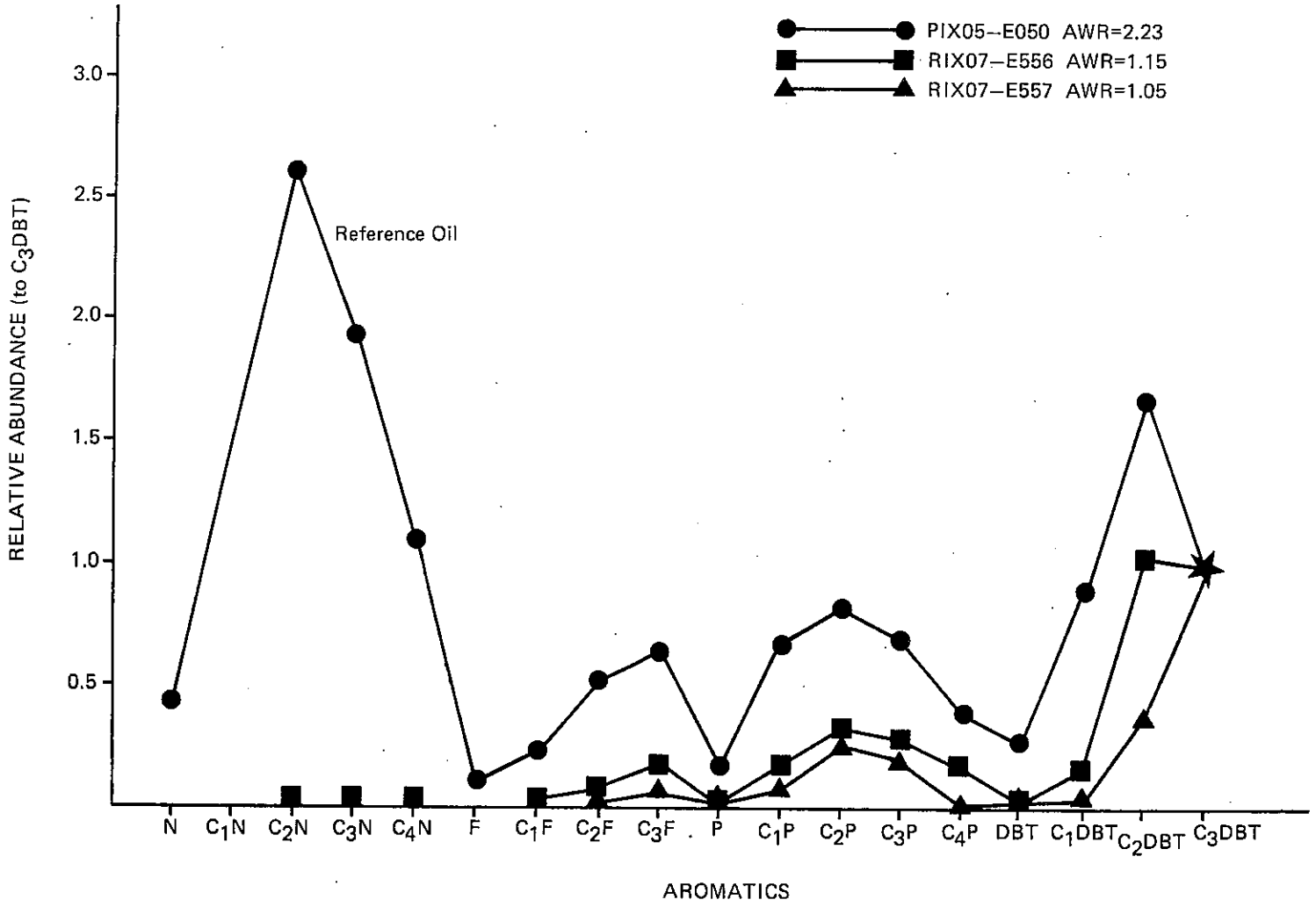

Figure 9. Relative abundance of aromatics of microlayer samples.

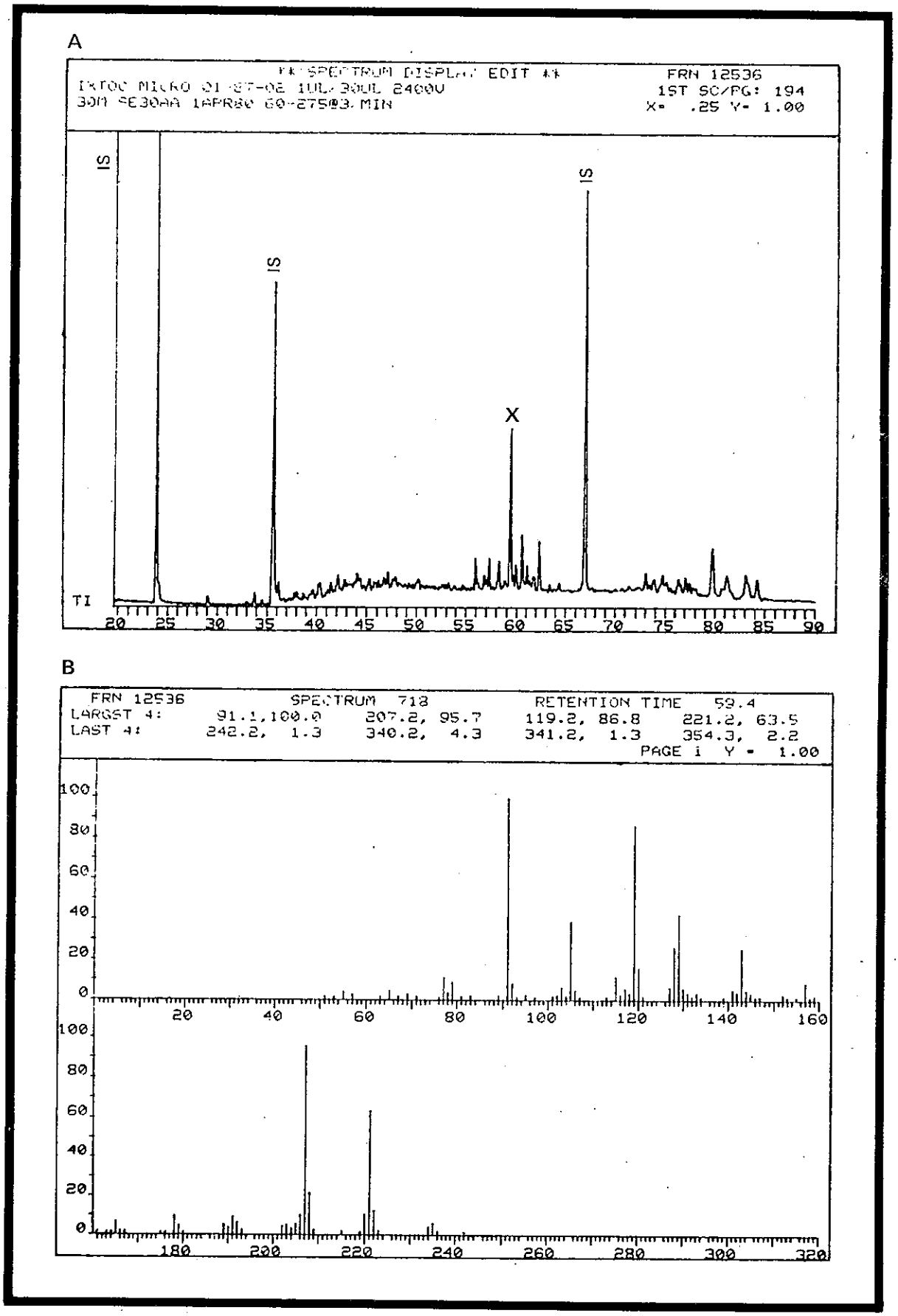

Figure 10. A. Total ionization chromatogram of a surface microlayer sample collected downwind of a mousse raft at Station RIX 10. B. Mass spectrum of the compound marked X in the chromatogram above.

3.2 Seawater/Particulates

3.2.1 General

There are several ways of viewing the data on the suite of seawater (whole water, dissolved and particulate hydrocarbons) samples. The following section addresses both quantitative and compositional comparisons between water column samples through a water column profile down to 20 m at each station. For ease of visual presentation and sample comparison, the capillary GC traces and GC/MS data (e.g., Figure 11) have been transformed to graphical data displays (GDD's) (e.g., Figure 12), which include key quantitative information on each sample fraction, levels of key individual components within each fraction, and key parameter ratios, which describe the extent of evaporation /dissolution (SHWR, AWR) and biodegradation (ALK/ISO). These ratios can be used to diagnose the factors influencing observed sample compositions. The AWR of seawater samples should be compared to that of the reference oil and fresh mousse (2.2 - 2.5). Values less than those of the fresh mousse result from a relative loss of naphthalene and fluorene compounds by evaporation and dissolution. Values greater than the reference values, as consistently occur with whole seawater samples, arise from a coincidence of the dissolved and particulate plumes, resulting in greater relative concentrations of the more soluble biaromatic hydrocarbons and, hence, a higher AWR.

Tables 4 and 5 present all relevant information on hydrocarbon fraction concentrations and values of the key diagnostic parameter ratios for seawater and particulate samples. Details of GC and GC/MS analyses of whole water, particulate, and dissolved samples are presented on the GDD that appear throughout this report.

Quantitative values should be viewed with the caveat that significant quantities of oil sorb to walls of water samplers in areas of maximum concentrations (i.e., PIX 05, PIX 10), and hence measured concentrations at these stations may be underestimated.

3.2.2 Station PIX 01

Water samples obtained from this control station contain varying quantities (ND-70 µg/L) of paraffinic tar, an ubiquitous petroleum contaminant in the Gulf of Mexico and in pelagic systems in general (Jeffrey et al., 1974; Butler et al., 1973). The particulate hydrocarbons are roughly equivalent to the whole water in terms of concentrations and hydrocarbon distributions. The GDD's indicate that, although the paraffinic tar contribution dominates the sample, n-alkanes of a phytoplanktonic source (n-C_{15}, n-C_{17}, n-C_{19}; Clark and Blumer, 1967) are present in significant abundances (Figure 13). The samples contain sizeable unresolved complex mixtures (UCM) characteristic of some pelagic tar (Butler et al., 1973) but lack any detectable aromatic hydrocarbons.

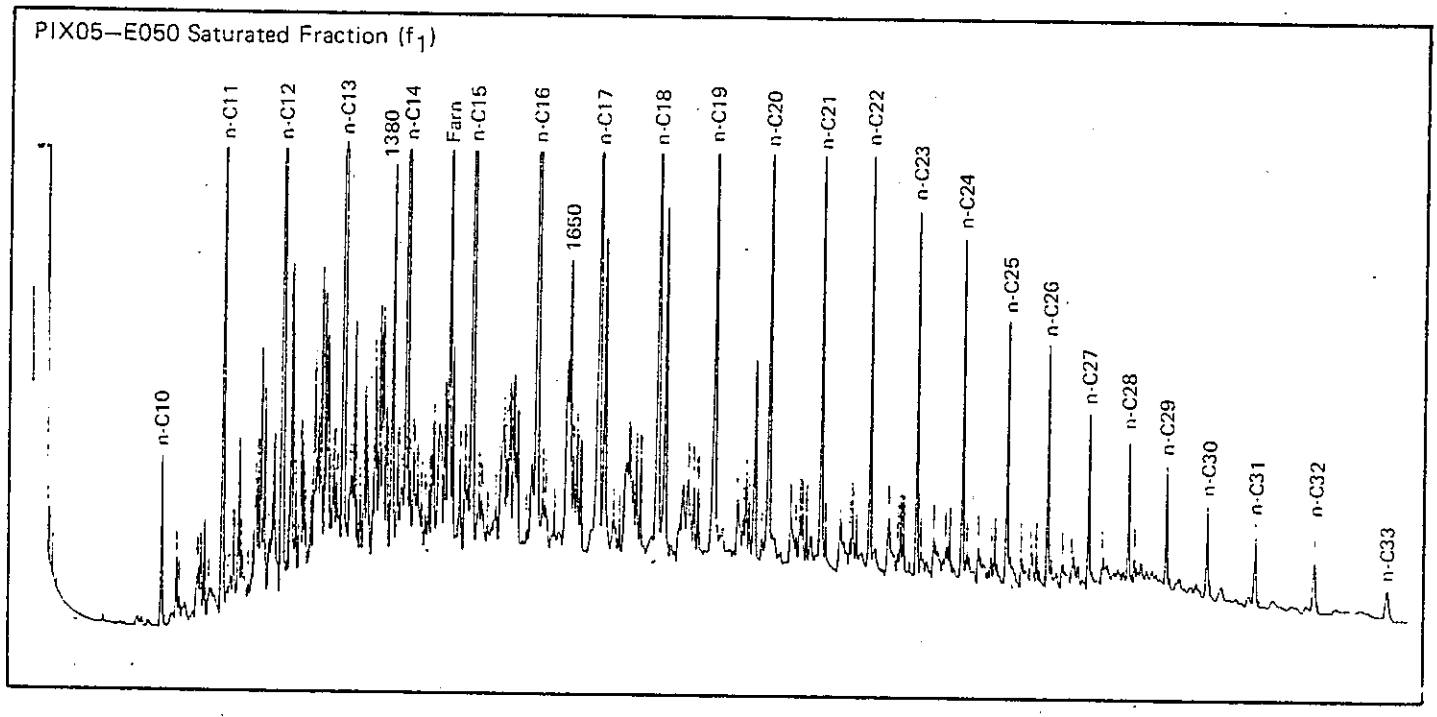

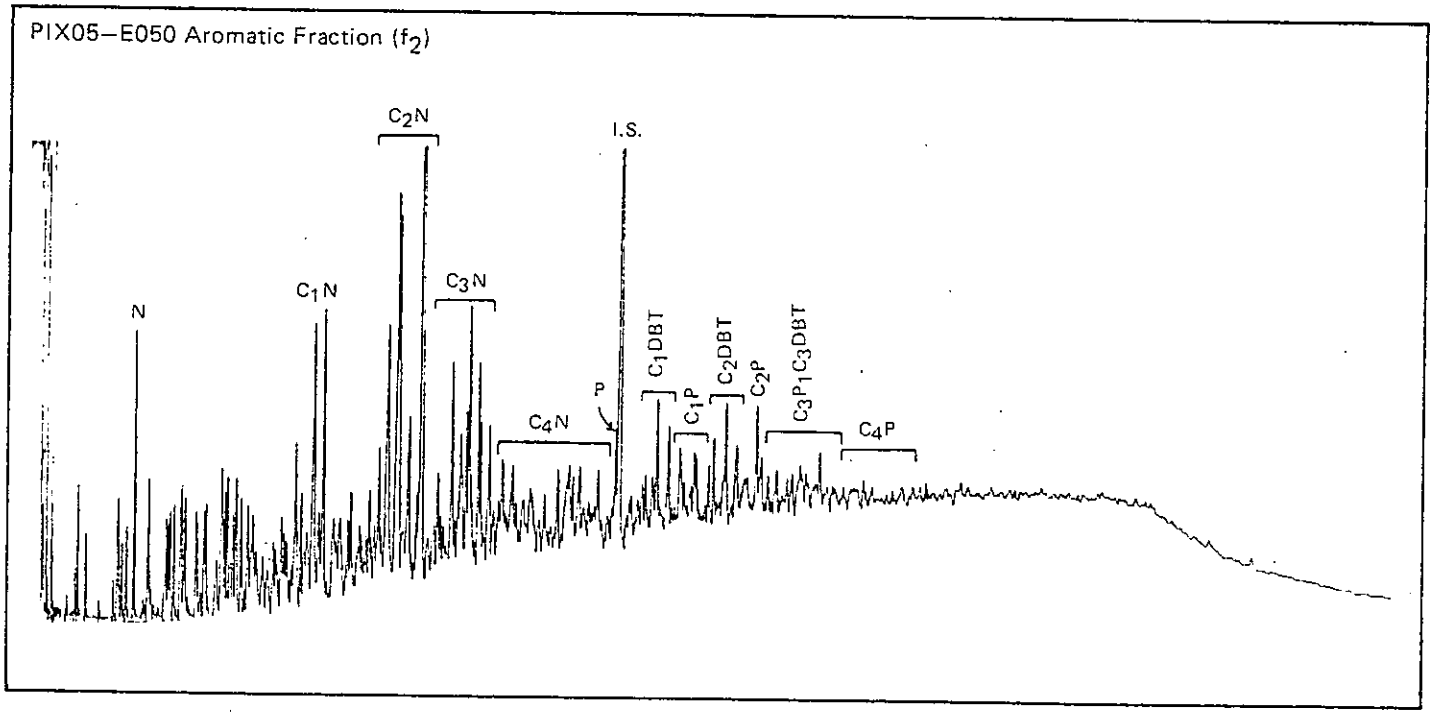

Figure 11. Glass capillary gas chromatograms of "reference oil."

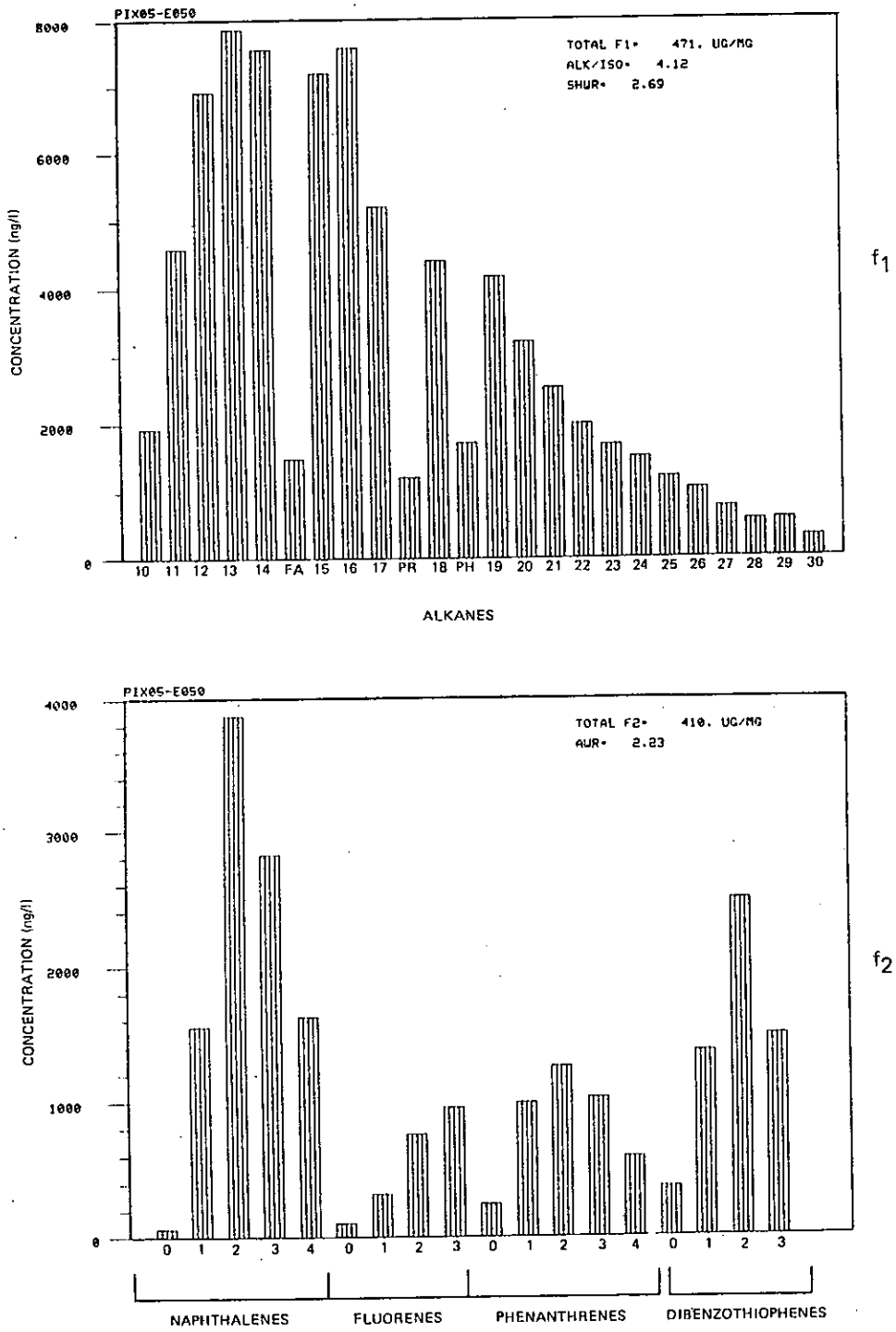

Figure 12. Station PIX 05 - reference mousse.

Table 4. Water column whole water and filterable (dissolved) hydrocarbon data summary.

Station & Sample	Water Depth (m)	Distance from well-head (km)	Gravimetric f_1 (µg/L)	Gravimetric f_2 (µg/L)	Gravimetric f_3 (µg/L)	ALK/ISO[1]	SHWR[1]	AWR[1]
PIX 01 E025	1	Control	10.1	ND	ND	--	--	--
E021	4	Control	ND	ND	ND	--	--	--
E014	14	Control	ND	ND	ND	--	--	--
PIX 02 E046	2	Control	11.1	5.0	7.4	--	--	--
E041	6	Control	16.0	5.0	7.5	--	--	--
E036	16	Control	ND	ND	ND	--	--	--
PIX 14 E163	1	44.0	3.4	< 1.0	91.0	4.2	1.45	--
PIX 12 E122	6	23.0	26.0	40.0	24.5	--	1.12	5.12
E119	20	23.0	31.0	29.0	35.0	2.2	1.33	--
PIX 08 E100	6	22.0	277.5	51.0	63.5	3.5	1.25	1.60
E099	6 (Fil)[2]	22.0	38.0	38.0	165.0	--	--	8.84
E095	16	22.0	292.0	20.9	83.0	3.6	1.78	2.52
E094	16 (Fil)	22.0	29.0	31.0	69.0	--	--	--
E090	19	22.0	26.0	34.0	29.0	4.2	1.27	1.59
E088	19 (Fil)	22.0	ND	ND	ND	--	--	--
PIX 15 E180	2 (Fil)	16.0	19.0	30.4	35.9	--	1.19	--
E176	6 (Fil)	16.0	26.0	19.5	39.5	--	1.44	--
E172	20 (Fil)	16.0	8.9	7.2	35.9	--	1.00	1.24
E182	40	16.0	49.0	28.0	36.5	--	1.22	--
PIX 15 E181	2	16.0	96.0	76.0	138.0	3.5	1.35	--
E173	20	16.0	32.0	19.0	188.0	--	1.23	--
PIX 11 E111	6	12.0	221.0	174.0	66.0	3.7	1.73	2.91
E108	20	12.0	74.0	46.0	28.0	3.5	1.50	3.09
PIX 10 E106	2	0.8	4,170.0	2,840.0	858.0	4.5	2.17	2.80
E104	2 (Fil)	0.8	65.0	51.5	28.0	3.6	1.28	6.66
PIX 05 E066	2	0.5	1,000.0	800.0	350.0	3.9	1.37	1.90
E061	6	0.5	1,550.0	1,050.0	102.0	4.8	1.65	3.16
E056	20	0.5	348.0	271.0	451.0	2.8	1.44	--
PIX 07 E072	1	2.3 (east of	49.0	45.0	72.0	3.2	1.04	--
E071	6	2.3 wellhead)	45.0	72.0	47.0	3.0	1.02	--

[1]See text for explanation.

[2]Fil indicates filterable or dissolved material.

Table 5. Water column particulate hydrocarbon data summary.

Station & Sample	Water Depth (m)	Approximate Distance From Well (km)	Gravimetric f_1(µg/L)	Gravimetric f_2(µg/L)	Gravimetric f_3(µg/L)	ALK/ISO[1]	SHWR[1]	AWR[1]
PIX 01 E013/E024	1	Control	35.0/<1.0	<1.0/<1.0	8.4/ 8.1	--	--	--
E018/E019	4	Control	19.3/<1.0	<1.0/<1.0	<1.0/17.4	--	--	--
E015/E013	14	Control	<1.0/<1.0	<1.0/<1.0	8.9/<1.0	--	--	--
PIX 02 E044/E047	2	Control	3.0/<1.0	3.0/<1.0	--	3.3		
E042/E039	6	Control	<1.0/<1.0	<1.0/<1.0	<1.0/<1.0	--		
E034/E036	16	Control	<1.0/<1.0	<1.0/<1.0	<1.0/<1.0	--		
PIX 14 E160	1	44.0	9.1	2.0	28.8	--	1.14	1.01
E161	1	44.0	6.8	6.0	12.0	4.0	1.24	--
E157	6	44.0	1.5	<1.0	6.7	5.6	1.11	1.01
E156	6	44.0	2.4	1.0	20.4	4.6	1.08	1.00
E151	14	44.0	5.0	10.0	17.7	4.7	1.14	1.00
E150	14	44.0	9.8	9.1	13.2	3.5	1.28	1.11
PIX 08 E097	6	22.0	98.7	60.5	25.1	3.2	1.52	1.54
E096	6	22.0	84.4	41.7	30.0	4.8	1.36	1.22
E091	16	22.0	46.7	34.4	7.2	4.4	1.63	1.24
E089	19	22.0	6.7	12.8	19.0	3.3	1.16	1.02
E086	19	22.0	7.2	7.8	6.1	4.4	1.13	--
PIX 15 E179	2	16.0	64.3	45.1	29.6	3.6	1.58	1.43
E178	2	16.0	93.3	60.9	66.1	3.7	1.73	1.40
E175	6	16.0	75.8	43.7	29.0	3.7	1.77	1.39
E174	6	16.0	39.3	28.7	22.1	3.8	1.73	1.40
E170	20	16.0	21.7	9.3	9.7	2.7	1.33	1.24
E171	20	16.0	29.4	14.1	17.0	2.8	1.30	1.28
PIX 10 E105	2	0.8	3,350.0	2,860.0	582.0	4.8	2.54	2.14

[1]See text for explanation.

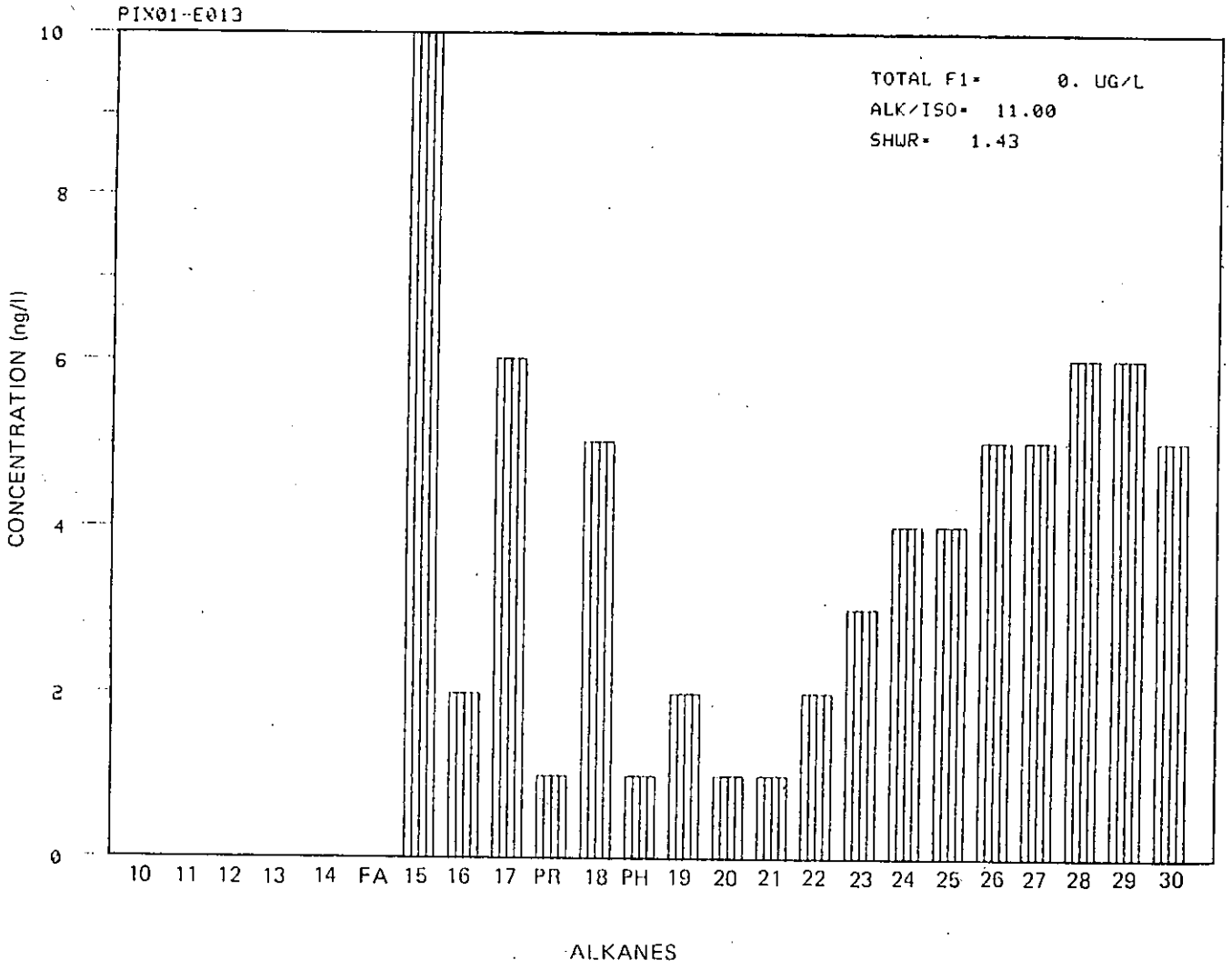

Figure 13. Station PIX 01 - particulate hydrocarbons (f_1).

3.2.3 Station PIX 02

This second control station, located closer to the well, contained lower total concentrations of hydrocarbons but a relatively greater contribution of $n\text{-}C_{15}$ and $n\text{-}C_{17}$, planktonic alkanes (Figure 14), to the hydrocarbon assemblage throughout the top 20 m. Small quantities (1-10 ng/L) of naphthalene, phenanthrene, and their mono-substituted homologues were observed in the particulate sample from the surface (2 m). A petroleum source seems unlikely for these aromatics, due to the sparsity of alkylated members of the two- and three-ringed aromatic series. A more likely source would be a combustion (pyrogenic) source perhaps related to trace amounts of shipboard contamination.

3.2.4 Station PIX 14

Petroleum hydrocarbons associated with the IXTOC-I blowout were detected in the subsurface water at this station located 44 km from the wellhead. A vertical profile of the compositional changes of the saturated particulate hydrocarbons (1-14 m) is shown in GDD's (Figure 15). Concentrations of petroleum-associated components increase with depth. Small-scale spatial heterogeneities are apparent in the lack of consistent compositional characteristics of the samples at a given depth (Table 5). Compositional patchiness is noted especially in the SHWR (Table 5), which varies from 1.1 to 1.3. A suite of substantially weathered (AWR = 1.0-1.1) aromatic hydrocarbons characterizes the particulates at 14 m with total f_2 fraction concentrations 10 µg/L and individual alkylated fluorenes, phenanthrenes, and dibenzothiophenes present in concentrations from 1 to 30 ng/L (Figure 15).

3.2.5 Station PIX 12

Significant quantities (60-70 µg/L) of petroleum hydrocarbons were present at this station. Only two whole water samples (unfiltered), at 6 and 20 m, were collected and analyzed. Total hydrocarbon levels were similar at both 6 and 20 m. Compositionally, all the samples appeared to be a combination of weathered tar and a dissolved-type distribution of alkyl benzenes and naphthalenes (Figure 16) with individual aromatic components in the 20-100 ng/L range. This station appears to lie on the outer edge of the subsurface distribution of large amounts of dispersed petroleum from the wellheat (Fiest and Boehm, this symposium).

The exact relation of the observed weathered hydrocarbon distribution to the main subsurface oil plume is difficult to determine. The preponderance of soluble aromatics in the whole water at PIX 12 results in a high AWR (5.1), characteristic of the filterable (dissolved) hydrocarbons at stations closer to the well. This may indicate that detectable subsurface oil, remote from the blowout, is comprised of a diluted dissolved hydrocarbon plume, confirming spectrofluorometric-derived conclusions (Fiest and Boehm, this symposium). Saturated hydrocarbons at a depth of 20 m are less weathered (SHWR = 1.33) than those at 6 m (SHWR = 1.12), which appear similar in composition to surface mousse from the area (PIX 08, RIX 07, see Table 2).

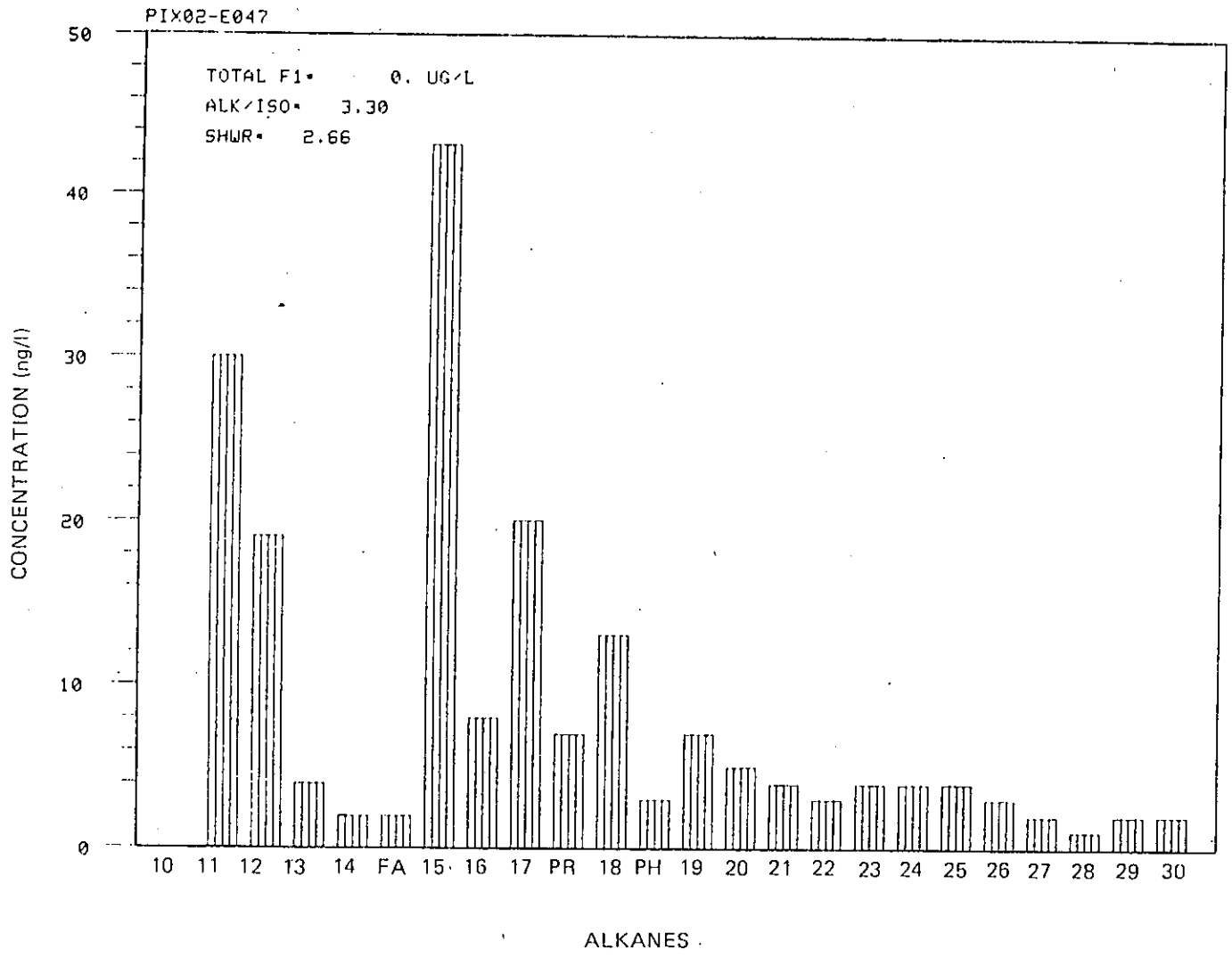

Figure 14. Station PIX 02 - particulate hydrocarbons (f_1).

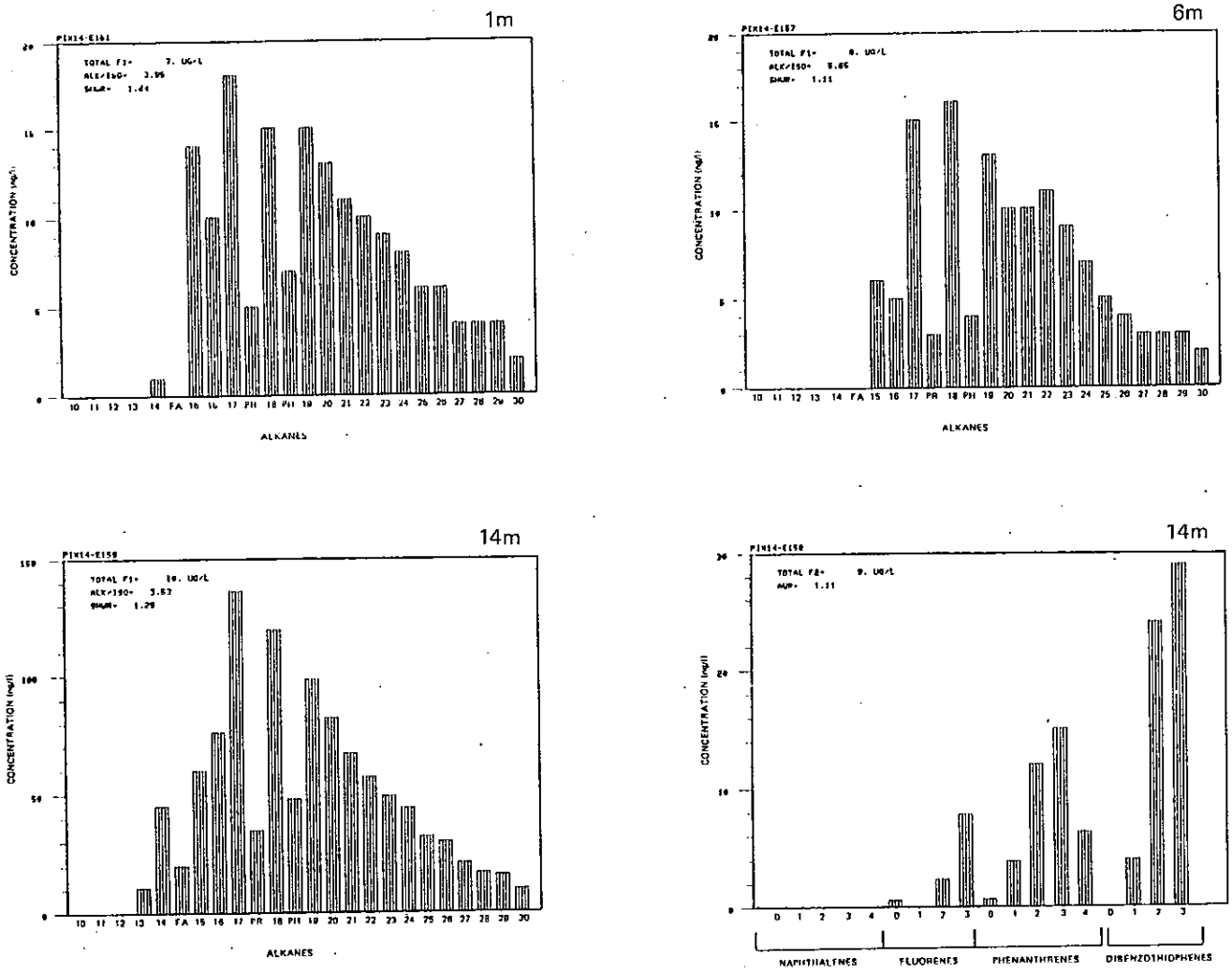

Figure 15. Station PIX 14 - particulate hydrocarbons.

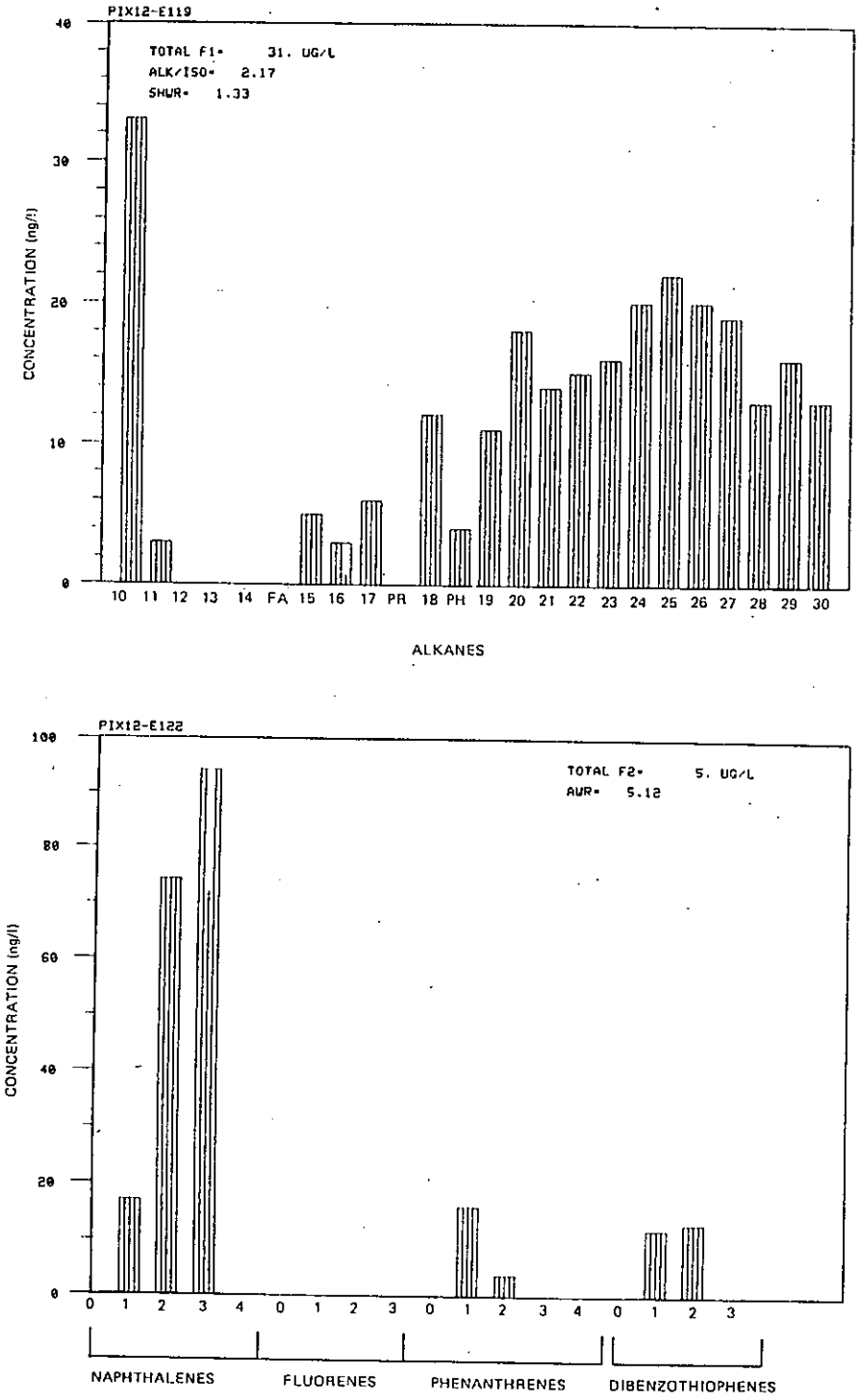

Figure 16. Station PIX 12 - whole seawater hydrocarbons (f_1, f_2).

3.2.6 Station PIX 08

This station, located at the edge of the particulate oil plume, was intensely sampled. Vertical profiles (6, 16, and 19 m) of whole water samples and particulate material were obtained simultaneously with acoustic reflectance profiling (Walter and Proni, this symposium). A dissolved (filtered) hydrocarbon sample was obtained at 6 m.

At 6 m, the whole water contained considerable quantities of IXTOC-I petroleum hydrocarbons, 280 µg/L of saturated (f_1), and 51 µg/L of aromatic hydrocarbons. The saturate fraction contained a composite of oil that had been weathered by physical/chemical processes ($\sim$80 g/L) (SHWR = 1.25) and a large amount ($\sim$200 µg/L) of paraffinic tar characterized by UCM and high-molecular weight paraffins. Individual aromatic hydrocarbons were present at levels from 40 to 600 ng/L, with the naphthalene and dibenzothiophene families dominating. The simultaneous presence of significant quantities of naphthalenes in a sample containing a weathered saturate fraction in the C_{10} to C_{17} range suggests that the whole water sample consists of significant quantities of both dissolved and particulate hydrocarbons. GDD presentations of whole water compositions are presented in Figure 17.

The filtered (dissolved) sample from this depth (6 m) contained only small quantities of saturated hydrocarbons but sizeable quantities of naphthalene (50 ng/L) and its C_1 through C_4 alkylated homologues (dimethyl naphthalene = 530 ng/L). Trimethyl and tetramethyl benzene compounds were present at the 200-500 ng/L level. Only very small quantities of other aromatic families (e.g., phenanthrenes) were present (see Figure 18), indicating the predominance of truly dissolved aromatic hydrocarbon compounds.

The particulate oil (Figure 19) at this depth consisted of whole oil ($f_1 \simeq 100$ µg/L, $f_2 \simeq 60$ µg/L), which was less weathered than oil at stations farther away from the blowout. Considerable quantities of n-C_{11} to n-C_{17} alkanes were present (SHWR = 1.4-1.5). The aromatic spectrum is similar to the oil at the wellhead except for a $\simeq$60% depletion of the two-ringed aromatics, probably through dissolution of the naphthalenes, relative to the dibenzothiophenes. Naphthalene and methyl naphthalene were absent in the particulate samples, indicating that these compounds are present in seawater most likely in a dissolved form.

At 16 m, IXTOC-I oil was found in the whole water sample in greater concentrations (three to four times; f_1 = 292 µg/L; f_2 = 209 µg/L) than in the surface water. Low-molecular weight compounds were present in both the saturate and the aromatic fractions (SHWR = 1.8; AWR = 2.5), with the naphthalenes dominating the aromatic spectrum (Figure 17). The compositions of both the f_1 (Figure 20) and f_2 fractions are nearly identical to that of the reference wellhead dispersion sample (see Figure 12).

The particulate oil at 16 m was very different in character than in the whole water. Low-molecular weight alkanes, while still present, were depleted (SHWR = 1.6). The absolute concentrations of particulate oil were much lower in the whole water, probably owing more to patchiness in the water column than to a preponderance of dissolved material in the water column. However, qualitatively the unsubstituted and methyl naphthalenes appear to be associated with the dissolved fraction, as the particulate aromatics are primarily

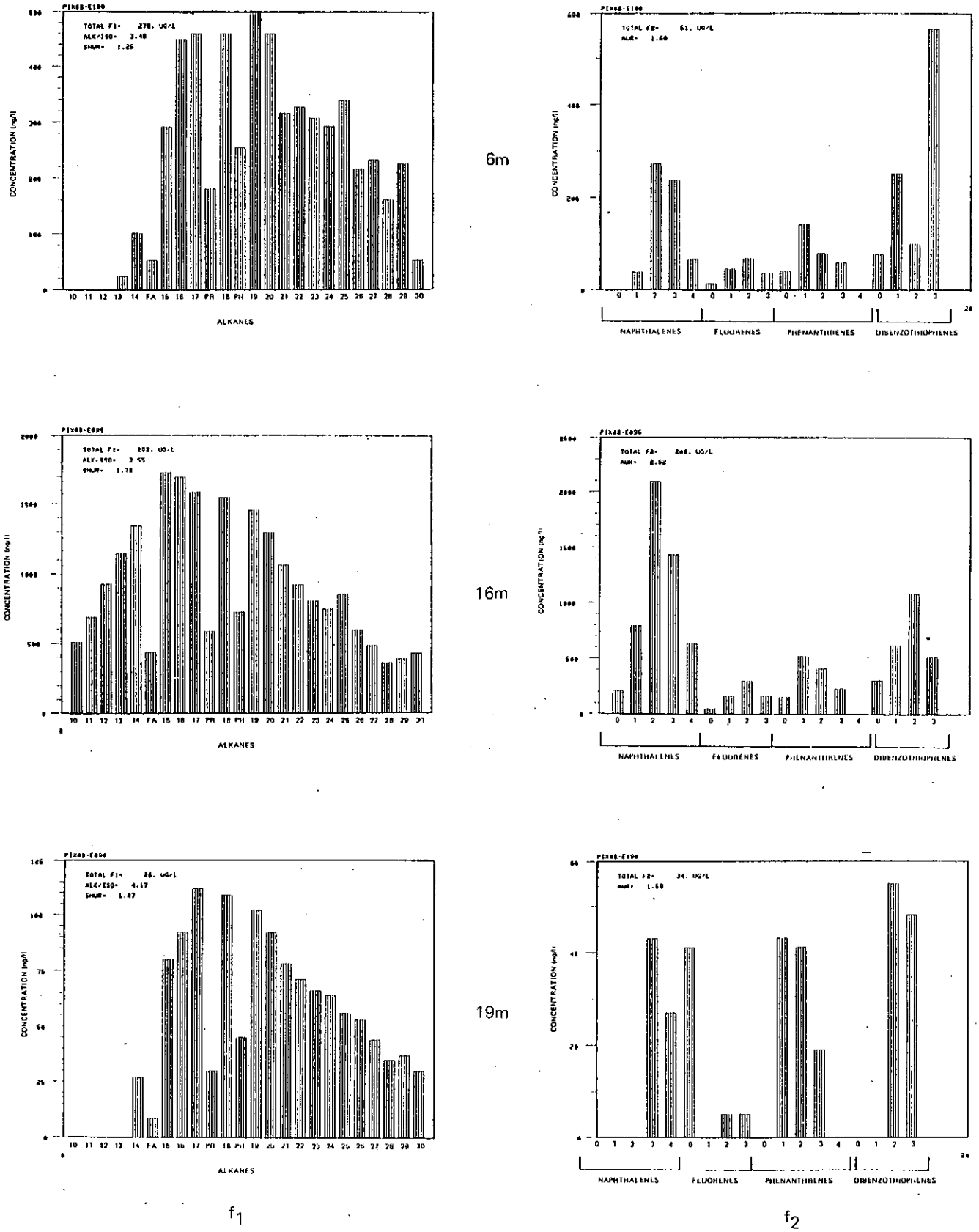

Figure 17. Station PIX 08 - whole water hydrocarbons (f_1, f_2).

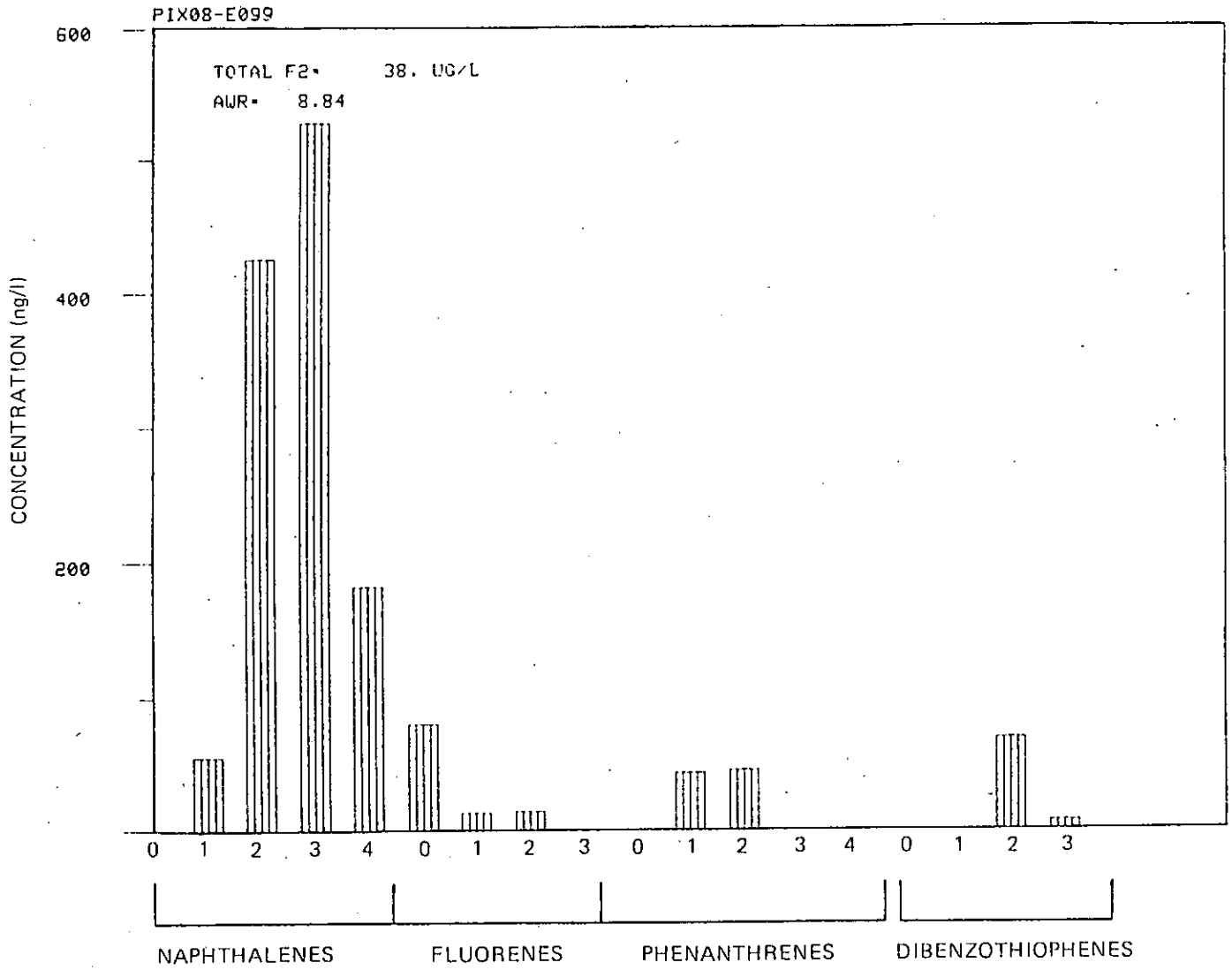

Figure 18. Station PIX 08 - dissolved hydrocarbons (f_2).

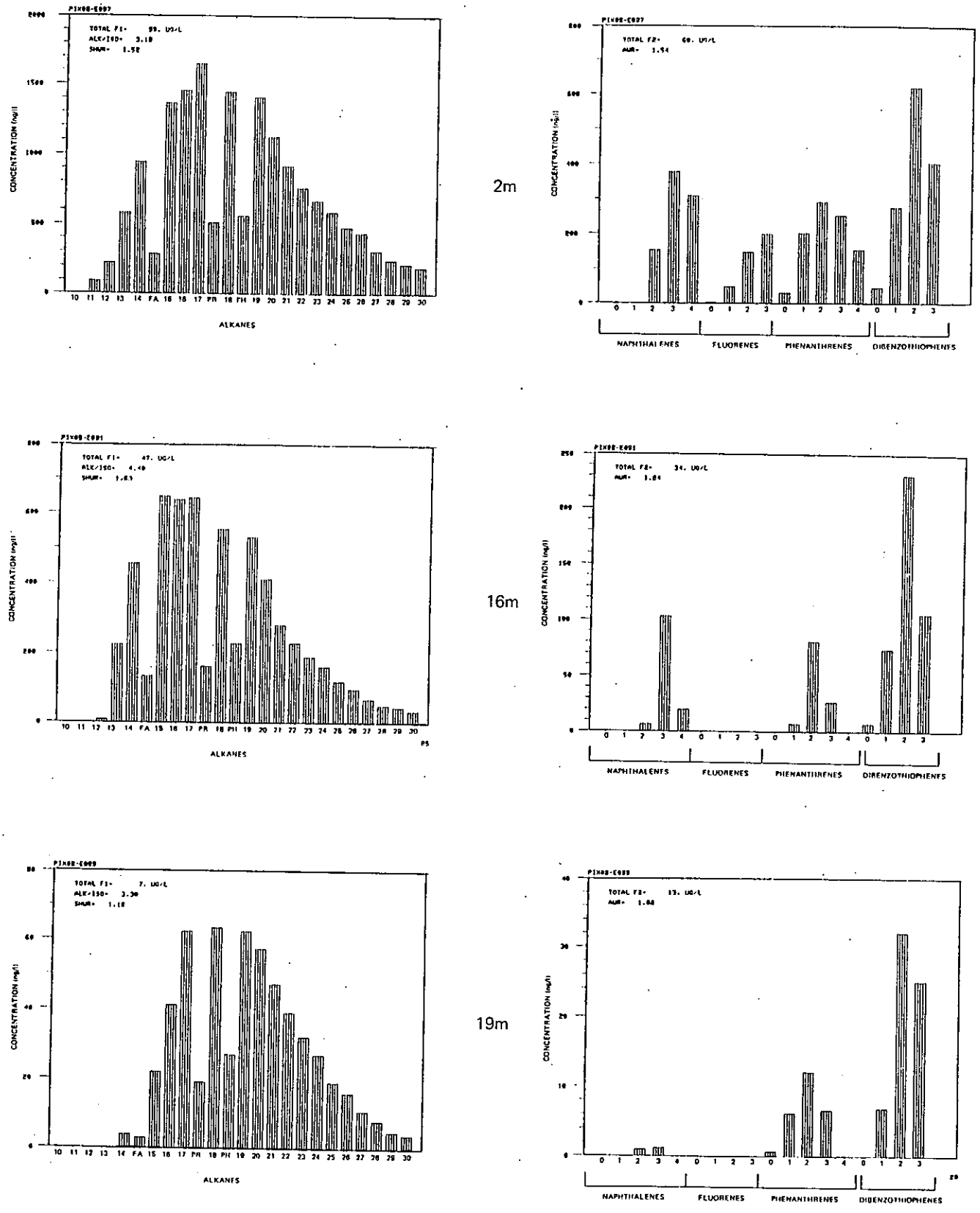

Figure 19. Station PIX 08 - particulate hydrocarbons (f_1, f_2).

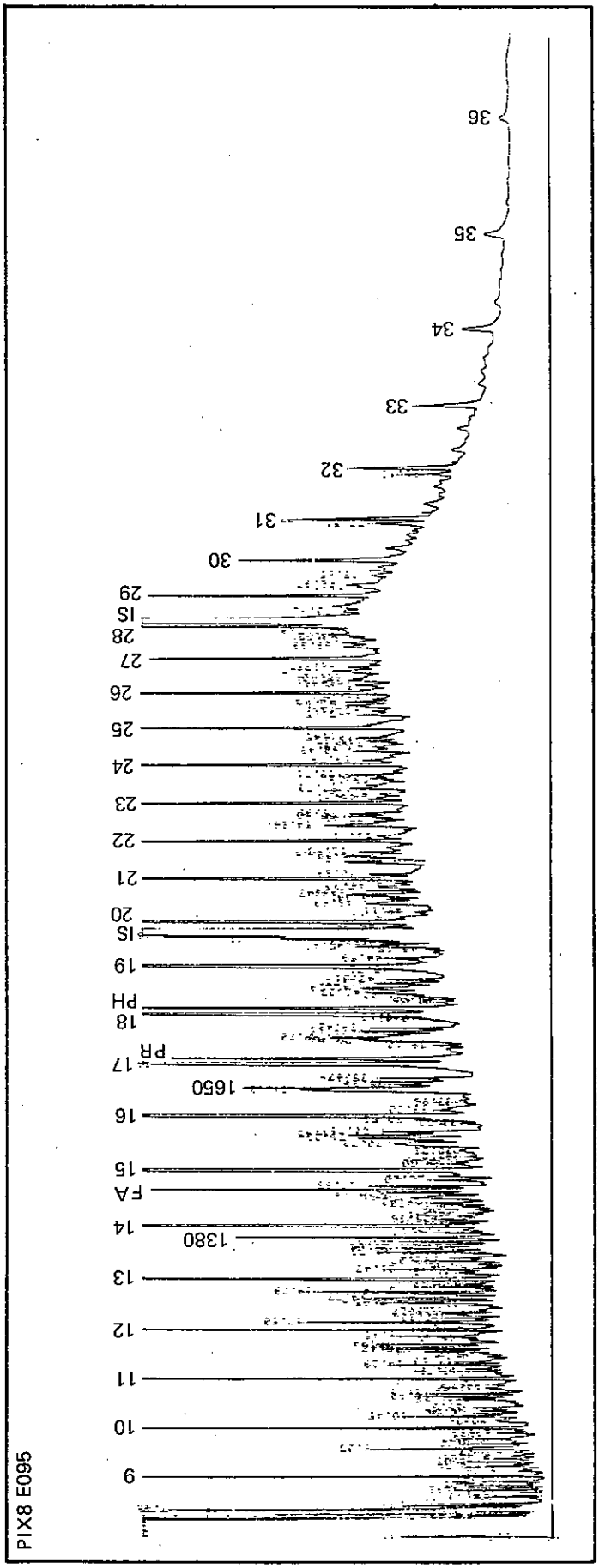

Figure 20. Saturated hydrocarbons in whole water, Station 8, 16 m, in subsurface plume (9-36=n-alkanes; 1380, FA, 1650, PR, PHY=isoprenoids; I.D. - internal standards).

comprised of dibenzothiophenes (10-200 ng/L), phenanthenes (7-100 ng/L), and C_2, C_3, and C_4 substituted naphthalenes (7-100 ng/L) (AWR = 1.2). Naphthalenes, completely absent from the particulate samples, were quite abundant in the whole waters. Phenanthrenes and dibenzothiophenes dominated the particulate aromatic fraction, while naphthalenes, phenanthrenes, and dibenzothiophenes were all present in the whole waters. Presumably, although not directly measured, the naphthalenes are associated with a dissolved form.

At 19 m, the concentrations of hydrocarbons were much lower than in the 16 m sample, thus indicating a sharp discontinuity in subsurface oil layers at this station. The 19-m whole water sample was depleted in both light aliphatic (SHWR = 1.3) and aromatic (AWR = 1.6) compounds relative to the 16 m whole water sample. It is qualitatively similar to the 6-m sample (above the apparent enriched 16-m layer), but in somewhat lesser concentrations (Table 4). Particulate hydrocarbons at 19 m, however, were found in much lesser concentrations than at 6 or 16 m and were compositionally more weathered (SHWR = 1.1-1.2; AWR = 1.0) than the particulates above, thus indicating a quantitative and qualitative (compositional) gradient with depth-decreasing concentration and increased weathering.

The particulate, whole water, and dissolved (filterable) petroleum hydrocarbons appear to reflect significant compositional differences related to both size fractionation and chemical weathering. A subsurface plume consisting of light aromatic and light aliphatic (n-C_{10} to n-C_{17}) compounds in the whole water sample and not in macroparticulates suggests that a dissolved and/or microparticulate (colloidal) dispersion dominates this plume.

3.2.7 Station PIX 15

Whole water and particulate petroleum hydrocarbons were sampled at this station from 2, 6, and 20 m. At 2 m depth, the quantity of hydrocarbons in the particulate phase approximately equals that in the whole water (f_1 whole = 96 µg/L; f_1 particulate = 93 µg/L). In contrast to Station PIX 08, the dissolved fraction of this sample set contains only small quantities of saturate and aromatic hydrocarbons. The compositions of the whole water and the particulate samples are not equivalent, though, with the amount of weathering of the light end (n-C_{10} to n-C_{17}) being greater in the whole water samples (SHWR = 1.35; Figure 21) than in either of the surface particulate samples (1.6-1.7; Figure 22). The ALK/ISO ratio of the samples equals 3.5 and 3.7 for the whole water and the particulates, respectively, indicating insignificant microbial degradation (reference oil = 4.1) at 2 m.

Replication between the two filtered particulate samples collected at 2, 6, and 20 m is quite good (Figure 22), indicating minimal quantitative and qualitative differences related to sampling. Sampling replication results indicate the following coefficients of variation (standard deviation/mean) for the following parameters: aliphatics (f_1) = ± 10%; aromatics (f_2) = ± 30%; individual compounds = ± 30%. These values are not typical for the entire study region, as the more hydrocarbon-rich water samples exhibited greater patchiness.

The particulate samples at 6 m are qualitatively and quantitatively similar to those at 2 m. Particulate saturate hydrocarbons were present in

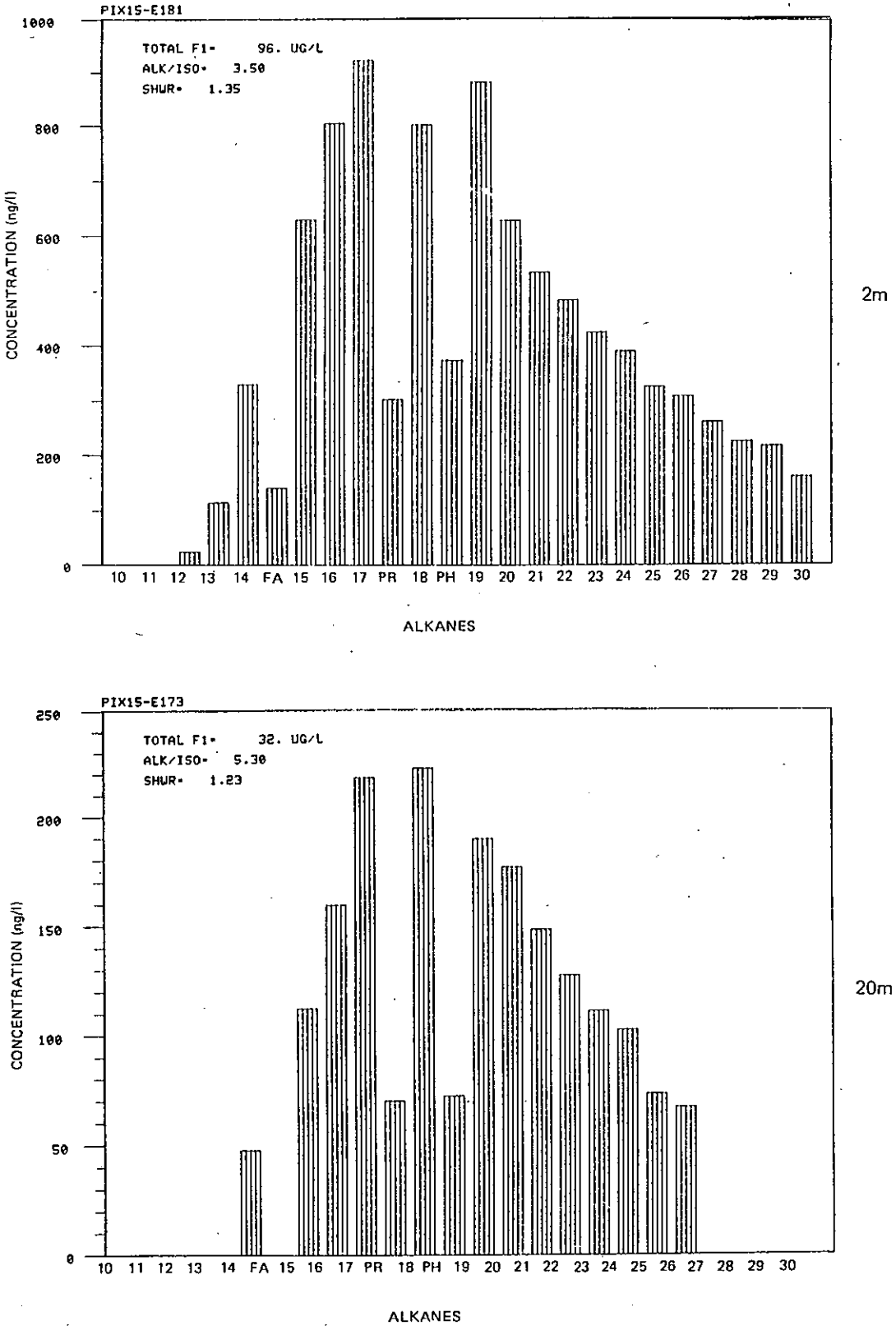

Figure 21. Station PIX 15 - particulate hydrocarbons (f_1).

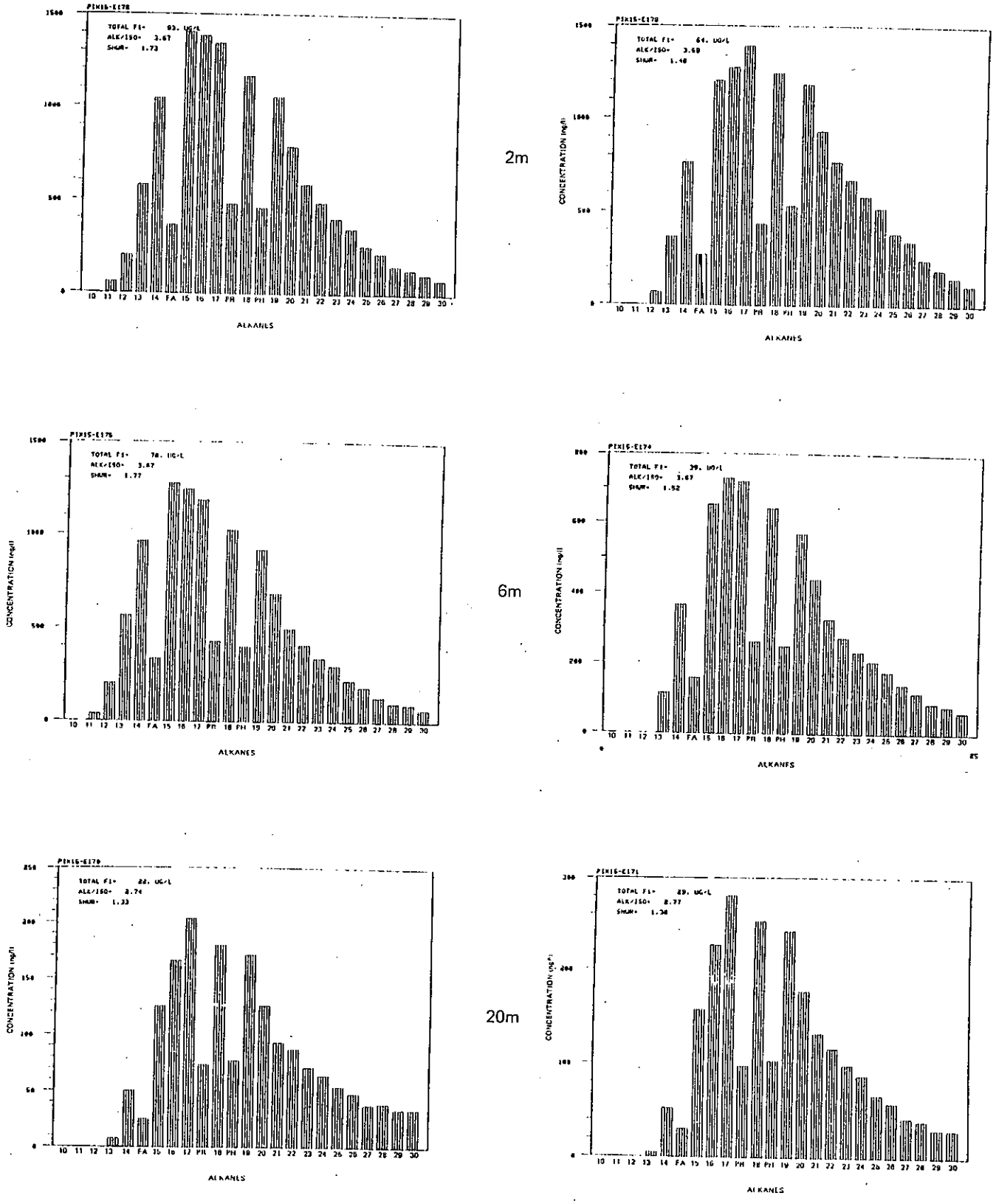

Figure 22. Station PIX 15 - particulate hydrocarbons (f_1).

concentrations of 40-76 µg/L, while the total aromatic fraction ranged from 29 to 44 µg/L. The aromatic hydrocarbon spectra (Figure 23) is dominated by the phenanthrenes (~220 ng/L) and dibenzothiophenes (~ 330 ng/L), with significant quantities of alkylated naphthalenes (~ 90 ng/L) and fluorenes (~ 80 ng/L) present. Saturated hydrocarbons in the particulates have weathered only to the point where SHWR = 1.7. This pattern represents an intermediate weathering stage, in which substantially more material in the n-C_{12} to n-C_{17} range is present than in most other particulate samples in the study. This relative enrichment of light saturated hydrocarbons in the 2- and 6-m samples is significant in terms of relating composition to lateral transport of subsurface oil (see Discussion).

At 20 m, a different picture emerges. Particulate hydrocarbons at this depth are substantially "older" in terms of weathering, which is indicated by a lower ALK/ISO ratio (equals 2.7 and 2.8 for the replicates) due to slight biodegradation and a lesser SHWR (1.3) due to increased evaporation/dissolution. The aromatic fraction (Figure 23) is depleted in the C_1 and C_2 naphthalene compounds as well and consists mainly of dibenzothiophenes (~ 160 ng/L) and phenanthrenes (~100 ng/L). Absolute saturate particulate hydrocarbon concencentrations are 22-30 µg/L and aromatics are 9-14 µg/L, significantly lower than in the surface (< 6 m) waters. Thus, the water column profiles reveal not only less material with depth but also a more weathered version of IXTOC-I oil.

3.2.8 Station PIX 11

Whole seawater samples collected with GO-FLO bottles at 6 and 20 m at this station, located approximately 10 km from the wellhead, revealed fresh oil with abundant naphthalenes (~ 3,400 ng/L; Figures 24 and 25) at the near surface. The AWR equals 3.0, indicating that naphthalenes are dominant to a greater extent than in the reference mousse, again demonstrating that significant quantities of dissolved naphthalenes influence the whole water composition. The total aromatic fraction and saturate fraction concentrations are 174 and 221 µg/L, respectively, in the 6-m sample. Saturated hydrocarbons contain relatively unweathered alkanes n-C_{10} to n-C_{17} (SHWR = 1.5-1.7). At 20 m, the composition of the sampled oil is identical to that at the surface, although of less concentration (f_1 = 74 µg/L; f_2 = 46 µg/L).

3.2.9 Station PIX 10

This station, located closer to the blowout site (< 0.8 km), was sampled at the surface (2 m) for dissolved, particulate, and whole water hydrocarbons. This sample set reveals perhaps the clearest picture of qualitative and quantitative partitioning of oil between the dissolved and particulate phases. Comparison of compositional patterns (Figures 26, 27, 28) reveals basic information on the qualitative partitioning process and also on the relative kinetics of weathering. Particulate hydrocarbons are comprised of the component distributions shown in Figures 26B, 27B, and 28B. By comparison, the dissolved (filterable) fraction (Figures 26C, 27C, 28C) contains primarily naphthalenes (and alkyl benzenes) in the aromatic fraction, with only small quantities of other aromatics. Alkane distributions of the dissolved material exhibit a component distribution with a maximum at n-C_{18}.

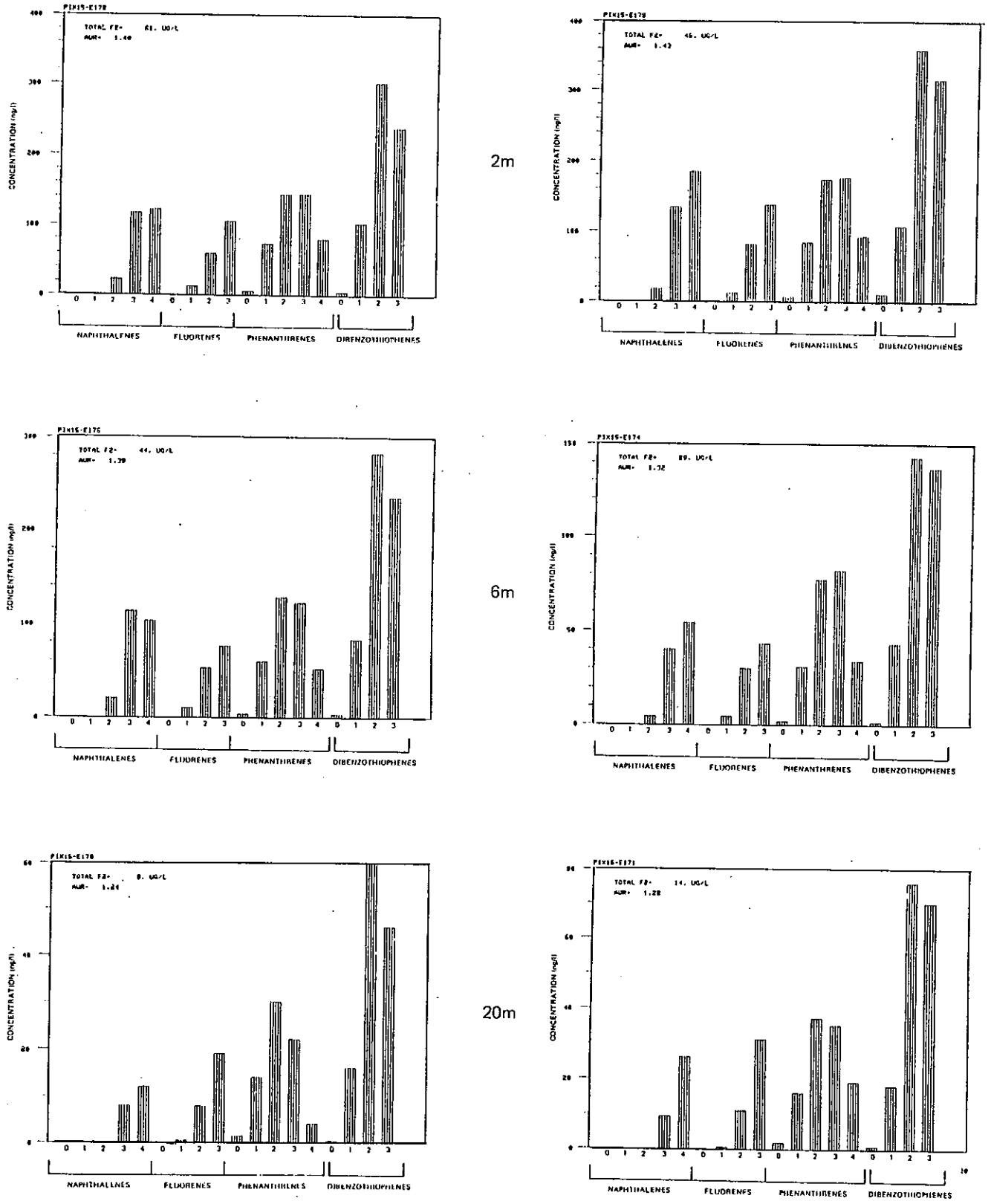

Figure 23. Station PIX 15 - particulate hydrocarbons (f_2)

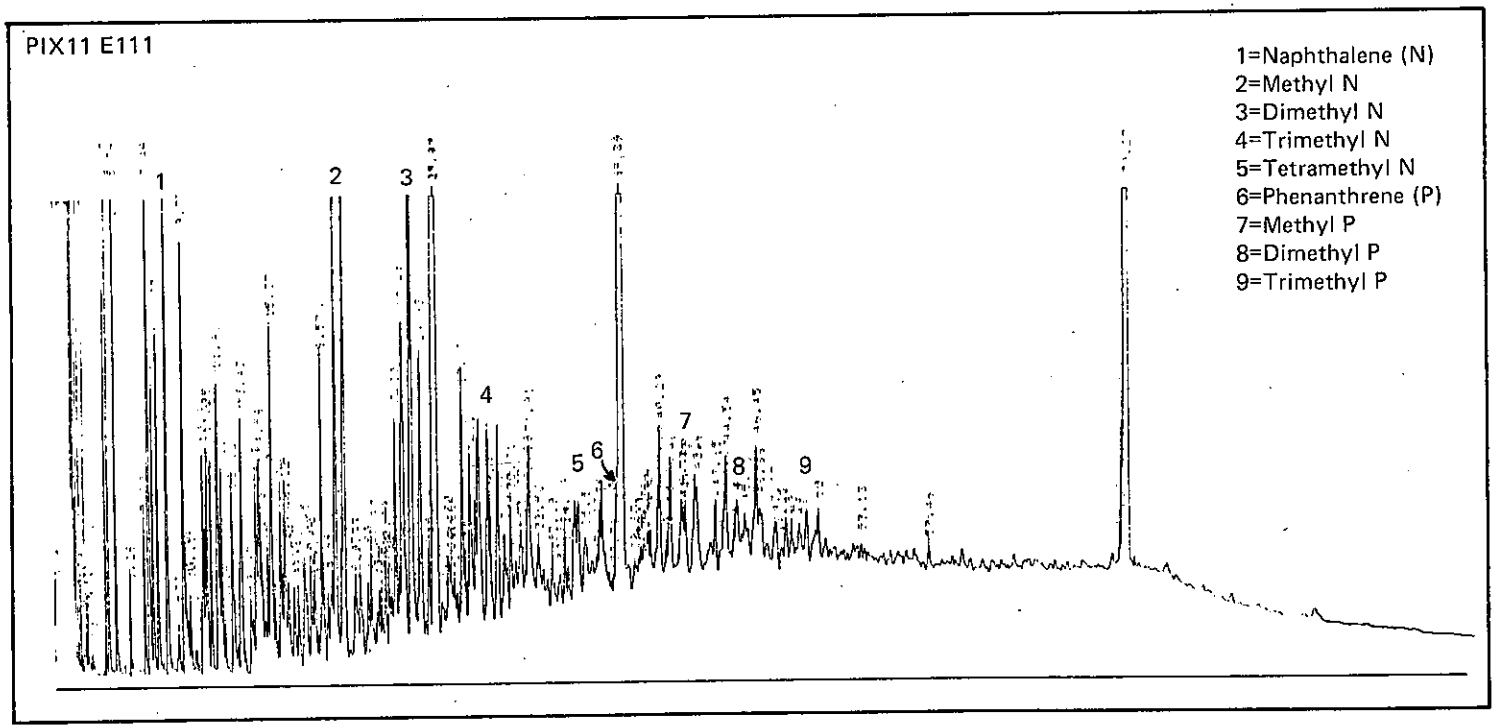

Figure 24. Aromatic hydrocarbons in whole water from PIX 11; 6 meters depth.

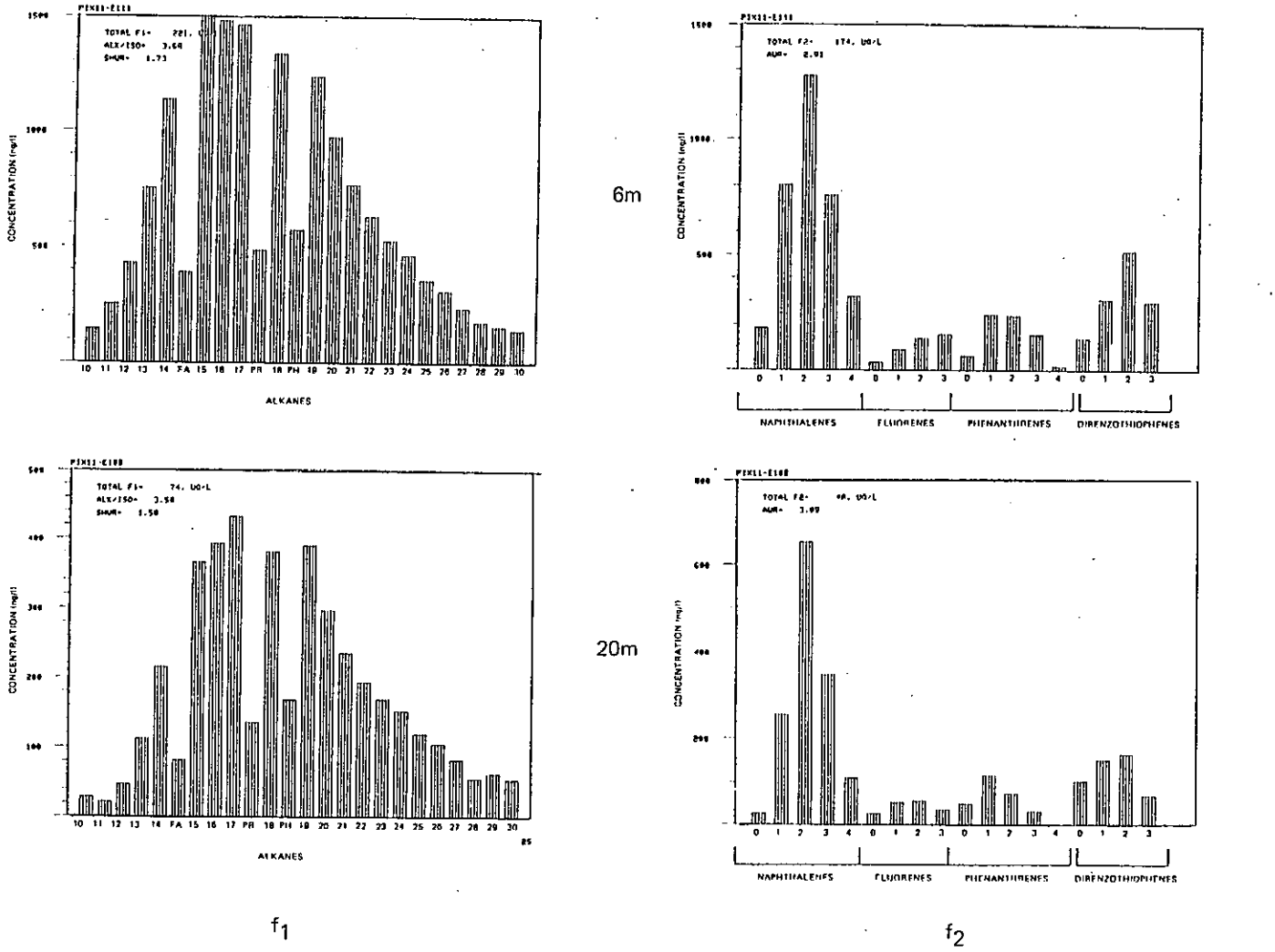

Figure 25. Station PIX 11 - whole water hydrocarbons (f_1, f_2).

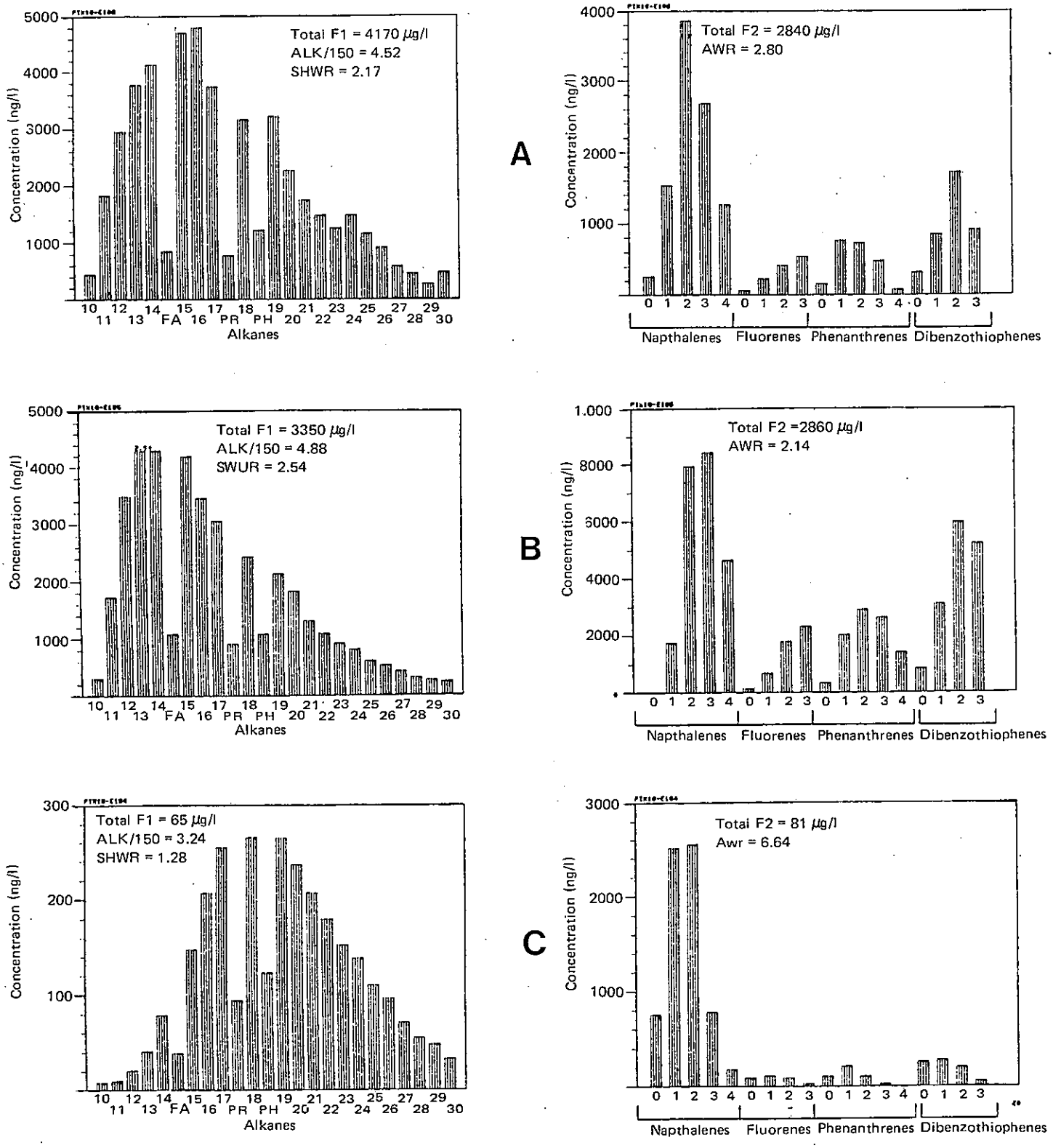

Figure 26. Station PIX 10 - whole seawater at 2 m depth (A), particulate (B), and dissolved (C) hydrocarbons (f_1, f_2).

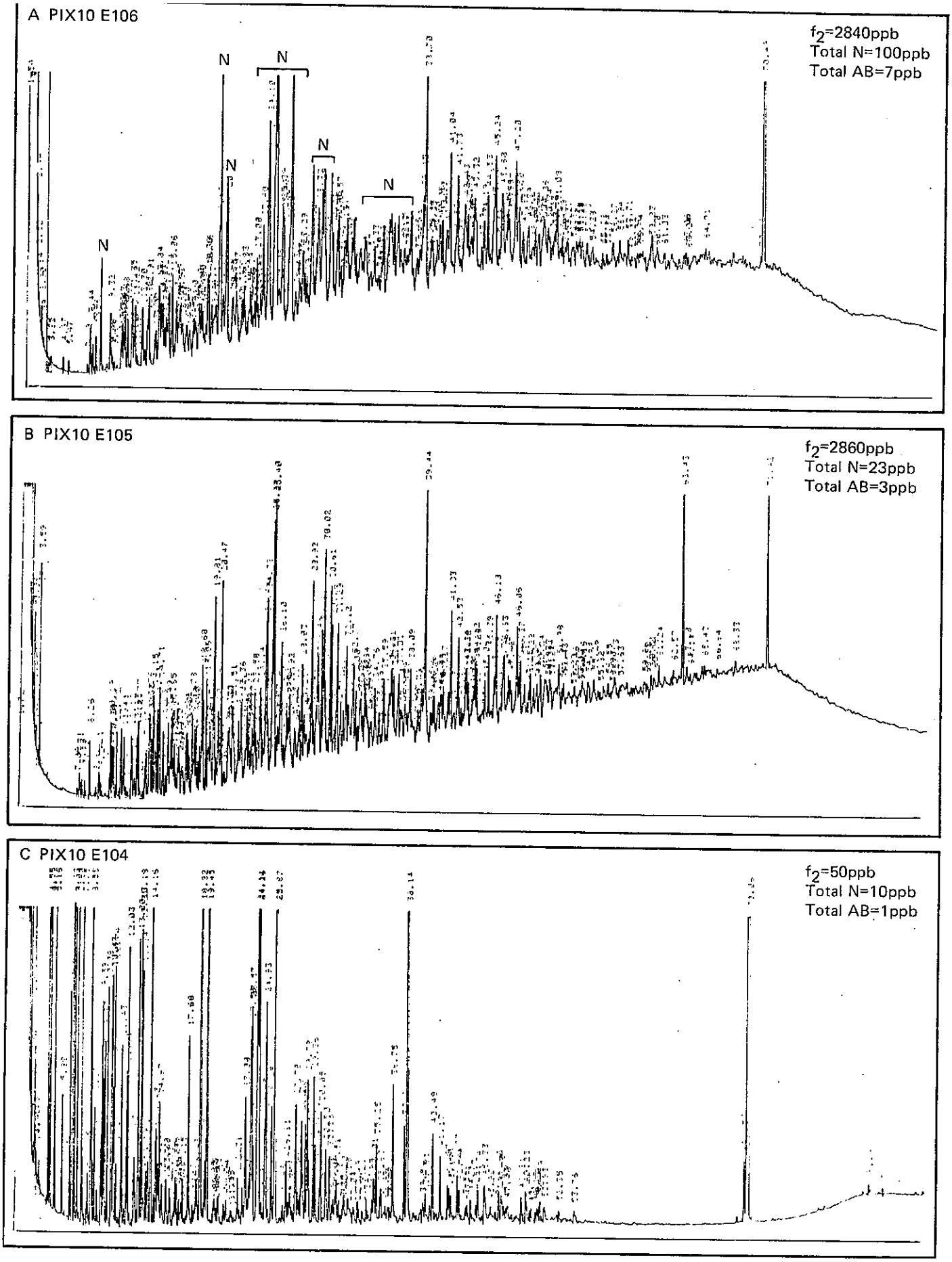

Figure 27. Aromatic hydrocarbons in whole water (A), particulate (B), and dissolved (C) fractions from PIX 10 at 2 m depth (N= naphthalenes; AB=alkyl benzenes).

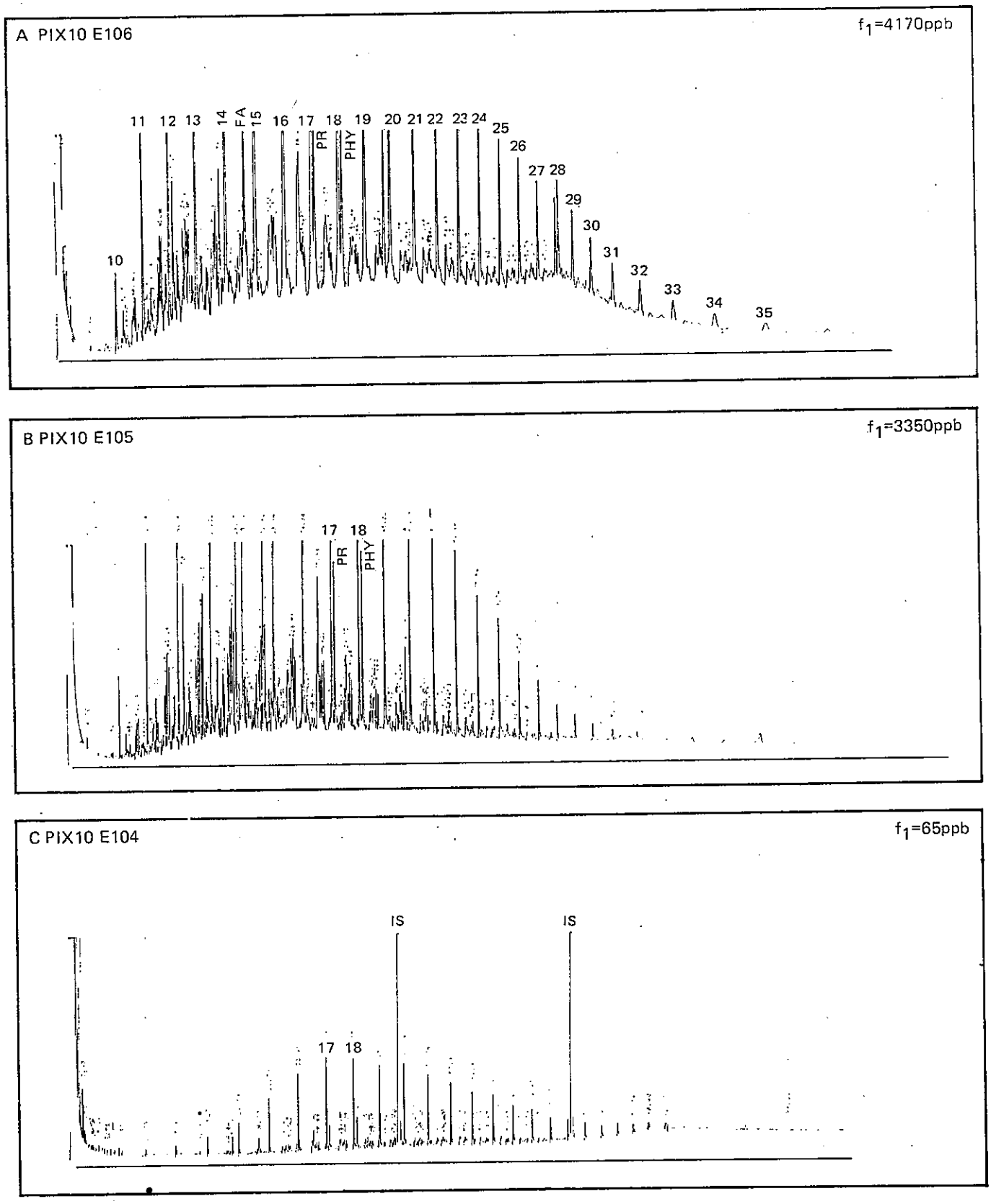

Figure 28. Saturated hydrocarbons in whole water (A), particulate (B), and dissolved (C) fractions from Station PIX 10 at 2 m depth.

While the naphthalenes appear to have partitioned into the dissolved phase, the low-molecular weight alkanes (n-C_{10} to n-C_{13}) are still associated with the particulate phase. The whole water aromatic fraction reflects the sum of the naphthalene-rich dissolved phase and the particulate phase wherein fluorenes, phenanthrenes, and dibenzothiophenes are important (Figure 26A). The whole water saturate fraction is nearly identical to the particulate sample. Thus, aromatic and saturate fractions behave quite independently from each other and appear to partition at different rates.

Concentrations of petroleum in the water column at PIX 10 are roughly 7,000 µg/L of total petroleum, with levels of alkyl benzenes ad naphthalenes at 6.5 and 100 µg/L, respectively. Much of these light aromatics exist in a filterable (dissolved) state.

3.2.10 Station PIX 05

Three samples of whole water were obtained at this station located 0.5 km from the blowout site. Samples obtained at 2, 6, and 20 m differed significantly in their compositions and concentrations (Figure 29). Saturated and aromatic concentrations were approximately the same at 2 and 20 m (200-400 µg/L) but were higher at 6-m depth (~ 1,150 µg/L). The 2-m sample exhibited a decreased abundance of naphthalene compounds relative to dibenzothiophenes, perhaps indicating a "stripping" of soluble aromatics from the oil during its ascent from the sea bed. This fact is further supported by the alkyl benzene distribution in the water column. The concentration of C_3, C_4, and C_5 alkyl benzenes in the top 20 m was much higher at 6 m (~ 1,200 ng/L) compared with ~200 ng/L at 20 m and ~50 ng/L at 2 m. The 6-m samples also contained more low-boiling alkanes (SHWR = 1.7) compared to samples above (2 m = 1.4) and below (20 m = 1.4), implying a midwater-enriched layer, perhaps a source of laterally advected plumes observed at stations farther from the well.

3.2.11 Station PIX 07

Whole (unfiltered) water column samples taken on the "upwind" side of the wellhead where no observable surface slick was noted contained small quantities of weathered paraffinic oil (~ 40 µg/L). Material collected at this station was much older than most other particulates collected and may represent a maximum weathering state of particulates. Note that biodegradation appears to have slightly affected the alkane to isoprenoid ratio (Table 4), and hence the saturate composition of the 6-m sample, to the same extent as for the 20-m PIX 15 particulates.

4. DISCUSSION

4.1 Surface Oil/Microlayer

Despite the lack of a strong correlation between the petroleum hydrocarbon composition of the surface oil samples and the distance between the sampling stations and the blowout, a pattern of progressive weathering of the surface oil samples is evident. Surface oil can weather to varying extents by

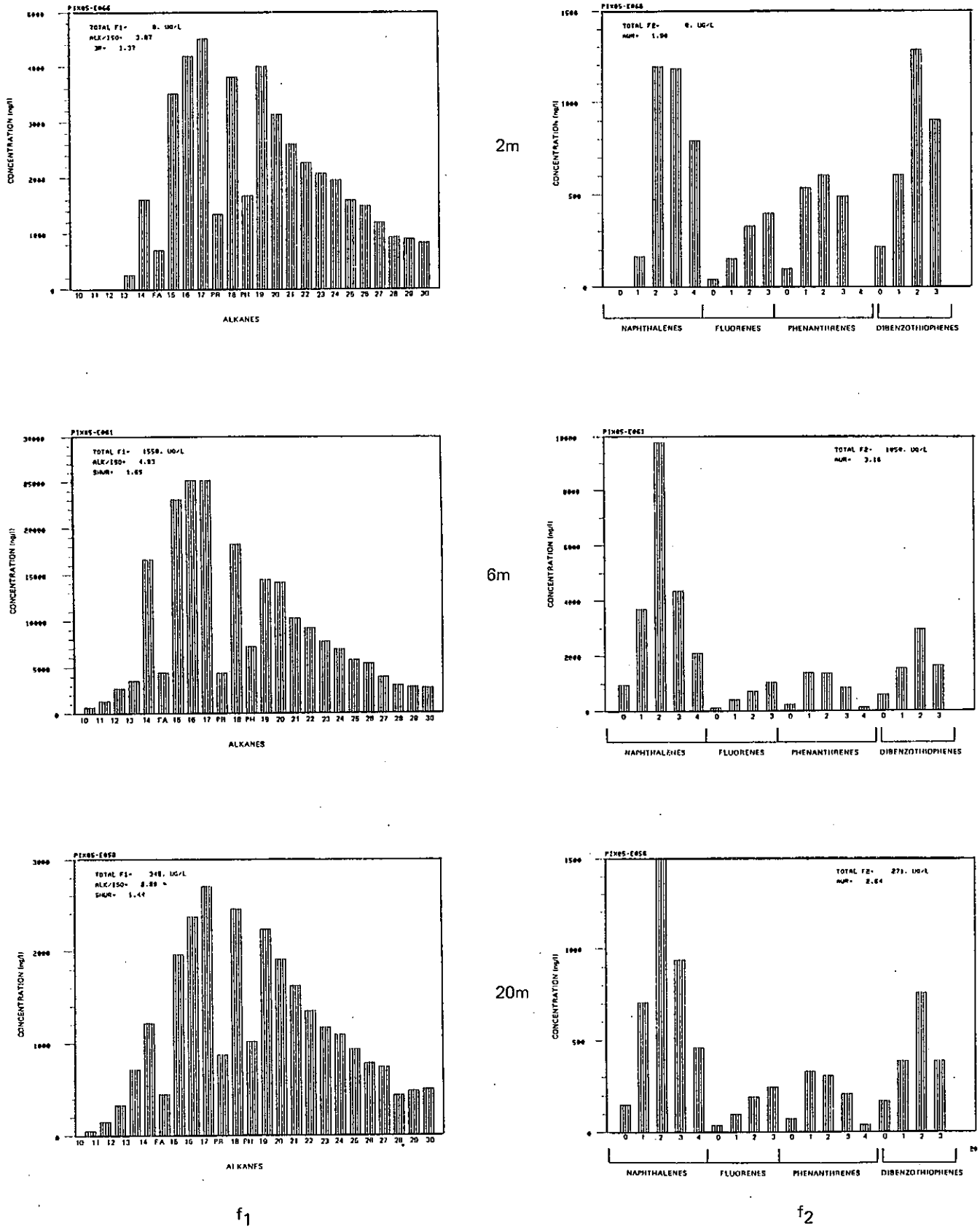

Figure 29. Station PIX 05 - whole seawater hydrocarbons (f_1, f_2).

evaporation, dissolution, microbial degradation, and photochemical oxidation, which are mediated by physical processes (e.g., mixing, emulsification). The relative importance of each of these processes can be deduced by comparing the chemical composition of surface oil, emulsified oil mousse, and microlayer samples.

The oil that reached the ocean surface at the IXTOC-I blowout had already progressed through the early stages of weathering. The high shear at the ocean bottom where the oil was released strongly mixed the oil with seawater and formed an oil-in-water dispersion. Seawater had begun dissolving the low-boiling saturated and aromatic hydrocarbons, and the gaseous components had formed bubbles that either rose to the surface, where they burned in the fire at the sea surface, or were released to the atmosphere, or were transported laterally for some distance in the subsurface waters (Brooks et al., this symposium).

Two samples collected at stations PIX 05 and PIX 10 were the least weathered surface oil samples found and are assumed to be representative of oil that had recently surfaced. The oil in these samples had formed an oil-in-water emulsion that had a watery consistency and strongly adhered to objects that they contacted. Alkanes from n-C_9 to n-C_{32} and substituted aromatics with one, two, and three rings predominated in gas chromatograms of these samples. By comparing the petroleum hydrocarbon compositions of other surface oil samples with that of the reference samples collected at the well blowout, the sequential weathering of the oil can be deduced.

Whereas evaporative weathering causes an equivalent depletion of saturate and aromatic compounds with low boiling points, dissolution preferentially depleted low-boiling aromatics relative to saturate compounds due to the much larger solubilities of the aromatics. The nearly equivalent loss of both saturate and aromatic hydrocarbons with low similar boiling points and different solubilities suggests that evaporation is the predominant weathering mechanism influencing the composition of mousse samples.

The ratio of an aromatic compound (methyl dibenzothiophene) to an alkane (n-C_{17}) with equivalent boiling points but different solubilities can be used to evaluate the relative importance of dissolution. This ratio is 0.39 in the reference oil and decreases to no less than 0.20 in any of the mousse samples. For those samples with C_1DBT/n-C_{17} equal to approximately 0.20, roughly 70% of the n-C_{17} has been lost by evaporation. If we can assume that C_1DBT is evaporated similarly to n-C_{17}, then approximately 70% of the C_1DBT in the original oil has been lost by evaporation, 15% by dissolution, and 15% remains. In the most weathered samples collected near the well, dissolution is shown to be an important but secondary weathering mechanism for the mousse samples.

The extent of microbial degradation of the mousse samples can be followed with the ALK/ISO ratio, which is designed to approach zero as n-alkanes are preferentially depleted relative to branched alkanes by bacterial action. This ratio is 4.1 in the reference oils and is no lower than 3.0 in virtually all of the mousse samples. We conclude that a significant biochemical depletion of the n-alkanes in the mousse is not occurring. The primary reason for the lack of microbial weathering appears to be related to the low concentrations of nutrients in the underlying water, although some chemical

inhibition by photo-decomposition products of the oil cannot be ruled out (Larson et al., 1979). Samples of mousse collected as far north as the Texas coast show little evidence of microbial degradation. The absence of observed degradation as a result of microbial activity contrasts with other coastal spills, e.g., AMOCO CADIZ, for which microbial degradation played an important role in the weathering of the oil (Atlas et al., 1980).

The tar sample collected at station RIX 13 off Tampico, Mexico, is anomalous in that extensive microbial degradation of a surface oil sample was found. The apparent enhancement of microbial activity associated with this sample may have resulted from its association with floating algae in a windrow. Nutrients may have been released from decomposing plant matter or fixed by blue-green algae and hence introduced to the microenvironment of the tarball, thereby enhancing microbial degradation.

Another important weathering pathway for the oil in the mousse patches was the emission of material to a surface sheen surrounding the mousse patches. This mechanism by which oil was transferred from the mousse to thin surface film was observed for all patches of mousse that were encountered. From the helicopter, the sheen associated with the mousse patch was often more visible than the patches of mousse associated with it. The hydrocarbons in the microlayer are more extensively evaporated than were hydrocarbons in the mousse sample, as a result of the much greater surface area/volume of the microlayer. The more extensive loss of the aromatics relative to saturates, as evidenced in the C_1DBT/n-C_{17} ratio, is most likely a result of dissolution and/or photo-decomposition of the aromatics in the microlayer.

4.2 Seawater/Particulates

Whole water, particulate, and filterable hydrocarbons are operationally defined in this study, with particulate material being that trapped on a Gelman A/E glass fiber filter (98% retention of particles greater than or equal to 0.3 µm), and dissolved and/or colloidal material being that which passes through the filter. Although the operational definition does not permit rigorous interpretation of results in terms of physical/chemical realities, the particulate and filterable fractions will behave differently, primarily due to the greater surface area and lesser buoyancy of the latter as well as to the fact that significant quantities (estimated to be $\geq$ 50% of the filterable fraction) of hydrocarbons passing the filter are truly dissolved. Compositionally, all material passing the filter is similar to the "water-soluble fractions" used by many researchers in evaluating acute and sublethal toxicities. The submicron colloidal material can be viewed as having a large surface area to volume ratio, which promotes rapid dissolution.

It also should be noted that this study addresses "high-molecular weight" hydrocarbon distributions - saturated hydrocarbons larger than n-C_{10} (decane) and aromatics with higher boiling points than the ethyl (or dimethyl) benzenes. Thus, the results from this study should be viewed as complementary to those of the volatile and gaseous hydrocarbons in subsurface waters (Brooks et al., this symposium).

Throughout the evaluation of the results of this study, it should be kept in mind that the time lag between whole water and particulate/dissolved

samplings was considerable ($\sim$ 30 min). Thus, heterogeneities in the water column may explain any lack of "additivity" of particulate plus dissolved and whole waters.

The gas chromatograms of filtered seawater reveal aromatic compositions quite different from the particulate material and quite similar to those of laboratory-prepared water soluble fractions (e.g., Zurcher and Thuer, 1978; see Figure 27C). The filtered seawater contains relatively greater quantities of the more soluble alkyl benzenes and naphthalenes, compared with phenanthrenes and dibenzothiophenes (AWR $\geq$ 6). Particulate oil, on the other hand, is comprised of an aromatic hydrocarbon distribution similar to that of a weathered mousse, but depleted in the lower boiling aromatic compounds and enriched in phenanthrene and dibenzothiophene homologs. Any unresolved material (UCM) is usually associated with the particulate fraction, virtually absent from the filterable (dissolved) fraction, and sporadically observed in the whole water samples.

Whole water samples are consistently enriched in light aromatic compounds relative to wellhead oil or overlying weathered mousse. The explanation is not to be found entirely in the dissolved fraction, which contains only as much as 20% of the total light aromatics found in whole water. Shaw and Reidy (1979) found that a marked chemical fractionation of crude oil occurred upon dispersion; the resultant whole water dispersion apparently contained filterable material (colloidal and dissolved) enriched in light aromatics and depleted in saturates (alkanes). The authors showed an important relationship between mixing energy, chemical, and physical size fractionation. Such a relation appears to dictate the whole water chemistry in samples taken under the surface plume. The 15-20 m thick acoustic scattering layer (Walter and Proni, this symposium) is characterized by an aromatic-enriched whole water hydrocarbon assemblage and a slightly aromatic-depleted set of particulate samples. The whole water probably consists of small particles among colloidal/dissolved plume, and the particulates probably consist of larger particles slightly depleted in aromatics relative to surface mousse.

It is clear from the set of samples at PIX 10 (Figures 27 and 28) that most of the water-borne petroleum is in a particulate (droplet) form. One to two percent of the total f_1 and f_2 fraction concentrations of the whole water sample is "dissolved" or passes the filter. Some of this "dissolved" oil may not be truly dissolved, but judging by the grossly different aromatic hydrocarbon profiles of the dissolved and particulate matter (Figure 27), we assume most of the aromatics passing the filter to be in a dissolved or solubilized form. While significant amounts of the naphthalenes and alkyl benzenes (20-50%) may have partitioned into the dissolved phase, the filtered sample contains little indication of low-molecular weight (n-C_{10} to n-C_{15} alkanes). The saturated components at PIX 10 and in subsurface waters in general are associated with the particulate phase. Thus, the saturates and aromatics within a petroleum hydrocarbon mixture are exhibiting different dissolution kinetics. Similar disparate behavior is consistently observed in laboratory studies (e.g., Boehm and Quinn, 1975; Zurcher and Thuer, 1978). While the dissolved fractions represent only one to two percent of the total oil concentration in the water column, the dissolved alkyl benzenes, naphthalenes, methyl naphthalenes, and total naphthalenes represent 15, 30, 16, and 7 percent of their respective whole water concentrations.

The areal distributions and vertical profiles of the concentration and composition of subsurface dissolved and particulate oil within the blowout's major impact area (0-70 km from the wellhead) during 11-27 September are not simple functions of decreasing concentrations and increasing weathering with time (distance) from the blowout site. Small-scale spatial heterogeneity, both quantitative and compositional, of the subsurface oil-rich plumes, observed especially at Station PIX 08, indicates that the chemical observations are influenced by weathering kinetics rather than equilibria. What seems to be quite apparent is that a significant part of the subsurface petroleum hydrocarbon distributions is decoupled from surface mousse. That is to say that significant amounts of oil injected into the water column from the sea bed blowout probably remain in the water column for significant periods of time, presumably depending on droplet size, buoyancy, and water-column hydrography. Laboratory studies (Shaw and Reidy, 1979) have shown that important compositional differences occur as particle size decreases; small particles (submicron) are enriched in the more toxic components of crude oils (i.e., light aromatics). Once at the surface, little exchange occurs via dissolution of hydrocarbons from the surface slick to the water column. This does not imply that major hydrographic forces such as wind-induced turbulence could not drive oil back onto the water column. However, the particulate hydrocarbons in the water column are consistently, significantly different from the overlying mousse/oil. Furthermore, whole water samples beneath the surface oil slick contain greater relative quantities of low-boiling aromatic hydrocarbons (e.g., alkyl benzenes, naphthalenes, fluorenes) than does the surface oil, implying 1) subsurface transport of "fresh" oil plumes or dissolved gaseous hydrocarbon, or 2) vertical mixing of surface oil down to 20 m with resultant fractionation (dissolution) of soluble components. These two hypotheses are pursued below.

4.3 Interrelationships between Mousse, Seawater, and Water-borne Particulates

The relative hydrocarbon compositions of the surface oil/mousse, whole water, and particulate oil can be evaluated graphically (Figure 30) by considering two key parameter ratios: the saturated hydrocarbon weathering ratio (SHWR) and the aromatic hydrocarbon weathering ratio (AWR), both previously defined in the Results section. One of the significant findings of this study was the determination that biodegradation was nearly inoperative in the open sea except in very specialized microenvironments (see below). Therefore, as the ratio of alkanes to isoprenoids (ALK/ISO) remains nearly constant at 3.5-4.5 for all samples, the SHWR and AWR, which are functions of evaporation and dissolution, appear to tell nearly the entire weathering "story" in the water column within 50 km of the blowout and over hundreds of kilometers at the sea surface. Photochemical weathering, which is important in the tropical climate of the IXTOC blowout, probably becomes the major process acting on the surface oil beyond 100 km or so from the wellhead. It is not known how photochemical changes in the oil's composition compete with evaporation/dissolution in changing these parameter ratios.

A plot of SHWR vs. AWR (Figure 30) illustrates interesting and consistent weathering relationships between the various sample types. Weathering presumably proceeds in a step-wise fashion (similar to distillation stages) down the weathering curves (Figure 31). The size of the steps is dictated by reaction kinetics. The SHWR/AWR curves represent pseudo-equilibria for the three sample types.

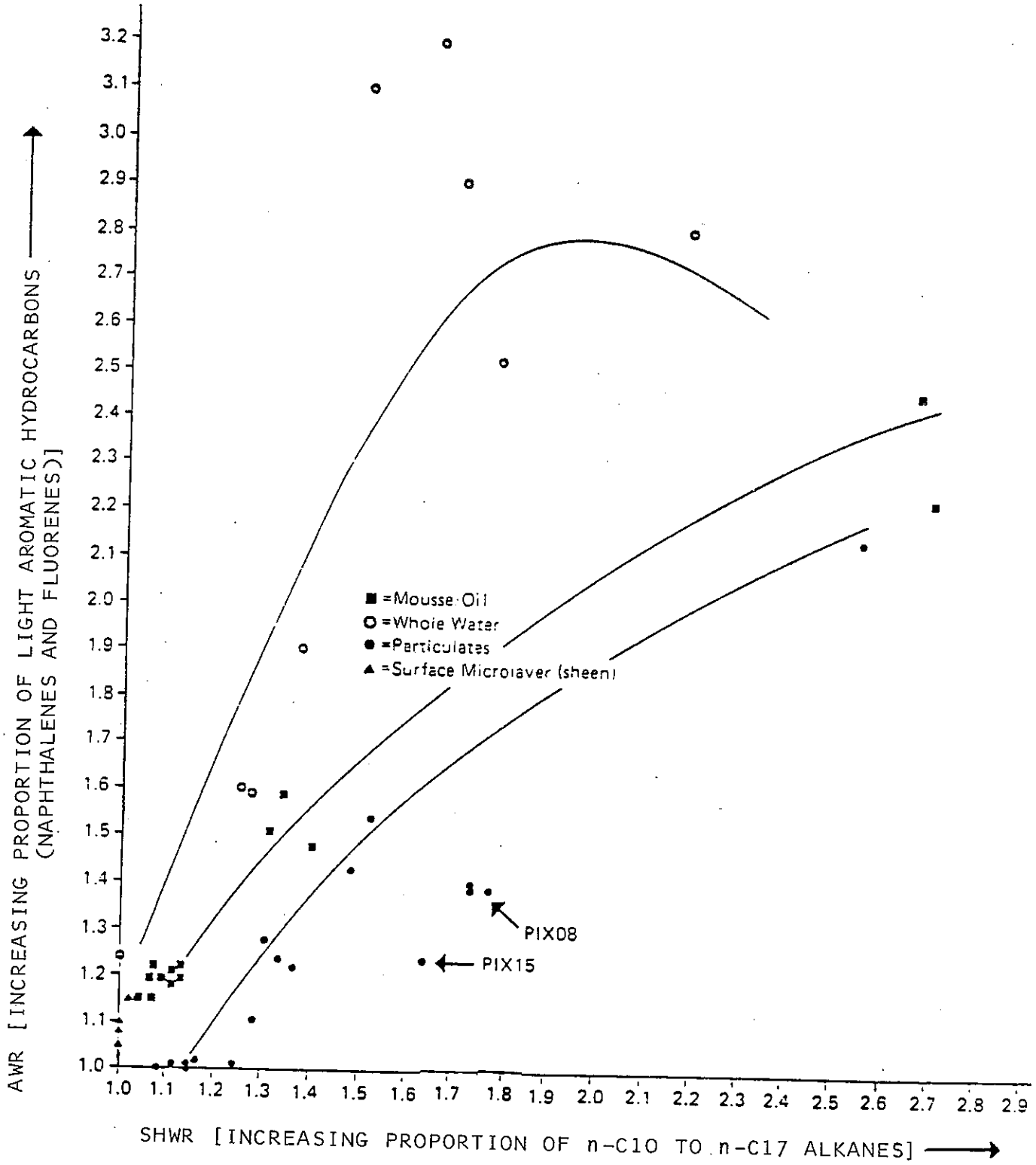

Figure 30. Weathering of various types as indicated by relative saturated and aromatic weathering parameters.

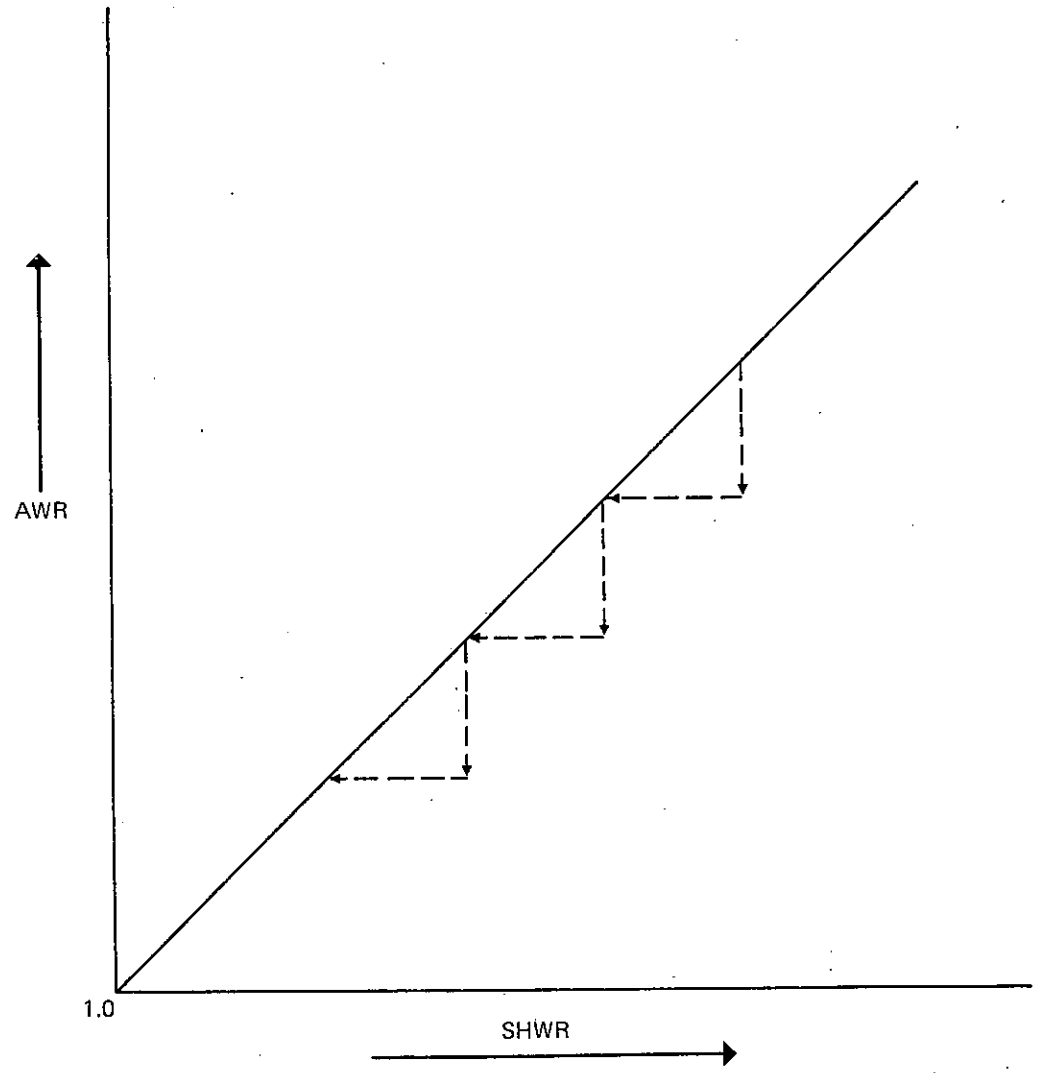

Figure 31. Ideal stepwise weathering behavior of each sample type.

According to the formulation of these ratios, weathering begins at a composition equivalent to oil introduced at the blowout site and continues in a direction approaching the origin (i.e., SHWR and AWR = 1.0). The highly weathered microlayer samples form the weathered "end-member." Although it is difficult to determine the age of the samples due to mixing of old oil with newly introduced oil in the study region, it is possible to consider each weathering curve as defining the weathering age of the oil. Fitting this data to established mathematical weathering models could then yield information on weathering rates.

On the SHWR vs. AWR plot, samples of each type are clustered in distinct groups and lie along weathering lines. Mousse samples form one weathering population of compositions intermediate to whole water and particulate samples. Dissolved samples are greatly enriched in light aromatics and depleted in aliphatics relative to all samples, and thus they lie off the vertical scale of Figure 30 (e.g., AWR = 6-8, SHWR = 1.3). Particulate samples are significantly depleted in light aromatics relative to mousse samples. A secondary population of particulate samples characterizes PIX 15 (2 and 6 m) and PIX 08 (16 m) samples due to rapid aromatic weathering, which perhaps is attributable to the different exposure history of these related samples. These particulate samples apparently are depleted in two-ring aromatics and "enriched" in n-C_{10} to n-C_{12} aliphatics (most notably n-C_{12}, n-C_{13}, and n-C_{14}) relative to the main population of particulates. Whole water at this station, on the other hand, is characterized by a large enrichment of light aromatic hydrocarbon concentrations, presumably related to a coexistence of dissolved (colloidal) oil plumes with macro-(> 1 μm) particles.

The processes that account for the whole waters' greater relative light aromatic hydrocarbon composition compared to source material most likely involve the stripping of petroleum aromatics (naphthalenes and fluorenes) upon initial ascent to the surface and continually along the path of movement. The stripped materials (along with neutrally buoyant oil particulates) are then advected away from the blowout site. Thus, we believe that a dissolved or colloidal enriched particulate plume of material is being transported laterally to PIX 08 or beyond and concurrently is being markedly diluted by seawater.

4.4 Subsurface Oil Plumes

Whole water, particulates, and mousse are most similar in composition near the wellhead (Table 6), where great turbulence keeps the water column well mixed and weathering processes have not had much effect. At more distant stations, whole waters consistently show aromatic enrichment relative to overlying mousse, presumably due to one or several processes. Significant quantities of oil may remain subsurface, where evaporative loss of aromatics is greatly decreased. This results in the "containment" of high levels of aromatics, which can be lowered by dilution and diffusion but weather as a separate population of oil. Alternatively, particles of surface mousse may be mixed down to 20 m, large particles may rise back to the surface, and smaller particles may remain at depth and coexist with aromatic material stripped from larger particulates prior to their ascent back to the surface.

Table 6. Relative compositions of oil mousse particulates and whole water.

	Mousse		Particulate		Whole Water	
Station	SHWR	AWR	SHWR	AWR	SHWR	AWR
PIX 05	2.13-2.69	1.19-2.23	--	--	1.65	3.16
PIX 10	2.66	2.46	2.54	2.14	2.17 1.28	2.80 6.66(F)
PIX 11	1.43	--	--	--	1.5-1.73	2.91
PIX 15	1.29	--	(2 m) 1.48-1.73 (6 m) 1.73-1.77 (20 m) 1.30-1.33	1.40-1.43 1.39-1.40 1.24-1.28	1.35	--
PIX 08	1.11	1.21	(6 m) 1.36-1.52 (16 m) 1.63 (19 m) 1.13-1.16	1.22-1.54 1.24 1.02	1.25 -- 1.78 1.27	1.60 8.84 (F) 2.52 1.59
PIX 14	1.36	1.52	(1 m) 1.14-1.24 (6 m) 1.08-1.11 (14 m) 1.14-1.28	1.01 1.00 1.00-1.11	1.45	--
PIX 07			--	--	1.04	--
RIX 13						
PIX 12	--	--	--	--	1.12-1.33	5.12

It is difficult to separate the two phenomena near the well, but the existence and ultimate separation of the subsurface oil mass from the surface mousse plume occurs at or before reaching PIX 08. The vertical profiles of subsurface hydrocarbons obtained by pumping water from depths less than 20 m suggest the existence of vertical quantitative and qualitative (compositional) discontinuities, which can be connected horizontally (laterally) between stations along the axis of advection (Figure 32).

On the "up current" side of the well, water at PIX 07 was relatively uncontaminated by IXTOC-I although small amounts (50-75 µg/L) of particulate oil were observed at 6 m while none was sampled at 20 m. GO-FLO bottle samplings at PIX 11, located 9 km from the wellhead and in the plume, indicated that petroleum hydrocarbons were more abundant at 6 m (400 µg/L) than at 20 m depth (120 µg/L), although compositionally both were identical, exhibiting "typical" whole water characteristics: enhanced naphthalenes (AWR = 3.0), an undegraded alkane distribution (ALK/ISO = 3.7), and an aliphatic distribution showing only slight weathering (evaporation) of light aliphatic components.

A decreasing concentration gradient with increasing depth was observed at PIX 15. The concentration of hydrocarbons observed in the particulate fraction at 2, 6, and 20 m ranged from 100-150 µg/L at 2, 60-100 µg/L at 6, and 30 µg/L at 20 m. The top 6 m appear uniform compositionally. However, the particulate aliphatic hydrocarbon distribution at 20 m reflects a small but significant amount of biodegradation (ALK/ISO $\simeq$ 2.5) and the depletion of naphthalene compounds (AWR = 1.2-1.3) relative to the 6-m samples (AWR = 1.7-1.8). Such a decreasing gradient may reflect differences between oil particulates within the main 2-15 m) subsurface oil mass and those at the bottom (underside) of these lenses.

The water column hydrocarbon profile at PIX 08 reveals a striking discontinuity at 10-15 m, at which depth a subsurface intrusion of aromatic-rich material and particulate (aromatic-depleted, saturated enriched) hydrocarbons, the sum total resembling fresh oil, is observed. The vertical profiles of whole water is strikingly offset at the 16-m sampling depth (Figure 32), implying a large intrusion of dissolved, or colloidal (microparticulate) oil at this level or great small-scale spatial heterogeneity within this subsurface layer. Macroparticulate concentrations (> 1 µm) show only a minor increase in concentration, perhaps due to sampling heterogeneities (i.e., patchiness).

Support for the existence of subsurface plumes comes from an evaluation of the vertical profiles shown in Figure 32. The whole water samples at Station PIX 11 ($\sim$ 12 km from the wellhead) contain what we consider to be relatively unweathered, "fresh" oil (SHWR = 1.7 and AWR = 2.9) and similar to PIX 05 and PIX 10 samples. No vertical compositional gradients are evident. The nature of the PIX 11 samples is very similar to the whole water sampled at 16 m at PIX 08 ($\sim$ 22 km from the wellhead) and quite unlike the petroleum in whole water samples taken at 6 and 19 m at this station, both of which contain a more weathered hydrocarbon "assemblage." No whole water samples were obtained from PIX 15 (between PIX 11 and PIX 08). However, the striking anomalous nature of the PIX 15 and PIX 08 (10 m) particulates, previously mentioned, apparently links the subsurface oil at these two stations. The above relationships, in addition to the higher apparent concentrations of

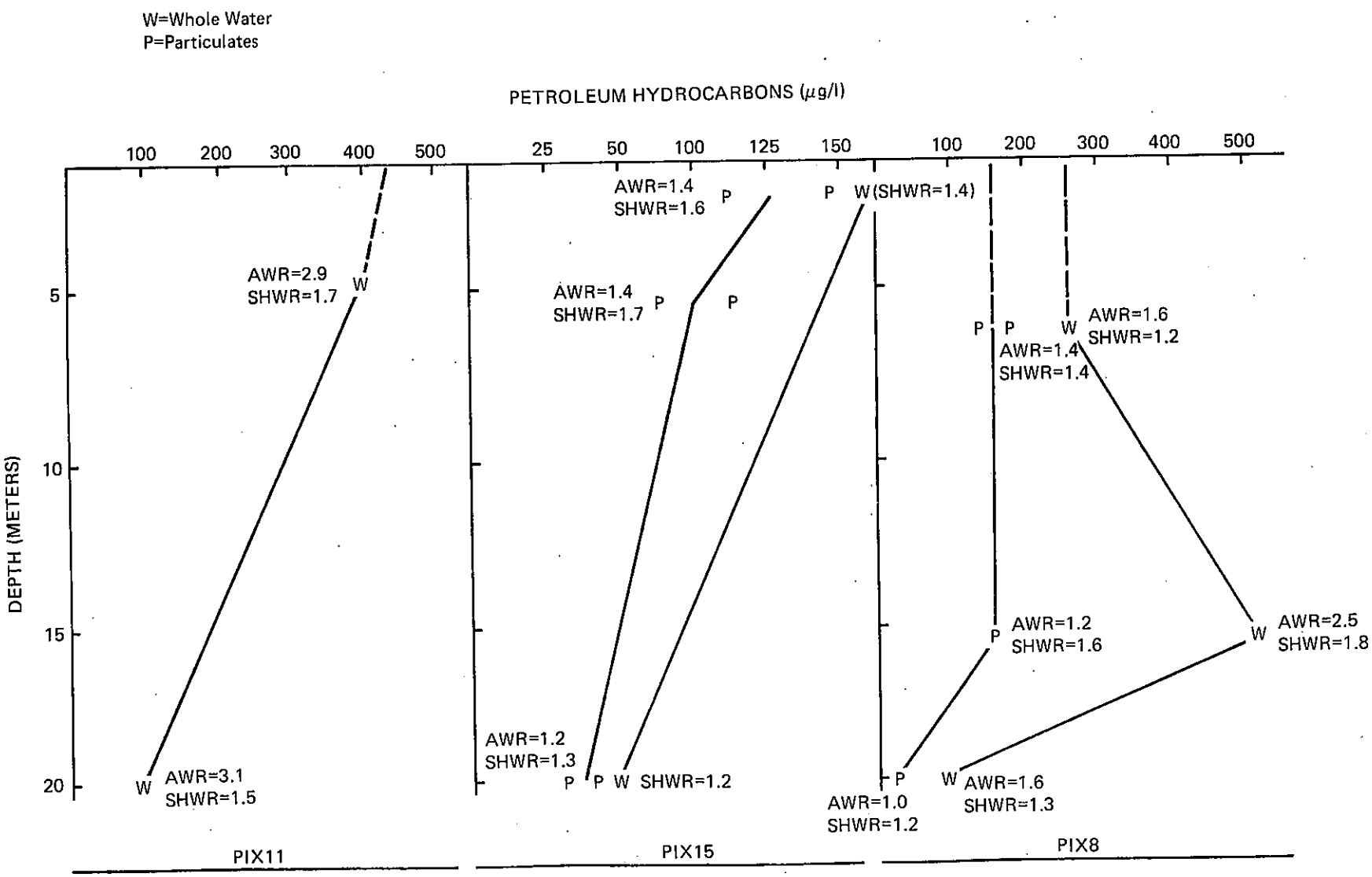

Figure 32. Vertical profiles of petroleum hydrocarbons in seawater.

particles/droplets at the PIX 08, 10-m level, as revealed by acoustical reflectance measurements (Figure 33; see Walter and Proni, this symposium), strongly suggest the existence of a laterally advected subsurface petroleum plume.

4.5 Horizontal Concentration Gradients: Solubility and Toxicity Considerations

Horizontal variations in hydrocarbon concentrations indicate, quite expectedly, that concentrations of oil in the water column generally decrease with increasing distance from the wellhead (Table 7). That most of the subsurface water-borne hydrocarbon movement was toward the northeast and east at the time of this research cruise is verified by the occurrence of only low levels of particulate hydrocarbons in the water column just to the west of the blowout location (PIX 07). Along the axis of movement of the surface oil plume, concentrations of total hydrocarbons and of the lower-boiling, more soluble and volatile components (e.g., naphthalene) decrease due to seawater dilution.

In general, the weathering processes resulted in decreasing SHWR and AWR values with increasing distance from the wellhead. The major exceptions occurred within the less weathered, petroleum-rich subsurface plume at PIX 08. The weathering of saturates caused a change in the SHWR from 2.5 to 1.0 over the length and time of transit of the oil from the wellhead to approximately PIX 14. The weathering of aromatic compounds in the particulates caused a change in the AWR from 2.2 to 1.0. These data potentially could be used to define weathering rates if subsurface current speeds were accurately known ($\simeq$ 0.5-1.0 knots).

Concentrations of some of the more toxic compounds - alkylated benzenes, naphthalene, and methyl naphthalene - appeared in the water column in sizeable concentrations, but did not appear to approach solubility levels at all stations investigated (Table 8). It is assumed that enough dilution was achieved so that actual levels of aromatic hydrocarbons with boiling points greater than that of trimethyl benzene were well below (three orders of magnitude) published solubility values for benzenes and naphthalenes (Eganhouse and Calder, 1976; McAuliffe, 1966; Sutton and Calder, 1975).

Water soluble aromatics may have sublethal effects on marine organisms at concentrations of 0.01-0.1 ppm, lethal toxicities at 0.1-1.0 ppm for larval stages, and acutely lethal consequences at 1-100 ppm (Moore and Dwyer, 1974). Individual hydrocarbons vary considerably in their solubility and toxicity (Anderson et al., 1974). Toxic levels of crude oils range from 4-100 ppm for crude oil emulsions and from several hundred micrograms per liter (ppb) to the ppm range (Tatem et al., 1978) for the water soluble fraction. Although the determination of sublethal effects and toxicities has received a tremendous amount of attention during the last decade, the details of this topic are beyond the scope of this work. Toxicity is a complex function of the developmental stage of an organism as well as of environmental parameters (e.g., temperature). The concentrations of individual hydrocarbons in the dissolved form (0.01-3 ppb) observed in this study appear to lie below the toxic range, even in the acute impact zone. However, the total concentrations of water-borne alkyl benzenes and naphthalene compounds in whole water fall in the 0.5-500 ppb range, and concentrations of total water-borne oil dispersions lie in

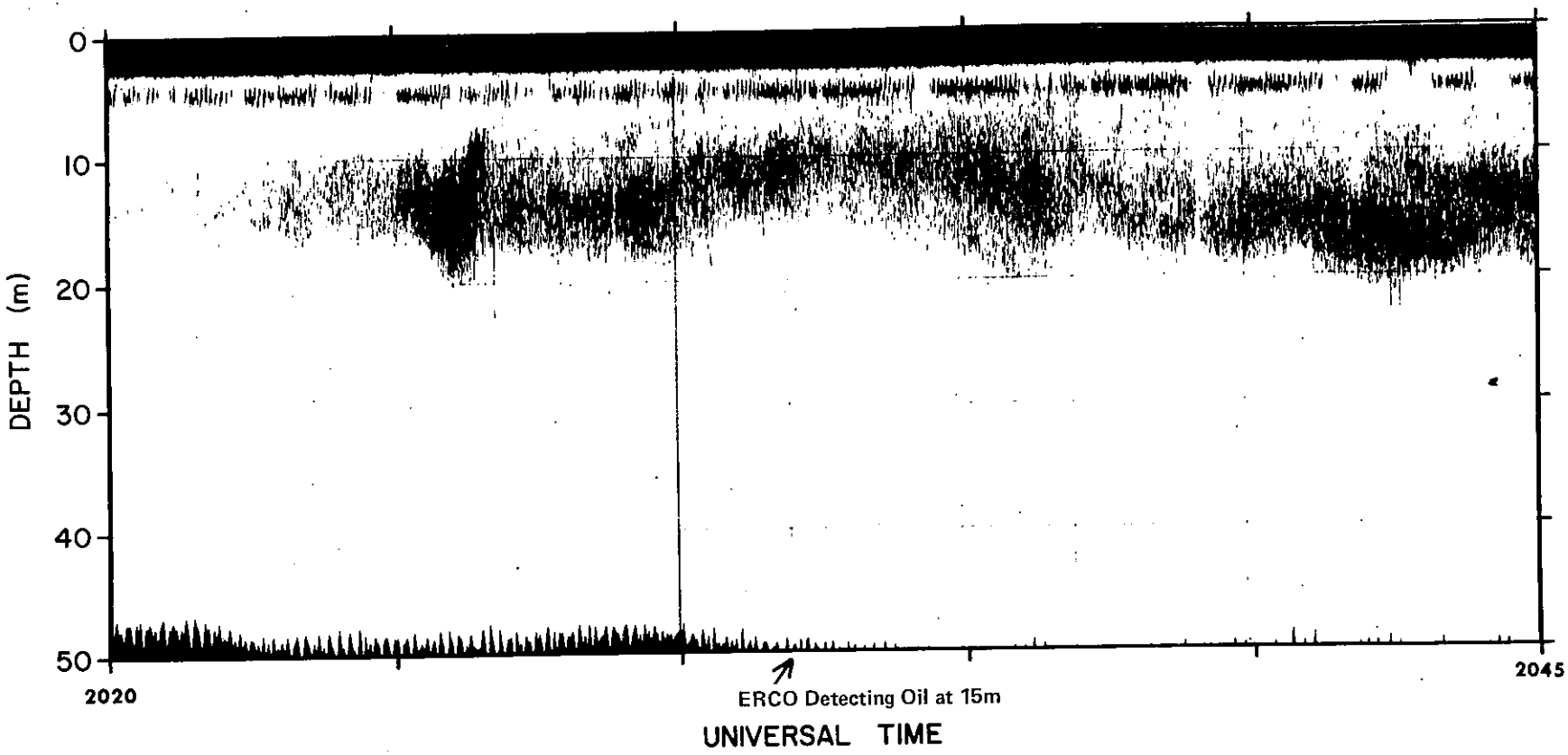

Figure 33. Acoustical reflectance data from PIX 8 (from Walter and Proni, 1980).

Table 7. Summary of hydrocarbon concentrations and compositional properties along a horizontal axis.

Station	Sampling Date	Approximate Distance from Well (km)	Total Hydrocarbon (µg/L)	ALK/ISO[1]	SHWR[1]	AWR[1]	Total Naphthalenes (ng/L)
PIX 07	9/18/79	3	nd-40(W)	3.0	1.04	--	nd
PIX 10	9/19/79	1	6500(P) 7000(W)	4.8 4.5	2.54 2.17	2.14 2.80	23,500 98,000
PIX 11	9/19/79	12	200-400(W)	3.6	1.6	3.0	3,000
PIX 15	9/21/79	21	15-175(W) 80-200(P)	3.5 3.6	1.35 1.3-1.8	-- 1.3-1.4	10 250
PIX 08	9/18/79	29	60-400(W) 50-150(P)	3.5-4.2 3.5-4.5	1.3-1.8 1.1-1.6	1.6-2.5 1.0-1.5	100-5000 100-850
PIX 14	9/20/79	45	10-20(P)	3.5-4.5	1.1-1.3	1.0-1.1	nd

[1]See text for explanation.

W = whole water.

P = particulates.

Table 8. Observed concentrations of hydrocarbons compared with their solubilities.

Compound	Approximate Solubility in Seawater at 25°C (mg/L)	Observed Concentration Range within 20 km Distance from Blowout (µg/L)
Trimethyl benzenes	30-40	.050 - 2.00 (W) 0 - 0.60 (D)
Tetramethyl benzenes	10-20	0 - 3.0 (W) 0 - 0.4 (D)
Naphthalene	30	0.02 - 3.0 (W) 0.06 - 0.8 (D)
Methyl naphthalene	25	0.05 -15.0 (W) 0.01 - 2.5 (D)
Dimethyl naphthalene	2	0.04 -38.0 (W) 0.01 - 2.6 (D)
Phenanthrene	1	0.02 - 1.6 (W) 0.01 - 0.4 (D)
Petroleum	----	100-10,000

D = dissolved (filterable)

W = whole water

the 100-10,000 ppb (0.1-10 ppm) range; both fall well within the range of observable effects on marine organisms.

4.6 Lack of Significant Microbial Degradation

A significant finding of this study was the lack of change in the composition of surface oil/mousse, microlayer oil, and subsurface oil attributable to microbial degradation. Only in specialized microenvironments (i.e., within windrows containing plant matter) did microorganisms appear to degrade oil particles, probably due to the availability of nutrients otherwise in very low quantities in the study region. The low level of nutrients in the water column (Berberian, personal communication) apparently accounted for the insignificance of microbial degradation as a major weathering factor in the water column. Degradation of oil appears to proceed in the sediments (Boehm and Fiest, this symposium), but at a slower rate than observed at the AMOCO CADIZ spill (Atlas et al., 1980).

4.7 Subsurface Oil Budget in Wellhead Region

Concentrations of petroleum in the top 20 m of the water column within ~25 km of the wellhead, beneath the surface oil mass, exceed maximum values observed at the EKOFISK-BRAVO (300 µg/L; Grahl-Nielsen, 1978) blowout, and the AMOCO CADIZ (350 µg/L, Calder et al., 1978) and ARGO MERCHANT (450 ppb; Grose and Mattson, 1977) tanker spills. The total amount of IXTOC-I petroleum hydrocarbons estimated to be in the top 20 m of water within 25 km of the well at the time of this sampling cruise equals 20,000 gallons = 70×10^6 grams, or approximately 1% of that observed on the surface as mousse. Therefore, we hypothesize that for this type of blowout one can assume that of the total volume of oil discharged, about 1% of the high molecular weight hydrocarbons spilled will be present in the water column for considerable distances from the wellhead. Of this material, about 90% will be particulate and about 10% dissolved and/or colloidal in nature.

5. CONCLUSIONS

The results of this study indicate that:

(1) large- and small-scale heterogeneities are characteristic of surface mousse and subsurface water hydrocarbon concentrations and compositions along the apparent axis of movement of spilled oil from the IXTOC-I blowout;

(2) whole water samples are markedly enriched in light aromatics relative to other aromatic components (phenanthrenes, dibenzothiophones), presumably due to the presence of considerable quantities of soluble solubilized, or colloidal material in the water column;

(3) particulate hydrocarbons, although comprising the bulk of the total hydrocarbon mass (95%) in subsurface oil, account for considerably less (80%) of the light aromatic, the rest being found in the sub-particulate or dissolved phase;

(4) surface mousse and subsurface water and particulate oil exhibit separately definable but interrelated weathering sequences involving stepwise changes in aromatic and saturate compositions;

(5) approximately 1% of the total oil spilled will be present in the subsurface (2-20 m) zone within a 25 km distance from the blowout source;

(6) significant vertical quantitative and compositional structure is present in these subsurface plumes;

(7) subsurface oil plumes may be transported laterally for considerable distances, becoming less concentrated due to dilution but relatively richer in naphthalenes and other low-boiling, toxic aromatic hydrocarbons due to dissolution, solubilization or accommodation of particulate oil in seawater;

(8) biodegradation of water-borne petroleum did not occur to any significant extent; thus physical/chemical weathering dominates, evaporation and dissolution occurring within 50 km of the wellhead, and thereafter photo-chemical changes presumably playing a major relative role in altering the oil's composition;

(9) a significant quantity of oil (perhaps ½ 50%) remains offshore as neutrally buoyant petroleum residues existing at the sea surface or at density discontinuities in the water column as small particles, according to our hypothesis.

6. ACKNOWLEDGEMENTS

The authors would like to thank Keith Hausknecht, Jack Barbash, and George Perry of ERCO for their invaluable help in collecting and processing samples aboard the RESEARCHER and the PIERCE under the most difficult of sampling conditions. The officers and crew of both research vessels and the scientific party aboard all deserve thanks and praise for a well-executed pioneering research effort.

We also acknowledge the valuable assistance of Dr. Ed Overton, Mr. Larry McCarthy, and associates at the University of New Orleans Center for Bio-Organic Studies, for performing extractions on large volume water samples and for acting as a reference/distribution library for mousse samples. Adria Elskus, John Yarko, Neil Mosesman, and Ann Jefferies assisted with phases of the analytical work.

Finally and perhaps most importantly, we thank the support and efforts of Dr. Donald Atwood and Dr. George Harvey of NOAA/AOML, Dr. John Farrington of Woods Hole Oceanographic Institution, and Ms. Judith Roales and Dr. Lou Butler of NOAA/Office of Marine Pollution Assessment (OMPA), on behalf of the entire IXTOC research team. Our research was supported by Contract No. NA80RAC00054 from NOAA/OMPA.

7. REFERENCES

Anderson, J. W., J. M. Neff, B. A. Cox, H. E. Tatum, and G. M. Hightower (1974): Characteristics of dispersions and water soluble extracts of crude and refined oils and their toxicity to estuarine crustaceans and fish. Mar. Biol., 27: 75-88.

Atlas, R. M., P. D. Boehm, and J. A. Calder (1980): Chemical and biological weathering of oil from the AMOCO CADIZ spillage within the littoral zone. Estuar. Coast. Mar. Sci. (submitted).

Boehm, P. D. (1980): The decoupling of dissolved, particulate, and surface microlayer hydrocarbons in northwestern Atlantic continental shelf waters. Mar. Chem. (in press).

Boehm, P. D., J. E. Barak, D. L. Fiest, and A. Elskus (1980): A chemical investigation of the transport and fate of petroleum hydrocarbons in littoral and benthic environments: the TSESIS oil spill. Mar. Environ. Res. (submitted).

Boehm, P. D., and D. L. Fiest (1978): Analyses of water samples from the TSESIS oil spill and laboratory experiments on the use of the Niskin Bacteriological Sterile Bag sampler. Final Report, Contract No.: 03-A01-8-4178, National Oceanic and Atmospheric Administration, Boulder, Co.

Boehm, P. D., J. Perry, and D. Fiest (1978): Hydrocarbon chemistry of the water column of Georges Bank and Nantucket Shoals, February-November 1977. In: The Wake of the ARGO MERCHANT: Proceedings of a Symposium Held January 11-13, 1978, Center for Ocean Management Studies, University of Rhode Island: 58-64.

Boehm, P. D., and J. G. Quinn (1975): The solubility behavior of No. 2 fuel oil in seawater. Mar. Poll. Bull., 5: 101-105.

Boehm, P. D., W. G. Steinhauer, D. L. Fiest, N. Mosesman, J. E. Barak, and G. H. Perry (1979): A chemical assessment of the present levels and sources of hydrocarbon pollutants in the Georges Bank region. In: Proceedings, 1979 Oil Spill Conference, American Petroleum Institute, Washington, D.C.: 333-344.

Brooks, J. M., B. B. Bernard, T. C. Sauer, Jr., and H. Abdel-Reheim (1978): Environmental aspects of a well blowout in the Gulf of Mexico. Environ. Sci. Technol., 12: 695-702.

Butler, J. N., B. F. Morris, and J. Sass (1973): Pelagic tar from Bermuda and the Sargasso Sea. Special Publication No. 10, Bermuda Biological Station for Research.

Calder, J., J. Lake, and J. Laseter (1978): Chemical composition of selected environmental and petroleum samples from the AMOCO CADIZ spill. In: The AMOCO CADIZ oil spill - a preliminary scientific report, W. Hess (Ed)., NOAA/EPA special report, NOAA, Boulder Co: 21-84.

Clark, R. C., and M. Blumer (1967): Distribution of paraffins in marine organisms and sediments. Limnol. Oceanogr., 12: 79-87.

Eganhouse, R. P., and J. A. Calder (1976): The solubility of medium-molecular-weight aromatic hydrocarbons and the effects of hydrocarbon cosolutes, and salinity. Geochim. Cosmochim. Acta, 40: 555-561.

Farrington, J. W., and P. A. Meyers (1975): Hydrocarbons in the marine environment. In: Environmental Chemistry, Vol. 1, G. Eglinton, (Ed.), The Chemical Society, United Kingdom: 109-136.

Gagosian, R. B., J. P. Dean, Jr., R. Hambun, and O. C. Zafiriou (1979): A versatile interchangeable chamber seawater sampler. Limnol. Oceanogr., 24: 583-588.

Garrett, W. D. (1965): Collection of slick-forming materials from the sea surface. Limnol. Oceanogr., 10: 602-605.

Gordon, D. C., Jr., and P. D. Keizer (1974): Hydrocarbons in seawater along the Halifax-Bermuda section: lessons learned regarding sampling and some results. In: Marine Pollution Monitoring (Petroleum). NBS Special Publication No. 409, National Bureau of Standards, Washington, D.C.: 113-116.

Grahl-Nielsen, O. (1978): The Ekofisk Bravo blowout: petroleum hydrocarbons in the sea. In: Proceedings of the Conference on Assessment of Ecological Impacts of oil spills, 14-17 June 1978, Keystone, Colorado, American Institute of Biological Sciences, Washington, D.C.: 476-487.

Grose, P. L., and J. S. Mattson, Eds. (1977): The ARGO MERCHANT oil spill - a preliminary scientific report. U.S. Department of Commerce, NOAA/ERL, Boulder, Co.

Jeffrey, L. M., W. E. Pequegnat, E. A. Kennedy, A. Vos, and B. M. James (1974): Pelagic tar in the Gulf of Mexico. In: National Bureau of Standards, Special Publication No. 409, Washington, D.C.: 233-236.

Kolpack, R. L., and N. B. Plutchak (1976): Elements of mass balance relationships for oil released in the marine environment. Proceedings of Symposium on Sources, Effects and Sinks of Hydrocarbons in the Aquatic Environment, 9-11 August, Keystone, Co., American Institute for Biological Sciences, Washington, D.C.

Larson, R. A., T. L. Bott, L. L. Hunt, and K. Rogenmuser (1979): Photo-oxidation products of a fuel oil and their anti-microbial activity. Environ. Sci. Technol., Vol. 13, No. 8: 965-969.

Leinonen, P. J., and D. Mackay (1977): Mathematical model of the behavior of oil spills on water with natural and chemical dispersion. Prepared for Fisheries and Environment Canada and published as Economic and Technical Review Report No. EPS-3-EC-77-19.

Mackay, D., I. Buist, R. Mascarenhas, and S. Paterson (1979): Oil spill processes and models. Report to Environmental Protection Service (Arctic Marine Oil Spill program) D-SS contract No. 0655-KE304-8-0680.

MacKay, D., and S. Paterson, Eds. (1978): Oil spill modeling. Proceedings, workshop held in Toronto, Canada, 7-8 November 1978, Publication EE-12, Institute for Environmental Studies, University of Toronto, Toronto, Canada.

Mattson, J. S., and P. L. Grose (1979): Modeling algorithms for the weathering of oil in the marine environment. Final Report, Research Unit No. 499, Outer Continental Shelf Environmental Assessment Program, NOAA, Boulder, Co.

McAuliffe, C. (1966): Solubility in water of paraffin, cycloparaffin, olefin, acetylene, cycloolefin, and aromatic hydrocarbons. J. Phys. Chem., 70: 1267-1275.

McAuliffe, C. D., G. P. Canevari, T. D. Searl, and J. C. Johnson (1980): The dispersion and weathering of chemically treated crude oils on the sea surface. In: Proceedings, International Conference and Exhibition: Petroleum and the Marine Environment, 27-30 May 1980, Monaco.

Moore, S. F., and R. L. Dwyer (1974): Effects of oil on marine organisms: A critical assessment of published data. Water Resources, 8: 819-827.

Patton, J. S., M. W. Riger, P. D. Boehm, and D. L. Fiest (1980): The IXTOC-I oil spill: flaking of surface mousse in the Gulf of Mexico. Science (submitted).

Payne, J. R., J. R. Clayton, Jr., B. W. de Lappe, P. L. Millikin, J. S. Parkin, R. K. Okazaki, E. F. Letierman, and R. W. Risebrough (1977): Hydrocarbons in the water column. Southern California Baseline Study, Vol. III, Report 3.2.3 to the Bureau of Land Management, Washington, D.C.: 207 pp.

Shaw, D. G, and S. K. Reidy (1979): Chemical and size fractionalization of aqueous petroleum dispersions. Environ. Sci. Technol., 13: 1259-1263.

Smith, J. E., Ed. (1968): Torrey Canyon Pollution and Marine Life. A report by the Plymouth Laboratory of the Marine Biological Association of the United Kingdom. Cambridge University Press, Cambridge, United Kingdom: 194 pp.

Sutton, C., and J. A. Calder (1974): Solubility of higher-molecular-weight n-paraffins in distilled water and seawater. Environ. Sci. Technol., 8: 654-657.

Sutton, C., and J. A. Calder (1975): Solubility of alkyl-benzenes in distilled water and seawater at 25°C. J. Chem. Engr. Data, 20: 320-322.

Tatem, H. E., B. A. Cox, and J. W. Anderson (1978): The toxicity of oils and petroleum hydrocarbons to estuarine crustaceans. Estuar. Coast. Mar. Sci., 6: 365-373.

Zsolnay, A. (1978): Caution in the use of Niskin bottles for hydrocarbon samples. Mar. Poll. Bull., 9: 23-24.

Zurcher, F., and M. Thuer (1978): Rapid weathering processes of fuel oil in natural waters: analyses and interpretations. Environ. Sci. Technol., 12: 838-843.

PHOTO-CHEMICAL OXIDATION OF IXTOC-I OIL

Edward B. Overton, John L. Laseter, Wayne Mascarella,
Christine Raschke, and Ileana Nuiry
Center for Bio-Organic Studies
University of New Orleans
New Orleans, Louisiana 70122

John W. Farrington
Woods Hole Oceanographic Institution
Woods Hole, Massachusetts 02543

1. INTRODUCTION

The weathering of petroleum and petroleum products in the marine environment has been intensively investigated. Some of the recognized processes of weathering are evaporation, dissolution, emulsification, microbial degradation, uptake and discharge by marine organisms, and chemical and photochemical decomposition. The first apparent compositional changes in petroleum on sea surfaces are due to evaporation and dissolution, the rates of which are dependent on temperature, wind velocities, and the chemical composition of the spilled oil. With time after a spill, the other weathering processes play an increasingly important role in the environmental degradation of the oil.

Degradation induced by sunlight may involve various interrelated processes, such as:

1. Photooxidation of aliphatic and aromatic compounds by oxygen and sunlight interaction.

2. Photodecomposition--a process of fragmentation of organic molecules by light.

3. Polymerization--formation of long-chain, high-molecular-weight, hydrocarbon-type materials by the action of light.

The action of these processes on petroleum is collectively not well understood, although it is apparent that they are interrelated. Among all of the different photochemical processes studied, only photooxidation has received much attention. Preliminary reports concerning the chemical changes of petroleum during the weathering process began to appear during the late 1960's. Armstrong et al. (1966) suggested that ultraviolet radiation was responsible for the oxidation of organic matter at the surface of the sea. An overall review of seawater photochemistry was presented by Zafiriou (1977). Berridge et al. (1968) speculated that the oxidation of petroleum would lead to the formation of oxygenated products such as carboxylic acids, alcohols, peroxides, sulfoxides, and related molecular species. Using infrared techniques, Kawahara (1969) demonstrated that sunlight indeed had a chemical effect on petroleum.

Definite laboratory evidence of the photooxidation of petroleum hydrocarbons was obtained by Freegrade et al. (1971), using mercury lamps with various selected wavelengths shorter than 600 nm. The products, determined by relatively non-specific chemical analytical methods, appeared to be organic acids and esters. Most important, however, was the observation that the destruction of oil slicks was related to quantum efficiency and intensity at different wavelengths (the intensity and amount of light absorbed).

One of the more important observations necessary for the understanding of the reaction mechanism of photochemical weathering of petroleum was made by Pilpel (1973). They reported that photosensitizers, such as 1-naphthol and other naphthalene derivatives, play an important role in the photodecomposition

of oils by accelerating the process. The use of 1-naphthol as a photosensitizer during the photooxidation of n-alkanes and alkylbenzenes floating on water generated various oxygenated products, such as alcohols, peroxides, and hydroperoxides. These oxidative reactions may lead to the formation of oxygenated products during such photochemical reactions. The influence of photosensitizers on the photooxidation of petroleum also indicates that the reactions may depend on the formation of a "reactive oxygen" (singlet oxygen) from molecular oxygen. Moreover, these investigations established the fact that the photooxidation of oils plays an important role in the formation of polymeric products (tar) and that the high viscosity of oil restricts the diffusion of oxidation products across the oil-water interface.

Burwood and Speers (1974) reported that light and atmospheric oxygen were clearly required for the formation of sulfoxides and phenols from crude oils. They proposed the formation of such oxidized products by a photo-initiated radical mechanism involving hydroperoxides. Some reactions involving second-order kinetics were predicted for the photochemical weathering of oil by Majewski and O'Brien (1974).

Studies in our laboratory (Patel et al., 1978) have verified that oxygenated products can be generated from aromatic molecules, such as phenanthrene, under simulated environmental conditions; further, these reactions require the participation of singlet oxygen. The mechanism for singlet oxygen formation is shown in Table 1. The conversion of ground-state oxygen ($^3O_2$) to its excited singlet state (S) ($^1O_2$) may be achieved by a process known as sensitization, and sensitizers such as certain porphyrins and polycyclic aromatic hydrocarbons (e.g., perylene) are particularly useful. While two sensitization mechanisms have been suggested, they have the same first two steps: excitation of the sensitizer (S) to its singlet state (designated S*) by absorption of a photon of light (h, usually in the visible region) and subsequent intersystem crossing to the triplet state of the sensitizer (steps a and b).

The next step (step c) involves the formation of excited singlet oxygen by transfer of energy from the excited sensitizer to the ground-state triplet oxygen. In this process the sensitizer returns to the ground state and is available for excitation and a repeat performance.

Table 2 illustrates the photooxidation products that our laboratory has recently reported for phenanthrene. As can be seen, there is a wide variety of products, including 9,10-epoxy-9,10-dihydrophenanthrene, as well as thirteen related molecules. It is interesting to note that the 9,10-epoxide and several others are primary metabolites of phenanthrene. Such photodecomposition pathways may serve as models for the higher-molecular polycyclic aromatic hydrocarbons found in petroleum. More recently we reported the presence of a series of alkyl-substituted dibenzothiophene-5-oxides and trace levels of corresponding sulfone in mousse samples collected along the coast of France following the AMOCO CADIZ oil spill (Overton, 1979). Laboratory experiments (Patel et al., 1979) carried out using Arabian medium crude oil similar to the AMOCO CADIZ spilled oil indicated that the formation of oxidized dibenzothiophenes could occur under simulated environmental conditions through a photocatalyzed process. It can be seen from the few examples that sunlight does not necessarily

Table 1. Mechanism for singlet oxygen formation.

Mechanism		State
STEP (a)	Absorption of light	$h + s \text{ ---- } {}^1S^*$
STEP (b)	Intersystem crossing	${}^1S^* \text{---} {}^3S^*$
STEP (c)	Energy transfer from triplet excited ground state (triplet) oxygen	${}^3S^* + {}^3O_2 \text{ ---}$ $S^* + {}^1O_2^*$ $({}^2 \text{ or } {}^1)$

Table 2. Photooxidation products from phenanthrene after 9 hours of irridiation.

NO.	NAME OF PRODUCT	FORMULA	MOL. WT.
1	Fluorene	$C_{13}H_{10}$	166
2	Fluorenone	$C_{13}H_8O$	180
3	Dibenz[b,d]oxepin	$C_{14}H_{10}O$	194
4	2,2'-diformylbiphenyl	$C_{14}H_{10}O_2$	210
*5	2'-formylbiphenyl-2-carboxylic acid	$C_{14}H_{10}O_3$	226
7	3,4-benzocoumarin	C H O	196
*8	diphenic acid	$C^{13}H^8\ O^2$	242
*9	9-phenanthrol	$C^{14}H^{10}O^4$	194
10	9,10-phenanthrenequinone	$C^{14}H^{10}O$	208
*11	diphenic acid anhydride	$C^{14}H^8O^2$	224

*These compounds were observed as their corresponding methylated derivatives.

cause the degradation of petroleum hydrocarbons into simpler molecules; on the contrary, it initially transforms them into material of greater complexity.

Not only is sunlight important as a mechanism in the removal of spilled petroleum hydrocarbons from the environment, but recent evidence shows that the resulting products have biological activity. For example, toxic effects of Number 2 fuel oil on various marine organisms (e.g., grass shrimp, sheephead minnow, channel catfish, and bluegill) were found to increase upon exposure to ultraviolet (UV) light (Scheier and Gominger, 1976). The phytotoxicity of Kuwait crude oil on marine plankton communities has been found to increase following illumination (Larson et al., 1976). Of course, whether or not such processes have any significant impact under actual spill conditions remains to be demonstrated.

This paper describes the results of the analysis of the following samples: products from the simulated laboratory photooxidation of IXTOC oil; the polar hydrocarbons produced in the microcosm experiments (Buckley and Pfaender, this report); and the polar compounds found in an environmental sample collected at PIX10. The data presented herein represent initial interpretations of extremely complex gas chromatographic mass spectrometric information. Much additional work and further laboratory experimentation will be needed to fully elucidate the complex chemical processes that degrade petroleum in the marine environment. These data are presented as a portion of the investigation of the IXTOC-I oil spill. Their significance will be fully understood only after synthesis with the results of other investigators who are studying this incident, as well as future research.

2. EXPERIMENT

In order to investigate the effect of photooxidation on the IXTOC-I crude, several environmental simulation experiments were performed. These experiments consisted of exposing petroleum samples to sunlight, air, and synthetic seawater. The seawater was subsequently examined for trace photochemical products using gas chromatography/mass spectrometry. The oil used in the experiments was obtained by extracting the petroleum from oil/water mixtures collected in the immediate vicinity of IXTOC-I (station PIX05). Because this recovered oil was only briefly in contact with the environment, it was considered to be representative of the wellhead oil and was the closest to an actual wellhead sample that was available. Seawater for use in the simulation was prepared from a commercially available mix (Rila Marine Mix, Rila Products, Teaneck, N.J.) and high-purity, reagent-grade water. This synthetic seawater was free of contamination by the organic compounds of interest. Many uncertainties that could have arisen from the use of natural seawater were thus eliminated. Reaction vessels were constructed of glass crystallizing dishes 150 mm in diameter and 75 mm deep (Pyrex #3140) covered with 150 mm x 150 mm x 3.5 mm fused quartz glass plates. These quartz lids are transparent in the actinic blue to near-UV wavelengths of sunlight. The lids were held approximately 5 mm above the upper edge of each dish by small glass spacers to allow the free passage of air.

The petroleum samples were exposed to simulated environmental conditions in the following manner. Five hundred ml of synthetic seawater were placed in the dish. A solution of one gram of petroleum in 100 ml of heptane was then added. The heptane would later evaporate, leaving a thin film of petroleum evenly dispersed on the surface of the synthetic seawater. The dish was covered with the quartz lid. A control dish was prepared by wrapping an identical dish of oil on seawater with aluminum foil. The exposure dish and its companion control dish were then carried to the roof of the laboratory for exposure to sunlight and air. While on the roof a degree of temperature control was provided by placing the dishes in shallow steel trays containing water to a depth of three cm. Typically, after a four-day rooftop exposure to direct sunlight and air the dishes were removed and their contents processed for analysis.

The analytical schemes used to process these samples, shown in Figures 1, 2, and 3, consisted of extraction, fractionation and derivatization. The samples were first separated into aqueous and oily fractions by dissolving any residual petroleum or tarry polymeric material floating on the seawater in approximately 50 ml of a 1:1 solution of toluene-dichloromethane, and then separating the two liquid phases in a separatory funnel. The synthetic seawater was extracted with two 30-ml portions of dichloromethane. This extract contained neutral organic compounds introduced into the seawater from the petroleum. The pH of the seawater was lowered to 3 by the addition of a sufficient volume of one-molar hydrochloric acid solution. The seawater was then extracted with two more 30-ml portions of dichloromethane. This extract contained acidic organic compounds (carboxylic acids, phenols, etc.) found in the seawater. The pH of the seawater was then raised to 11 by the addition of one-molar sodium hydroxide solution. The seawater was finally extracted with two 30-ml portions of dichloromethane. This final extract contained any basic organic compounds found in the seawater. Each of the fractions was dried with anhydrous sodium sulfate and concentrated to a convenient volume in a rotary evaporator. The acidic extract was derivatized with diazomethane to facilitate GC/MS analysis (Overton et al., this report). Each experiment yielded ten fractions for analysis: the "tar," acidic, derivatized acidic, basic, and neutral fractions from each pair of experimental and control dishes.

Extraction and analytical schemes applied to samples collected on the cruises and from the microcosm experiments are given in detail by Overton et al. (this report).

3. RESULTS

3.1 Simulated Environmental Photooxidation

Photographs of the experiment are shown in Figures 4, 5, 6, and 7. Figures 4 and 5 show the exposed IXTOC oil over artificial seawater at the start of the experiment and after one day of exposure to bright sunlight. Figure 6 compares the exposed and control experiment after four consecutive days of exposure. Notice that the control shows no visual evidence of change, while

PHOTOCHEMISTRY EXTRACTION SCHEME

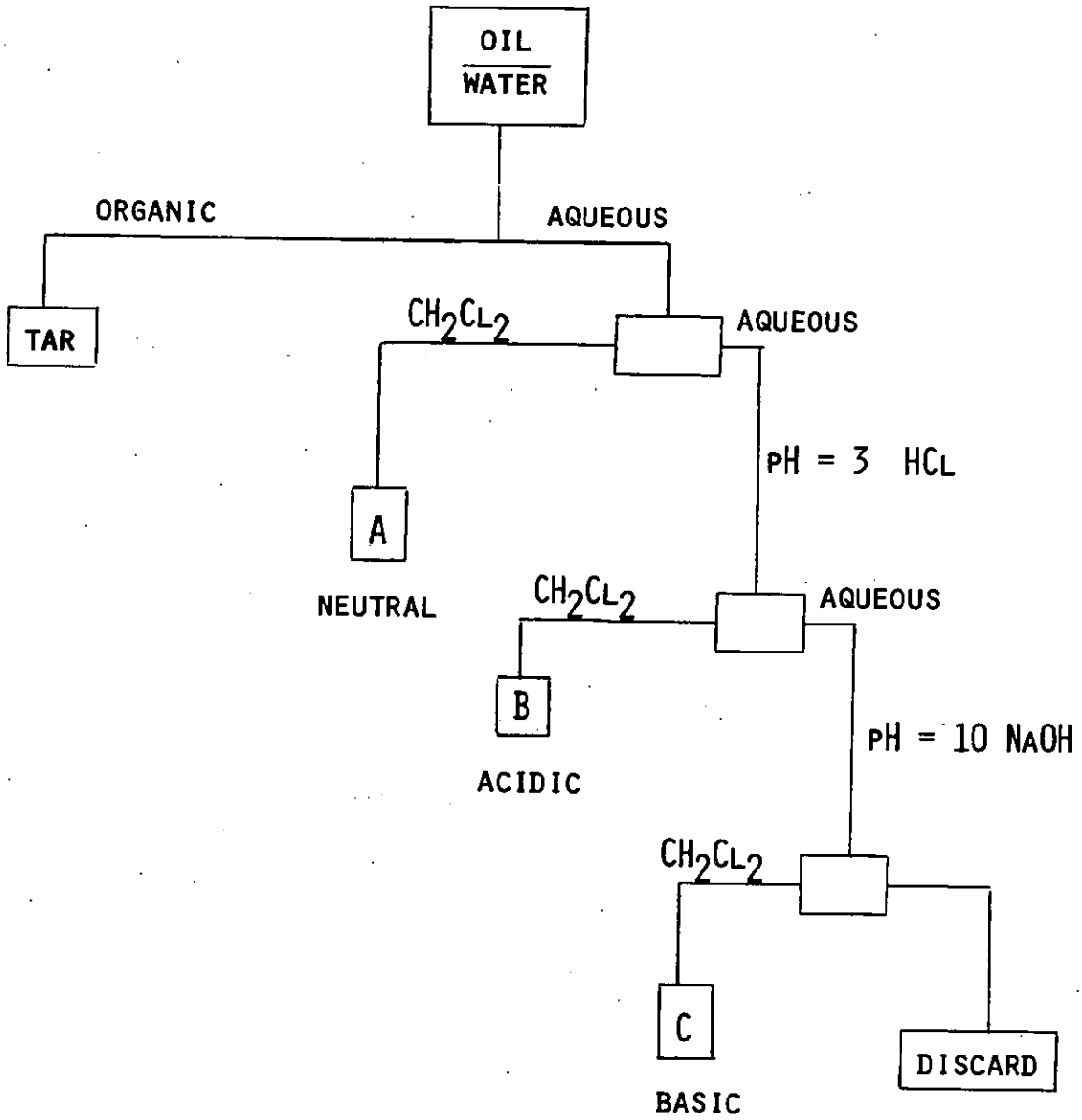

Figure 1. Diagram of the extraction scheme used for analysis of samples from the simulated laboratory photooxidation of IXTOC-I crude oil.

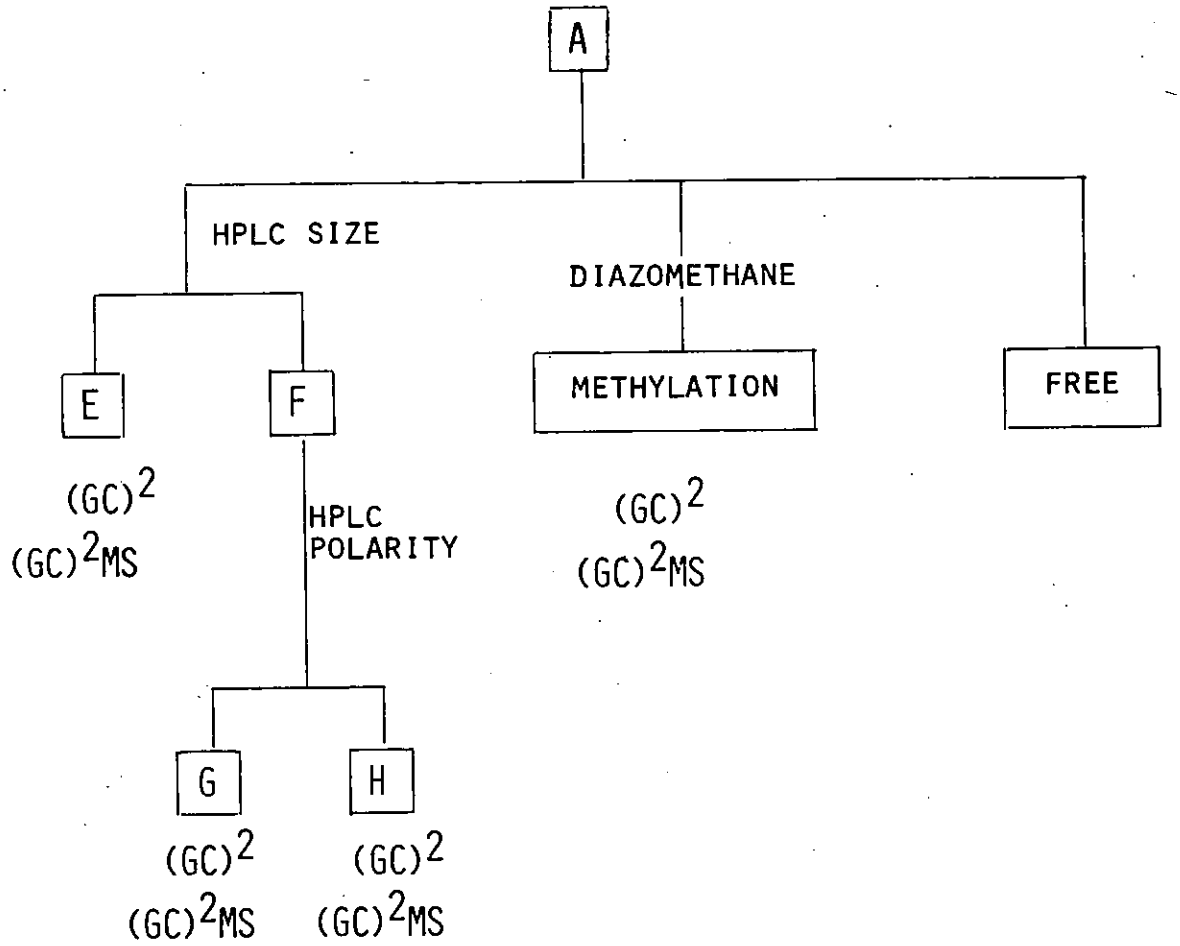

Figure 2. Schematic diagram of the analytical procedures used to analyze the neutral fraction from the simulated laboratory photooxidation of IXTOC crude oil.

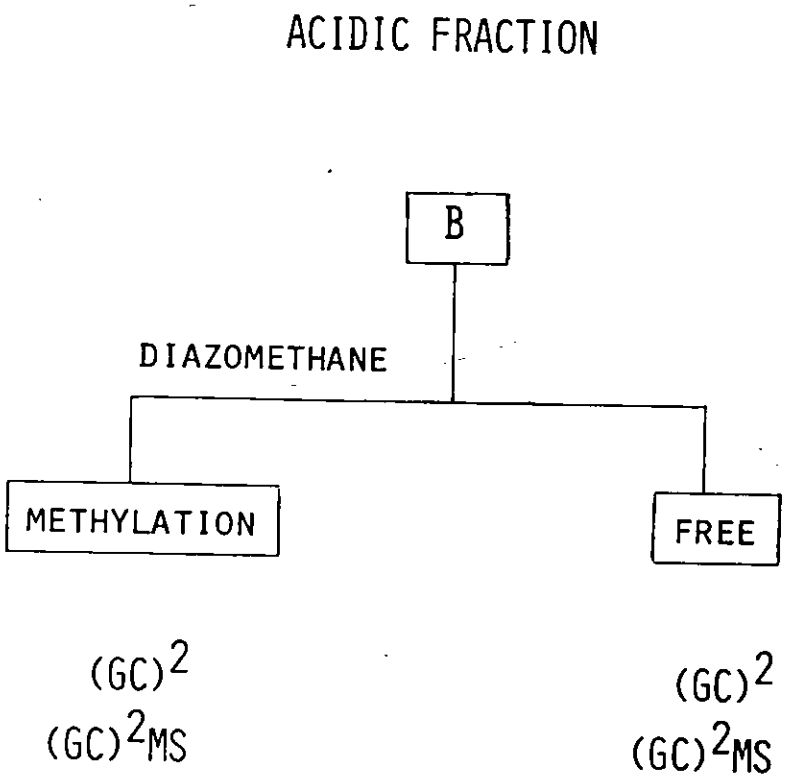

Figure 3. Schematic diagram of the analytical procedures used to analyze the neutral fraction from the simulated laboratory photooxidation of IXTOC crude oil.

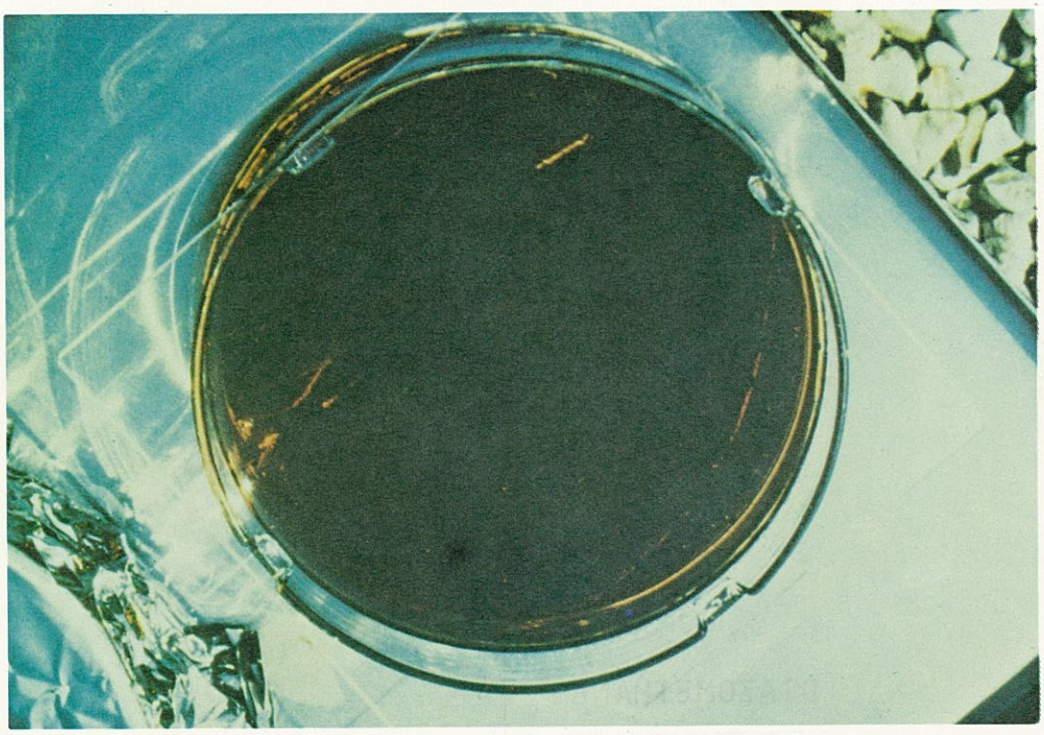

Figure 4. Photograph of the simulated environmental photolysis of IXTOC oil floating on artificial seawater before being exposed to bright sunlight.

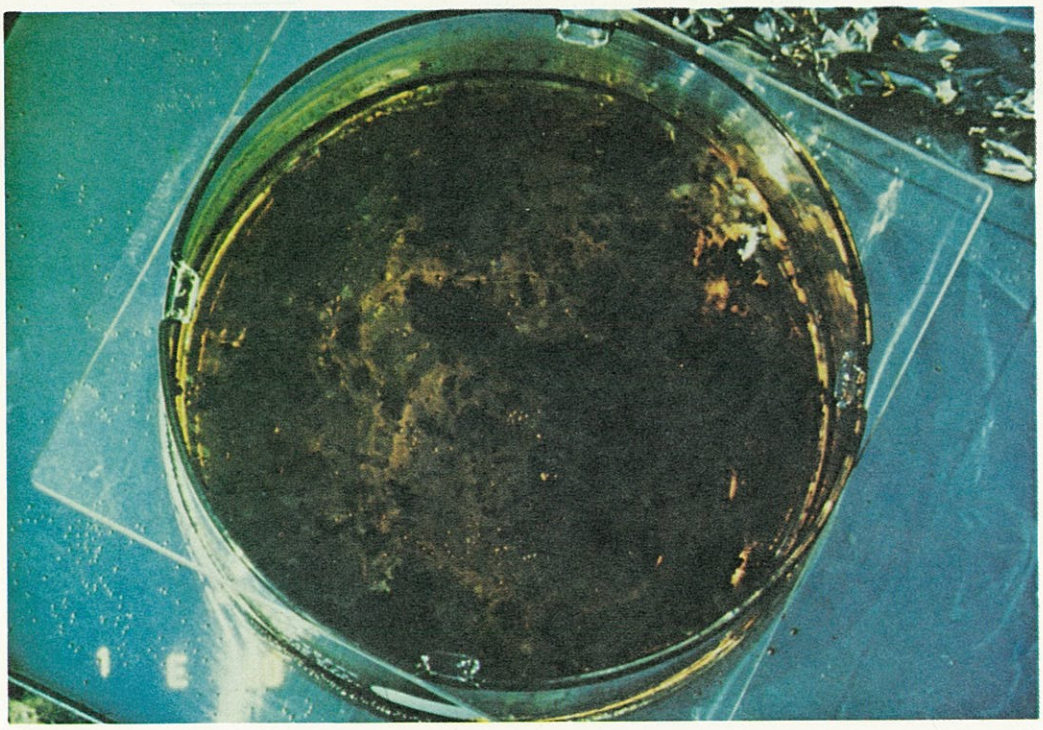

Figure 5. Photograph of the simulated environmental photolysis of IXTOC oil floating on artificial seawater after one day of exposure to bright sunlight.

Figure 6. Photograph of the exposed and control (dark) simulated environmental photolysis of IXTOC oil on artificial seawater after four consecutive days of exposure to bright sunlight.

Figure 7. Photograph of the crust that formed from IXTOC oil after four days of exposure to bright sunlight.

the exposed oil has been completely degraded into residual tarry material and flakes. Figure 7 is a closeup photograph of the light brown crust that formed after exposure to bright sunlight for four days. A crust similar in color was reported on oil-and-water emulsions seen floating in the Gulf of Mexico.

Figures 8, 9, and 10 show glass-capillary gas chromatographic (GC^2) data for the HPLC-fractionated neutral extracts (A) of the control and exposed IXTOC oil. Figure 8 compares the HPLC saturate fractions of the exposed and control neutral extracts. The control data resemble that for fresh oil and contains normal hydrocarbons from n-C_{11} to n-C_{32}. The data for the exposed sample, however, contain no hydrocarbons below n-C_{15}. The distribution of saturated hydrocarbons is distinctly different from that which would be expected from evaporative weathering. Notable is the absence of hydrocarbons below n-C_{15} and the relatively large quantity of n-C_{15}. Figure 9 shows chromatographic data from the control and exposed HPLC aromatic nonpolar fractions. The control sample contains quantities of the lower-molecular-weight aromatic compounds such as the naphthalenes. The exposed sample did not contain appreciable quantities of the lower-molecular-weight aromatics, but the aklylated phenanthrenes and dibenzothiophenes were present in relatively higher concentrations. The quantities of all aromatic hydrocarbons were much lower in the exposed water column sample than in the control extract. Figure 10 shows chromatographic data for the HPLC polar aromatic fraction. The exposed fraction contains substantially more compounds than the control fraction. An unresolved mixture was also evident in the exposed fraction.

Chromatographic data from the unfractionated acid extraction of both the control and the exposed water column samples are given in Figure 11. Qualitatively, the control extract appears very similar to the neutral extract; however, it contains substantially smaller quantities of hydrocarbons. The exposed extract is considerably altered when compared to the control. The chromatographic data indicate small quantities of hydrocarbons in the extract and large quantities of polar compounds. This extract was methylated with the gas phase diazomethane procedure described by Overton et al. (this report). The chromatographic data of the methylated, exposed extract are given in the bottom chromatogram in Figure 11. The most notable change in the chromatographic data between the methylated and unmethylated extracts is in the sharp, more symmetrical peak shapes in the methylated sample. This indicates that polar compounds have been derivatized to substances more amenable to gas chromatographic analysis.

The methylated acid extract was analyzed by glass-capillary gas chromatography-mass spectrometry and found to contain numerous oxygenated hydrocarbons derived from the IXTOC oil. Figure 12 shows the reconstructed ion chromatogram (RIC) and several of the structured oxidized hydrocarbons found in a 10-minute portion (15 to 25 minutes) of the glass-capillary gas chromatographic-mass spectrometric (GC^2MS) run. Most notable are the large quantities of the n-C_9, n-C_{10} and n-C_{11} fatty acid methyl esters (FAME's). Also present were a number of branched chain FAME's. Since singlet oxygen does not generally oxidize saturated hydrocarbons directly, other mechanisms must be used to explain the presence of the FAME's. One possible explanation involved the action of oxidized aromatic intermediates, such as hydroperoxides, to form fatty acids from the saturate hydrocarbons. Also, ground-state oxidation could form these

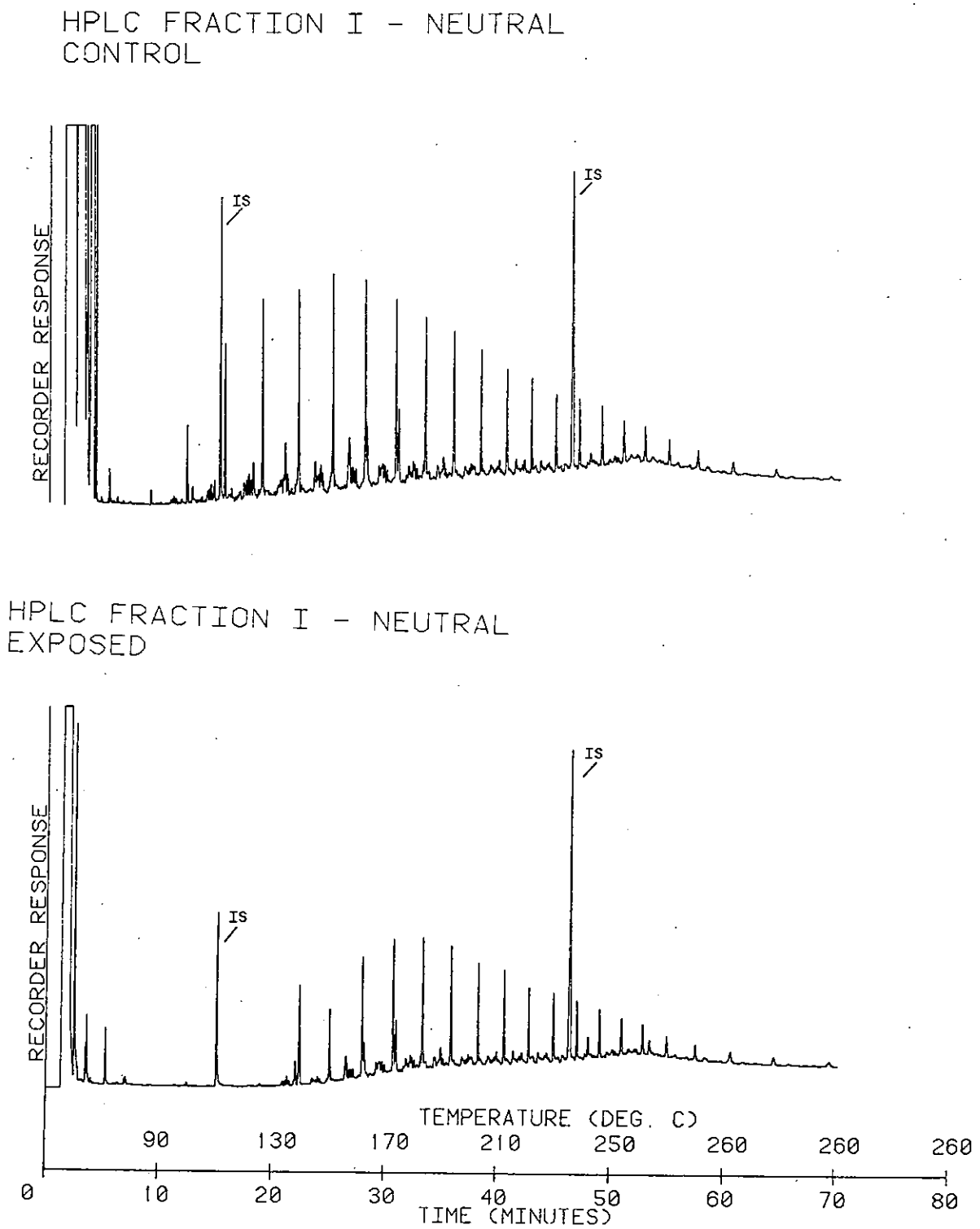

Figure 8. Glass capillary gas chromatographic data of the HPLC fraction I (saturate) of the neutral extract from the control (no sunlight) and exposed (sunlight) simulated laboratory photolysis experiment.

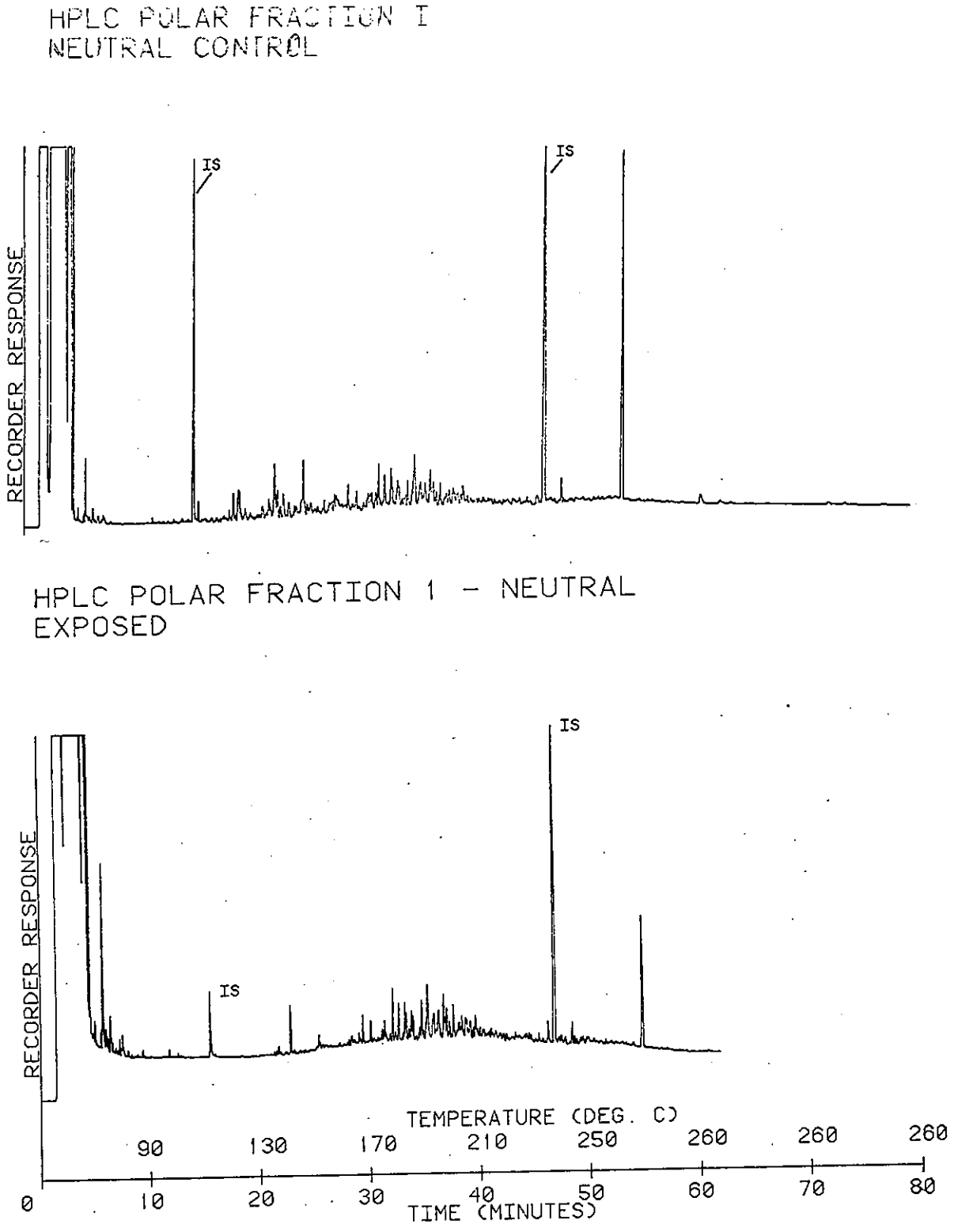

Figure 9. Glass capillary gas chromatographic data of the HPLC polar fraction 1 (aromatic) of the neutral extract from the control (no sunlight) and exposed (sunlight) simulated laboratory photolysis experiment.

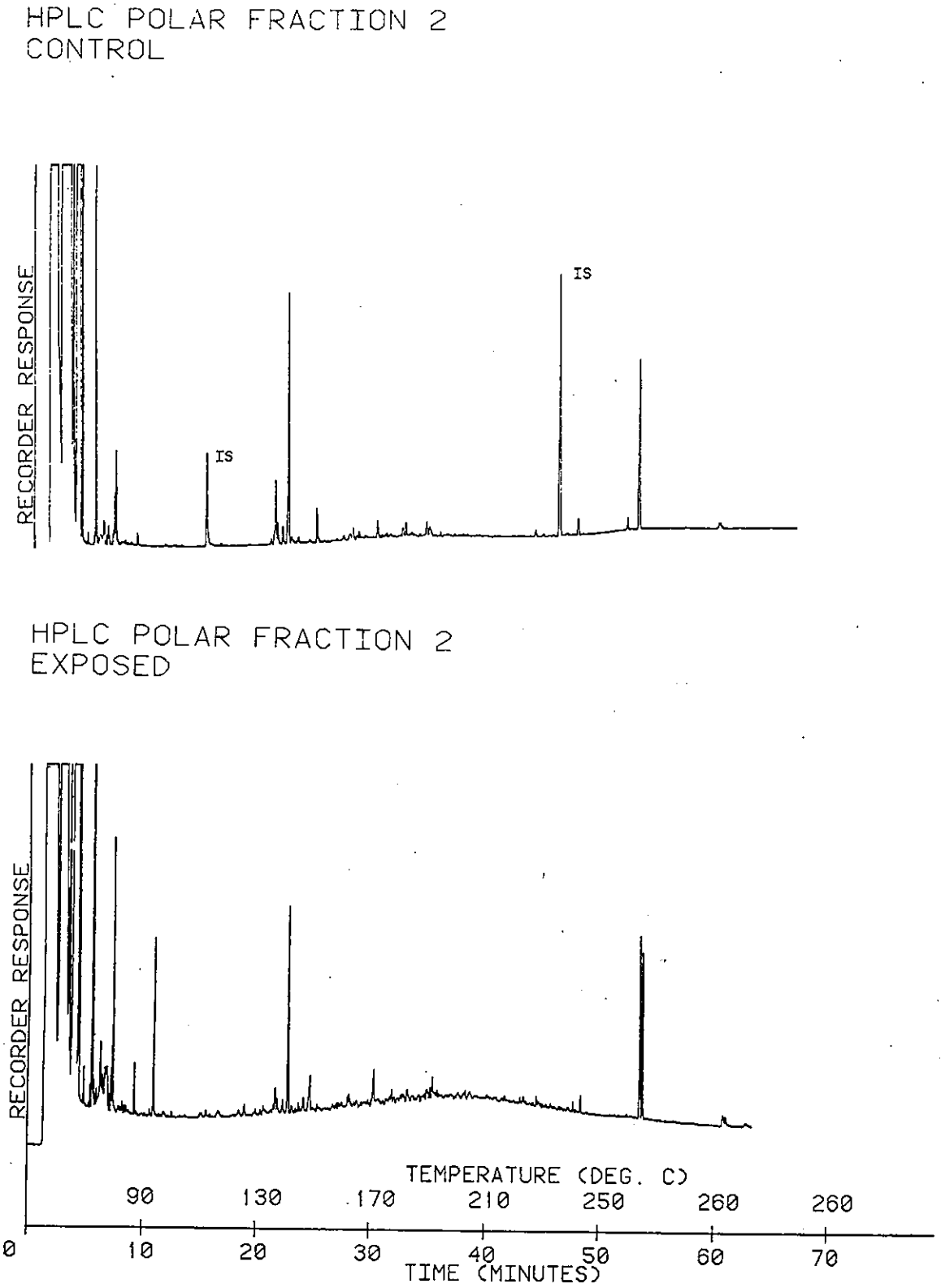

Figure 10. Glass capillary gas chromatographic data of the HPLC polar fraction 2 (polar aromatic) of the neutral extract from the control (no sunlight) and exposed (sunlight) simulated laboratory photolysis experiment.

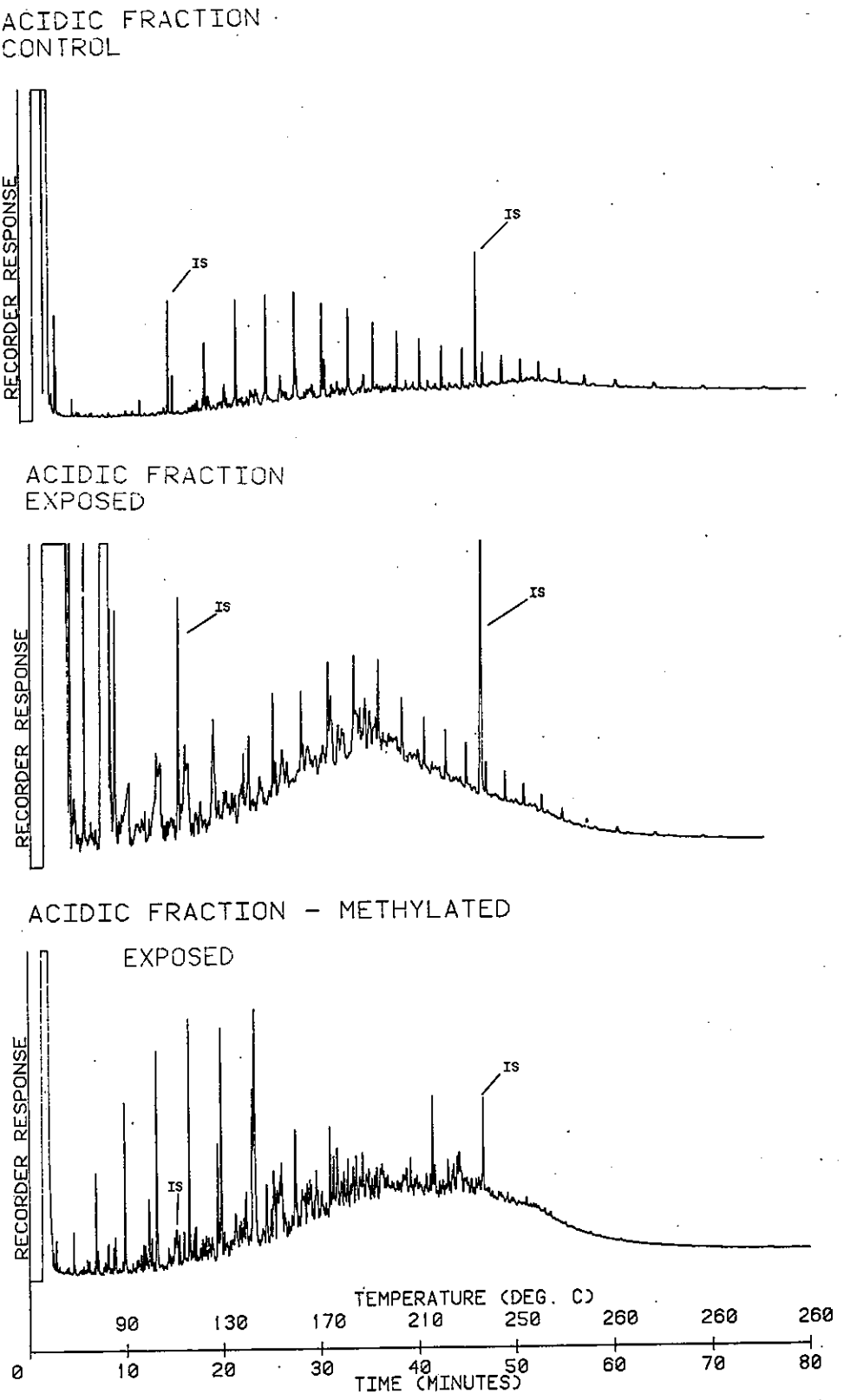

Figure 11. Glass capillary gas chromatographic data from the acid extract of the control (top), exposed (middle) and methylated exposed (bottom) photooxidation experiment.

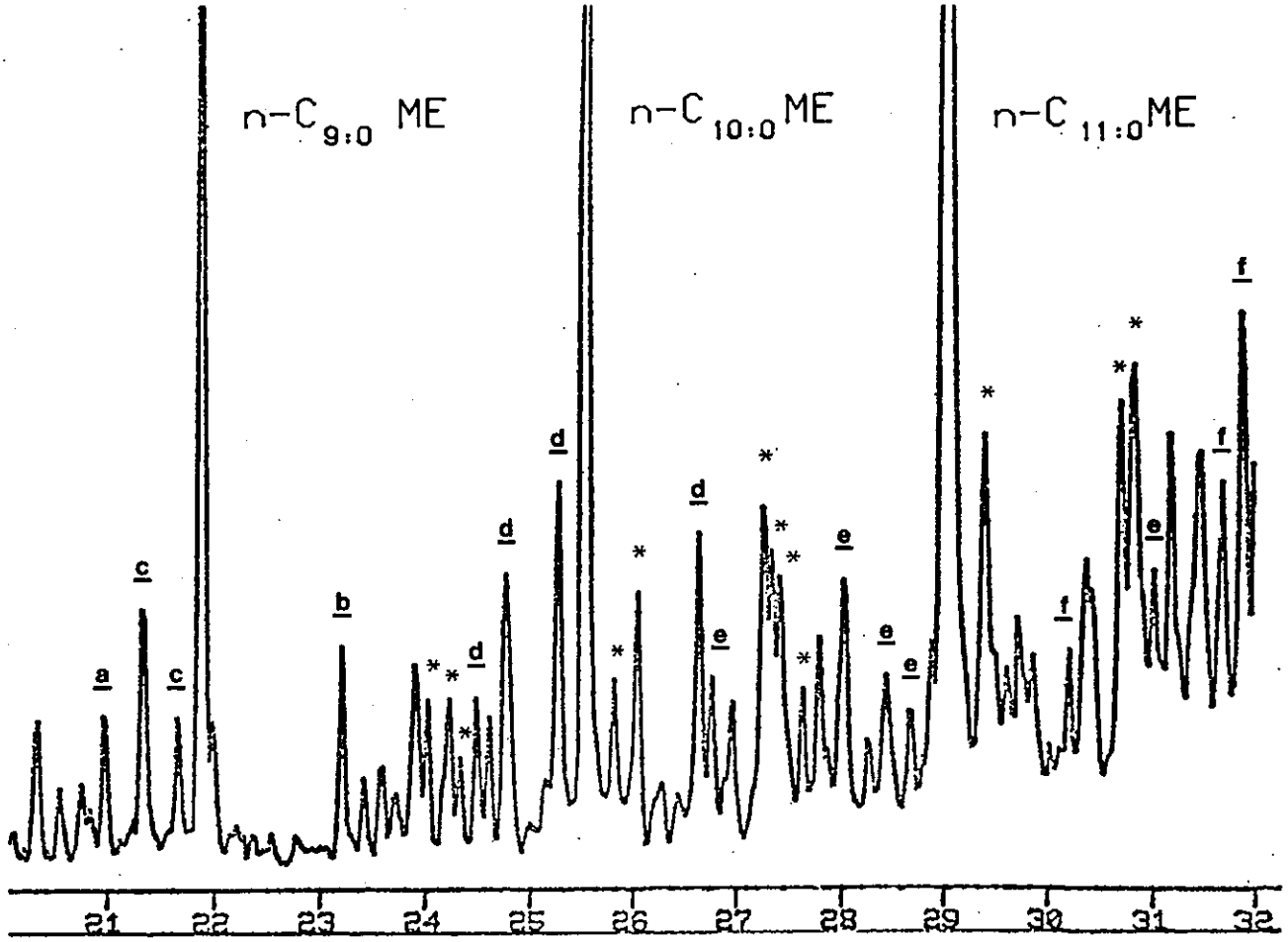

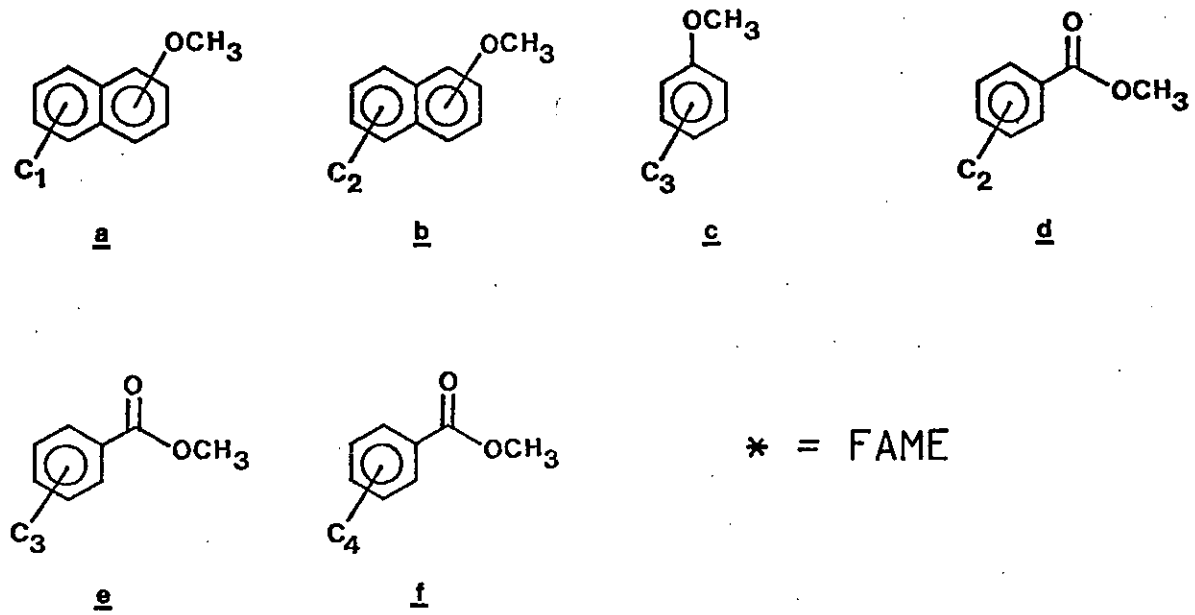

Figure 12. Reconstructed ion chromatogram of a 10-minute portion (15 minutes to 25 minutes) of the GCMS analysis of the methylated acid extract from the exposed simulated photooxidation experiment. The identifications and molecular structures of certain major components are indicated on the figure.

compounds, but this mechanism does not seem probable since virtually no fatty acids were found in the control sample. Much additional work must be done before an unequivocal explanation can be given for the sources of these substances.

Another interesting facet of the fatty acid formation is the absence of larger-molecular-weight fatty acids. Although water solubility may account for the absence of these substances, this reason is not entirely suitable for explaining the large quantities of the C_9, C_{10}, and C_1 fatty acids and the very small quantities of the C_{12} and larger fatty acids.

Other oxidized hydrocarbons found in the acidic extract were derived from oxidation of aromatic precursor molecules. For example, the C_1 and C_2 alkylated naphthols were identified in the extract. Also present were a number of substituted benzoic acids as well as substituted naphthoic, phenanthroic, benzothiophenoic, and dibenzothiophenoic acids. It is interesting to note that while alkyl fluorenes were present in IXTOC oil, no alkyl fluorenic acids were found in water column samples. Figure 13 shows the extracted ion current profiles (EICP) for the parent (186), parent-31 (155), and parent-59 (127) ions in the mass spectra of napthoic acid. These data indicate that the two C_1 alkylated naphthalene components in the IXTOC oil have been oxidized on the side chain.

The following is a brief summary of the major oxidized hydrocarbons found from simulated environmental photolysis experiments using IXTOC crude oil:

normal fatty acids (C_7 to C_{11})

branched fatty acids (C_9 to C_{12})

alkyl phenols

alkyl benzoic acids (C_1 to C_6)

alkyl naphthols

alkyl naphthoic acids

alkyl phenanthroic acids

phenanthrol

alkyl benzothiophenoic acids

alkyl dibenzothiophenoic acids

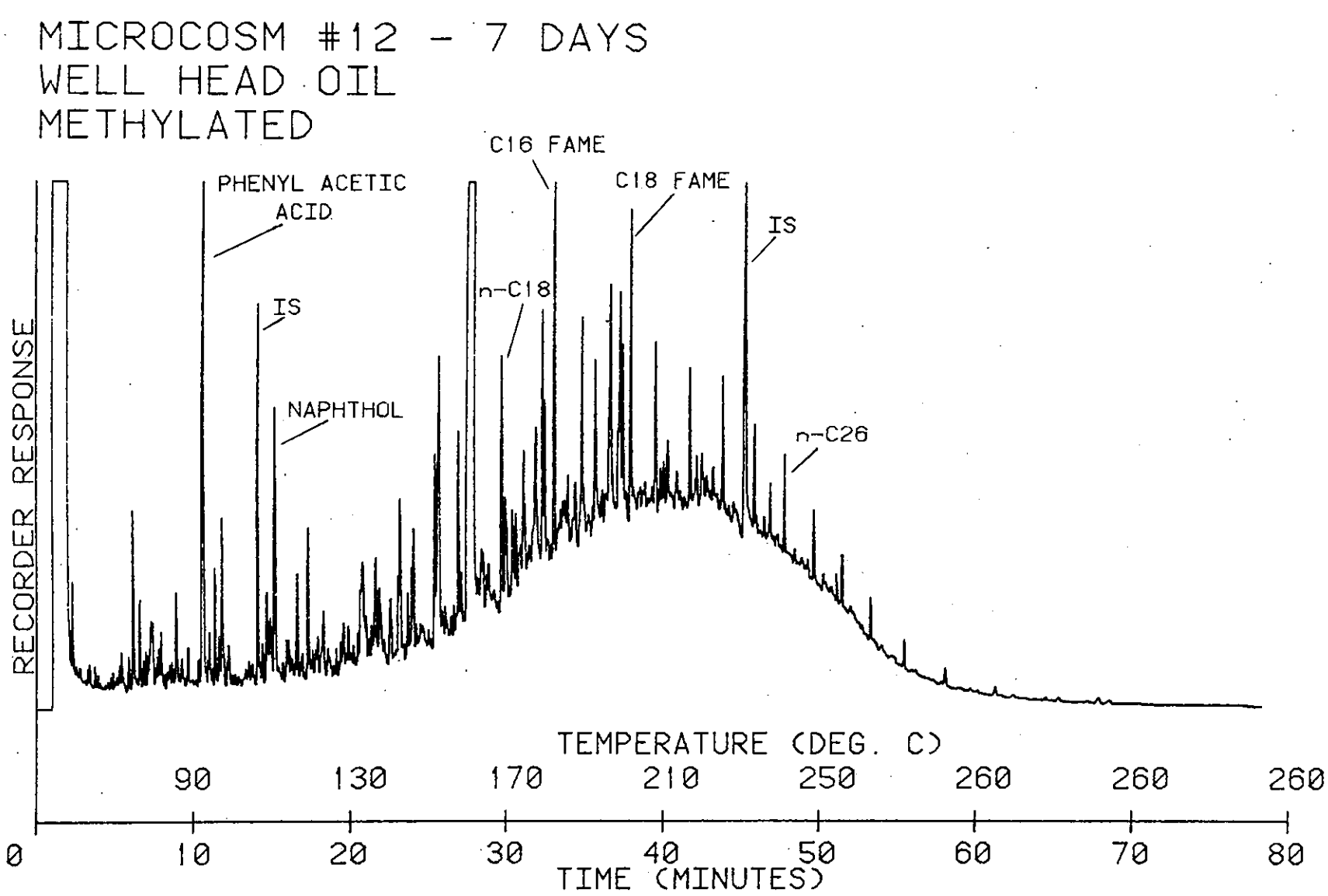

Figure 13. Glass capillary gas chromatographic data from the methylated acid extract of the water column sample taken from the day-7 microcosm experiment utilizing fresh wellhead oil.

2.2 Microcosm Experiments

Results from our chemical analysis of samples from the various microcosm experiments have been described by Overton et al. (this report). This previous report did not include the results of detailed analysis of polar oxidized products of microbial origin. Results of our analysis of polar oxidation products are presented herein. Figure 14 shows the chromatographic data for the methylated whole-water acid extract from the microcosm experiment utilizing fresh wellhead oil. The extract was analyzed by GC^2MS and found to contain numerous methyl derivatives of oxygenated hydrocarbons in addition to the saturate and aromatic compounds normally found in petroleum samples. The oxygenated hydrocarbons included the following classes of compounds:

fatty acids ($\underline{n}$-C_{16} predominating)

alkyl benzoic acids (C_1 to C_6)

alkyl phenols

phenylacetic acid

alkyl methoxybenzoic acids

alkyl benzene diacids

alkyl naphthols

alkyl naphthoic acids

alkyl phenanthroic acids

phenanthrol

alkyl benzothiophenoic acids

alkyl dibenzothiophenoic acids

Qualitatively, the most abundant oxidized hydrocarbons were the fatty acids and alkyl benzoic acids. Quantitatively, the single most abundant oxidized hydrocarbon was a substance that did not give a molecular ion on GCMS analysis. High-resolution mass spectral analysis indicated that the base peak in its spectrum was due to the $C_9H_7O_3^+$ ion, and this is strong evidence that the substance is a one-aromatic ring diacid. The extract contained many other oxidized compounds that are as yet not identified. Mass spectral data indicate that these substances contain oxygenated functional group, but their identity is not readily apparent. No fluorenoic acids were identified in the sample.

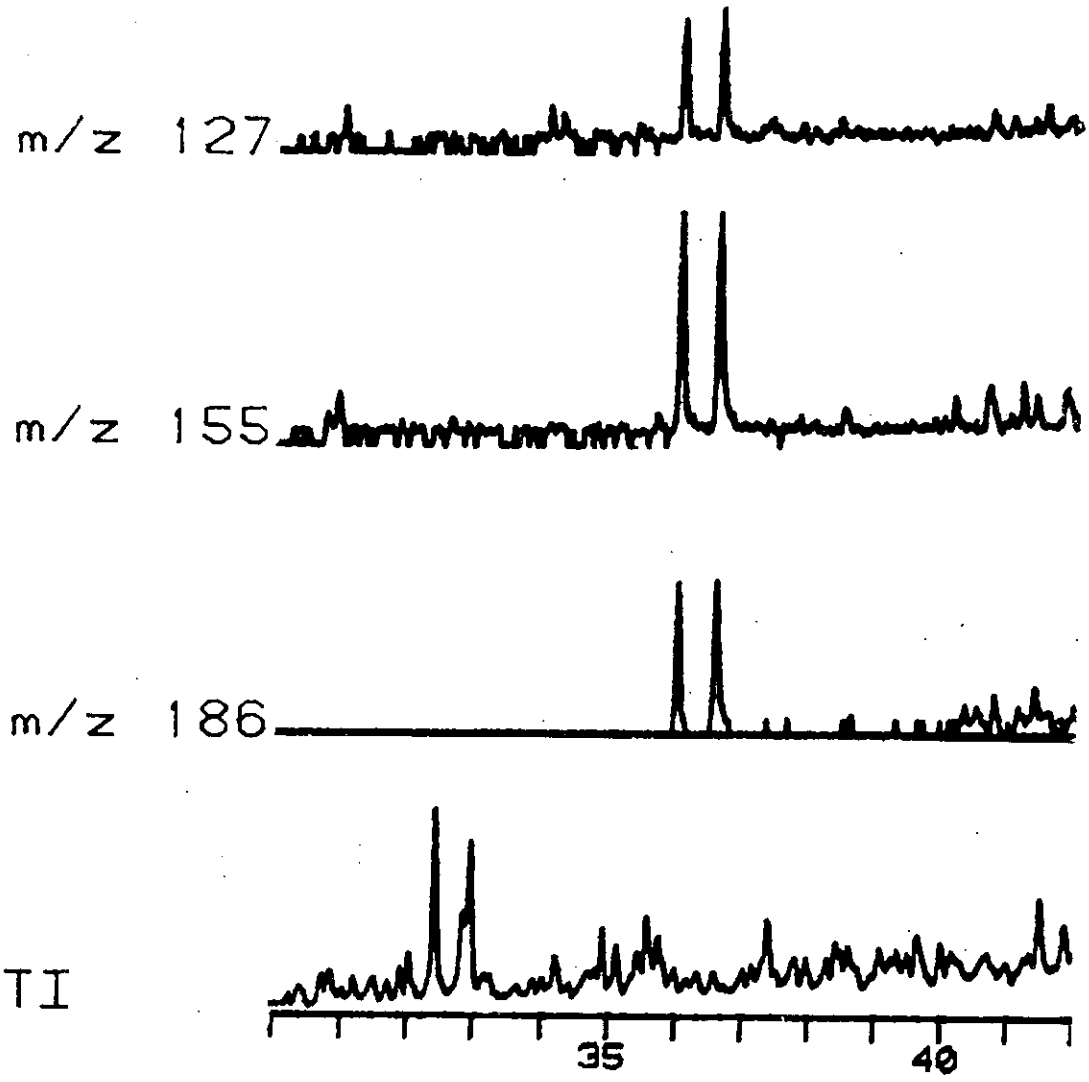

Figure 14. Extracted ion current profiles of the parent (186), parent-31 (155), and parent-59 (127) from the GC^{2}MS analysis of the acid extract of a whole water column sample from the microcosm experiment, utilizing fresh wellhead oil after seven days of incubation. Ions 186, 155, and 127 represent, respectively, the molecular weight of naphthanic acid, loss of the methyloxy group from the parent, and loss of the methyloxy acidic functional group from the parent.

2.3 Comparison Between Photochemical and Microbial Oxidation Products

Microbial and photochemical oxidations should produce many of the same classes of oxidized organic compounds. Microbial processes, however, are more selective and should favor the oxidation of specific isomers. Photooxidative processes are expected to exhibit less selectivity in their oxidation reaction. These broad generalizations are gross oversimplifications of extremely complex reaction mechanisms that are not fully understood at the present time. Therefore, we believe it to be useful to present data that compare the alkyl homolog distributions of major oxidation products of aromatic hydrocarbons from IXTOC oil produced by both microbial and photochemical processes.

The major aromatic oxidation products include alkyl benzoic, naphthoic, and phenanthroic acids. Figures 15 to 29 show extracted ion current profiles from the GC^2MS analysis of the methylated acid extracts of a day-7 microcosm experiment and the simulated laboratory photooxidation experiment. The ions plotted in the extracted ion current profiles are those characteristic of the specific homologs being studied. Compounds detected in the mass chromatograms have been identified as homologs by background subtracted mass spectra.

Figures 15 to 21 show the extracted ion current profiles for benzoic acid and its C_1, C_2, C_3, C_4, C_5, and C_6 homologs. The most prominent ion in the mass spectra of these compounds appears at parent-31, which represents facile loss of the methoxy group. It must be recognized that ions chosen for display in the extracted ion current profiles are not characteristic of just the benzoic acids; therefore, both background subtracted mass spectra and retention times were used to identify the homolog distributions for the microcosm and photochemical experiments. Figure 22 shows the relative quantities of the homologs of benzoic acids in the microcosm and photochemical experiments and the homolog distribution of alkylated benzenes in the IXTOC oil. These data were quantified from extracted ion current profiles of rapid-scanning (one second cycle time) GC^2MS data and must be considered in light of the inherent inaccuracies of this type of quantification. The data in Figures 15 to 22, however, clearly show interesting trends. For example, the homolog distribution for the C_3 to C_6 family of alkyl benzoic acids generally varies significantly between the microcosm and photochemical experiments, while the homolog distribution for the parent C_1 and C_2 homologs is quite similar. The relative quantities of the alkyl benzoic acids are minimal for the C_4 homologs but relatively more abundant for lower and higher homologs. This bimodal quantitative distribution is not evident in the homolog distribution of alkyl benzenes in the parent IXTOC oil. The alkyl benzoic acids may not all be derived from the same family of precursor compounds, and this could account for the abundant distribution.

Figures 23 to 25 show the extracted ion current profiles for naphthoic acid and its C_1 and C_2 homologs in the microcosm and photochemical experiments. The extracted ion plots (186, 200, 214) are representative of the parent ions for these compounds. In all cases, the homolog distribution is significantly different when comparing microbial processes and photooxidations. Figure 26 shows the quantitative distribution for the alkyl naphthoic acid from the microcosm and photochemical experiment and the alkyl naphthalenes in IXTOC

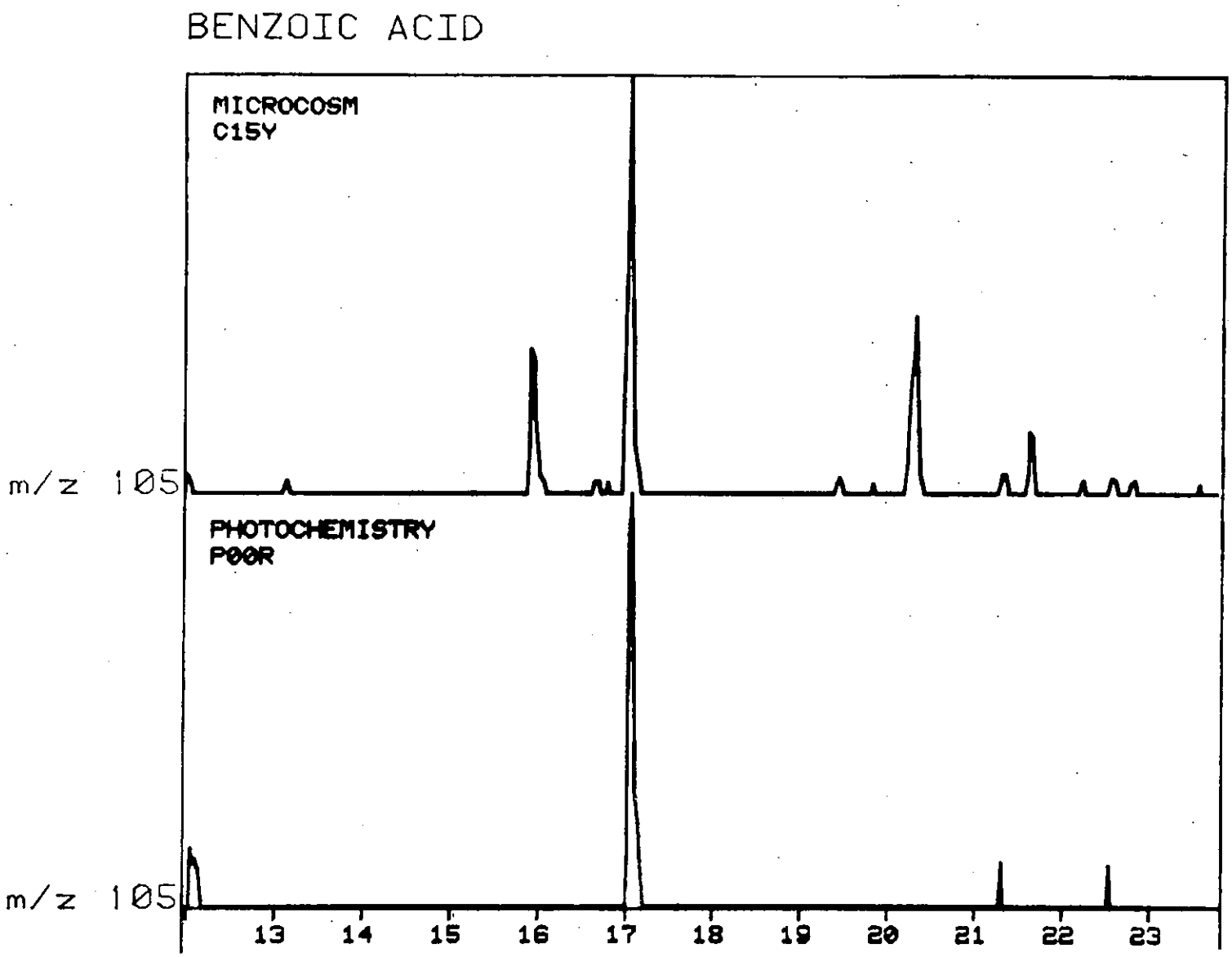

Figure 15. Extracted ion current profiles from the GC^2MS analyses of: top methylated acidic extract from a microcosm experiment utilizing fresh wellhead oil after seven days of incubation; bottom-methylated acidic extract of the water column sample from a simulated environmental photooxidation experiment after exposure to 32 hrs of bright sunlight. 105 is characteristic of the P-31 ions in the mass spectra of benzoic acid.

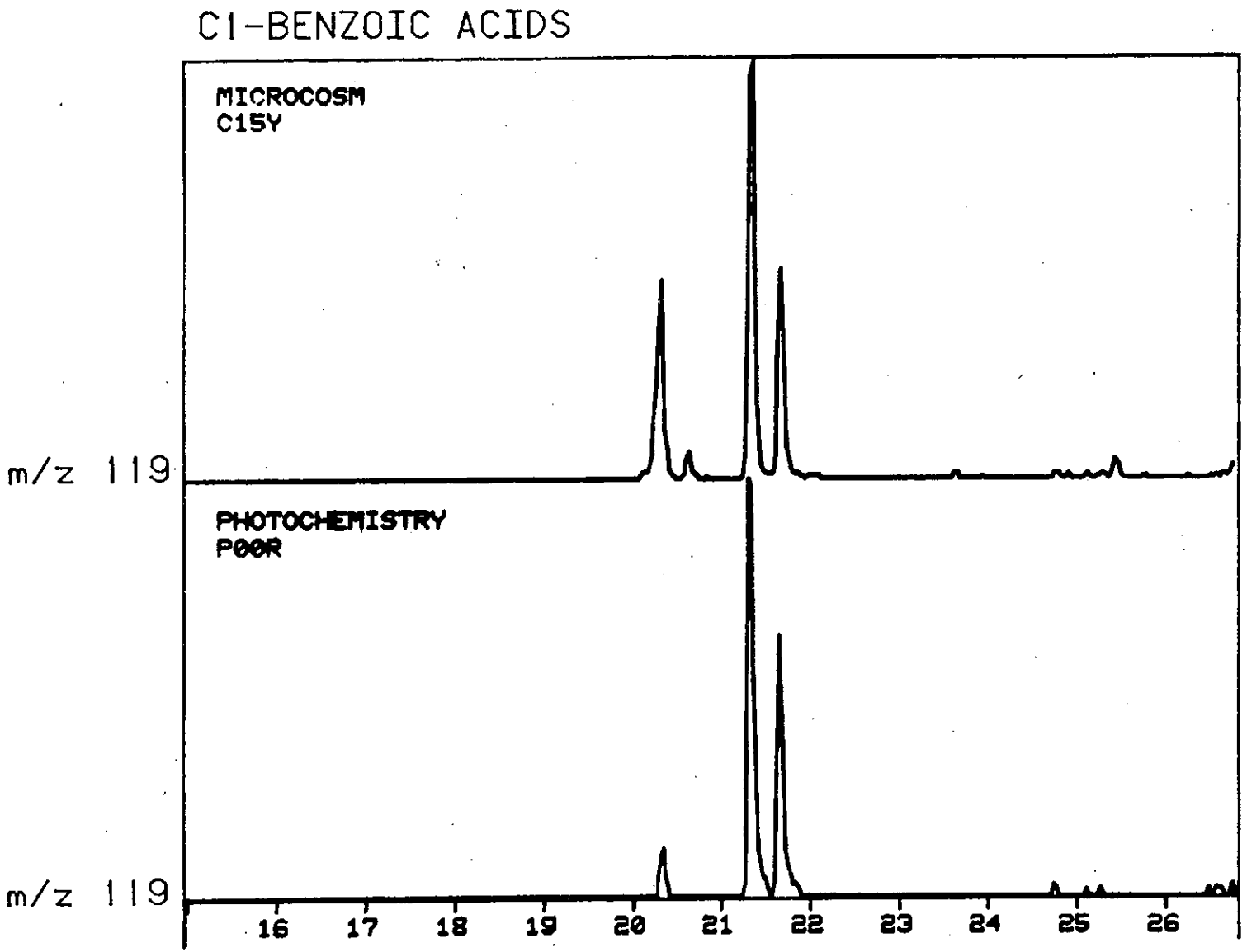

Figure 16. Extracted ion current profiles from the GC^2MS analyses of: top methylated acidic extract from a microcosm experiment utilizing fresh wellhead oil after seven days of incubation; bottom-methylated acidic extract of the water column sample from a simulated environmental photooxidation experiment after exposure to 32 hrs of bright sunlight. 119 is characteristic of the P-31 ions in the mass spectra of C_1 benzoic acids.

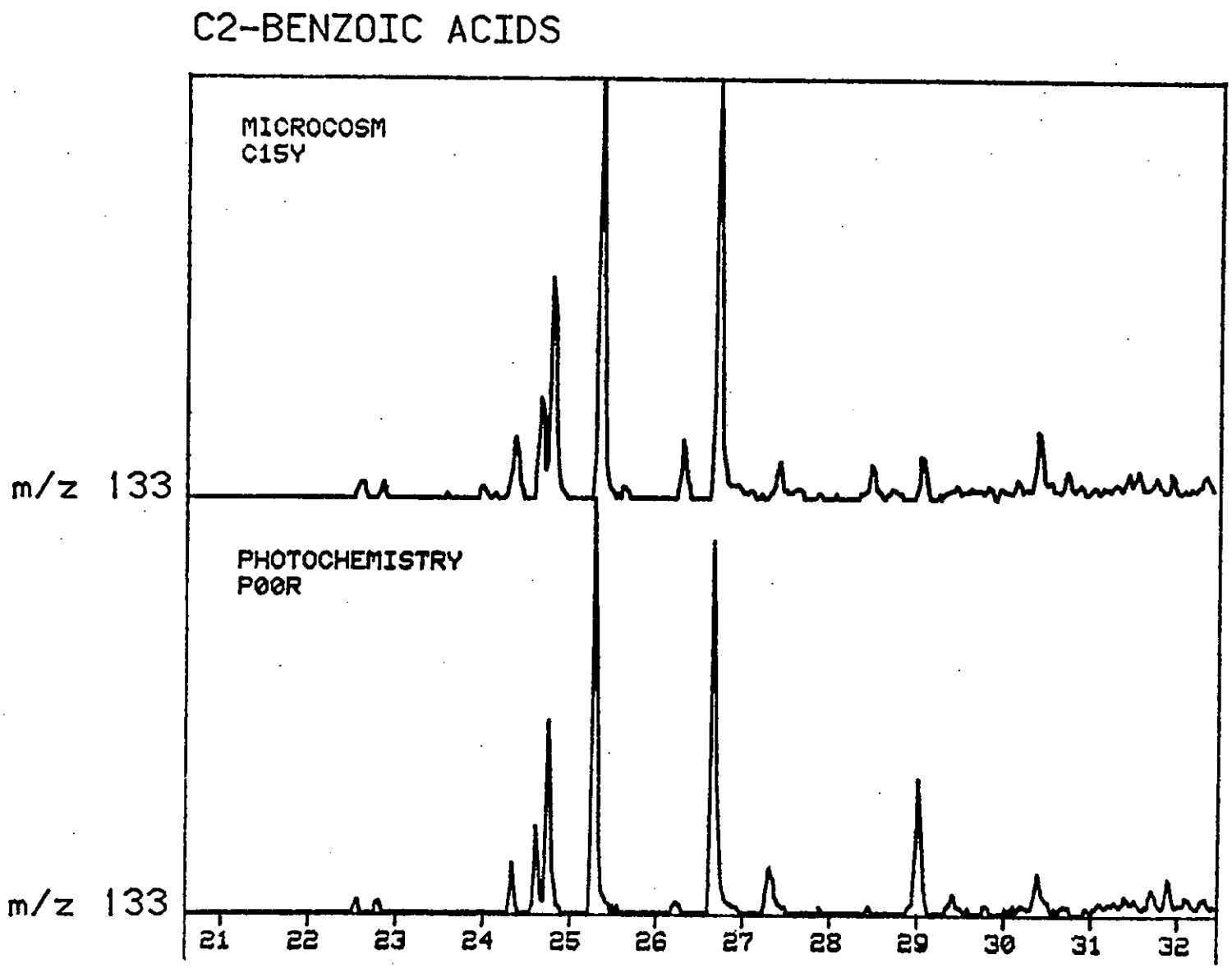

Figure 17. Extracted ion current profiles from the GC^2MS analyses of: top methylated acidic extract from a microcosm experiment utilizing fresh wellhead oil after seven days of incubation; bottom-methylated acidic extract of the water column sample from a simulated environmental photooxidation experiment after exposure to 32 hrs of bright sunlight. 133 is characteristic of the P-31 ions in the mass spectra of C_2 benzoic acids.

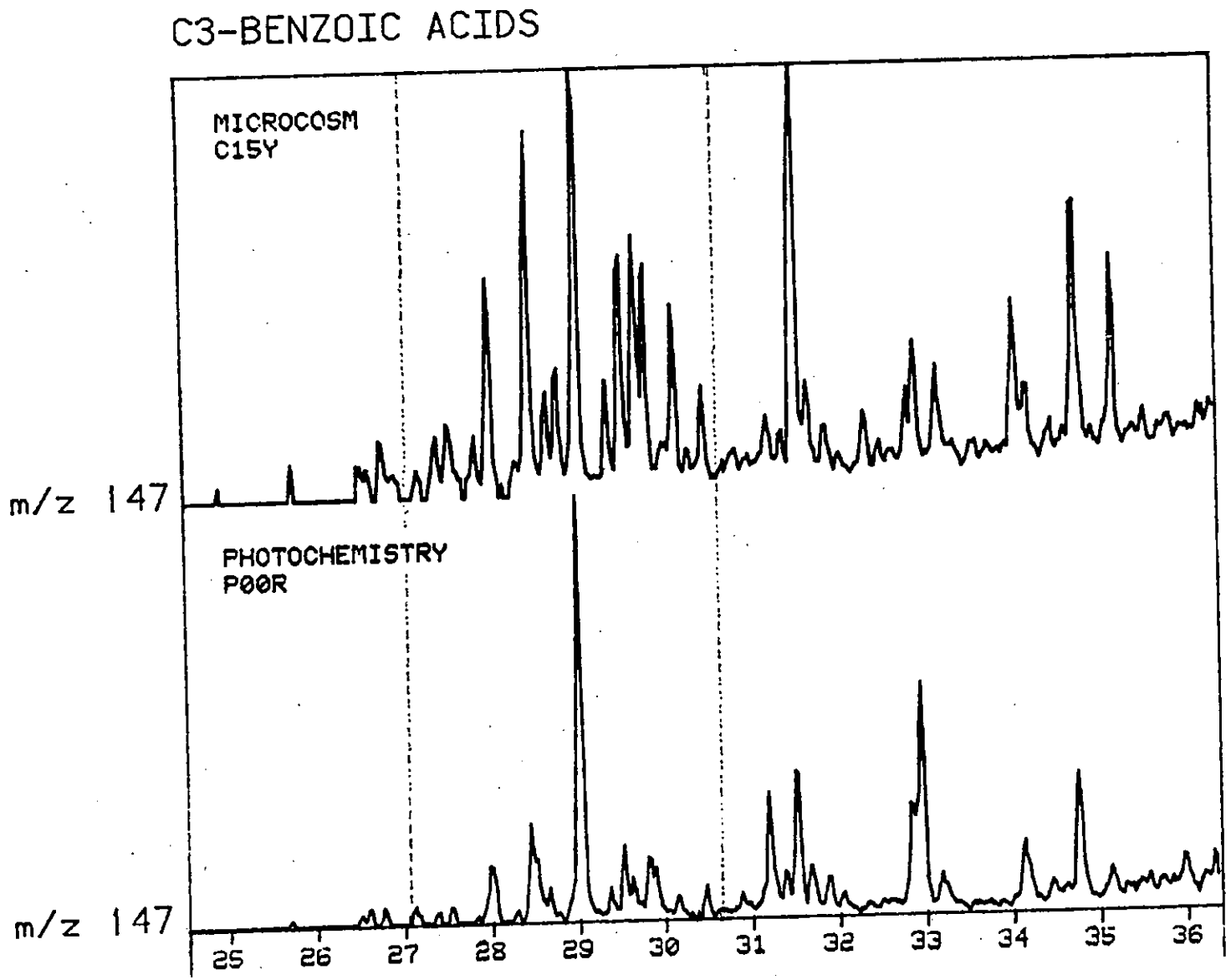

Figure 18. Extracted ion current profiles from the GC^2MS analyses of: top methylated acidic extract from a microcosm experiment utilizing fresh wellhead oil after seven days of incubation; bottom-methylated acidic extract of the water column sample from a simulated environmental photooxidation experiment after exposure to 32 hrs of bright sunlight. 147 is characteristic of the P-31 ions in the mass spectra of C_3 benzoic acids.

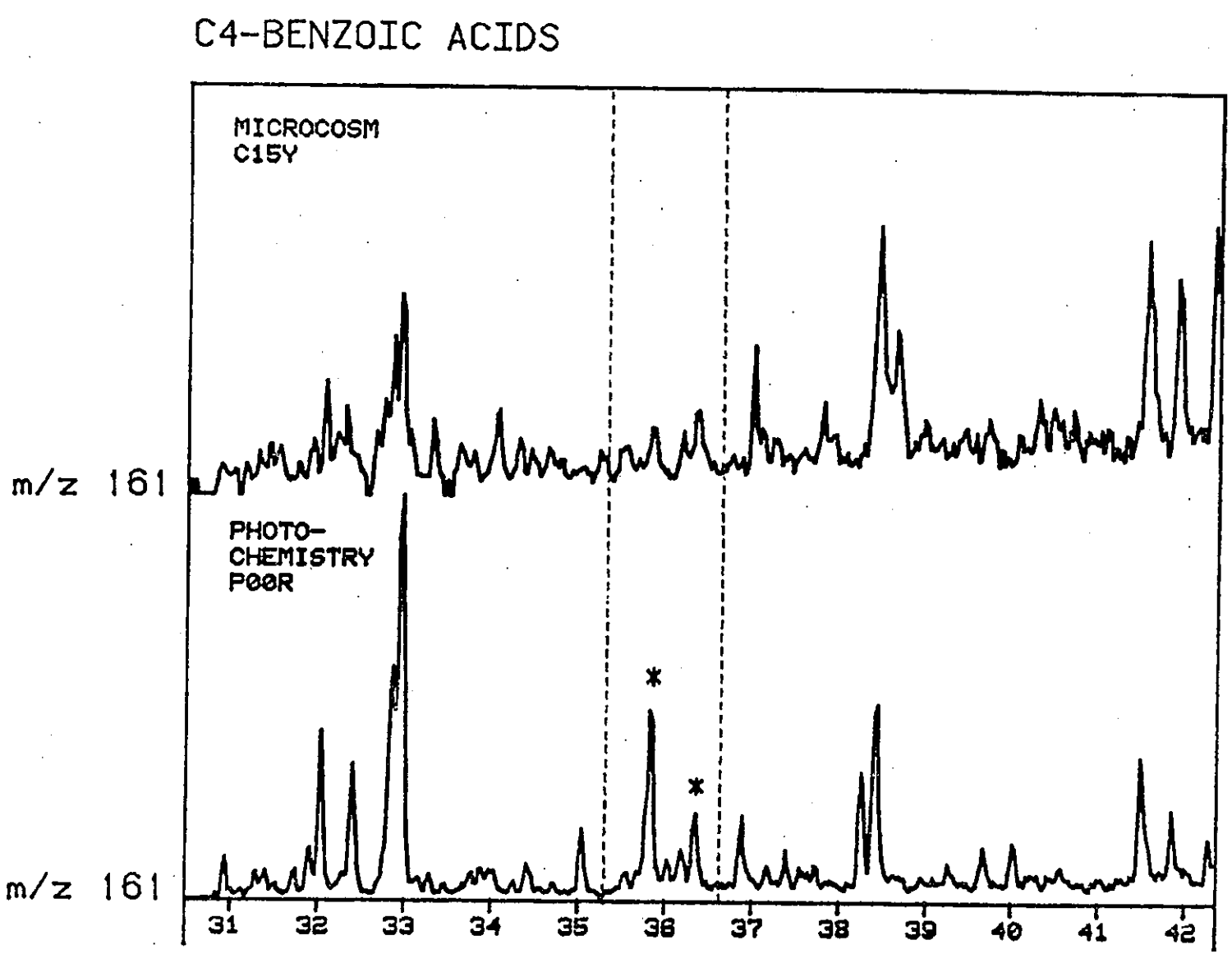

Figure 19. Extracted ion current profiles from the GC^2MS analyses of: top methylated acidic extract from a microcosm experiment utilizing fresh wellhead oil after seven days of incubation; bottom-methylated acidic extract of the water column sample from a simulated environmental photooxidation experiment after exposure to 32 hrs of bright sunlight. 161 is characteristic of the P-31 ions in the mass spectra of C_4 benzoic acids.

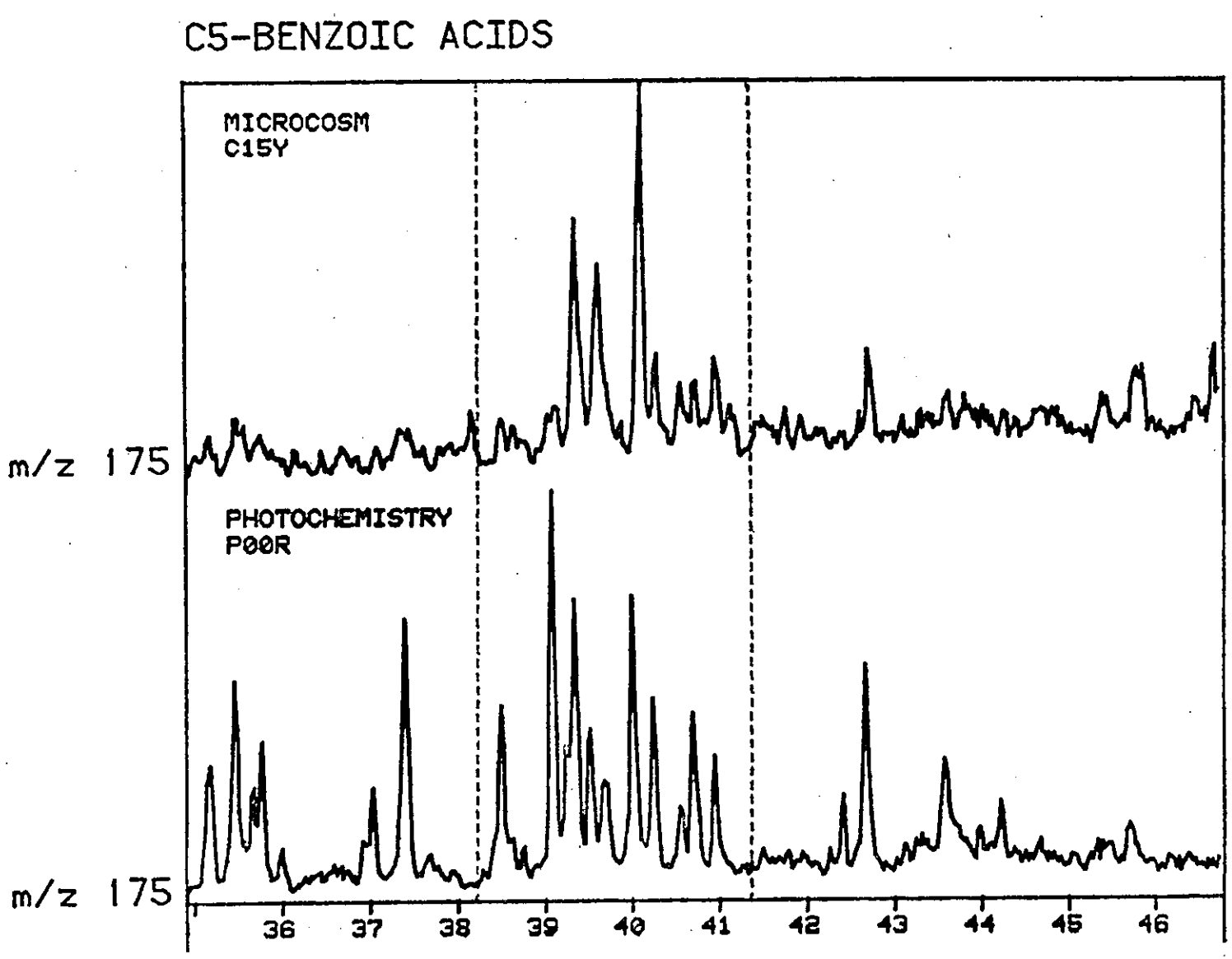

Figure 20. Extracted ion current profiles from the GC^2MS analyses of: top methylated acidic extract from a microcosm experiment utilizing fresh wellhead oil after seven days of incubation; bottom-methylated acidic extract of the water column sample from a simulated environmental photooxidation experiment after exposure to 32 hrs of bright sunlight. 175 is characteristic of the P-31 ions in the mass spectra of C_5 benzoic acids.

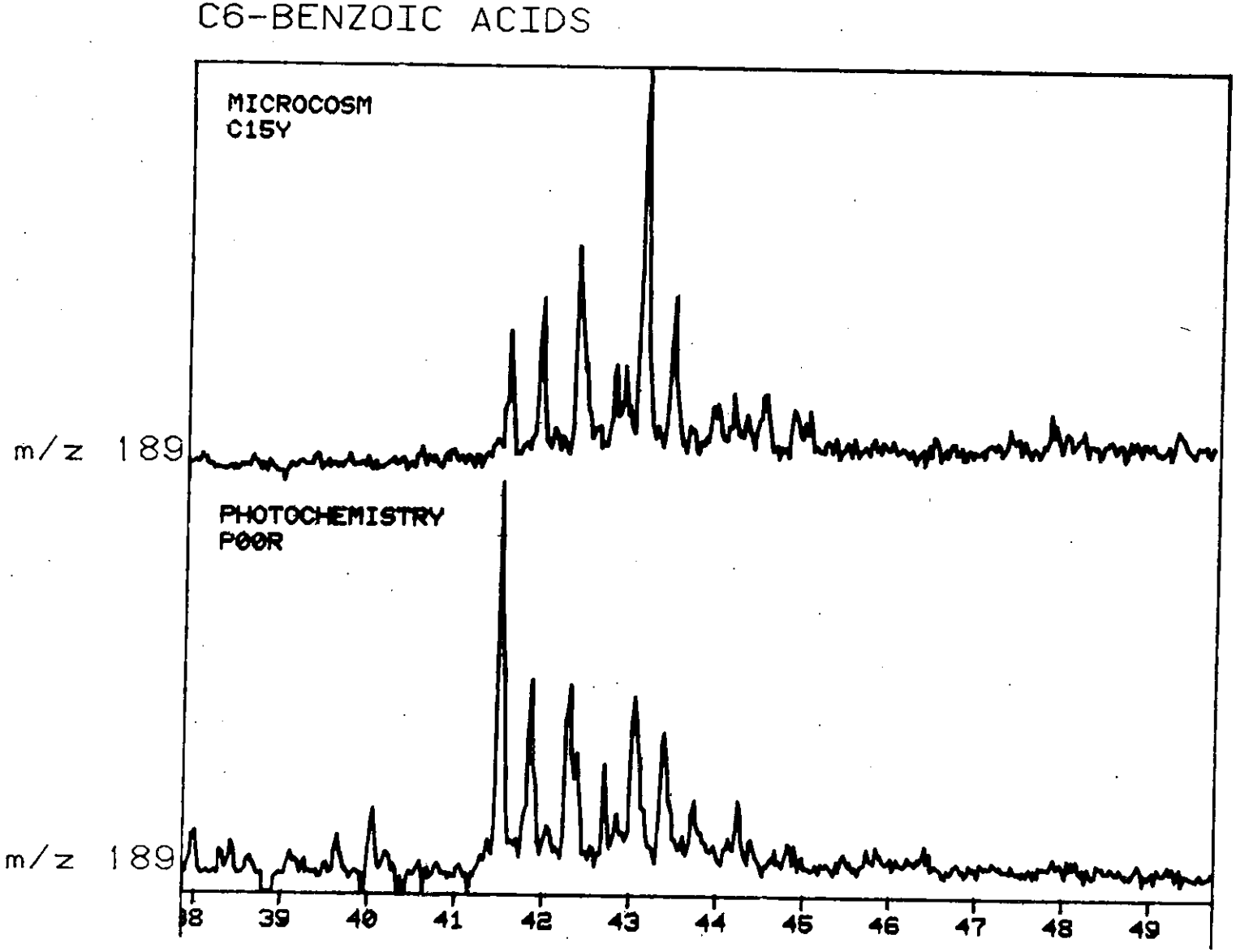

Figure 21. Extracted ion current profiles from the GC^2MS analyses of: top methylated acidic extract from a microcosm experiment utilizing fresh wellhead oil after seven days of incubation; bottom-methylated acidic extract of the water column sample from a simulated environmental photooxidation experiment after exposure to 32 hrs of bright sunlight. 189 is characteristic of the P-31 ions in the mass spectra of C_6 benzoic acids.

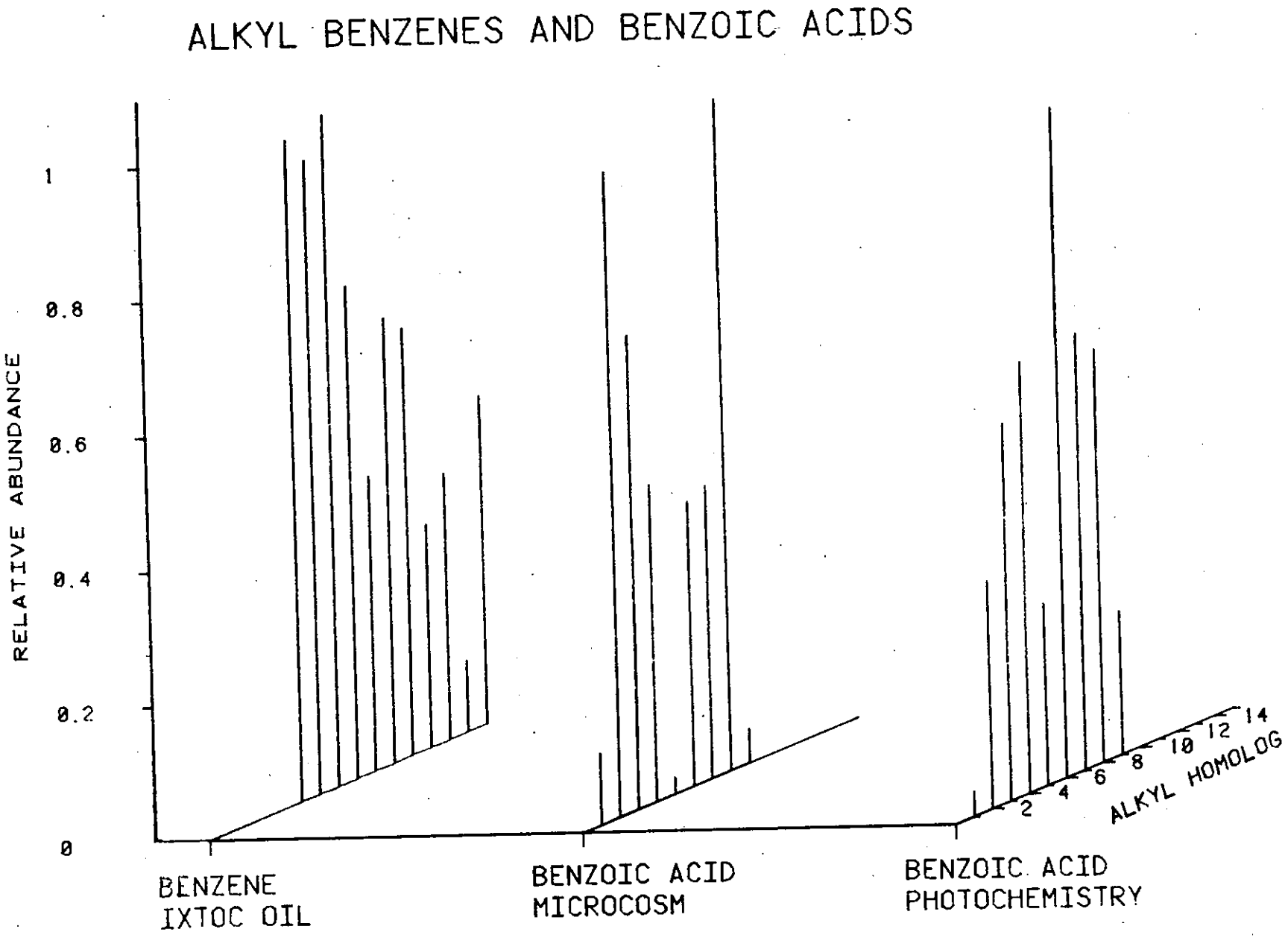

Figure 22. Three-dimensional diagram showing the relative quantities of the alkyl benzoic acid from the microcosm and photochemical experiments and the alkyl benzenes in the IXTOC oil.

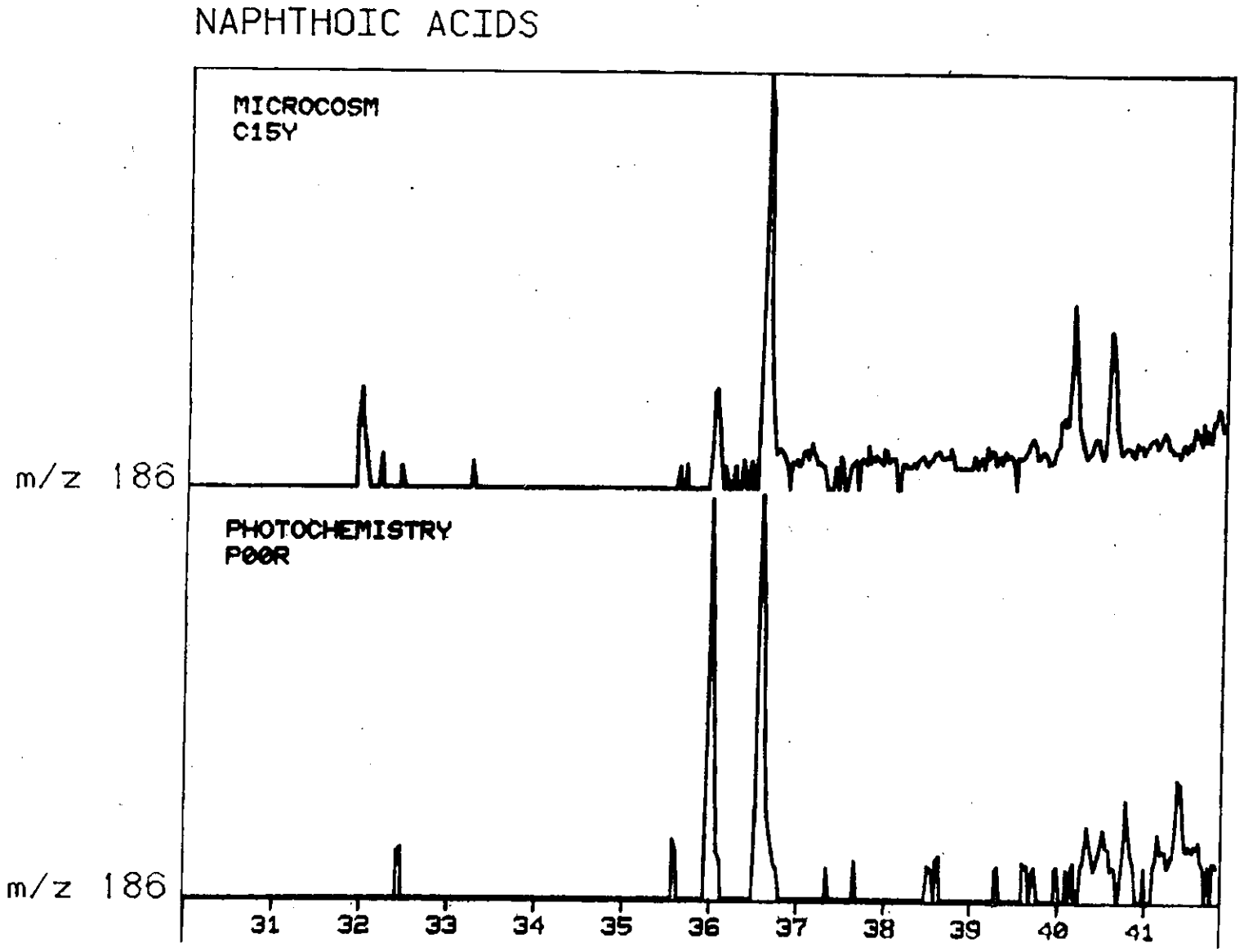

Figure 23. Extracted ion current profiles from the GC^2MS analyses of: top methylated acidic extract from a microcosm experiment utilizing fresh wellhead oil after seven days of incubation; bottom-methylated acidic extract of the water column sample from a simulated environmental photooxidation experiment after exposure to 32 hrs of bright sunlight. 186 is characteristic of the parent ions in the mass spectra of naphthoic acids.

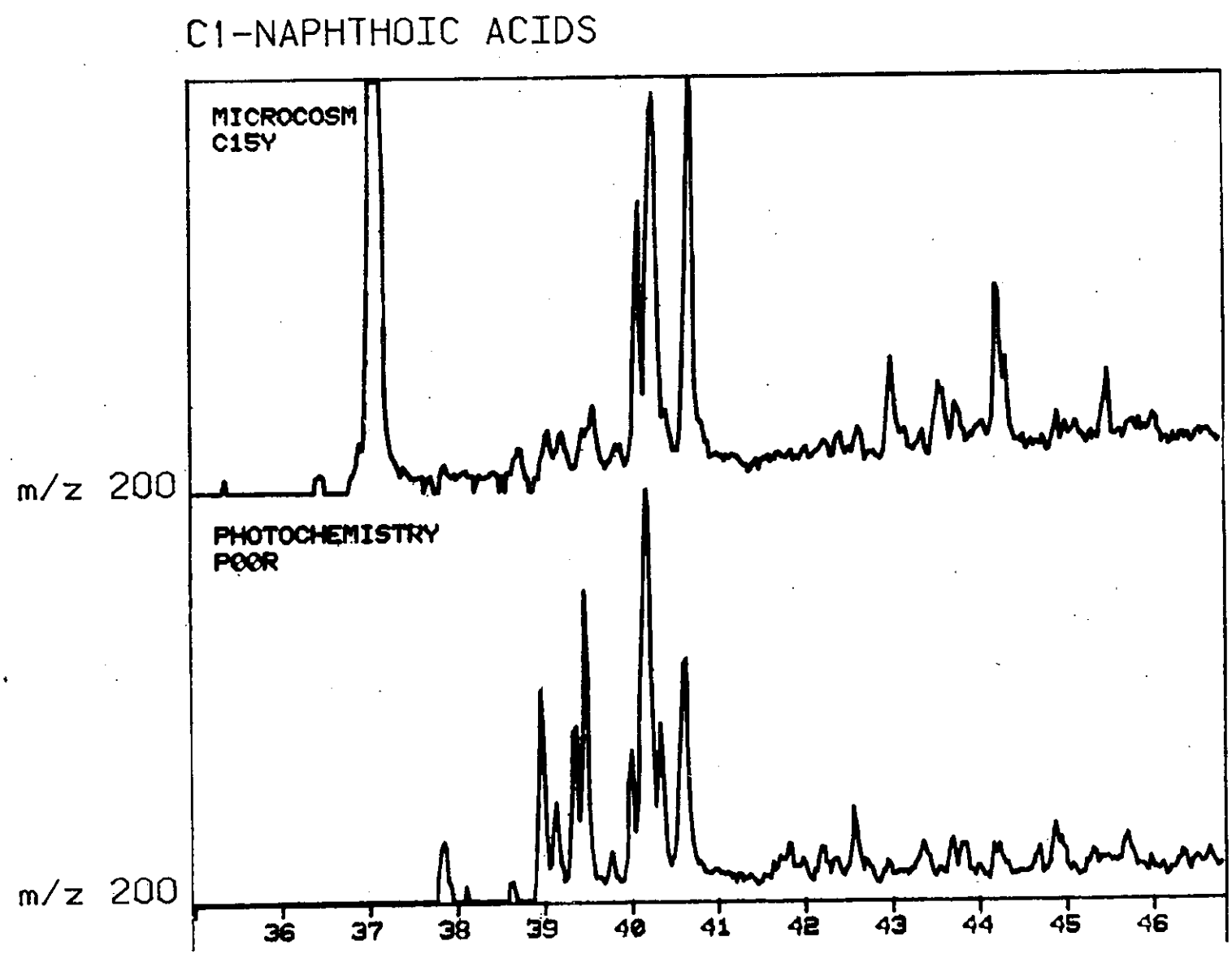

Figure 24. Extracted ion current profiles from the GC^2MS analyses of: top methylated acidic extract from a microcosm experiment utilizing fresh wellhead oil after seven days of incubation; bottom-methylated acidic extract of the water column sample from a simulated environmental photooxidation experiment after exposure to 32 hrs of bright sunlight. 200 is characteristic of the parent ions in the mass spectra of C_1 naphthoic acids.

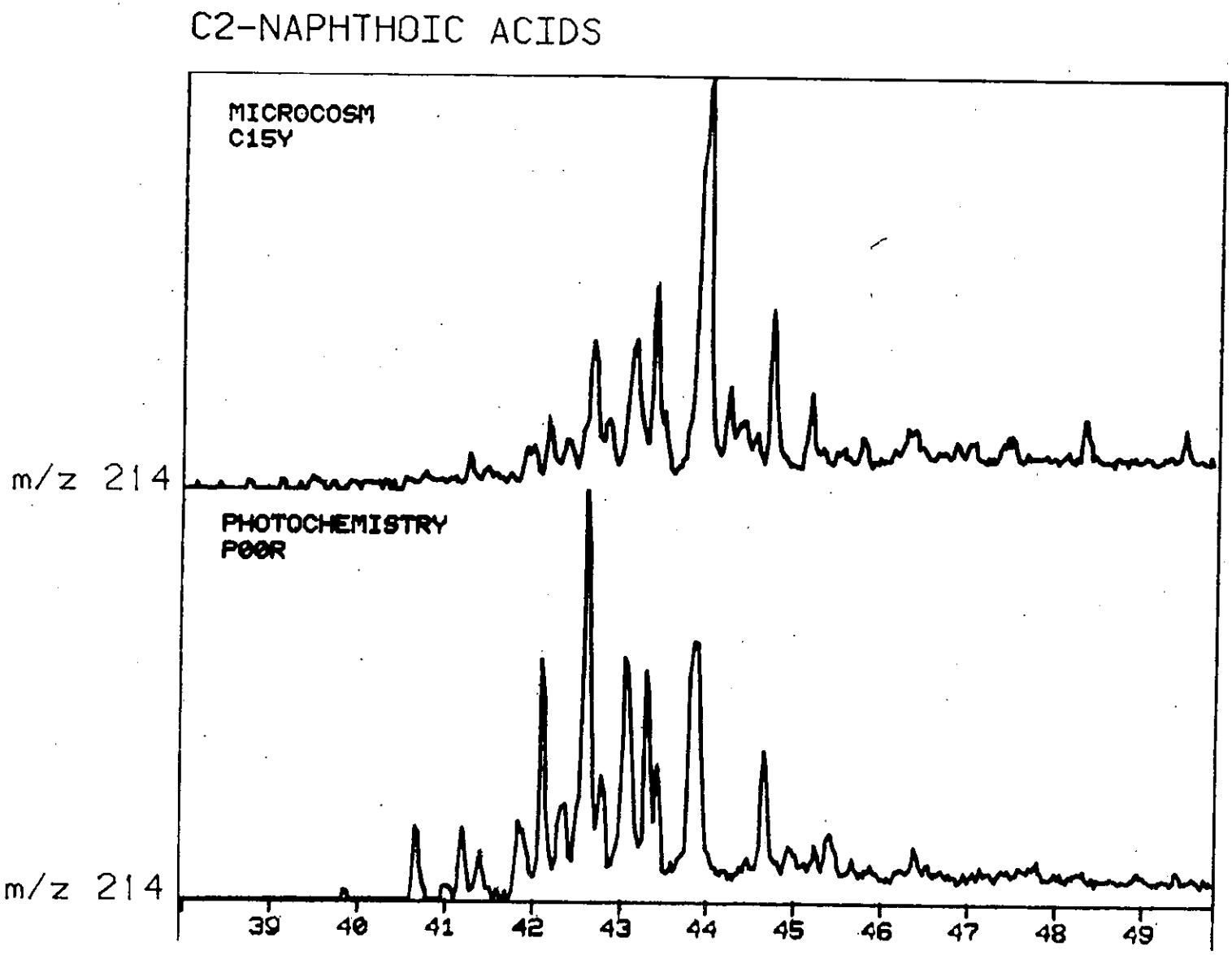

Figure 25. Extracted ion current profiles from the GC^2MS analyses of: top methylated acidic extract from a microcosm experiment utilizing fresh wellhead oil after seven days of incubation; bottom-methylated acidic extract of the water column sample from a simulated environmental photooxidation experiment after exposure to 32 hrs of bright sunlight. 214 is characteristic of the parent ions in the mass spectra of C_2 naphthoic acids.

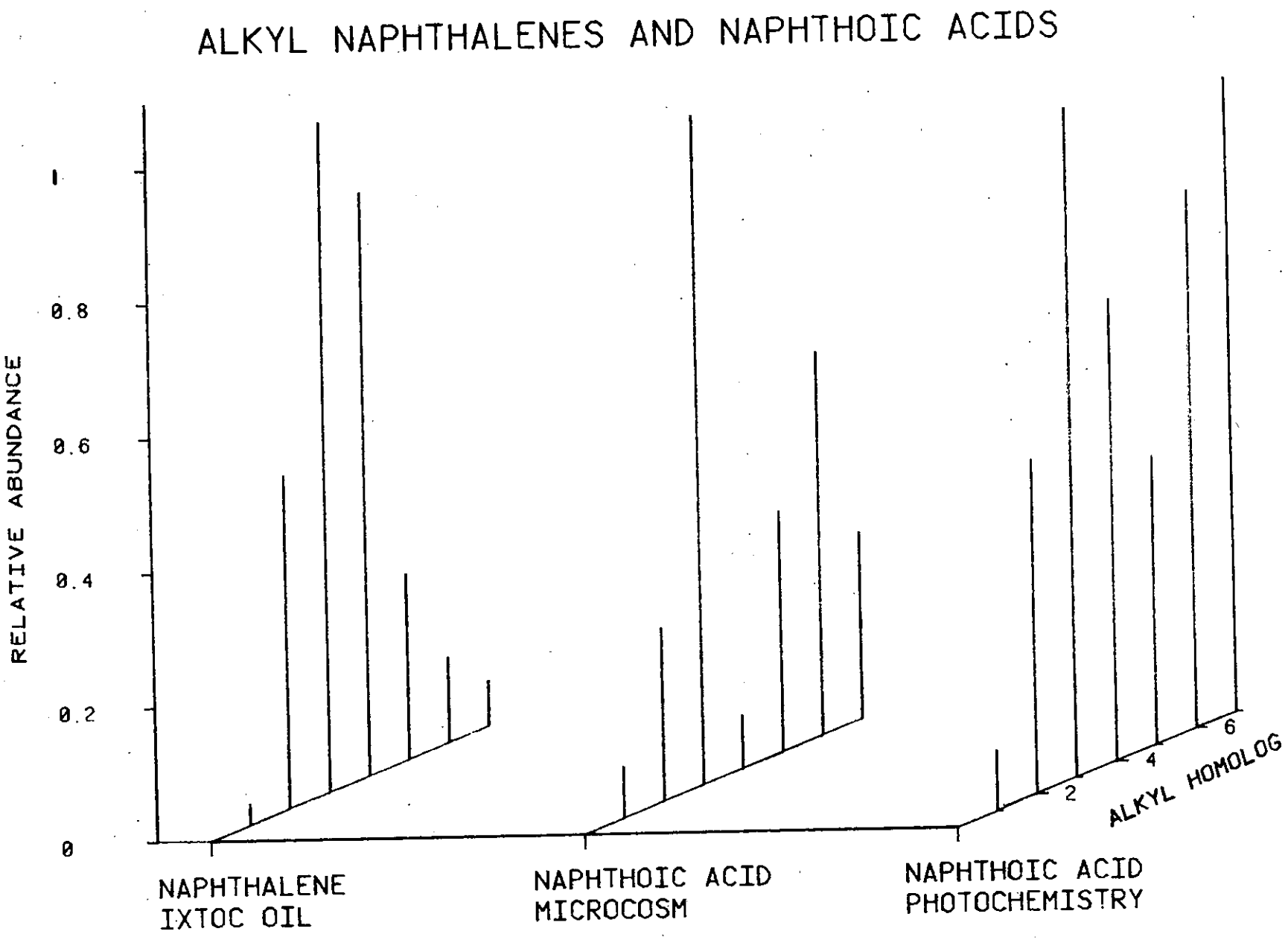

Figure 26. Three-dimensional diagram showing the relative quantities of the alkyl naphthoic acids in the microcosm and the alkyl naphtholenes in the IXTOC oil.

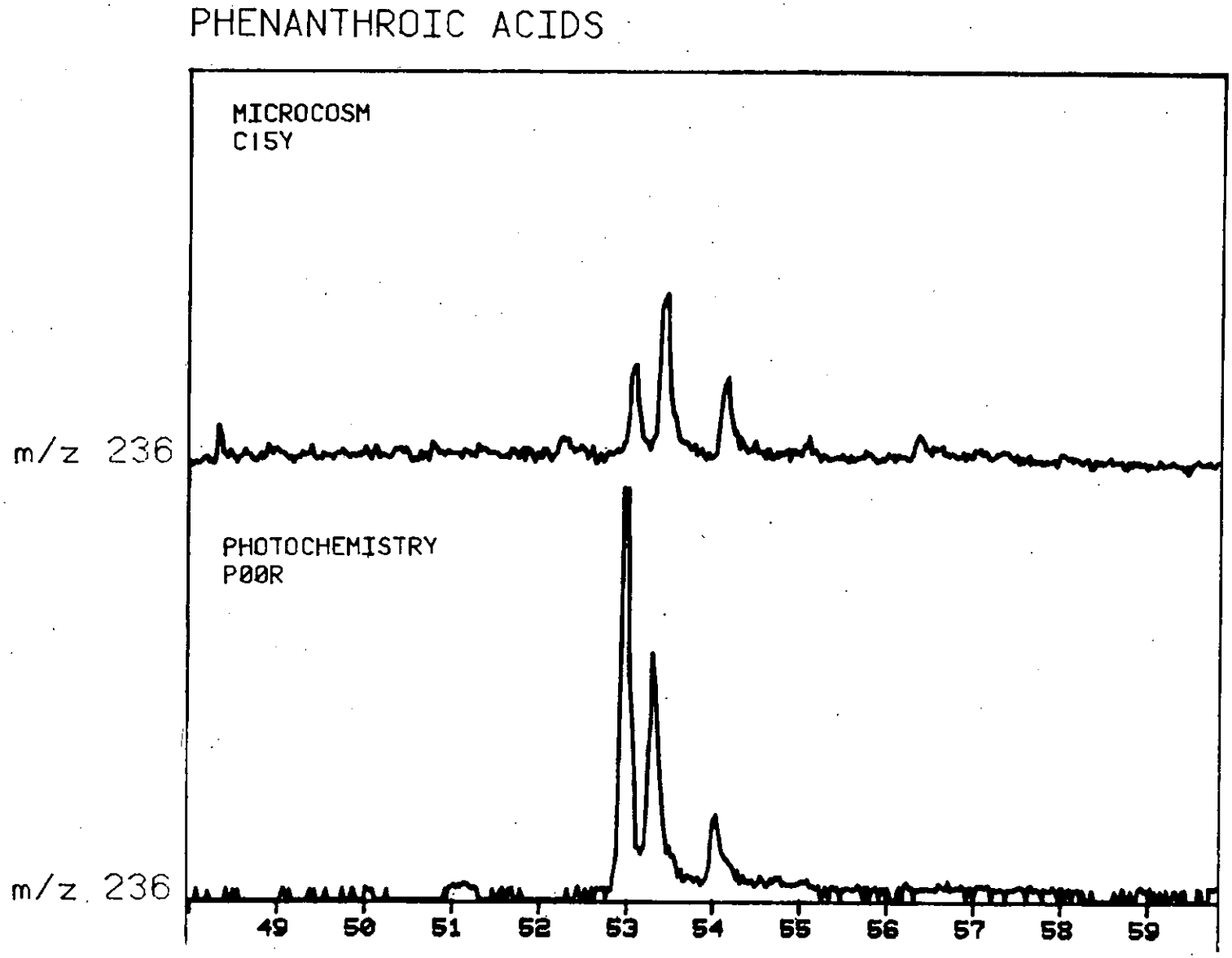

Figure 27. Extracted ion current profiles from the GC^2MS analyses of: top methylated acidic extract from a microcosm experiment utilizing fresh wellhead oil after seven days of incubation; bottom-methylated acidic extract of the water column sample from a simulated environmental photooxidation experiment after exposure to 32 hrs of bright sunlight. 232 is characteristic of the parent ions in the mass spectra of phenanthroic acids.

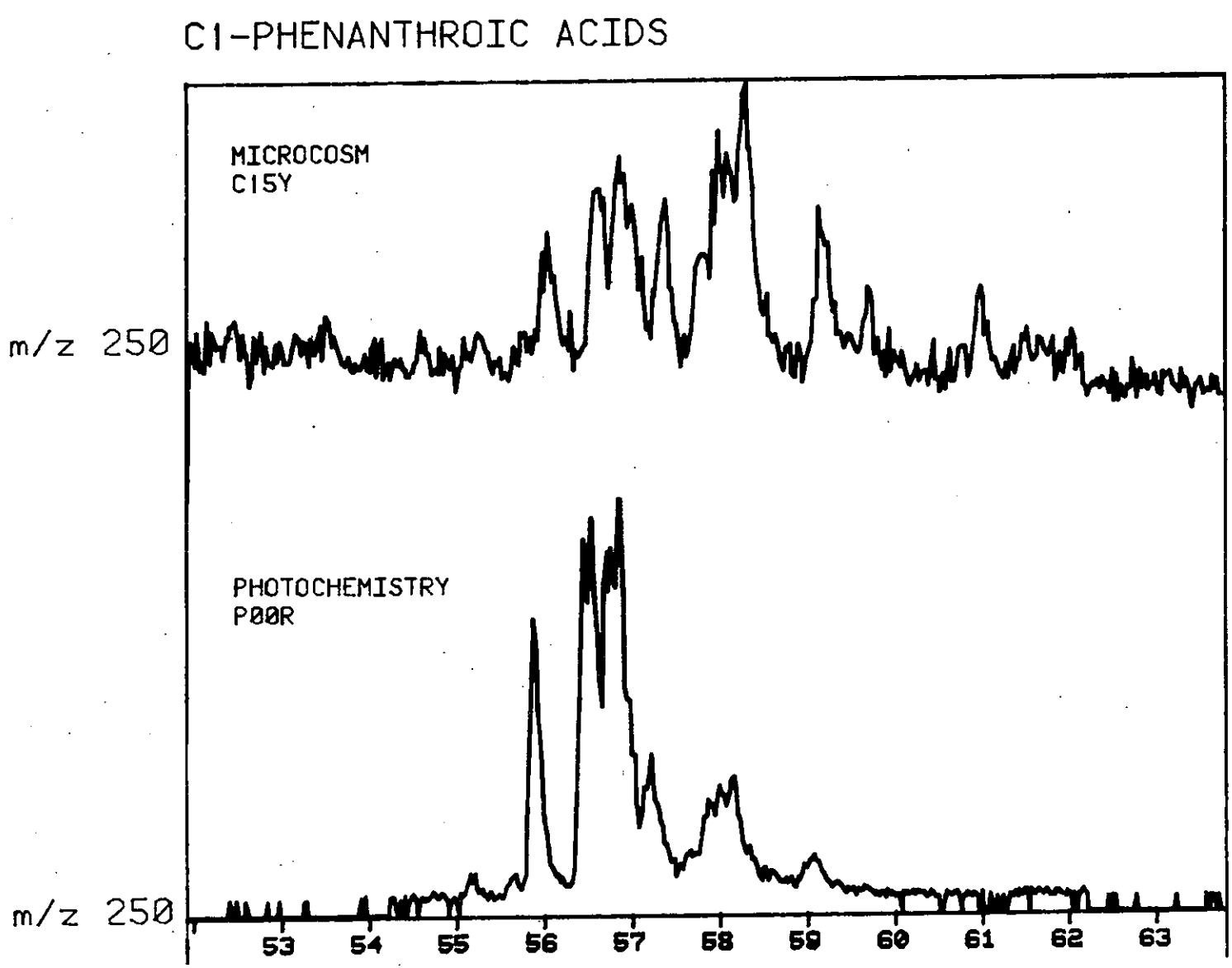

Figure 28. Extracted ion current profiles from the GC^2MS analyses of: top methylated acidic extract from a microcosm experiment utilizing fresh wellhead oil after seven days of incubation; bottom-methylated acidic extract of the water column sample from a simulated environmental photooxidation experiment after exposure to 32 hrs of bright sunlight. 250 is characteristic of the parent ions in the mass spectra of phenanthroic acids.

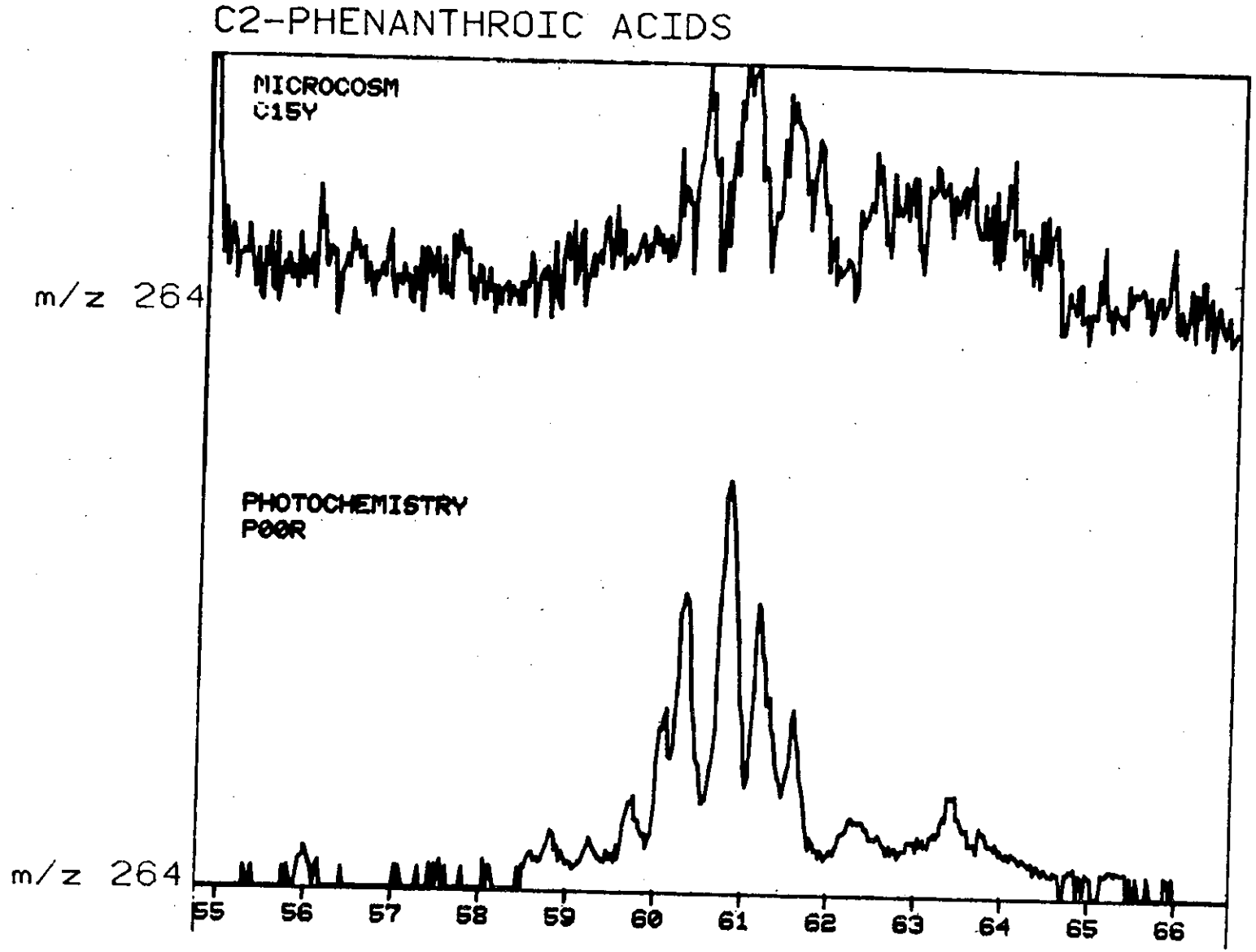

Figure 29. Extracted ion current profiles from the GC^2MS analyses of: top methylated acidic extract from a microcosm experiment utilizing fresh wellhead oil after seven days of incubation; bottom-methylated acidic extract of the water column sample from a simulated environmental photooxidation experiment after exposure to 32 hrs of bright sunlight. 264 is characteristic of the parent ions in the mass spectra of phenanthroic acids.

oil. A bimodal homolog distribution is observed for the alkyl naphthoic acids but not for the alkyl naphthalene homologs.

Figures 27 to 29 show the extracted ion current profiles for phenanthroic acid and its C_1 and C_2 homologs. The C_2 homologs were present only in very low concentrations. The ions used are characteristic of the parent ions for these compounds.

It is important to recognize that standard compounds are not available for most of these alkyl aromatic acids, and their mass spectra do not contain enough structural information to identify specific homologs. These data are presented to illustrate the differences between microbial and photooxidation processes when using identical starting oil. Identification of specific isomers must await further research.

2.4 Whole-Water-Column Samples

The acid extracts of whole-water-column samples were analyzed by GC^2MS techniques, and numerous oxidized hydrocarbons were identified. In general, the major oxidized compounds were fatty acids and esters of phthalic acid. Several whole-water samples appeared to contain elevated levels of these substances, along with other oxidized hydrocarbons. For example, Figure 30 shows the chromatographic data from the methylated acidic extract of a whole-water sample collected at PIX10. The sample contained elevated levels of fatty acids and phthalates when compared to other samples collected in the vicinity of the blowout. It contained many other oxygenated hydrocarbons in addition to many phthalate esters not normally found in Gulf waters (Giam, 1977). Table 3 lists the esters of phthalic acid found in the sample. Those esters commonly found in marine and other samples are indicated with asterisks. The source of these numerous phthalate compounds is unknown, although they appear to be associated with anthropogenic activity. The use of dispersants or other surfactants near the site or time of sampling had not been reported. However, a petroleum-based Mexican product, Kay Dispersant, was sprayed from a boat approximately 15 miles from the wellsite (G. P. Lindblom, private communication), but the time of application has not yet been determined. The product was not sprayed during the time that these samples were obtained. Phthalate compounds are presumably useful as dispersants and may have originated from this or other applications in the area of the wellhead. The sample contained evidence of other oxidized hydrocarbons, but because of the presence of the large quantities of phthalate esters, the source of these oxidized aromatic hydrocarbons is uncertain. The sample extract also contained low-molecular-weight fatty acids similar to those obtained from laboratory photolysis of IXTOC oil. The concentration of these fatty acids was very low. Thus the concentrations of other oxidation products are expected to be below detection limits, using the quantity of sample collected in the field.

After preliminary analysis of data from water column samples and the photooxidation experiments, we hypothesize that hydrocarbons from the IXTOC oil are being degraded by the action of sunlight at the water's surface. The hydrocarbons may be oxidized through the action of triplet oxygen or by some

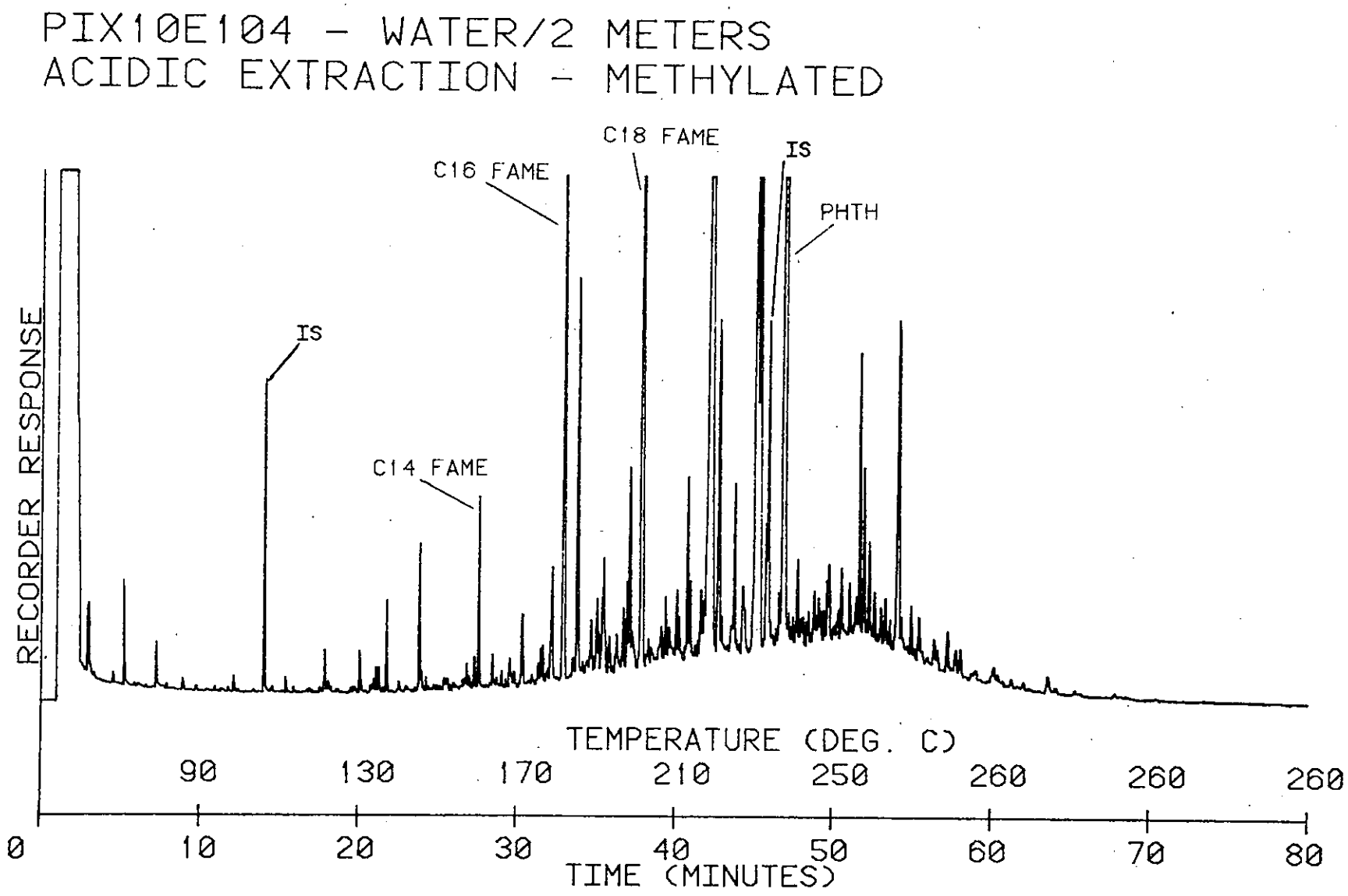

Figure 30. Glass capillary gas chromatographic data from methylated acid extract of a whole water sample collected at PIX 05.

Table 3. Phthalate esters identified in PIX 10E104 (2 m).

*Bismethyl phthalate
Bisethyl phthalate
Methylpentyl phthalate
Ethyl alkyl phthalate
Bis(2-methyl)propyl phthalate
*Bisbutyl phthalate
Ethylbenzyl phthalate
Methylhexyl phthalate
Butyloctyl phthalate
Alkyl benzyl phthalate
*Bis(2-ethylhexyl) phthalate
Bisoctyl phthalate

*Phthalate esters observed at 2 m in control stations and laboratory experiments.

type of free radical reaction. Oxidation would increase the polarity of the hydrocarbons and cause them to become more water soluble. Because of their enhanced water solubility, the oxidized products become diluted in the water column to below ordinarily detectable levels. We believe that the 20-liter water samples collected at most stations are probably marginal with respect to sample size for analysis of oxygenated hydrocarbons. A combination of larger sample sizes and more efficient extraction techniques should be applied in future research efforts to find photooxidized products of petroleum in the marine environment.

3. SUMMARY

These data, as stated above, have yet to be fully interpreted, and additional analyses and experiments are needed to obtain a reasonably complete understanding of the role of photochemical and microbial reactions in weathering of spilled oil. However, the data and initial interpretations present clear evidence for the formation of oxygenated compounds during such reactions. While these oxidations were suspected, as stated in the Introduction, analytical chemistry evidence for most of the compounds reported here was limited or nonexistent before our investigations.

The similarity of classes of compounds resulting from microbial and photochemical attack on mixtures of petroleum compounds is an important finding. The differences in the relative distributions within these classes of compounds (i.e., the benzoic and naphthoic acids) demonstrate that the pathways of reactions leading to the compounds are specific for particular types of reactions.

Clearly the biological and photochemical processes can occur simultaneously during and after oil spills in the field. This is "a priori" a complicated set of interweaving reactions. The control experiences reported here and the few field measurements for oxygenated reaction products comprise an initial step in what must be a long series of experiments and investigations. These experiences are important not only to predictive or hindcast modeling of the fate of petroleum compounds, but also, as indicated in the Introduction, to understanding short-term and long-term effects of oil on marine organisms or ecosystems.

4. ACKNOWLEDGMENTS

The authors would like to thank Maryann Maberry, Shelley Antoine, Rene Surgi, Cathy Cummings, Albertina Rhyans, Larry Clinton, Patrick Remele, and Frank Stone for technical assistance; Paulette Brooks and Diane Trembley for typing the manuscript; Richard Berry and Ildefonso DeLeon for editorial assistance; Fred Pfeander and Earl Buckley for samples from the microcosm experiments, and Don Atwood and George Harvey of AOML for technical support. This work was partially supported by NOAA contract number NA 79RAC00145.

5. REFERENCES

Armstrong, F. A. J., P. M. Williams, and J. D. H. Strickland (1966): Photooxidation of organic matter in sea water by ultra-violet radiation, analytical and other applications. Nature, 211: 481-483.

Berridge, S. A., R. A. Dean, R. G. Fallows, and R. Fish (1968): The properties of persistent oils at sea. J. Inst. Petrol., 54:

Burwood, R., and G. C. Speers (1974): Photooxidation as a factor in the environmental dispersal of crude oil. Estuar. Coastal Mar. Sci., 2: 117-135.

Freegrade, M., C. G. Hatchard, and C. A. Parker (1971): Oil spill at sea: Its identification, determination and ultimate fate. Laboratory Practice, 20: 35-40.

Giam, C. S., Ed. (1977): Pollutant effects on marine organisms. Lexington Books, Massachusetts, Toronto: 32-33.

Kawahara, R. K. (1969): Identification and differentiation of heavy residual oil and asphalt pollutants in surface waters by comparative ratios of infrared absorbences. Environ. Sci. Technol., 3: 150-153.

Larson, R. A., L. L. Hunt, and D. W. Blankenship (1976): Toxic hydroperoxides: Photochemical formation from petroleum constituents. AIBS Symp. on Sinks of Hydrocarbons in the Aquatic Environment, Washington, D.C.

Majewski, J., and J. O'Brien (1974): A kinetic study of fuel oil undergoing photochemical weathering. Environ. Lett., 7: 145-161.

National Academy of Sciences (1973): Petroleum in the marine environment. Workshop on Inputs, Fates and Effects of Petroleum in the Marine Environment, Airlie, Virginia, May 21-25.

Overton, E. B., J. R. Patel, and J. L. Laseter (1979): Chemical characterization of samples from the AMOCO CADIZ oil spill. 1979 Oil Spill Conference (Prevention, Behavior, Control, Clean-up).

Patel, J. R., S. W. Mascarella, E. B. Overton, and J. L. Laseter (1979): Monitoring the photooxidation of crude oil by gas chromatography-mass spectrometry system. Extracted ion current profiles of dibenzothiophenes and their sulfoxides. Presented at 27th Annual Conference on Mass Spectrometry and Allied Topics, Amer. Society of Mass Spectrometry, Seattle.

Patel, J. R., J. McFall, G. W. Griffin, and J. L. Laseter (1978): Toxic photogenated products generated under environmental conditions from phenanthrene. EPA Symp. on Carcinogenic Polynuclear Aromatic Hydrocarbons in the Marine Environment, Pensacola Beach, Florida, August 14-18, 1978.

Pilpel, N. (1973): Sunshine on a sea of oil. New Scientist, 59: 636-644.

Scheier, A., and D. Gominger (1976): A preliminary study of the toxic effects of irradiated vs. non-irradiated water soluble fractions of #2 fuel oil. Bull. Environ. Contam. Toxicol., 16: 595-603.

Zafiriou, O. C. (1977): Marine organisms photochemistry previewed. Mar. Chem., 5: 497-522.

CHEMISTRY AND NATURAL WEATHERING OF VARIOUS CRUDE OIL FRACTIONS FROM THE IXTOC-I OIL SPILL

Alfonso V. Botello and Sylvia Castro-Gessner
Centro de Ciencias del Mar y Limnologia, UNAM
Apartado Postal 70 - 305
Mexico 20, D.F.

ABSTRACT

The preliminary results of the natural weathering of the crude oil spilled by the IXTOC-I well in the Campeche Bank area is presented. Glass capillary gas chromatography analyses were done on the saturated and aromatic fractions of the original crude oil, and the presence of certain compounds were confirmed by the GC-MS coupled system.

The results show that the samples collected in the vicinity of the spill have 95% or more of the total hydrocarbons, in contrast with some other samples that lost up to 60% in hydrocarbon content due to the high natural weathering process.

1. INTRODUCTION

The introduction of chemical pollutants to the marine environment represents a serious problem for mankind, and also for the marine ecosystem with which mankind is closely related.

In recent years much information has been published about the dispersion in the marine environment of pollutants such as heavy metals, pesticides, and industrial chemical wastes that have been detected in zones as far as the Antarctic (Goldberg, 1976). In the present day the introduction of fossil hydrocarbons to the marine environment is of great importance, due primarily to the recent accidental oil spills.

Mexico, in the midst of its increasing industrialization and exploitation of its natural and mineral resources, could not avoid an accident such as the spill of the IXTOC-I well on the Campeche Bank. Since then, the spill has liberated great quantities of crude oil into the Gulf of Mexico.

In countries located in the temperate and cold zones where the great majority of oil accidents have occurred, much scientific literature has been published, and the effects (some of them harmful) of the fossil hydrocarbons on marine organisms have been analyzed (Blumer et al., 1970; Blumer and Sass, 1972; Gordon and Prouse, 1973; Jacobson and Boylan, 1973; Parker and Menzel, 1974; Pulich et al., 1974). In the case of Mexico the results cannot be compared easily with those of other geographic areas since this was the first spill in a tropical zone where the oceanographic and biological conditions are not equivalent to those in other latitudes.

2. MATERIALS AND METHODS

The samples of crude oil analyzed were collected near the IXTOC-I well and at different distances from the spill during an oceanographic cruise conducted by the staff of the Centro de Ciencias del Mar y Limnologia, University of Mexico, July 20-24, 1979. The ship used was the ONJUKU, belonging to the Departamento de Pesca (Figure 1).

After collection, the samples were separated and purified in hydrocarbon fractions, principally the saturated and aromatic fractions, using a chromatographic column 60 cm long by 3 cm wide, packed with silica gel (Woelm) with grade 1 activity. The fractions were eluted with 500 ml of hexane, 500 ml of benzene, and 500 ml of methane, respectively. After the elution the fractions were dried completely to obtain the dry weight of each of them, as well as the percent concentrations of crude oil in the original samples.

The analysis of the fractions was determined by gas chromatography, using a Perkin-Elmer Model 910 chromatograph. It was equipped with an ionization flame detector and a capillary column 30 m long and 0.25 mm internal diameter which was siliconized with OV-101. This instrument was equipped with a linear temperature programmer which was programmed from 70° to $255^{o}C$ with an increase of $3^{o}C$/minute.

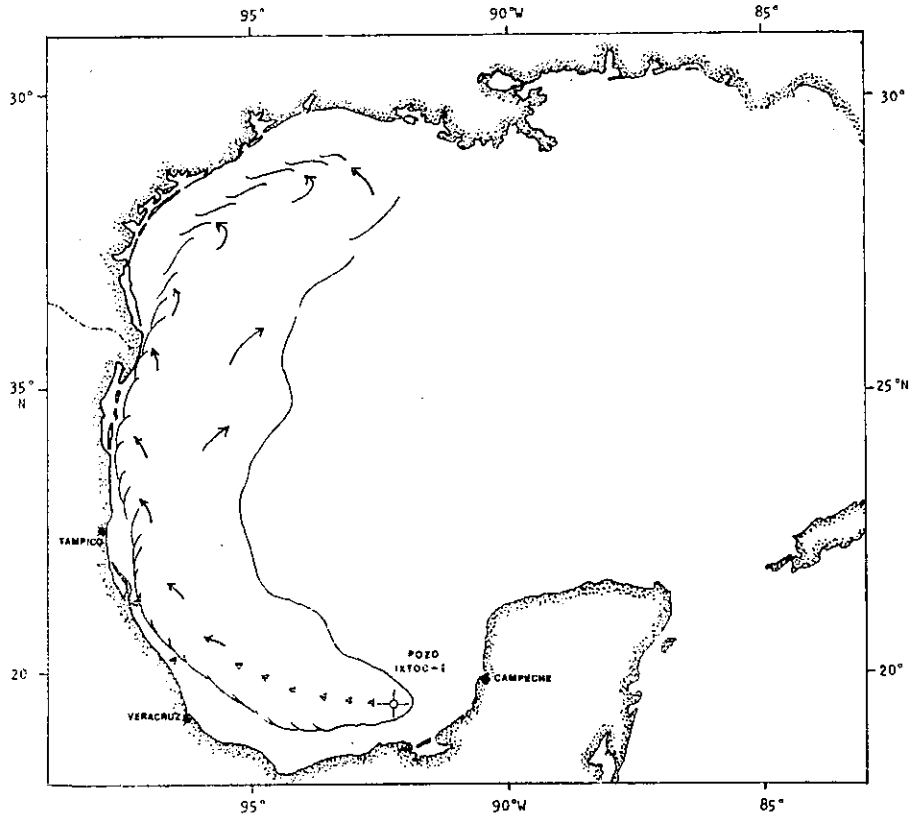

Figure 1. Sampling sites for the crude oil spilled by the IXTOC-I well in the Campeche Bank area.

A Finnigal GC-MS Series 4000 (Incos Data System) was used to identify the structure of the isomeres present in the samples and to confirm the presence of some polycyclic aromatic compounds. The temperature was programmed from $80^{o}C$ up to $250^{o}C$ using a 60 m glass capillary column WCOT (SP 2100).

3. RESULTS AND DISCUSSION

Table 1 gives the percent composition of saturated and aromatic hydrocarbons in samples of different "ages" or residence time in the Gulf of Mexico, from those collected near the spill to those collected approximately seven or eight weeks after their arrival on the north coasts of Veracruz and Tampico. The samples collected near the origin of the spill contain approximatley 95% of the total hydrocarbons (saturated and aromatic fractions). The percentage decreases as the distance increases from the origin of the spill, losing up to 60% or more of the total hydrocarbons. This is true especially of those samples that have remained for a long time in the sea. This is important from an ecological point of view since the weathering or natural degradation that acts upon the spilled crude oil in the Gulf of Mexico is high if compared with the spills that have occurred in temperate and cold zones. In the latter zones, weathering is low and so the hydrocarbons remain for years in these latitudes (Blumer and Sass, 1972; Sanders et al., 1972; Gundlach, 1977; Keizler et al., 1978).

Since the IXTOC-I oil spill occurred in a tropical area (Bank of Campeche), there are factors that produce high weathering when interacting, the most important being

(1) Evaporation
(2) High photochemical oxidation
(3) Intense solar radiation
(4) High temperatures
(5) Great metabolic activity of marine organisms

The above observations agree with those of Blumer et al. (1973) and Butler (1975) and seem to be confirmed by the analysis of the crude oil chromatograms of the nearly original fractions (40 hours after the spill) and those that arrived on the Tampico coasts after eight weeks.

Figure 2 shows the saturated fraction chromatogram containing the normal paraffins, from those with a low molecular weight such as the n-undecane (C_{11}), to n-pentatriacontane (C_{35}), the highest peak being n-tridecane (C_{13}). The isoprenoids pristane and phytane are also present. The pristane/phytane ratio was 1.2 and the OEP value (odd-even predominance) was 1.0, which agrees with previously reported values for the crude oils that have not had a remarkable weathering (Scalan and Smith, 1970).

After seven weeks we observe in the saturated fraction the almost total loss of the normal paraffins with carbon chains C_{11} to C_{15} (only those with C_{16} to C_{31} carbons) remaining in the collected tars (Figure 2B). This loss coincides with the results obtained by Macko et al., (1980), following the behavior of a spill that occurred along the Texan coast. After fifteen weeks, the saturated fraction degraded up to 90% of its original components. Paraffins with high molecular weights, C_{25} to C_{32}, remained.

Table 1. Hydrocarbon Percent Composition of the Various Crude Oil Samples from the IXTOC-I Spill.

Sample No.	% Saturates	% Aromatics	% Total Hydrocarbons	Age
1	45	52	97	40 hours
2	52	34	88	1 week
3	41	35	76	1-1/2 weeks
4	30	46	76	2 weeks
5	19	15	34	6 weeks
6	15	13	28	7 weeks
7	11	13	24	8 weeks

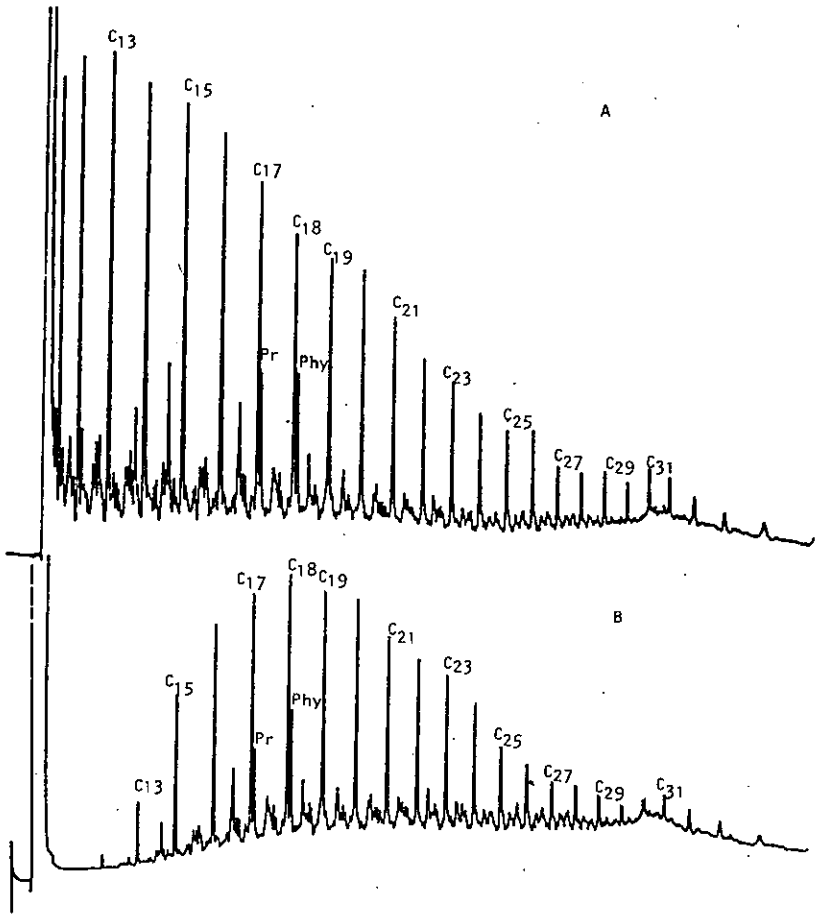

Figure 2. Gas chromatograms of the saturate fraction of a mousse sample collected 40 hours after the IXTOC-I blowout (A) and in Tampico Beach after seven weeks (B).

The aromatic fraction (Figure 3) is composed of aromatic hydrocarbons such as benzene, naphthalenes, phenantrenes, and their methyl-substituted homologs. Biphenyl groups, fluorene and dibenzothiophenes are also present. Besides these compounds a complex mixture of unresolved and unidentified (UCM) small peaks are observed.

With regard to the aromatic fraction which represents the greatest ecological importance due to its high toxicity, it is observed in the chromatograms (Figure 3b) that after seven weeks the light aromatic compounds have been almost totally lost. The compounds are primarily those belonging to the group of naphthalenes, that due to their solubility, are highly toxic for the marine organisms, especially for the planktonic and benthic species (Vernberg and Vernberg, 1974; Lockwood, 1976).

Therefore, the aromatic fraction shows an evolutionary pattern different from that of the saturated fraction since there is a very rapid loss of benzenes and naphthalenes primarily. Nevertheless, the most substituted compounds (C_3-naphthalenes and C_3-phenanthrenes) remain in the analyzed samples for longer periods of time than their original compounds or their analogous less substituted compounds; moreover, there is a remarkable increase in the mixture of unresolved peaks (UCM). The degrading patterns of both fractions (aromatic and saturated) are similar to those previously reported by other authors (Mayo et al., 1978; Teal et al., 1978), but in the samples from the IXTOC-I well the loss of the different compounds seems to be much more rapid.

Gibson (1977) suggests that the decrease in the aromatic compounds is the result of a combination of factors, such as dissolution, diffusion, evaporation, absorption on sediments, and attack by microorganisms. Other important factors that are apparent in tropical seas are photooxidation and transport due to water and wind currents.

Figures 4 ans 5 show the chromatograms of the aromatic fractions, obtained in the GC-MS coupled system (Finigan 4000 Incos Data System), corresponding to the samples with less residence time (40 hours) in the ocean (Figures 4a and 5a), compared with those that already present a certain degree of weathering (four weeks; Figure 4b), and those collected in the northern part of Veracruz with approximately ten weeks of residence time (Figure 5b). A high content of aromatic compounds is characteristic in the samples, mainly benzene-substituted compounds (methyl-, dimethyl-, and trimethyl-naphthalenes), phenantrenes, anthracenes, thiophenes, dibenzothiophenes, and its methyl-substituted homologous (methyl-, dimethyl-, and trimethyl-dibenzothiophenes).

It is remarkable that, after four weeks, and even eleven weeks, of weathering of the samples, a high proportion of these compounds is lost; however, they remain in low concentrations in the samples due to their high chemical stability as detected in the chromatograms through the GC/MS coupled system. The peaks for naphthalene (M/E = 128), methylnaphthalene (M/E = 142), dimethylnaphthalene (M/E = 156), and trimethylnaphthalene (M/E = 170) are shown in Figure 6. Figure 7 shows the peaks corresponding to phenantrene (M/E = 178), dibenzothiophene (M/E = 184), methylphenantrene (M/E = 192), methyldibenzothiophene (M/E = 198), dimethylphenantrene (M/E = 206), dimethyldibenzothiophene (M/E = 212), trimethylphenantrene (M/E = 220), and trimethyldibenzothiophene (M/E = 226). Figures 8 and 9 represent the mass spectra for

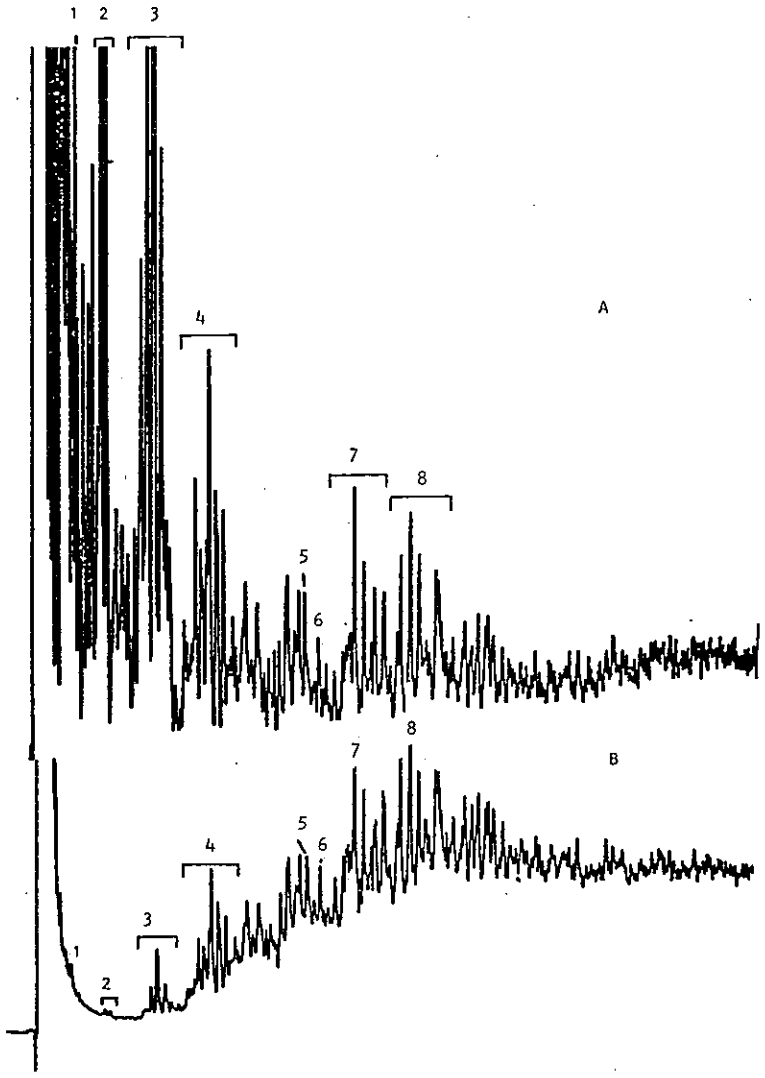

Figure 3. Gas chromatograms of the aromatic fraction of a mousse sample collected 40 hours after the IXTOC-I blowout (A) and in Tampico Beach after seven weeks (B).

1 = naphthalene; 2 = methylnaphthalenes; 3 = dimethylnaphthalenes; 4 = trimethylnaphthalenes; 5 = dibenzothiophene; 6 = phenantrene; 7 = methylphenatrenes, methyldibenzothiophenes; 8 = dimethylphenantrenes, dimethyldibenzothiophenes.

Figure 4.

GC/MS chromatogram of the aromatic fraction corresponding to samples with 40 hours (A) and four weeks (B) of residence time in the Gulf of Mexico waters.

1 = naphthalene; 2 = methylnaphthalene; 3 = dimethylnaphthalenes; 4 = trimethylnaphthlenes; 5 = dibenzothiophene; 6 = phenantrene; 7 = methylphenantrenes, methyldibenzothiophenes; 8 = dimethylphenantrenes, dimethyldibenzothiophenes; 9 = dimethylbenzothiophenes; 10 = dimethylphenantrenes; 11 = trimethylbenzothiophenes; 12 = trimethylphenantrenes.

Fig. 4

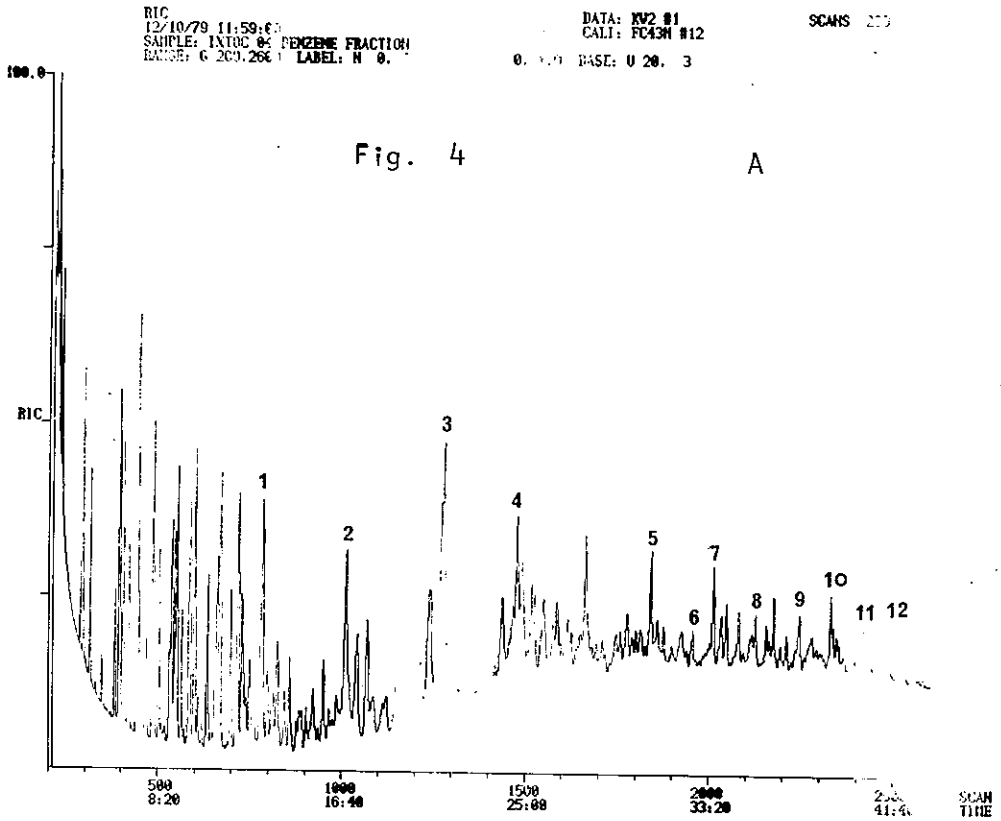
RIC
DATA: KV2 #1
CALI: FC43M #12
SCANS
BASE: U 20. 3
100.0
RIC
1
2
3
4
5
6
7
8
9
10
11
12
500
8:20
1000
16:40
1500
25:00
2000
33:20
SCAN
TIME

A

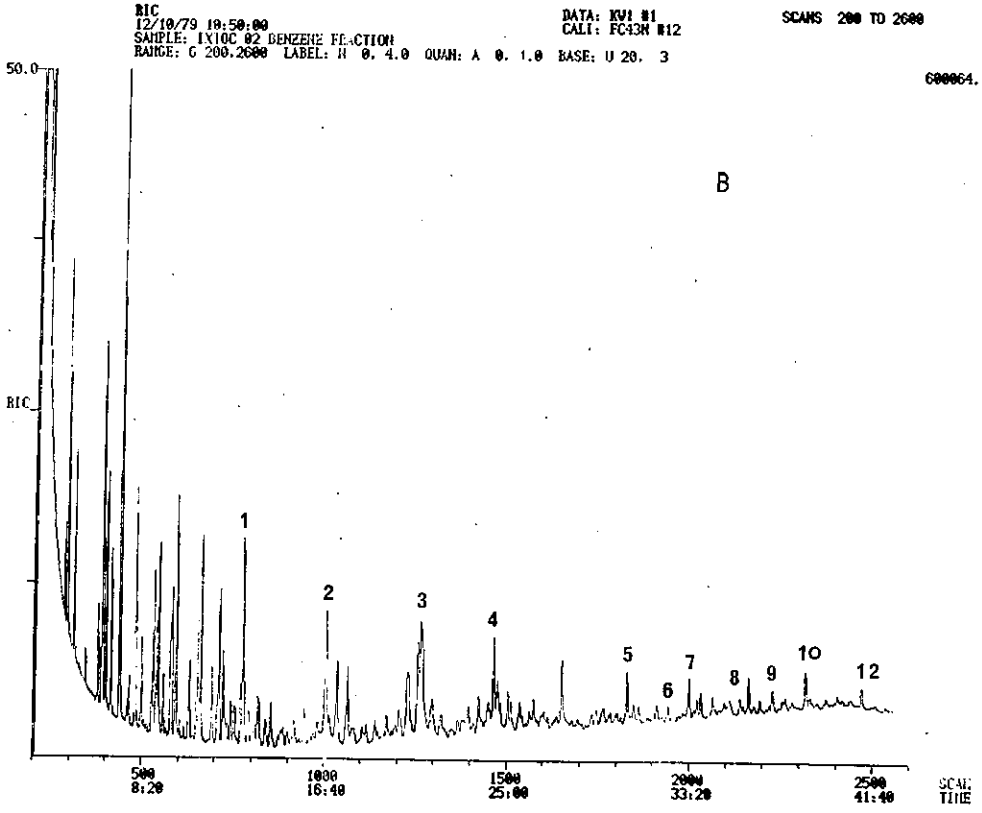
RIC
12/10/79 10:50:00
SAMPLE: IX10C 02 BENZENE FRACTION
RANGE: G 200.2600 LABEL: H 0. 4.0 QUAN: A 0. 1.0 BASE: U 20. 3
DATA: KV1 #1
CALI: FC43M #12
SCANS 200 TO 2600
600864.
50.0
RIC
1
2
3
4
5
6
7
8
9
10
12
500
8:20
1000
16:40
1500
25:00
2000
33:20
2500
41:40
SCAN
TIME

B

Figure 5.

Chromatogram of the aromatic fractions corresponding to samples with 40 hours (A) and ten weeks (B) of residence time in the Gulf of Mexico waters.

1 = naphthalene; 2 = methylnaphthalene; 3 = dimethylnaphthalenes; 4 = trimethylnaphthalenes; 5 = dibenzothiophene; 6 = phenantrene; 7 = methylphenantrenes, methyldibenzothiophenes; 8 = dimethylphenantrenes, dimethyldibenzothiophenes; 9 = dimethylbenzothiophenes; 10 = dimethylphenantrenes; 11 = trimethylbenzothiophenes; 12 = trimethylphenantrenes.

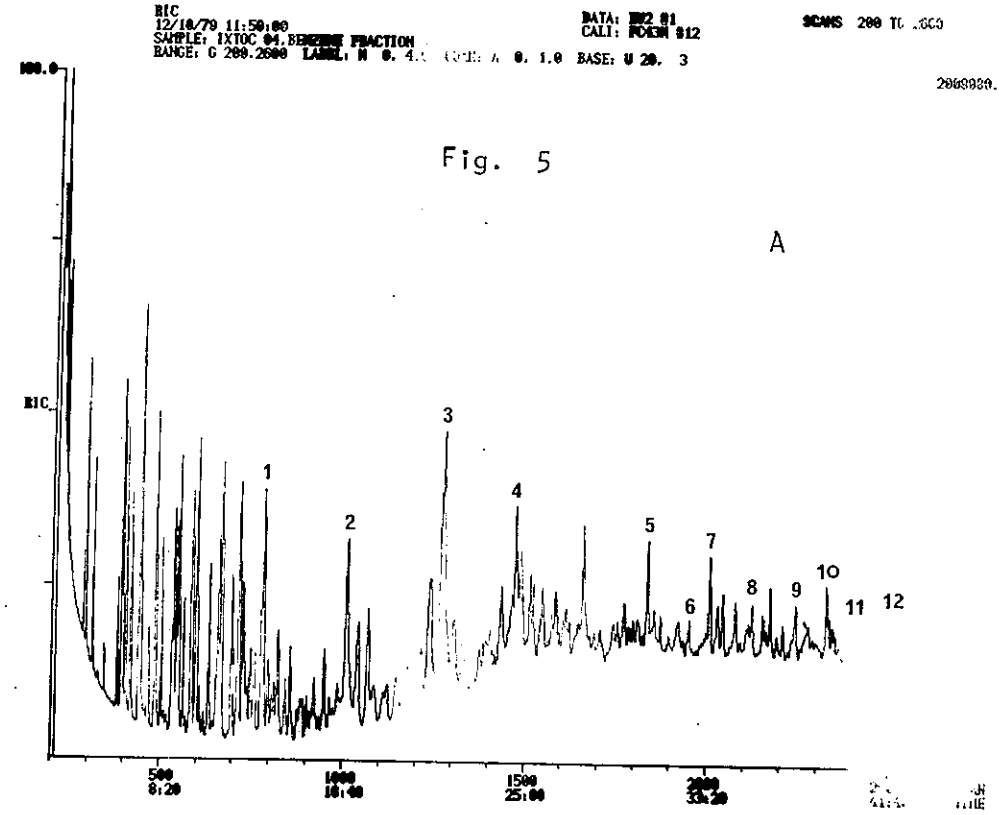
RIC
12/10/79 11:50:00
SAMPLE: IXTOC 04.BENZENE FRACTION
RANGE: G 200.2600 LABEL: N 0. 4.
BASE: U 20. 3
SCANS 200 TO
2009930.
100.0
RIC
1
2
3
4
5
6
7
8
9
10
11
12
500
8:20
1000
16:40
1500
25:00
2000
33:20

Fig. 5

A

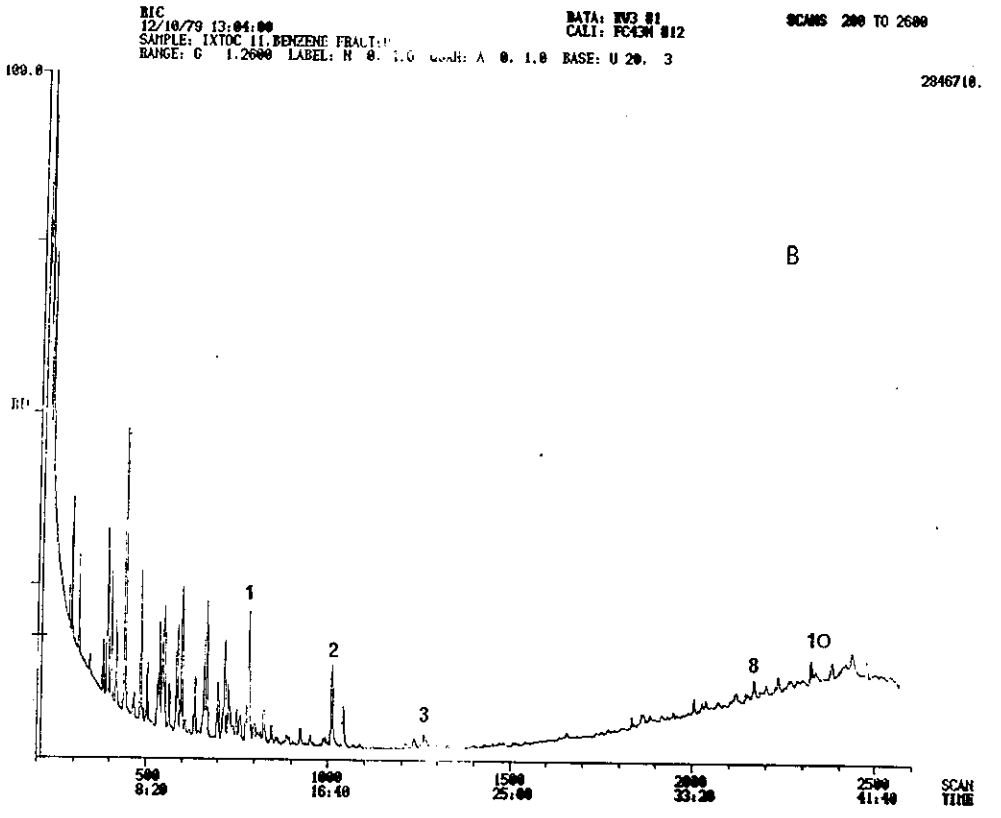
RIC
12/10/79 13:04:00
SAMPLE: IXTOC 11.BENZENE FRACT
RANGE: G 1.2600 LABEL: N 0. 1.0
BASE: U 20. 3
SCANS 200 TO 2600
2846710.
100.0
1
2
3
8
10
500
8:20
1000
16:40
1500
25:00
2000
33:20
2500
41:40
SCAN
TIME

B

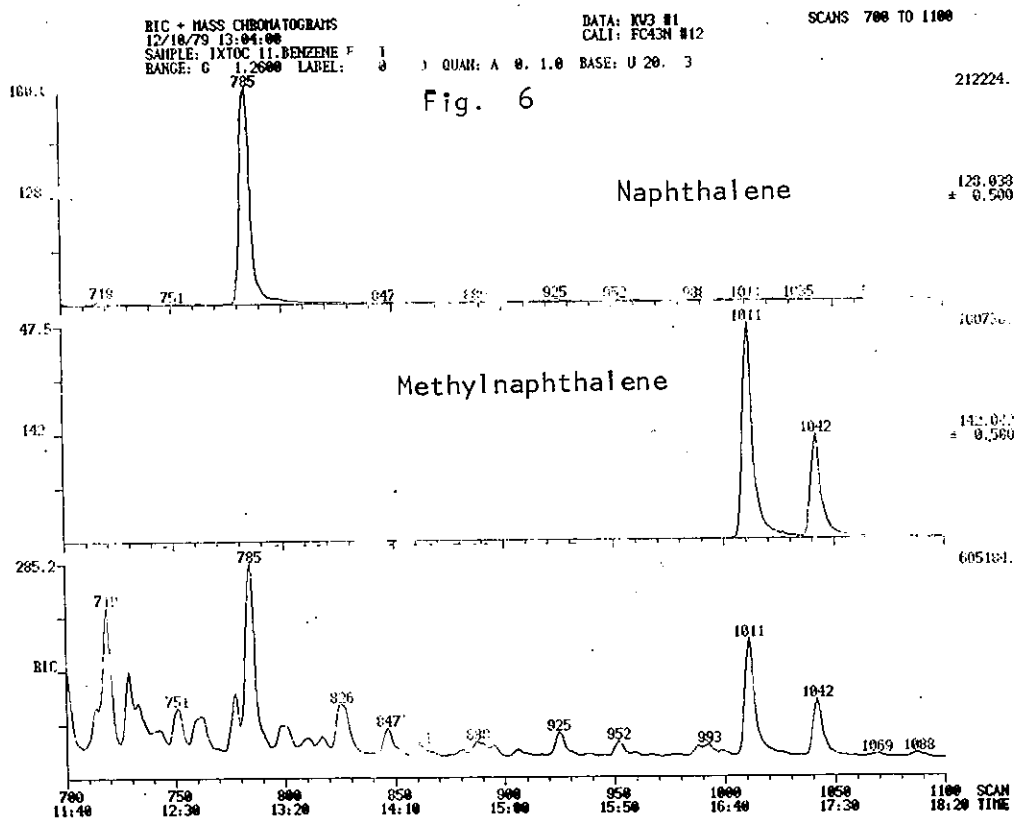
Naphthalene
Methylnaphthalene
BIC
SCAN TIME

Fig. 6

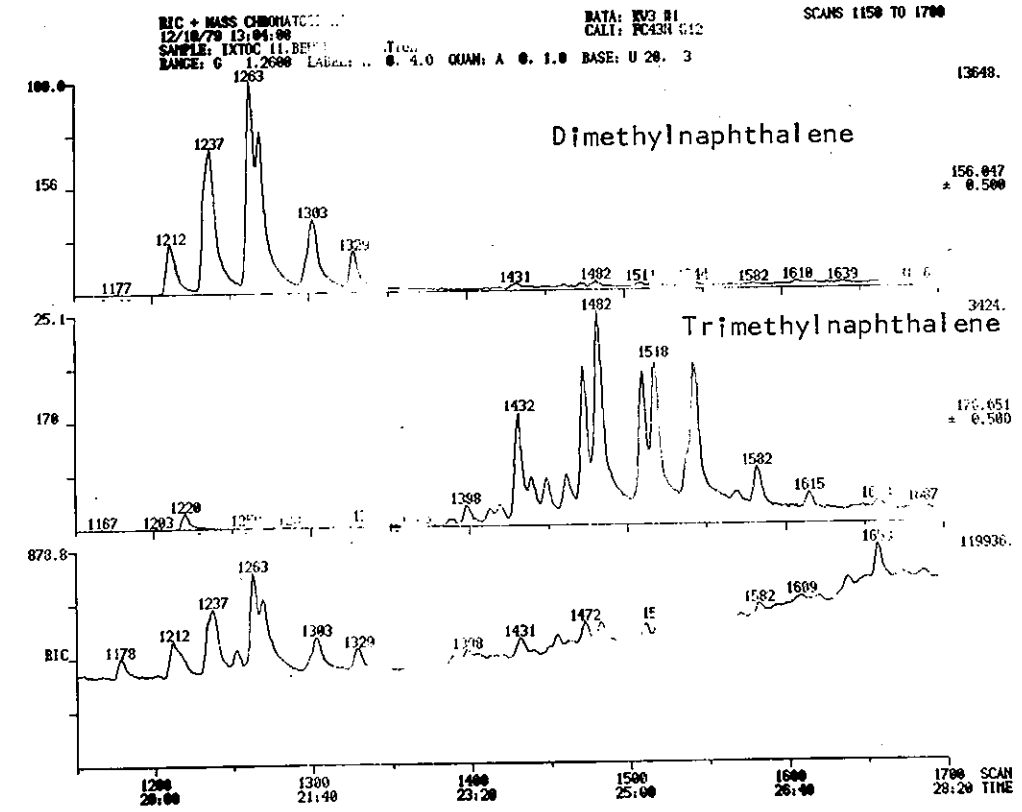
Dimethylnaphthalene
Trimethylnaphthalene
BIC
SCAN TIME

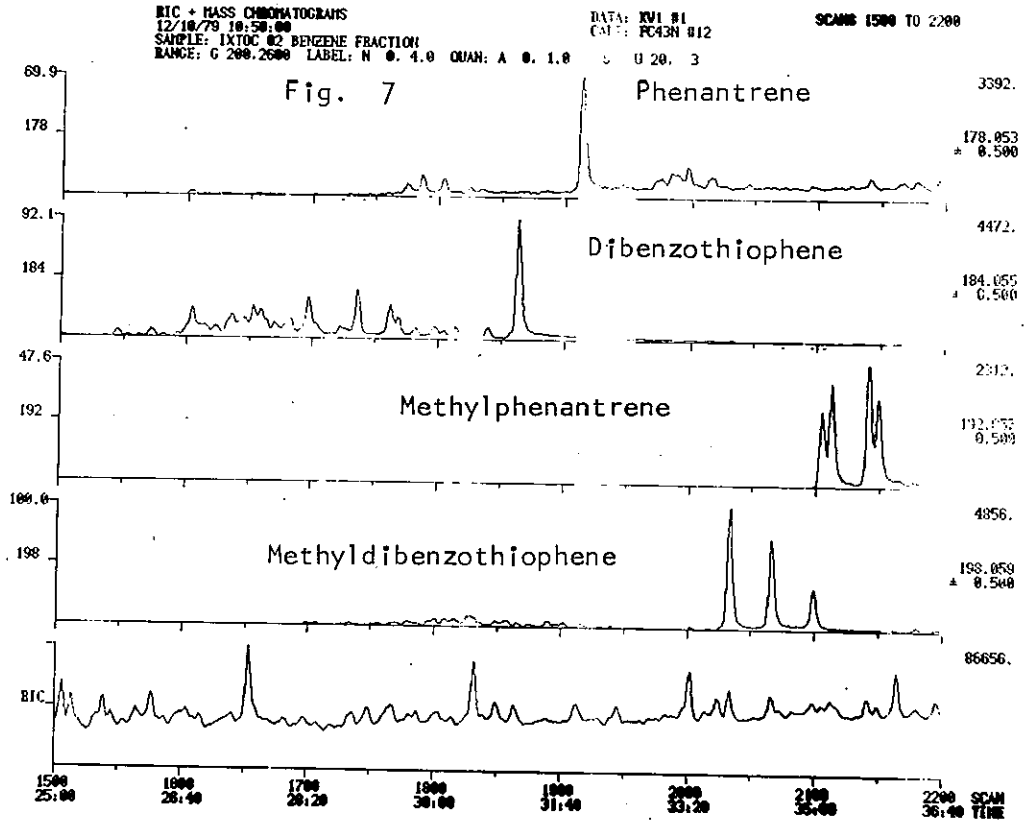
Fig. 7
Phenantrene
Dibenzothiophene
Methylphenantrene
Methyldibenzothiophene
BIC
SCAN TIME

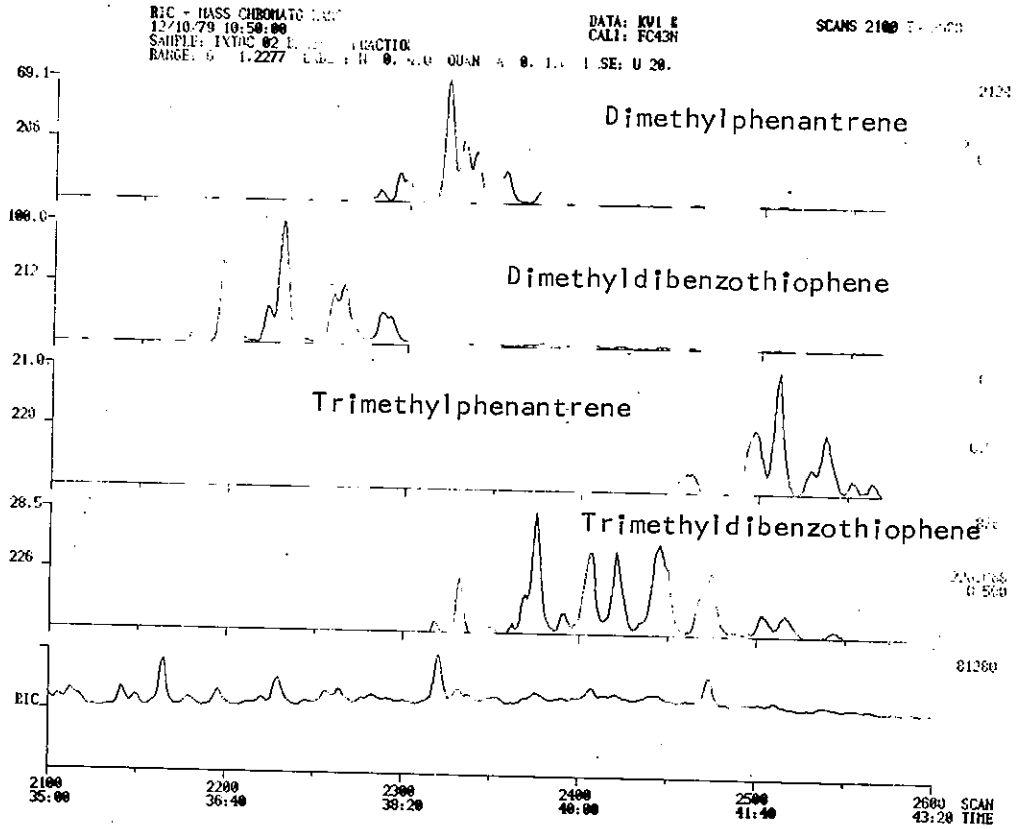
Dimethylphenantrene
Dimethyldibenzothiophene
Trimethylphenantrene
Trimethyldibenzothiophene
BIC
SCAN TIME

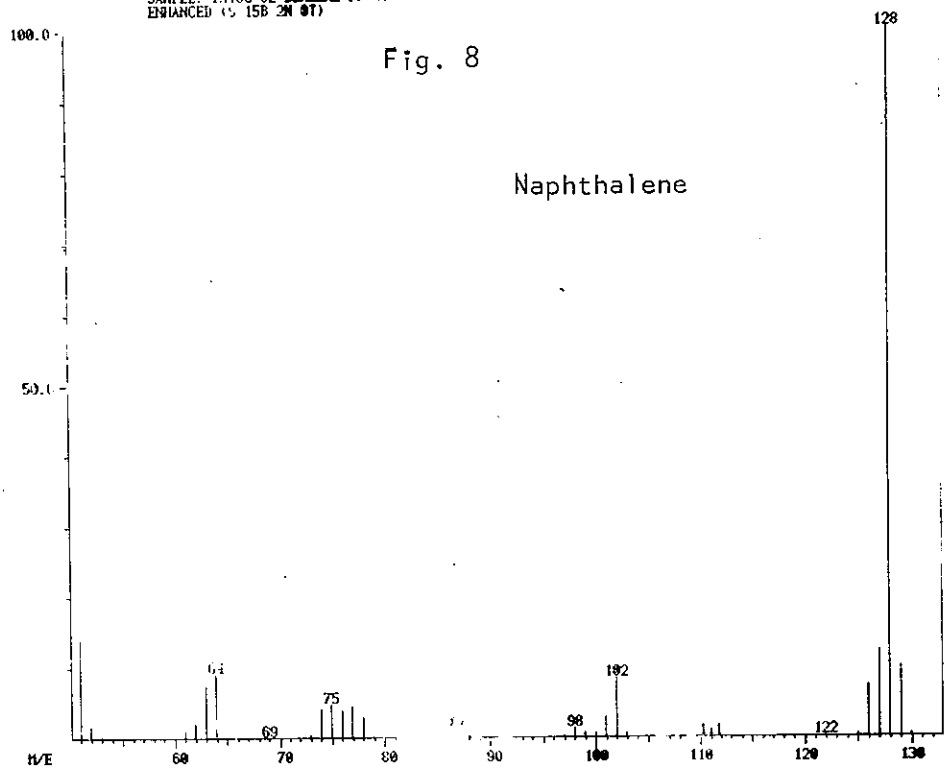
MASS SPECTRUM
12/10/79 10:50:00 + 12:58
SAMPLE: IXTOC 02 BENZENE FRACT
ENHANCED (5 15B 2N 0T)
DATA: KV1
CALI: FC43
BASE M/E: 128
RIC: 106012.
Naphthalene
128
102
75
69
98
122
M/E
60
70
80
90
100
110
120
130

Fig. 8

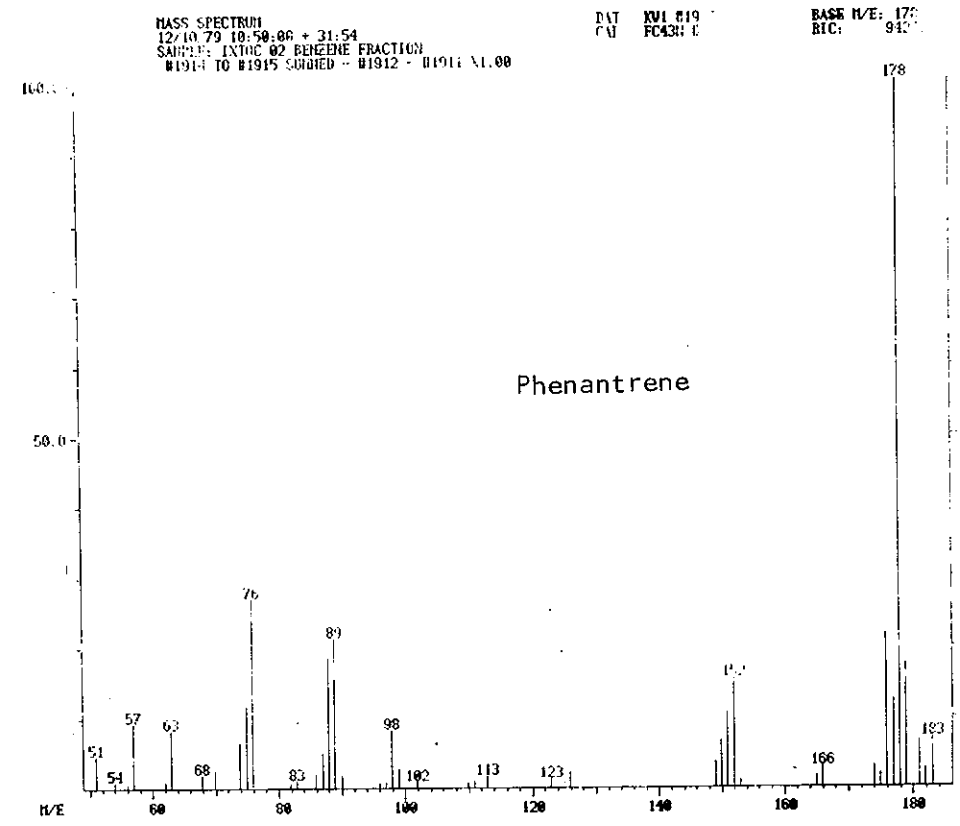
MASS SPECTRUM
12/10/79 10:50:06 + 31:54
SAMPLE: IXTOC 02 BENZENE FRACTION
DAT KV1 #19
CAL FC43
BASE M/E: 178
RIC:
Phenantrene
178
76
89
57
63
98
51
54
68
83
102
113
123
166
183
M/E
60
80
100
120
140
160
180

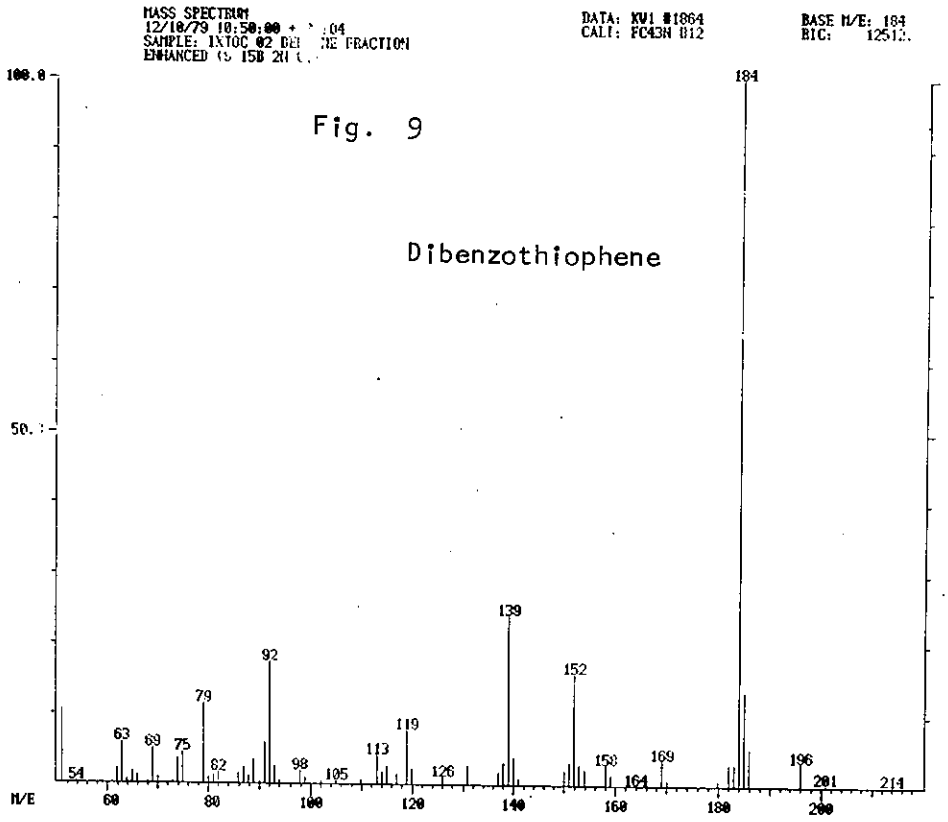

Fig. 9

Dibenzothiophene

naphthalene, phenantrene, and dibenzothiophene, respectively, from the sample with longer residence time. In spite of natural weathering acting upon this sample, the compounds previously mentioned remained unaltered during considerable periods of time (Macko et al., 1980).

Stable Isotope Ratio:

In regard to the values of the carbon isotopic ratio in the samples of spilled oil analyzed, we observe a rate of values from δC^{13} = -27.1 °/oo to -27.5 °/oo, the average being δC^{13} = -27.3 °/oo. Measurements also were done in the saturated and aromatic fractions from the original crude oil. Corresponding average values of δC^{13} = -27.7 °/oo for the saturated compounds (n-paraffins) and of δC^{13} = -27.1 °/oo for the aromatic compounds (Table 2).

All the values mentioned are in accordance with the values obtained by Calder and Parker (1968) for crude oils and gases such as butane, propane and ethane (δC^{13} = -25 °/oo to -32 °/oo), and with the reported values by the same authors for the products derived from the petrochemical industry (δC^{13} = -27.3 °/oo to -30.7 °/oo). The high natural weathering shown by the crude oil from the IXTOC-I well is relevant from the point of view of the hydrocarbon geochemistry, because its carbon isotope ratio was almost unaltered and its behavior was similar to that of the crude oil spilled along the Texas coasts (Macko et al., 1980). In that case, after two years of natural weathering the variation from the original crude oil was only 0.08 °/oo.

Table 2. δC^{13} Values for Representative Samples of Fresh and Weathered IXTOC-I Oil.

Sample No.	Whole Oil	Saturates	Aromatics	NSO*
1	-27.3	-27.8	-27.0	-26.8
2	-27.5	-27.6	-27.0	-26.8
3	-27.3	-27.6	-27.1	-27.1
4	-27.1	-27.7	-27.0	-27.1
5	-27.4	-27.6	-26.9	-26.8
6	-27.2	-27.5	-26.9	-26.7
7	-27.0	-27.4	-26.8	-26.4

δC^{13} = values reported relative to the PDB standard

*NSO = Compounds eluted from silica gel with methanol often containing nitrogen sulfur, or oxygen.

4. BIBLIOGRAPHY

Blumer, M., M. Erhardt, and J. H. Jones (1973): The environmental fate of standard crude oil. Deep-Sea Res., 20: 239-259.

Blumer, M., and J. Sass (1972): Oil pollution: Persistence and degradation of spilled fuel oil. Science, 176: 1120-1122.

Blumer, M., G. Souza, and J. Sass (1970): Hydrocarbon pollution of edible shellfish by an oil spill. Mar. Biol., 5: 195-202.

Butler, J. N. (1975): Evaporite weathering of petroleum residues: The age of pelagic tar. Mar. Chem., 3: 9-21.

Calder, J. A., and P. L. Parker (1968): Stable carbon isotope ratios as indices of petrochemical pollution of aquatic systems. Environ. Science and Tech., 2, p. 535.

Gibson, D. T. (1977): Biodegradation of aromatic petroluem hydrocarbons. In: Fate and Effects of Petroleum Hydrocarbons in Marine Ecosystems and Organisms. D. A. Wolfe (Ed.), Pergamon Press, Inc., New York: 36-46.

Goldberg, E. D. (1976): The Health of the Oceans. The UNESCO Press, Paris: 173 pp.

Gordon, D. C., Jr., and N. J. Prouse (1973): The effects of three oils on marine phytoplankton photosynthesis. Mar. Biol., 22: 329-333.

Gundlach, R. E. (1977): Oil tanker disasters. Environment, 19(9): 16-27.

Jacobson, S. M., and D. B. Boylan (1973): Effect of sea water soluble fraction of kerosene on chemotaxis in a marine snail. Nature, 241: 213-215.

Keizer, P. D., T. P. Ahern, J. Dale, and J. H. Vandermeulen (1978): Residues of Bunker C Oil in Chedabucto Bay, Nova Scotia, six years after the Arrow Spill. Jour. Fish. Board. Canada, 35(5): 528-535.

Lockwood, A. P. M. (Ed.) (1976): Effects of Pollutants on Aquatic Organisms. Cambridge University Press. Cambridge, England: 183 pp.

Macko, A. S., P. L. Parker, and A. V. Botello (1980): Persistence of spilled oil in a Texas salt marsh. Environ. Pollut., Series (B) (in press).

Mayo, D. W., D. S. Page, J. Cody, and E. Sorenson (1978): Weathering characteristics of petroleum hydrocarbons deposited in fine clay marine sediments, Searsport, Maine. Jour. Fish. Res. Board Canada, 35(5): 552-562.

Mironov, O. G. (1970): The effect of oil pollution on the flora and fauna of the Black Sea. FAO Tech. Conf. Mar. Poll. Rome, Paper E-92.

Parker, P. O. L., and D. Menzel (1974): Effects of pollutants on marine organisms. In: Workshop on Effects of Pollutants on Marine Organisms. Sydney, British Columbia, Canada, August 11-14, 1974: 46 pp.

Pulich, W., K. Winters, and C. Van Baalen (1974): The effects of a No. 2 fuel oil and two crude oils on the growth and photosynthesis of microalgae. Mar. Biol., 28: 87-94.

Sanders, H. L., J. F. Grassle, and G. R. Hampson (1972): The west Falmouth oil spill 1: Biology. Woods Hole Oceanographic Institute Tech. Rept. No. 72-20 (unpublished).

Scalan, R. S., and J. E. Smith (1970): An improved measure of the odd-even predominance in the normal alkanes of sediment extracts and petroleum. Geochim. Cosmochim. Acta., 34: 611-620.

Teal, J. M., K. Burns, and J. Farrington (1978): Analysis of aromatic hydrocarbons in intertidal sediments resulting from two spills of No. 2 fuel oil in Buzzards Bay, Massachusetts. Jour. Fish. Res. Board Canada, 35(5): 510-520.

Vernberg, F. J., and W. B. Vernberg (1974): Pollution and Physiology of Marine Organisms. The Academic Press: 492 pp.

MICROBIAL DEGRADATION OF HYDROCARBONS IN MOUSSE FROM IXTOC-I

Ronald M. Atlas, George Roubal, Anne Bronner, John Haines
Department of Biology
University of Louisville
Louisville, Kentucky 40292

1. INTRODUCTION

Microorganisms play a major role in the removal of hydrocarbon pollutants from marine ecosystems. Important factors that influence the rates of biodegradation include: the qualitative and quantitative composition of the microbial community; the chemical composition of the oil; the physical state of the oil; temperature; oxygen concentrations; and nutrient concentrations, especially nitrogen and phosphorus. For a general review of the interactions of microorganisms and petroleum hydrocarabons, see Bartha and Atlas (1977) or Colwell and Walker (1977). The present report deals specifically with a case study aimed at examining the role of microorganisms in the degradation of hydrocarbons in "mousse," i.e., the stable oil-water emulsion formed from the IXTOC-I well blowout in the Bay of Campeche, Gulf of Mexico.

2. MATERIALS AND METHODS

2.1 Sample Collection

Surface water samples (top 1 m) were collected during the period September 14-23, 1979, at 13 sites shown in Figure 1. Samples were collected with either a Niskin butterfly sterile water collector (General Oceanics, Miami, Florida) or a clean bucket in areas of heavy oil accumulation. Samples were visually examined and the presence of oil or mousse was recorded.

2.2 Enumeration of Microbial Populations

Total numbers of microorganisms per ml of surface water were determined by direct count procedures (Daley and Hobbie, 1975). Portions of collected water samples were preserved with formalin, 1:1. Microorganisms in the preserved samples were collected on a 0.2 μm pore size Nuclepore filter that had been stained with irgalan black. The microorganisms were stained with acridine orange and viewed using an Olympus epifluorescence microscope. Cells stained orange or green were counted in 20 randomly selected fields and the mean concentration was determined.

Hydrocarbon-utilizing microorganisms were enumerated using a three-tube Most Probable Number (MPN) procedure (Atlas, 1979). Serial dilutions of water samples, prepared using Rila marine salts solutions, were inoculated into sealed serum vials containing 10 ml of Bushnell Haas broth (Difco) and 20 μl of South Louisiana crude oil spiked with ^{14}C hexadecane (sp. act. 10 μCi/ml oil). After 14 days of incubation at 25°C, the $^{14}CO_2$ (if any) in the head space was collected by flushing and trapping in oxifluor CO_2 (New England Nuclear) and quantitated by liquid scintillation counting. Vials showing $^{14}CO_2$ production (counts significantly above background) were scored as positive and the Most Probable Number of hydrocarbon utilizers per gram dry weight were calculated from standard MPN tables.

2.3 Hydrocarbon Biodegradation Potentials

Five-ml portions of water samples were placed into serum vials containing 20 μl filter sterilized South Louisiana crude oil spiked with ^{14}C hexadecane,

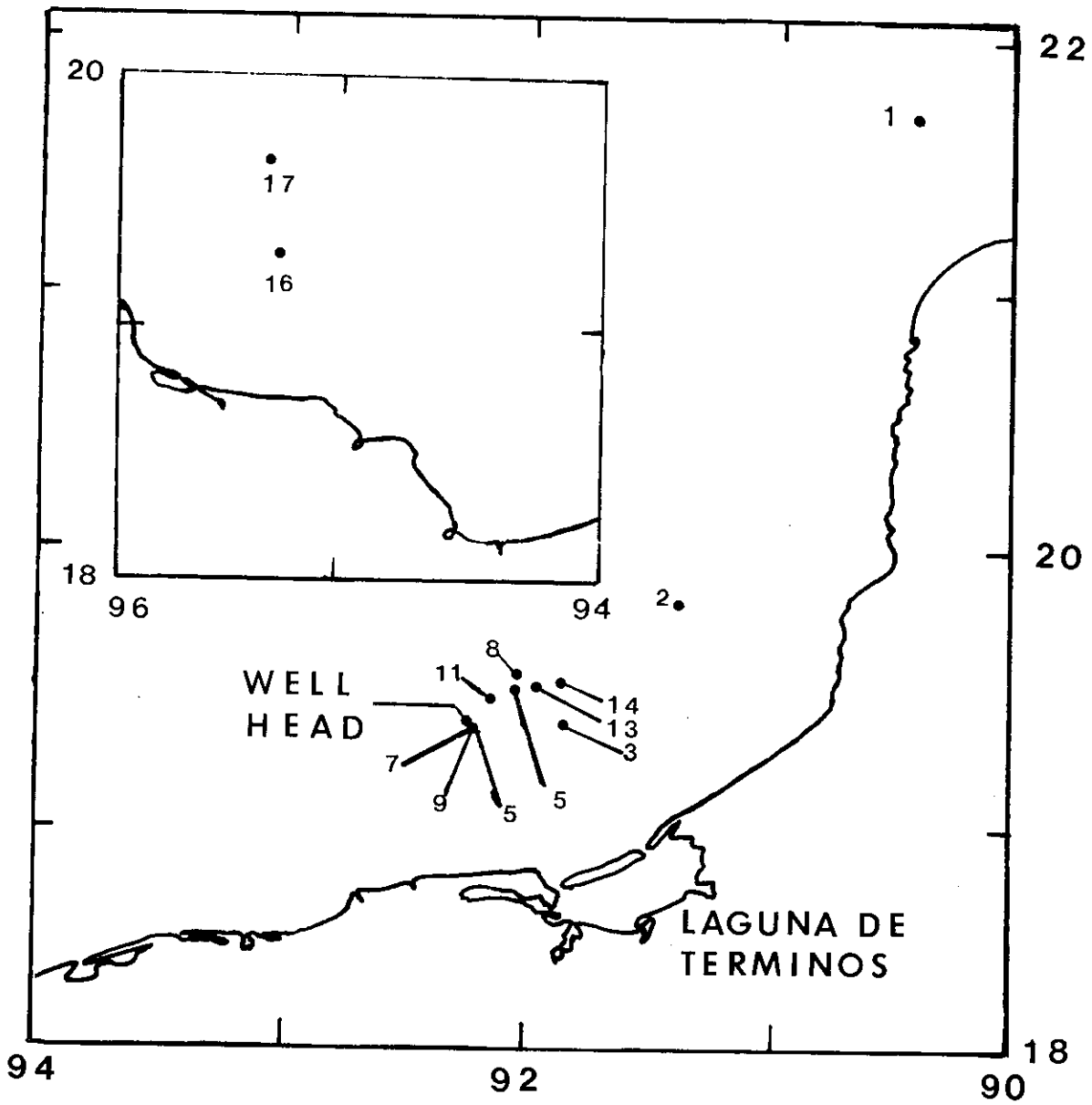

Figure 1. Chart showing sampling sites.

Table 1. Enumerations of microbial populations.

Site	Direct Count x 10^5 ml^{-1}	MPN-Hydrocarbon ml^{-1}
P1	1.5	0.3
P2	3.4	0.3
P3***	4.5	24.0
P5*	1.8	4.0
P7	2.8	4.0
P8	2.3	9.0
P8***	7.0	2400.0
P9***	2.2	2400.0
P11	2.5	4.0
P13***	1.7	24.0
P14	3.6	1.0
P14***	6.2	12000.0
P15**	4.2	46.0
P16	2.0	1.0
P17***	1.1	2400.0

*Oil, but no mousse, present in sample

**Mousse-tar particles in sample

***Heavy mousse-water mixture

^{14}C pristane, ^{14}C 9-methylanthracene, or ^{14}C benzanthracene (all specific activity ≈ 10 µCi/ml oil). The samples were incubated at 25°C. At 2, 10, and 30 days, further degradation was stopped by addition of KOH. All sample-substrate-time combinations were run in triplicate. The $^{14}CO_2$ produced from mineralization of the radio-labelled hydrocarbon was determined by acidifying the solution, flushing the headspace, trapping the $^{14}CO_2$ in 10 ml CO_2 oxifluor, and quantitating by liquid scintillation counting. Filter-sterilized controls were treated in a similar manner. The percent mineralization was calculated as $^{14}CO_2$ produced (above sterile control) divided by ^{14}C hydrocarbon added.

The above procedures measure the potential for complete microbial degradation of oil in a slick under natural conditions. Any partial or co-metabolic degradation would be detected by these procedures, as would any nutrient limitation. The influence of the physical state of the oil, such as within "mousse," will not be determined in these tests.

In a separate series of tests, five-ml portions of water samples were supplemented with NH_4NO_3 (final concentration 1 mM) and KH_2PO_4 (final concentration 1 mM) to remove nutrient limitations. These supplemented samples were added to serum vials containing 20 µl of South Louisiana crude oil spiked with ^{14}C hexadecane (specific activity 10 µCi/ml oil). After ten days of incubation, further degradation was stopped and the amount of $^{14}CO_2$ produced (^{14}C hexadecane mineralized) was determined as described above. Ratios of amounts of hydrocarbon mineralized with nutrient supplementation to amounts mineralized under natural conditions were calculated.

2.4 Oil - Mousse - Biodegradation - Mineralization

Mousse samples were collected at stations P5, P8, P14, and P17. Samples were weighed and "replicate" 5-g portions placed into 250 ml flasks, each containing 75 ml of water collected at the same site. Twenty-eight replicate flasks were established for each station. Four of the flasks from each station were fitted with sidearms and used to measure CO_2 production. Half of the flasks were treated with concentrated KOH to act as sterile controls. All flasks were incubated at 25°C on a rotary shaker at 50 rpm. CO_2 production was measured cumulatively by placing KOH in the sidearm flasks to trap CO_2. Periodically the KOH traps were recovered, $BaCl_2$ was added to precipitate $BaCO_3$, and the amount of CO_2 trapped was determined by titrating with 0.1 N HCl to a point of neutrality. Fresh KOH was added to the sidearms and the flasks were further incubated up to six months. During this time the mousse retained its physical integrity at least by visual observation.

After 2, 10, 20, 40, 90, and 180 days of incubation, oil was recovered from two active and two control flasks from each station. Extraction was with two sequential portions of methylene chloride. The basic analytical procedure described by Brown et al.(1979) was used. The extracts were transferred to pentane solvent by distillation at 44°C under a vigreaux reflux column. The volume was adjusted to 5 ml by evaporation under nitrogen. The extracts were subjected to column chromatography to split the extracts into aliphatic (f_1) and aromatic (f_2) fractions. Columns were prepared by suspending silica gel 100 (E. M. Reagents, Darmstadt, W. Germany) in CH_2Cl_2 and transferring the suspension into 24-ml burets with teflon stopcocks to attain a 15-ml silica

gel bed. The CH_2Cl_2 was washed from the columns with three volumes pentane. 2.5-ml portions of the extracts in pentane were applied to the columns, drained into the column bed, and allowed to stand three to five minutes. The aliphatic fraction (f_1) was eluted from the column with 25 ml pentane. After 25 ml pentane had been added to the column, 5 ml of 20% (v/v) CH_2Cl_2 in pentane was added and allowed to drain into the column bed. Fraction f_1 was 30 ml. The aromatic fraction (f_2) was eluted from the column with 45 ml of 40% (v/v) CH_2Cl_2 in pentane.

The fractions of each extract were then concentrated to about 5 ml at 35°C and transferred quantitatively to clean glass vials. Fractions f_1 and f_2 were prepared for analysis by gas chromatography or gas chromatography-mass spectrometry. An internal standard, hexamethyl benzene (Aldrich Chem. Co., Milwaukee, Wisconsin), was added to each sample. In fraction f_1, hexamethyl benzene (HMB) was present at 12.6 ng/µl; in fraction f_2, HMB was present at 25.2 ng/µl.

Fraction f_1 was analyzed by GC on a Hewlett-Packard 5840 reporting GC with FID detector. The column was a 30-m, SE54 grade AA glass capillary (Supelco, Bellefonte, PA). Conditions for chromatography were injector, 240°C; oven 70°C for two minutes to 270°C at 4°C/min. and hold for 28 minutes; FID, 300°C; and carrier, He at 25 cm/sec. A valley-valley integration function was used for quantitative data acquisition. Response factors were calculated using n-alkanes (C_{10}-C_{28}), pristane, and phytane standards.

Fraction f_2 was analyzed with a Hewlett-Packard 5992A GC-MS. Conditions for chromatography were injector, 240°C; oven 70°C for two minutes to 270°C at 4°C/min. and hold for 18 minutes. Data was acquired using a selected ion monitor program. Thirteen ions were selected for representative aromatic compounds. The ions monitored were 128, 142, 147, 156, 170, 178, 184, 192, 198, 206, 212, 220, and 226. The representative compounds were naphthalene, methyl naphthalene, HMB as an internal standard, dimethyl naphthalene, trimethyl naphthalene, phenanthrene, dibenzothiophene, methyl phenanthrene, methyl dibenzothiophene, dimethyl phenanthrene, dimethyl dibenzothiophene, trimethyl phenanthrene, and trimethyl dibenzothiophene, respectively. The dwell time per ion was 10 m/sec. Instrument response factors were calculated by injecting known quantities of unsubstituted and C_1 and C_2 substituted authentic compounds and determining the integrated response for each compound. These values were used to extrapolate for quantitation of isomers and C_3 substituted compounds.

3. RESULTS

3.1 Enumerations

The results of enumerations of microbial populations are shown in Table 1. There was no significant difference in total microbial biomass (direct count) between samples with visible oil and those from control sites. The highest direct counts did occur at sites P8 and P14, where mousse was present; direct counts at these sites were two to four times those at controls sites P1 and P2. In other cases, however, direct counts at sites with mousse (e.g., P9, P13, and P17) were not higher than at the control sites.

In contrast to the total microbial biomass there was a significant positive correlation between numbers of hydrocarbon-utilizing microorganisms (MPN - Hydrocarbon) and the visible presence of mousse in the sample. At control sites P1 and P2, concentrations of hydrocarbon utililzers in the surface waters were less than 1 per ml. The sample with oil and no mousse collected at site P5 had a concentration of four hydrocarbon utilizers per ml, which was an order of magnitude above the eastern control sites but was not significantly different from other sites in the vicinity of the wellhead. Samples with visible mousse had significantly elevated counts of hydrocarbon utilizers. In samples with mousse-tar particles, counts of hydrocarbon utilizers were 10^1-10^2/ml. In samples with heavy mousse accumulations, counts of hydrocarbon utilizers were 10^1-10^5 ml. The highest concentration of hydrocarbon utilizers occurred in a sample collected at site P14. High concentrations of hydrocarbon utilizers also were found at sites P8, P9, and P11. There appeared to be a relatively tight association between elevated numbers of hydrocarbon utilizers and water in direct contact with mousse. At sites P8 and P14, surface water samples were collected with and without the presence of visible mousse. In both cases, the counts in the samples with mousse were several orders of magnitude higher than in the samples without the mousse.

3.2 Hydrocarbon Biodegradation Potentials

The hydrocarbon biodegradation potentials without added nutrients are shown in Tables 2-5 for hexadecane, pristane, 9 methylanthracene, and benzanthracene, respectively. In these experiments the radio-labelled hydrocarbon tracer had the same specific activity relative to the amount of oil added. The tracer was within an oil slick, not within mousse. The amount of hydrocarbon added (16 mg) was in excess of levels of hydrocarbons contained in the water samples. The amount of hydrocarbon degraded to CO_2 was very low for all of the hydrocarbons tested. For hexadecane, which is considered to be a very readily biodegraded hydrocarbon, generally less than 1% was mineralized during 30 days of incubation. The greatest degradation of polynuclear aromatics measured was 0.2% mineralized during 30 days, and in most cases no mineralization of either 9 methyl anthracene or benzanthracene could be detected.

A possible cause for the limited hydrocarbon degradation was the availability in the water samples of nitrogen- and phosphorus-containing nutrients, which are necessary to support microbial oil degradation. This indeed appears to be the case. A comparison of the percent hexadecane mineralized during ten days of incubation with and without nutrient supplementation is shown in Table 6. The extent of mineralization was one to two orders of magnitude higher with nutrients added than under natural conditions (Table 7). The extent of hydrocarbon mineralization with nutrients added was 9% at both control sites P1 and P2 and between 13 and 28% at sites nearer the wellhead. Unlike the enumeration results, there was no significant correlation between biodegradation potentials, with or without added nutrients, and visible mousse present in the sample. The maximal rates of complete hydrocarbon degradation for the natural situation appears to be 3 mg/day/liter of surface water, based on hexadecane and assuming 1% mineralization during ten days for all hydrocarbons in the oil. For the nutrient supplemented situation, maximal rates could be 80 mg hydrocarbon mineralized/day/liter; this could occur if there was extensive mixing to

Table 2. Natural biodegradation potential for hexadecane.

Site	10-Day % Mineralization	30-Day % Mineralization
P1	0	0.3
P2	0	0.5
P3***	0	0
P5*	0.1	0.1
P7	0.3	1.2
P8	0.5	1.0
P8***	1.1	2.5
P9***	0.5	0.8
P11	0.5	0.5
P13**	0.2	0.3
P14	0.2	1.0
P14***	0.3	1.2
P15**	---	0.1
P16	0.2	0.3
P17***	0.3	1.6

*Oil, but no mousse, present in sample

**Mousse-tar particles present in sample

***Heavy mousse-water mixture

Table 3. Natural biodegradation potential for pristane.

Site	10-Day % Mineralization	30-Day % Mineralization
P1	0.2	0.7
P2	0.4	0.5
P3***	0	0
P5*	0.4	1.0
P7	0.3	1.2
P8	0.3	0.4
P8***	1.1	2.0
P9***	0.6	1.0
P11	0.4	0.8
P13**	0.4	1.0
P14	0.2	0.4
P14***	0.7	1.3
P15**	0.4	1.0
P16	0.3	1.0
P17***	0.6	1.2

*Oil, but no mousse, present in sample

**Mousse-tar particles present in sample

***Heavy mousse-water mixture

Table 4. Natural biodegradation potential for 9-methylanthracene.

Site	10-Day % Mineralization	30-Day % Mineralization
P1	0	0
P2	0	0
P3***	0	0
P5*	0	0
P7	0	0
P8	0	0.2
P8***	0	0.2
P9***	0	0.2
P11	0	0.2
P13**	0	0
P14	0	0.1
P14***	0	0
P15**	0	0
P16	0	0
P17***	0	0.2

*Oil, but no mousse, present in sample

**Mousse-tar particles

***Heavy mousse-water mixture

Table 5. Natural biodegradation potential for benzanthracene.

Site	10-Day % Mineralization	30-Day % Mineralization
P1	0	0
P2	0	0
P3***	0	0
P5*	0	0
P7	0	0
P8	0	0
P8***	0	0.2
P9***	0	0
P11	0	0
P13***	0	0
P14	0	0
P14***	0	0
P15	0	0
P16	0	0
P17***	--	--

*Oil, but no mousse, present in sample

**Mousse-tar particles present in sample

***Heavy mousse-water mixture

Table 6. Natural and non-nutrient limited biodegradation potentials for hexadecane during 10-day incubation.

Site	Nutrient-Limited (Natural) % Mineralization	Non-Nutrient (N,P-supplemented) % Mineralization
P1	0.2	9.0
P2	0.3	9.0
P5*	0.1	17.0
P7	0.3	15.0
P8	0.5	17.0
P8***	1.1	23.0
P9***	0.5	15.0
P11	0.5	18.0
P13**	0.2	26.0
P14	0.2	13.0
P14***	0.2	27.0
P15**	0.1	23.0
P16	0.2	13.0
P17***	0.3	28.0

*Oil only, no mousse present

**Mousse-tar particles in sample

***Heavy mousse-water mixture

Table 7. Ratio of non-nutrient limited (N,P supplemented) to natural biodegradation potentials.

Site	Nutrient Limited (Natural)
P1	45
P2	30
P5*	215
P7	50
P8	34
P8***	21
P9***	25
P11	36
P13**	130
P14	65
P14***	135
P15**	300
P16	65
P17***	100

*Oil, but no mousse, present in sample

**Mousse-tar particles in sample

***Heavy mousse-water mixture

prevent nutrient depletion in the vicinity of the oil in areas of the Gulf of Mexico, where productivity is not severely limited by available concentrations of nitrogen and phosphorus.

3.3 Mousse Hydrocarbon Biodegradation

The evolution of CO_2 from the degradation of mousse hydrocarbons at sites P5, P8, P14, and P17 is shown in Figure 2. Higher rates of CO_2 production were found for mousse collected at sites P14 and P17 than for that at the other sites. Sites P14 and P17 are relatively distant from the wellhead, and the mousse from these sites was presumed to be of the oldest age. The lowest rates of CO_2 production were found for mousse samples from site 5. It is not known whether these samples truly represent young mousse or, more likely perhaps, they represent older mousse that was blown back past the wellhead and coated with fresh oil. The rates of CO_2 production convert to mineralization rates of 1 mg hydrocarbon converted to CO_2/day/liter of water for site P5 and 2.5 mg hydrocarbon mineralized/day/liter of water for sites P14 and P17. The rates of mineralization of hydrocarbons in the mousse thus appear to be of the same order of magnitude as rates of hydrocarbon mineralization measured in the ^{14}C radio-labelled natural hydrocarbon degradation potential experiments. It should be noted, however, that a maximum of only 0.7% of the mousse actually added in the flasks was mineralized during the 180-day incubation. Thus the percent degradation of hydrocarbons in the mousse was lower than would be predicted from the biodegradation experiments.

While there was a continuous gradual evolution of CO_2, changes in the relative concentrations of hydrocarbons in the mousse, indicative of biodegradation, did not generally appear until the 120-day sampling (Tables 8-11) occurred. A high degree of variability in the relative concentrations of hydrocarbons in the mousse was detected in replicate samples. In all cases, however, the concentrations of n-alkanes in freshly collected mousse were higher than those of pristane and phytane. Following 180 days of incubation, the ratios of n-alkanes to isoprenoid hydrocarbons were reduced, but only for mousse from site 5 were the n-alkanes reduced to concentrations below those of the isoprenoid hydrocarbons. The changes in the overall composition of the oil indicate some preferential degradation of n-alkanes over isoprenoid hydrocarbons and reflect the overall low percentage of degradation of hydrocarbons in the mousse added to each flask.

Analyses of the aromatic fraction have not been completed, but those samples analyzed (representative results shown in Tables 12-15) indicate that biodegradation of the aromatic fraction occurred during the incubation period. The dimethyl and trimethyl phenanthrenes appeared to be among the most persistent compounds in the aromatic fraction of the mousse and generally increased in importance relative to even substituted dibenzothiophenes during the 180-day incubation period.

4. DISCUSSION

There was a significant elevation (several orders of magnitude) in counts of hydrocarbon-utilizing microorganisms in association with mousse formed from

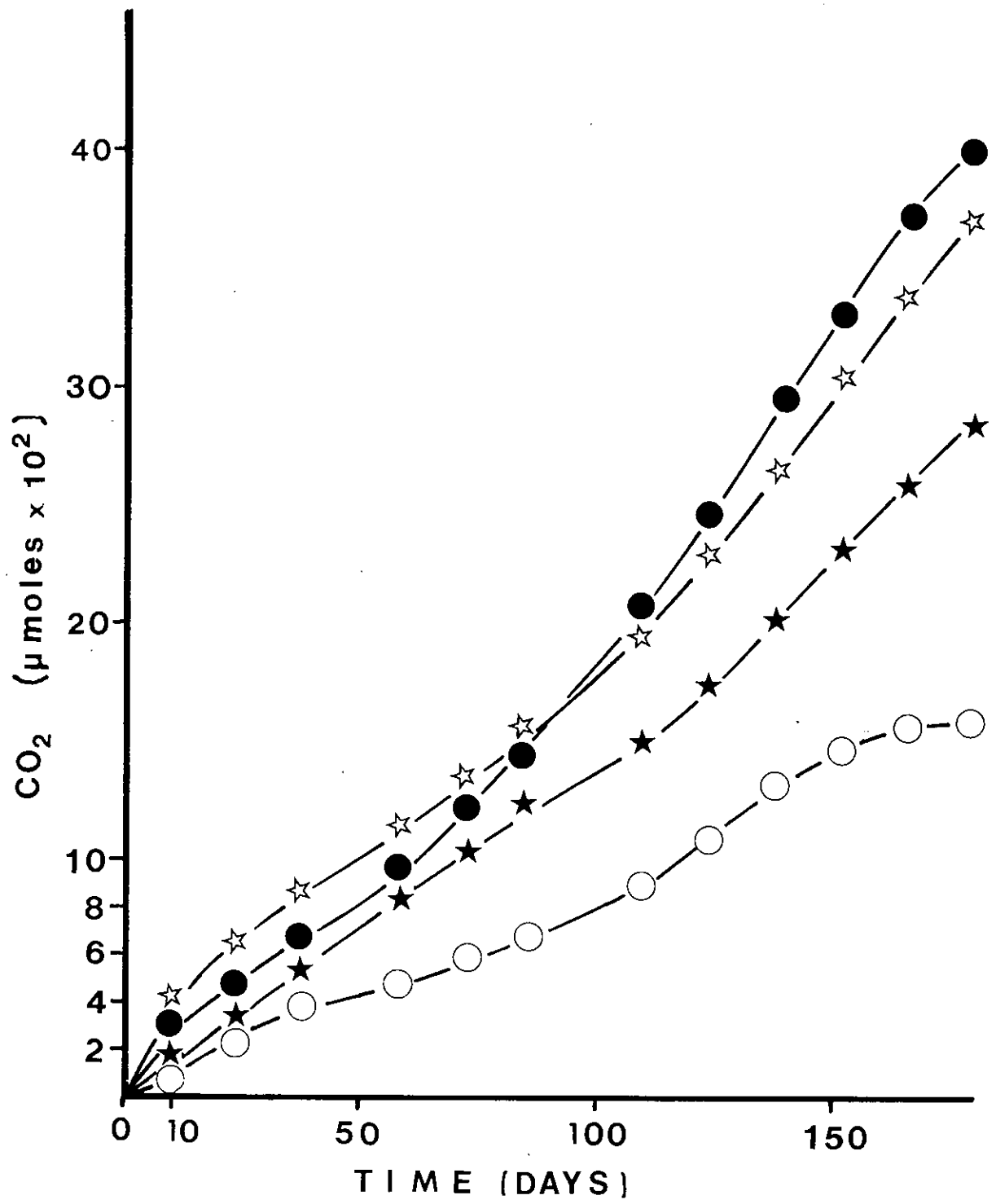

Figure 2. CO_2 production from mousse collected at several sites in the Gulf of Mexico. Open circle: site P5; closed star: site P8; closed circle: site P14; open star: site P17.

Table 8. Analysis of saturate hydrocarbons from mousse from site P5.

	Ratio to Phytane					
	Incubation Time (Days)					
Compound	0	10	20	40	120	180
C14	---	---	---	---	---	---
C15	0.4	1.1	1.0	---	---	---
C16	0.9	2.1	1.7	0.8	---	---
C17	1.6	2.6	2.2	1.4	---	---
Pristane	0.5	---	0.6	---	0.5	0.4
C18	2.9	3.4	3.2	2.2	---	---
Phytane	1.0	1.0	1.0	1.0	1.0	1.0
C19	3.4	3.0	2.9	2.1	0.4	---
C20	3.9	3.1	3.1	2.3	0.7	0.5
C21	3.7	2.9	2.8	2.0	0.7	0.6
C22	3.6	2.6	2.7	1.7	0.7	0.6
C23	3.6	2.6	2.4	1.7	0.6	0.6
C24	3.5	2.8	2.5	1.6	0.7	0.5
C25	2.8	2.1	2.0	1.1	0.4	0.4
C26	2.8	2.1	2.9	1.1	0.4	0.3
C27	2.1	1.7	1.2	0.8	---	---
C28	2.0	2.8	1.5	1.0	0.4	0.4

Table 9. Analysis of saturate hydrocarbon fraction from site P8.

	Ratio to Phytane					
	Incubation Time (Days)					
Compound	0	10	20	40	120	180
C14	---	---	---	0.1	---	---
C15	0.3	0.3	0.2	0.3	0.2	---
C16	0.8	0.7	0.6	0.8	0.6	0.5
C17	1.4	1.3	1.2	1.6	1.8	1.0
Pristane	0.5	0.4	0.4	0.6	0.5	0.4
C18	2.7	2.5	2.3	3.2	2.4	2.0
Phytane	1.0	1.0	1.0	1.0	1.0	1.0
C19	3.3	3.0	2.7	4.7	2.9	2.4
C20	3.5	3.3	3.2	4.1	3.3	2.9
C21	3.2	3.1	3.0	3.9	3.1	2.6
C22	3.2	3.2	3.0	3.7	3.3	2.6
C23	3.6	3.1	2.8	3.8	3.0	2.5
C24	3.0	2.9	2.8	3.5	3.0	2.5
C25	2.3	2.4	2.3	2.5	2.4	2.0
C26	2.6	2.3	2.3	2.6	2.6	2.1
C27	1.7	1.8	1.8	2.1	1.9	1.7
C28	1.8	1.4	1.7	1.9	1.9	1.7

Table 10. Analysis of saturate hydrocarbon fraction from site P14.

	Ratio to Phytane					
	Incubation Time (Days)					
Compound	0	10	20	40	120	180
C14	0.4	0.3	0.4	0.4	0.3	---
C15	1.0	1.0	1.0	0.9	0.8	0.2
C16	1.4	1.5	1.5	1.5	1.2	0.5
C17	1.8	2.0	1.9	1.8	1.5	0.7
Pristane	0.6	0.5	1.1	0.6	0.6	0.6
C18	2.6	2.8	2.7	2.5	2.3	1.2
Phytane	1.0	1.0	1.0	1.0	1.0	1.0
C19	2.5	2.6	2.8	2.2	2.4	1.3
C20	2.6	2.8	2.8	2.5	2.3	1.3
C21	2.4	2.6	2.6	2.3	2.1	1.1
C22	2.3	2.7	2.4	2.2	2.0	1.1
C23	2.1	2.4	2.4	2.0	1.9	---
C24	2.1	2.4	2.4	2.1	1.9	1.0
C25	1.8	1.8	2.2	1.6	1.7	0.9
C26	1.9	1.9	1.9	1.6	1.4	1.1
C27	1.3	1.2	3.5	1.2	1.1	0.6
C28	1.2	1.3	1.2	1.2	1.1	0.8

Table 11. Analysis of saturate hydrocarbon fraction from site P17.

	Ratio to Phytane					
	Incubation Time (Days)					
Compound	0	10	20	40	120	180
C14	---	---	---	---	---	---
C15	0.3	---	2.0	0.2	0.1	---
C16	0.8	3.7	0.7	0.6	0.4	0.3
C17	1.4	1.5	1.3	1.2	0.8	0.6
Pristane	0.4	0.4	0.4	0.5	0.5	0.4
C18	2.6	2.7	2.5	2.2	1.6	1.4
Phytane	1.0	1.0	1.0	1.0	1.0	1.0
C19	3.1	3.2	3.2	2.8	2.2	1.5
C20	3.6	3.6	3.6	3.0	3.1	2.2
C21	3.5	3.7	3.2	3.1	2.5	2.0
C22	3.4	3.6	3.2	2.9	2.5	2.2
C23	3.1	3.5	3.2	2.5	2.3	2.2
C24	3.1	3.5	3.2	2.4	2.3	2.2
C25	2.4	2.8	2.5	3.4	1.8	1.9
C26	2.8	2.9	2.7	2.3	1.9	2.2
C27	1.9	2.1	2.0	1.6	1.2	1.7
C28	1.9	1.9	2.0	1.7	1.7	1.7

Table 12. Analysis of aromatic fraction of mousse collected at site P5.

	Ratio to Methyl Dibenzothiophene				
	Incubation Time (Days)				
Compound	0	10	20	40	180
Naphthalene	---	---	---	---	---
C1-Naphthalene	---	---	---	---	---
C2-Naphthalene	0.2	---	---	---	---
C3-Naphthalene	0.5	0.1	---	---	---
Phenanthrene	0.1	0.1	---	0.2	---
C1-Phenanthrene	1.1	0.9	---	2.3	---
C2-Phenanthrene	72.7	21.5	0.7	36.9	++
C3-Phenanthrene	35.4	7.8	---	13.9	++
Dibenzothiophene	0.1	0.1	---	---	---
C1-Dibenzothiophene	1.0	1.0	1.0	1.0	---
C2-Dibenzothiophene	2.1	1.7	2.4	2.1	++
C3-Dibenzothiophene	1.1	0.7	0.5	0.7	++

++ = barely detectable

Table 13. Analysis of aromatic fraction of mousse collected at site P8.

	Ratio to Methyl Dibenzothiophene		
	Incubation Time (Days)		
Compound	0	120	180
Naphthalene	---	---	---
C1-Naphthalene	---	---	---
C2-Naphthalene	0.1	---	---
C3-Naphthalene	0.3	0.1	0.5
Phenanthrene	0.1	---	0.7
C1-Phenanthrene	1.0	---	---
C2-Phenanthrene	9.8	77.5	167.6
C3-Phenanthrene	5.1	51.1	185.9
Dibenzothiophene	0.1	---	0.2
C1-Dibenzothiophene	1.0	1.0	1.0
C2-Dibenzothiophene	1.8	7.6	15.6
C3-Dibenzothiophene	0.9	4.3	16.2

Table 14. Analysis of aromatic fraction of mousse collected at site P14.

	Ratio to Methyl Dibenzothiophene					
	Incubation Time (Days)					
Compound	0	10	20	40	120	180
Naphthalene	---	---	---	---	---	---
C1-Naphthalene	0.0	---	0.4	---	---	---
C2-Naphthalene	1.6	0.1	---	0.0	---	---
C3-Naphthalene	2.2	0.5	1.0	0.2	0.3	1.5
Phenanthrene	0.2	0.1	0.0	0.2	---	---
C1-Phenanthrene	0.9	1.0	0.8	1.6	0.2	---
C2-Phenanthrene	6.9	19.1	17.2	30.8	33.0	121.4
C3-Phenanthrene	3.1	6.9	10.1	15.6	15.5	108.7
Dibenzothiophene	0.3	0.1	---	0.0	---	---
C1-Dibenzothiophene	1.0	1.0	1.0	1.0	1.0	1.0
C2-Dibenzothiophene	1.3	1.3	1.7	1.4	2.8	6.7
C3-Dibenzothiophene	0.5	0.5	0.8	0.6	1.3	4.1

Table 15. Analysis of aromatic fraction of mousse collected at site P17.

	Ratio to Methyl Dibenzothiophene		
	Incubation Time (Days)		
Compound	0	20	180
Naphthalene	---	---	---
C1-Naphthalene	---	---	---
C2-Naphthalene	0.1	---	---
C3-Naphthalene	0.5	0.4	---
Phenanthrene	0.1	---	---
C1-Phenanthrene	1.0	---	---
C2-Phenanthrene	9.6	123.7	85.0
C3-Phenanthrene	2.4	156.8	490.4
Dibenzothiophene	0.1	---	---
C1-Dibenzothiophene	1.0	1.0	1.0
C2-Dibenzothiophene	1.7	8.1	68.1
C3-Dibenzothiophene	1.0	5.4	93.7

oil released from the IXTOC-I well in the Gulf of Mexico. This rise represented a shift within the microbial community; there was no significant elevation in total microbial biomass. Similar selective increases in concentrations of hydrocarbon utilizers have been reported in most cases following oil spills; they have been noted by the authors of this report in previous studies of marine and inland oil spills, including concentrations in sediments impacted by the AMOCO CADIZ oil spill.

Despite the elevated populations of hydrocarbon utilizers, rates of hydrocarbon degradation appear to be slow. Unlike previous reports in the literature concerning the fate of crude oil in the Gulf of Mexico (e.g., Kator et al., 1971), which would indicate extensive degradation within 24 hours, this study shows that the complete biodegradation to CO_2 of hydrocarbons in mousse from IXTOC-I was of the order of less than 5% per year. There was evidence for a relatively severe nutrient limitation to extensive oil biodegradation. Although nutrient levels were not measured by the present authors, the comparison of natural and nutrient-stimulated rates of hydrocarbon mineralization strongly suggests that concentrations of available nitrogen and phosphorus in the Bay of Campeche surface waters were very low.

The hydrocarbon composition of mousse collected near the wellhead (site P5) and at some distance from the wellhead (sites P14 and P17) did not show evidence of extensive microbial modification of the hydrocarbons in the mousse. Unlike analyses of hydrocarbons in sediments impacted by mousse from the AMOCO CADIZ spill, where n-alkane to isoprenoid hydrocarbon ratios shifted rapidly from four to less than one within a few weeks following the spill, the n-alkane to phytane ratios generally remained greater than one in mousse collected in the Gulf of Mexico, even following extensive incubation. A decrease in the n-alkane to isoprenoid hydrocarbon ratio is taken as evidence of biodegradation, since microorganisms usually degrade straight chain alkanes more rapidly than branched alkanes.

There is some difficulty in establishing appropriate units for degradation rates of hydrocarbons in mousse. Compared to oil slicks, a lower percentage of hydrocarbon was found to be completely degraded to CO_2 in the mousse, although absolute rates of CO_2 evolution extrapolated to comparable volumes of seawater were not different between hydrocarbons in oil slicks and hydrocarbons in mousse. It is likely that hydrocarbons in large mousse accumulations are not as rapidly degraded as oil available in slicks or in fine emulsions within the water column, due to unfavorable surface area-to-volume relationships and poor transport of nutrients to hydrocarbons within large accumulations of mousse. It seems safe to conclude that the evidence indicates that biodegradation of hydrocarbons in mousse floating on surface waters in the Gulf of Mexico was severely limited; it was occurring but at low rates. As a result, sufficient time existed for transport of the mousse in relatively undegraded states to other systems, such as benthic or intertidal sediments. Evidence for long-term mineralization of the hydrocarbons in the mousse was found, but it is likely that extensive degradation will occur in systems with greater availability of nutrients such as in coastal lagoons and estuaries, where the oil may be transported and deposited.

5. REFERENCES

Atlas, R. M. (1979): Measurement of hydrocarbon biodegradation potentials and enumeration of hydrocarbon utilizing microorganisms using carbon-14 hydrocarbon-spiked crude oil. In: Native Aquatic Bacteria: Enumeration, Activity and Ecology, J. W. Costerton and R. R. Colwell (Eds.), STP 695, ASTM, Philadelphia, PA: 196-204.

Bartha, R., and R. M. Atlas (1977): The microbiology of aquatic oil spills. Adv. Appl. Microbiol., 22: 225-266.

Brown, B. W., L. S. Ramos, B. J. Friedman, and W. D. Macleod (1979): Analysis of trace levels of petroleum hydrocarbons in marine sediments using a solvent/slurry extraction procedure. NBS Special Publication 519, Washington, D.C.: 161-167.

Colwell, R. R., and J. D. Walker (1977): Ecological aspects of microbial degradation of petroleum in the marine environment. CRC Crit. Rev. Microbiol., 5: 423-445.

Daley, R. J., and J. E. Hobbie (1975): Direct counts of aquatic bacteria by a modified epifluorescence technique. Limnol. Oceanogr., 20: 875-882.

Kator, H., C. H. Oppenheimer, and R. J. Miget (1971): Microbial degradation of a Louisiana crude oil in closed flasks and under simulated field conditions. In: Prevention and Control of Oil Spills, American Petroleum Inst., Washington, D.C.: 287-296.

DETAILED CHEMICAL ANALYSIS OF IXTOC-I CRUDE OIL AND SELECTED ENVIRONMENTAL SAMPLES FROM THE RESEARCHER AND PIERCE CRUISES

E. B. Overton, L. V. McCarthy, S. W. Mascarella, M. A. Maberry
S. R. Antoine, and J. L. Laseter
Center for Bio-Organic Studies
University of New Orleans
New Orleans, Louisiana 70122

J. W. Farrington
Woods Hole Oceanographic Institution
Woods Hole, Massachusetts 02543

1. INTRODUCTION

The cruises of the RESEARCHER and PIERCE were designed to collect scientific data and samples that will be used to extend our understanding of the long-term fates and effects of spilled petroleum hydrocarbons in the marine environment. This scientific venture takes advantage of the research opportunities afforded by the IXTOC-I spill and is of particular significance since it is the only major spill studied to date that occurred in a temperate climate. The samples collected from the cruises were analyzed as a "team effort" by a selected group of university and private laboratories. This paper describes preliminary observations resulting from the analyses performed at the University of New Orleans' Center for Bio-Organic Studies. It must be emphasized that the data presented herein require further analysis, interpretation, and synthesis with the results of other investigators before the significance of this research can be fully understood. We have included raw gas chromatographic and gas chromatographic-mass spectrometric data for examination by those who are associated with oil spill research, so that these results may be fully viewed and interpreted in the broadest possible context. While tabular data are easiest for scientists not familiar with the specific project to understand, they inevitably omit important results that can be obtained only by careful review of all data from a set of analyses.

Our program was designed to accomplish the following: (1) detailed characterization of fresh IXTOC-I crude oil; (2) detailed characterization of weathered IXTOC-I oil; (3) analyses of selected environmental samples to determine the effects of weathering on IXTOC-I oil; (4) laboratory photolysis of IXTOC-I oil; (5) determination of the photochemical oxidation products from IXTOC-I oil, and (6) analysis of samples from the Bacterial Microcosm Experiment for selected hydrocarbons and degradation products of the IXTOC oil. This paper will describe the results of 1, 2, 3, and 6.

2. ANALYTICAL METHODOLOGY

2.1 Fractionation

The general philosophy in our laboratory concerning the analysis of environmental samples is to keep chemical treatment of the sample extract to a minimum. Unfortunately, environmental samples are of such complexity that the extracts must be simplified into subfractions prior to instrumental analysis. Figure 1 diagrams the various fractionation schemes that were used in analyzing samples from the IXTOC-I blowout.

2.1.1 Neutral Extraction

The neutral extract is functionally defined as that portion of the sample that will dissolve in or be extracted by nonpolar organic solvents (such as hexane or methylene chloride). The neutral extracts are fractionated by any one of three fractionation schemes.

Silica Gel Fractionation. The standard analytical fractionation scheme involves liquid-solid absorption chromatography using activated silica gel as

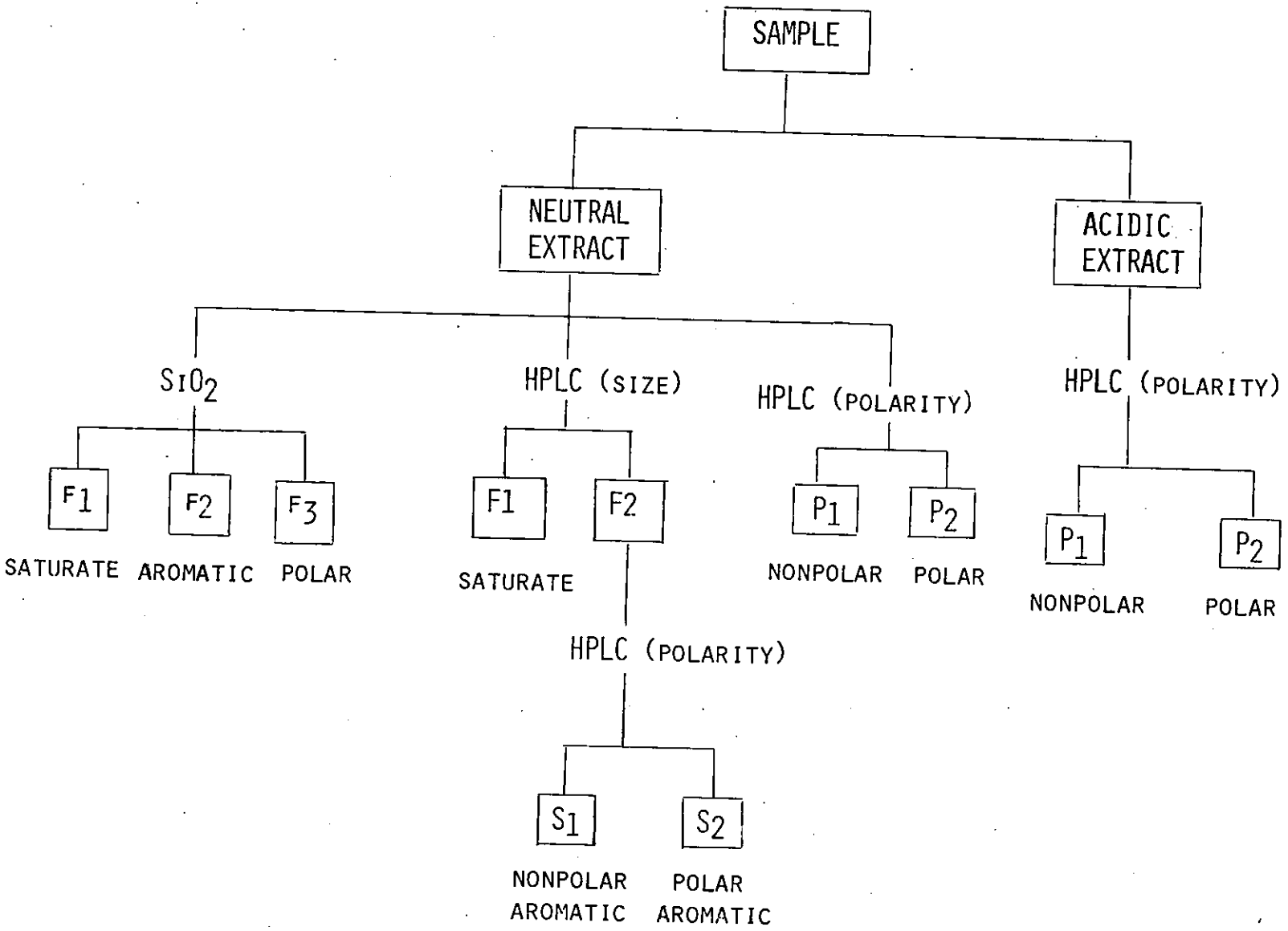

Figure 1. Schematic diagram of the various fractionation schemes used in the analysis of environmental samples from the IXTOC-I oil spill.

the solid substrate. By increasing the polarity of the eluting solvent, successively more polar subfractions can be eluted from silica gel columns. Nonpolar solvents, such as hexane, will elute saturated-type hydrocarbons and produce an f_1 fraction; a mixture of 30% methylene chloride in hexane will elute slightly more polar compounds (such as the aromatic hydrocarbons) and produce an f_2 fraction. A polar solvent, such as methanol, will elute polar compounds from the silica gel column and produce an f_3 fraction.

Silica gel fractionation is tried and proven for analysis of the saturate (f_1) and aromatic (f_2) fractions but is not entirely suitable for analysis of more polar compounds. For example, silica gel is used as a catalyst in the synthesis of certain types of oxidized hydrocarbons (McKillop and Young, 1979). The catalytic activity is a serious disadvantage when silica gel is used as a fractionation medium in the analysis of oxidized aromatic compounds. To overcome the inherent limitations in the use of silica gel fractionation of environmental samples, we have developed alternative techniques that represent more gentle and more effective separation methods. These techniques involve the use of high-pressure liquid chromatography (HPLC). Throughout our study, HPLC fractionation techniques applied only to samples shown to contain interesting features using the more conventional silica gel fractionation techniques.

HPLC Size and Polarity Separation. The HPLC fractionation technique separates extracts using a two-dimensional chromatographic scheme. The first step separates samples according to the principle of size-exclusion chromatography. This separation sequence is followed by additional fractionation involving either a normal or a reverse-phase absorption chromatographic procedure. This two-dimensional fractionation technique produces essentially the same types of fractions as are produced by silica gel chromatography, but the fractions are cleaner and less subject to catalytic decomposition. Also, certain fatty acid compounds are separated from the polar aromatic compounds. This is significant, since the fatty acids are ubiquitous in the marine environment and interfere in the analysis of polar and oxidized aromatic hydrocarbons. The HPLC fractionation scheme is flexible in that several additional subfractions, which are not normally obtainable from silica gel column chromatography, can easily be generated from the sample extract. Also, the fractions are separated using nonaqueous solvent systems, and this facilitates their analysis by glass-capillary gas chromatographic $(GC)^2$ and glass-capillary gas chromatographic-mass spectrometric (GC^2MS) techniques. Aprotic solvents are also essential for derivatization of polar fractions.

Figure 2 shows the computer-reconstructed glass capillary gas chromatograms of the saturate and aromatic fractions of a mousse sample collected at RIX 10, using both the silica gel and the HPLC fractionation schemes. Careful examination of these data indicates that our HPLC fractionation reproduces essentially the same types of fractions as can be obtained from silica gel columns. There are important differences, however, between these two techniques. The HPLC fraction II is substantially cleaner and has a less pronounced unresolved mixture than the aromatic fraction from silica gel columns. This cleaner fraction facilitates more detailed GC^2 and GC^2MS analysis of this important fraction.

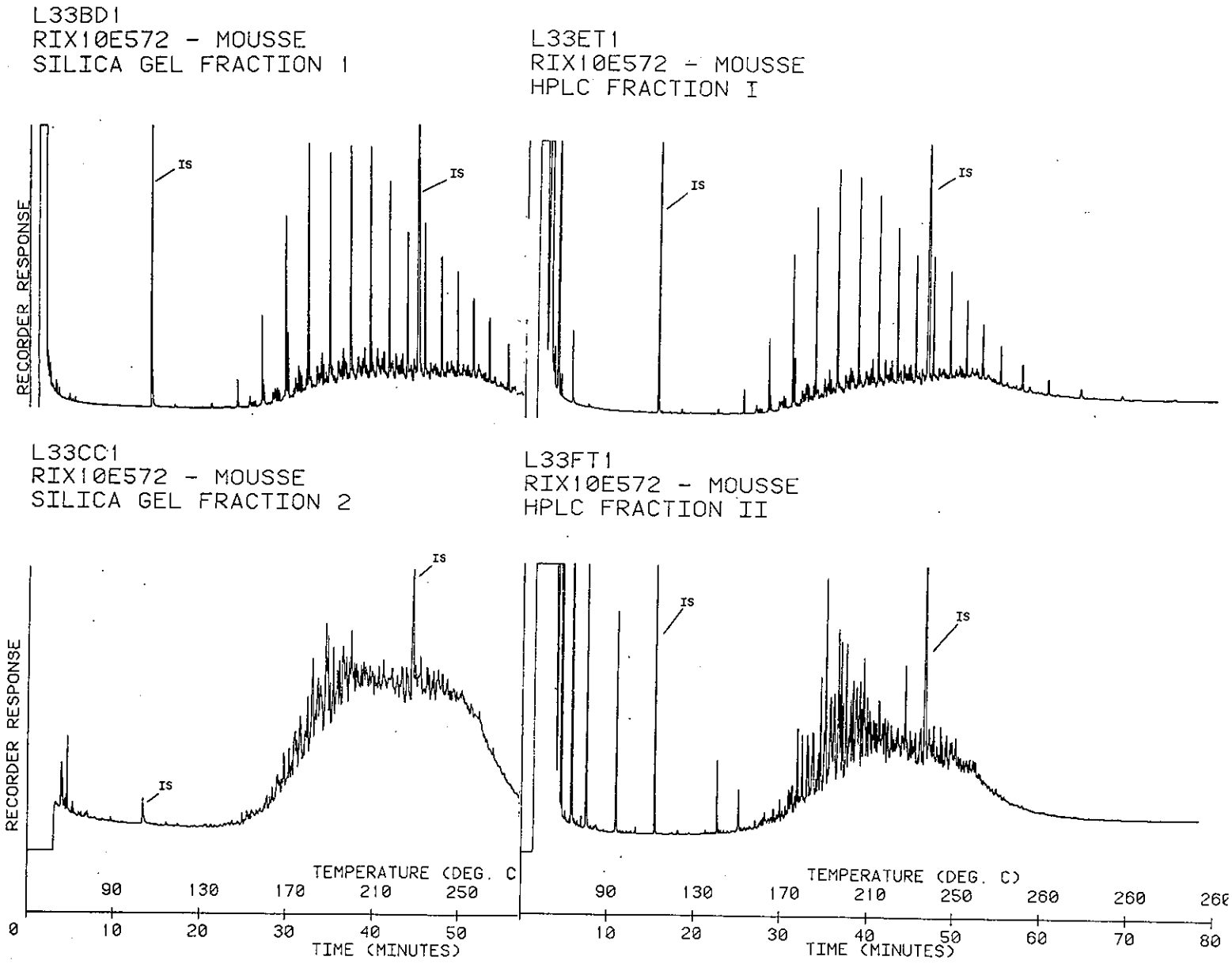

Figure 2. Glass capillary gas chromatograms of the saturate and aromatic fractions of a RIX 10 mousse sample that was fractionated using both the standard silica gel column chromatography (left) and the HPLC fractionation schemes (right). The first internal standard, MBT, elutes with approximately the same retention time as 2-methylnaphthalene. The second internal standard, DTP, elutes between n-C_{24} and n-C_{25}.

HPLC Polarity (only) Separation. Certain of the samples from this study were fractionated into polar and nonpolar fractions using only HPLC absorption chromatography.

2.1.2 Extraction of Bases

Sample extracts also can be liquid-liquid partitioned to extract organic compounds with various functional groups. For example, extraction of mousse samples against 1M HCl solutions will partition certain nitrogen-containing hydrocarbons as the hydrochloride salt. The salts are then neutralized and re-extracted into organic solvents prior to GC^2 and GC^2MS analysis.

2.1.3 Acid Extractions

Water samples can be acidified and then extracted with organic solvents. This sequential extraction scheme, which follows the neutral extraction of water column samples, is designed to extract those hydrocarbons that are ionized (or dissociated) at neutral pH's. Organic compounds that are extracted by these techniques include phenols and carboxylic acids.

2.1.4 Special Methylation Procedure

Figure 3 diagrammatically shows the additional analytical methods applied to sample fractions. If fractions have compounds that should not contain easily dissociated hydrogen ions, they are analyzed directly by GC^2, using simultaneous general (flame-ionization) and element specific (S or N) detectors, and/or GC^2MS.

Certain fractions contained organic compounds with replaceable hydrogen ions. These fractions were derivatized with a diazomethane procedure especially developed for analysis of environmental samples. The procedure is a gentle gas-phase methylation technique that minimizes side-reaction products and contamination. Diazomethane is generated by a two-phase reaction between sodium hydroxide and N-nitroso-N-methyl urea (Schwartz and Bright, 1974). The sample extract is placed on celite and the diazomethane gas is passed over the extract. The methylated extract is then washed off the substrate and subjected to GC^2 and GC^2MS analysis.

2.2 Gas Chromatography

All gas chromatographic separations were achieved using SE-52 wall-coated open tubular glass capillary columns made in-house according to the procedures of Grob (Grob et al., 1979). The columns were generally 30 m in length, 0.3 mm ID, and had a helium flow rate of 3 ml/min. The columns were installed in Hewlett-Packard 5711 gas chromatographs and temperature programmed from 50°C to 250°C at 4°C/min. Eluting peaks were detected by several methods: (1) generalized flame ionization detector (FID); (2) simultaneous FID and Hall electrolytic conductivity detector (HECD) in either the nitrogen or sulfur mode (McCarthy et al., 1980); and (3) a mass spectrometer interfaced directly to the gas chromatographs.

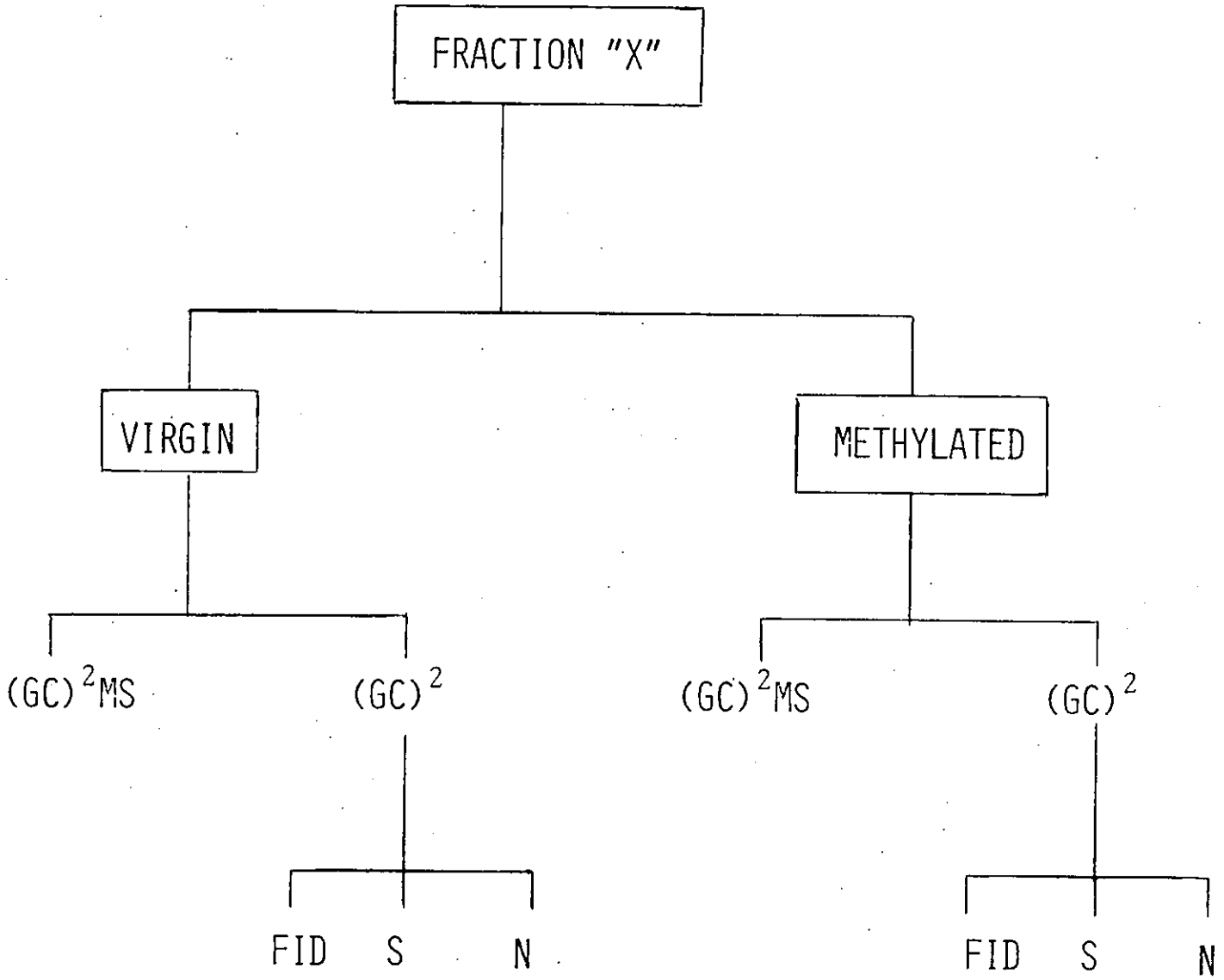

Figure 3. Schematic diagram of the various analytical techniques applied to fractions from the IXTOC-I oil spill.

2.3 Mass Spectrometry

Three types of mass spectrometers were used in this work: a Varian/MAT 311A high-resolution mass spectrometer; a duPont 21-491 double-focussing mass spectrometer; and a Hewlett-Packard (HP) 5985 quadrupole mass spectrometer. Most routine GC^2MS runs were done on the HP 5985 instrument. Raw GC^2MS data was written on magnetic tape in the compressed Hewlett-Packard/Environmental Protection Agency (HPEPA) format. Special software routines, which were written in-house, read the HPEPA-formatted data into an INCOS GC^2MS data system (Steele, et al., 1980). This unique software allows GC^2MS data generated on the HP 5985 to be treated by the advanced algorithms of the INCOS data system. All GC^2MS analyses performed on the quadrupole instrument were done using a mass spectral cycle time of one second, so that accurate quantification could be obtained from mass spectral data of individual eluting compounds. Mass spectral identifications were based on a combination of matches with authentic standards, matches with data in the Environmental Protection Agency/National Bureau of Standards/National Institute of Health (EPA/NBS/NIH) Mass Spectral Library, manual interpretation of mass spectral data, and the use of retention time comparisons between standards and unknowns for those compounds exhibiting ambiguous mass spectral fragmentation patterns.

All GC^2 and GC^2MS raw data are stored in digital form on either magnetic discs or tapes and are available for future examination.

2.4 Standards

Prior to GC^2 and GC^2MS analysis, each fraction was spiked with two internal standards that elute at different times during a run. The internal standards, methylbenzothiazole (MBT) and ditolylpyridine (DTP), were chosen to give responses with the element-specific detectors. Also, the use of two internal standards facilitates alignment between GC^2 runs and between GC^2 and GC^2MS analysis. The first internal standard, MBT, elutes with approximately the same retention time as 2 methylnaphthylene. The second internal standard, DTP, elutes between n-C_{24} and C_{25}. Table 1 indicates the concentration of internal standards in micrograms per gram (ppm) used to spike sample fractions prior to GC^2 and GC^2MS analysis. The values given in the table are representative of concentrations of individual components (assuming equal response factors) in the sample fractions.

3. RESULTS

3.1 Unweathered Oil (Control Sample)

Figure 4 contains diagrams of the molecular structures of various hydrocarbons and non-hydrocarbons found in the IXTOC oil.

3.1.1 Aromatic Hydrocarbons

Figure 5 is a computer-generated plot of the simultaneous glass-capillary gas chromatograms using the FID and sulfur-specific detectors of the size-

Table 1. Internal standard concentrations for GC[2] analysis. (The internal standard was spiked to indicate the amount, in μg per gram, of individual components in specific sample fractions.)

Figure Number		Internal Standard Amt. (ppm) (First Internal Std. - MBT)
2	top left	5140
	top right	5790
	bottom left	257
	bottom right	278
4	top and bottom	1020
7	top and bottom	.012
8	top and bottom	.012
14	top	585
	middle	140
	bottom	292
15	top	4560
	middle	146
	bottom	115
16	top	600
	middle	60
	middle	60
	bottom	16.8
17	top	7.2
	bottom	16.8
18	top	.001
	bottom	.0005
21	top left	3.08
	top right	3.08
	bottom left	1800
	bottom right	1800
22	top left	3.08
	top right	3.08
	bottom left	.005
	bottom right	.005
23	top left	.005
	top right	.002
	bottom left	.005
	bottom right	.003

Table 1. (Continued)

Figure Number		Internal Standard Amt. (ppm) (First Internal Std. - MBT)
24	top left	.300
	top middle	.625
	top right	.625
	middle left	.294
	middle middle	.613
	middle right	.613
	bottom left	.283
	bottom middle	.589
	bottom right	.589
25	top	46.2
	botom	5560
26	top left	3.08
	top right	3.08
	bottom left	556
	bottom right	556
27	top	.125
	middle	.092
	bottom	.062
28	top	.062
	bottom	.030
29	top	.125
	middle	.250
30	top	.062
	middle	.333
	bottom	.062
31	top	.125
	middle	.114
	bottom	.062
32	top	.062
	middle	.114
	bottom	.030
33	top	.062
	bottom	5330
34	top	.030
	bottom left	533
	bottom right	533

Table 1. (Continued)

Figure Number		Internal Standard Amt. (ppm) (First Internal Std. - MBT)
35	top	.250
	bottom	10600
36	top left	.062
	top right	.062
	bottom left	1060
	bottom right	1060
37	top	.062
	bottom	5780
38	top	.030
	bottom left	578
	bottom right	578
39	top	.032
	middle	.032
	bottom	.032
40	top left	.032
	top right	.038
	bottom left	.040
	bottom right	.095

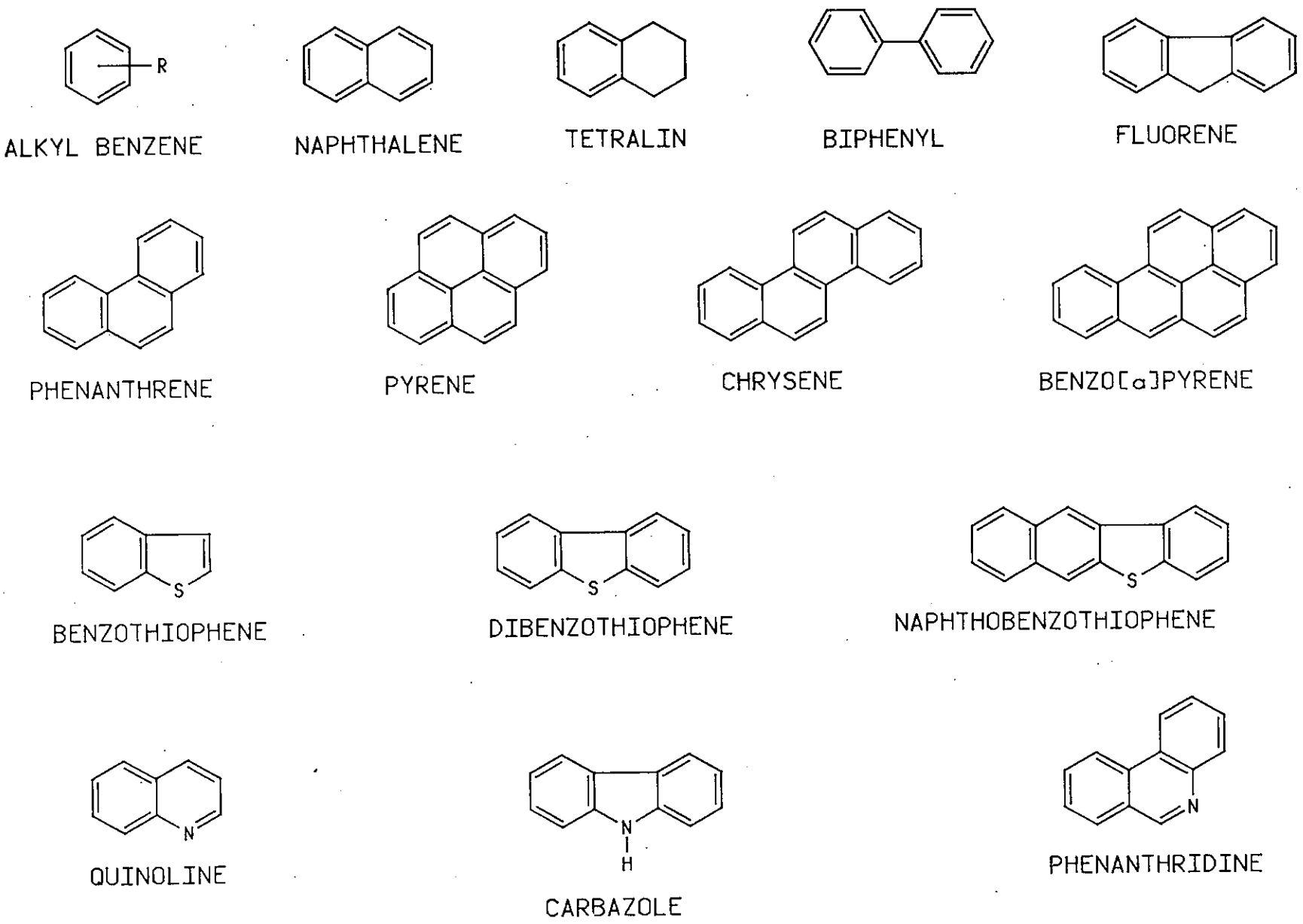

Figure 4. Diagrams of the molecular structures of the various aromatic hydrocarbons and nonhydrocarbons identified in IXTOC-I oil.

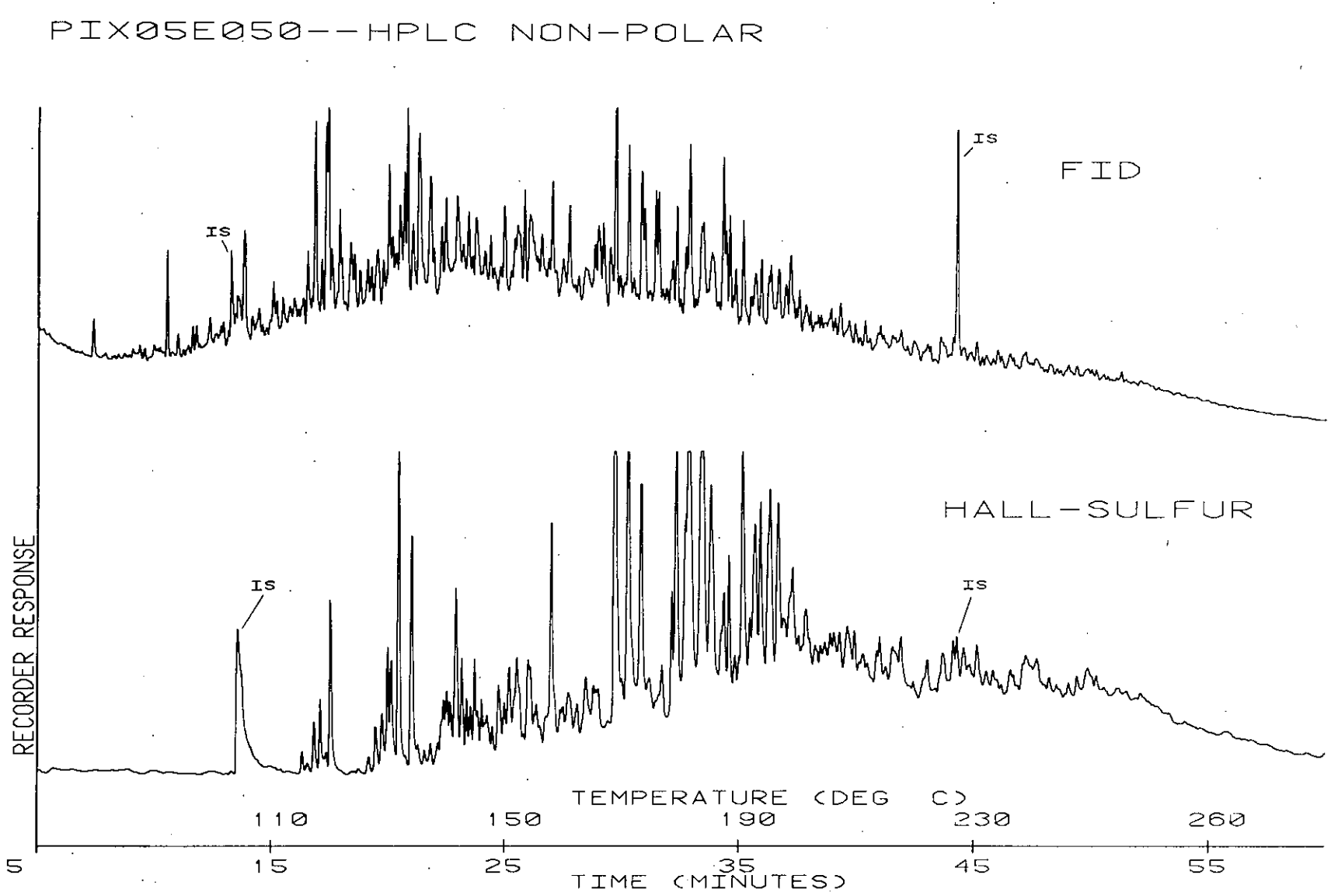

Figure 5. Glass capillary gas chromatograms using the FID (top) and the Hall sulfur-specific (bottom) detectors of the HPLC fractionated nonpolar extract of a fresh oil sample collected at PIX 05. The first internal standard, MBT, elutes with approximately the same retention time as 2-methyl-naphthalene.

separated nonpolar fraction (S1) of the fresh oil collected at site PIX 05. This sample represents the freshest, most unweathered oil collected during the cruises. It was sampled close to the wellsite at 0.75 nautical miles downstream from the discharge in the plume. The following aromatic hydrocarbons and homologs were identified via mass spectrometry in this sample:

alkylated benzenes	(to at least C_6 alkyl homologs)
naphthalenes	(to C_4 alkyl homologs)
naphthenoaromatics	(to C_3 alkyl homologs)
biphenyls	(to C_3 alkyl homologs)
fluorenes	(to C_3 alkyl homologs)
phenanthrenes	(to C_3 alkyl homologs)
the pyrene family	(202 family - to C_3 alkyl homologs)
the chrysene family	(228 family - to C_3 alkyl homologs)
the benzopyrene family	(252 family - to C_3 alkyl homologs)

3.1.2 Sulfur-Containing Compounds

The following sulfur-containing compounds were detected by the Hall electrolytic conductivity detector and identified via mass spectrometry:

benzothiophenes	(to the C_3 alkyl homologs)
dibenzothiophenes	(to the C_3 alkyl homologs)
benzonaphthylthiophenes	(to the C_3 alkyl homologs)

Other sulfur compounds were detected in the sulfur chromatogram but have not, as yet, been identified by mass spectrometry.

Figure 6 shows the extracted ion current profiles (EICP) representative of benzonaphthylthiophene (234) and its C_1 (248), C_2 (262), and C_3(276) alkyl homologs. Background-subtracted mass spectra are also given for the parent compound and typical C_1 to C_3 alkyl homologs. The parent (P), parent minus 1 (P-1), parent plus 1 and 2 (P+1, P+2), and parent minus 15 (P-15) are important ions used to identify these substances. Mass spectral background subtracting techniques did not completely remove ion resulted from coeluting components in these complex analyses.

3.1.3 Nitrogen-Containing Compounds

Figures 7 and 8 show the computer-generated plots of the simultaneous FID and nitrogen-specific detector gas chromatograms of the polar and nonpolar fractions of the acid extract of oil collected at PIX 05. These chromatograms visually illustrate the numerous nitrogen-containing organic compounds found

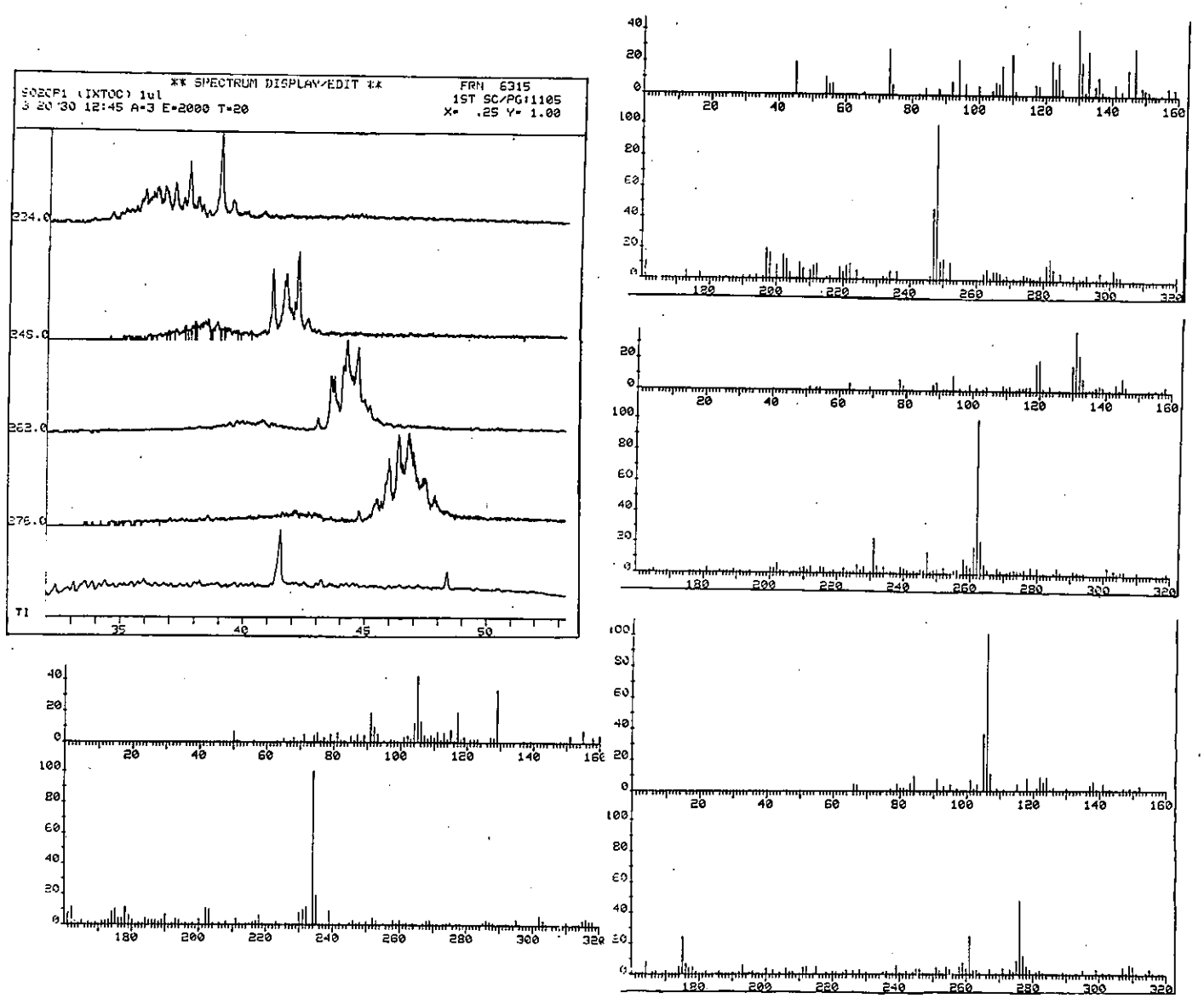

Figure 6. Extracted Ion Current Profiles and representative background subtracted mass spectra for the naphthylbenzothiophenes and their C_1, C_2 and C_3 alkylated homologs.

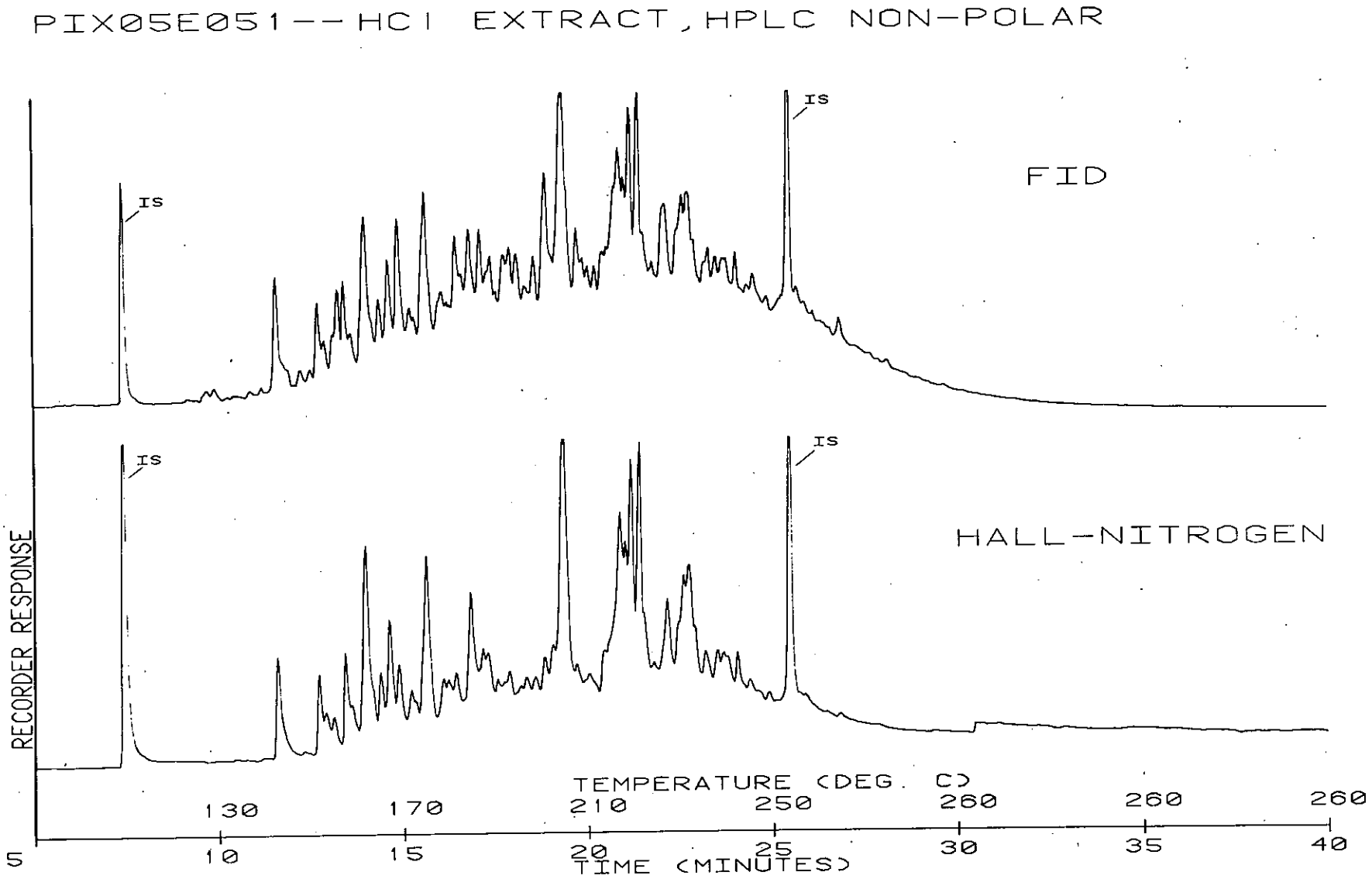

Figure 7. Glass capillary gas chromatograms using the FID (upper) and Hall nitrogen-specific (lower) detector of the hydrochloride extracts, HPLC fractionated, nonpolar fraction of the fresh oil sample collected at PIX 05.

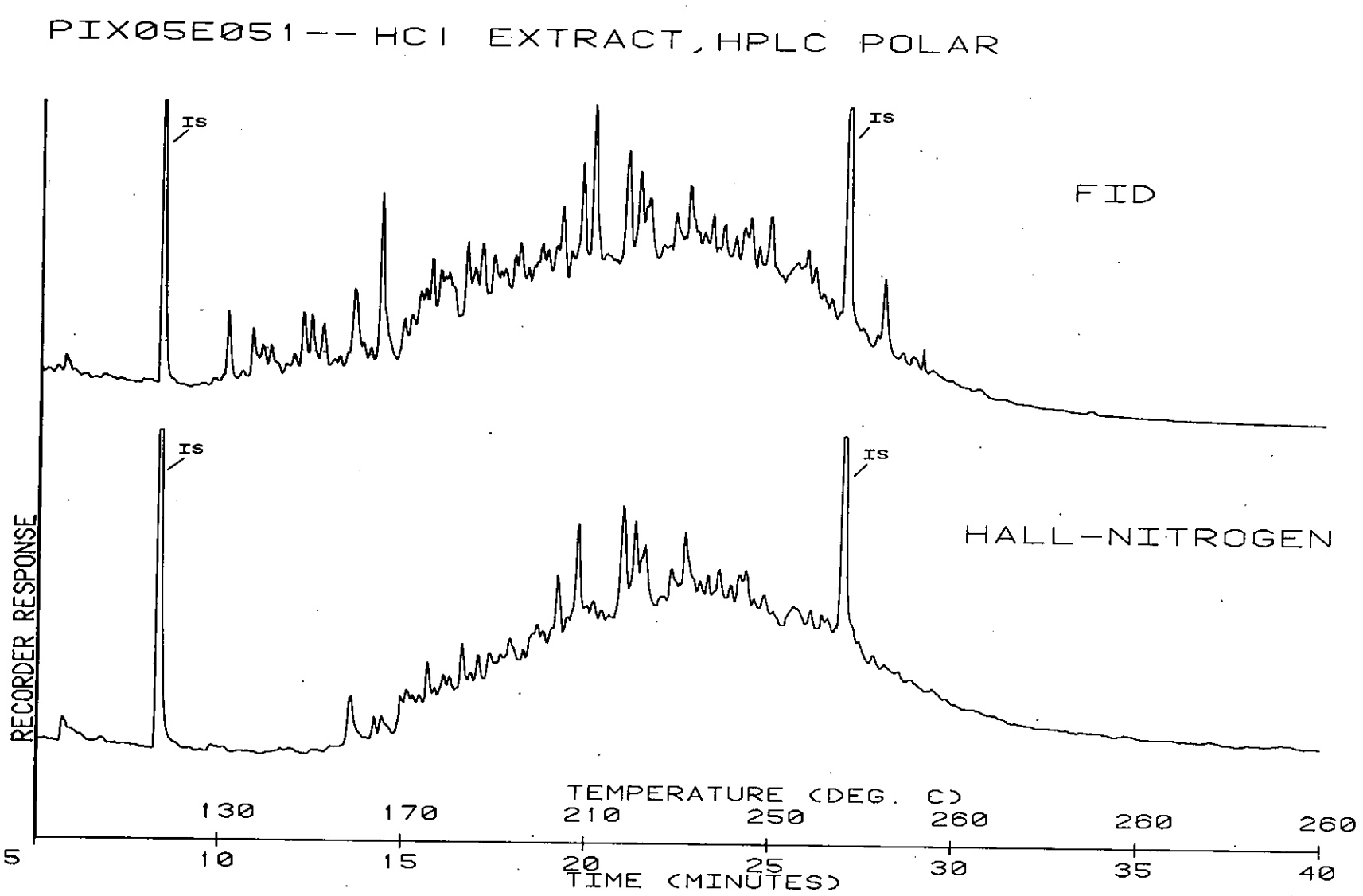

Figure 8. Glass capillary gas chromatograms using the FID (upper) and Hall nitrogen-specific (lower) detector of the hydrochloride extracts, HPLC fractionated, polar fraction of the fresh oil sample collected at PIX 05.

in this oil. Many of these compounds belong to the quinoline (129), phenanthridine (179), and carbazole (167, emperical formula of $C_{12}H_9N$) families of nitrogen azaarenes. Other nitrogen-containing compounds are not, as yet, completely identified.

Figure 9 shows the EICP for the C_2 (195), C_3 (209), C_4 (223), and C_5 (237) alkyl homologs of carbazole, together with the background-subtracted mass spectra of representative compounds for each group of alkyl homologs. Although the amounts of individual components were extremely low, important features in the spectra are evident. Most alkyl homologs of these aromatic heterocycles exhibit prominent parent ions along with intense ions at P-1 and P-15. The base peak in the spectrum is often determined by the positions of alkyl substitution. For example, Figure 10 shows the molecular ion region in the spectra of the four C_3 alkyl homologs of carbazole. Although background-subtraction routines tend to alter the ion intensities in the mass spectra from complex chromatograms such as these and do not always remove ions from coeluting substances, this figure clearly shows the influence of alkyl substitution on the mass spectra of the C_3 carbazoles. While these specific compounds are not in the EPA/NBS/NIH mass spectral library, their mass spectra generally agree with published mass spectra of other substituted azaarenes (Draper and MacLean, 1968).

Figure 11 shows the EICP and representative mass spectra from the f_3 fraction of IXTOC-I oil. The EICP is for ions with masses of 179, 193, 207, 221, and 235, which are characteristic of three-ring aromatic compounds (i.e., phenanthridine) and their alkyl homologs containing a nitrogen atom in the ring structure. The single peak in the 207 EICP is not characteristic of the alkyl homolog distribution pattern to be expected if the compound was a member of the phenanathridine family of azaarenes. The mass spectrum tends to support this conclusion, since P-1 and P-15 ions are not present. This peak probably represents the parent compound in a new series of azaarenes with molecular formula of $C_{15}H_{13}N$. Because of the small quantities of the compound present and the absence of extensive molecular fragmentation, unequivocal identification of this substance is difficult.

Figure 12 shows the EICP and representative mass spectra for the series 171, 185, 199, 213, and 227. The major peak eluting in the 171 mass chromatogram (EICP) appears to be a C_3 alkylated quinoline. The parent C_1 and C_2 homologs of quinoline were not detected in this fraction. Other homologs were detected in the mass chromatograms (EICP) for ions 185, 199, and 213. Figure 13 shows four background-subtracted mass spectra with parent ions of 185. Examination of this data reveals that certain of the compounds with molecular weights of 185 may not be homologs of the quinoline series of azaarenes and may represent other ring-structure azaarenes. Also, depending on the position of alkyl substitution, the base peak in the spectra of certain alkyl homologs can be found at P-1.

3.2 Weathered Oil-Water Emulsions (Mousse Samples)

Detailed GC^2 and GC^2MS analyses of a number of mousse samples were performed in order to determine the effects of weathering on these samples. Whenever possible, the mousse samples were classified by visual identification and manually separated into an outer crust (which was the more heavily

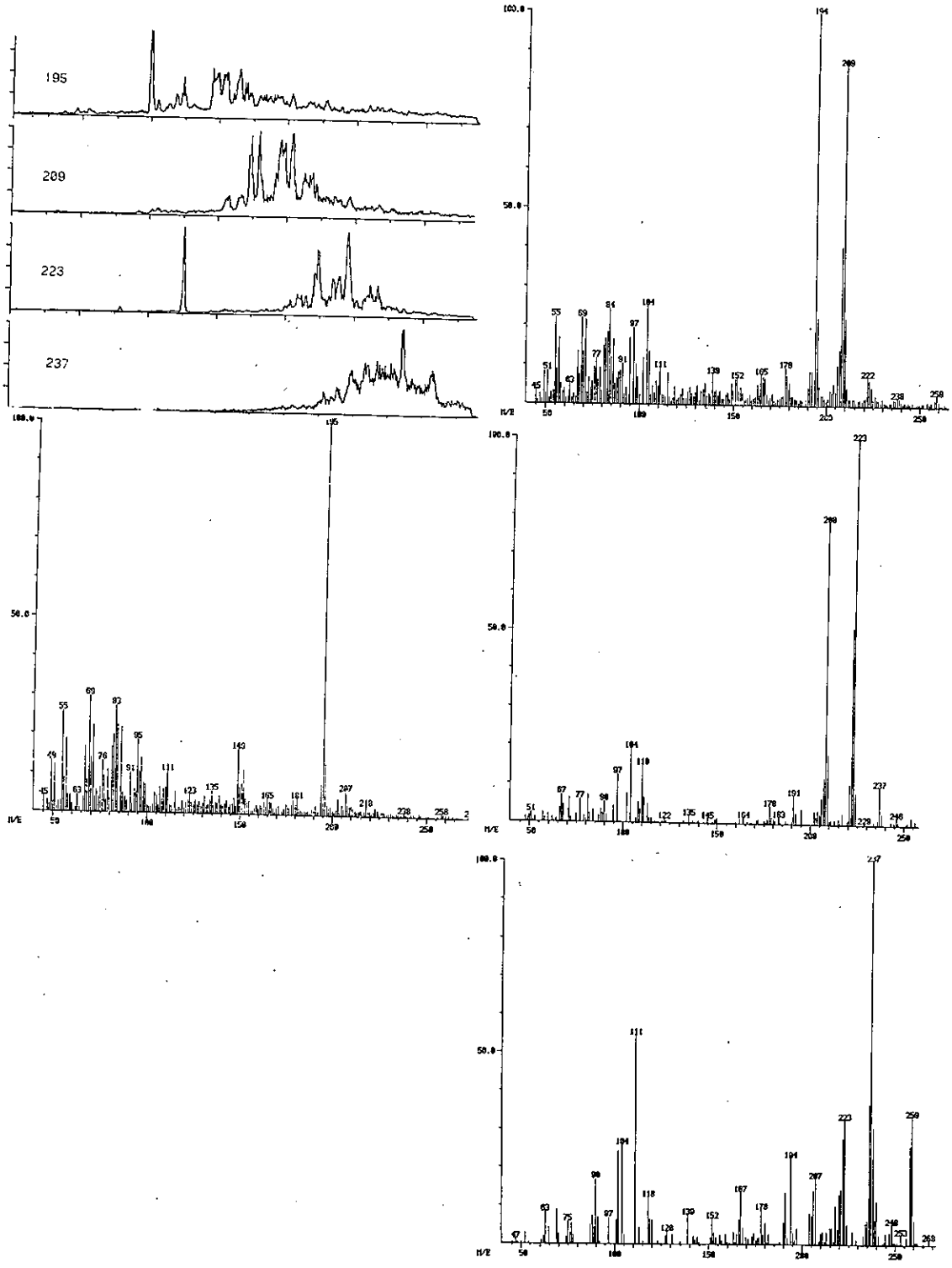

Figure 9. Extracted Ion Current Profiles and representative background-subtracted mass spectra for members of the carbazole family of nitrogen-containing aromatic compounds (195-C_2 carbazoles, 209-C_3 carbazoles, 223-C_4 carbazoles, 237-C_5 carbazoles).

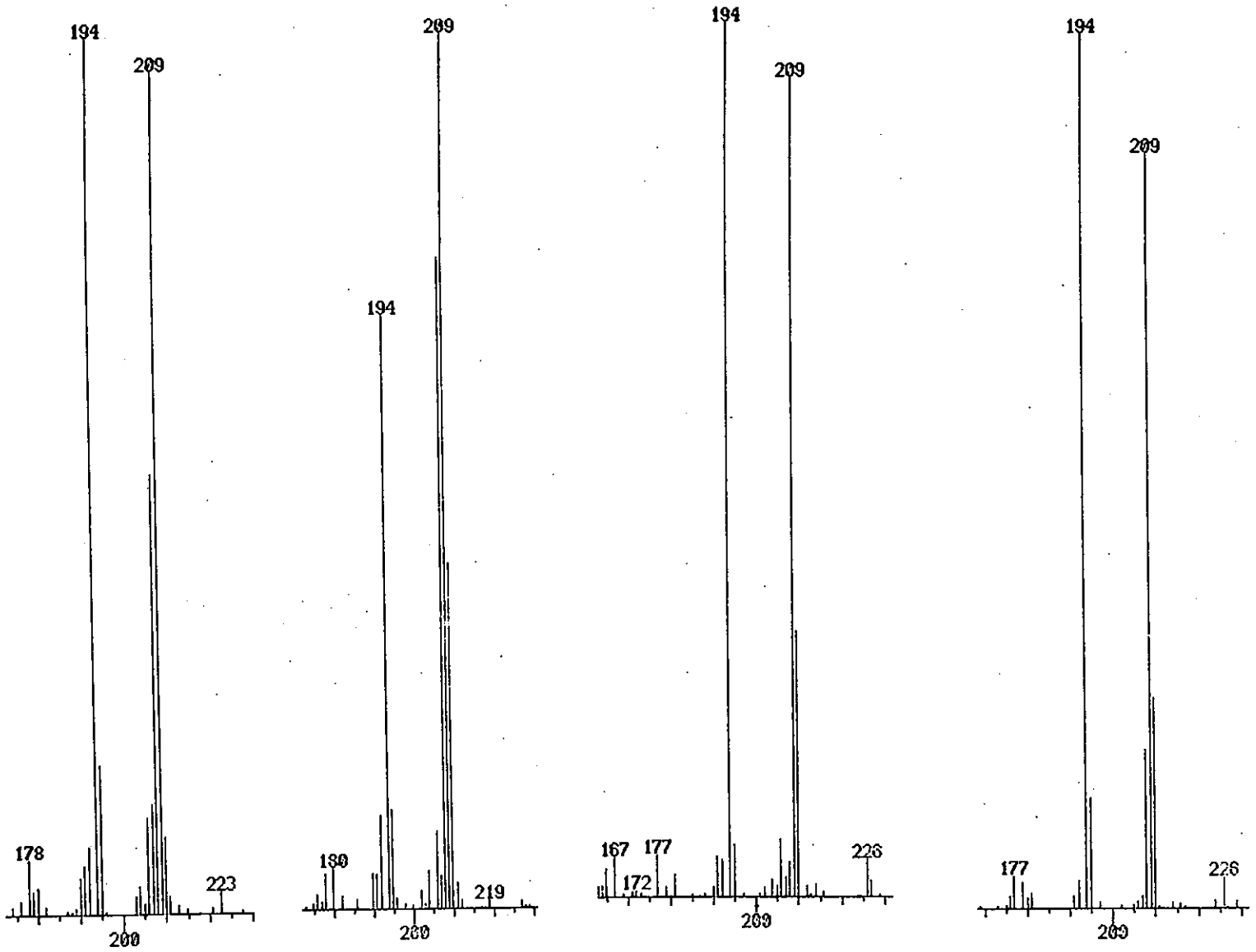

Figure 10. Background-subtracted mass spectra of four homologs of the C_3 alkylated carbazole family of nitrogen-containing azaarenes.

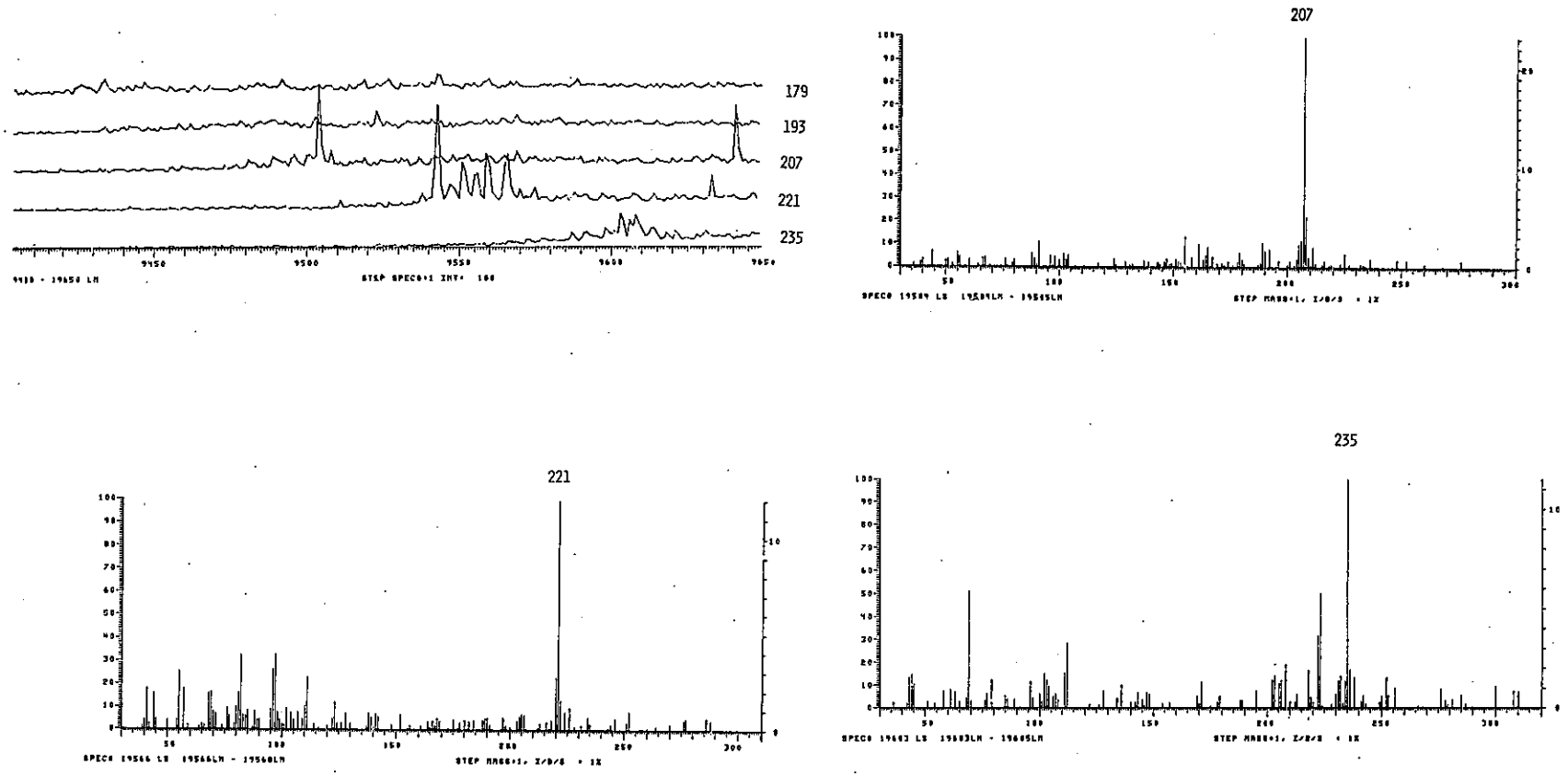

Figure 11. Extracted Ion Current Profiles and representative background-subtracted mass spectra for the phenanthridine family of azarenes (179-parent phenanthridine, 193-C_1 phenanthridine, 207-C_2 phenanthridine, 221-C_3 phenanthridine, 235-C_4 phenanthridine).

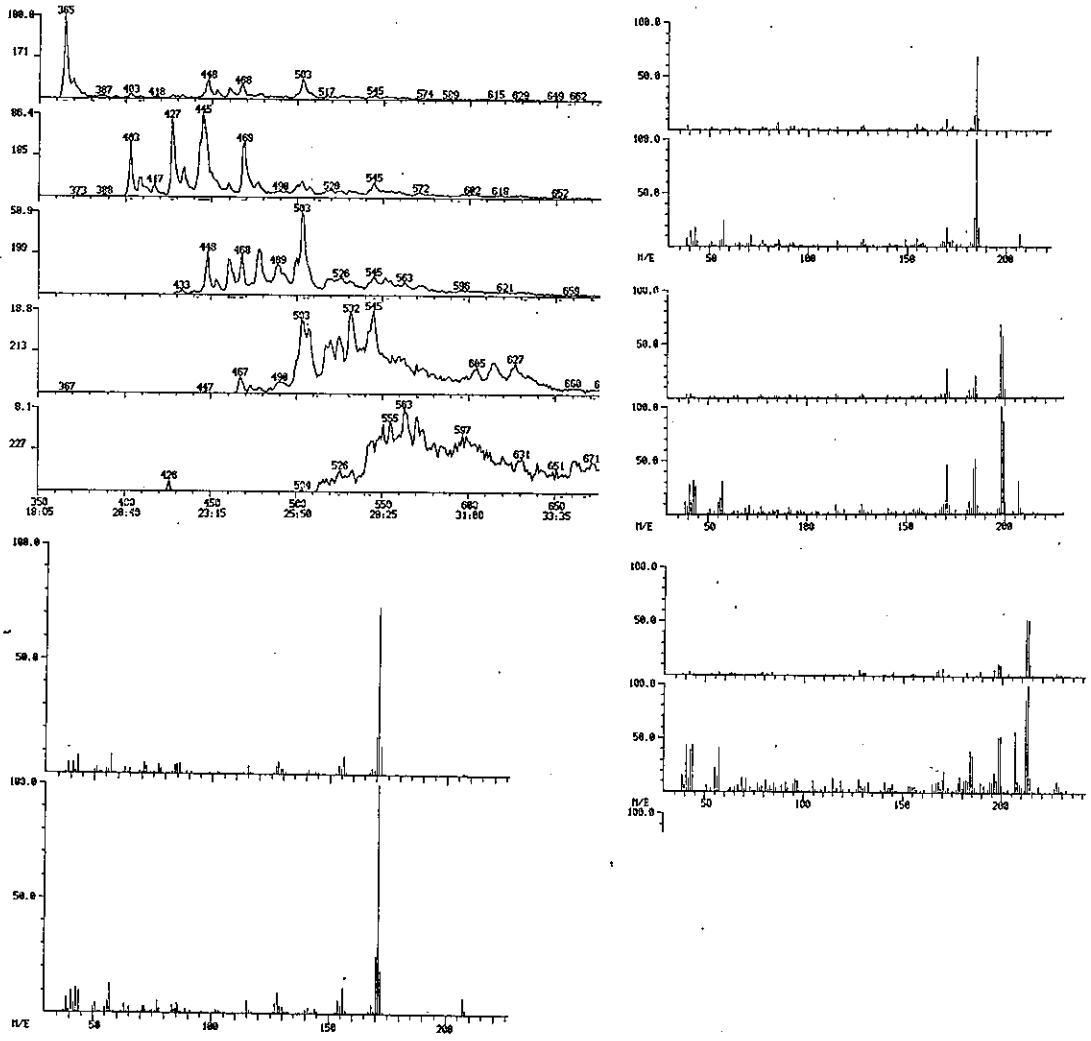

Figure 12. Extracted Ion Current Profiles and representative background subtracted mass spectra for the alkylated quinoline family of azarenes (171-C_3 quinoline, 185-C_4 quinoline, 199-C_5 quinoline, 213-C_6 quinoline, 227-C_7 quinoline).

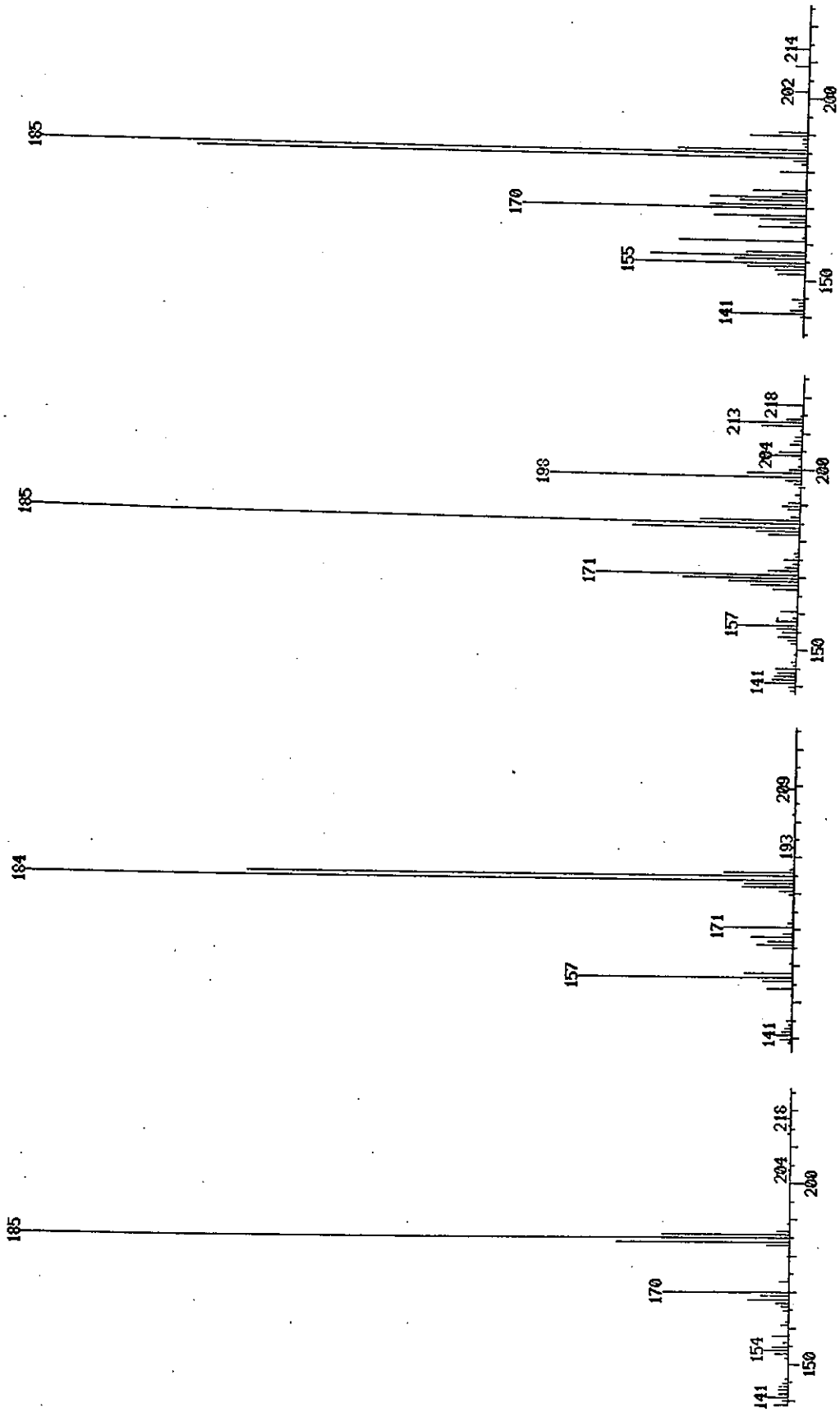

Figure 13. Background-subtracted mass spectra of four azaarenes with molecular weight of 185.

weathered portion of the sample) and the less-weathered inner material. Typical data are presented in this report. Figures 14 and 15 show the computer-reconstructed glass capillary gas chromatograms of the f_1, f_2, and f_3 fractions of the mousse sample collected off the beach at RIX 23. This particular mousse had a well defined outer crust and a less weathered inner structure. Figure 14 shows the data for the outer crust, while Figure 15 shows the equivalent data from the less weathered inner portion of this mousse sample.

3.2.1 Saturate (f_1) Fraction

Examination of Figures 14 and 15 reveals that the f_1 fractions are qualitatively very similar. The lower molecular weight n-alkanes up to C_{17} have been lost to evaporation. Quantitatively, the inner structure sample was substantially richer in these saturate compounds.

3.2.2 Aromatic (f_2) Fraction

Examination of the aromatic or f_2 fractions, however, reveals some interesting differences between these two samples. The outer crust is essentially devoid of all aromatic compounds. This is also evident in the sulfur-specific chromatograms, which show essentially no sulfur-containing compounds in this fraction. Examination of the f_2 fraction for the inner structure (Figure 15) reveals aromatic profiles that are similar to those of oil samples that have been weathered for a relatively short period of time. The inner structure has lost most of the naphthalenes and the parent compounds of phenanthrene and dibenzothiophene. The sample still retains small quantities of the C_1 homologs and most of the C_2 and C_3 homologs of phenanthrene and dibenzothiophene. The sulfur-specific chromatogram, which shows small quantities of the C_1 dibenzothiophenes, larger quantities of the C_2 and C_3 dibenzothiophenes, and naphthylbenzothiophene, substantiates these observations.

3.2.3 Polar (f_3) Fraction

Examination of the f_3 fractions in Figures 14 and 15 reveals a small unresolved mixture characteristic of weathering in the f_3 fraction of the inner material. It is interesting to note that most of the more polar oxidized aromatic compounds were not present in the f_3 fraction of this mousse crust. In virtually all of the mousse samples that we have analyzed, there were only very small quantities of polar compounds in the f_3 fraction. This was somehwat unexpected, since at the start of the study we had anticipated that as the aromatic compounds of petroleum became oxidized or otherwise degraded by the various weathering processes we would notice an increase in the more polar substances in the f_3 fraction. Our preliminary data suggest that as these compounds are oxidized by environmental processes, they become more water-soluble and are leached into the environment rather than accumulating in or remaining in the mousse samples.

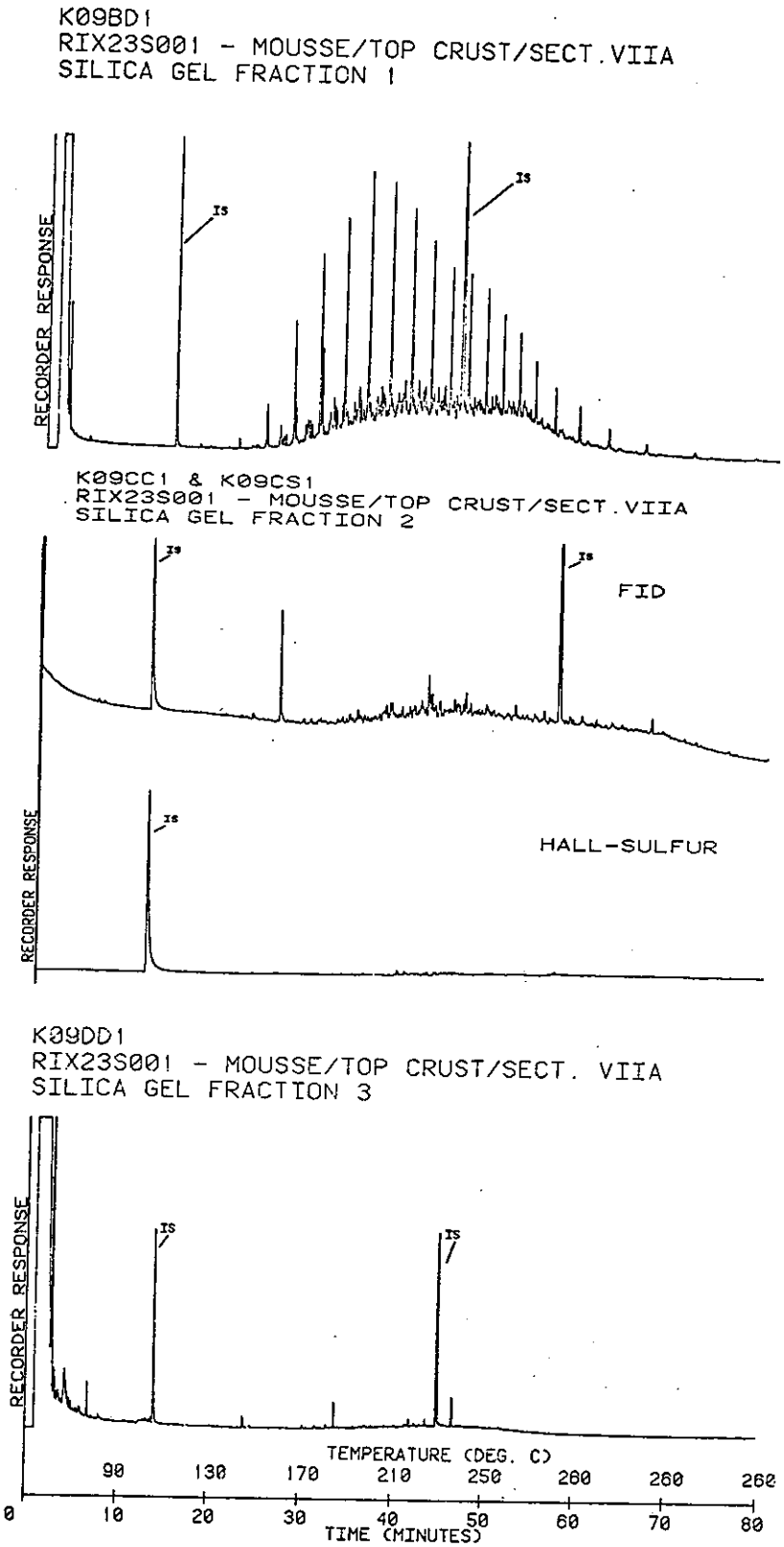

Figure 14. Glass capillary gas chromatograms of the saturate (f_1), aromatic (f_2, FID and sulfur-specific), and polar (f_3) fractions of a mousse (weathered outer crust) sample collected at RIX 23. The first internal standard, MBT, elutes with approximately the same retention time as 2-methyl-naphthalene. The second internal standard, DTP, elutes between $\underline{n}$-C_{24} and $\underline{n}$-C_{25}.

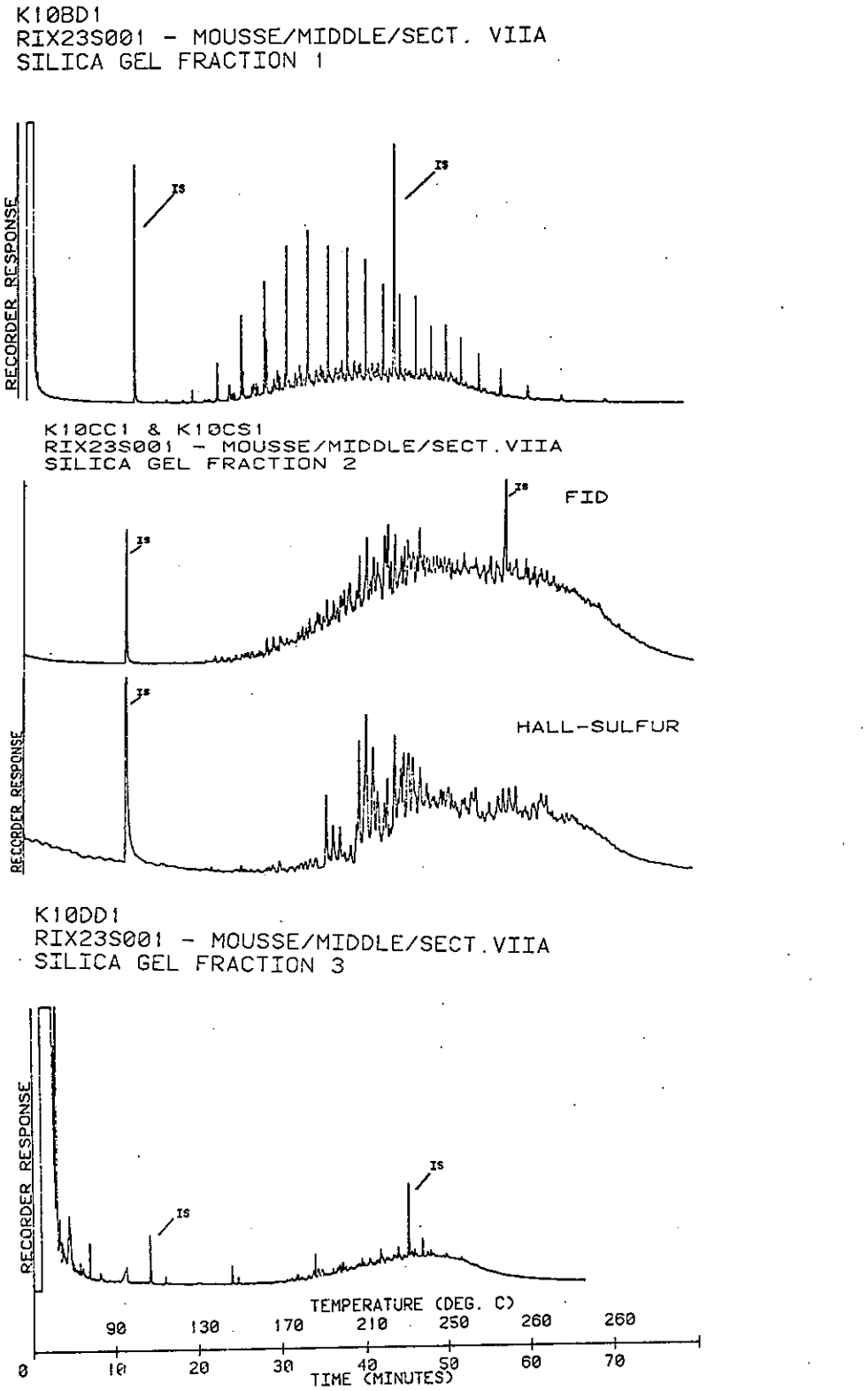

Figure 15. Glass capillary gas chromatograms of the saturate (f_1), aromatic (f_2), FID and sulfur-specific), and polar (f_3) fractions of the less weathered inner structure of the mousse sample collected at RIX 23. The first internal standard, MBT, elutes with approximately the same retention time as 2-methylnaphthalene. The second internal standard, DTP, elutes between $\underline{n}$-C_{24} and $\underline{n}$-C_{25}.

3.3 Air/Sea Interface Samples

Figure 16 shows the reconstructed glass-capillary gas chromatograms of the saturate, aromatic and polar fractions of an air-sea interface sheen collected with a Teflon disc at RIX 06. The f_1 and f_2 fractions appear similar to those that would be expected from mousse samples that have been weathered. The f_3 fraction, however, shows a pronounced unresolved mixture with several resolvable components at very small concentrations. We think that these polar components are the result of environmental weathering at the air-sea interface and have not yet been leached into the water column. Figure 17 compares the polar f_3 fractions of air-sea interface samples taken at control site RIX 02 and at site RIX 06. There are numerous polar compounds that are absorbed onto the Teflon disc at both locations. These are predominantly fatty acids and phthalate-type compounds. However, the sheen sample from RIX 06 shows a prominent unresolved mixture along with many other compounds that were not evident at the control site. GC^2MS analysis of this sample revealed the presence of substituted phenols and the sulfoxides of dibenzothiophenes as well as other aromatic compounds, fatty acids, and phthalates. Some of these compounds undoubtedly have resulted from environmental weathering or environmental oxidation of aromatic compounds in the spilled IXTOC oil.

3.4 Whole Water Column Samples

3.4.1 Neutral and Acid Extracts

A large number of whole water column samples were analyzed during the course of this study. In addition to the neutral extraction, several water column samples were acidified to a pH of three and then re-extracted with methylene chloride. This was an attempt to extract the phenols and acid-type compounds that would represent the oxidized products of aromatic compounds.

Figure 18 shows the neutral and acidic extract of a water column sample from control site PIX 02. As expected, these samples contained numerous compounds of biogenic origin, such as the fatty acids, the C_{16} fatty acid being predominant. Several phthalates also were observed in these samples.

Figures 19 and 20 are three-dimensional (3D) quantitative plots that display the concentrations in parts-per-million (ppm) of several major components in both the neutral and the acid extracts, respectively, of various water samples. The fatty acids are those of biogenic origin and the phthalates are the dibutyl and diethylhexyl. The stations are plotted according to distance from the well site, with the control stations at the far left and stations near the well site at the right end of the 3D plot. The neutral extract contains elevated levels of diethylhexyl phthalate in roughly equal concentrations (except for PIX 05 and PIX 10). These quantities generally agree with those reported previously in the literature (Giam, 1977). The acid extract contained elevated levels of fatty acids at sites RIX 05, PIX 08, and PIX 10, while the other stations contained the same quantities of fatty acids that were found at the control sites PIX 01 and RIX 02. The reason for these elevated levels is not obvious at the present time.

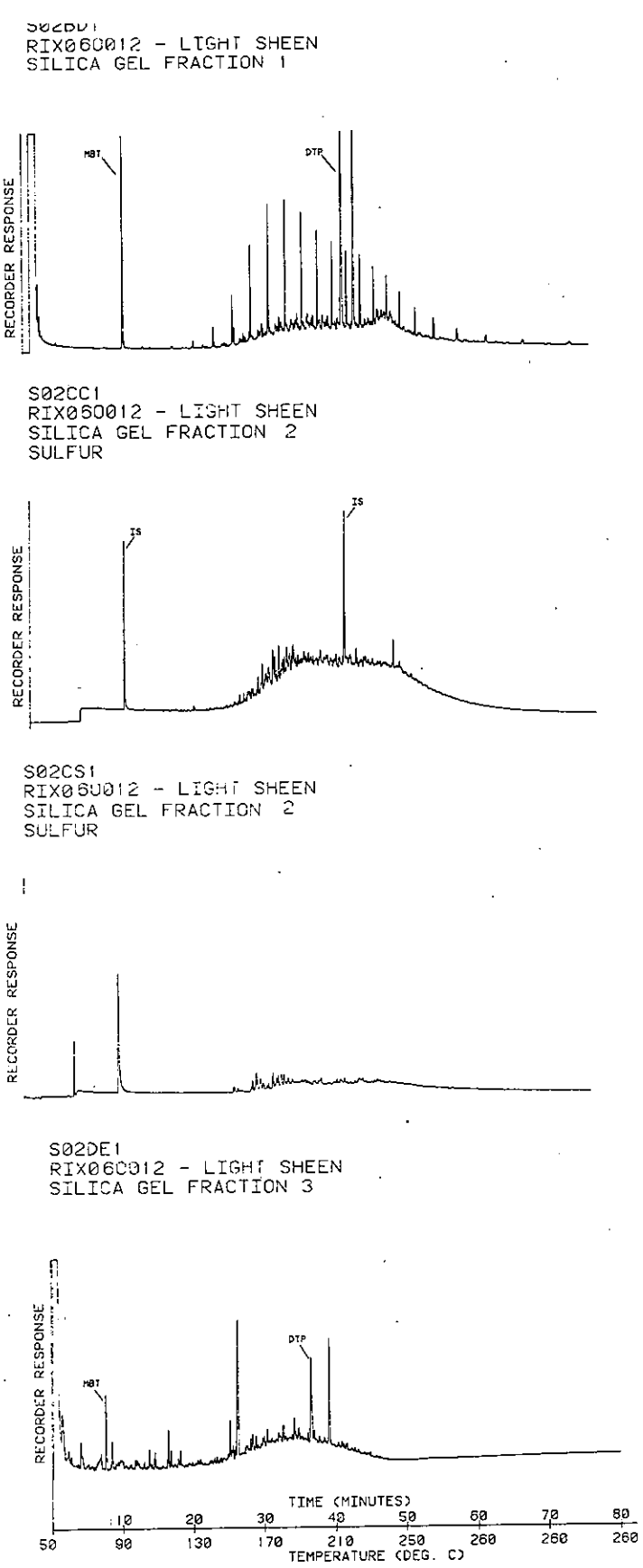

Figure 16. Glass capillary gas chromatograms of the saturate, aromatic (FID and sulfer-specific detector), and polar fractions of a light sheen sample collected with a Teflon disc at station RIX 06. The first internal standard, MBT, elutes with approximately the same retention time as 2-methylnaphthalene. The second internal standard, DTP, elutes between $\underline{n}$-C_{24} and $\underline{n}$-C_{25}.

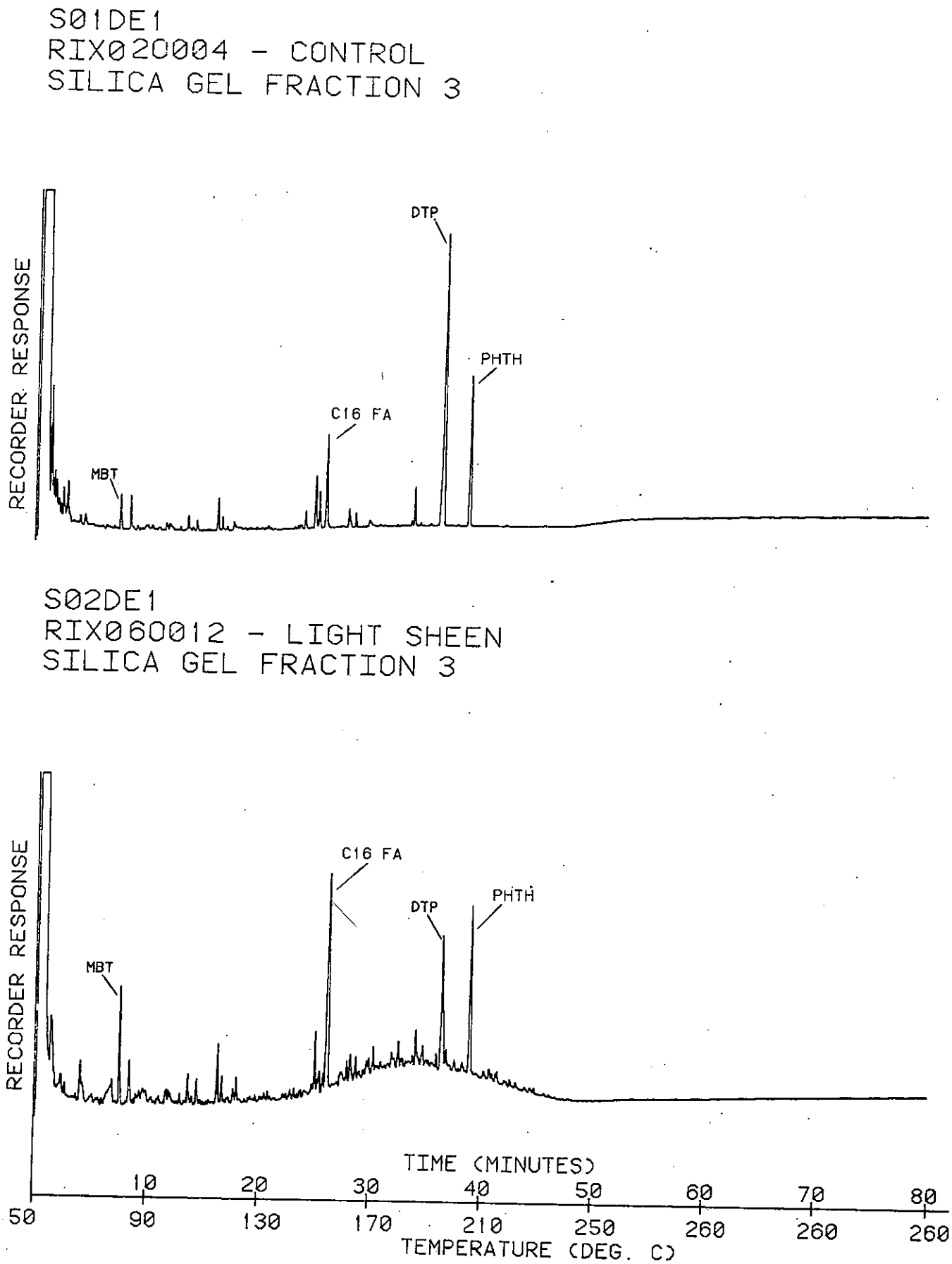

Figure 17. Glass capillary gas chromatograms of the polar (f_3) fraction of sheen samples collected by Teflon disc at control station RIX 02 (upper) and station RIX 06 (lower).

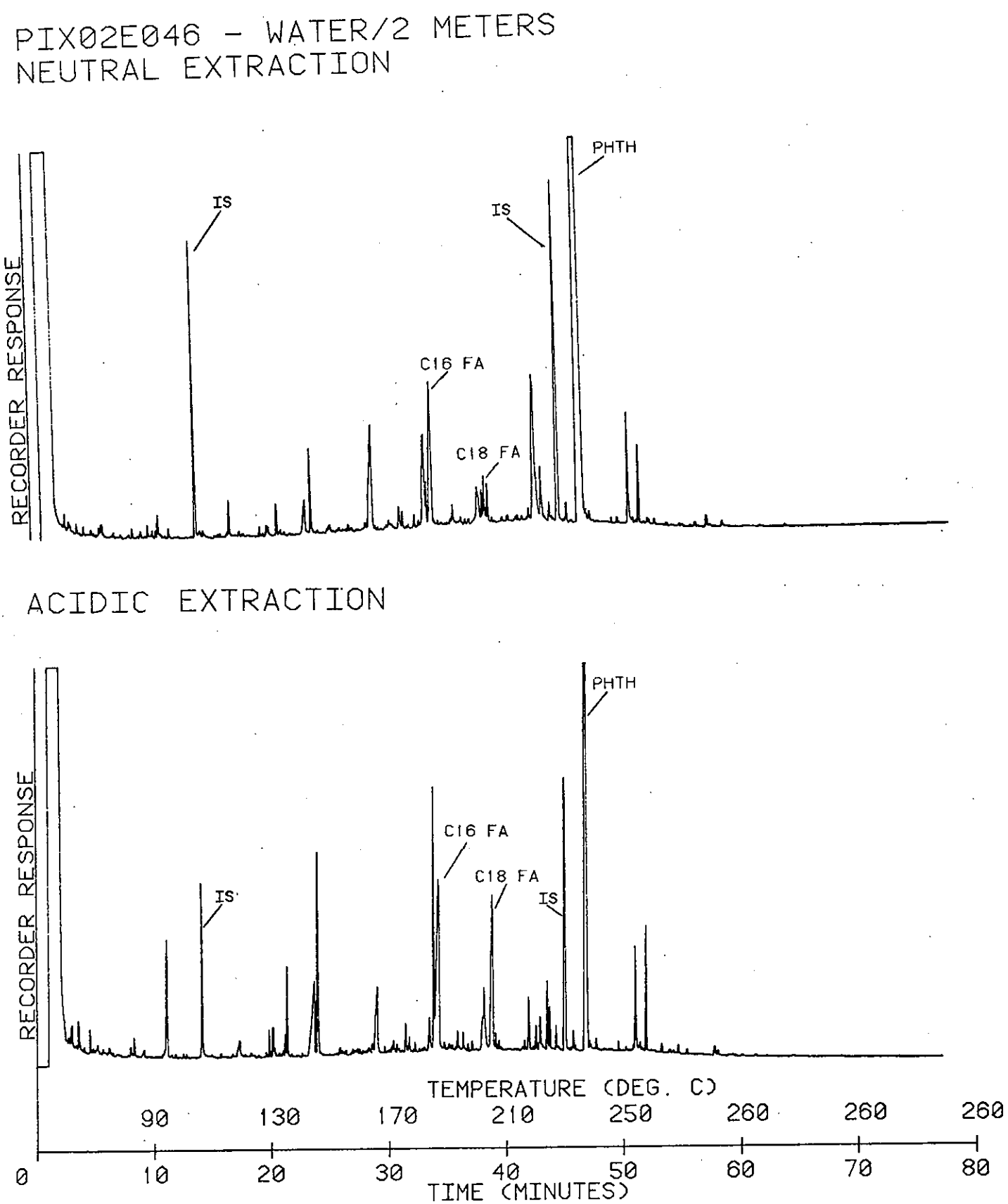

Figure 18. Glass capillary gas chromatograms of the neutral (upper) and acidic extracts (lower) of a whole water sample collected at control site PIX 02. The first internal standard, MBT, elutes with approximately the same retention time as 2-methylnaphthalene. The second internal standard, DTP, elutes between $\underline{n}$-C_{24} and $\underline{n}$-C_{25}.

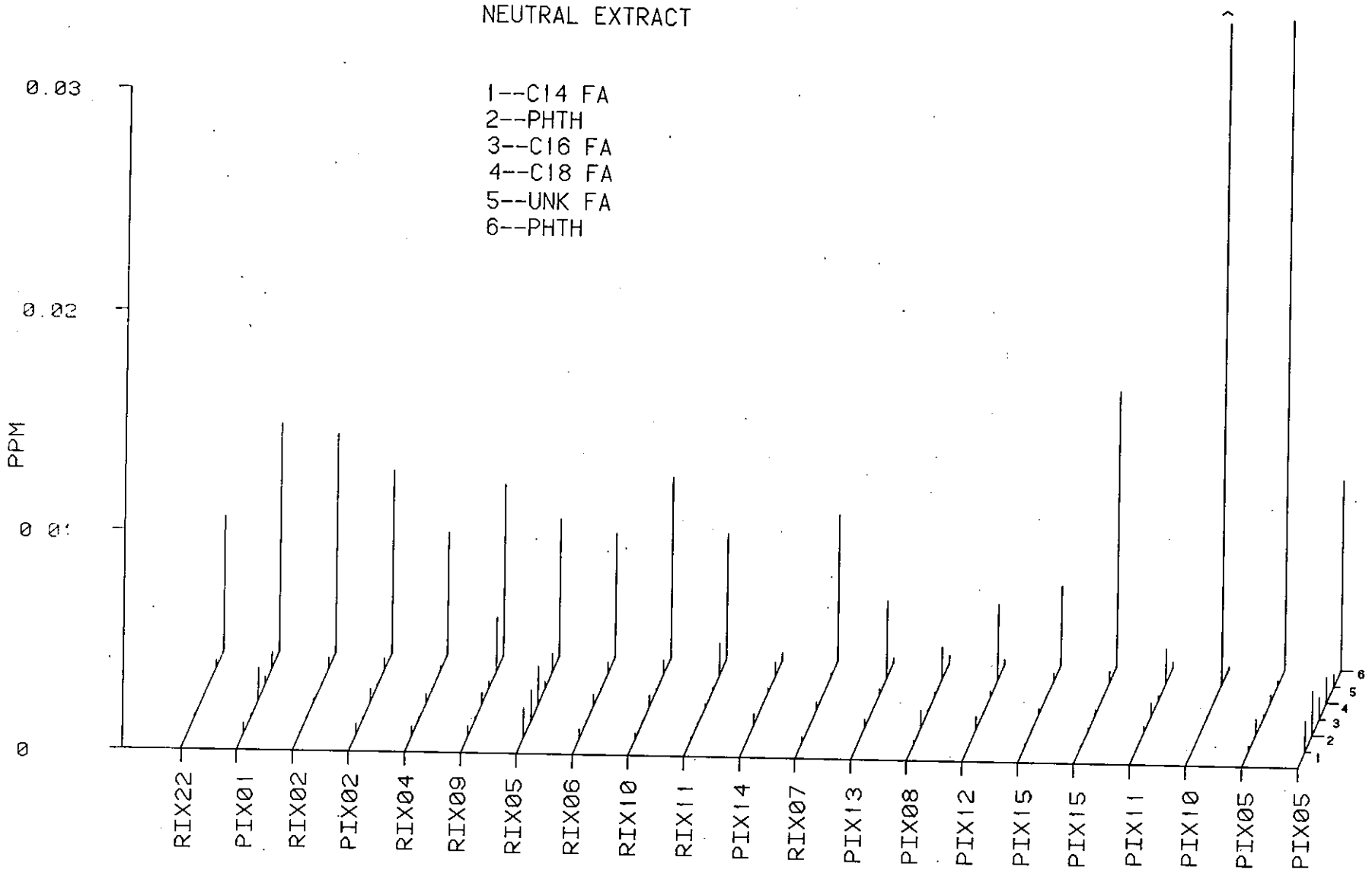

Figure 19. Three-dimensional plot comparing the concentrations (vertical axis) at several stations (horizontal axis) of the major organic compounds in the neutral extract of whole water samples (axis into the page). Samples near the well site are plotted to the right while samples farthest from the well site are plotted to the left.

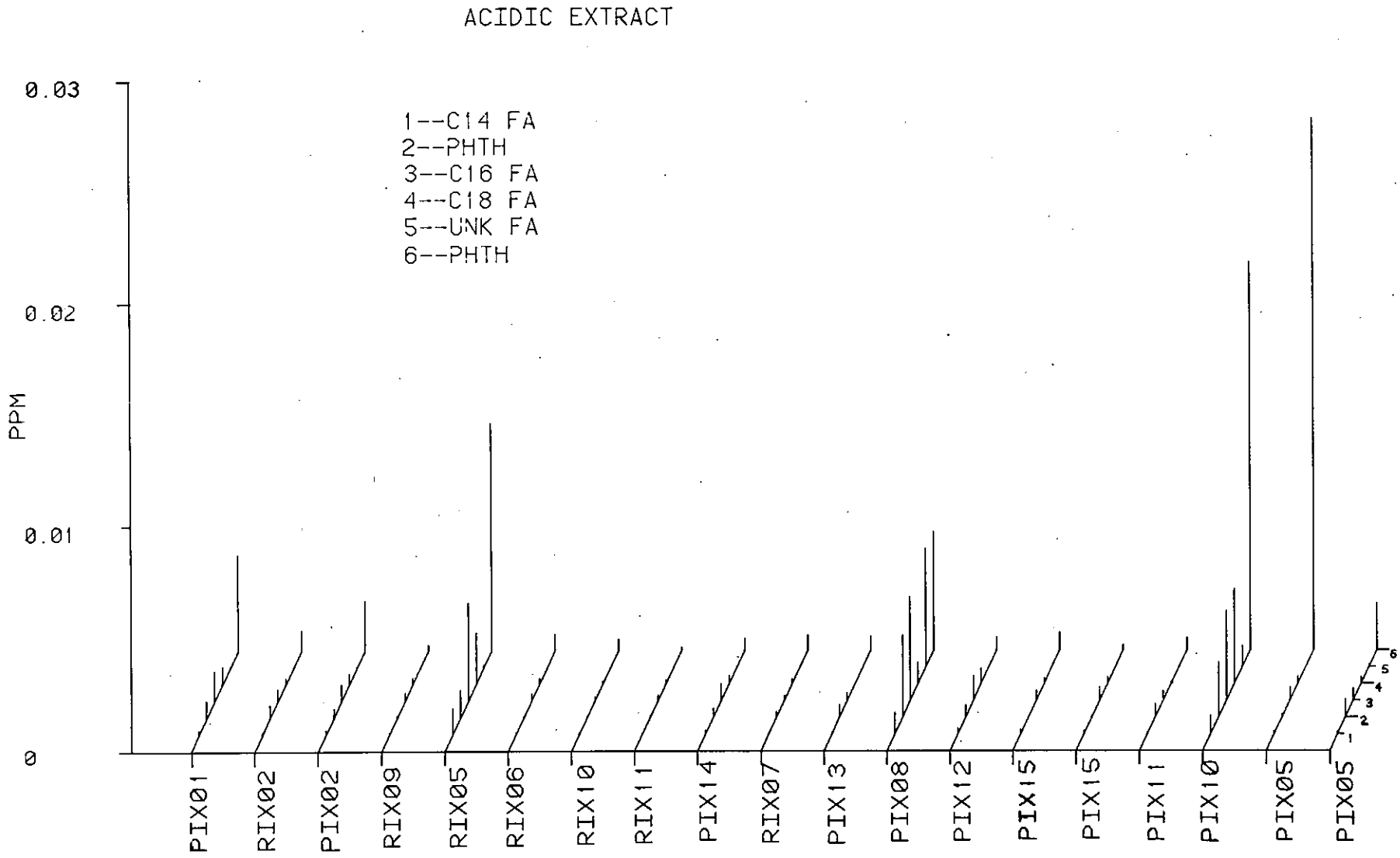

Figure 20. Three-dimensional plots showing the concentration (vertical axis) at several stations (horizontal axis) for six components detected in the acidic extract of whole water samples. Stations near the wellhead are plotted to the right while stations farthest from the wellhead are plotted to the left.

3.4.2 Aromatic Fractions

Figure 21 shows a computer-reconstructed gas chromatogram of the aromatic fraction with the FID and sulfur-specific traces of a water sample at PIX 05 and a sample of fresh crude oil collected subsurface by divers for PEMEX (personal communication, Sra. Amada Cortes Rubio). The sulfur-specific traces appeared to be identical in the two samples and showed the presence of the benzothiophenes, dibenzothiophene, and small quantities of napthylbenzothiophene. The FID trace showed differences in the early-eluting portion of the runs. Many of the alkylated benzene compounds are less abundant in the PIX 05 sample. These alkylated benzene compounds are the more volatile (and water soluble) of the aromatics and presumably were lost from the PIX 05 sample by the time of collection. Assuming that the well discharged the same composition of oil, the data show that even in the PIX 05 sample collection close to the well site, initial weathering had already changed the composition of the oil.

Figure 22 shows comparative data between the fresh oil-in-water sample at PIX 05 (both the FID and the sulfur-specific chromatograms) and a 2-m water column sample taken at PIX 10. Examination of the data from the sample taken at PIX 10 indicates that quantities of the more soluble aromatic alkylated benzenes and small quantities of the alkylated naphthalenes, and benzothiophenes were present in the water column. Since the high molecular weight aromatic compounds were absent, we believe that these data indicate that there was soluting of these aromatic compounds in the water column sample, as opposed to some type of colloidial oil/water mixture apparent in other whole water samples that we have examined.

3.4.3 Methylated Fractions

Figure 23 shows the reconstructed glass-capillary chromatograms of the unfractionated neutral and acidic extract of the PIX 10 sample. It also shows these sample extracts after methylation by the gentle diazomethane procedure developed for the project. The methylated acidic extract was a very heavy run and contained numerous fatty acids and an unusually large number of phthalate compounds not found in other water column samples. The data from this sample will be discussed in greater detail in another paper.

3.5 Sediment Samples

Figure 24 shows the raw chromatographic data for our analysis of three sediment samples collected off the Brownsville, Texas, Gulf coast. Examination of this data indicates only very low (less than 1 ppm), if any, levels of petroleum hydrocarbons in these samples.

3.6 Microbial Degradation (Microcosm) Experiment

A series of laboratory experiments was performed onboard the RESEARCHER to determine the effects of microbial degradation on the IXTOC oil. These experiments are described in detail in the paper by Buckley and Pfeander (this symposium). Three types of oil samples were incubated in the dark for a

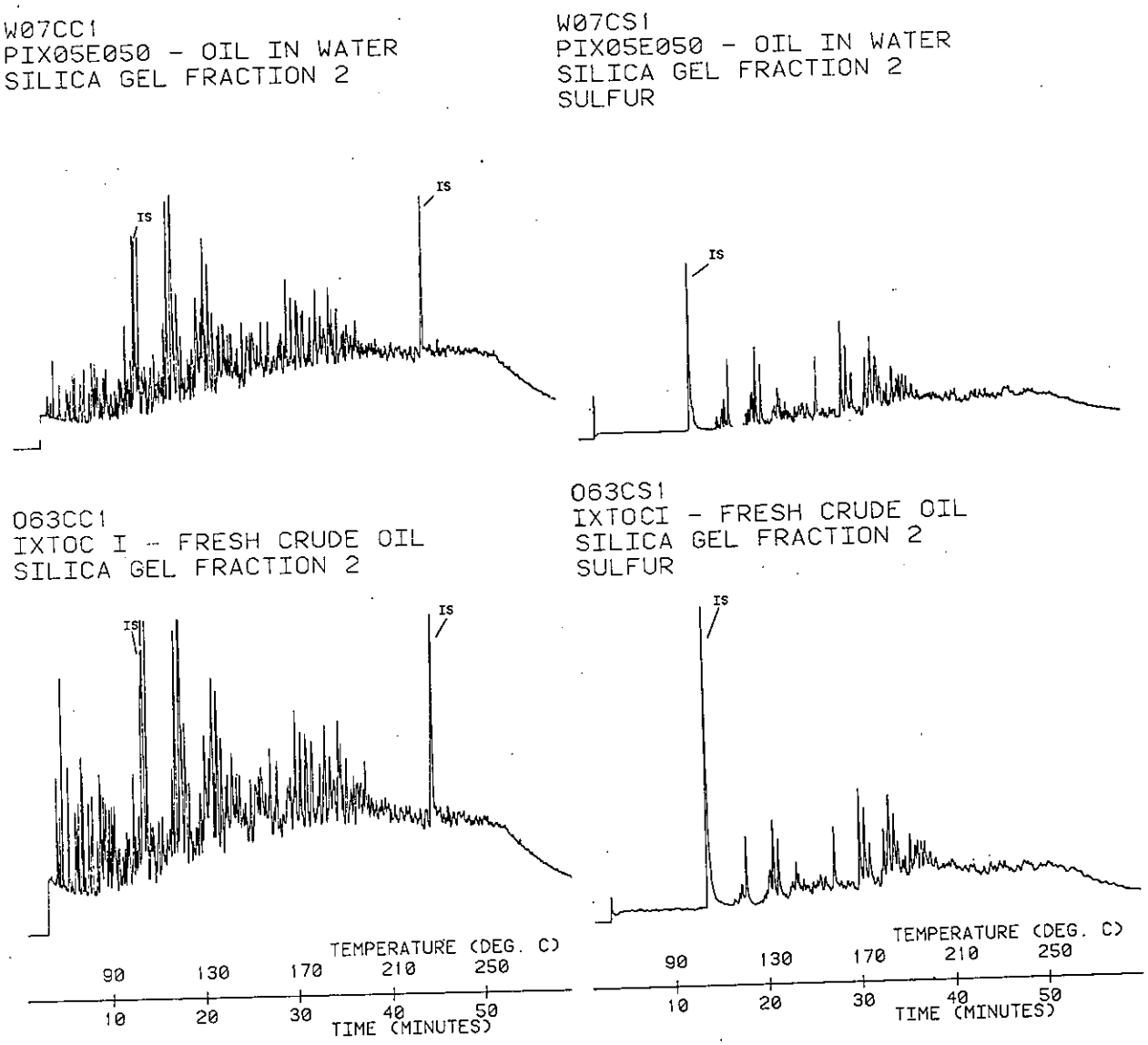

Figure 21. Glass capillary gas chromatograms using the FID and sulfur-specific detectors for the aromatic fractions of the fresh oil collected at PIX 05 and a sample of fresh crude collected subsurface by divers. The first internal standard, MBT, elutes with approximately the same retention time as 2-methylnaphthalene.

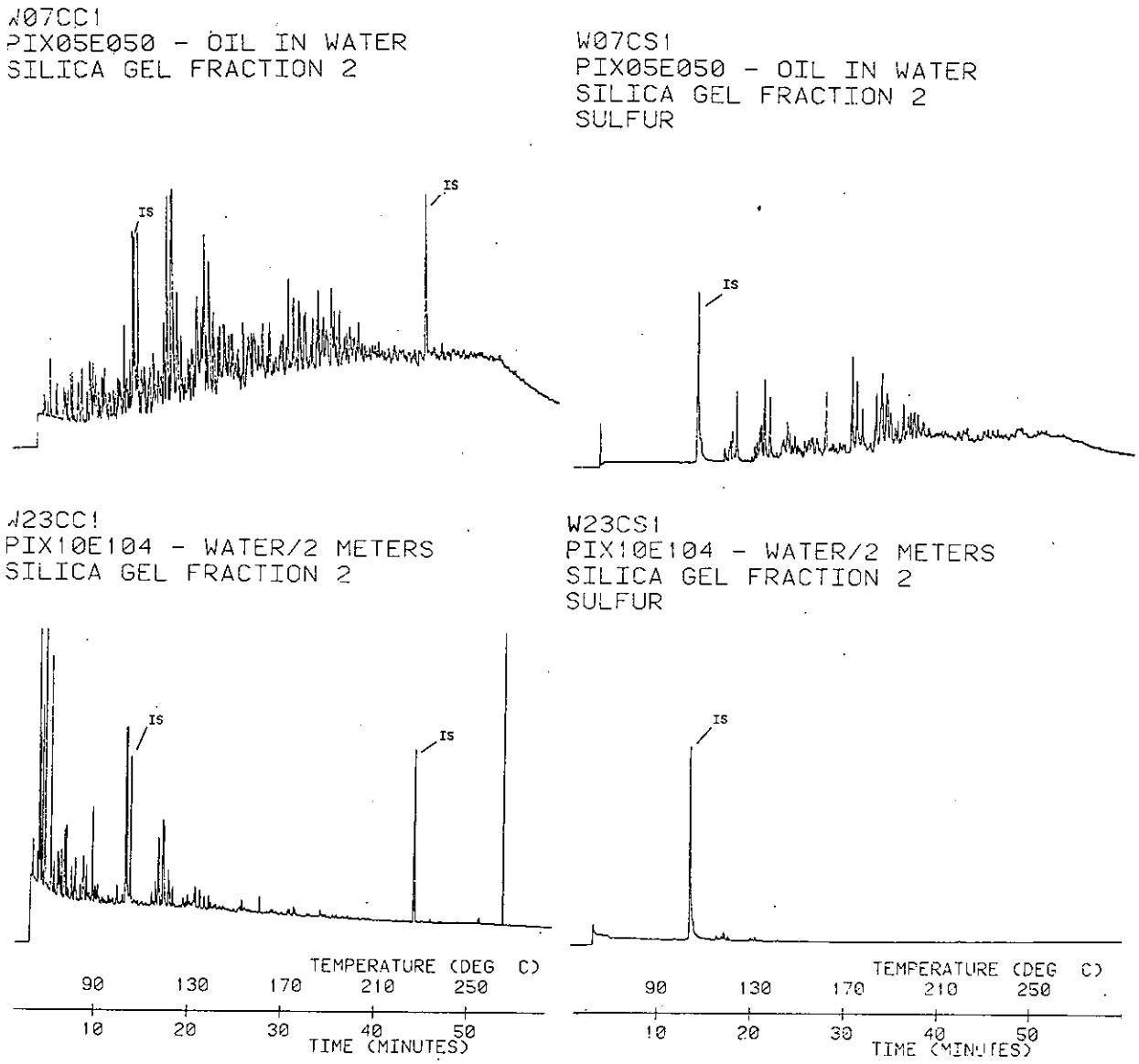

Figure 22. Glass capillary gas chromatograms using the flame ionization and sulfur-specific detectors for the aromatic fractions of the fresh oil and water samples collected at PIX 05 and the neutral extract of a 2 m whole water sample collected at PIX 10. The first internal standard, MBT, elutes with approximately the same retnetion time as 2-methylnaphthalene.

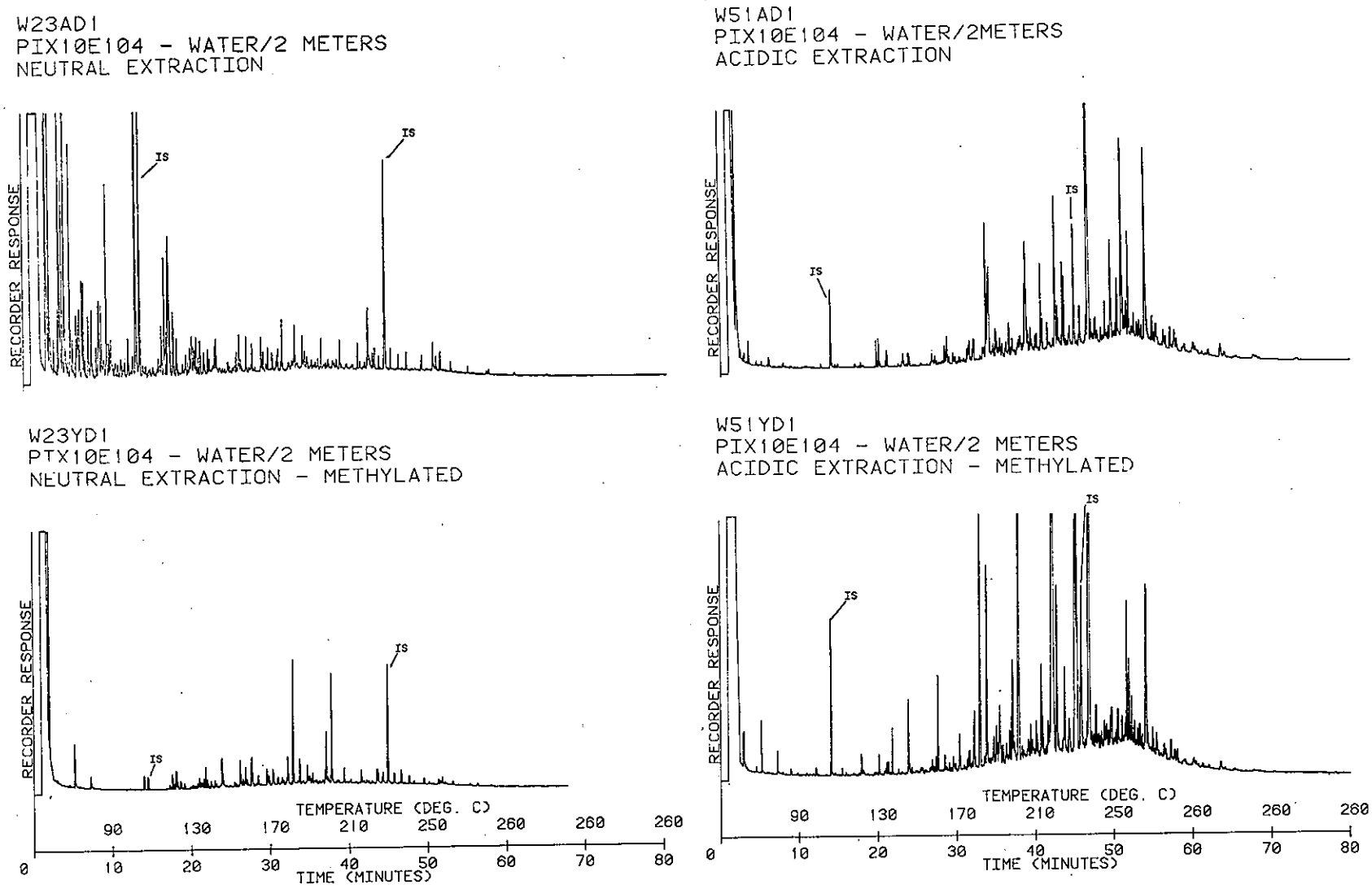

Figure 23. Glass capillary gas chromatograms of the neutral and acidic extract, both free and methylated, of a whole water sample collected at PIX 10. The first internal standard, MBT, elutes with approximately the same retention time as 2-methylnaphthalene.

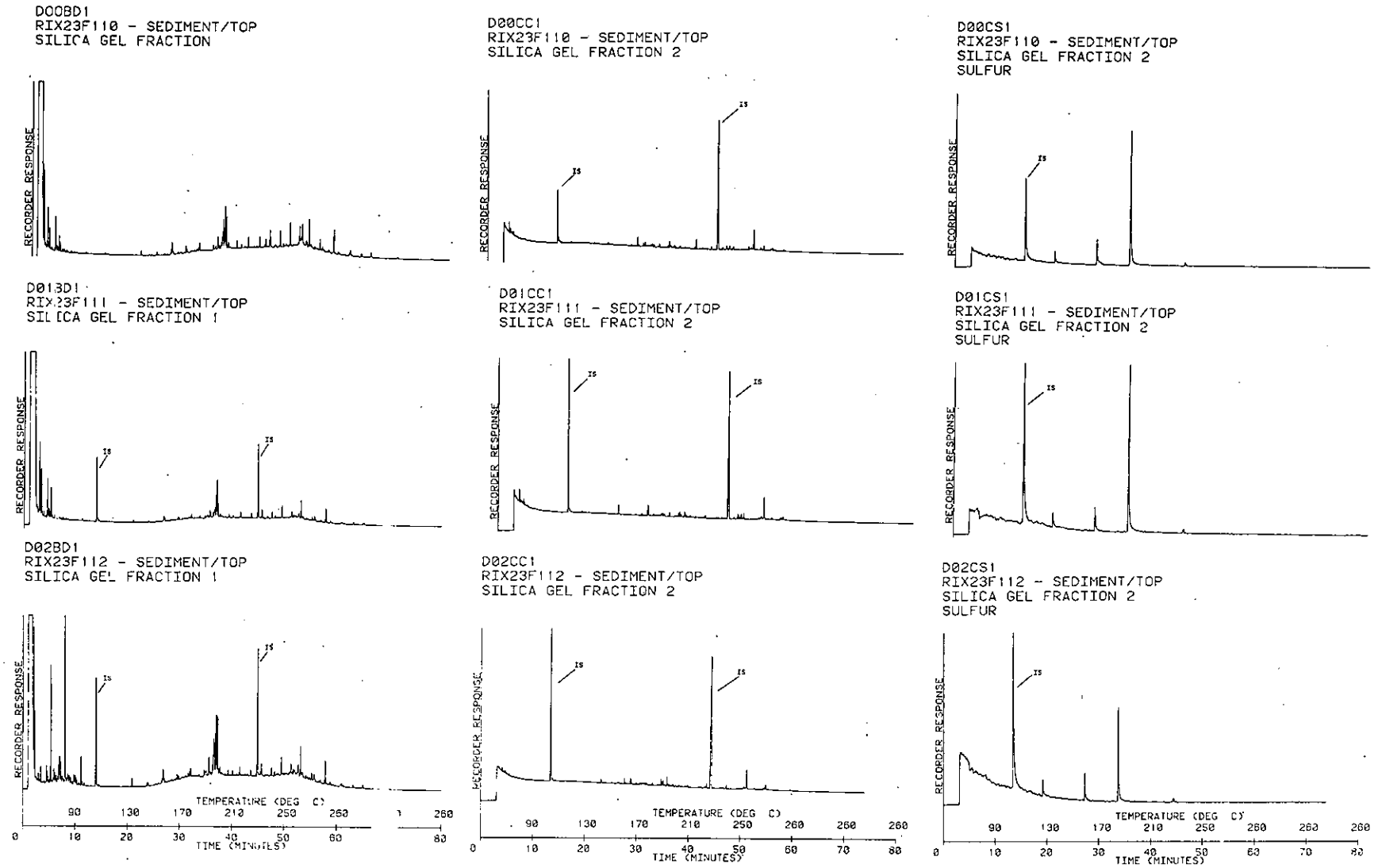

Figure 24. Glass capillary gas chromatograms of the saturate and aromatic fractions (flame ionization and sulfur-specific detectors) of surface sediment collected along a transect near station RIX 23. The first internal standard, MBT, elutes with approximately the same retention time as 2-methylnaphthalene. The second internal standard, DTP, elutes between $\underline{n}$-C_{24} and $\underline{n}$-C_{25}.

period of seven days over Gulf water collected at Station RIX 09. The types of oil used for these experiments included oil droplets collected at RIX 07 that were similar in appearance to those collected at PIX 05, a relatively fresh mousse (or oil and water emulsion sample) collected at RIX 06, and a mousse collected off the beach at the south end of Padre Island, Texas.

The data shown in Figures 25 through 40 attempt to highlight several interesting comparisons discovered during analysis of samples from these microcosm experiments. The first comparison, illustrated by the data in Figures 25 and 26, considers the chemical composition of the microcosm oils before and after exposure for seven days. The second comparison, illustrated by the data in Figures 26 and through 32, highlights the differences in the water column composition between the control day, exposed day zero, and exposed day seven for the three types of microcosm experiments (using fresh oil, fresh mousse, and Texas beach mousse). The third comparison, shown in Figures 33 to 38, considers the differences in chemical composition between the water column extracts and the oil floating above the water column after seven days of incubation. The final microcosm experiment data presented in this report concern an examination of the more polar organic compounds produced by the experiment.

3.6.1 Composition of Oil Samples Before and After Exposure

Figure 25 shows a comparison of the saturate (f_1) fractions of the fresh oil collected at PIX 05 and the fresh oil taken from the microcosm experiment after seven days of incubation. From examination of these data we can see that the saturate fraction readily lost the more volatile components, as would be expected simply due to evaporative weathering. Figure 26 shows the FID and sulfur-specific chromatograms from the aromatic (f_2) fraction of fresh oil taken at PIX 05 and fresh oil after seven days of incubation. Examination of these data shows that, as expected, the microcosm oil samples had lost the lower molecular weight aromatics, predominantly the alkylated benzenes and naphthalenes. The sulfur-specific chromatogram showed that quantities of the benzothiophenes and the dibenzothiophenes were still present at day seven in the weathered oil. Comparison data between the starting materials and the day seven oils are not available for other types of microcosm oils.

3.6.2 Composition of Water Columns Before and After Exposure

Figures 27-32 show saturate (f_1) and aromatic (f_2) water column data for the control day, day zero, and day seven for the three types of microcosm experiments using the different starting oil samples. These chromatographic data were developed from the acid extracts of the water column under the various types of oils that were incubated for the respective time periods. The most dramatic differences between day zero and day seven were observed for the microcosm experiment using fresh mousse (Figures 29 and 30). Notice that there are substantial unresolved mixtures in the water column on day seven, for both the saturate and aromatic fractions. These observations are in agreement with the data given at this symposium by Dr. Pfaender and Mr. Buckley, who observed increased microbial activity in the fresh mousse microcosm experiment, compared with the weathered beach mousse and the fresh wellhead oil experiments.

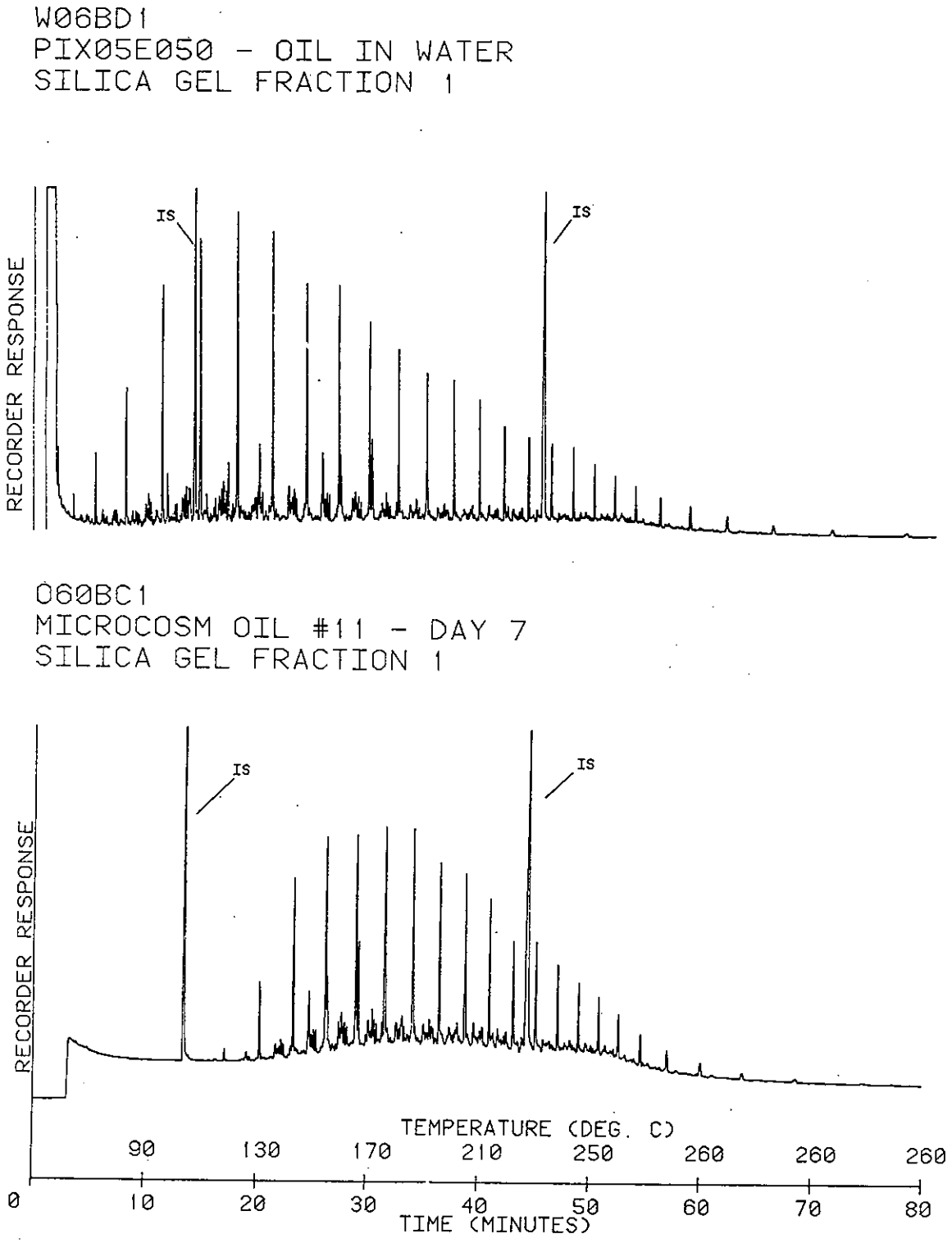

Figure 25. Comparison of the glass capillary gas chromatographic data of the saturate fractions of a fresh oil and water sample collected at PIX 05 (upper) and the fresh microcosm oil samples after seven days of incubation (lower). The second internal standard, DTP, elutes between $\underline{n}$-C_{24} and $\underline{n}$-C_{25}.

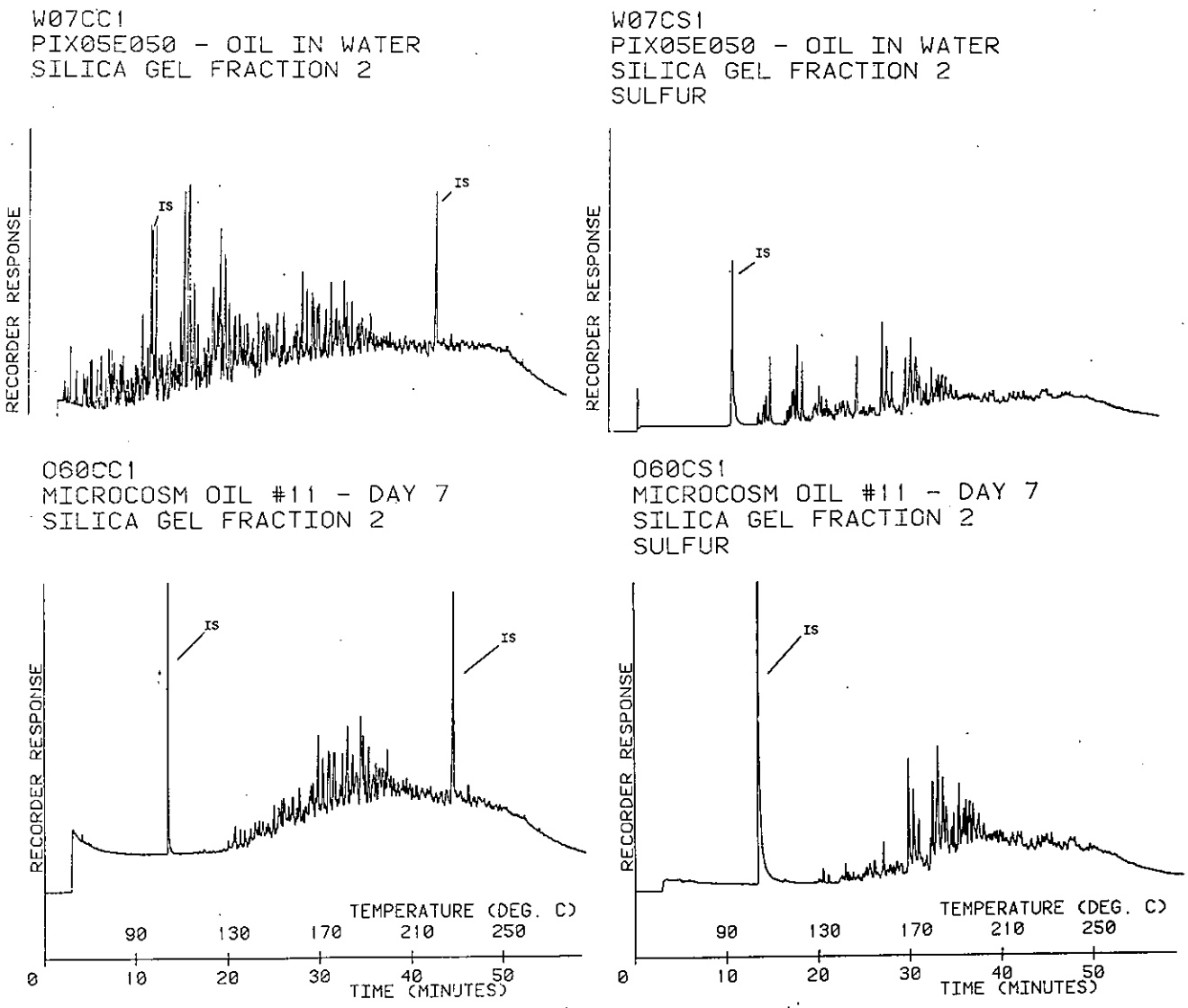

Figure 26. Comparison of the gas capillary gas chromatographic data from the microcosm experiment using fresh mousse. Upper trace shows data for the aromatic fraction of the water column extract, day seven. Lower trace shows the aromatic fraction of the microcosm oil after seven days of incubation. The first internal standard, MBT, elutes with approximately the same retention time as 2-methylnaphthalene.

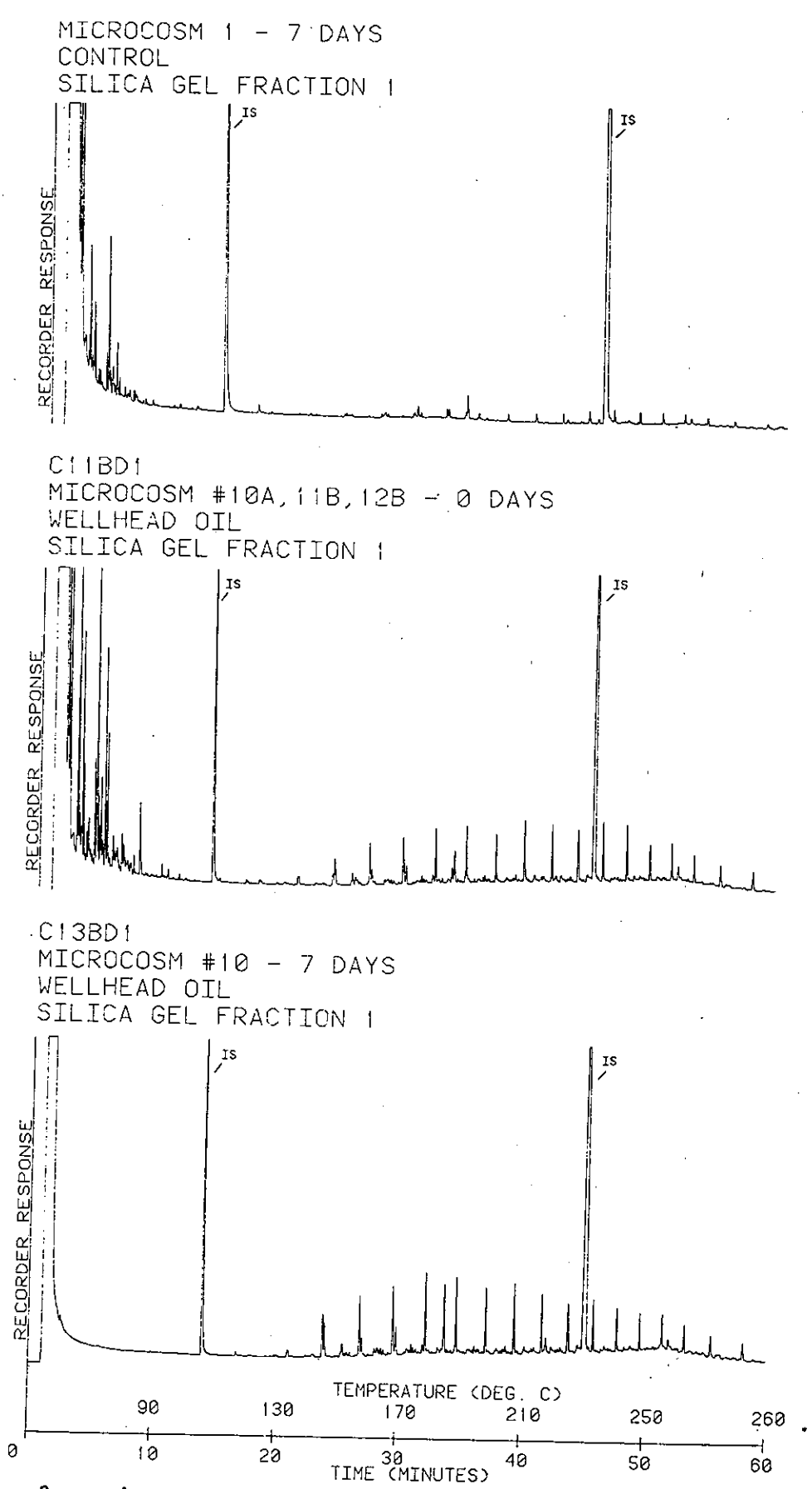

Figure 27. Comparison of the glass capillary gas chromatographic data of the saturate fraction from the water column extract from the microcosm control on day seven, and the fresh wellhead oil on days zero and seven of the microcosm experiment. The second internal standard, DTP, elutes beteen $\underline{n}$-C_{24} and $\underline{n}$-C_{25}.

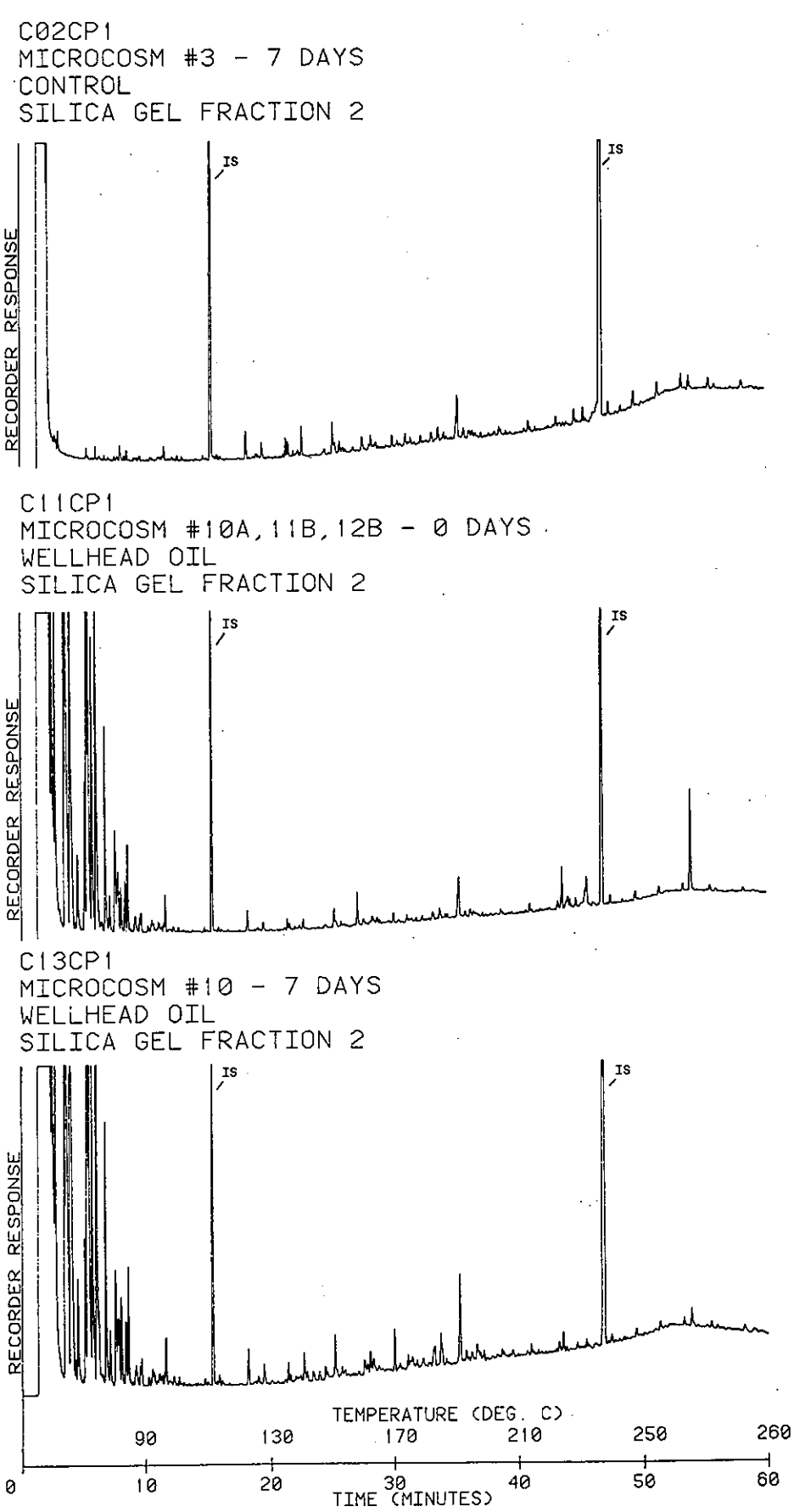

Figure 28. Comparison of the glass capillary gas chromatographic data of the aromatic fraction from the control and the fresh wellhead oil on days zero and seven of the microcosm experiment. The first internal standard, MBT, elutes with approximately the same retention time as 2-methylnaphthalene.

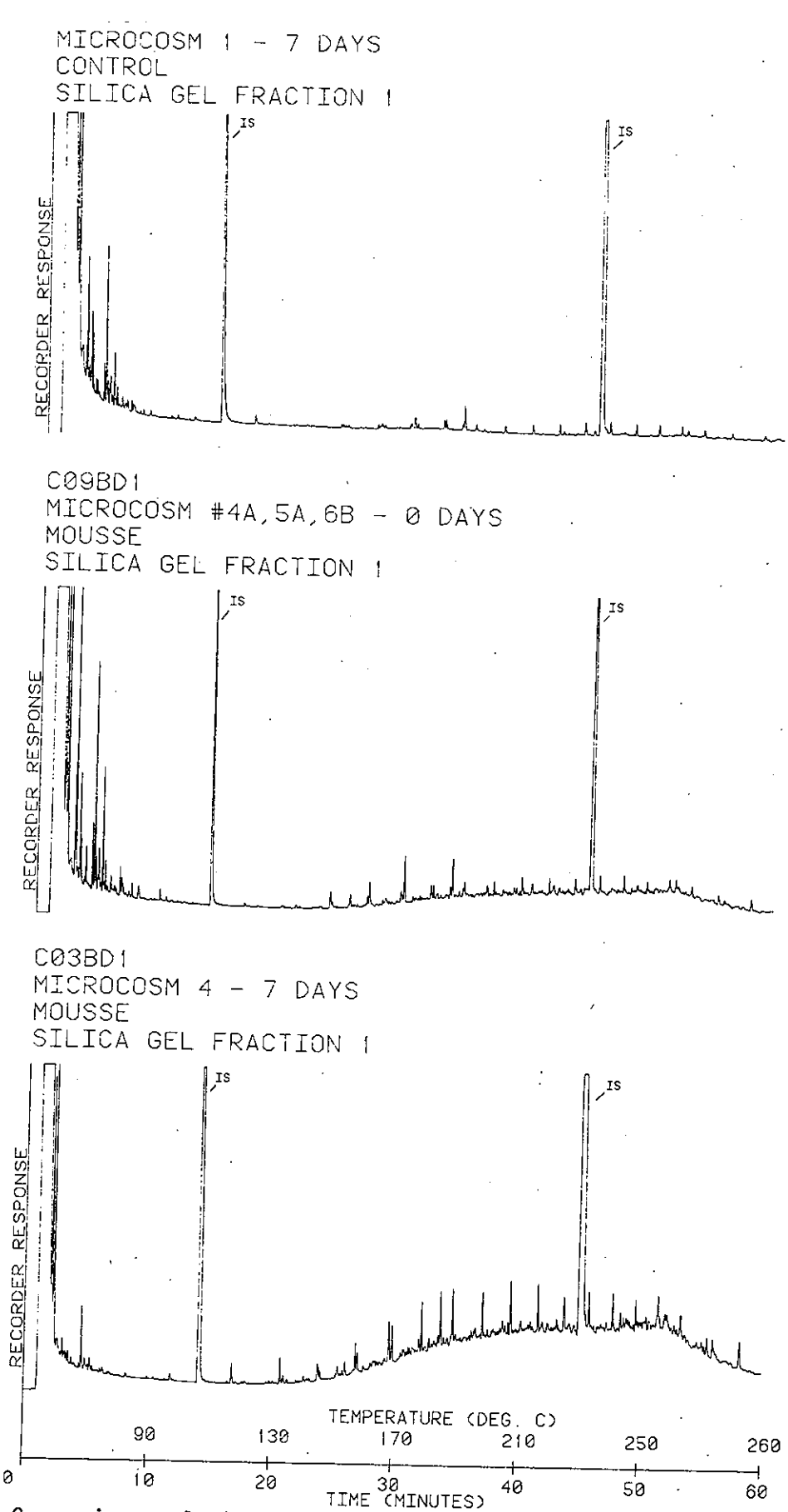

Figure 29. Comparison of the glass capillary gas chromatographic data of the saturate fraction from the control and the microcosm experiment utilizing fresh mousse from days zero and seven. The second internal standard, DTP, elutes between $\underline{n}$-C_{24} and $\underline{n}$-C_{25}.

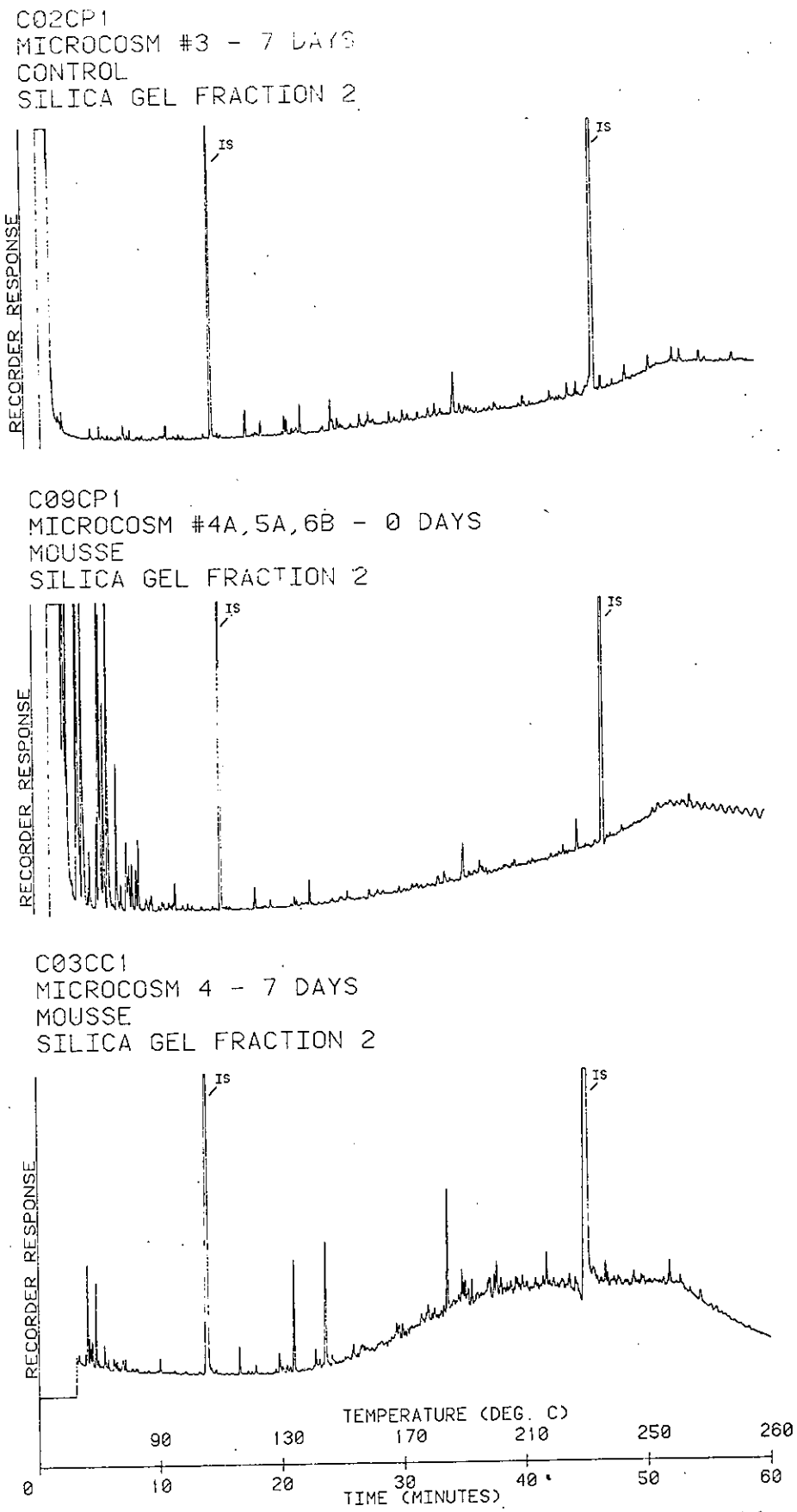

Figure 30. Comparison of the glass capillary gas chromatographic data of the aromatic fraction from the control and the microcosm experiment using fresh mousse from days zero and seven. The first internal standard, MBT, elutes with approximately the same retention time as 2-methylnaphthalene.

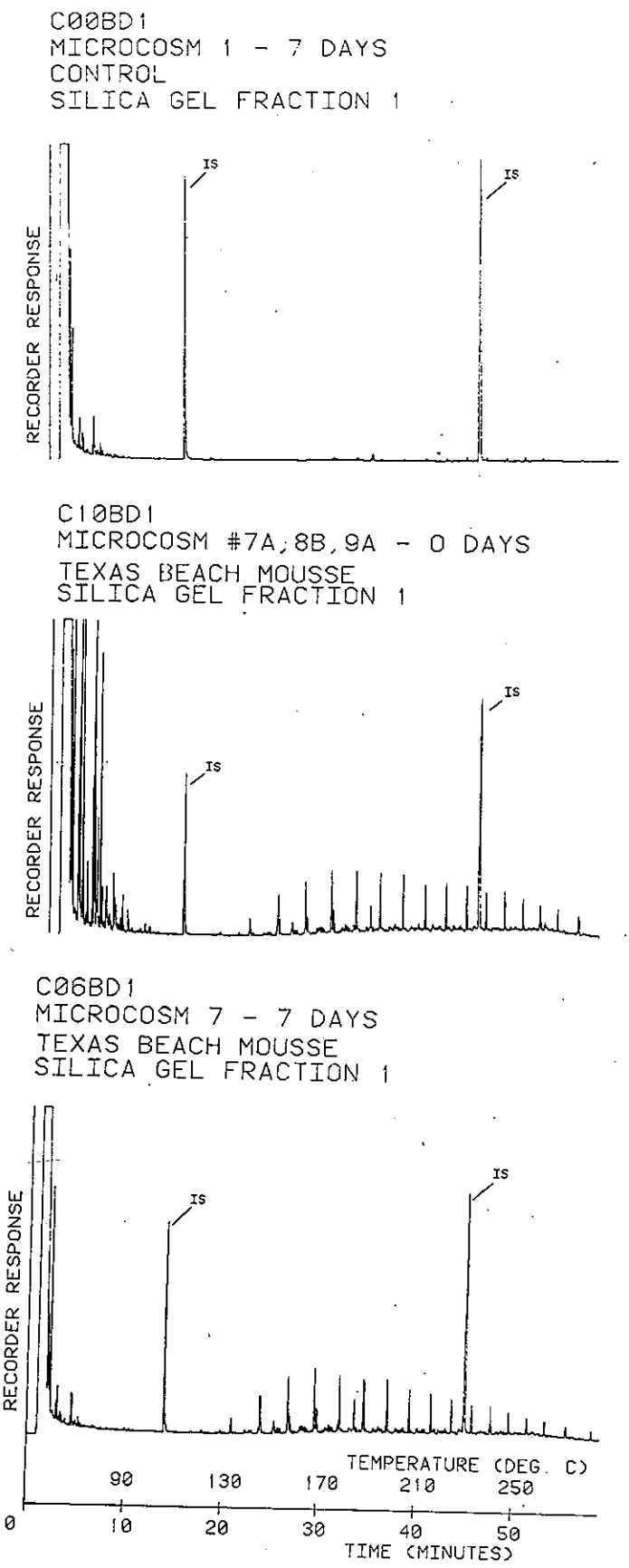

Figure 31. Comparison of the glass capillary gas chromatographic data of the saturate fraction from the control and the microcosm experiment using fresh Texas beach mousse from days zero and seven. The second internal standard, DTP, elutes between $\underline{n}$-C_{24} and $\underline{n}$-C_{25}.

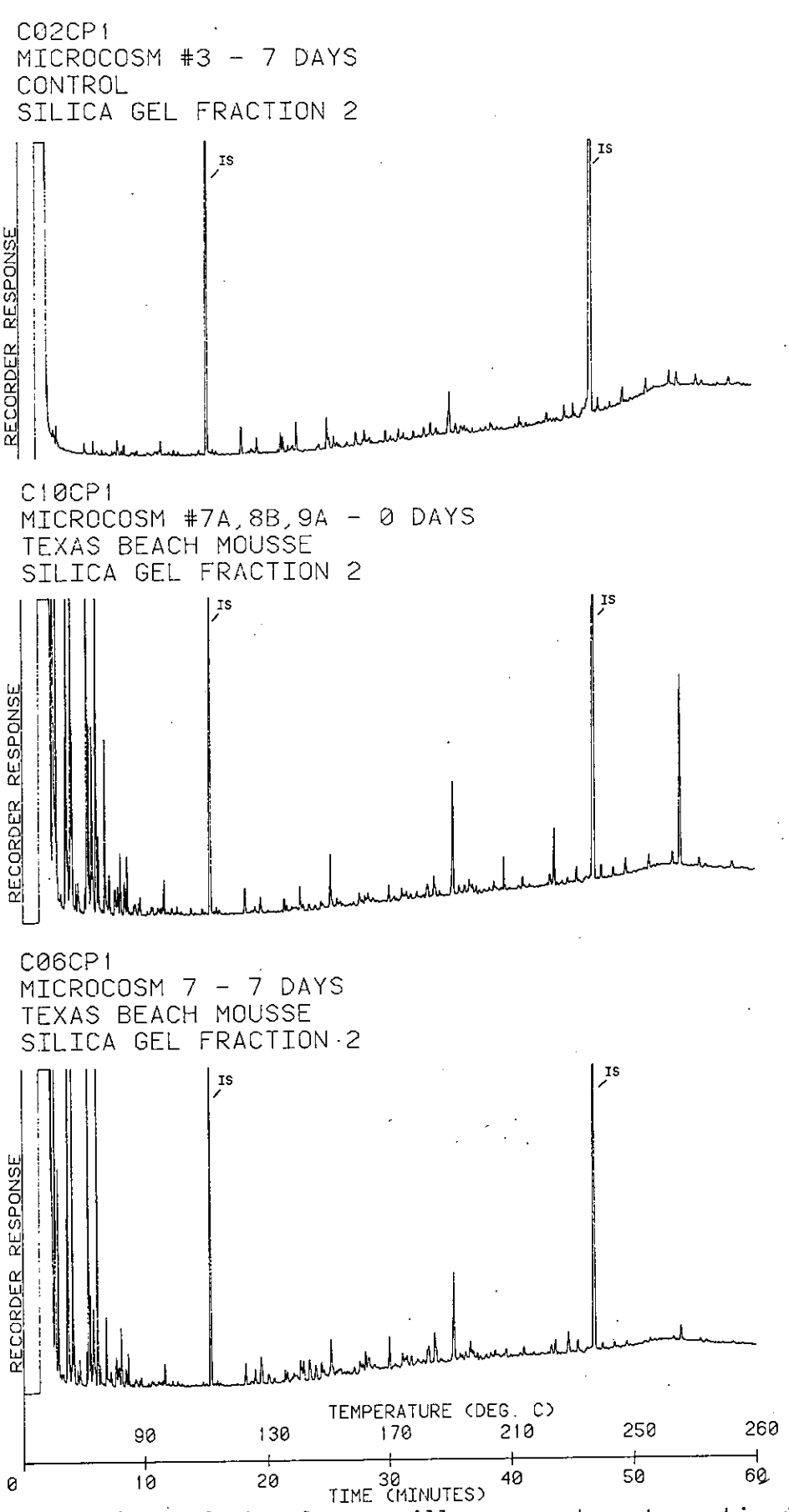

Figure 32. Comparison of the glass capillary gas chromatographic data of the aromatic fraction from the control and the microcosm experiment using Texas beach mousse from days zero and seven. The first internal standard, MBT, elutes with approximately the same retention time as 2-methylnaphthalene.

3.6.3 Comparison of Oil Samples and Associated Water Columns after Exposure

Figures 33-38 show a comparison between the saturate (f_1) and aromatic (f_2) fractions of the day-seven microcosm water samples and the saturate and aromatic fractions of the oil above the water column samples for the three types of oil used in the experiments. The day-seven oil samples did not exhibit advanced weathering characteristics, but this is not surprising since concentrations of the oils used in the microcosm experiment were so high that weathering might not be observed. The data in Figures 35-36 substantiate the earlier observation that the microcosm experiment using fresh mousse experienced the greatest amount of alteration. An interesting point, however, is that while the mousse sample exhibited an unresolved mixture, the sulfur-specific chromatogram showed the presence of the benzothiophenes in addition to the dibenzothiophenes. This is not characteristic of weathered mousse samples. However, these compounds were not present in the water column from this experiment.

3.6.4 Polar Compounds

Figure 39 shows the day-seven HPLC fraction 1 and polar fractions 1 and 2 from the water column extract of the microcosm experiment with fresh wellhead oil. Examination of the data in polar fraction 2 (equivalent to silica gel fraction f_3) indicates the presence of a substantial unresolved mixture as well as a number of resolvable polar compounds. Figure 40 shows the HPLC fraction 1 and polar fraction 2 (both free and methylated) for this same microcosm experiment. Examination of the data for the saturate fraction (HPLC I) indicated a number of biogenic fatty acids that elute between the normal hydrocarbons in the methylated chromatogram. The chromatogram of the methylated polar fraction 2 reveals a number of resolvable compounds. GCMS analysis indicated that the largest peaks are oxidized aromatic compounds, such as naphthols and substituted benzoic acids. The mass spectral data for this fraction will be discussed in greater detail in the subsequent paper.

4. SUMMARY

(1) Fresh IXTOC oil contained the following aromatic hydrocarbons:

- alkylated benzenes (to, at least, the C_6 homolog)
- naphthalene and alkylated napthalenes
- alkylated naphthenoaromatics
- alkylated biphenyls
- fluorene and alkylated fluorenes
- phenanthrene and alkylated fluorenes
- alkylated members of the pyrene family
- alkylated members of the chrysene family
- alkylated members of the benzopyrene family.

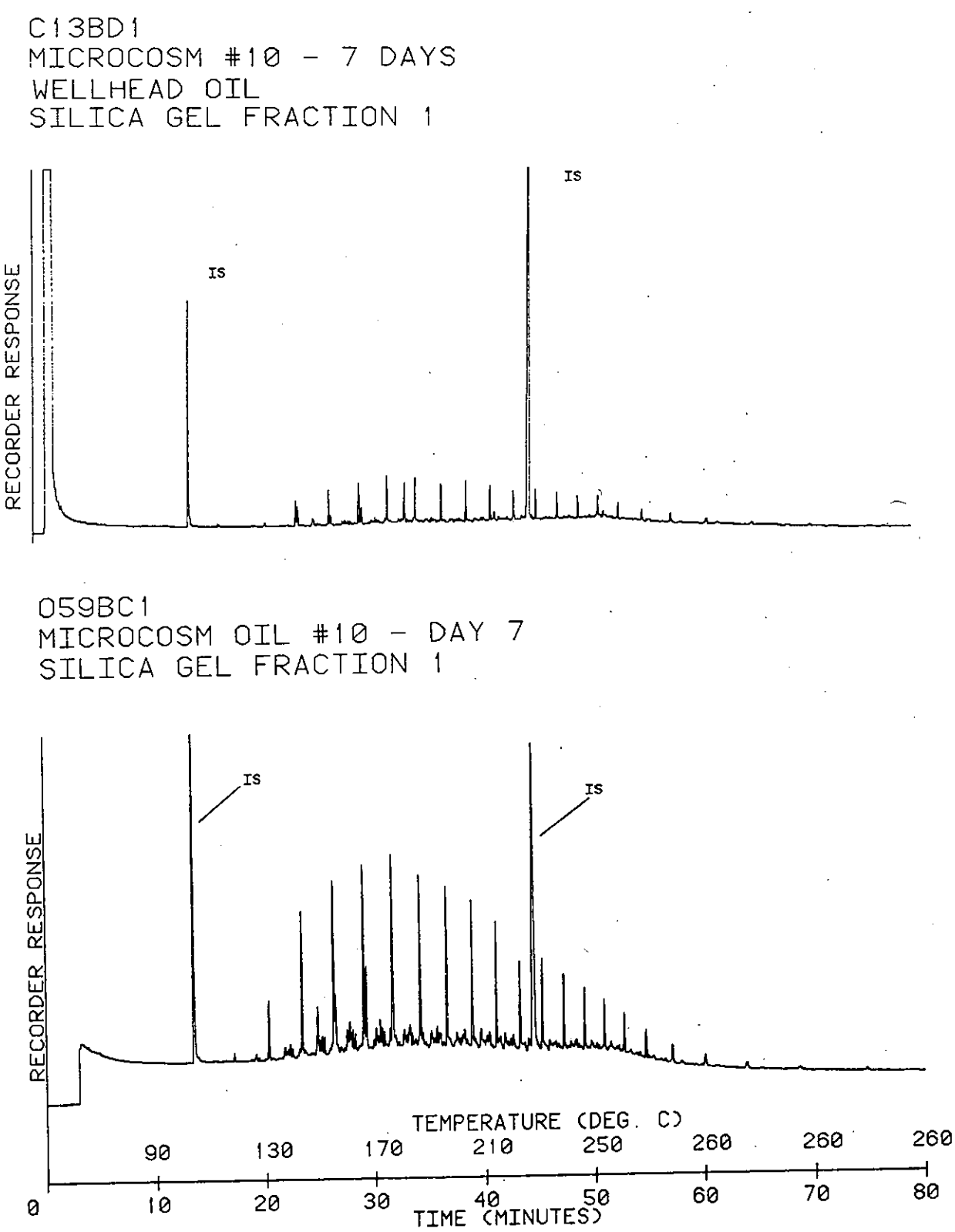

Figure 33. Comparison of the glass capillary gas chromatographic data of the microcosm experiment using fresh wellhead oil. The upper trace is the data from the saturate fraction of the water column extract. The bottom trace is data from the saturate fraction of the microcosm oil after seven days of incubation. The second internal standard, DTP, elutes between $\underline{n}$-C_{24} and $\underline{n}$-C_{25}.

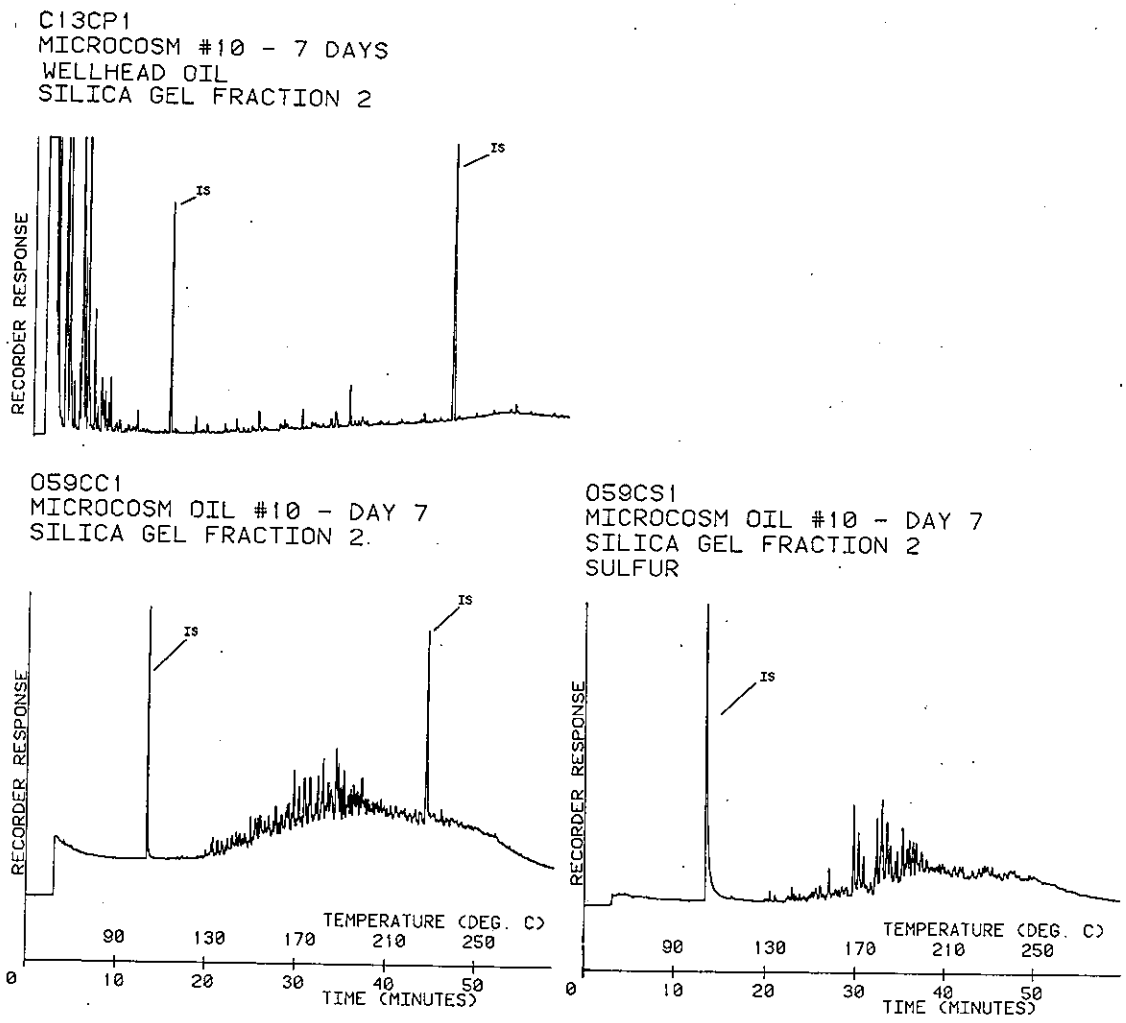

Figure 34. Glass capillary gas chromatographic data for the aromatic fraction of the microcosm experiment using fresh wellhead oil. Upper trace shows data for the aromatic fraction of the water column extract day seven. Bottom trace shows the generalized FID and sulfur-specific detector data for the aromatic fraction of the microcosm oil after seven days of incubation. The first internal standard, MBT, elutes with approximately the same retention time as 2-methylnaphthalene.

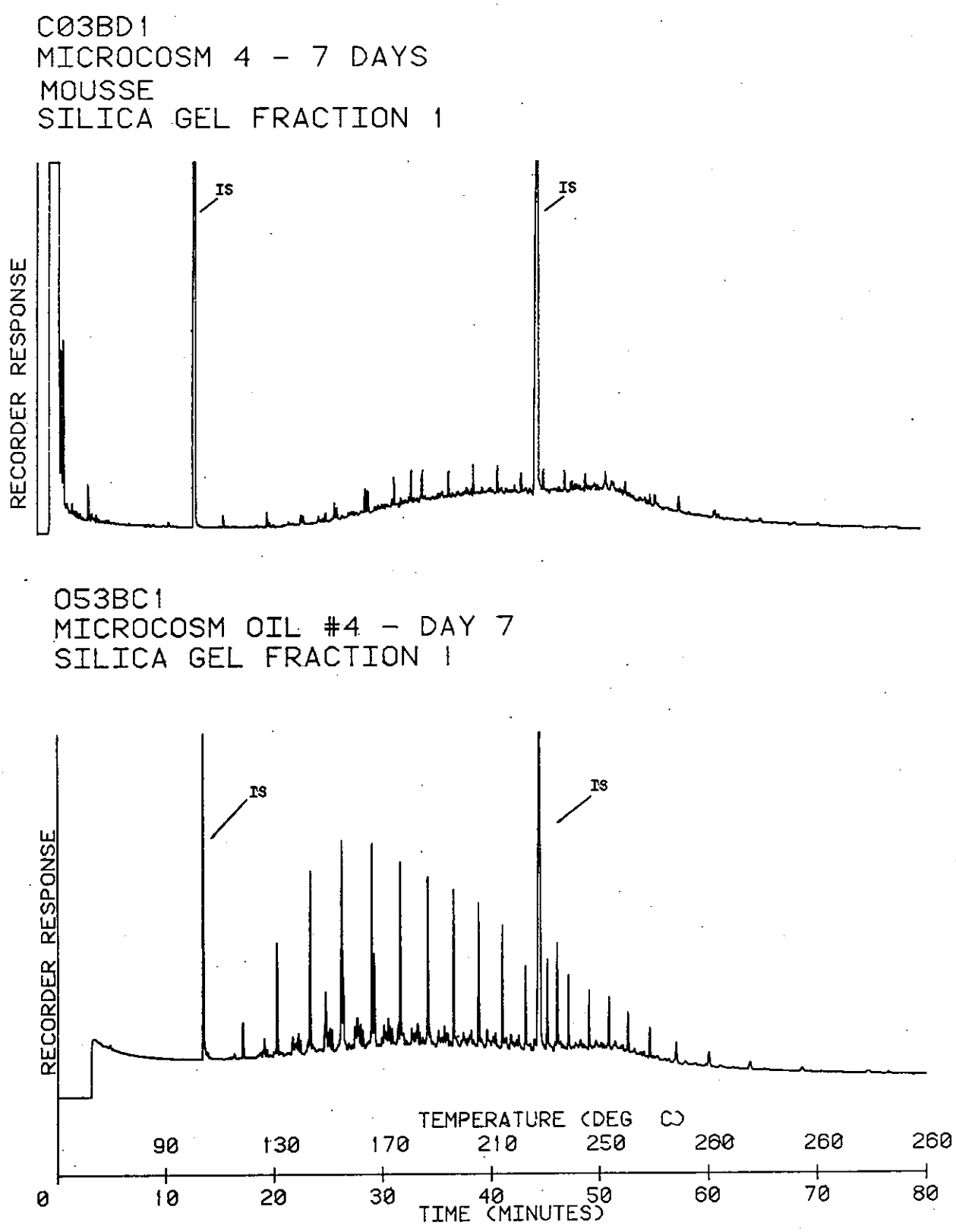

Figure 35. Comparison of the glass capillary gas chromatographic data of the microcosm experiment using fresh mousse. Upper trace is the data from the saturate fraction of the water column extract. Bottom trace is data from the saturate fraction of the microcosm oil after seven days of incubation. The second internal standard, DTP, elutes between $\underline{n}$-C_{24} and $\underline{n}$-C_{25}.

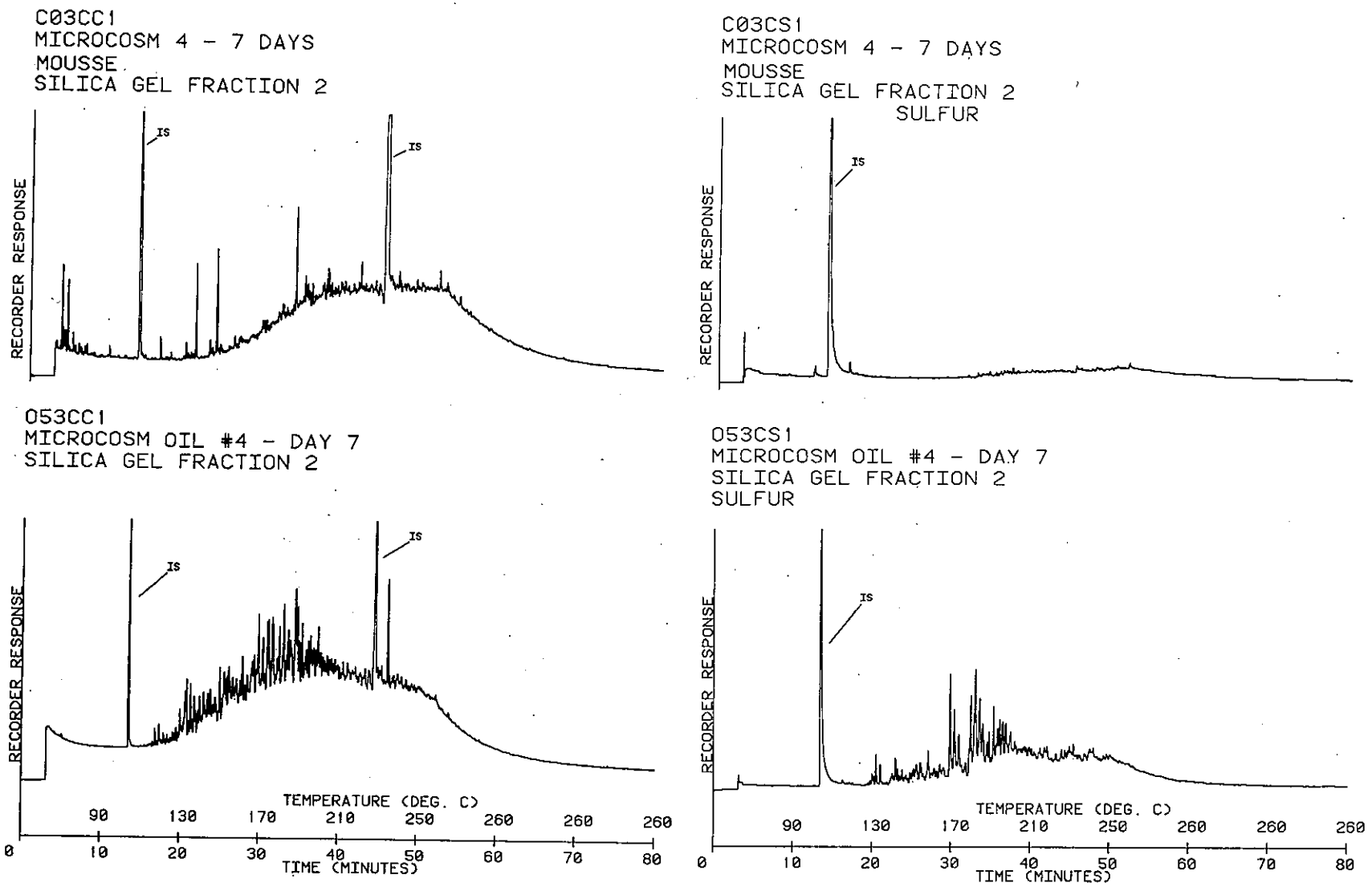

Figure 36. Comparison of the glass capillary gas chromatographic data from the microcosm experiment using fresh mousse of the aromatic fractions. Upper traces are the FID and the sulfur-specific detectors for the aromatic fraction of the water column extract. Lower extracts are the FID and sulfur-specific chromatograms of the aromatic fraction of the microcosm oil after seven days of incubation. The first internal standard, MBT, elutes with approximately the same retention time as 2-methylnaphthalene.

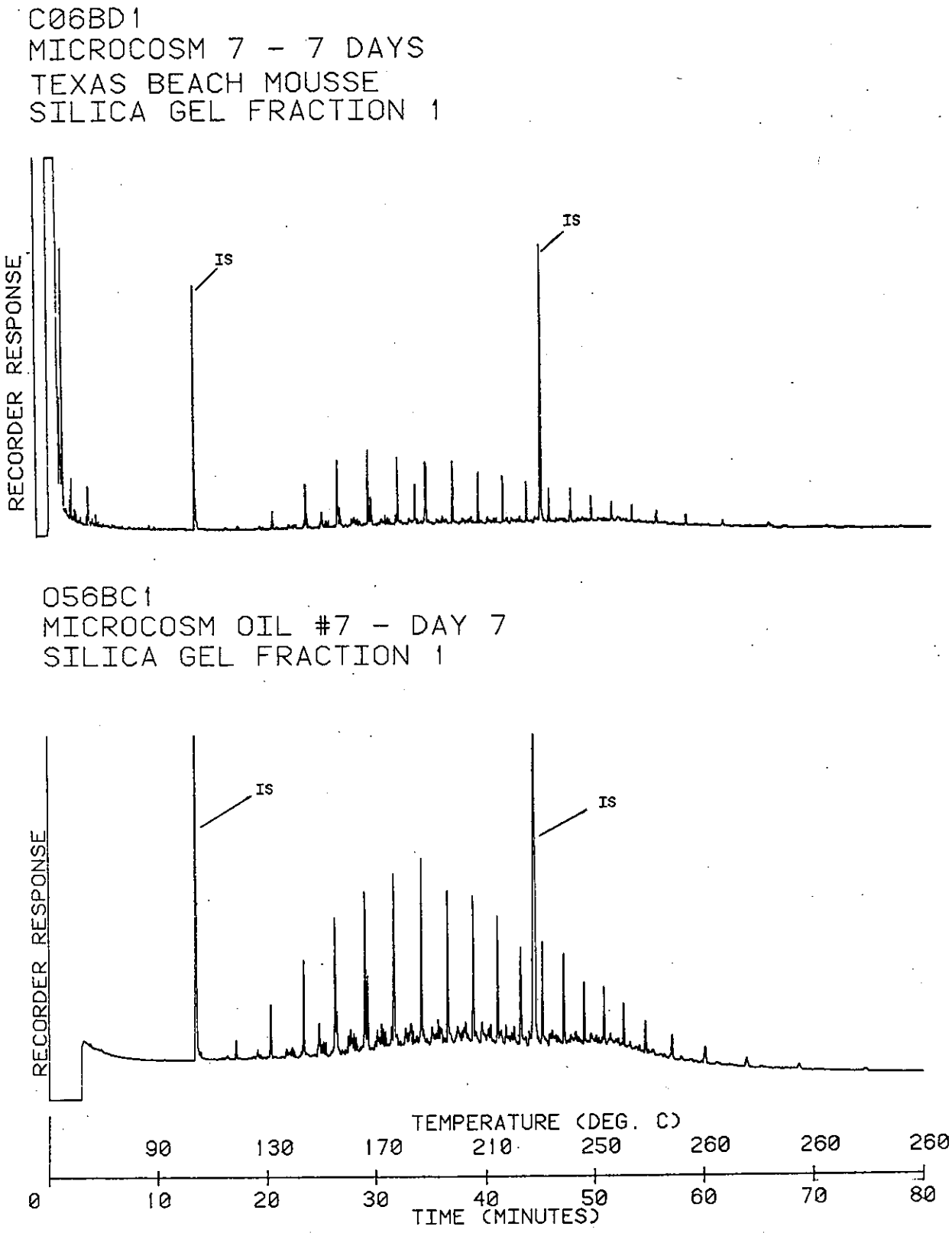

Figure 37. Comparison of the glass capillary gas chromatographic data from the microcosm experiment using Texas beach mousse. Upper trace shows the saturate fraction of the water column extract after seven days of incubation. Lower trace shows the saturate fraction of the microcosm oil after seven days of incubation. The first internal standard, MBT, elutes with approximately the same retention time as 2-methylnaphthalene.

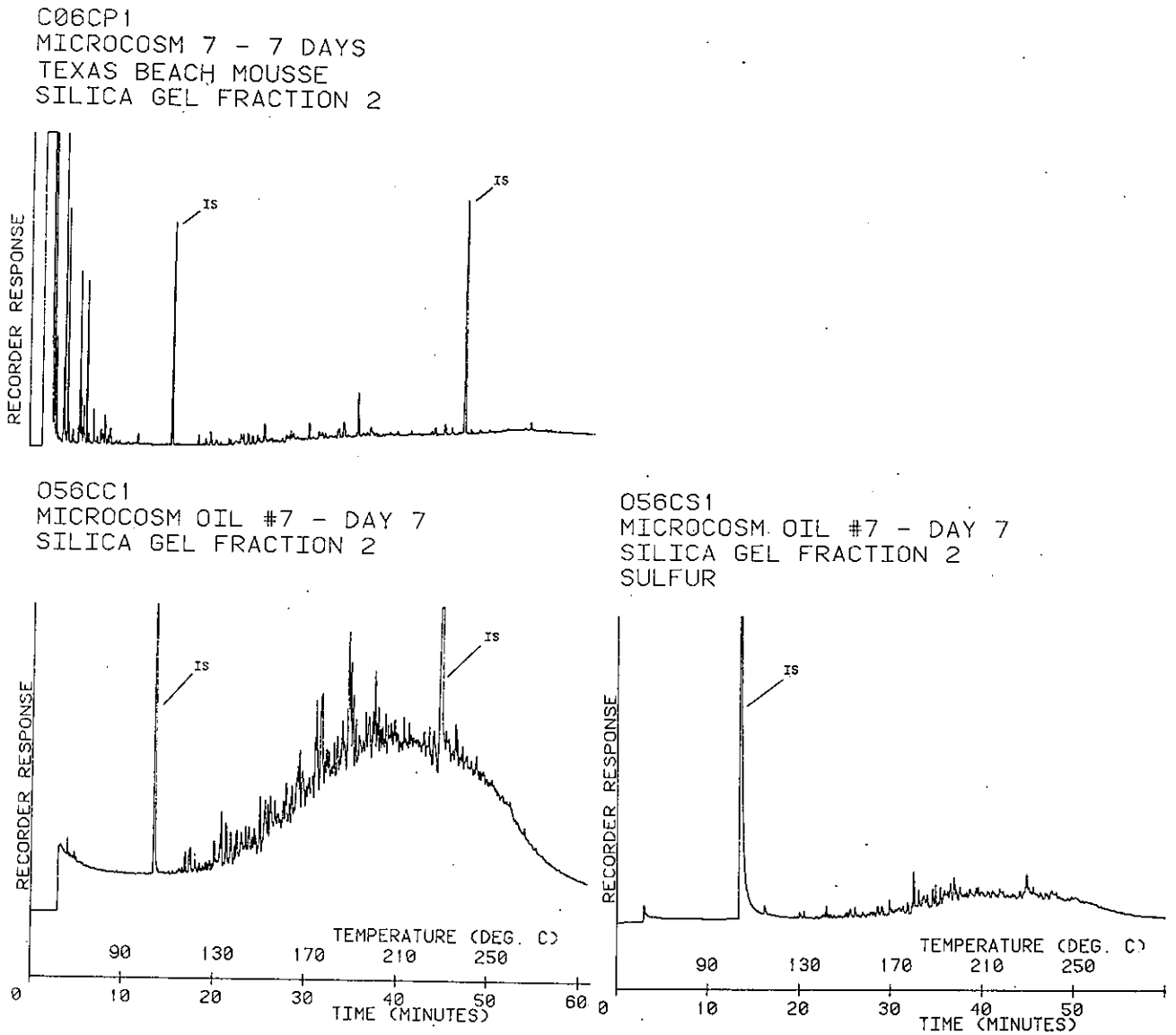

Figure 38. Glass capillary gas chromatographic data from the microcosm experiment using Texas beach mousse. Upper trace shows the aromatic fraction of the water column extract after seven days of incubation. Lower trace shows the aromatic fraction of the generalized and sulfur-specific detectors of the microcosm oil after seven days of incubation. The first internal standard, MBT, elutes with approximately the same retention time as 2-methylnaphthalene.

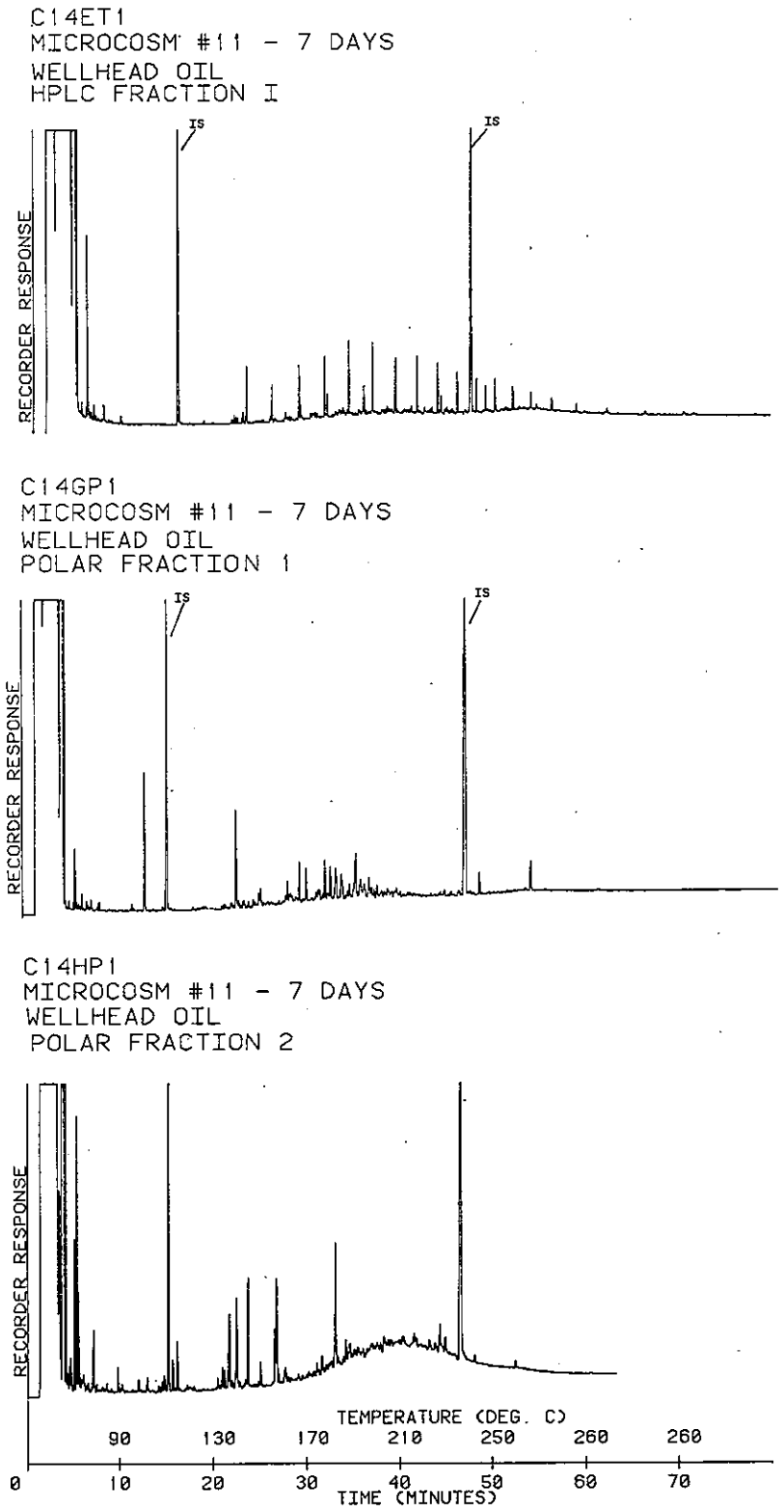

Figure 39. Glass capillary gas chromatographic data from the HPLC fraction 1 (saturate), high pressure polar fraction 1 (aromatic), and HPLC polar fraction 2 (polar) from the water column extract of the microcosm experiment using fresh wellhead oil after seven days of incubation. The first internal standard, MBT, elutes with approximately the same retention time as 2-methylnaphthalene. The second internal standard, DTP, elutes between $\underline{n}$-C_{24} and $\underline{n}$-C_{25}.

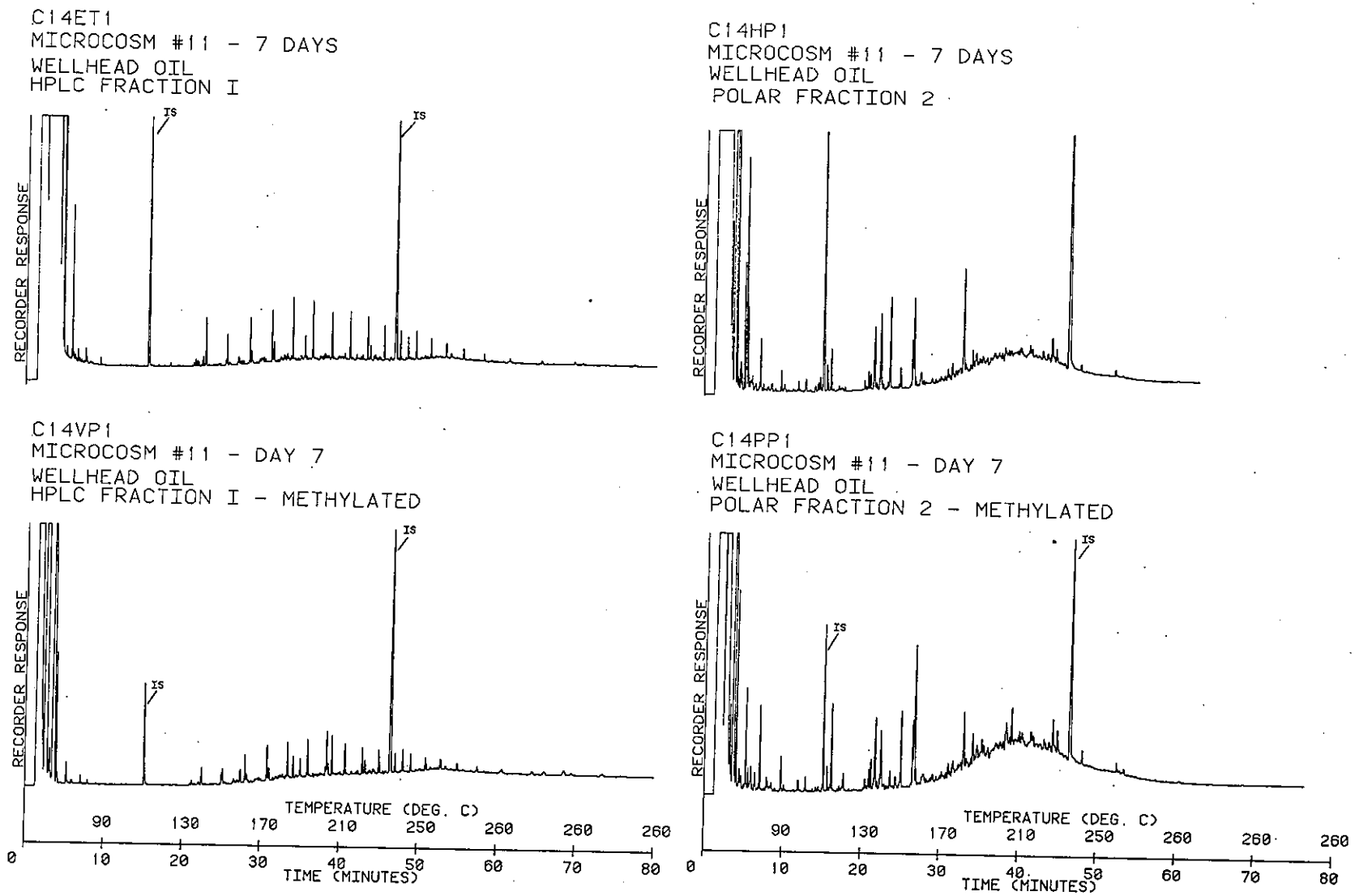

Figure 40. Glass capillary gas chromatographic data from the microcosm experiment using fresh wellhead oil of the HPLC fraction 1 and polar fraction 2. Upper traces show the data of the unmethylated fraction. Lower traces show the data after the samples have been subjected to methylation with diazomethane. The first internal standard, MBT, elutes with approximately the same retention time as 2-methylnaphthalene. The second internal standrad, DTP, elutes between $\underline{n}$-C_{24} and $\underline{n}$-C_{25}.

(2) The oil contained the following families of sulfur-containing aromatic hydrocarbons:

- benzothiophene and its alkylated homologs
- dibenzothiophene and its alkylated homologs
- naphthalylbenzothiophene and its alkylated homologs

(3) The oil contained the following families of nitrogen-containing aromatic compounds:

- alkylated quinolines
- alkylated carbazoles
- alkylated phenanthridine
- others

(4) No oxygen-containing aromatic compounds were observed in the IXTOC oil.

(5) Mousse samples appeared to be generally devoid of oxidized aromatic hydrocarbons.

(6) Air-water interface samples contained elevated levels of polar oxygenated products.

(7) Water column samples contained large quantities of fatty acids and phthalates and low concentrations of IXTOC hydrocarbons.

(8) Microcosm samples contained oxidized hydrocarbons of microbial origin.

5. ACKNOWLEDGMENTS

The authors would like to thank Chris Raschke, Ileana Nuiry, Rene Surgi, Cathy Cummings, Albertina Rhyans, Larry Clinton, Patrick Remele, and Frank Stone for their technical assistance; Paulette Brooks and Diane Trembley for their typing of the manuscript; Paul Boehm and Dave Fiest of ERCO and Jim Payne of SAI for supplying samples; Fred Pfeander and Earl Buckley for providing samples from the microcosm experiment; Sra. Amada Cortes Rubio for providing a sample of IXTOC oil collected subsurface by divers; and Don Atwood and George Harvey of AOML for technical support. This work was partially supported by NOAA contract number NA 79RAC00145.

6. REFERENCES

Draper, P.M., and D.B. MacLean (1968): Mass spectra of alhylquinolines. Canadian J. Chem., 46: 1487-1497.

Draper, P.M., and D.B. MacLean (1970): Mass spectra of some deuterium labelled dimethylquinolines. Canadian J. Chem., 48: 738-745.

Giam, C.S., Ed. (1977): Pollutant effects on marine organisms. Lexington Books, D. C. Heath and Co., Lexington, Mass., p. 3.

Grob, K., G. Grob, and K. Grob, Jr. (1979): Deactivation of glass capillary columns by silylation. J. High Resolution Chromatog. and Chromatog. Comm., 1: 31-35.

McCarthy, L.V., E. B. Overton, M.A. Maberry, and J.L. Laseter (1980): Glass capillary gas chromatography using simultaneous FID and Hall element specific detection (in preparation).

McKillop, A., and D.W. Young (1979): Organic synthesis using supported reagents - Part II: Synthesis, 79: 481-500.

Schwartz, D.P., and R.S. Bright (1974): A column procedure for the esterification of organic acids with diazomethane at the microgram level. Analyt. Biochem., 61: 271-274.

Steele, C.F., E.B. Overton, and J.L. Laseter (1980): A system-independent data transfer and storage scheme for GCMS data (submitted).

ACOUSTIC OBSERVATIONS OF BIOLOGICAL VOLUME SCATTERING IN THE VICINITY OF THE IXTOC-I BLOWOUT

Michael C. Macaulay, Kendra Daly, and T. Saunders English
Department of Oceanography
University of Washington
Seattle, Washington 98195

1. INTRODUCTION

A chemical oceanography cruise to the area of the IXTOC-I blowout in the Gulf of Mexico allowed us to sample on a not-to-interfere basis at times and locations that were convenient to the chemical studies. We intended to use quantitative acoustic methods to observe, as volume scattering strength, the distribution and abundance of zooplankton in relation to the oil. Samples were to be taken with nets to identify probable target animals to enhance the interpretation of the acoustic observations.

2. METHODS

Acoustic observations and net catches were made in the Bay of Campeche, Gulf of Mexico, aboard the G. W. PIERCE from 14 to 22 September 1979. The acoustic records and net catches were returned for analysis to the Department of Oceanography, University of Washington.

2.1 Field Methods

Eleven acoustic observations were made at 10 stations (Table 1), using a Ross Laboratories 200A Fineline echosounder operating at a frequency of 105 kHz. The pulse length was 0.4 msec with a repetition rate of 2 per second. On station, a 10° transducer was lowered just below the water surface. At some stations, oil accumulated on the transducer face, requiring frequent removal for cleaning.

Paper chart recordings, or echograms, of the incoming signals were made continuously on station for immediate examination. The detected output of the acoustic system returning from the water column was heterodyned to produce a modulated output amplitude of 5 kHz, which was directed to an analog recorder for later digitization and analysis.

The receiver sensitivity, including the transducer, was -88 db/re 1 mv, and the source level was 228.3 db/re 1 μ pascal. The transducer had a beam half-angle of 3° at the -3 db, or half power, point.

Twenty-four net samples were taken at 9 stations near noon or midnight (Table 1). A 0.75 m ring net and a 1 m Tucker trawl (Tucker, 1951) were used. The mesh for both nets was 571μ m; the open area ratio of mesh to mouth was 8:1 for the ring net and 4:1 for the Tucker trawl.

The ring net was towed vertically from near the bottom to the surface. The Tucker trawl was used in double-oblique tows reaching near the bottom. A flow meter was mounted on the top trawl bar to measure the volume of water filtered. Only two samples were taken before the trawl was lost from a defective wire on the winch.

The net catches were collected along the edge of the oil plume, rather than directly under the oil, in an attempt to keep the nets as clean as

Table 1. Acoustic and 0.75 m ring net observations and estimates of the relative odor of oil and the visible presence of oil on the surface during day and night in the Gulf of Mexico, 14 to 22 September 1979.

STATION NUMBER	TIME	OBSERVATION NET	OBSERVATION ACOUSTIC	OIL ODOR	OIL SURFACE	NORTH LATITUDE	WEST LONGITUDE	DEPTH (m)
PIX-01	Night	X	X	0	0	21°41.0'	90°25.0'	32
PIX-02	Night	X	X	0	0	19°48.8'	91°21.7'	29
PIX-07	Night	X				19°23.8'	92°11.2'	45
PIX-08	Day	X	X	2	2	19°27.7'	92°04.5'	35
PIX-09	Night	X	X	1	2	19°24.7'	92°13.1'	48
PIX-11	Day		X	0	1	19°27.5'	92°08.0'	40
PIX-12	Day	X	X	0	0	19°32.3'	92°04.0'	56
PIX-13	Day		X	0	1	19°13.0'	91°56.0'	52
PIX-14	Night	X	X			19°33.9'	91°51.0'	49
	Day	X	X	1	0.5	19°32.7'	91°49.4'	49
PIX-15	Night	X				19°31.6'	92°04.9'	48
	Day	X	X	2	0.5	19°29.6'	92°03.2'	50
PIX-16	Day	X	X	0	0	19°15.6'	95°12.2'	1830

possible. When tarballs and patches of mousse did make contact with the net, it was soaked in a degreasing detergent, scrubbed, and washed down with clean water.

The samples were preserved with 10% buffered formalin.

2.2 Laboratory Methods

The computer system for acoustic processing consisted of a data collecting subsystem and a numerical analysis subsystem. The collected subsystem treated the analog data by converting the 5 kHz amplitude modulated signal from the sounder to an envelope, using a precision envelope detector. The envelope detector was adjusted to give 1 v DC output for a 1 v peak-to-peak 5 kHz input. The envelope-detected signal was digitized at a 10 kHz rate to produce a measurement of the returning echo every 0.75 m, assuming a sound velocity of 1500 m/sec. The procedure was repeated on the signal to the bottom or to 200 m. The measurements were then sent to the analysis subsystem for computation of volume scattering strength at depth intervals of interest. The collection subsystems then digitized a new signal and waited until the numerical analysis was completed for the previous signal before sending new data.

The analysis subsystem converted the measured voltage levels to volume scattering strengths by means of the equation:

$$RL = SL - 20 \log r - 2\alpha r + TS + 10 \log(c\tau/2) - DI$$

rearranging terms;

$$TS = RL - SL + 20 \log r + 2\alpha r - 10 \log(c\tau/2) + DI$$

where the parameters are: TS = volume scattering strength (db/m_3); RL = reverberation level; SL = source level; r = range (m); α = attenuation of sound; c = sound velocity; τ = pulse length (seconds); DI = directivity index.

The acoustic analysis examined profiles of volume scattering strength through the entire water column and in a layer between 10 and 15 m. Seven 0.75 m depth increments in the layer were measured for two pulses to compute a mean and 95% confidence interval estimates for each station.

Descriptions of surface oil and the odor of oil were used to estimate rough concentrations at the stations. A scaled value of 2 indicates a strong concentration, and 0 indicates no observed concentration (Table 1). The estimates of concentrations were used in a multiple regression analysis of volume scattering strength on oil odor, surface oil, and distance from the well.

The net catches either were counted entirely or were subsampled. An entire catch was counted if there appeared to be fewer than 100 animals in the most abundant taxonomic category. Larger catches were divided with a Folsom plankton splitter (McEwen et al., 1954) to provide an aliquot portion with about 100 of the most abundant animals. The copepods were identified from one

sample at each station; other organisms were identified from all samples. Animals longer than 5 mm were measured.

3. RESULTS

The quantitative acoustic methods provided measurements of volume scattering strength at several stations. The net catches provided identifications and indications of abundance of planktonic animals in the water column.

3.1 Volume Scattering Strength

The echograms at all stations showed concentrations of targets, or scattering layers, at intermediate depths between the surface and bottom (Figure 1). There was almost always a layer between 10 and 20 m, but it varied over time at a station. The profiles of volume scattering strength reveal large differences among stations (Figure 2). The profile at night at station 14 did not differ greatly from the profile during the day, so the night observation was not considered further.

The mean volume scattering strength of duplicate pulses quantified in the layer from 10 to 15 m differs among stations (Figure 3). Stations 8, 15, and 16 appear distinctly different from the other stations. Station 16, which was significantly different statistically from stations 8 and 15, was far removed from all other stations and positioned over relatively very deep water.

Frequently, distributions of volume scattering strengths also differed among stations (Figure 4). The upstream stations 1 and 2 were intended to serve as controls. Stations 11, 12, 13, and 14 appeared much like the controls; stations 8, 9, 15, and 16 differed from the controls. Stations 8 and 15 were close together and at both stations the oil fumes were so concentrated that masks were required while sampling. Station 9 was near the well and had a moderate oil odor and heavy surface oil.

The multiple regression analysis identified the oil fumes as the statistically significant variable associated with a change in volume scattering strength (Table 2). The surface oil was associated with a small effect; the distance from the well was relatively unimportant.

3.2 Planktonic Animals

A wide variety of planktonic animals appeared in the net catches (Appendix I). The abundance of organisms in the vertical ring net catches was tabulated (Appendix II). At most stations and times, the copepods and chaetognaths were dominant numerically and by percentage (Tables 3 and 4).

At station 8, the animals were covered with oil. There was some oil on the organisms at station 9. There were some small tarballs in the net catches at stations 12, 14, and 15, but very little oil on the animals. There was one small tarball in the net catch at station 16.

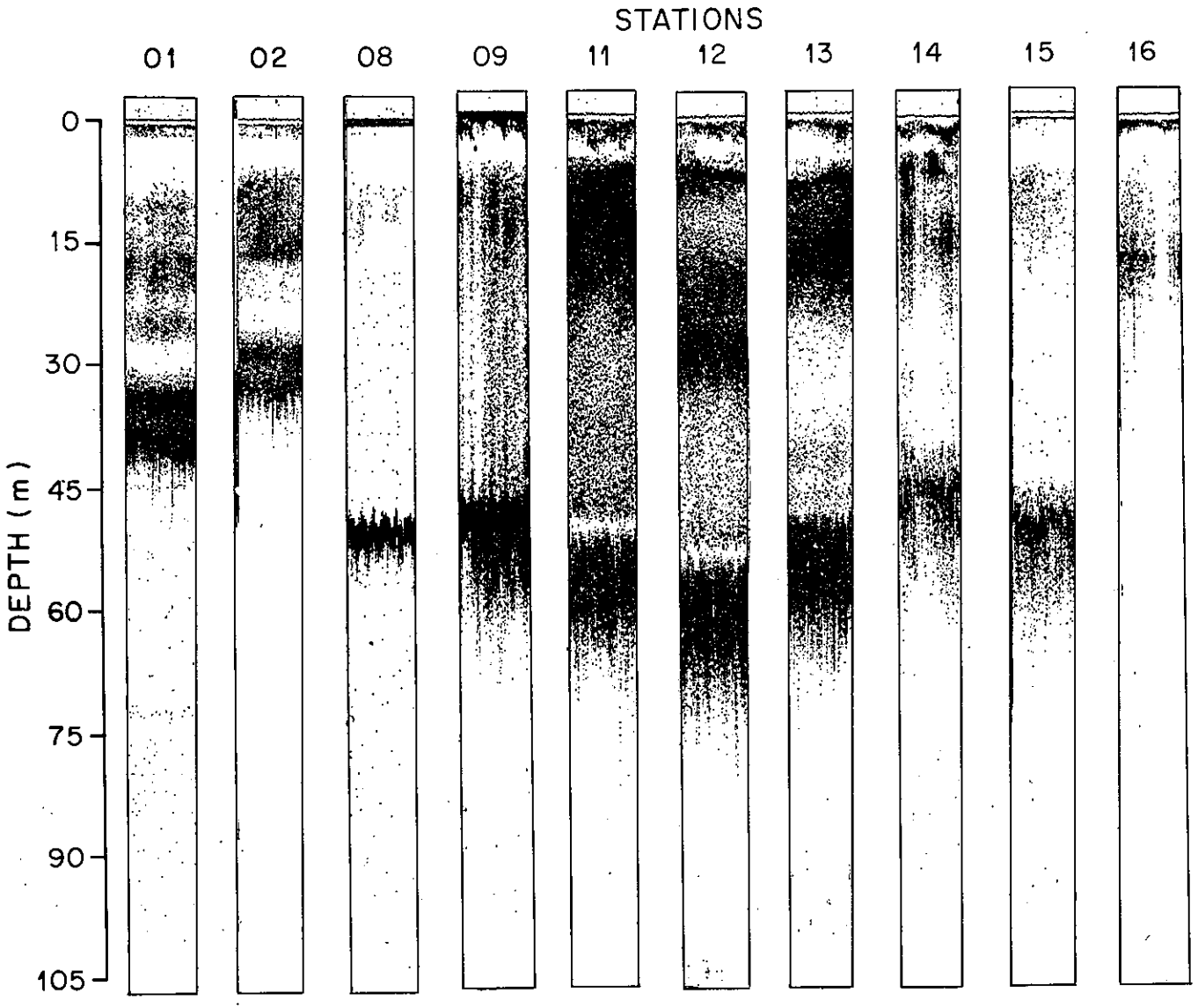

Figure 1. Echograms of 1-min. duration at stations in the Gulf of Mexico, 14 to 22 September 1979.

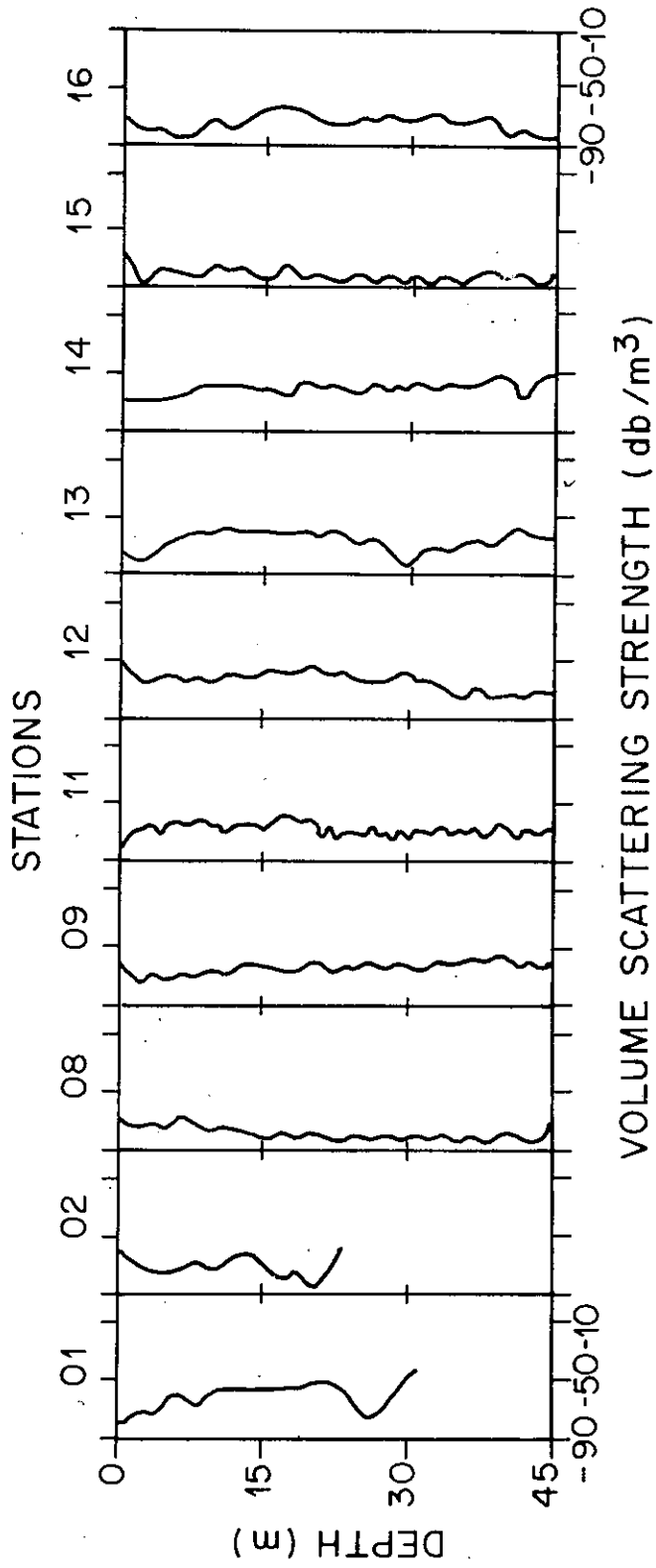

Figure 2. Volume scattering strength profiles at stations in the Gulf of Mexico, 14 to 22 September 1979.

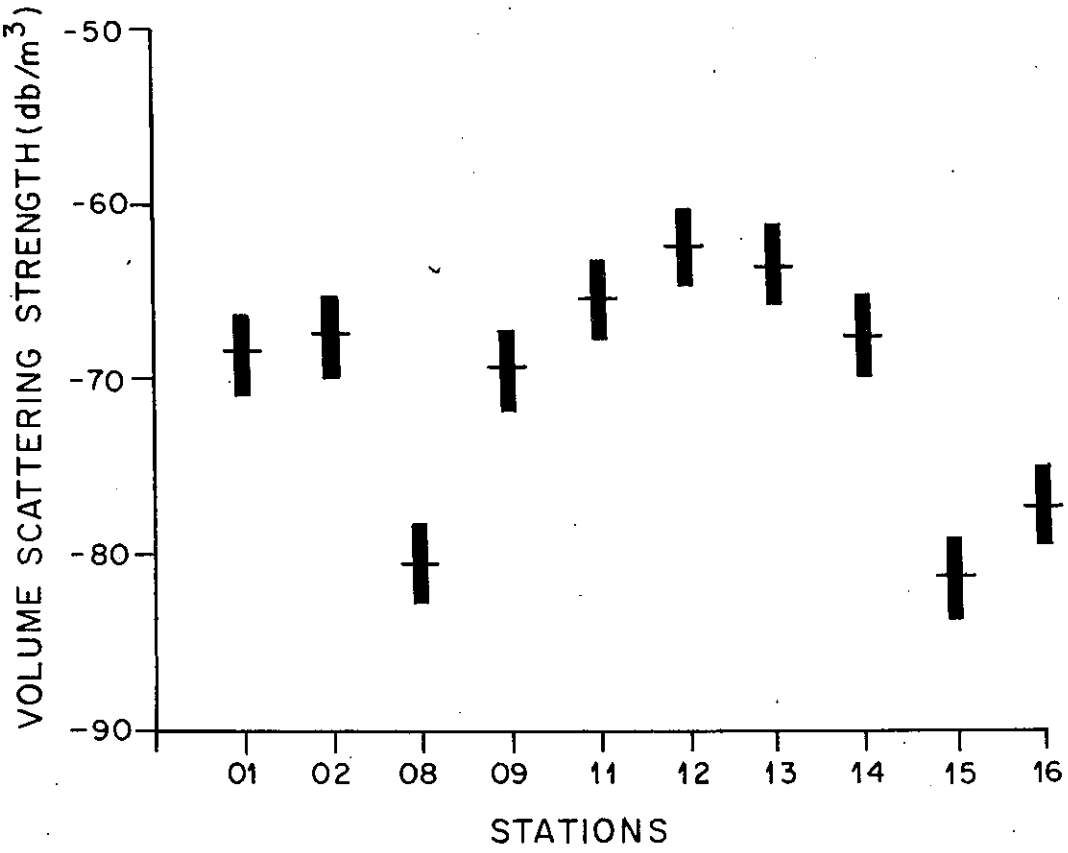

Figure 3. Mean volume scattering strength and 95% confidence interval estimates at stations in the Gulf of Mexico, 14 to 22 September 1979.

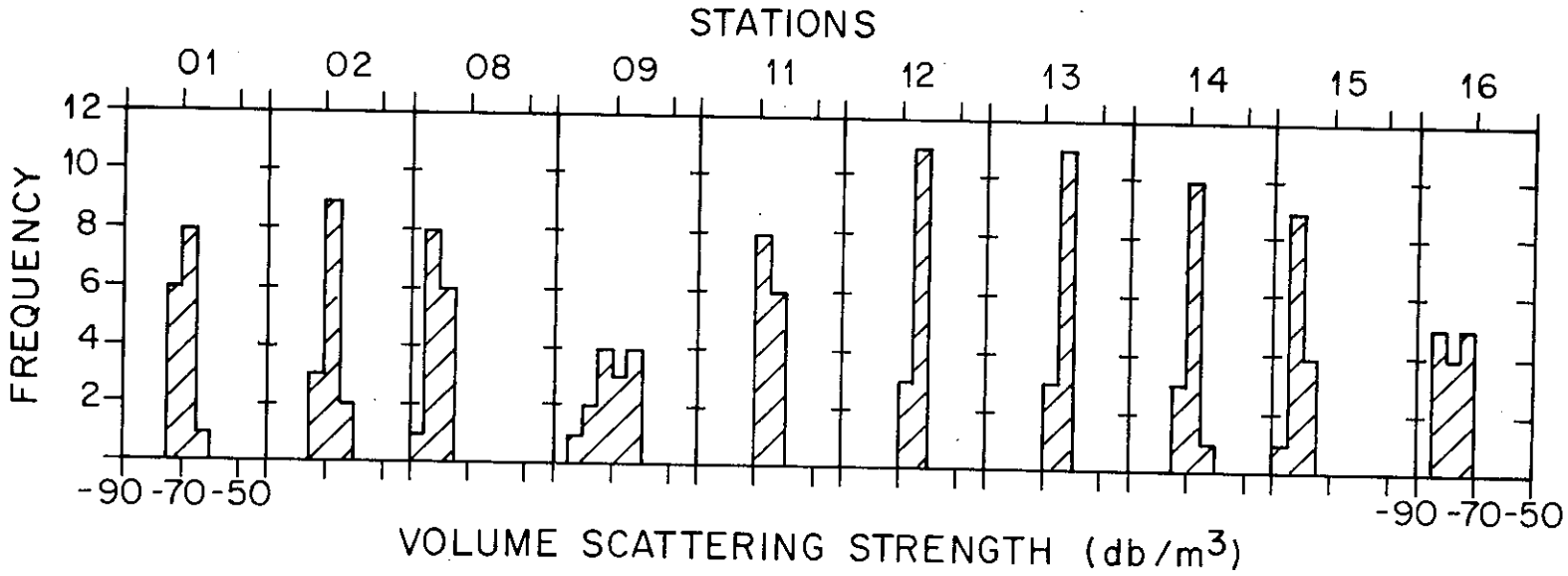

Figure 4. Frequency distributions of volume scattering strength at stations in the Gulf of Mexico, 14 to 22 September 1979.

Table 2. Multiple regression coefficients relating volume scattering strength to the independent variables of oil odor, surface oil, and distance from the well.

Variable	Coefficient
Oil odor	-8.00
Surface oil	0.23
Distance	-0.03

Table 3. Abundance, as number/m^3, of animals caught in a 0.75 m ring net in the Gulf of Mexico, 14 to 24 September 1979.

Taxa	Stations										
	1 night	2 night	7 night	8 day	9 night	12 day	14 day	14 night	15 day	15 night	16 day
Medusae		54.38	1.10	0.50	1.03	0.63	0.34	0.50	0.03	0.09	0.07
Siphonophora	0.50	2.73	3.60	2.77	4.19	1.39	8.87	3.47	2.97	3.65	3.25
Polychaeta	2.03	0.47	0.07	0.07	0.15	0.05	0.05	0.15	0.03	0.03	0.07
Gastropod larvae	0.24	0.78	0.52	0.28	0.70	0.25	0.81	0.94	0.17	0.60	0.33
Heteropod	0.08		0.20	0.12	0.15		0.11	0.05		0.03	0.05
Pteropod	0.16	0.08	0.33	0.09	1.47	0.07				0.03	0.12
Cladocera	0.24	0.70					0.11	0.05		0.15	
Ostracoda	2.19	0.08		0.02	0.04					0.03	0.51
Copepoda	15.67	2.34	14.22	5.85	7.87	5.83	6.51	10.20	4.61	7.43	2.98
Stomatopoda	0.73	0.39	0.07	0.13	0.18	2.08	0.34	0.20	0.10	0.15	0.05
Mysidacea	1.06	1.25		0.02		0.05	0.03	0.15		0.06	
Cumacea	0.65	5.94	0.07					0.10			
Amphipoda	1.87	6.56	0.97	0.17	0.33	0.05	0.39	0.20	0.03	0.03	0.22
Decapoda-shrimp larvae	4.14	35.94	0.84	0.95	2.43	1.13	0.83	1.19	0.64	1.90	0.71
-phyllosoma larvae	0.08				0.04						
-crab adults & larvae	5.03	3.91	0.33	0.41	1.66	0.88	1.25	1.73	0.65	1.05	0.82
Brachiopoda		0.03	0.13	0.15	0.11		0.05	0.05	0.05	0.15	0.02
Echinodermata larvae	0.49	0.23	1.04	1.34	0.92	0.30		0.25	0.08	0.36	0.07
Chaetognatha	6.01	3.91	9.09	7.01	10.99	4.01	10.33	14.75	2.15	10.60	8.70
Larvacea	0.16	0.08			0.04						
Thaliacae	4.63			0.02	0.40	0.05		0.10		0.09	0.07
Fish eggs	1.79	1.80	0.84	0.76	0.29	0.44	0.55	1.04	0.40	0.78	0.22
Fish larvae	1.87	0.31	2.27	0.54	4.49	0.76	0.19	1.29	0.13	3.20	0.28
TOTAL	49.62	121.91	35.69	21.20	37.48	17.97	30.76	36.41	12.04	30.41	18.54

Table 4. Percent occurrence of animals caught in a 0.75 m ring net in the Gulf of Mexico, 14 to 24 September 1979.

	Stations										
	1	2	7	8	9	12	14		15		16
Taxa	night	night	night	day	night	day	day	night	day	night	day
Medusae		45	3	2	3	4	1	1	< 1	< 1	< 1
Siphonophora	1	2	10	13	11	9	29	10	25	12	19
Polychaeta	4	< 1	< 1	< 1	< 1	< 1	< 1	< 1	< 1	< 1	< 1
Gastropod larvae	< 1	1	1	1	2	1	3	3	1	2	1
Heteropod	< 1		< 1	< 1	< 1		< 1	< 1			< 1
Pteropod	< 1		1	< 1	4	< 1				< 1	1
Cladocera	< 1	1					< 1	< 1		1	
Ostracoda	4	< 1		< 1	< 1					< 1	3
Copepoda	31	2	40	27	21	36	21	28	38	25	14
Stomatopoda	1	< 1	< 1	1	< 1	1	1	1	1	1	< 1
Mysidacea	2	1		< 1		< 1	< 1	< 1		< 1	
Cumacea	1	5	< 1					< 1			
Amphipoda	4	5	3	1	1	< 1	1	1	< 1	< 1	1
Decapoda-shrimp larvae	8	29	3	4	7	7	3	3	5	62	3
-phyllosoma larvae	< 1				< 1						
-crab adults & larvae	10	3	1	3	4	5	5	5	5	4	3
Brachiopoda		< 1	< 1	1	< 1			< 1	< 1	< 1	< 1
Echinodermata larvae	1	< 1	3	6	2	2		1	1	1	< 1
Chaetognatha	12	3	25	33	29	25	34	40	20	35	50
Larvacea	< 1	< 1			< 1						
Thaliacae	9			< 1	1	< 1		< 1		< 1	< 1
Fish eggs	4	1	2	4	1	3	2	3	3	3	1
Fish larvae	4	< 1	6	3	13	5	1	4	1	11	1

No striking diel differences in net catches were observed. Neither patterns of occurrence of animals nor length-frequencies of animals appeared to correlate with or help explain the acoustic results.

4. DISCUSSION

The quantitative acoustic observations indicate relationship between distributions of volume scattering strength and oil from the IXTOC-I blowout. The surface oil appeared to have little effect, while the presence of a strong oil odor was associated with marked changes in the quantity and quality of volume scattering strength.

Two adjacent stations, 8 and 15, had strong oil fume odors and were similar in the intensity and range of volume scattering strength. Stations 8 and 15 had reduced scattering in the -75 to -60 db range that characterized the two control stations and the five other stations at similar shallow depths. Stations 8 and 15 also had increased scattering in the -90 to -75 db range. One conclusion is that some component of the oil was associated with a reduction in abundance of a type of animal normally present in that area of the Gulf of Mexico. Another conclusion is that some sound scattering targets, possibly oil droplets or small tarballs, were present in the water columns at stations 8 and 15, and perhaps at station 9 near the well.

The echograms at 105 kHz were not sufficient to distinguish between stations, as the paper charted record showed a sound scattering layer at each station. The quantitative acoustic methods were necessary to document differences in volume scattering strength among stations.

The sizes of planktonic animals caught with the ring net did not appear to be correlated with the acoustic observations. The acoustic target animals recorded at 105 kHz probably were larger and more active and should have been sought with the 1 m Tucker trawl or an even larger net. Those organisms would be of a size capable of moving moderate distances to avoid undesirable products in the water column.

This study was limited in several ways. The cruise track did not provide replicate samples in areas affected by several levels of concentrations of oil. Without a towed or hull-mounted transducer, we could not make acoustic observations underway and were limited to observations on station. Multiple frequencies might have allowed better acoustic identification and partitioning of oil products in the water column. Large multiple opening-closing nets would have allowed partitioning target animals in the water column and correlating animals with the observed changes in volume scattering strength. Realtime acoustic analyses would enhance sampling design by suggesting where to sample most effectively with nets to document differences in the distribution and abundance of animals in the water column. Further, acoustic observations of differences in volume scattering strength could be effectively used to select locations and depths where samples should be taken for chemical determinations.

Our results obtained on the cruise, even using hastily assembled and marginally adequate borrowed equipment, demonstrated that some aspects of the extent of areas affected by oil spills can easily be determined by quantitative acoustic methods. More detailed descriptions could be obtained by observing continuously with multiple acoustic frequencies and by access to more sophisticated acoustic processing systems. The identity and population characteristics of affected organisms can certainly be determined with adequate nets. While some work needs to be done to learn how best to conduct acoustic and net studies related to oil, a vastly improved program could be carried out when the next oil spill occurs.

5. ACKNOWLEDGMENTS

Gayle A. Heron aided in the identification of copepods. Leanne Stahl identified the fish larvae.

6. REFERENCES

McEwen, G. F., M. W. Johnson, and T. R. Folsom (1954): A statistical analysis of the performance of the Folsom Plankton Sampler Splitter, based upon test observations. Archiv fur Meteorologie, Geophysik and Bioklimatologie Ser. A, 7: 502-527.

Tucker, G. H. (1951): Relation of fishes and other organisms to the scattering of underwater sound. J. Mar. Res., 10: 215-238.

Appendix I. Animals collected in the Gulf of Mexico, 14 to 22 September 1979.

PROTOZOA

- Foraminifera
- Radiolaria

CNIDERIA

- Hydrozoa
  - Medusae
  - Siphonophora
- Anthozoa

ANNELIDA

- Polychaeta

MOLLUSCA

- Gastropoda
  - Mesogastropoda
    - Pterotracheid heteropods
    - Atlantid heteropods
  - Thecosomata
    - *Creseis* spp.
    - *Carolinia* spp.
    - *Diacria* sp.
    - *Hyalocyclix* sp.
  - Gymnosomata
- Pelecypoda
- Cephalopoda

ARTHROPODA

- Crustacea
  - Cladocera
    - *Penilia* spp.
  - Ostracoda
  - Copepoda
    - Calanoida
      - *Nannocalanus minor* (Claus)
      - *Undinula vulgaris* (Dana)
      - *Eucalanus monachus* (Giesbrecht)
      - *Eucalanus mucronatus* (Giesbrecht)
      - *Rhincalanus cornutus* (Dana)
      - *Euchaeta marina* (Prestandrea)
      - *Scolecithrix danae* (Lubbock)
      - *Temora stylifera* (Dana)
      - *Centropages violaceus* (Claus)
      - *Centropages* sp.
      - *Haloptilus paralongicirrus* Park

Appendix I. (Continued)

- *Candacia curta* (Dana)
- *Candacia pachydactyla* (Dana)
- *Paracandacia simplex* (Giesbrecht)
- *Candacia* spp.
- *Pontella meadii* Wheeler
- *Pontella mimocerami* Fleminger
- *Labidocera acutifrons* (Dana)
- *Labidocera nerii* (Krøyer)
- *Labidocera scotti* Giesbrecht
- *Pontellopsis villosa* Brady
- Pontellidae spp.
- *Acartia* sp.

Harpacticoida

Cyclopoida

- *Sapphirina stellata* Giesbrecht
- *Sapphirina* spp.
- *Copilia mirabilis* Dana
- *Corycaeus speciosus* Dana
- *Corycaeus* sp.

Cirripedia

Stomatopoda

Mysidacea

Cumacea

Tanaidacea

Isopoda

Amphipoda

- Hyperiidea
- Gammaridea
- Caprellidea

Euphausiacea

Decapoda

Penaeidea

- *Solenocera* sp.
- *Penaeus* spp.
- *Sicyonia* spp.
- *Acetes* sp.
- *Lucifer faxoni* Bourradaile
- *Lucifer typus* Milne Edwards

Caridea

- *Processa* sp.
- *Leptochela* spp.
- *Lysmata* sp.
- Palaemoninae
- Alpheidae
- Scyllaridea
- Thalassinidea (*Callianassa* spp.)

Appendix I. (Continued)

- Anomura
  - Galatheidae
  - Porcellanidae
  - Paguridae
  - Albunidae
- Brachyura
  - Dorippidae
  - Leucosiidae
  - Raninidae
  - Portunidae
    - *Portunus ordwayi* (Stimpson)
  - Pinnotheridae

BRACHIOPODA

ECHINODERMATA

CHAETOGNATHA

CHORDATA

- Larvacea
- Thaliacea
- Teleostei
  - Elopidae
  - *Opichthus gomesi* (Costelnau)
  - *Sardinella anchovia* Valenciennes
  - *Anchoa hepsetus* (Linnaeus)
  - *Synodus* sp.
  - *Bregmaceros atlanticus* Goode and Bean
  - *Cypselurus* sp.
  - Holocentridae
  - *Pseudopriacanthus altus* (Gill)
  - *Caranx* sp.
  - *Coryphaena hippurus* Linnaeus
  - Pomadasyidae
  - Sparidae
  - Scianidae
  - *Sphyraena* sp.
  - *Gobionellus* sp.
  - *Auxis thazard* (Lacépède)
  - *Euthynnus alletteratus* (Rafinesque)
  - *Thunnus* sp.
  - *Scorpaena* sp.
  - *Bothus ocellatus* (Agassiz)
  - *Etropus crossotus* Gordon and Gilbert
  - *Syacium* sp.
  - Soleidae
  - *Symphurus* sp.
  - *Acanthostracion quadricornis* (Linnaeus)
  - *Sphoeroides* sp.

Appendix II. Abundance, as number/m^3, of animals caught in a 0.75 m ring net in the Gulf of Mexico, 14 to 24 Sep 1979.

Taxa	Stations										
	1 night	2 night	7 night	8† day	9Ψ night	12Ψ day	14Ψ day	14Ψ night	15Ψ day	15Ψ night	16 day
Foraminifera				P*							
Radiolaria				P					P		P
Medusae		54.38	1.10	0.50	1.03	0.63	0.34	0.50	0.03	0.09	0.07
Siphonophora	0.50	2.73	3.64	2.78	4.19	1.39	8.87	3.47	2.97	3.65	3.25
Anthozoan larvae								0.05			
Polychaeta	2.03	0.47	0.07	0.07	0.15	0.05	0.05	0.15	0.03	0.03	0.07
Gastropoda larvae	0.08	0.31	0.46	0.23	0.59	0.23	0.76	0.94	0.17	0.60	0.12
Echinospira larvae	0.16			0.07	0.07		0.05			0.03	0.10
Heteropoda, pterotracheids								0.05			0.02
Heteropoda, Creseis sp.	0.08		0.20	0.11	0.15		0.11				0.02
Pteropoda, Diacria sp.	0.16		0.33	0.07	0.70	0.05				0.03	0.10
Pteropoda, Carolinia sp.											0.02
Pteropoda, Hyalocyclix sp.					0.70	0.02					
Pteropoda, gymnosomes					0.04						
Pterpoda		0.08		0.02	0.04						
Pelecypoda larvae		0.47	0.07			0.02					
Cephalopoda larvae					0.04						0.10
Cladocera, Penilia sp.	0.24	0.70					0.11	0.05		0.15	
Ostracoda spp.	2.19	0.08		0.02	0.04					0.03	0.51
Nannocalanus minor			3.57	0.78	2.65	0.88	2.80	2.72	0.99	1.92	0.90
Undinula vulgaris	12.66	0.47	3.51	0.39	0.74	0.28	1.38	0.79	1.09	1.74	0.34
Eucalanus monachus		1.72	2.14	1.56	1.84	0.56	0.79	3.02	0.64	1.92	0.27
Eucalanus mucronaius					0.22						
Rhincalanus cornuius					0.07			0.05			

Appendix II. (Continued)

Taxa	Stations										
	1 night	2 night	7 night	8† day	9Ψ night	12Ψ day	14Ψ day	14Ψ night	15Ψ day	15Ψ night	16 day
Euchaeta marina	0.24		0.78	1.10	0.44	1.53	0.37	1.73	0.89	0.66	0.07
Scolecithrix danae			0.65	0.39	0.52	0.51	0.21	0.89	0.45	0.12	0.15
Temora stylifera			0.33	0.39	0.59	0.05	0.58	0.10	0.15	0.60	0.07
Centropages violaceus	0.08					0.23					
Centropages sp.											0.34
Haloptilus paralongicirrus											0.05
Candacia curta						0.05			0.05		
Candacia pachydactyla	0.16		0.39	0.39	0.29	0.09		0.10			
Paracandacia simplex						0.05					
Candacia spp.							0.16	0.10			
Pontella meadii											
Pontella mimocerami											
Labidocera acutifrons			0.84		0.07	0.05		0.05	0.05		
Labidocera nerii	0.57										
Labidocera scotti											0.02
Pontellopsis villosa											0.02
Pontellidae spp.			0.20	0.07							
Acartia sp.	0.16		0.07								
Harpacticoida sp.											
Sapphirina stellata			0.20	0.20		0.05	0.05	0.15	0.05	0.12	0.05
Sapphirina spp.			0.13								
Copilia mirabilis	0.89	0.08	1.04	0.39	0.22	0.88	0.16	0.45	0.25	0.30	0.10
Corycaeus speciosus			0.33	0.20	0.22	0.65		0.05		0.06	0.02
Corycaeus sp.			0.07								0.02

Appendix II. (Continued)

Taxa	Stations										
	1 night	2 night	7 night	8† day	9Ψ night	12Ψ day	14Ψ day	14Ψ night	15Ψ day	15Ψ night	16 day
Other unidentified spp.	0.89	0.08									0.02
Cirripedia larvae										0.03	0.21
Stomatopoda larvae	0.73	0.39	0.07	0.13	0.18	0.21	0.34	0.20	0.10	0.15	0.05
Mysidacea spp.	1.06	1.25		0.02		0.05	0.03	0.15		0.06	
Cumacea spp.	0.65	5.94	0.07					0.10			
Tanaidacea spp.											
Isopoda spp.											0.04
Amphipoda, hyperid spp.	0.16	0.08	0.52	0.17	0.33	0.05	0.39	0.10	0.03	0.03	0.22
Amphipoda, gammarid spp.	1.71	4.53						0.10			
Amphipoda, caprellid spp.		1.95	0.46								
Euphausiacea larvae	0.81						0.13	0.05	0.03		0.05
Penaeidae larvae	0.08			0.04				0.05		0.21	0.05
Solenocera larvae	0.08						0.05			0.06	0.08
Penaeus larvae			0.07	0.02		0.02					0.02
Sicyonia larvae											
Acetes larvae				0.02				0.05			
Lucifer faxoni	0.33	33.44	0.58	0.28	0.99	0.19	0.16	0.15	0.03		0.02
Lucifer typus	0.08			0.04	0.04						
Sergestidae larvae											
Processa larvae	0.08										
Leptochela spp.	0.65	0.08		0.02		0.02					
Lysmata larvae			0.07	0.04							0.02
Palaemoninae larvae										0.03	
Alpheidae larvae								0.05		0.06	

Appendix II. (Continued)

Taxa	Stations										
	1 night	2 night	7 night	8† day	9Ψ night	12Ψ day	14Ψ day	14Ψ night	15Ψ day	15Ψ night	16 day
Caridean juveniles & larvae	2.44	2.42	0.07	0.30	0.63	0.30	0.29	0.40	0.12	0.15	0.20
Scyllaridae juveniles	0.08										
Phyllosoma larvae	0.08				0.04						
Thalassinidae larvae											
Callianassa larvae	0.41		0.07	0.17	0.77	0.60	0.34	0.50	0.50	1.38	0.10
Galatheidae zoeae	0.08										0.10
Porcellanidae zoeae									0.03		
Paguridae zoeae	0.33	0.23		0.15	0.22	0.07				0.06	
Albuneidae zoeae	0.33				0.04		0.03	0.05	0.07	0.06	0.10
Anomura zoeae				0.02	0.04	0.09	0.08	0.10	0.05	0.09	0.02
Anomura megalopae			0.13	0.04	0.11	0.02			0.12	0.09	
Dorippidae zoeae	0.33						0.05				0.09
Leucosiidae zoeae cf.	0.33	0.16				0.07		0.10			0.10
Raninidae zoeae	0.16					0.02					0.04
Portunus ordwayi	0.49										
Portunidae megalopae	0.16			0.11	0.70	0.16		0.40	0.12	0.39	
Pinnotheridae sp.											
Pinnotheridae zoeae		0.47			0.07		0.65	0.30		0.15	0.02
Brachyura zoeae	2.76	3.05	0.20		0.29	0.44	0.42	0.79	0.22	0.21	0.29
Brachyura megalopae	0.08			0.09	0.18		0.03		0.03		0.05
Brachipoda larvae	0.49	0.03	0.13	0.15	0.11		0.05	0.05	0.05	0.15	0.02
Echinodermata larvae		0.16	0.91	0.91	0.40	0.16		0.20	0.03	0.24	0.07
Ophiopluteus late larvae		0.08	0.13	0.43	0.52	0.14		0.05	0.05	0.12	
Chaetognatha spp.	6.01	3.91	9.09	7.01	10.99	4.01	10.33	14.75	2.15	10.60	8.70

Appendix II. (Continued)

Taxa	Stations										
	1 night	2 night	7 night	8† day	9Ψ night	12Ψ day	14Ψ day	14Ψ night	15Ψ day	15Ψ night	16 day
Larvacea	0.16	0.08			0.04						
Thaliacea	4.63			0.02	0.40	0.05		0.10		0.09	0.07
Ophichthus gomesi larvae			0.13		0.07		0.05			0.03	0.02
Sardinella anchovia larvae	0.65										
Anchoa hepsetus larvae			0.07			0.02			0.03		
Synodus larvae											
Bregmaceros atlanticus young & larvae					0.11			0.10			
Cypselurus larvae	0.16										
Holocentridae larvae											
Pseudopriacanthus altus larvae											
Carangidae larvae		0.08		0.02			0.03				
Caranx sp. young				0.02							
Coryphaena hippurus larvae											
Pomadasyidae larvae	0.16										
Sparidae larvae											
Scianidae larvae											
Sphyraena larvae	0.08										
Gobiidae young & larvae				0.07	0.11			0.05	0.03	0.06	0.10
Gobionellus larvae			1.88	0.11	3.60	0.46	0.03	1.04		2.67	
Auxis thazard larvae				0.02							
Euthynnus alletteratus larvae				0.02							
Thunnus? larvae			0.07	0.07							
Scorpaena larvae											
Bothidae young & larvae		0.16		0.04	0.11	0.07	0.03			0.03	

Appendix II. (Continued)

Taxa	Stations										
	1 night	2 night	7 night	8† day	9Ψ night	12Ψ day	14Ψ day	14Ψ night	15Ψ day	15Ψ night	16 day
Bothus ocellatus larvae							0.03				
Etropus crossotus larvae											
Syacium larvae				0.02		0.07	0.03		0.05	0.03	0.10
Soleidae											
Symphurus larvae				0.02							
Acanthostracion quadricornis larvae											
Sphocroides larvae	0.08										
Non-elongate fish larvae	0.73	0.08	0.13	0.07	0.11	0.02		0.05	0.03	0.03	0.05
Elongated fish larvae				0.07	0.37	0.02		0.05		0.36	
Leptocephalus larvae						0.09					
Fish eggs, unidentified	1.71	1.80	0.84	0.74	0.26	0.44	0.55	1.04	0.37	0.75	0.22
Fish eggs, *Synodus* sp.	0.08			0.02	0.04				0.03	0.03	

†The numbers are an average of three hauls, except for the copepods which were identified from only one haul.

ΨThe numbers are an average of two hauls, except for the copepods which were identified from only one haul.

*P = present.

ACOUSTIC OBSERVATIONS OF SUBSURFACE SCATTERING DURING A CRUISE AT THE IXTOC-I BLOWOUT IN THE BAY OF CAMPECHE, GULF OF MEXICO

Donald J. Walter and John R. Proni
Atlantic Oceanographic and Meteorological Laboratories
National Oceanic and Atmospheric Administration
15 Rickenbacker Causeway
Miami, Florida 33149

ABSTRACT

In September 1979 the Ocean Acoustics Group of NOAA's Atlantic Oceanographic and Meteorological Laboratories (AOML) participated in a study of the subsurface oil plume created by the blowout of the IXTOC-I oil platform. Preliminary data from this study suggest that: (1) high-frequency sound (20 kHz and 200 kHz) can detect subsurface oil; (2) assuming that the subsurface acoustical reflectors are of oil origin, a substantial quantity of oil is present at various depths within the water column; (3) after the passage of Tropical Storm Henri, most of the oil resided within the top 20 m or so of the water column; (4) density stratification within the water column that existed prior to the passage of Tropical Storm Henri had significant influence upon the subsurface distribution of the oil; (5) at least some of the oil exists in a physical state such that it is subject to certain oceanic dispersal processes that appear to be similar to that of dilute, small particulate concentrations observed elsewhere.

1. INTRODUCTION

In September 1979 the NOAA Ship R/V RESEARCHER and the contract vessel R/V PIERCE (Tracor Marine) undertook a study in the vicinity of the IXTOC-I blowout to determine the fate and effects of oil spilled in the Bay of Campeche and the Gulf of Mexico (see Figures 1 and 2). Multidisciplinary studies would be conducted that would pay special attention to chemical and biological fates of the spilled oil and its subsequent interaction with the marine environment.

The AOML Acoustics Group was given a twofold task during the study. First, the group would employ high-frequency acoustics to attempt detection and tracking of subsurface oil-related materials; second, it would coordinate the activities of the scientists on board the RESEARCHER and the PIERCE. The R/V PIERCE, on which the acoustics were employed, was to serve as the major sampling platform in oil-bound waters, especially within the oil plume itself.

2. HISTORY

One of the most difficult measurements to be taken during oil spills or blowouts is the subsurface concentration of the oil. The IXTOC-I exploratory well blowout provided an opportunity to determine whether or not high-frequency sound could be used to map the subsurface distribution of the oil. The AOML Ocean Acoustics Group has been using high-frequency sound for a number of years (Proni et al., 1976; Newman et al., 1977) to detect and determine the subsurface concentration field of materials such as sewage sludge, pharmaceutical wastes, and dredge material dumped or placed into the oceanic water column.

Prior to this experiment it was not known whether or not high-frequency sound could be used to detect oil with oil in the physical form or state that it would assume within the water column. Evidence as to the physical form that the oil would assume when released directly from the ocean bottom into the water column under high pressure is sparse. Further, evidence as to the evolution of the physical form of the oil as it is dispersed in time and space within the water column is also extremely sparse.

Within the oil industry, sound in the low-frequency range up to two or three kHz has been used to detect suboceanic oil deposits. These deposits are detectable because of the acoustic impedance change caused by the reflecting liquid oil. It has also been possible to detect gas and oil seeps using 12-kHz sound (Geyer and Sweet, 1974). Nevertheless, it is not clear that the escaping oil would be in or evolve into a physical state that could reflect sound and hence could be detectable.

During the summer of 1979 it was reported that large patches of oil originating from the IXTOC-I wellsite were approaching the coastline of southern Texas. Initial environmental concern was focused on these floating patches and their possible effect on resort and fishing areas within the region. However, subsequent to the spill and cleanup efforts, on numerous occasions off the

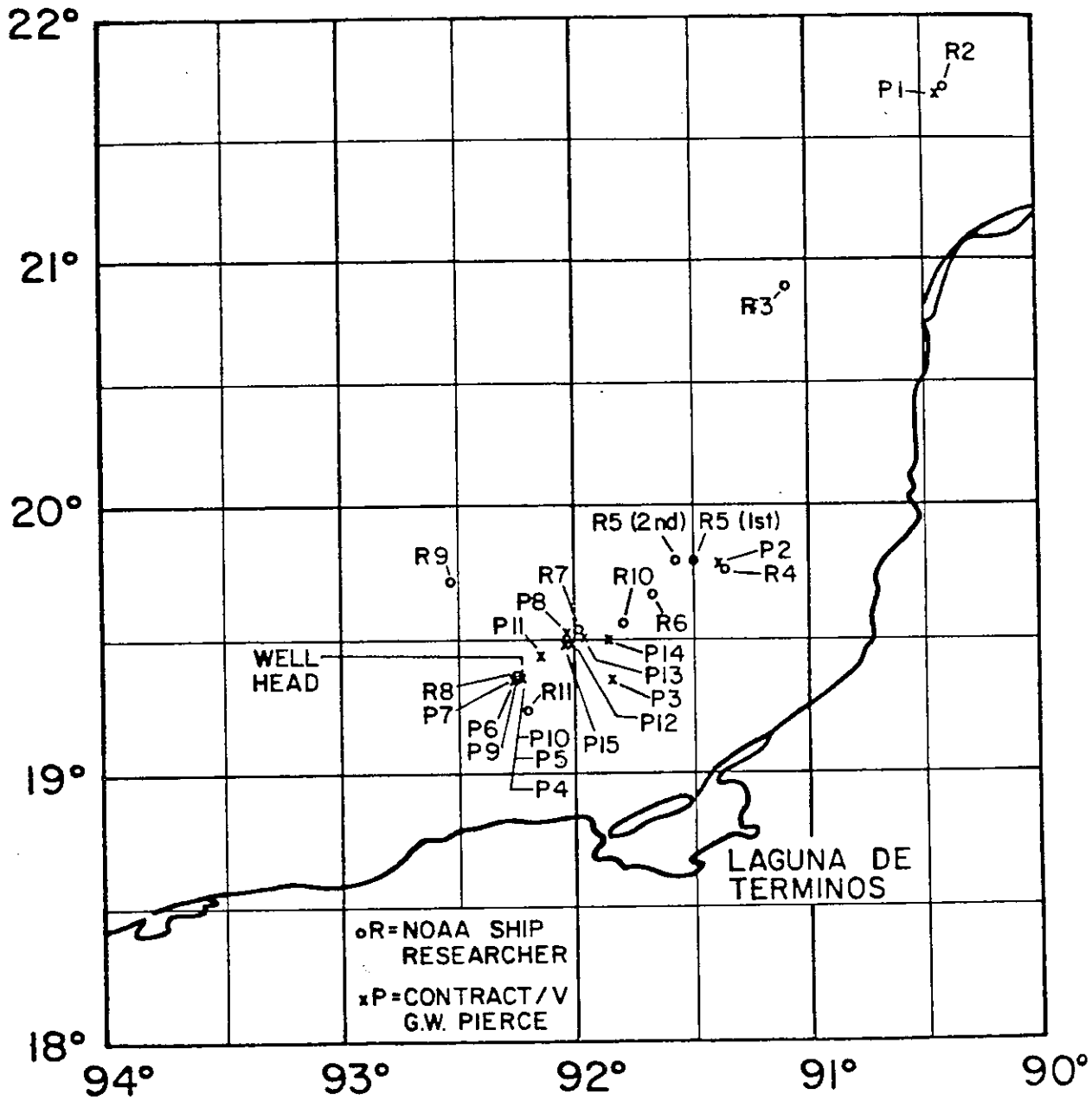

IXTOC-I
CAMPECHE OIL SPILL CRUISE
11-27 SEPTEMBER 1979
EXPANDED WELLHEAD REGION

Figure 1. Map of IXTOC study area.

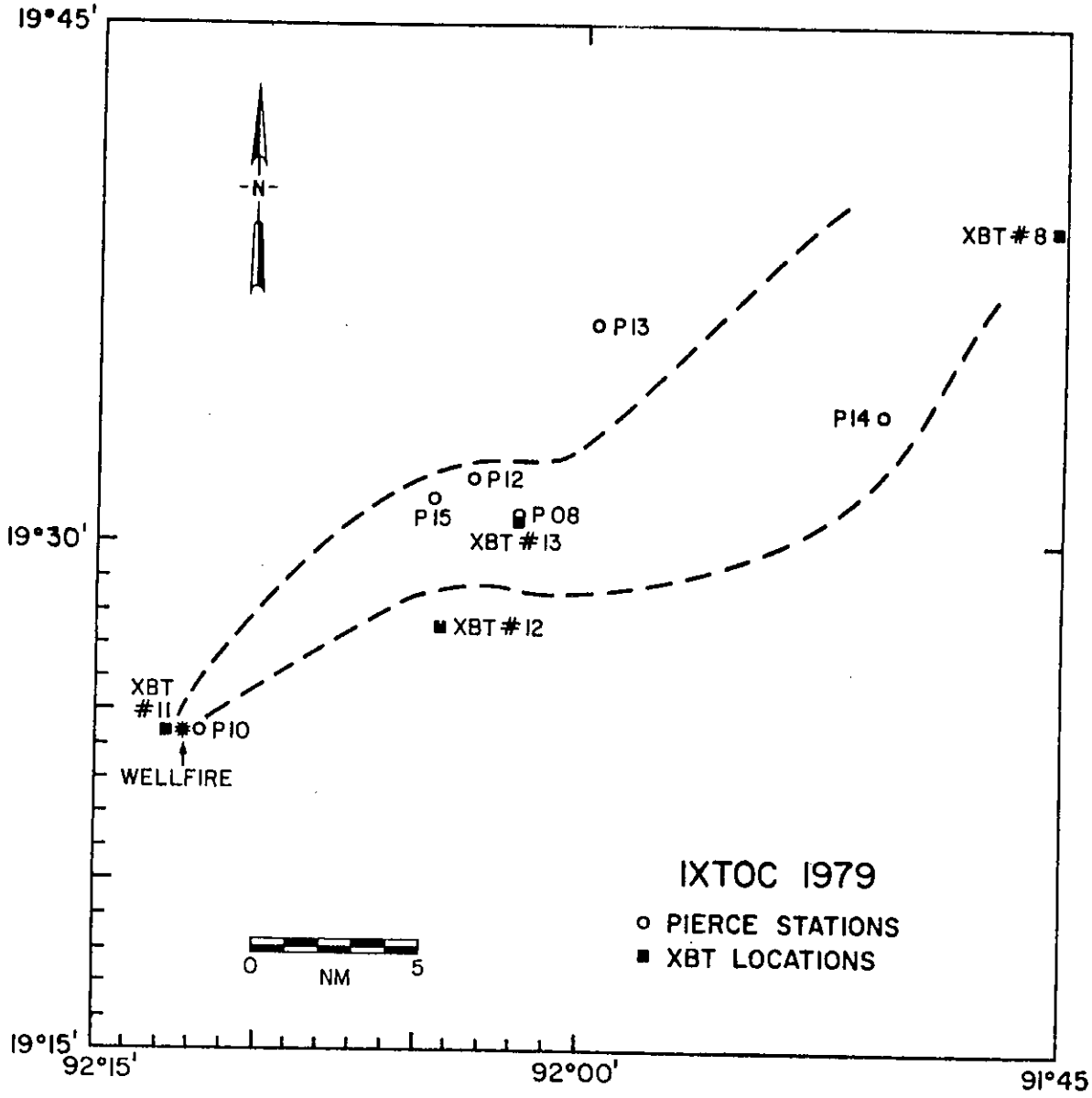

Figure 2. Enlarged map with PIERCE stations, XBT locations and plume limits as determined by helicopter overflight 9-19-80.

Texas coast, divers reported observations of tar balls suspended in the water column, generally at a depth of about 12 m (OSIR, 1980).

At the time few means, if any, were available for detecting the presence of subsurface tar balls. Obtaining a representative sample of these tar balls would be very difficult indeed using standard sampling apparatus for discrete point sampling.

The Coast Guard was successful in trapping some submerged tar balls in a heavy nylon net, which was deployed beneath an oil boom installed in the Port Mansfield Cut. It is not known whether any attempt was made by the Coast Guard or other authorities to determine if the material captured by this net was indeed transported from the IXTOC well area.

3. PHYSICAL SETTING

The R/V PIERCE arrived at the study area at about the time that rough seas were developing due to Tropical Storm Henri. In fact, sampling operations were conducted for only one day after arrival at the wellsite. The captain of R/V PIERCE reported 5-7 m seas.

Nevertheless, well defined stratification was present in the water column at the time of arrival of the R/V PIERCE. A typical shallow water temperature structure is clearly present in XBT #8 (Figure 3), to a depth of about 9 m, at which point the onset of a strong thermocline begins. The upper area of this thermocline (density interface) commonly serves as an area of accumulation for particulates and a variety of organisms. It is therefore likely that if tar balls were in fact suspended in the water column they would be suspended on an interface such as this. After the passage of Henri, the water column was completely mixed, as can be seen from XBT #11, Figure 3.

4. METHODS

Two acoustic frequencies (20 and 200 kHz) were to be used during this experiment; however, due to problems encountered with the 200-kHz tow body, only data obtained with the 20-kHz system will be discussed at this time.

The 20-kHz system transmitted a 1-KW, 1-ms-long acoustic pulse from a transducer with a beam width of 12°x18°, installed in a hydrodynamically designed tow body. The teardrop-shaped tow body is designed to be towed outboard of the ship at a depth of about 2 m. This system was successfully used in previous studies of pollution problems, such as ocean dumping of sewage sludge, dredge spoil, and pharmaceutical wastes, and also was used for detecting the presence of strong density interfaces in the water column. It was felt that if the tow body were employed for this study it would be a possible means of detecting and tracking subsurface oil and/or tar balls, if in fact they were originating from the IXTOC wellsite.

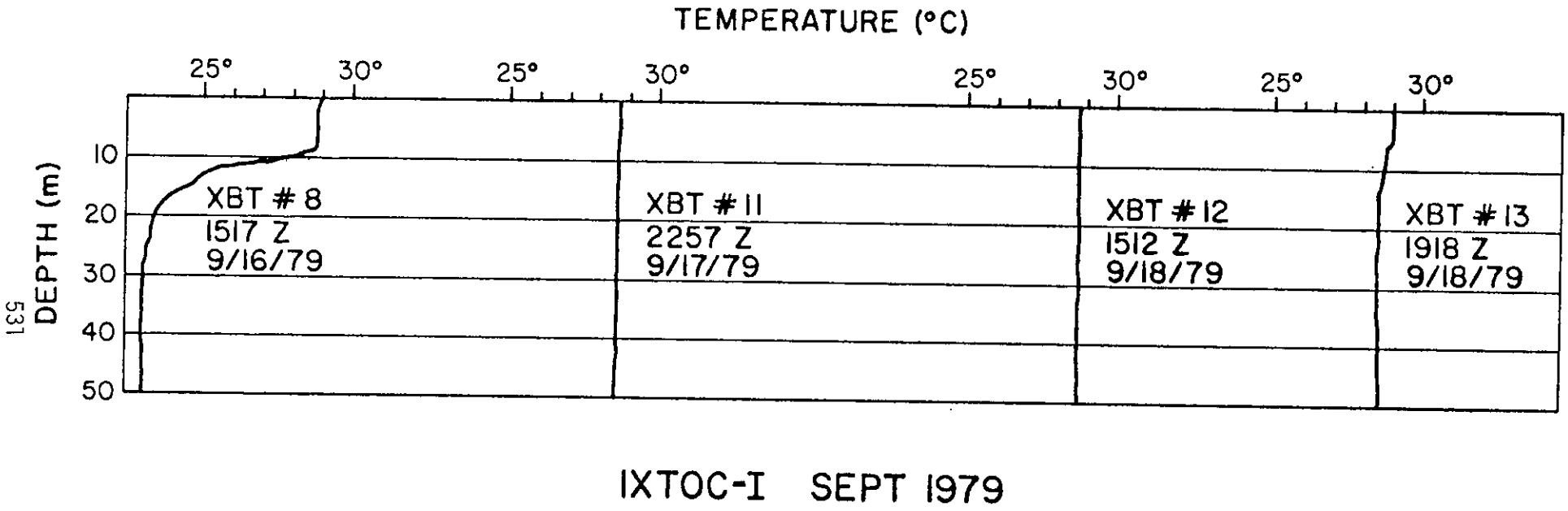

Figure 3. XBT traces comparing water structure before and after passage of Tropical Storm Henri.

The tar balls would become heavier than the surrounding water and sink until they encountered an interface strong enough to inhibit penetration. The probability of this penetration would, of course, depend on the physical characteristics of the tar balls. The interfaces are generally considered to be common regions from which acoustic reflections occur, especially when particulate matter is suspended upon the interface.

5. DISCUSSION

Figure 4 is a photo of acoustic data obtained approximately 5 NM from the blowout. Attention is drawn to the presence of two distinct layers of acoustical reflectors, one in the 10 to 15 m depth range and the other in the 20 to 25 m depth range. Layers such as these are typical in stratified bodies of water and have been associated with dispersion characteristics of wastes disposed of in the marine environment (Proni et al., 1976).

Temperature stratification such as that shown in Figure 3 (XBT #8) is generally considered to have a significant influence on the vertical distribution of acoustical scatterers associated with these events. In a typical ocean dumping scheme, scatterers precipitate until they encounter a density interface strong enough to inhibit any further sinking. They then remain buoyed on this interface until events occur which will either allow them to be propelled through it or mix with the remainder of the surrounding water. They are then influenced by typical oceanic dispersal processes that occur in local waters.

Both of the layers in Figure 4, one from 10 to 15 m and the other from 20 to 25 m, are detected quite easily by the acoustical system. The shallower layer detected between 10 and 15 m seems to be intermittent in its appearance in that it is detectable only for short periods of time. The deeper layer, however, was detected at this time and persisted, although at a different depth, for several hours afterward.

It can be seen in the photograph in Figure 5, taken after passage of the storm, that no subsurface layering was detected at this time. Evidently the turbulence created by the storm was successful in mixing the water column to the point where no isopycnal layering existed.

In comparing Figures 4 and 5, attention is drawn to the change in acoustical backscatter in the upper 20 m of the water column. This change denotes a large difference in the volume of material present within these regions of the water column. Using this as evidence, it may be concluded that, prior to the storm, isopycnal layering was present and did account for numerous manifestations of subsurface acoustical reflectors that could be associated with the IXTOC blowout. However, as a result of turbulent mixing created by the storm, no isopycnal layering was present immediately after its passage through the area. Evidence shows that for some time after the storm's passage, material expelled from the well remained in the upper 20 m of the water column and did not disperse along any subsurface boundaries. However, as winds diminished and

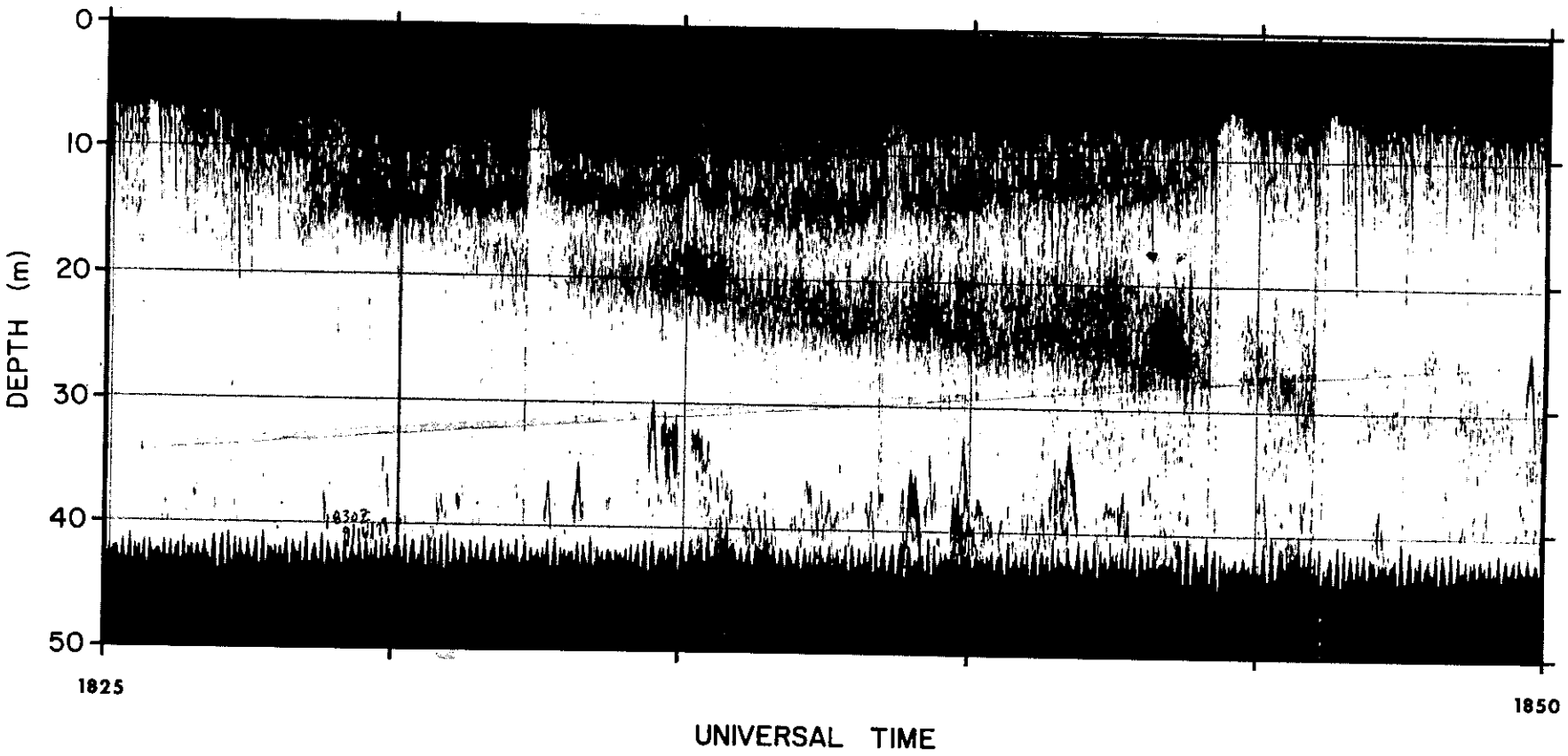

Figure 4. Acoustic data obtained approximately 30 miles northeast of the blowout. (Vertical scale = depth in meters, horizontal scale = universal time.)

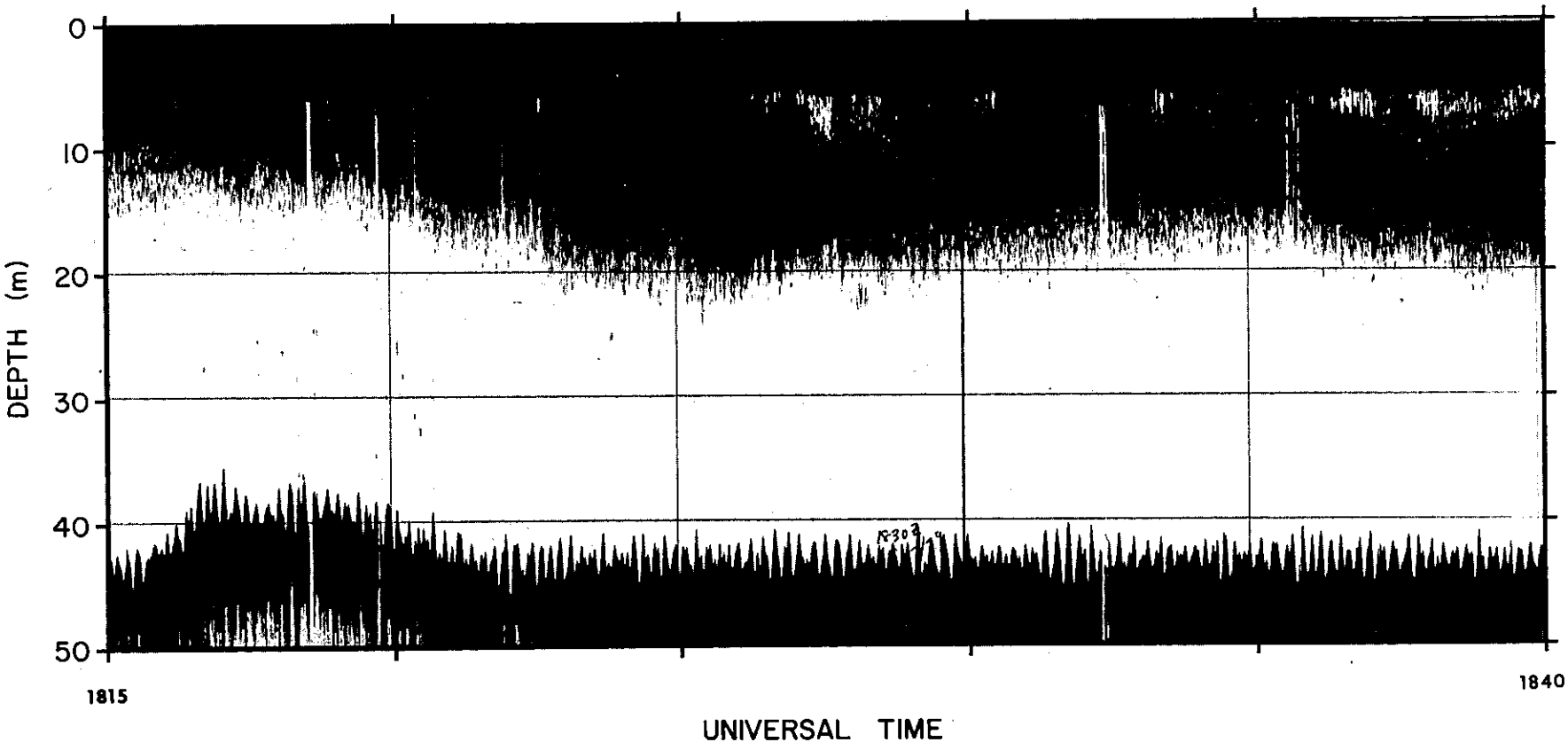

Figure 5. Acoustic data taken on station P05 approximately 0.5 nautical mile from the blowout.

seas calmed, the surface waters began to rewarm and the water column again tended to become stratified.

In Figure 3 (XBT #13) a change can be detected in both the surface temperature and the temperature structure of the water column below it. Although a strong temperature gradient is not present, consideration must be given to the overall change in the water column temperature structure and to the possible effect that this may have on the dispersion and/or buildup of material that may be detected acoustically on reflective layers.

In Figure 6 subsurface scattering from a discrete layer has been detected again with the acoustical system. These data were obtained two days after the storm's passage and during the time when water column stratification had begun (Figure 3, XBT #13). A comparison of the location (depth) of the acoustical layer and the multiple depth layers in XBT #13 indicates that a consistency exists in the 5 to 20 m depth region. There is an indication that a subsurface mixed layer was present between 5 and 15 m depth. A layer such as this could serve as a transport mechanism to material that had been entrapped within it.

Chemical samples taken at the time (2032Z; Figure 2, P08) by Energy Resources Company show increased concentration of hydrocarbons within the region indicated by the acoustic layers in Figure 6 (Boehm and Feist, this volume).

Other instances of subsurface layering occurred two days later (Figure 7) in the same general location (Figure 2, P15). The proximity of these and other occurrences in this location indicates that a phenomenon associated with the subsurface scattering may be an indicator that subsurface degradation of hydrocarbons is dependent on both time and mixing processes associated with their distribution throughout the water column.

Data obtained 3/10 mile from the wellhead indicate that, prior to stopping for station P10 (Figure 3), the ship made a transect across an interface associated with the plume of oil being expelled from the blowout at the time.

Figure 8 shows significant evidence that a crossing was made by the R/V PIERCE from an area containing large quantities of acoustically reflective targets to an area having much smaller quantities of these targets. During this passage, especially at 1050 U.T., the acoustic record indicates that acoustic return was higher within and at the edge of the plume than that encountered outside the plume. This phenomenon has been observed previously and has been associated with the distribution characteristics of various types of ocean waste disposal practices. Similarities are found when comparing these data. Of particular interest is the buildup of acoustically reflective material at the edges of plumes (Figures 8 and 9).

As previously mentioned, Figure 8 is a photograph of acoustic data obtained during a transect of the oil plume edge by the R/V PIERCE. Figure 9, on the other hand, is a transect of a plume edge of pharmaceutical wastes observed during a dump study off of Puerto Rico.

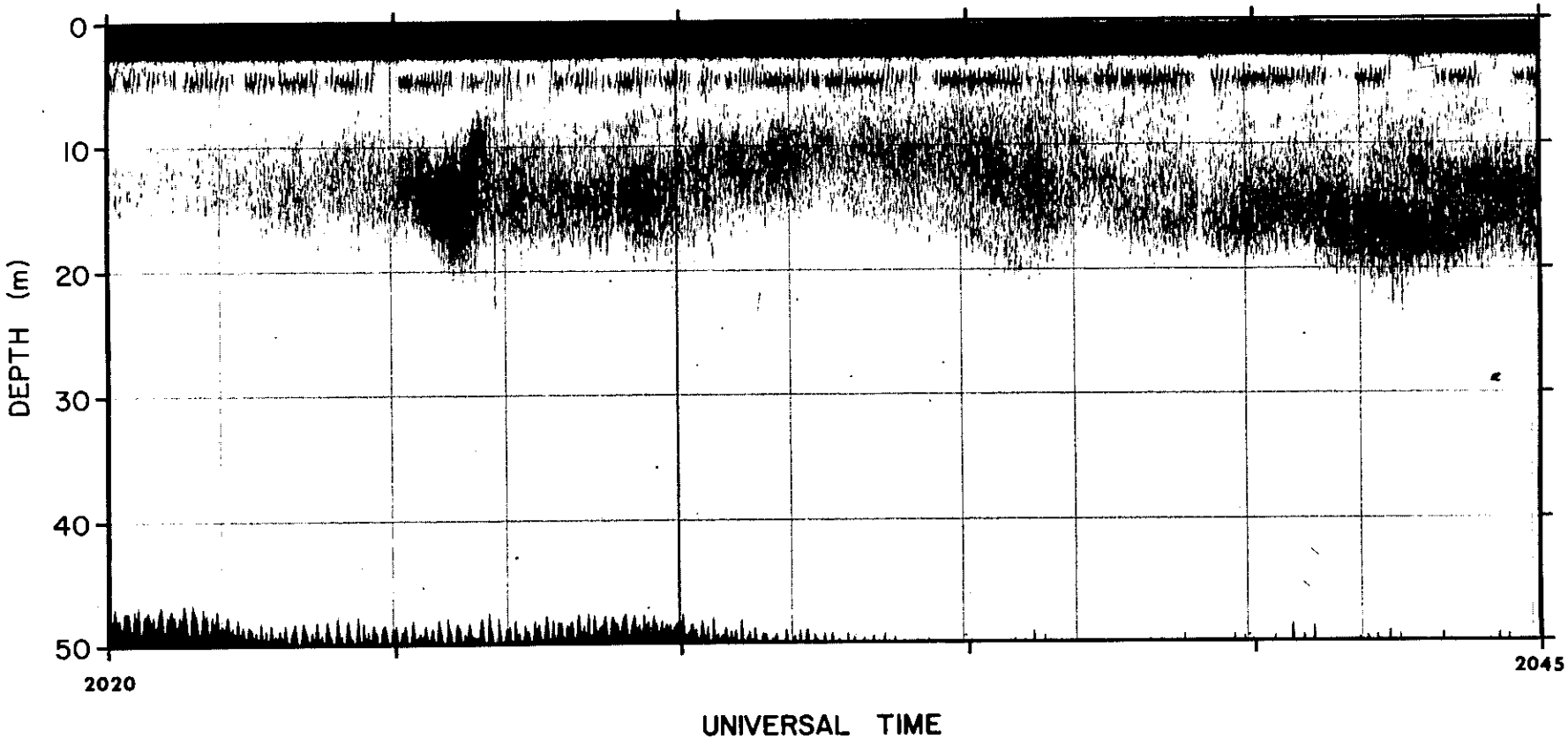

Figure 6. Acoustic data taken on station P08 approximately 12 nautical miles from the blowout.

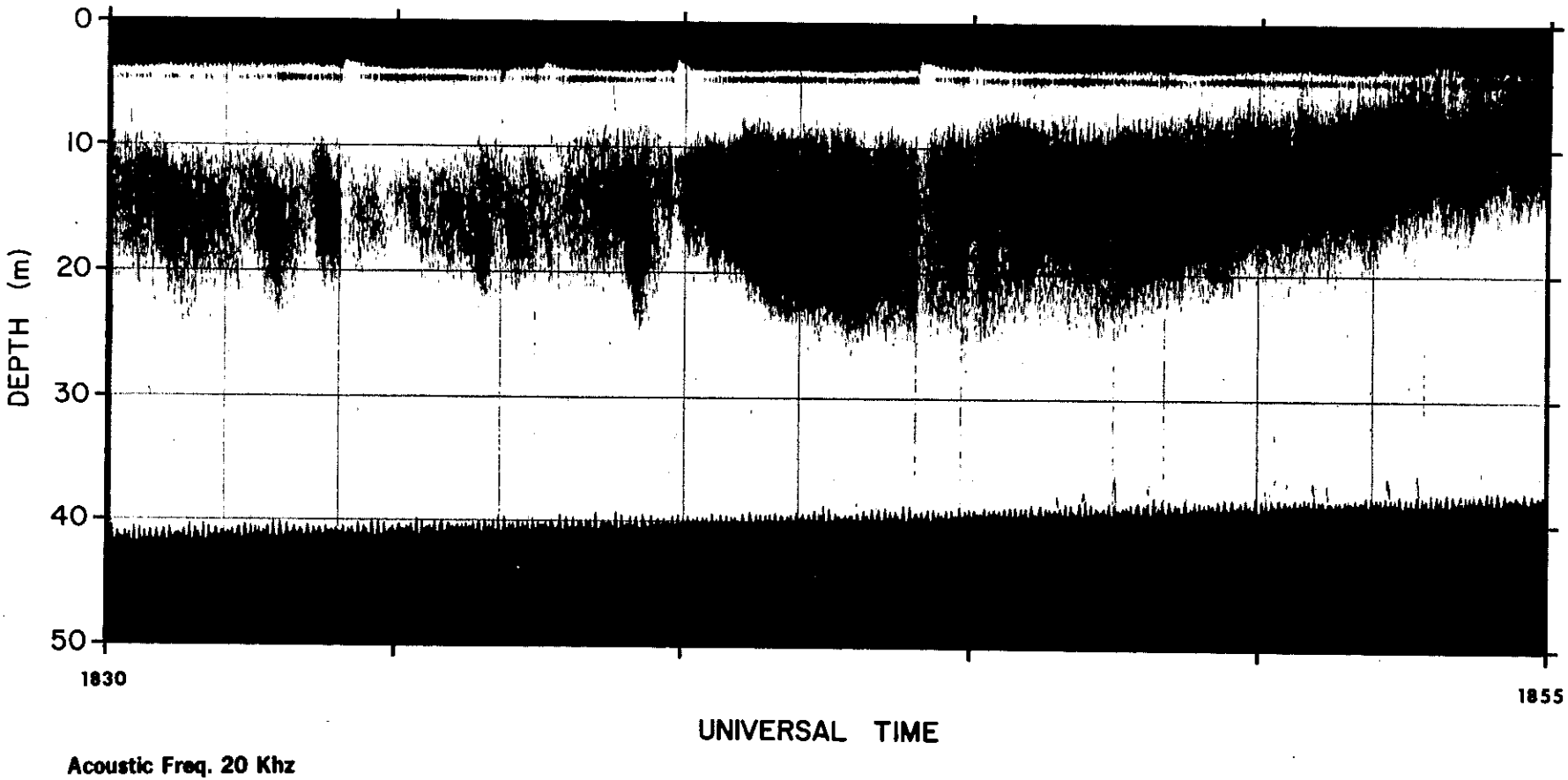

Figure 7. Acoustic data taken on station P15, 10 nautical miles from the blowout.

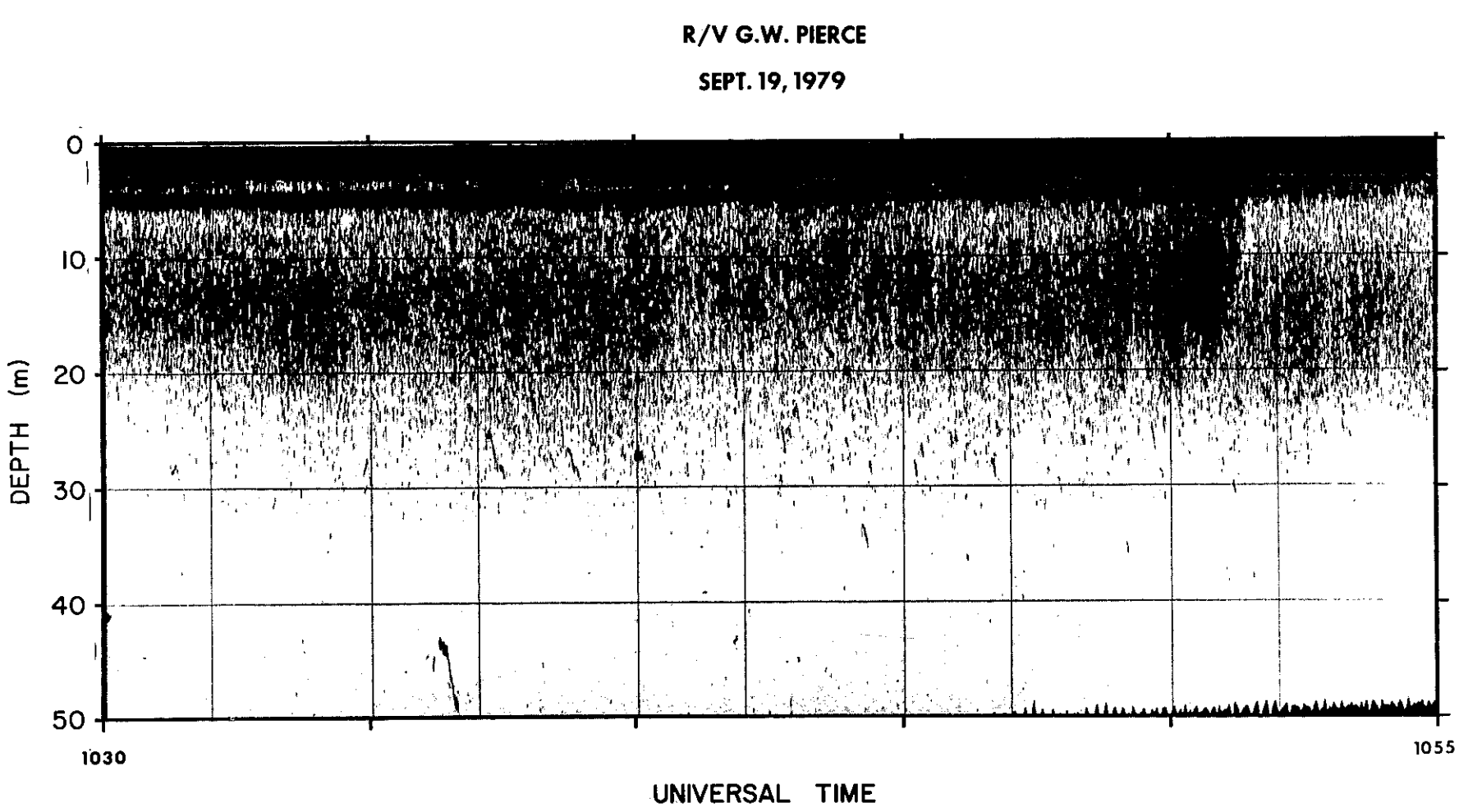

Figure 8. Acoustic data taken while underway and crossing edge of surface oil plume.

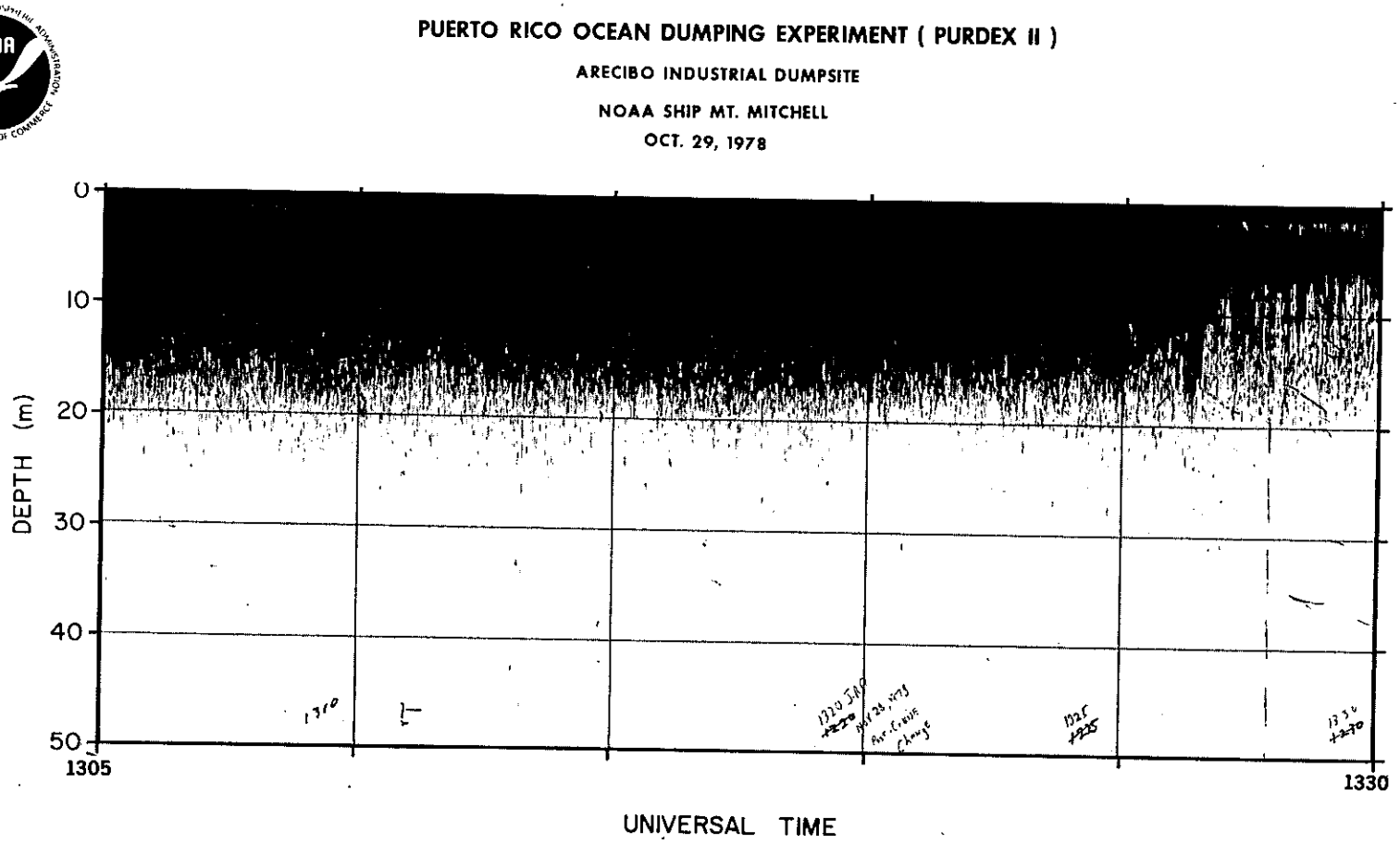

Figure 9. Acoustic data taken while underway and crossing edge of surface pharmaceutical waste plume. (Puerto Rico Ocean Dumping Experiment II, October 1978.)

Attention is directed here to the interface detected at approximately 1327. At this time there was a distinctive change in the volume of reflected signal very similar to the change referred to previously in Figure 8. Although electronic settings were different in each case, the qualitative similarities in the distribution of reflectors is obvious.

6. CONCLUSIONS

Acoustic data have been presented which indicate that subsurface layering was in evidence at stations and transits taken in the oil plume outward from the blowout. Of particular interest is the subsurface layering associated with Figures 6 and 7 observed at stations P08 and P15, respectively (Figure 3). Both of these stations are located within a 10-12 mile range of the blowout.

A comparison is made of IXTOC data and data obtained from a previous study that indicate obvious changes in acoustic backscatter at a plume boundary. The similarities of the acoustic properties at these interfaces indicate that in some instances various types of plumes may have similar dispersional characteristics. In any case, it is felt that acoustics can be used as a tool for indicating the presence of subsurface distributions associated with hydrocarbons. Further testing and sampling techniques should be developed that can be utilized in the future for more synoptic analyses of the subsurface distribution of hydrocarbons in the water column, whether this presence is due to natural or man-made seeping or spillage.

7. ACKNOWLEDGMENTS

The authors wish to acknowledge the cooperation and assistance of Captain Jim Scott and the crew of the R/V PIERCE. Special thanks also go to NOAA Corps Lt. Cdr. Bruce Arnold and Seaman Eddie Ward for their diligent efforts to insure that operations were run smoothly and safely. And finally we thank W. Paul Dammann and Antonio Puig for their help in securing the acoustic data.

8. REFERENCES

Geyer, R. A., and W. E. Sweet (1974): Naturally occurring hydrocarbons in the Gulf of Mexico and Caribbean Sea. Ocean 74 Proceedings, 1: 289-300, IEEE Publishing Co., New York.

Newman, F. C., J. R. Proni, and D. J. Walter (1977): Acoustic imaging of the New England shelf-slope water mass interfaces, Nature, 269, 5631: 790-791.

Newman, F. C., J. R. Proni, and D. J. Walter (1978): Some high-frequency acoustical observations of oceanic fronts, EOS, Transactions, AGU, 59, 4: 302.

Oil Spill Intelligence Report (OSIR) (1980): Special Report: IXTOC I, Vol. III, No. 1, 1-36. January 4, 1980 Newsletter. Center for Short-Lived Phenomena, Cambridge, MA.

Proni, J. R., F. C. Newman, R. L. Sellers, and C. Parker (1976): Acoustic tracking of ocean-dumped sewage sludge, Science, 193: 1005-1007.

RESPONSE OF THE PELAGIC MICROBIAL COMMUNITY TO OIL FROM THE IXTOC-I BLOWOUT: I. *IN SITU* STUDIES

Frederic K. Pfaender and Earle N. Buckley
Department of Environmental Sciences and Engineering
University of North Carolina
Chapel Hill, North Carolina 27514

Randolph Ferguson
Beaufort Laboratory
Southeast Fisheries Center
National Marine Fisheries Service
Beaufort, North Carolina 28516

1. INTRODUCTION

The ability of microorganisms to degrade crude oil and various petroleum products has been well known for years. Many different types of microorganisms have been shown to be capable of using various fractions of oil as sole sources of carbon and energy, growing at the expense of the oil. For many years, people have studied the response of oil-degrading bacteria to the presence of oil in different environments. Some of these studies, such as those conducted in Dr. Atlas' laboratory in North Carolina, have been very sophisticated and have demonstrated that a generalized response to oil pollution is an enrichment of the number of oil-degrading bacteria. There have been relatively few studies, however, on the impact of oil on the total microbial community. These few studes do tend to indicate that the effects on the entire community are relatively subtle and reflect some changes in the types of organisms present, principally a shift in metabolic patterns of the community to organisms capable of degrading oil. In addition, there have been some indications that certain types of community functions, such as the degradation of cellulose, can be inhibited by the presence of low concentrations of crude or refined petroleum products.

A topic of significant discussion among aquatic microbial ecologists is the role that microorganisms play in oceanic ecosystems. There would probably be little disagreement that microbes are important in the cycling of nutrients, which in turn is important to supporting primary productivity. Microorganisms also serve as food for consumer species and as enrichers of the nutrient value of suspended particles. Their role as degraders of organic material also may serve an important function in the carbon chemistry of the ocean. All of these roles contribute to the well-being and proper functioning of oceanic ecosystems. Therefore, it is important to understand the effect that oil may have on this community. The IXTOC-I blowout provided a unique opportunity to study the effects of petroleum on the pelagic microbial community, and to determine what, if any, detrimental effects may occur. Most prior studies have examined the impact of spilled oil on coastal areas where much more dramatic effects could be expected.

An objective of our study was to examine the effect of IXTOC oil on the pelagic microbial communities' composition and activity as a function of distance from the source of the oil. Community numbers, size and shape distributions, types present, and metabolic activities were examined. Another objective was to examine the *in situ* rates of hydrocarbon degradation in the water column that had been influenced by the spilled oil. Microcosm studies also were conducted to examine the effects of oil on these same community characteristics, using oils that had aged to different extents and were added to a non-impacted community.

2. EXPERIMENT

Over the last few years, microbial ecologists have come to realize that no single parameter adequately characterizes the entire microbial community. The

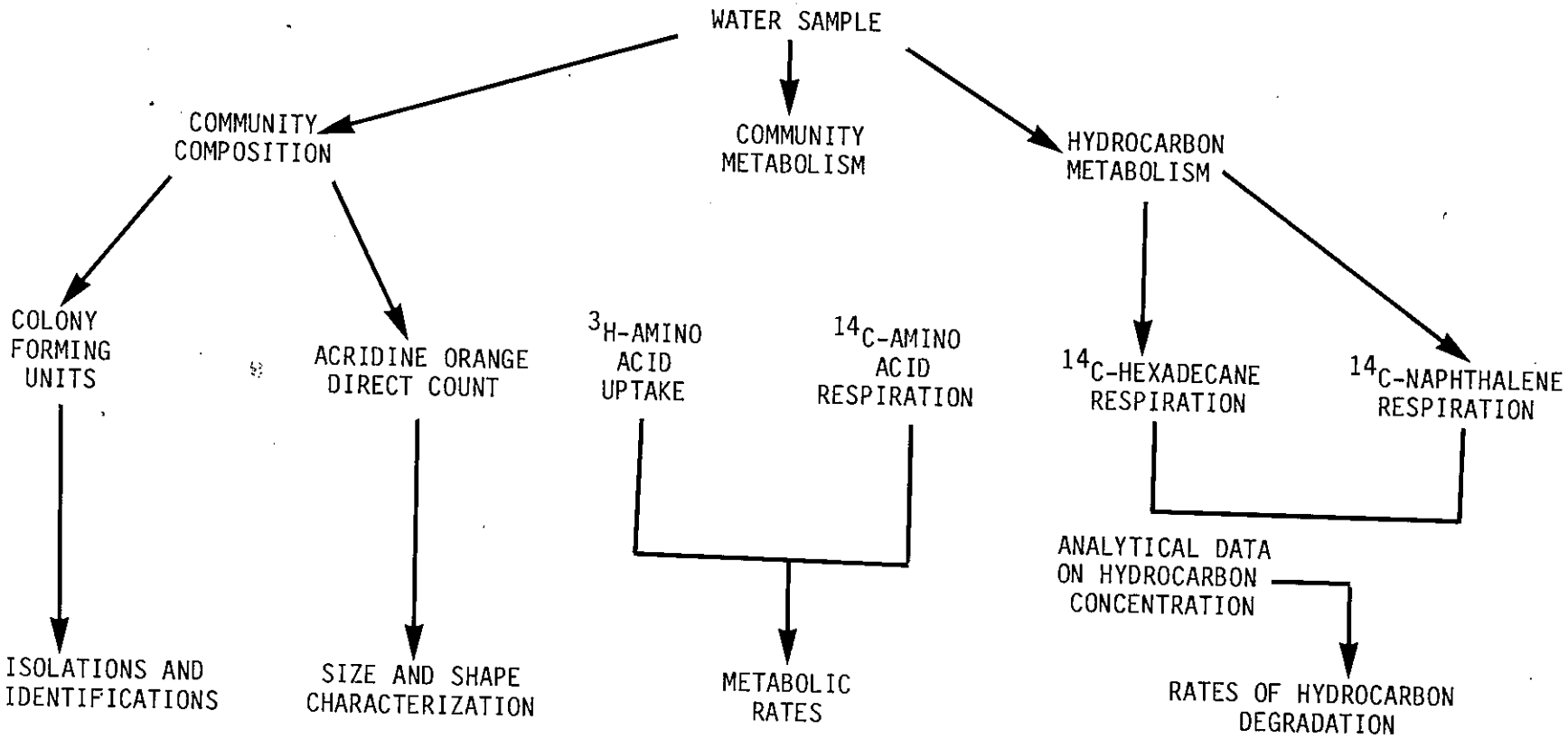

Figure 1. Community characterization.

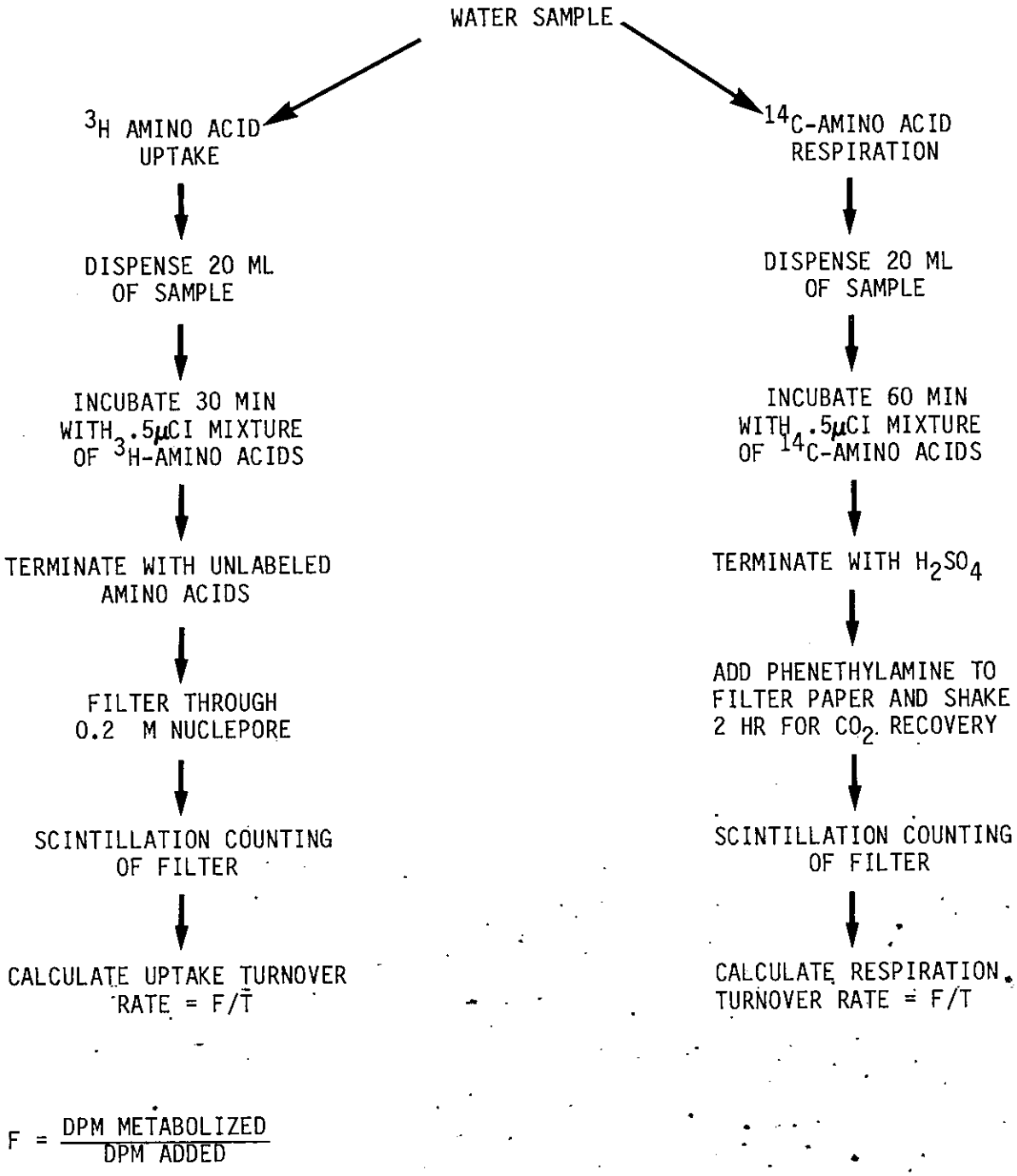

Figure 2. Heterotrophic activity measurement.

produced from the metabolism of the amino acids. Again, this is a tracer and the results are presented in terms of the turnover times for the natural amino acid concentration by natural population of microorganisms.

For measurement of the degradation of hydrocarbons, a technique was selected that would yield information about the natural rates of hydrocarbon metabolism. Many previous studies, starting with Zobell over 40 years ago, have shown that confining ocean water in a container dramatically increases the number and activity of the microorganisms present. This means that HC degradation rates obtained by experiments in which the microbial community is confined would be higher than the rates obtained under natural conditions. This would make the extrapolation of such results back to the environment especially difficult. Since these bottle effects are unavoidable in any study involving incubation for periods longer than approximately 12 hours, a major constraint was to keep the incubation period short.

The technique used, which was developed in our laboratory,involved the use of radio-labeled hexadecane as a representative of the aliphatic fraction of the oil, and C-14-labeled naphthalene was used as a surrogate for the aromatic fraction (Figure 3). These labeled hydrocarbons were added to samples from the environment, and the respiration of the substrates was measured over a six-hour period. Because analytical data were available for hydrocarbons in the waters from which these samples were obtained, it was possible to calculate an actual rate of metabolism. This rate represents the velocity of the metabolism of the hydrocarbons to CO_2 by the microbial community present in the water sample. The turnover time for the hydrocarbon concentration present was calculated and represents an estimate of how long it would take the community present to metabolize concentrations of hydrocarbons present.

It is important to keep in mind that these estimates can be calculated in a number of different ways, depending upon the hydrocarbon concentration used. In the present study, the respiration of hexadecane and the total aliphatic hydrocarbon concentrations were used to calculate the rates of aliphatic metabolism. This seemed justified, since microorganisms are not selective in the specific aliphatic hydrocarbons that they metabolize. In other words, the microorganism will metabolize C-12 through C-22 hydrocarbon without being selective to any particular isomer. The data also could have been presented in terms of rates of metabolism of hexadecane, but since the microorganisms were not selected, this rate probably would underestimate what would be occurring under natural conditions. Likewise, the metabolic rate or velocity for naphthalene is based upon the concentration of total aromatic metabolism. The microorganisms probably are somewhat more selective than with aliphatics, but the ring hydroxylation enzymes, which are necessary for the metabolism of aromatic hydrocarbons, probably are not completely selective.

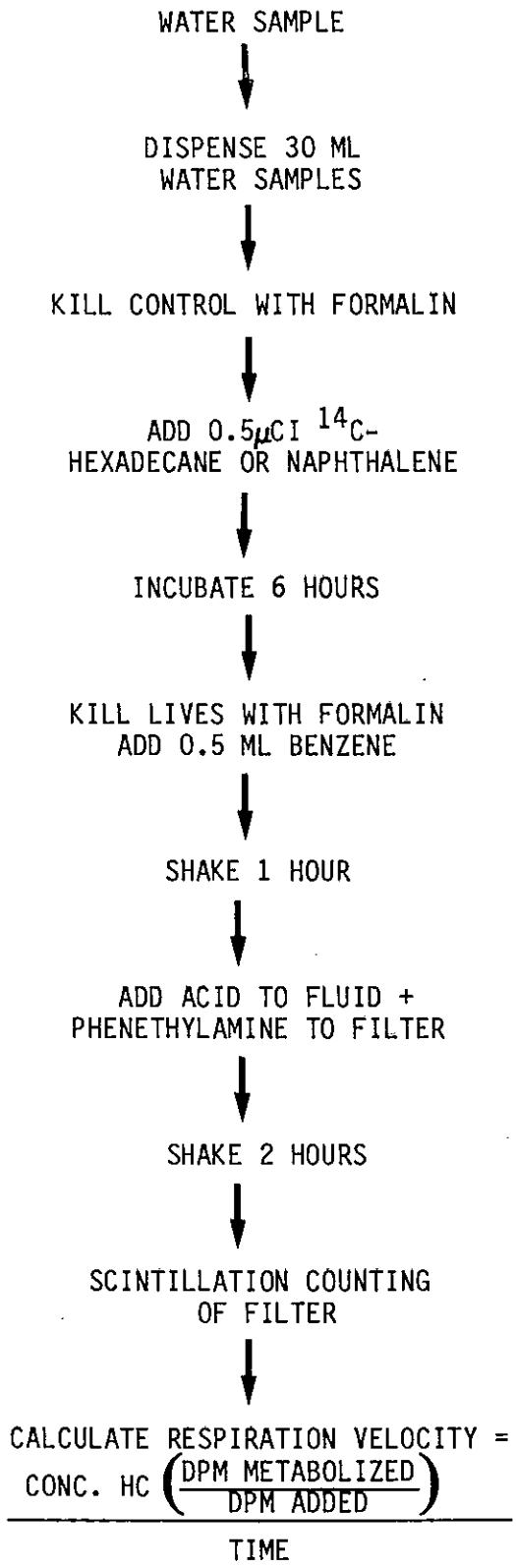

Figure 3. Hydrocarbon metabolism measurement.

3. RESULTS

3.1 Sample Site

Figure 4 gives sample locations. Water samples were obtained using sterile bag samplers. Samples from clean water areas were taken aboard the R/V NOAA Ship RESEARCHER, while those near the well head were taken by George Roubal on board the contract vessel G. W. PIERCE and transferred to the RESEARCHER. In all cases, the samples were processed in less than two hours from the time they were removed from the sea. Samples were taken from four areas at different distances from the well head, and two sites were at considerable distances in supposedly clean water areas (RIX02, RIX22). At each site, samples were taken from near the surface, at depths of approximately 10 m and 20 m.

3.2 Microbial Community Size and Composition

As seen in Table 1, AODC's do not change very much, regardless of whether oil is present or absent. There is also no major change with depth. The control station RIX02 shows somewhat lower counts than the oil-affected sites. Station RIX22 shows somewhat higher counts, which is probably a reflection of the influence of Rio Grande River inputs. The completion of statistical analyses of the data should determine whether these are significant changes. The size and shape characterization performed on the microscopic counts indicates that in all cases the majority of the cells are small, straight or curved rods (less than 1.2μ). The oil-impacted sites, however, are the only places where large rods appear, although they never constitute a high percentage of the total.

Although the total number of cells present does not appear to change appreciably, there are dramatic changes in the colony-forming unit counts (Figure 5). A short distance from the well head, surface counts begin to increase, reaching very high counts at 17 km. Near the well head, the influence of oil does not extend very deep, while at 17 km the effect impacts a larger part of the water column. At 27 km, the numbers are still slightly elevated, but they return to ambient, environmental levels by 37 km. This shows that there is a substantial change in the number of organisms that can grow under high nutrient conditions (oil) but that the increase is limited to areas very near the well head. The pattern that emerges from comparison of AODC/CFU is consistent with current thinking about the dynamics of oceanic microbial communities. This theory holds that enrichment leads to a change in the community, from one adapted to low concentrations of nutrients (probably do not grow on our media but are part of the AODC) to one that grows best under conditions of nutrient enrichment and do grow on media, hence increased CFU with constant AODC. The mousse from station RIX10, 40 km from the well head, contains approximately 4×10^6 CFU/gram, which represents over a 4-order-of-magnitude increase in number over the natural community, and two orders of magnitude over the highest oil-impacted water.

This change in the community is substantiated by the analysis of the bacterial isolates from these samples (Table 2). The arrows represent the

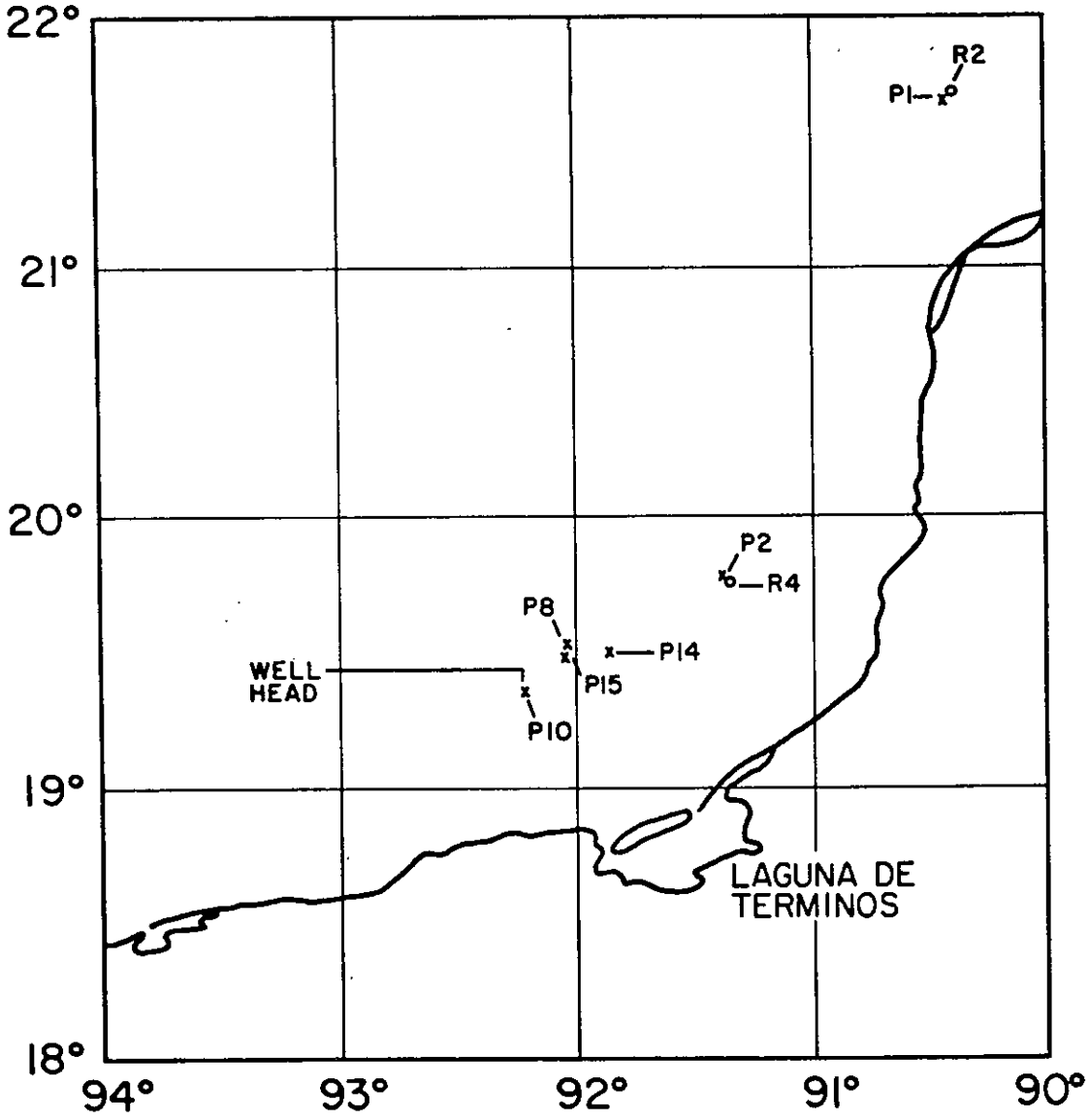

Figure 4. Sample sites.

Table 1. Microbial Numbers in Gulf of Mexico.

STATION	SITE (km from well head)	DEPTH (m)	COLONY-FORMING UNITS (per ml)	ACRIDINE ORANGE DIRECT COUNT ($X10^6$/ml)
PIX 10	0.5	2	773	1.01
		10	141	.88
		20	147	.93
PIX 15	27.4	2	38,665	.82
		10	34,500	.79
		20	16,230	.98
PIX 08	27.0	2	283	.73
		20	250	.71
PIX 14	37.0	2	78	1.14
		10	43	.78
		20	63	.92
RIX 02	300.0	2	151	.46
		10	123	.67
		20	231	.63
RIX 22	770.0	4	42	1.19
		20	37	.92
		40	102	1.03

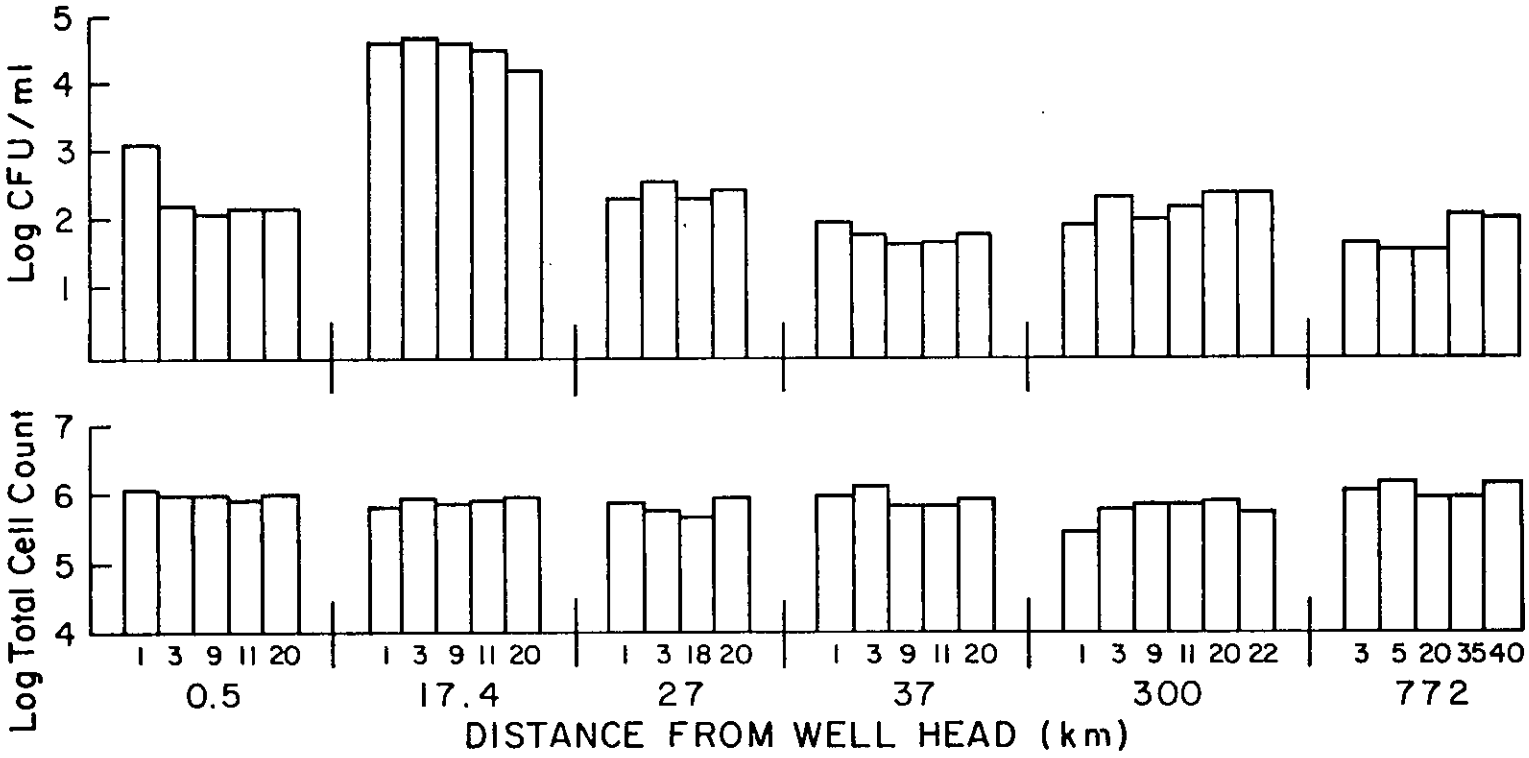

Figure 5. Colony-forming unit counts.

Table 2. Analysis of bacteria isolates.

Genera	Control Stations				Oil-influenced Stations								
	RIX02		RIX22		PIX10			PIX08		PIX14			RIX10
	Surface	20m	Surface	40m	Surface	10m	20m	Surface	20m	Surface	10m	20m	Mousse
Pseudomonas	37.6	41.6	29.75	36.0	0.2	37.0	55.0	19.0	9.9	34.0	18.2	19.4	56.6
Achromobacter	ND	ND	30.4	10.0	ND	ND	ND	ND	ND	ND	ND	ND	ND
Acinetobacter	8.2	1.1	ND	ND	1.6	2.7	2.7	ND	ND	7.2	7.3	10.4	5.9
Moraxella	6.1	2.6	ND	7.5	18.7	3.1	6.3	ND	ND	7.2	ND	ND	ND
Alcaligenes	--	3.4	17.2	14.0	1.4	10.8	11.7	11.0	ND	3.1	36.0	10.4	5.1
Flavobacterium	10.8	4.3	ND	ND	17.5	15.0	ND	41.0	9.9	9.1	7.3	14.9	10.3
Aeromonas	ND	1.5	ND	ND	2.6	6.3	2.7	ND	ND	ND	ND	ND	ND
Vibrio	ND	ND	ND	ND	ND	6.3	ND	ND	20.2	18.2	ND	ND	.3.3
Gram positive	9.2	2.5	ND	7.5	ND	ND	ND	ND	ND	ND	ND	ND	ND
Unidentified*	31.2	43.0	17.0	33.0	58.0	16.0	20.8	66.0	63.0	34.0	34.0	45.0	18.8

*Represents total of organisms not identified to genus level and those which did not grow on second transfer.

ND = No data.

directions of the changes and show that major shifts in community composition occur. Pseudomonas are the predominant organism at the control stations (30-40% of total), while at the well head they are inhibited at the surface (the same at 10 m and increased at 20 m). At greater distances there are fewer Pseudomonas; this impact shows up at greater depth, probably as a result of the spreading oil. Moraxella also seems to disappear from oil-impacted areas, while Flavobacterium becomes predominant at most sites. Members of the genus Vibrio appear only at sites influenced by oil. This organism, which is a fish and a potential human pathogen, seems to respond to organic pollution by increasing in number. For the same pattern, Vibrio, appearing only in the presence of organic enrichment, has been observed by Rita Colwell in her studies of pharmaceutical waste dumping in the ocean near Puerto Rico. The mousse is predominated by Pseudomonas, but they are of mostly different species from those found in the water. This may mean that once the mousse has formed, it represents a discrete microenvironment having different community composition, and, as the counts at distant stations indicate, having a smaller influence on water column populations.

3.3 Community Metabolic Activity

The data in Table 3 and Figure 6 show turnover times in days for ambient amino acid concentrations. The higher the number, the slower the metabolism.

Several striking features are revealed by these data. The most interesting feature is the almost total inhibition of amino acid respiration near the well head. There are two reasonable explanations for this observation. First, amino acids are constituents of proteins and probably would be metabolized for energy (i.e., to CO_2) only under conditions where no other energy-generating substrate is available or where amino acids are present in large quantities, being preferentially incorporated into new biomass. Therefore, the absence of amino acid respiration may reflect rapid growth in the presence of a large amount of metabolizable carbon source (oil). Secondly, there may be some inhibition by the oil. This appears to be a better explanation, since at the 17 km station we still have oil but amino acid respiration has increased. By the 17 km station, which is the site of the highest numbers, both uptake and respiration have increased severalfold, while oil concentration has decreased significantly. The apparent toxicity has been alleviated and metabolism is rapid. By 27 km, the uptake has decreased but respiration is high, which may reflect the fact that a population has grown on oil and now the oil concentration has decreased, and that the amino acids are being used for energy. By 37 km, both rates have decreased and respiration is higher, again indicating nutrient-poor conditions. At the control site, RIX02, the same pattern occurs: low uptake, high respiration, nutrient-poor conditions. At RIX22, the influence of the Rio Grande is seen again; more uptake occurs. Overall results seem to show that there is respiration inhibition near the well and a large increase in activity, followed by a return to the environmental level; this is consistent with the count data. The effects are restricted to the area immediately adjacent to well head area.

Table 3. Heterotrophic activity by Gulf of Mexico microbial community.

STATION	SITE[1] (km)	DEPTH (m)	AMINO ACID TURNOVER TIME (DAYS) UPTAKE	RESPIRATION
PIX 10	0.5	1	416	>400,000
		9	347	>400,000
		20	520	>400,000
PIX 15	17.4	1	181	152
		9	297	---
		20	116	187
PIX 08	27.0	1	3787	128
		3	1042	757
		18	502	730
PIX 14	37.0	1	833	372
		9	1388	555
		20	3472	413
RIX 02	300.0	3	1894	210
		9	817	254
		20	595	125
RIX 22	770.0	3	143	1,388
		35	298	353
		40	119	905

[1]Distance from well head.

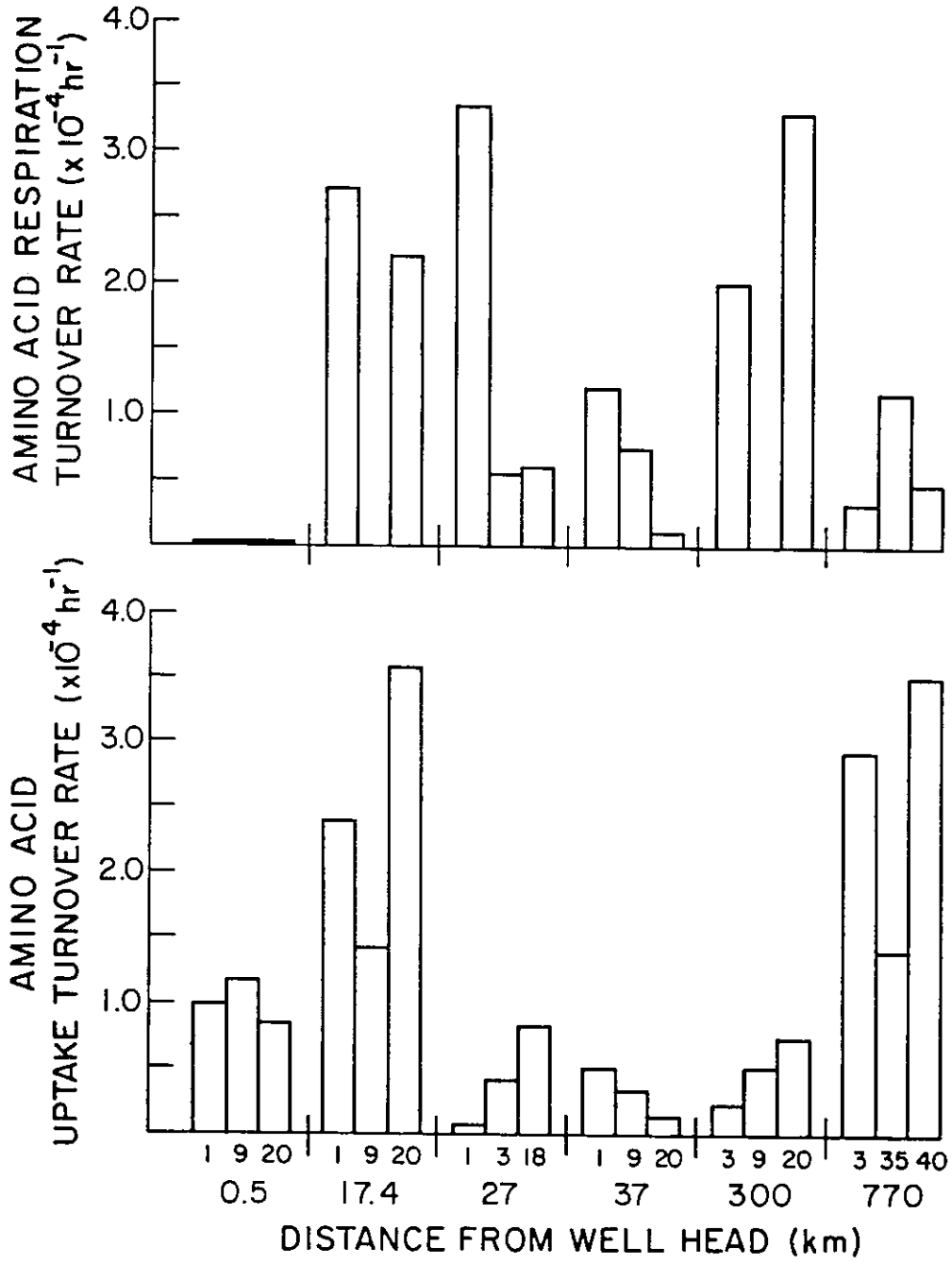

Figure 6. Turnover rates for amino acid concentrations.

3.4 Hydrocarbon Metabolism

The metabolism of hydrocarbons (Table 4) was investigated using a technique that yields results very similar to those expected under environmental conditions. Using the HC concentration for total aliphatics with hexadecane respiration data, and total aromatics with naphthalene respiration data, we have calculated metabolic velocities for the aliphatic and aromatic fractions of the oil, respectively. The results are expressed as turnover times, which is the concentration divided by the velocity. The length of time needed for that oil fraction to be metabolized at the rate measured is estimated. Again, the higher the turnover time, the slower the metabolism. Because chemistry data were available for only a few depths at each station, the asterisked values are those calculated using hydrocarbon concentrations from a depth other than that from which the water sample used in the metabolism study was taken.

The patterns seen are similar to the other microbiological parameters, with highest rates of aliphatic metabolism near the well head decreasing to near environmental levels moving away from the well head. Aromatic metabolisers appear to take longer to show high rates, probably because time is needed to induce a community of degraders; aromatics may not be so common in the water and therefore that ability may be rarer. The control stations show very low rates of metabolism.

The turnover time data indicate that the microbial community present has a high potential for the metabolism of hydrocarbons because the time required for breakdown is relatively short, even in the controls. Short turnover in controls is due to the fact that even at low rates, the low concentration can be metabolized rapidly.

These data indicate that microbial degradation of oil in the water can be very rapid, in contrast to the mousse, for which oxygen, N, and P may limit the speed of microbial utilization of the oil. The microbes are capable of significantly altering the hydrocarbon concentrations in relatively short periods.

4. CONCLUSIONS

(1) Spilled oil effects on the microbial community include:

a. Increases in numbers

b. Changes in the composition of the microbial community

c. Possible inhibition of amino acid respiration

d. Increases in metabolic activity

(2) The oil effects are restricted to areas very near the source of oil, and all parameters measured return to environmental levels within a short distance from the well.

(3) The aquatic microbial community is capable of rapid metabolism of the oil, which may be retarded when the mousse is formed. This could account for a large part of the decrease in oil. There needs to be more investigation of the mousse formation.

Table 4. Hydrocarbon metabolism rates.

STATION	SITE[1] (km)	DEPTH (m)	Hydrocarbon Respiration - µg/l/hr ALPHATIC[2]	Tt(HR)	AROMATIC[3]	Tt(HR)
PIX 10	0.5	1	44.30	94	1.58	1772.0
		9	21.70*	-	9.20*	304.0
PIX 15	17.0	1	0.36	266	2.18	34.8
		9	0.14	228	2.17*	8.85
		20	0.72	44	1.84	10.3
PIX 08	27.0	1	7.88*	35	6.44*	7.9
		3	--		2.51*	20.3
		18	.12	216	--	
PIX 14	37.0	1	--		0.65	70.7
		9	--		0.01*	320.0
		20	--		0.02	160.0
RIX 02	300.0	3	.05		.007*	157.0
		9	.09		.002*	550.0
		20	.04	30	.037	29.7
RIX 22	770.0	3	--		--	
		35	.01	200	.03	112.0
		40	.01	142	.02*	170.0

[1]Distance from well head.

[2]Calculations based on total aliphatic hydrocarbon concentration and metabolism of ^{14}C-hexadecane.

[3]Calculations based on total aromatic hydrocarbon concentrations and metabolism of ^{14}C-naphthalene.

*Calculated value using hydrocarbon concentration from depth other than that from which sample was taken.

RESPONSE OF THE PELAGIC COMMUNITY TO OIL FROM THE IXTOC-I BLOWOUT: II. MODEL ECOSYSTEM STUDIES

Earle N. Buckley, Frederic K. Pfaender, Kristine L. Kylberg
Department of Environmental Sciences and Engineering
University of North Carolina
Chapel Hill, North Carolina 27514

Randolph L. Ferguson
Beaufort Laboratory
Southeast Fisheries Center
National Marine Fisheries Service
Beaufort, North Carolina 28516

1. INTRODUCTION

The effects of oil on individual species of macroorganisms, phytoplankton, and zooplankton and on populations of these organisms have been studied extensively (Cowell, 1971; Hyland and Schneider, 1976; Nelsen-Smith, 1973). Little is known about the effects of petroleum hydrocarbons on natural populations of marine microorganisms. Partially because of the need to control spilled oil, most microbiological studies have been focused on the capacity of bacteria to degrade petroleum hydrocarbons (Atlas and Bartha, 1972a; Byron et al., 1970; Lee and Anderson, 1977; Miget et al., 1969; Soli and Bens, 1973; Walker et al., 1975a, b; Walker and Colwell, 1977; ZoBell and Prokop, 1966). However, batch culture experiments have demonstrated that dissolved oil fractions reduced growth rate and maximum cell density of individual strains of marine bacteria (Calder and Lader, 1976; Griffin and Calder, 1977). Oil inhibited D-glucose uptake and mineralization (Hodson et al., 1977) and total respiration (Atlas and Bartha, 1972b) of mixed populations of marine bacteria. Dietz et al. (1976) observed that crude oil enhanced bacterial biomass but decreased heterotrophic potential of marine bacteria in "bottle" experiments. In salt marsh microcosms, petroleum hydrocarbons increased the abundance of total bacteria and of cellulolytic bacteria but inhibited the utilization of crude fiber from Spartina alterniflora (Buckley, 1980).

The IXTOC-I well blowout in the Bay of Campeche, Gulf of Mexico, resulted in the largest accidental oil spill in maritime history. In contrast to other major oil spills, which occurred nearshore and resulted in significant environmental damage to coastal ecosystems (i.e., the groundings of the supertankers TORREY CANYON and AMOCO CADIZ, the Santa Barbara blowout), the pelagic communities of the Gulf of Mexico were most immediately and most heavily impacted by the oil released from IXTOC-I. The functions of heterotrophic bacteria in pelagic ecosystems include: (1) decomposition of photosynthetically produced and allochthonous organic matter, (2) cycling of nitrogen, phosphorus, sulfur, and other inorganic substrates, and (3) production of biomass through conversion of dissolved organic substances into bacterial protoplasm, thus making them available for the primary consumer species (Hoppe, 1976). Consequently, potential adverse effects of petroleum contamination on marine microbes and their metabolic activity could dramatically influence the productivity and energetics of the pelagic communities of the Gulf of Mexico.

The overall objective of the microbiological effects studies conducted on the RESEARCHER/PIERCE cruise was to assess the effects of oil from the IXTOC-I blowout on the structure and metabolic activity of the pelagic bacterial communities of the Gulf of Mexico. The work involved in-situ microbiological analyses (Pfaender et al., this report) and microcosm experiments. The objective of the microcosm experiments was to determine the effect of variously weathered oils on the indigenous microbial populations of unimpacted waters.

The advantages of the microcosm approach are: (1) it provides an experimental system that has discrete boundaries and is small enough to be conveniently subjected to experimental conditions (Gordon et al., 1969), (2) it allows the establishment of replicate ecosystems (Beyers, 1964), and (3) it simplifies the identification of operational mechanisms first in the experiment and later in nature (Margalef, 1967). The selection of microbiological

parameters measured, community abundance and composition, heterotrophic activity, and hydrocarbon utilization allowed for the identification and comparison of the response of the pelagic microbiota to oils of various "ages" from the IXTOC-I spill.

2. METHODS

2.1 Design of the Experimental System

The microcosm design was adapted from Buckley (1980). Briefly, sterile 3.8-l Nalgene polypropylene wide-mouth bottles (Sybron/Nalge, Rochester, N.Y.) were used for microcosms (Fig. 1). Each bottle was fitted with a 3-hole no. 15 Neoprene rubber stopper (Rhoades Rubber Corp.). Entering through the stopper were 1.0 ml glass pipettes. The air inlet tube extended to within 1 cm of the bottom of the bottle. The siphon tube was used for drawing samples from a point mid-depth in the initial water column. The gas outlet tube was extended to a point approximately 1.0 cm above the surface of the initial water column. Silent Giant® air pumps (Aquarium Pump Supply, Inc., Prescott, Ariz.) were used to aerate the microcosms. The air passed through Tygon tubing to an in-line cotton-filled trap, which functioned as a filter to prevent contamination of the sample water by atmospheric microorganisms, and on to a manifold consisting of T-shaped glass rods linking three bottles. Pinch clamps were used to equally distribute the air flow. During these experiments, the gas outlet was fitted with a trap containing sterilized cotton. This allowed equalization of gas pressure within the bottle with atmospheric pressure, but prevented atmospheric contamination of the sample water. The water was mixed by introducing a constant stream of bubbles from the air inlet, and by providing each microcosm with a 1" Teflon-coated magnetic stirring bar and stirring on a magnetic stirrer at approximately 300 RPM.

All incubations were done in the dark; each microcosm was covered with aluminum foil and a layer of duct tape. The temperature of the incubations was 25 ± 2°C.

Samples were drawn from the systems by attaching a 500-ml vacuum flask fitted with a one-hole rubber stopper containing a glass tube to Tygon tubing from the sample port, opening a clamp on the sample tube, and then applying a vacuum to the side-arm of the flask to siphon the required amount of sample water into the flask. The sample tube was enclosed, the flask removed, and the water remaining in the sample tube forced back into the microcosm by use of an air pump and manipulation of the pinch clamp on the sample tube.

2.2 Preparation of the Model Aquatic System

On 19 September, approximately 60 L of sample water were collected from a depth of 5 m at station RIX09, located 48 km northwest of the well site, using the glass Bodman bottle sampler. Sample water from two Bodman casts was combined and mixed into an 80-L-capacity sterile bag. Within one hour of collection, 3.6 L of mixed sample water were added to each of twelve microcosms.

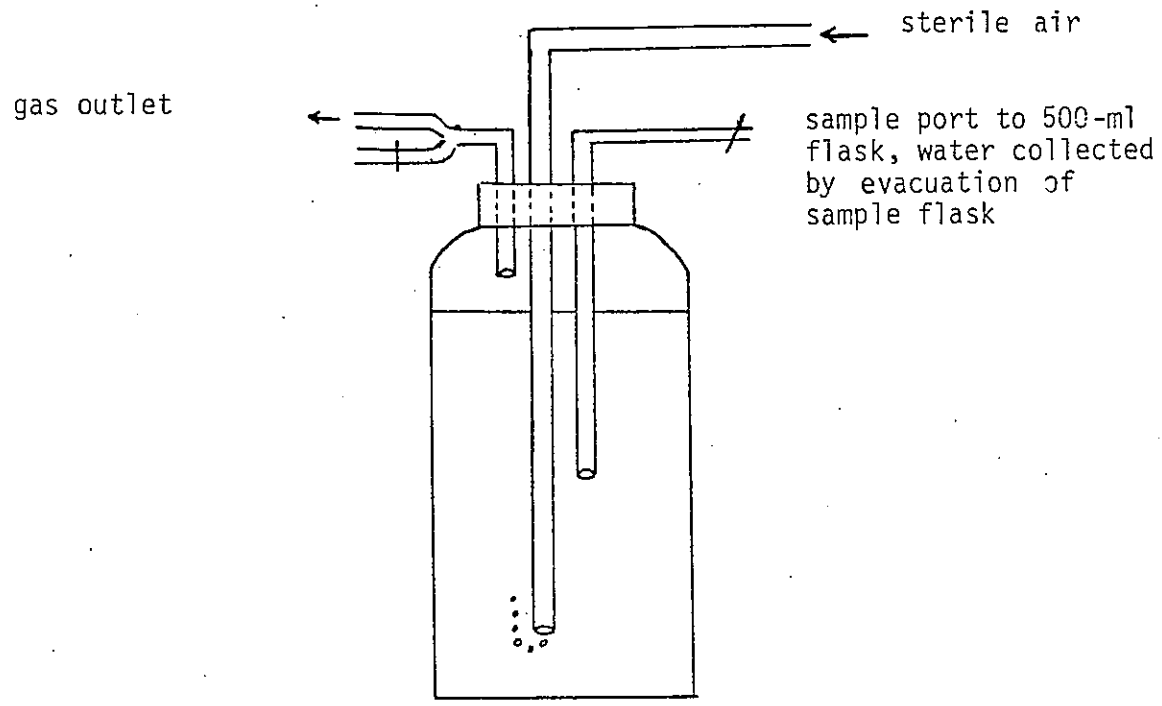

Figure 1. Microcosm design.

There were four oil treatment groups; each treatment group included three microcosms (Fig. 2). One set of microcosms (C) received no petroleum and served as a control. The microcosms of the second treatment group (WO) received fresh well oil that had been collected at RIX07, approximately 27 km from the wellhead and within the oil plume. The microcosms of the third treatment group (WM) received mousse collected at RIX06, 48 km northeast of the well. Mousse collected from a mousse patch off South Padre Island, Texas, by Roy Hahn of Texas A&M University was added to the fourth group of microcosms (TM). All oils were added within 30 minutes after the bottles were filled. The concentration of added oil and mousse was 1% (wt/vol). It should be noted that the mixing of the water column at no time resulted in oil particles or oil droplets being collected with the sample water. This indicates that while the mixing of the stirring bar provided homogeneously mixed samples of the water column, the bulk of the oil remained at the surface during the experiment. Hydrocarbon concentrations observed in the water thus resulted from dissolution of oil at the surface into the water column.

2.3 Subsampling Protocol and Analysis

Subsamples of the experimental water for chemical and microbiological analyses were taken during the collection of the sample water and at periodic intervals during the 7-day incubation period (Table 1). Samples drawn from the microcosms were processed immediately after being collected.

Microbiological community parameters measured included acridine orange direct counts of total cell number, colony-forming bacteria, uptake and respiration of amino acids, and respiration of n-hexadecane and naphthalene. During the enumeration of total cell numbers in all samples and in all counting fields, individual cells were measured using the smallest division (1.2 μ) of the counting grid. Differential counting of the bacterial colonies and isolation and identification of representative colony types were done on samples from the initial and final sampling times for all treatments. The techniques for all microbiological parameters measured are reviewed in Pfaender, et al. (this report).

Chemical analyses of water and oil from the microcosms were done by Dr. John Laseter and Dr. Ed Overton, University of New Orleans. The techniques for the chemical analyses are discussed in Laseter et al. (this report).

3. RESULTS AND DISCUSSION

3.1 Bacterial Abundance and Community Composition

All oil types caused an increase in total bacterial cell numbers relative to the control (Fig. 3). The initial density of cells in the sample water was 0.6×10^6 cells/ml.

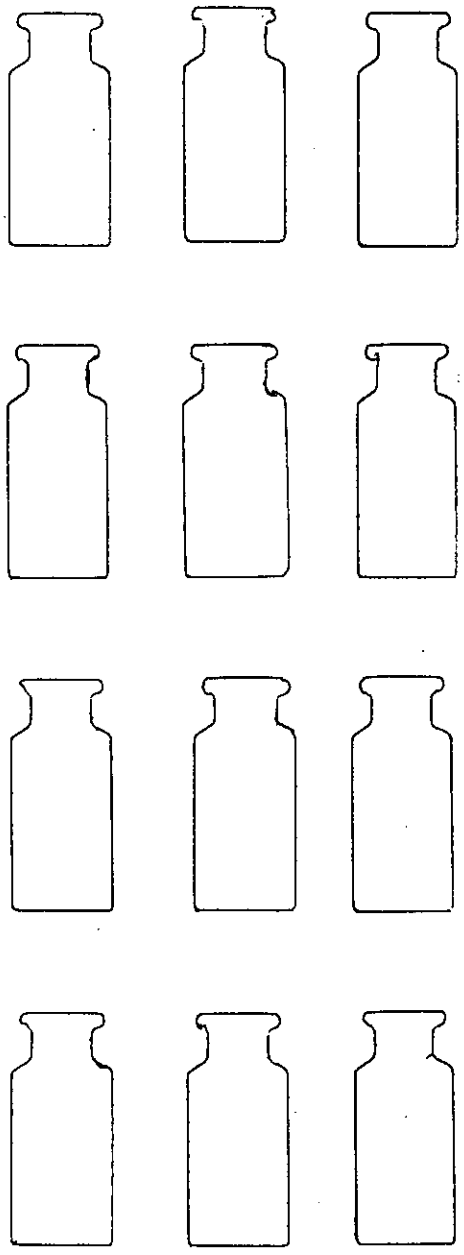

CONTROL (C)

WATER: 5 M, RIX09
OIL : NONE

WELL OIL (WO)

WATER: 5 M, RIX09
OIL : FRESH OIL, RIX07

WELL MOUSSE (WM)

WATER: 5 M, RIX09
OIL : MOUSSE, RIX06

TEXAS MOUSSE (TM)

WATER: 5 M, RIX09
OIL : MOUSSE, SOUTH PADRE ISLAND, TX

Figure 2. Experimental treatments of microcosm sample water.

Table 1. Sampling regime for microcosm experiment.

PARAMETER	DAY							
	0	1	2	3	4	5	6	7
Microbial Community:								
Total cells	+	+	+	+	+	+	+	+
Colony-forming units	+	+	+	+	+	+	-	+
Amino acid uptake	+	+	-	+	-	+	-	+
Amino acid respiration	+	-	-	+	-	+	-	+
Hexadecane metabolism	+	-	-	+	-	+	-	+
Naphthalene metabolism	+	-	-	+	-	+	-	+
Microbial Populations:								
Cell types	+	+	+	+	+	+	+	+
Differential colony counts	+	+	-	-	-	+	-	+
Identification	+	-	-	-	-	-	-	+
Chemistry:								
Hexadecane concentration	+	-	-	-	-	-	-	+
Naphthalene concentration	+	-	-	-	-	-	-	+

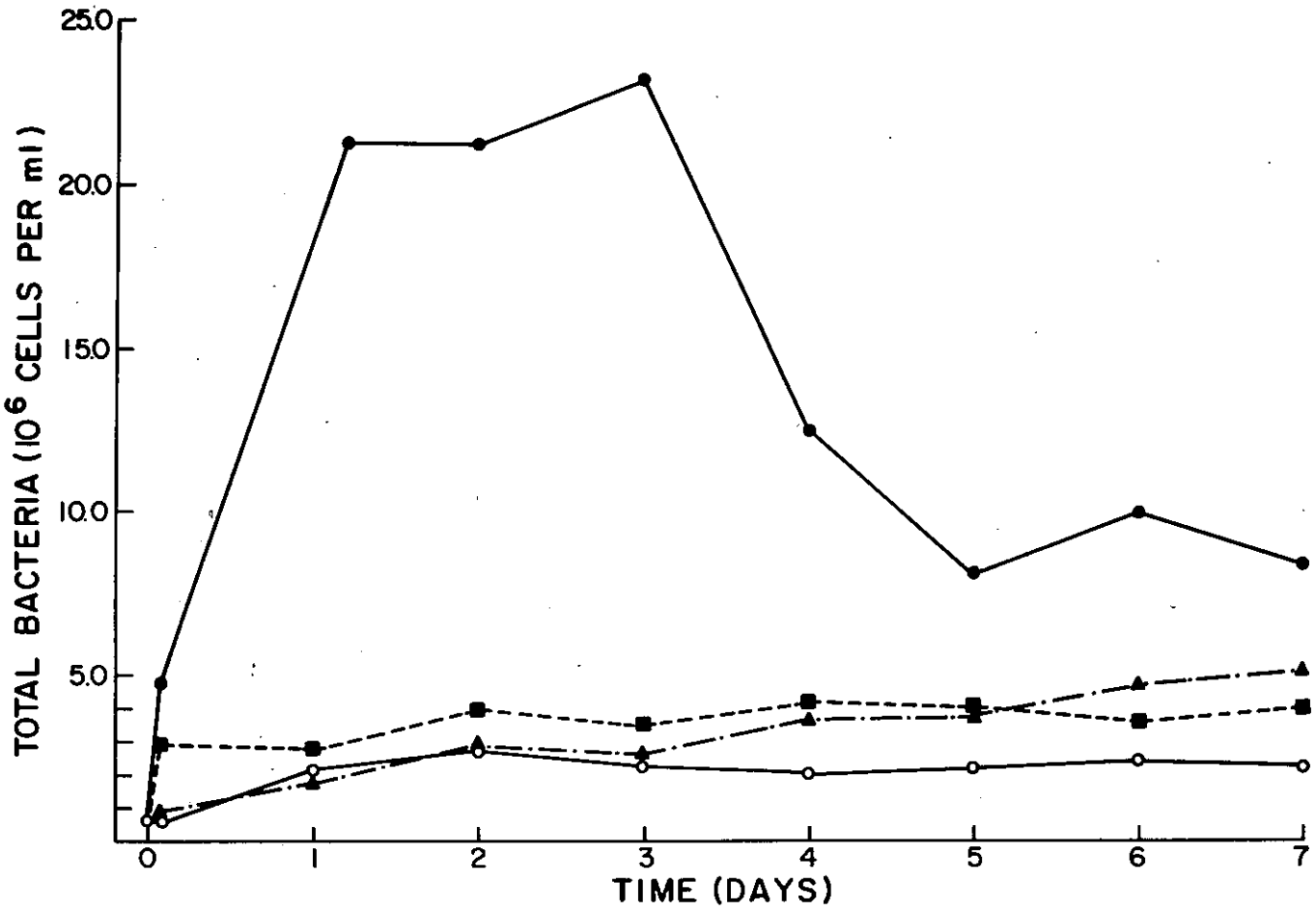

Figure 3. The response of total bacterial cell density to IXTOC-I oil: Control (○–○); Well mousse (●–●); Texas mousse (■--■); Well oil (▲–·–▲).

In the control microcosms, total cells exhibited a typical growth curve response to confinement: a phase of increase, a maximum stationary phase, a phase of decrease, and a phase of readjustment (ZoBell and Anderson, 1936). During the phase of increase, total cell density doubled twice to a maximum density of 2.7×10^6 cells/ml on day 2. The phase of decrease occurred between days 2 and 3. After day 3, total cell numbers fluctuated little; the mean total cell density for the phase of readjustment was 2.2×10^6 cells/ml.

In the oil and mousse microcosms, total cell density was increased within 1 h of addition of the hydrocarbons. In the one-hour samples, the number of total bacteria was 0.9×10^6 cells/ml in the WO microcosms, 4.75×10^6 cells/ml in the WM microcosms, and 2.94×10^6 cells/ml in the TM microcosms. The 1-h densities represent increases of 50%, 692%, and 390%, respectively, from the starting total cell numbers. This was most likely the result of the addition of bacteria to the water from the oil-associated microbial communities. Subsequent increases in total cell numbers probably were caused by inducement and stimulation of organisms in the presence of the hydrocarbons. The degree of stimulation and the rapidity of the response were dependent on oil type.

In the well mousse-amended microcosms, total bacteria increased to 21.28×10^6 cells/ml after 24 h and then stabilized until day 3. The mean cell density during the maximum stationary phase was 21.9×10^6 cells/ml. Between days 3 and 5, the total cell number decreased and re-equilibrated at a mean cell density of 818×10^6 cells/ml for the remainder of the incubation.

The greatest increase in total bacteria in the microcosms receiving Texas mousse occurred upon the addition of oil. Subsequently, total cell density did not change during the remainder of the initial 24-h incubation. Between days 1 and 2, the total bacteria increased to 4.0×10^6 cells/ml and subsequent fluctuations were small. After 48 h, the mean cell density was 3.9×10^6 cells/ml.

Although the addition of relatively fresh oil initially increased the abundance of suspended bacteria, total cell density in the WO microcosms was not significantly different from that in the control microcosms during the first 72 h of incubation. Only after day 3 was bacterial abundance enhanced; the final cell density in the WO microcosms was 5.1×10^6 cells/ml, the approximate density occurring in the WM microcosms after mousse addition.

Analysis of the cell type comprising the total bacteria demonstrates that, in conjunction with the enhancement of cell density, there were shifts within the bacterial communities. In the indigenous microbial community, rod-shaped cells less than 1.2 μ in length were predominant. After 24 h of incubation, rod-shaped cells greater than 2.4 μ in length were predominant in the control microcosms (Fig. 4).

After well mousse and Texas mousse were added, large (>2.4 μ) coccoid rods and S-shaped rods were observed in the samples from these treatment groups. In the well mousse amended microcosms, large coccoid and S-shaped cells accounted for over 50% of the total cells added to the oil. In contrast, only 15% of the bacteria added with the Texas mousse were these types of cells. However, after 24 h, 41.1% of the total cells in the Texas mousse exposed water were classified in these categories. The cell type composition in the water exposed to

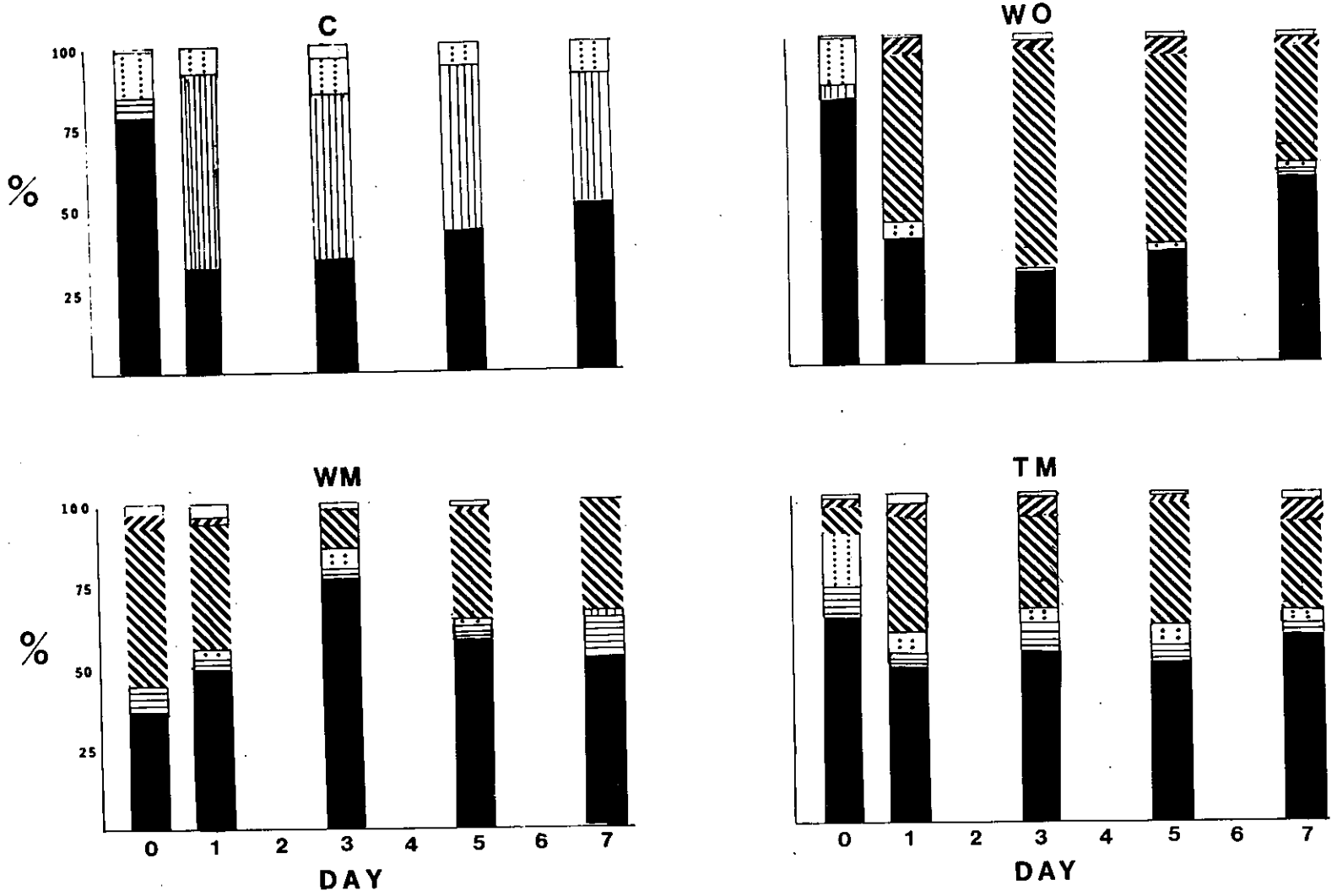

Figure 4. Fluctuations in the cell type composition of pelagic microbial communities exposed to IXTOC-I oil. C: control; WO: well oil; WM: well mousse; TM: Texas mousse (■ rod-shaped cells <1.2μ; ▤ rod-shaped cells 1.2-2.4μ; ▥ rod-shaped cells >2.4μ; □ cocci; ⊡ curved cells; ▧ large coccoid rods; ▨ large S-shaped cells).

well oil changed little after the addition of the hydrocarbons. By day 1, large coccoid rods and S-shaped cells were predominant.

The presence of particular cell types in the oiled microcosms that did not occur in the control water indicates that the oil selects for certain cell types within the community, thus causing shifts in the composition of the community. That oil enhances this shift is evidenced by the inducement of the coccoid and S-shaped rods in the WO microcosms after 24 h. The decrease in these cell types in the well oil exposed water may be a result of these bacteria associating with the oil as the oil ages. This association was demonstrated in the WM and TM treatment groups. This also supports in-situ data that indicate that the microbial community associated with mousse is distinct from the indigenous microbial community (Pfaender et al., this report).

Addition of oil also increased the abundance of culturable bacteria in the sample water (Fig. 5). The density of colony-forming bacteria in the original sample water was 5.0×10^2 CFU/ml. As with total cells, the greatest increase in CFU occurred following the addition of well mousse. The CFU density of 6.1×10^5 CFU/ml in the WM microcosms after 1 h represented a three-order-of-magnitude increase from the control water at 1 h. Texas mousse increased colony-forming bacteria over two orders of magnitude to 1.5×10^5 CFU/ml. The number of CFU in the well oil amended sample water increased threefold to 1.5×10^3 CFU/ml. If it is assumed that the enhancement of CFU density in the oiled microcosms was solely a result of the addition of CFU with the oil, bacteria originally associated with the well mousse accounted for 99.9% of the bacteria present in the water after 1 h. Texas mousse and well-oil-associated bacteria comprised 99.7% and 66.7% of the suspended bacteria in the respective treatment groups in the 1-h sample. Due to the large increase in CFU in the control water as a result of confinement alone, it was difficult to distinguish a treatment effect for the whole incubation period.

Addition of oil did result in the alteration of the generic composition of the sample water (Fig. 6). The unimpacted suspended community was predominated by Pseudomonas sp. and Alcaligenes sp. Following the addition of oil, regardless of type, Flavobacterium sp. and Vibrio sp. were increased and the percentage of Pseudomonas sp. was decreased. In the WO and WM microcosms, Flavobacterium was the predominant genus; Alcaligenes was the predominant genus in the TM microcosms. At the end of the incubation, Moraxella was the predominant genus in the control microcosms (Fig. 7). This effect of confinement was observed in all treatment groups. In the well oil amended microcosms, the percentage of Flavobacterium sp. and Vibrio sp. had changed little. Alcaligenes was the dominant genus in the WM microcosms after 5 days of incubation. Gram-positive organisms comprised a greater percentage of the Texas mousse exposed water. Thus, upon exposure to oil, the generic composition of the pelagic bacterial community was altered. The almost immediate restructuring of the indigenous community suggests that the oil and mousse are acting as a source of bacteria to the water. That the oil-associated microbial community is different from the suspended microbial community is noted by the increased occurrence of Flavobacterium sp. and Vibrio sp. in the oiled microcosms.

The occurrence of strains of Vibrio only in oil-exposed water may be significant. Colwell and Deming (1980) observed a similar relationship in the

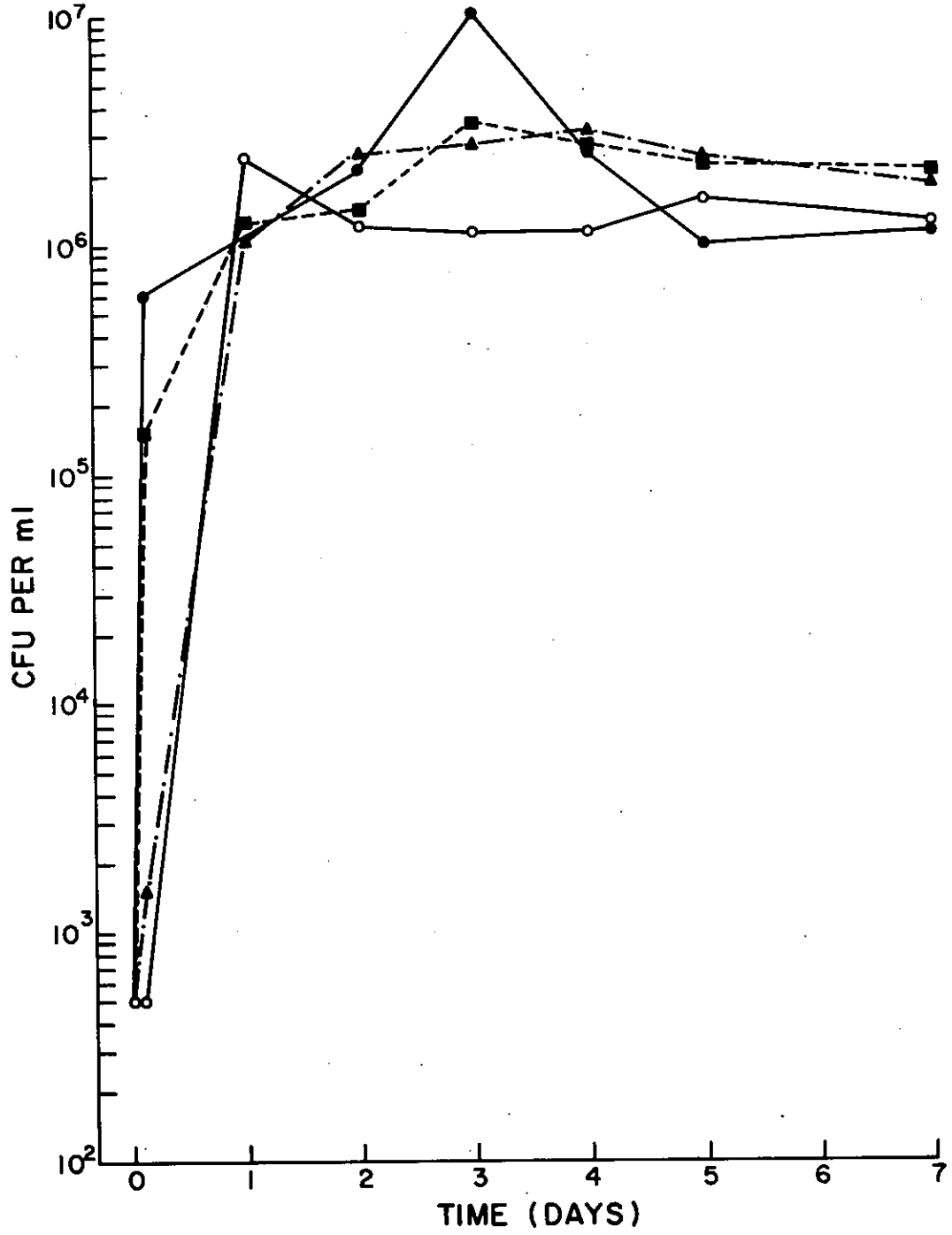

Figure 5. The response of colony-forming bacteria abundance to IXTOC-I oil: control (○—○); well mousse (●—●); Texas mousse (■--■); well oil (▲-·-▲).

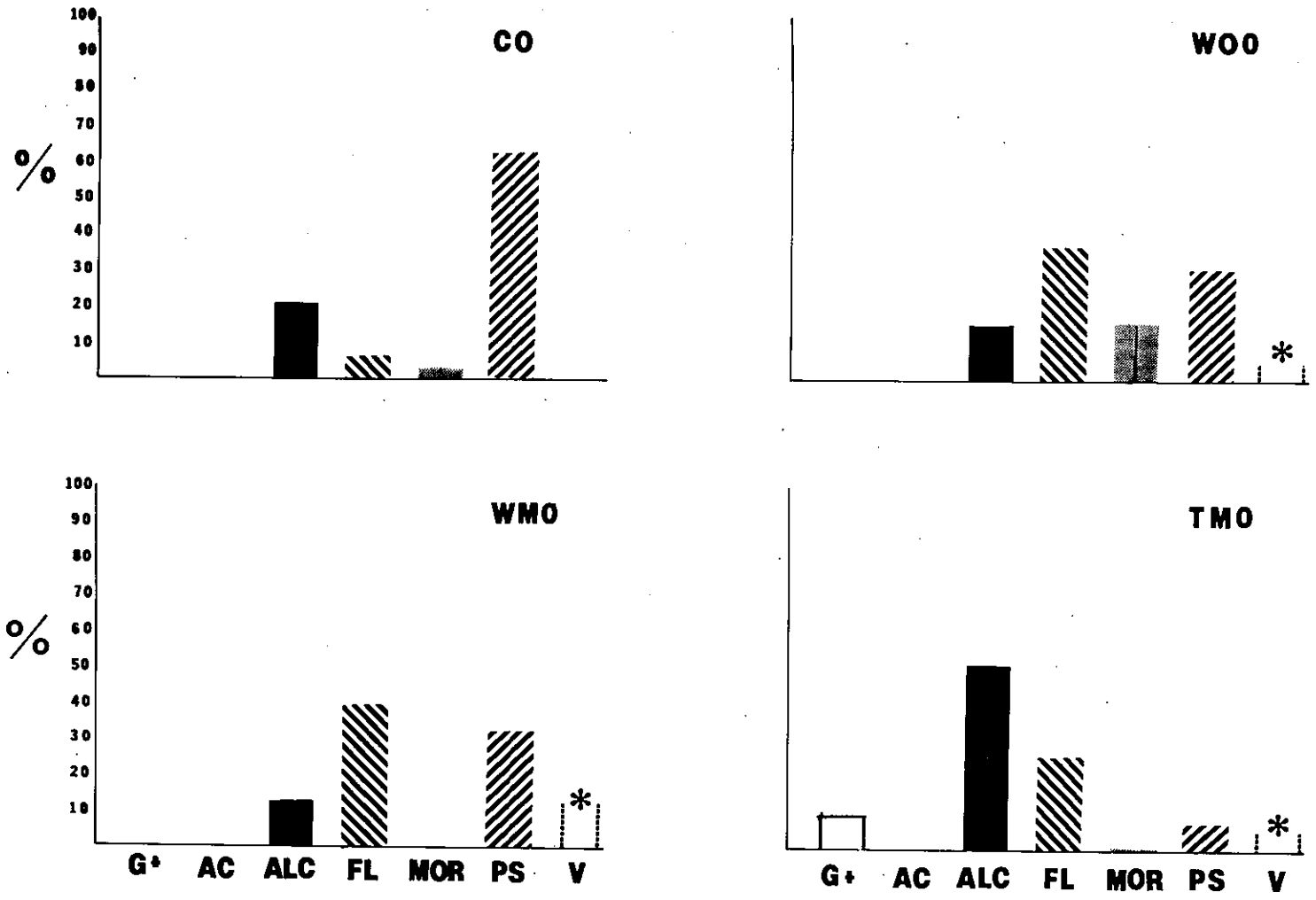

Figure 6. Generic composition of total colony-forming bacteria, initial samples. C: control; WO: well oil; WM: well mousse; TM: Texas mousse (G+, gram-positive bacteria; AC, Acinetobacter sp.; ALC, Alcaligenes sp.; FL, Flavobacterium sp.; MOR, Moraxella sp.; PS, Pseudomonas sp.; V, Vibrio sp., * underestimate due to growth characteristics).

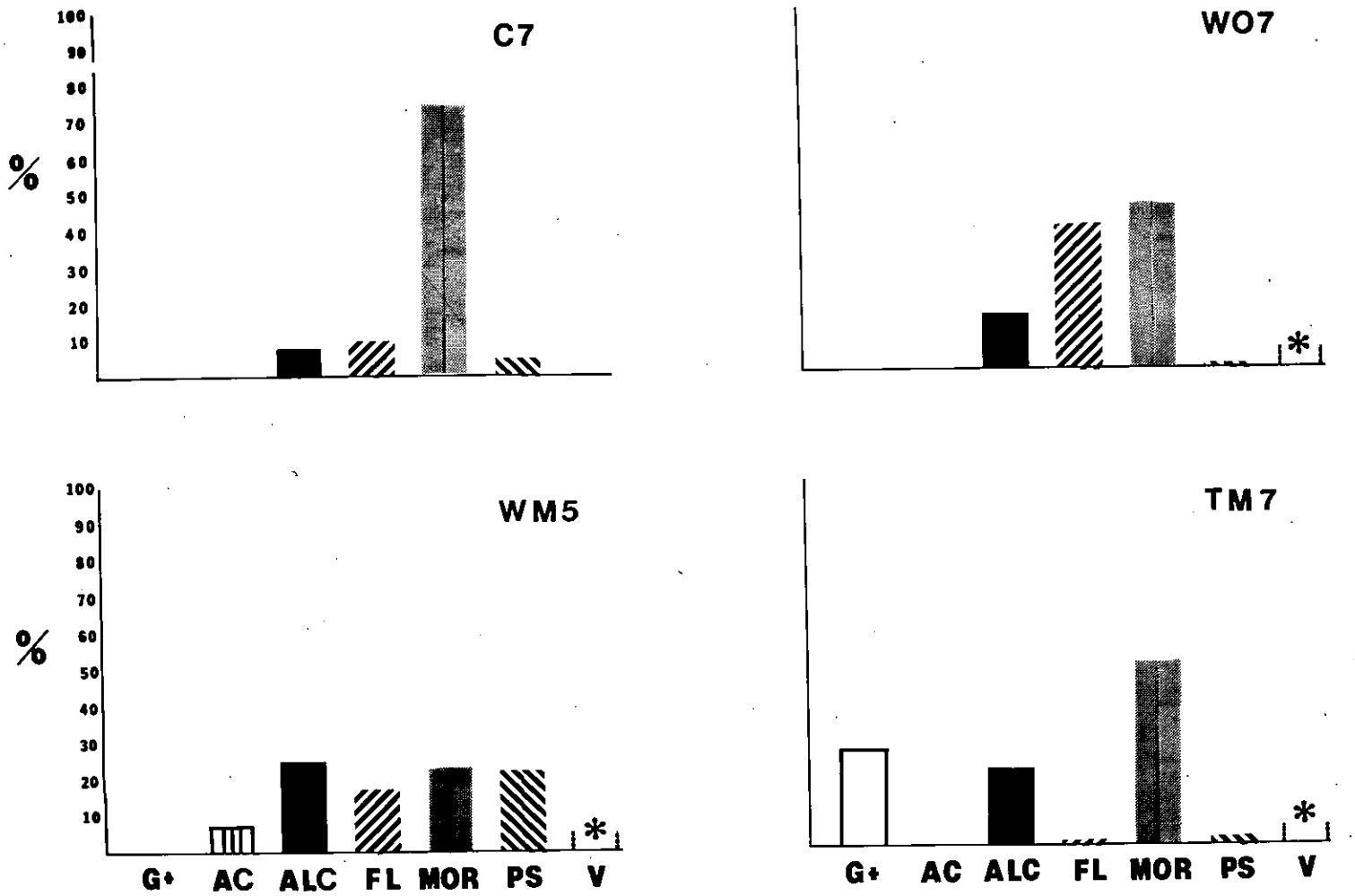

Figure 7. Generic composition of total colony-forming bacteria, final sampling (see Figure 6).

pharmaceutical waste dump sites off Puerto Rico. Within these ocean dumpsites, the predominant bacterial genus was Vibrio; in unimpacted waters, Pseudomonas was the predominant genus. Doubling times of 10-14 minutes have been recorded for some strains of Vibrio (Ulitzur, 1974), and many have exhibited a capability to degrade hydrocarbons (Buckley, 1980). Thus, selection of the oil for Vibrio sp. may promote the biological removal of the oil. However, the oil-mediated enhancement for Vibrio sp. could indirectly result in conditions hazardous to health if the selection process is nonspecific within the genus. The strains of Vibrio isolated in this study have been tentatively identified as Vibrio alginolyticus, which is the most commonly isolated Vibrio from marine pelagic systems (Baross and Liston, 1968). Species of Vibrio endemic to coastal marine systems include fish and human pathogens (Colwell, 1974). Enhancement of these organisms by oil intruding the coastal environment could create potential health hazards.

3.2 Heterotrophic Potential of the Microbial Community

Overall, the presence of oil increased the uptake of amino acids by the heterotrophic microbiota (Fig. 8). The enhancement of amino acid uptake was greatest and most rapid in the water exposed to well mousse. One hour after well mousse addition, the amino acid turnover rate increased from 0.25 x 10^{-3} h^{-1} to 4.4 x 10^{-3} h^{-1}. This may have resulted because of the large input of bacteria into the water from the mousse. However, the immediate stimulation of heterotrophic activity was not observed in the well oil or the Texas mousse amended microcosms. This suggests that the suspended microbiota in the microcosms subsequent to well mousse addition was better adapted to the conditions exerted by the well mousse on the water than the initial (1-h) microbial communities in the WO or TM microcosms. That the well mousse accounted for the largest percentage input of microbiota may have been a factor.

Oil-mediated stimulation of amino acid uptake in the Texas mousse microcosms did not occur until after day 1, and the turnover rate after readjustment was 50% lower than the final rate in the WM microcosms. The uptake of amino acids was depressed in the water exposed to well oil until day 5. Between day 5 and day 7, the turnover rate increased from 4.5 x 10^{-3} h^{-1} to 14.7 x 10^{-3} h^{-1}. Thus, the heterotrophic potential of the microbiota was not enhanced until after the controlling factors exerted by the oil on the bacteria had been sufficiently altered to promote amino acid uptake or after the microbiota in the water had adjusted to the input of petroleum hydrocarbons. Most likely, a combination of the alteration of the oil and the alteration of the microbiota was responsible for the enhancement of bacterial activity. In this respect it is noteworthy that stimulation did not occur until after 5 days of incubation; the rate of amino acid uptake in the day-5 sample from the WO microcosms was similar to the uptake rate in the WM microcosms following mousse addition, and the degree of stimulation was similar in both treatment groups.

The effects of the various oils on amino acid respiration were qualitatively similar (Fig. 9). In the mousse-exposed water, amino acid respiration was increased within an hour of the addition of mousse, and as with amino acid uptake, the stimulation was greater and more rapid in the water exposed to well mousse. Although the presence of well oil did not inhibit amino acid

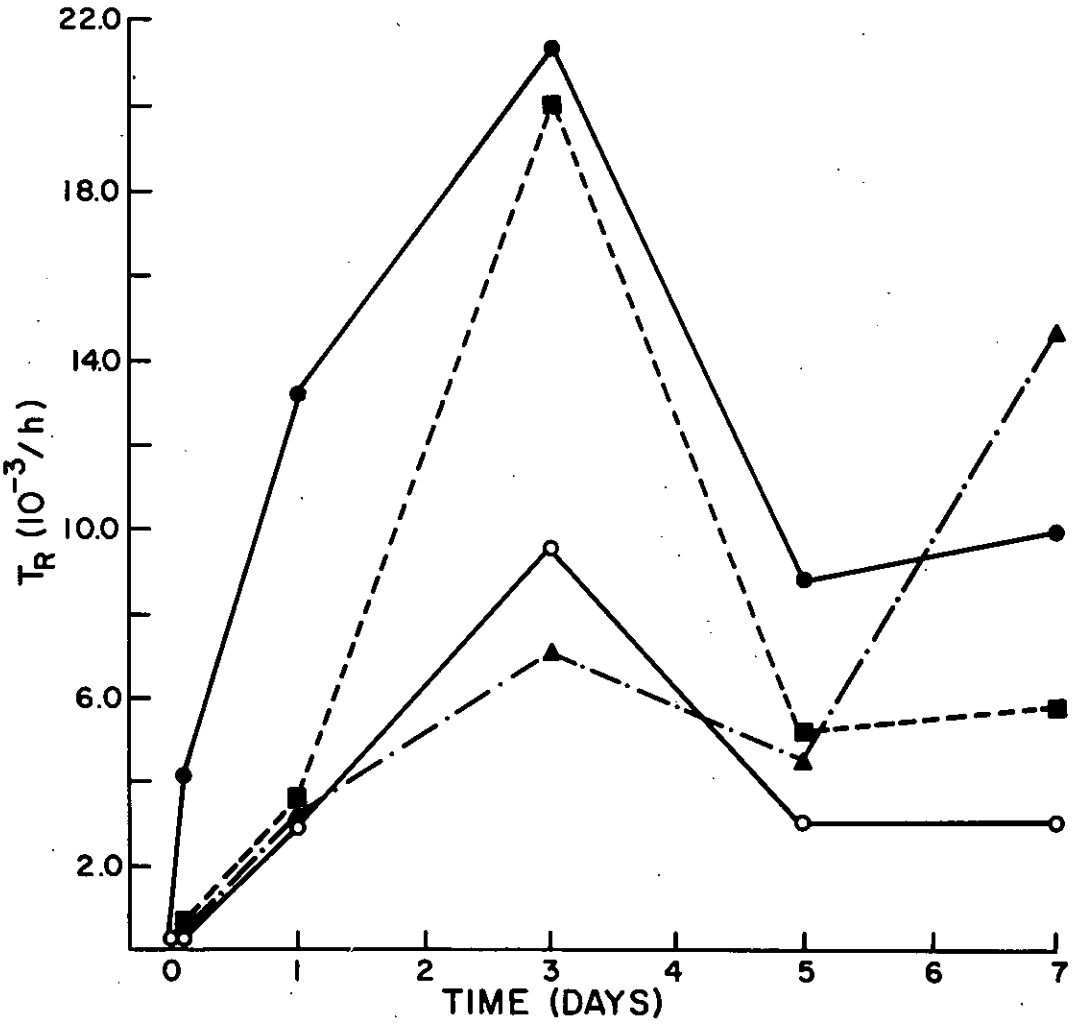

Figure 8. Effect of IXTOC-I oil on amino acid uptake. Control (○—○); well mousse (●—●); Texas mousse (■--■); well oil (▲-·-▲).

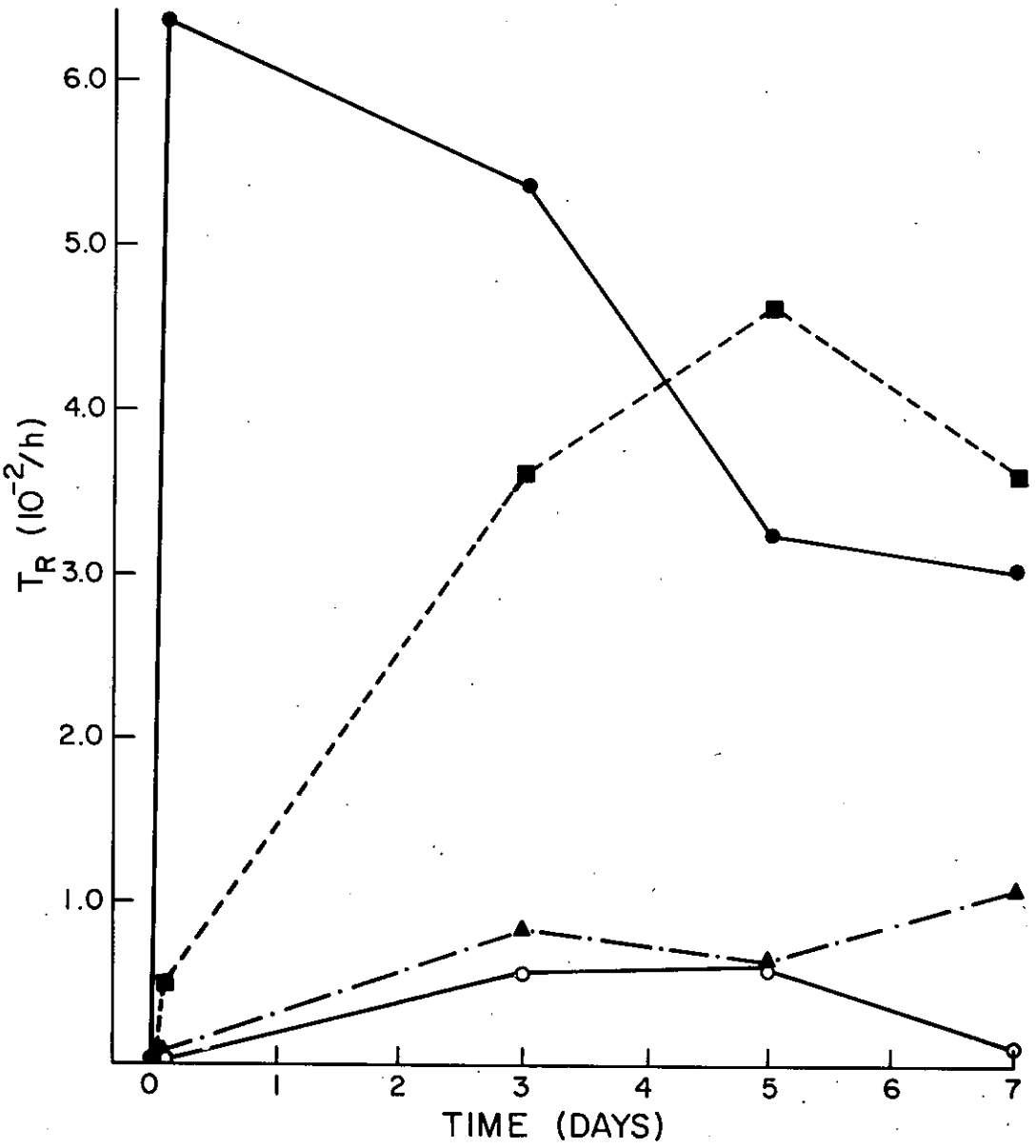

Figure 9. Effect of IXTOC-I oil on amino acid respiration. Control (○—○); well mousse (●—●); Texas mousse (■--■); well oil (▲-·-▲).

respiration, a significant enhancement of the respiration rate did not occur until after day 5, coincident with the stimulation of amino acid uptake.

3.3 Hydrocarbon Metabolism

In all of the oil-amended systems, the microbiota exhibited higher rates of hydrocarbon mineralization than in the control communities. It should be noted that rates of hydrocarbon metabolism were calculated using the concentrations of n-hexadecane and naphthalene in the sample water, which may cause an underestimation of the actual mineralization rate (Pfaender et al., this report). Despite the microbial mineralization of the oil in the microcosms, as indicated by the production of ^{14}C-CO_2 from ^{14}C-radiolabeled n-hexadecane and naphthalene, and by the appearance of partially oxidized aromatic compounds as metabolites of the bacterial degradative processes (Laseter, et al., this report), the concentration of hydrocarbons in the water column did not decrease throughout the experiment based on the concentration of both n-hexadecane and naphthalene at days 0 and 7 (E. Overton, University of New Orleans, personal communication). This suggests that: (1) the oil and mousse at the surface represent a large reservoir of hydrocarbons, which provides a constant supply of these compounds to the water within the microcosms, (2) the hydrocarbon concentrations in the water are at or near saturation, and (3) the limiting factor of concentration is the solubility of the oil into the water.

Hexadecane mineralization never exceeded 1.4×10^{-3} μg/L/h in the control water throughout the experiment (Fig. 10). Organisms in the water below the well mousse showed the greatest rate of hexadecane metabolism. Following the addition of the mousse, the rate of hexadecane mineralization was 0.2 μg/L/h, an increase of over two orders of magnitude from the rate in the original sample water. Hexadecane respiration was 0.5 μg/L/h during the cell density maximum and decreased to 0.2 μg/L/h by the end of the experiment. The addition of Texas mousse initially increased hexadecane metabolism by an order of magnitude (2.3×10^{-2} μg/L/h), but the mineralization rate decreased throughout the remainder of incubation. By day 7, the rate of hexadecane utilization in the TM microcosms was 2.5×10^{-3} μg/L/h, approximately 3 times greater than the mineralization rate in the control water. The well oil had no initial effect on hexadecane metabolism, but after day 5, the mineralization rate increased to 4.4×10^{-2} μg/L/h.

Naphthalene mineralization never exceeded 7.0×10^{-5} μg/L/h in the control water (Fig. 11). Addition of mousse or oil stimulated naphthalene respiration in all treatments. As with hexadecane metabolism, the well mousse stimulated naphthalene utilization most rapidly. After 1 h, the microbiota in the water exposed to well mousse were metabolizing naphthalene at a rate of 2.0×10^{-2} μg/L/h. This rate represents a three-order-of-magnitude increase from the rate in the original sample water, but it is an order of magnitude lower than the rate of hexadecane mineralization. During the cell density maximum, naphthalene respiration was approximately 0.2 μg/L/h; at the end of the incubation, the metabolism of naphthalene had decreased to 0.1 μg/L/h. Thus, after day 3, the mineralization rate of naphthalene was approximately half that for hexadecane. Texas mousse caused an initial increase in naphthalene metabolism to 2.4×10^{-3} μg/L/h; well oil initially increased naphthalene mineralization to

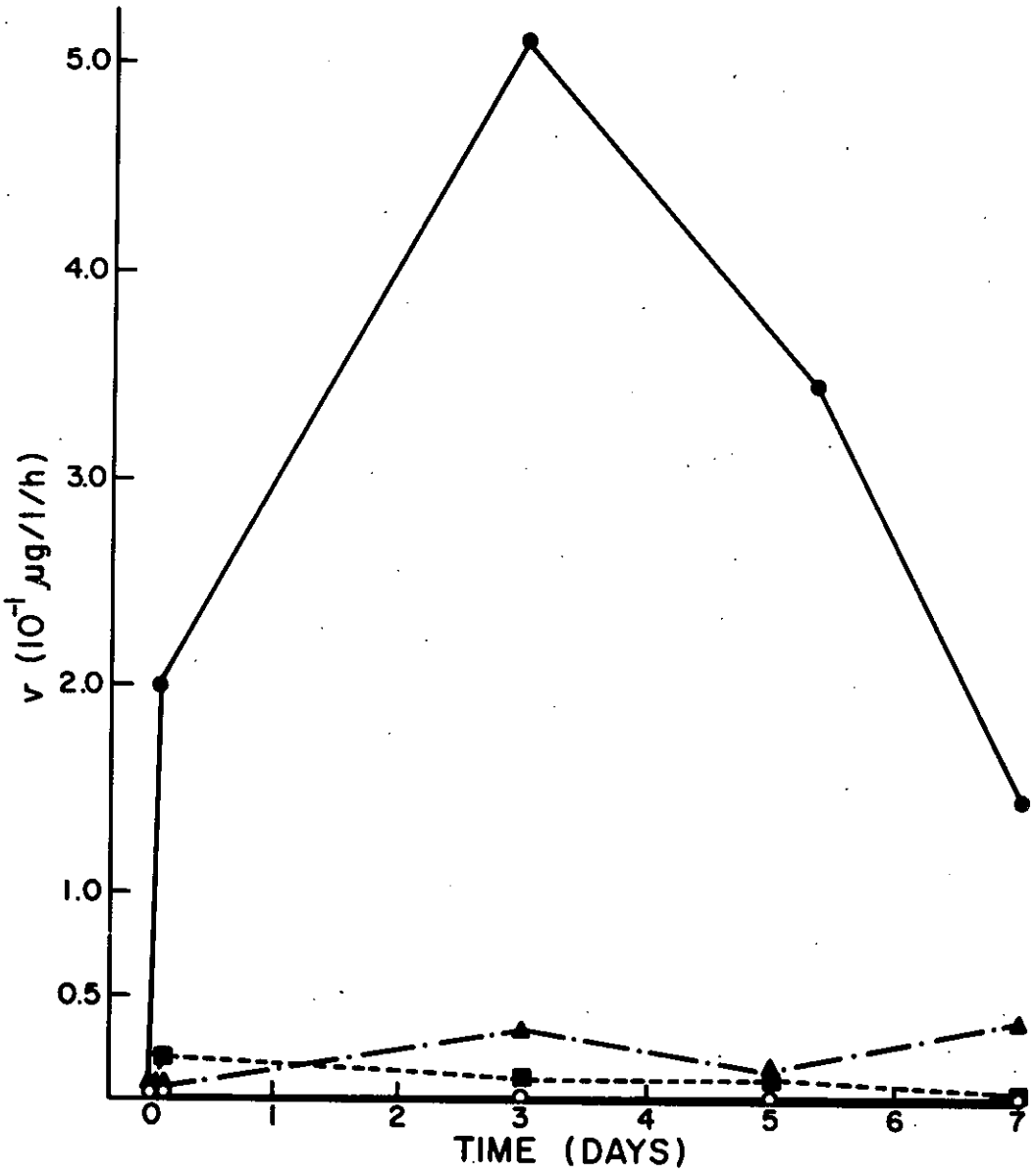

Figure 10. Effect of IXTOC-I oil on the mineralization rate of n-hexadecane. Control (○—○); well mousse (●—●); Texas mousse (■--■); well oil (▲-·-▲).

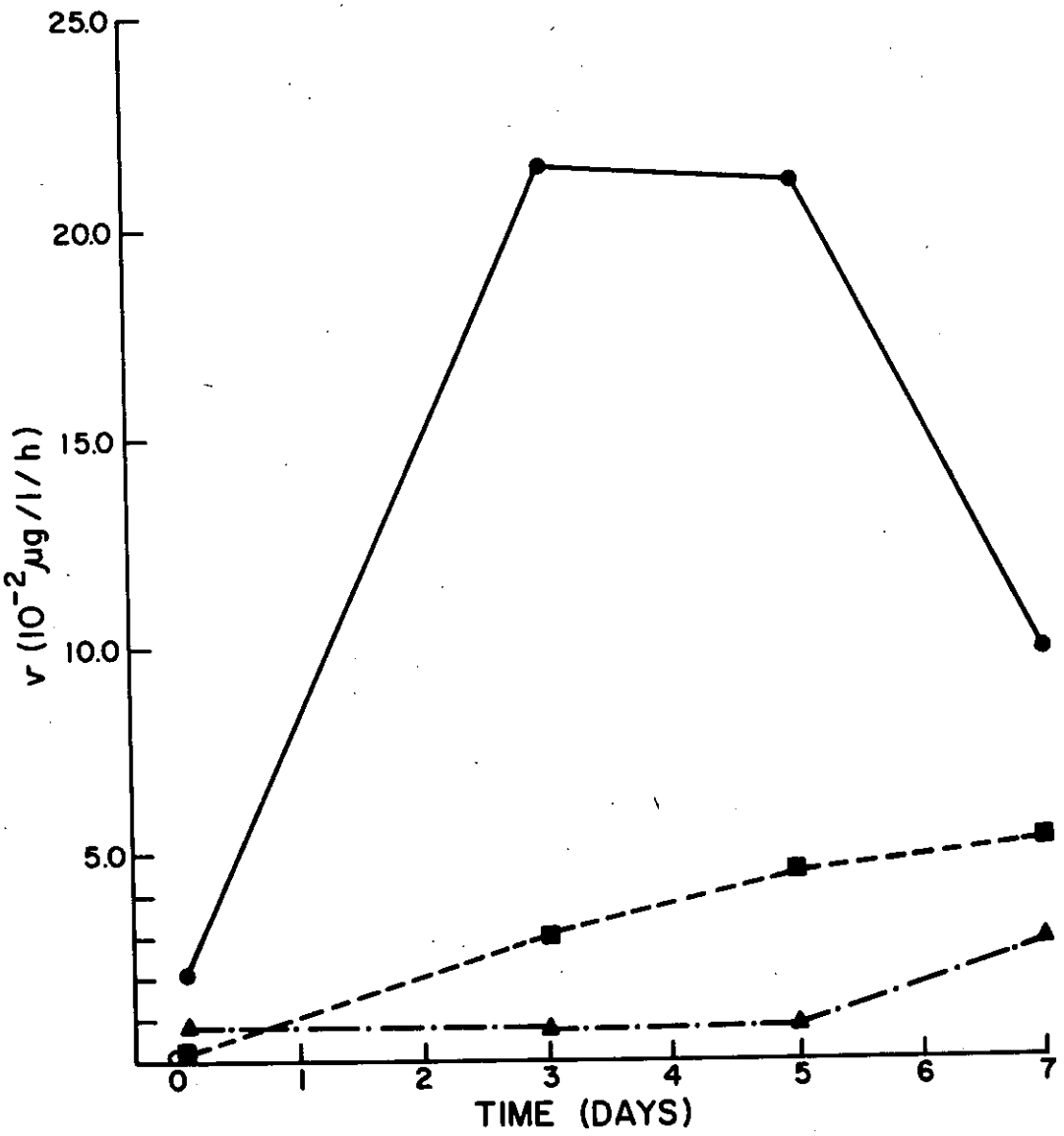

Figure 11. Effect of IXTOC-I oil on the mineralization rate of naphthalene. Control (○—○); well mousse (●—●); Texas mousse (■--■); well oil (▲-·-▲).

7.8×10^{-3} µg/L/h. Whereas naphthalene respiration did not increase again in the WO microcosms until after day 5, the rate of naphthalene metabolism in the Texas-mousse-impacted water increased throughout the incubation.

The mineralization rate of hexadecane was always greater than the rate of mineralization of naphthalene in samples from control, WM, and WO microcosms: it is well established that bacterial degradation of hydrocarbons is most rapid for straight-chain alkanes (McKenna and Kallio, 1965; Foster, 1962; Van der Linden and Thijsse, 1965). However, in the Texas mousse microcosms, the community was metabolizing naphthalene more rapidly than hexadecane by the end of the incubation period. This may be the result of a higher percentage of aromatic content in the more weathered Texas mousse. Chemical analyses of oil and water from the microcosms may help identify the mechanism of this effect.

5. SUMMARY

The responses of the microbial community to exposure to the various oils were (1) increased total bacterial cell density, (2) shifts in the generic composition (i.e., species predominance) and cell type distribution, (3) increased heterotrophic activity, in terms of amino acid uptake and respiration, (4) increased mineralization of n-hexadecane and naphthalene, and (5) the production of partially oxidized aromatic compounds as metabolites of the bacterial oxidation of the oil in the microcosms. The well mousse caused the most rapid and largest alterations in the sample water. This was initially due to the addition of bacteria from the mousse. These bacteria were already adapted to the presence of hydrocarbons from the mousse and consequently were capable of responding rapidly to the microcosm environment, which contained additional nutrients from the sample water and which was oxygenated continuously. These two factors, oxygen and nutrient limitation, are postulated to limit biodegradation in the mousse environment (Atlas et al., this report). In the well oil microcosm, a microbial community was induced from both the oil and sample water that was advantageous to the presence of oil. This suggests that the density of the well-oil-associated bacteria was considerably lower than the microbial density of the well mousse.

In consideration of the overall effect of the oil on the pelagic microbiota, the oil, in effect, molds the composition of the community by selecting for populations with favorable nutritional and physiological properties. But observations from this experiment suggest that the effect is not unidirectional; i.e., the bacteria in turn are able to modify the composition of their surroundings. At the end of the experiment, the physical characteristics of the fresh well oil were similar to those of fresh mousse. That the fresh mousse can serve as a good medium for microbial growth was observed by the enhancement of bacterial abundance, metabolic activity, hydrocarbon degradation, and the appearance of metabolites of microbial oxidation processes in the microcosms. In addition to being a source of carbon, the mousse can function as a source of surface area, which will further enhance microbial growth (ZoBell and Anderson, 1936). The alteration of the structure and metabolism of the initial community associated with the well oil

to a community similar to that initially associated with the well mousse suggests that the microbiota may play an important role in the conversion of fresh well oil into mousse.

In conclusion, the presence of oil had a profound influence in determining the composition and metabolic activity of the microbial communities within the microcosms; the metabolism of the community in turn may alter the physical and chemical properties of the oil. The presence of high numbers of bacteria associated with the oil may facilitate mousse formation.

6. REFERENCES

Atlas, R. M., and R. Bartha (1972a): Degradation and mineralization of petroleum by two bacteria isolated from coastal waters. Biotech. Bioeng., 14: 297-308.

Atlas, R. M., and R. Bartha (1972b): Biodegradation of petroleum in seawater at low temperatures. Can. J. Microbiol., 18: 1851-1855.

Baross, J., and J. Liston (1968): Isolation of Vibrio parahaemolyticus from the northwest Pacific. Nature, 217: 1263-1264.

Beyers, R. J. (1964): The microcosm approach to ecosystem biology. Amer. Biol. Teacher, 26: 491-498.

Buckley, E. N. (1980): The effects of petroleum hydrocarbons on metabolism of Spartina crude fiber by a salt marsh microbial community. Ph.D. Dissertation, University of North Carolina, Chapel Hill, NC, 320 pp.

Byron, J. A., S. Beastall, and S. Scotland (1970): Bacterial degradation of crude oil. Mar. Poll. Bull., 1: 25-26.

Calder, J. A., and J. H. Lader (1976): Effect of dissolved aromatic hydrocarbons on the growth of marine bacteria in batch culture. Appl. Environ. Microbiol., 32: 95-101.

Colwell, R. R. (1974): Vibrios and spirilla. In Handbook of Microbiology, A. I. Laskin and H. A. Lechevalier (Eds.), CRC Press, Inc., Cleveland, OH: 91-95.

Colwell, R. R., and J. Deming (1980): Effect of xenobiotic chemicals on marine microbial systems. Presented at the 80th Annual Meeting of the American Society for Microbiology, May 11-16, Miami Beach, FL.

Cowell, E. B., Ed. (1971): The Ecological Effects of Oil Pollution on Littoral Communities. Institute of Petroleum, London: 250 pp.

Dietz, A. S., T. Tuominen, and L. J. Albright (1976): Sublethal pollutant effects upon the native microflora of Georgia Strait. In Proc. 3rd Internat. Biodegradation Symp., Applied Sciences, New York, NY: 1083-1090.

Foster, J. W. (1962): Hydrocarbons as substrates for microorganisms. Antonie van Leeuwenhoek, 28: 241-274.

Gordon, R. W., R. J. Beyers, E. P. Odum, and R. G. Eagon (1969): Studies of a simple laboratory microecosystem: Bacterial activities in a heterophic succession. Ecology, 50: 86-100.

Griffin, L. F., and J. A. Calder (1977): Toxic effect of water-soluble fractions of crude, refined, and weathered oils on the growth of a marine bacterium. Appl. Environ. Microbiol., 33: 1092-1096.

Hodson, R. E., A. Azam, and R. F. Lee (1977): Effects of four oils on marine bacterial populations: Controlled ecosystem pollution experiment. Bull. Mar. Sci., 27: 119-126.

Hoppe, H. G. (1976): Determination and properties of actively metabolizing heterotrophic bacteria in the sea, investigated by means of microautoradiography. Mar. Biol., 36: 291-302.

Hyland, J. L., and E. D. Schneider (1976): Petroleum hydrocarbons and their effects on marine organisms, populations, communities, and ecosystems. In Proc. AIBS Symposium on Sources, Effects and Sinks of Hydrocarbons in the Aquatic Environment, Washington, DC: 463-506.

Lee, R. F., and J. W. Anderson (1977): Fate and effect of naphthalenes: Controlled ecosystem pollution experiment. Bull. Mar. Sci., 27: 127-134.

McKenna, E. J., and R. E. Kallio (1965): The biology of hydrocarbons. Ann. Rev. Microbiol., 19: 183-208.

Margalef, R. (1967): Laboratory analogues of estuarine plankton systems. In Estuaries, G. H. Lauff (Ed.), AAAS, Washington, DC: 757 pp.

Miget, R. J., C. H. Oppenheimer, H. I. Kator, and P. A. LaRock (1969): Microbial degradation of normal paraffin hydrocarbons in crude oil. In Proc. API/FWPCA Conf. on Prevention and Control of Oil Spills. API Publ. No. 4040, American Petroleum Institute, New York: 327-331.

Nelson-Smith, A., Ed. (1973): Oil Pollution and Marine Ecology. Plenum Press, New York, NY: 260 pp.

Soli, G., and E. M. Bens (1973): Selective substrate utilization by marine hydrocarbonoclastic bacteria. Biotech. Bioeng., 15: 285-297.

Ulitzur, S. (1974): Vibrio parahaemolyticus and Vibrio alginolyticus: Short generation-time marine bacteria. Microbiol. Ecol., 1: 127-135.

Van der Linden, A. C., and G. J. E. Thijsse (1965): The mechanisms of microbial oxidations of petroleum hydrocarbons. In Advances in Enzymology and Related Subjects of Biochemistry, Vol. 27, F. F. Nord (Ed.), Interscience Publishing Co., New York, NY: 469-546.

Walker, J. D., H. F. Austin, and R. R. Colwell (1975a): Utilization of mixed hydrocarbon substrate by petroleum-degrading microorganisms. J. Gen. Appl. Microbiol., 21: 27-39.

Walker, J. D., R. R. Colwell, and L. Petrakis (1975b): Evaluation of petroleum-degrading potential of bacteria from water and sediment. Appl. Microbiol., 30: 1036-1039.

Walker, J. D., and R. R. Colwell (1977): Role of autochthonous bacteria in the removal of spilled oil from sediment. Environ. Pollut., 12: 51-56.

ZoBell, C. E., and D. Q. Anderson (1936): Observations on the multiplication of bacteria in different volumes of stored seawater and the influence of oxygen tension and solid surfaces. Biol. Bull. Mar. Biol. Woods Hole, 71: 324-342.

ZoBell, C. E., and J. F. Prokop (1966): Microbial oxidation of mineral oils in Barataria Bay bottom deposits. Z. Allg. Microbiol., 6: 143-162.

APPENDIX I

Kinds and Numbers of Samples Collected

SAMPLE TYPE	NUMBER OF SAMPLES
Air Sample	37
Ammonia - NH_4^+	22
Microbiology, Acridine Orange Direct Counts of Bacteria	69
Bottom Sediment	98
Chlorophyll	82
Control H_2O	19
Control H_2O, Chlorophyll	18
Control H_2O, Extracted	3
Control H_2O, Low Molecular Weight Hydrocarbons	21
Control H_2O Particulates	6
Dead Fish	1
Hydrocarbon Biodegradation	19
Kjeldahl Analysis	2
Large Scale Hydrocarbon Biodegradation	4
Long Term Microcosm Study	12
Low Molecular Weight Hydrocarbon, H_2O	130
Microbiology	34
Microbiology - C^{14}, Amino Acid	15
Microbiology - C^{14}, Hexadecane	15
Microbiology - C^{14}, Naphthalene	15
Microbiology - H^3, Amino Acid	15
Microbiology - Plate Counts	32

SAMPLE TYPE	NUMBER OF SAMPLES
Mousse	93
Nutrients	100
Oil Covered Shell	1
Oil Patch	1
Oil/ Water Emulsion	2
Dissolved Oxygen	100
Particulates	31
Plankton	67
Purge Trap - Extracted - Filtered	7
Salinities	63
Sand, Beach	3
Sheen	112
Spanish Mackeral - Liver and Muscle	1
Surface Matter	10
Tar	26
Trace Metals (For Mexico)	12
Trace Organics	1
Volatile Hydrocarbons	68
Weed (Possibly Sugar Cane)	1
Whole H_2O	303

APPENDIX II

Explanation of Sample Code

An example and explanation of the Sample Code is as follows:

Example: RIX04A005

The first letter designates the ship from which the sample was taken;
'R' designates RESEARCHER and 'P' PIERCE.

The second and third letters designates the cruise; thus,
'IX' designates the IXTOC cruise.

The next two numbers of the Code designates the Station number; thus,
'04' indicates Station number 4.

The sixth character indicates who took the sample; thus,
'A' indicates the sample was taken by someone from AOML.

The other codes and their meaning are listed below:

A= AOML
B= Texas A&M University
E= Energy Resources Company,Inc.
F= Woods Hole Oceanographic Institution
K= Global Geochemistry Corporation
L= University of Louisville
M= Mexico
N= University of North Carolina
O= University of New Orleans
R= NOAA/NMFS/SEFC,BEAUFORT, N.C.
S= Science Applications,Inc.
W= University of Washington

The last three numbers indicate the sequential sample #; thus, '005'indicates the fifth sample taken by that "group."
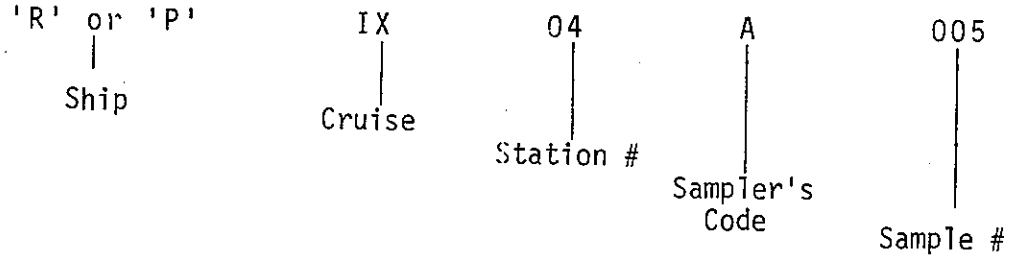
In summary the Sample Code Numbers indicate the following: